GEYSERS DATABASE LBL 1989

LBL-28618 1/3

LAWRENCE BERKELEY LABORATORY
EARTH SCIENCES DIVISION

A DATABASE FOR THE GEYSERS GEOTHERMAL FIELD

VOLUME I: TEXT AND MAIN FIGURES

SEPTEMBER 1989

G. S. BODVARSOOON, B. L. COX, P. FULLER, M. RIPPERDA,
H. TULINIUS, P. A. WITHERSPOON, N. GOLDSTEIN,
S. FLEXSER, K. PRUESS, AND A TRUESDELL

A DATABASE FOR THE GEYSERS GEOTHERMAL FIELD

Volume I: Text and Main Figures

Gudmundur S. Bodvarsson, B. Lea Cox, Peter Fuller, Mark Ripperda,
Helga Tulinius, Paul A. Witherspoon, Norman Goldstein,
Steve Flexser, Karsten Pruess and Alfred Truesdell*

Earth Sciences Division
Lawrence Berkeley Laboratory
University of California
Berkeley, California 94720

*U. S. Geological Survey
345 Middlefield Road
Menlo Park, California 94025

September 1989

This work was supported by the California State Lands Commission and by the U.S. Department of Energy under Contract No. DE-AC03-76SF00098.

Acknowledgements

The authors are indebted to the Division of Oil and Gas (R. Thomas and K. Stelling), the California State Lands Commission office in Sacramento (C. Priddy), the California State Lands Commission Office in Long Beach (P. Mount and J. Adams) and the Air Pollution Board for providing data from The Geysers field. We also thank Scott Gaulke and Sally Benson for their technical reviews. Significant contributions were made by U.C. Berkeley students Ali Barakat, Bjorna Goranson, Duc Nguyen and Jefferson Dolan. Word processing by Ellen Klahn and Leslie Fairbanks is appreciated, as is careful editing by Mary G. Bodvarsson. This work was supported by The California State Lands Commission and through U.S. Department of Energy Contract No. DE-AC03-76SF00098.

1.0. INTRODUCTION

In Fiscal Year 1985-86 the Earth Sciences Division of Lawrence Berkeley Laboratory (LBL) began a multi-year project for SLC to organize and analyze the field data from The Geysers. In the first year, most of the work concentrated on the development of a comprehensive database for The Geysers, and conventional reservoir engineering analysis of the data. Essentially, all non-proprietary data for wells at The Geysers have been incorporated into the database, as well as proprietary data from wells located on State leases. In following years, a more detailed analysis of The Geysers data has been carried out.

This report is a summary of the nonproprietary work performed in FY 1985-86. It describes various aspects of the database and also includes: review sections on Field Development, Geology, Geophysics, Geochemistry and Reservoir Engineering. It should be emphasized that these background chapters were written in 1986, and therefore only summarize the information available at that time. The appendices contain individual plots of wellhead pressures, degree of superheat, steam flow rates, cumulative mass flows, injection rates and cumulative injection through 1988 for approximately 250 wells. All of the data contained in this report are nonproprietary, from State and non-State leases. The production/injection and heat flow data from the wells were obtained from the California State Division of Oil and Gas (DOG) (courtesy of Dick Thomas). Most of the other data were obtained from SLC files in Sacramento (courtesy of Charles Priddy), or DOG files in Santa Rosa (courtesy of Ken Stelling).

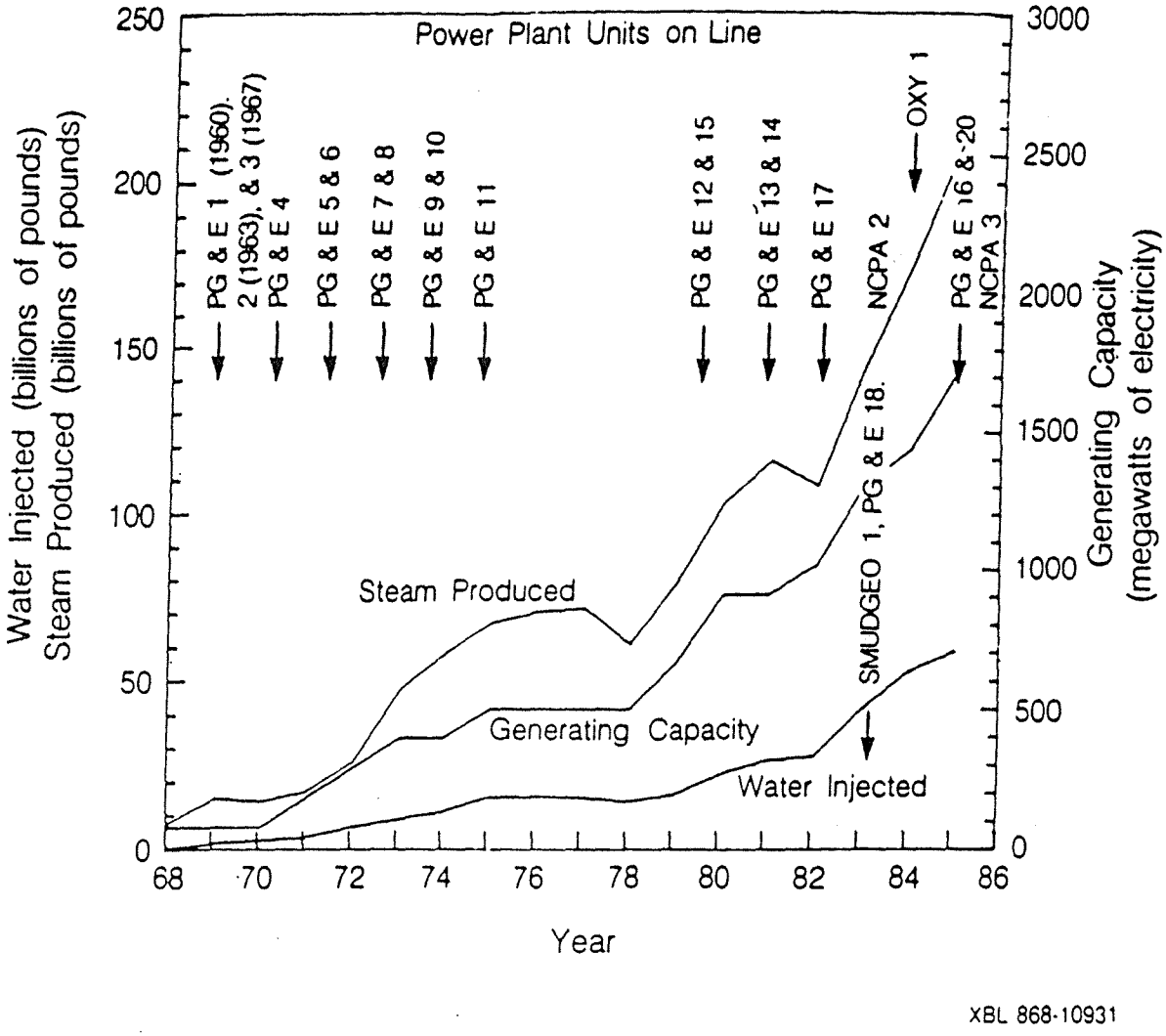

Figure 2-1. Cumulative steam production and water injection at The Geysers along with the electrical power production 1968-1986.

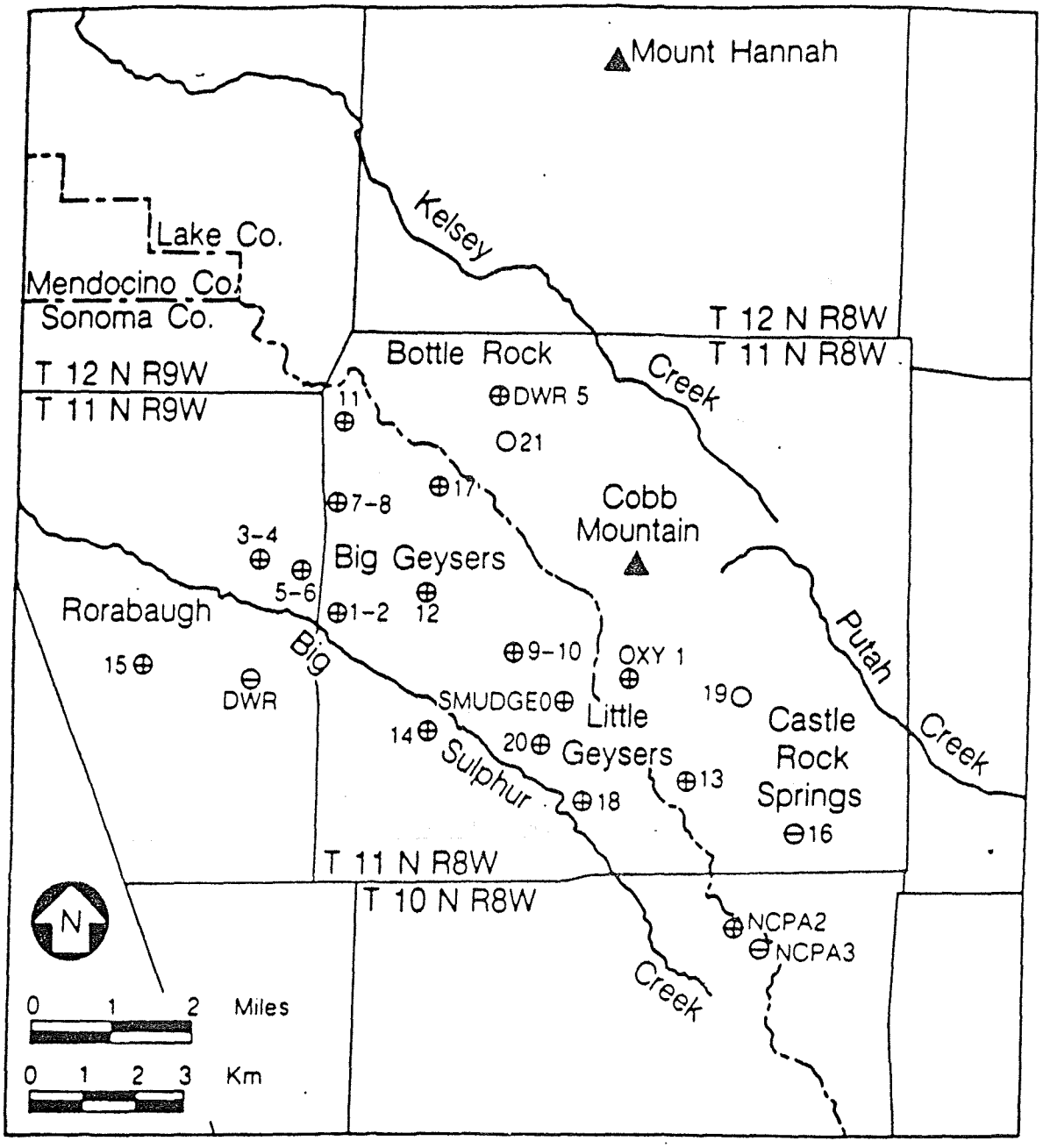

XBL 868-10949

Figure 2-2. Locations of power plants at The Geysers. Also shown are landmarks, rivers, and section and county lines.

Table 2.1. Geothermal power plants at The Geysers.

Plant Owner/Name	On Line	Primary Steam Supplier	Net MWe	Cum. Net MWe
PG&E 1-2	1960-82	Magma Thermal	24	24
PG&E 3-4	1967-68	Unocal Geothermal	54	78
PG&E 5-6	1971	Unocal Geothermal	106	184
PG&E 7-8	1972	Unocal Geothermal	106	290
PG&E 9-10	1973	Unocal Geothermal	106	396
PG&E 11	1975	Unocal Geothermal	106	502
PG&E 12	1979	Unocal Geothermal	106	608
PG&E 15	1979	Geo Operator Corp.	59	667
PG&E 13	1980	Freeport McMoran	133	800
PG&E 14	1980	Unocal Geothermal	103	909
PG&E 17	1982	Unocal Geothermal	110	1,019
PG&E 18	1983	Unocal Geothermal	110	1,129
NGPA 1	1983	Nocal Power Agency	106	1,235
SMUD 1	1983	Unocal Geothermal	65	1,309
OXY1	1984	Santa Fe Geothermal	80	1,380
PG&E 16	1985	Freeport McMoran	123	1,493
PG&E 20	1985	Unocal Geothermal	113	1,606
NCPA 2	1985-86	Nocall Power Agency	106	1,712
DWR 1	1985	Dept. Water Resources	52	1,764
CCPA 1-2	1988	Geooperator Corp.	130	1,894
Bear Canyon	1988	Freeport McMoran	20	1,941
Ford Flat	1988	Freeport McMoran	27	1,941
Aidlin	1989	Geo Energy Partners	20	1,961

Jack area; together they increased the total electric power production from this area to some 184 MW_e. Power plants 7 and 8 are located on State lease PRC 4596, close to the discovery well Ottoboni Federal 1, drilled by Union in 1966. Both of these 53 MW_e units came on-line in 1972. In 1975 and 1982 two 106 and 114 MW_e power plants, Units 11 and 17, also began commercial operation on PRC 4596. Thus, the total electrical production from PRC 4596 amounts to 326 MW_e.

Since 1973, most of the development in The Geysers area has been in the south-eastern part of the field, covering an area extending up to 5 miles southeast of the Big Geysers area. Units 9, 10, 12 and 14 produce from or close to another large State lease, PRC 4597. These units produce a total of 321 MW_e. All of the remaining power plants are farther to the southeast (Little Geysers) with the exception of Unit 15, which is located in the Rorabaugh area 1-2 miles southwest of the Sulphur Banks wellfield, and the DWR plant in the Bottle Rock area. At present, power plants PGE 13, PGE 18, NCPA 2 and 3, SMUD and OXY 1 are operating in or near the Little Geysers area, with a total generating capacity over 600 MW_e. Unit 13 is the largest unit at The Geysers, producing 135 MW_e.

Although Union-Magma-Thermal is the largest steam supplier at The Geysers, many other companies have drilled development wells that feed several of the power plants. In 1967, Geothermal Resources International (now GEO), began drilling wells in the Rorabaugh area. Seven wells were drilled by 1969, three of them producing steam equivalent to some 10 MW_e each. Further development in this area was conducted by Thermogenics Inc., resulting in a 59 MW_e generating unit (Unit 15), commencing operation in 1979 (Reed, 1982a). In 1969, Signal Oil and Gas Company began drilling in the Castle Rock Springs area, which at that time was a very large stepout to the southeast. Signal had drilled six wells in this area by 1971; the wells produced steam equivalent to some 30 MW_e (Garrison, 1972). Signal's interest in this area was acquired by Aminoil U.S.A., Inc., which contracted with PG & E to supply steam for Unit 13, a 135 MW_e unit that started commercial production in 1980. Aminoil also contracted with the Sacramento Municipal Utility District (SMUD) to provide steam for a 72 MW_e SMUD power plant north of

the Little Geysers area that came on-line in 1983. In 1984, Aminoil sold its interest at The Geysers to Phillips Petroleum Company, which then sold the properties a year later to the Freeport-McMoRan Resource Partnership (FMRP; Ken Stelling, personal communication, 1986).

Shell Oil Company started drilling in the southern part of The Geysers (south of Castle Rock Springs) in 1974. Shell made an agreement with the Northern California Power Agency (NCPA) to supply steam for two 55 MW_e NCPA power plants. NCPA 2 commenced operation in March 1983 and NCPA 3 in 1984. Shell later sold its interest to the Grace Geothermal Company, which then sold it to NCPA.

The McCulloch Geothermal Corporation (now MCR Geothermal Corporation) started drilling on leases in the northeastern part of The Geysers (Bottle Rock area) in 1976. The area proved to be productive and MCR agreed to provide steam for a 55 MW_e unit to be operated by the Department of Water Resources (DWR). This plant has been in operation for several years. MCR, in cooperation with DWR, has also been developing an area one mile south of Sulphur Banks (South Geysers), but construction of a power plant has been halted because of the lack of productive wells.

Occidental Geothermal Corporation started drilling north of Little Geysers in 1979. Many of the wells proved productive. Occidental has constructed an 80 MW_e power plant, which started commercial power production in 1984. Occidental sold its interests at The Geysers to the Santa Fe Geothermal Company, a subsidiary of the Kuwait Oil Company in 1985 (Ken Stelling, personal communication, 1986).

The development of The Geysers has continued at a fast rate through the 1980's, as clearly shown in Figure 2-1. The field has been extended to the northwest with the recent completion of the coldwater Creek power plants (GEO Operator Corp.). However, several plants that had been planned (PGE 21-24, for example) were canceled because of worries about the future availability of adequate steam supplies.

2.2. GEOLOGY

2.2.1. Regional Geology and Structure

The Geysers geothermal system is situated the northern California Coast Ranges, which are characterized by major northwest-trending, predominantly strike-slip faults of the San Andreas system (Figure 2-3). The basement lithology is composed of the late Mesozoic Franciscan assemblage, a diverse complex of marine metasedimentary and metaigneous rocks highly disrupted by continental margin subduction, structurally overlain by the approximately coeval, but much less disturbed marine sediments and ophiolites of the Great Valley sequence. The Franciscan and Great Valley units were deposited in widely separated basins, and were later juxtaposed across a major regional thrust fault, the Coast Range thrust, associated with subduction. Mid-Tertiary to Quaternary volcanic rocks are locally abundant in the Coast Ranges, and they are represented in the area of The Geysers by the predominantly Pleistocene Clear Lake volcanics, and by the Pliocene Sonoma volcanics. The Coast Ranges are highly complex structurally, a result of superposition of late Tertiary to Quaternary strike-slip and related tectonism upon the already complex subduction-related deformation of the Mesozoic units (McLaughlin, 1981).

Franciscan Assemblage

The Franciscan assemblage consists mainly of marine turbidite graywacke sandstones, with lesser but abundant chert, shale, greenstone, and serpentinized ultramafic rock, and with minor limestone and included blocks of eclogite and amphibolite. These rocks were formed west of or over an east-dipping subduction zone situated along the western margin of the continent in late Mesozoic time (McLaughlin and Pessagno, 1978). The detrital Franciscan rocks were probably derived from continental or island arc sources (McLaughlin, 1981), but there is debate concerning specific source areas due to their likely displacement or destruction by transform faulting and/or subduction (Jones et al., 1978).

The Franciscan assemblage is characterized by locally intense deformation, resulting in the occurrence of broken formations and melanges. The major deformation and metamorphism of the

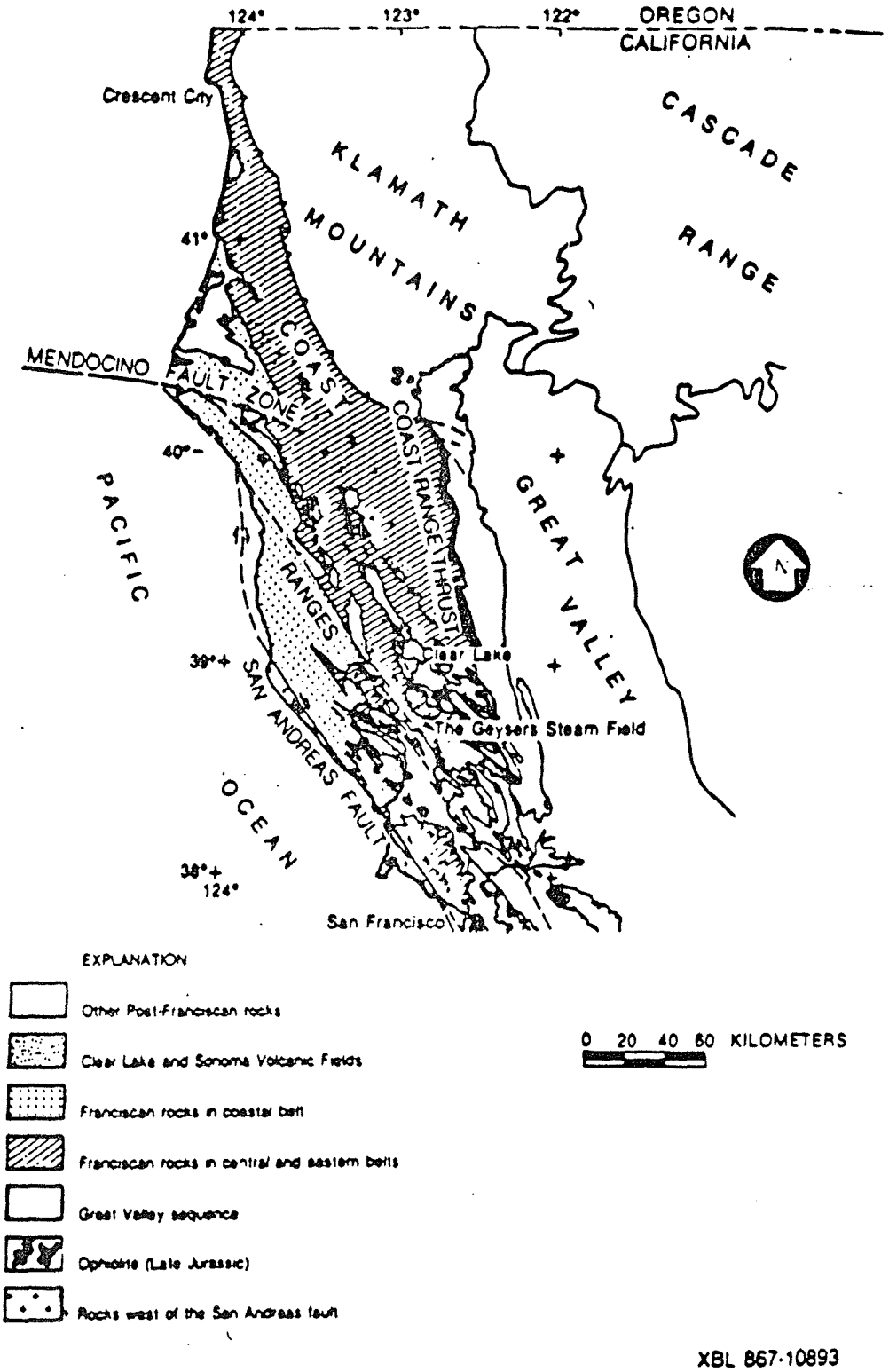

Figure 2-3. Location of Clear Lake and The Geysers in the Northern California Coast Ranges, showing generalized regional geology and major fault zones (after McLaughlin and Pessagno, 1978).

Franciscan took place in late Mesozoic and early Tertiary times, along an east-dipping subduction zone which stepped outward from the continent with time. Successively younger and more westerly slabs of Franciscan rocks were thrust beneath the hanging wall of the subduction zone, and metamorphism, ranging mainly from zeolite to blueschist facies, accompanied subduction. The easternmost slab of subducted Franciscan rock was juxtaposed against oceanic crust and overlying sediments comprising the Great Valley sequence, and this contact marks the Coast Range thrust (Figure 2-4) (Bailey et al., 1970). The age of this thrust has been determined by study of radiolaria in chert (McLaughlin and Pessagno, 1978) to have occurred after the start of the Cenomanian (late Cretaceous) 96 m.y.b.p (million years before present).

Three broad sub-units of the Franciscan in the northern Coast Ranges, the coastal, central, and eastern belts, have been recognized based on their degree of metamorphism and associated textural reconstitution (Blake et al., 1967), and they correlate with differences in age and lithology (Berkland et al., 1972; Jones et al., 1978). The three northwest-trending belts are progressively older from west to east, and early to mid-Tertiary ages have been reported for the coastal belt (Jones et al., 1978; Evitt and Pierce, 1975). Metamorphic grade generally increases from west to east also. The lithology of the coastal belt is typically graywacke metamorphosed to the low-grade blueschist facies minerals laumontite and pumpellyite; the eastern belt is largely graywacke metamorphosed to a higher grade assemblage characterized by lawsonite, with schistose and cataclastic textures. The lithology of the central belt is more diverse, and the varied assemblage of Franciscan rock types is well represented; broken formations and melanges are common, and metamorphic mineralogy and texture are intermediate between those of the other belts, with prehnite-pumpellyite grade metamorphism characteristic. The three sub-units of Franciscan rocks have probably been displaced relative to one another and to the structurally overlying Great Valley sequence by strike-slip motion (McLaughlin, 1981). On a smaller scale, they are cut into imbricate thrust slabs, which are folded and cut by steeply dipping strike-slip and normal faults.

In The Geysers area, outcrops consist mainly of the central belt of the Franciscan (Figure

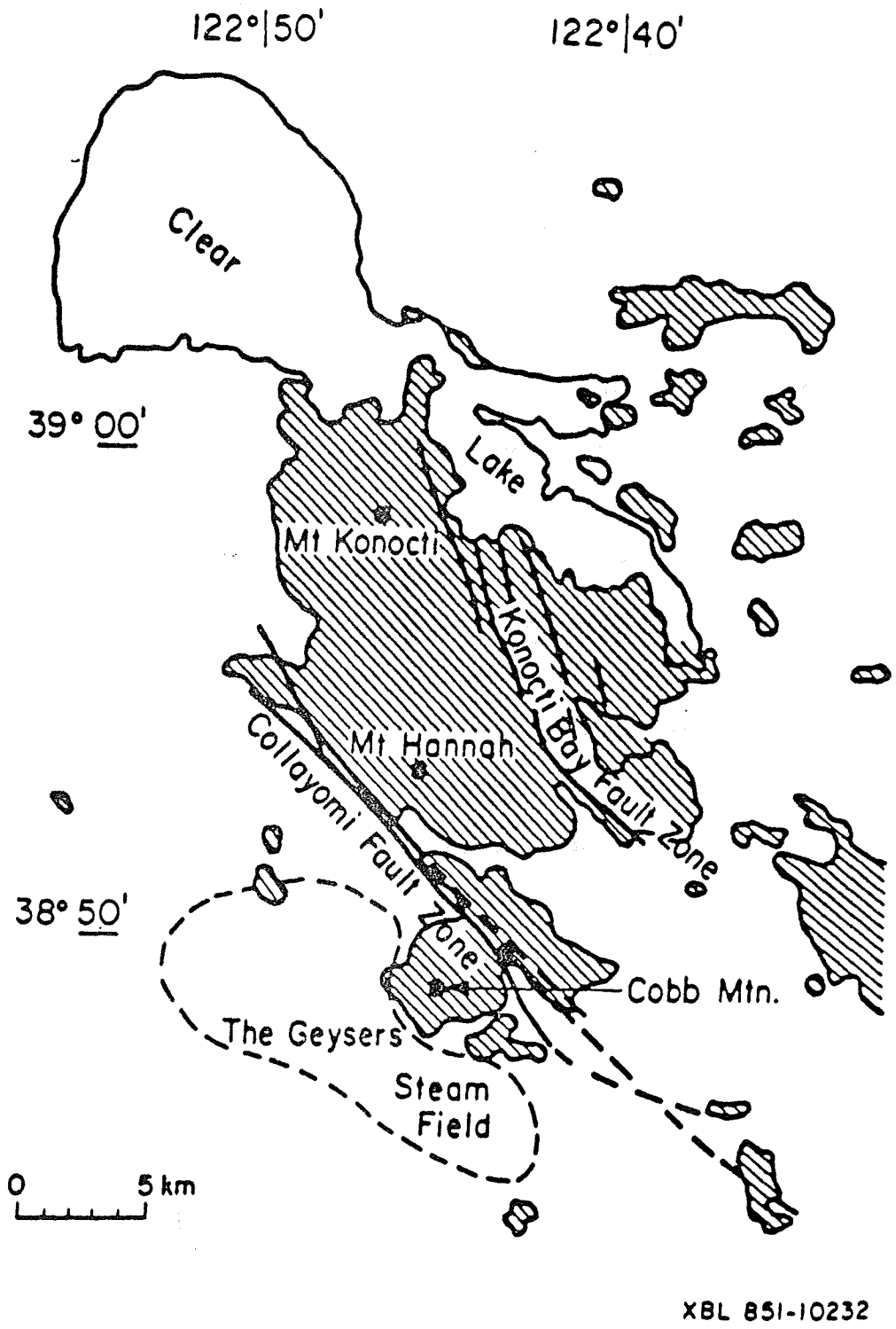

Figure 2-4. Generalized map of the Clear Lake volcanic field (shaded), with major fault zones and the approximate boundaries of The Geysers steam field (after Hearn et al., 1981).

2-5), which are characterized here and elsewhere by extensive landsliding (Berkland et al., 1972; Vantine, 1985; McLaughlin, 1978). Graywacke of this sub-unit and of the coastal belt serve as host rocks of the steam reservoir, while the more schistose rocks of the eastern belt probably play a lesser role (Thomas, 1981; McLaughlin, 1981).

Great Valley Sequence

The Great Valley sequence comprises lightly to moderately deformed marine sediments depositionally overlying an ophiolite sequence (oceanic crust) consisting of an upward progression from serpentinized peridotite to layered mafic plutonic rocks, volcanic rocks, and chert (Bailey et al., 1970). The Great Valley ranges in age from late Jurassic to late Cretaceous, and its sediments were deposited in an arc-trench gap or fore-arc basin environment near the western margin of the continent (McLaughlin, 1981; Dickinson, 1970). The ophiolite and basal sedimentary strata, late Jurassic in age, are significantly older than the Franciscan rocks which they structurally overlie across the Coast Range thrust. The thrust contact is nearly always marked by serpentinite, a component rock type of the Franciscan assemblage as well as of the Great Valley ophiolite. Franciscan serpentinite is characterized by a somewhat higher grade (actinolite-bearing) mineral assemblage than Great Valley serpentinite (Figure 2-5); on this basis, serpentinite at the thrust contact, and much of the serpentinite occurring in fault zones southwest of the thrust, has been assigned to the Great Valley ophiolite (McLaughlin and Pessagno, 1978).

In The Geysers area, the Great Valley sequence, with the exception of the above-mentioned serpentinite bodies, is not known to outcrop southwest of the Collayomi fault zone (the northeast boundary of the steam reservoir), and it does not play a significant role in the reservoir system.

Tertiary and Quaternary Volcanic Rocks

The Clear Lake volcanics are the youngest and most northwesterly of a line of late Tertiary and Quaternary Coast Range volcanic centers increasing in age to the southeast. They lie mainly to the north of the Collayomi fault zone and The Geysers steam field. Only one significant accumulation of Clear Lake volcanic rocks, the approximately 1 million-year-old silicic eruptions of

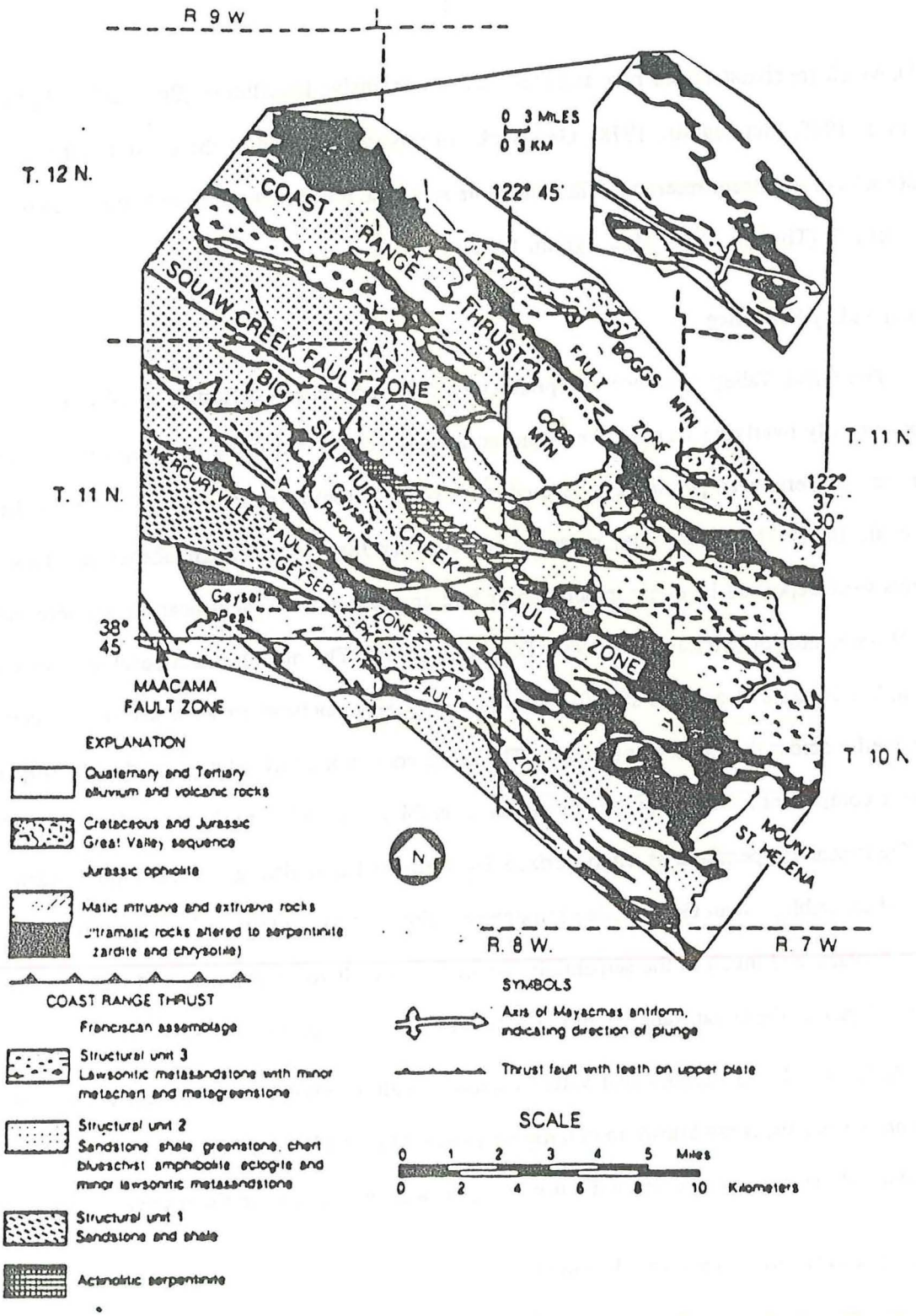

Figure 2.5. Geologic map of The Geysers steam field, showing major rock units, structural units, and fault zones. Structural units within the Franciscan are those of McLaughlin and Stanley (1976): Unit 1 comprises rocks of the coastal belt, Unit 2 of the coastal and central belts, and Unit 3 of the central and eastern belts. Line A-A' across the Big Sulphur Creek fault zone locates the cross-section shown in Figure 2-8 (after McLaughlin, 1977b).

Cobb Mountain (Donnelly-Nolan et al., 1981), and several scattered small eruptions, occur to the southwest of the fault zone (Figure 2-4). Intrusive rocks related to the Clear Lake volcanics have been intersected in drillholes, and these are discussed in a later section in connection with their implications as heat sources for the geothermal system.

The Clear Lake field comprises about 25 mi^3 (100 km^3) of volcanic rocks erupted in 100 to 200 separate eruptions and ranging in age from 2.1 m.y.b.p. to about 10,000 y.b.p. Domes and flows predominate, and pyroclastic eruptions are few. Overall, the volcanics span a complete range in composition from basalt to rhyolite, with a ratio of silicic to mafic rocks of about 3 to 2. In detail, four periods (possibly five) of major eruptive activity have been recognized, each beginning with one or more silicic eruptions; the oldest and youngest periods were dominated by mafic lavas and the intermediate periods by silicic lavas (Donnelly-Nolan et al., 1981). The oldest group of eruptions is widely dispersed, but each of the subsequent three groups is more localized geographically, and each occurs to the north of the preceding group (Hearn et al., 1981). The oldest of these three groups (1.1 to 0.8 m.y.b.p.) includes the eruptions of Mount Hannah and Cobb Mountain, straddling the Collayomi fault zone, while the youngest group (0.1 to 0.01 m.y.b.p.) was erupted along the eastern and southeastern arms of Clear Lake.

Hearn et al. (1981) and Futa et al. (1981) discuss the chemical and isotopic compositions of the volcanics, and these indicate that several of the mafic lavas had sources in the mantle. Assimilation of upper crustal rocks was a factor in the evolution of many of the basaltic rocks, as well as of the silicic rocks which were in part derived from them. Large shallow magma chambers may have been important in the development and eruption of some of the silicic magmas, but their role was not dominant. Pyroclastic eruptions comprise a minor portion of the volcanics, and it seems likely that ongoing tectonic disruption may have interfered with the development of large, stable chambers, and that faults have guided the ascent of at least some magma bodies to the surface (Hearn et al., 1981).

The Pliocene Sonoma volcanics occur entirely to the south and southeast of The Geysers, with the northernmost eruption located within 6 mi (10 km) of the boundary of the steam field.

The Sonoma volcanics range in age from 2.9 to at least 5.3 m.y.b.p. (Mankinen, 1972), and the gap between the last Sonoma and first Clear Lake eruptions is no more than 0.8 m.y. In contrast to the Clear Lake volcanics, the Sonoma volcanics include abundant small-scale ash flows, and are relatively free of quartz (Donnelly et al., 1977).

Structural and Tectonic Setting

The structural framework of the northern Coast Ranges is a composite of late Mesozoic to early Tertiary tectonism related to subduction, and late Tertiary to Quaternary right-lateral transform-related tectonism. The changeover to strike-slip tectonism represents a change from convergent to parallel plate motion at the margin of the North American plate; it corresponds with the initiation of contact between the North American and Pacific plates, and the consumption of the Farallon plate between them, in the subduction zone dipping to the east beneath the continent. The relative motions of the three plates are shown in Figure 2-6, and the triple junction, the point south of which motion at the edge of the North American plate has changed from subduction to right-lateral transform, can be seen migrating northward to its present location near Cape Mendocino. The time at which the triple junction was positioned at the latitude of The Geysers has been estimated at approximately 3 m.y.b.p. (McLaughlin, 1981; Atwater and Molnar, 1973).

In the Coast Ranges, subduction-related tectonism is responsible for the intense deformation characteristic of the Franciscan assemblage, and for thrusting of the Franciscan beneath the Great Valley sequence along the Coast Range thrust, and it is no younger than mid-Tertiary (McLaughlin, 1977a, 1981). It has also caused pervasive thrust faulting within the Franciscan assemblage, resulting in imbrication of the Franciscan rocks into a series of sub-parallel, low-angle thrust slabs of variable but predominantly north-to-northeasterly dip. The late Tertiary to Quaternary strike-slip tectonism is reflected, in the area of The Geysers, in several major west-to-north-northwesterly trending fault zones which dip steeply to the north or northeast, or are vertical, and are predominantly right-lateral. In addition, pervasive high-angle faults with reverse-slip components are present, cutting the Franciscan assemblage into a second set of

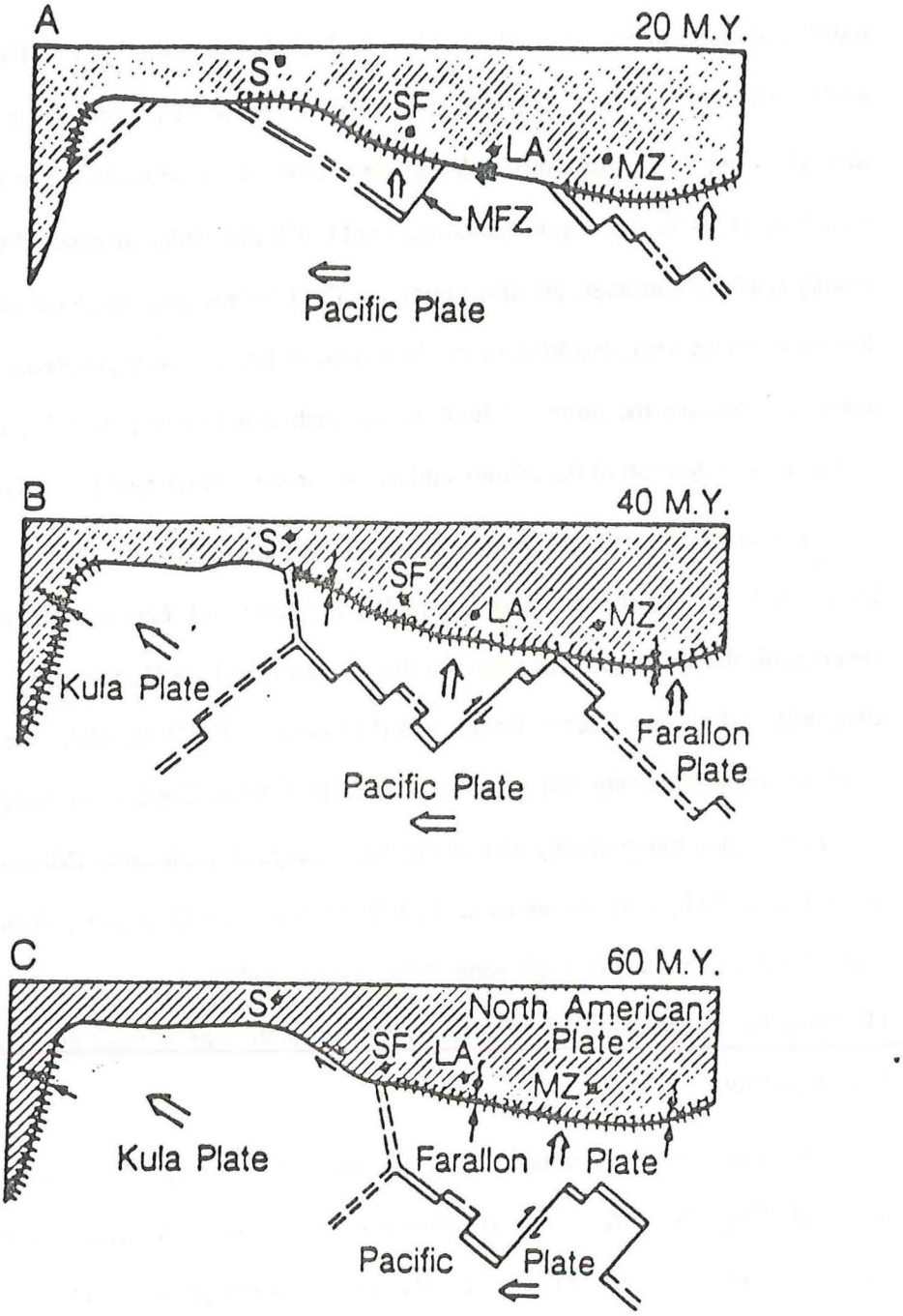

Figure 2.6. Schematic Cenozoic plate relationships along the western margin of North American at 20, 40 and 60 m.y.b.p. Motions of the Pacific, Farallon, and Kula plates (large arrows) are shown relative to the North American plate. Small arrows show direction of motion across plate boundaries; double lines are spreading centers and cross-hatching denotes subduction. The triple plate junction at the intersection of the Mendocino fault zone (MFZ) and the North American plate has continued to migrate northward during the past 20 m.y. to the present position of MFZ shown in Figure 2-3 (after Atwater, 1970).

imbricated, west-to-northwesterly trending fault blocks superimposed on the earlier-formed low-angle imbricate structure. These high-angle thrusts may be reverse-slip components of major, through-going strike-slip faults, and they determine, along with the major faults, the prevailing structural grain in the region (Thomas, 1981). Normal faults of small displacement, trending mainly north to northeast, are also present in The Geysers area. Regional late Cenozoic folding has occurred as well, resulting in the formation of broad, southeast-plunging folds. The steam reservoir occupies the northeast limb of one such structure, the complexly faulted Mayacmas antiform, an extension of the Diablo antiform to the south (McLaughlin, 1978, 1981).

The major fault zones in the area of The Geysers include the Mercuryville-Geyser Peak-Maacama fault zone to the southwest, the Big Sulphur Creek fault zone in the central part of the steam field, the Collayomi fault zone to the northeast, and the Konocti Bay fault zone further to the north in the Clear Lake volcanic field (Figures 2-4, 2-5, 2-7). Holocene right-lateral movement has occurred along and adjacent to the Big Sulphur Creek fault zone, along the Konocti Bay fault zone, and probably also along the Collayomi fault zone (McLaughlin and Stanley, 1975; Hearn et al., 1981; Donnelly et al., 1976). Large-scale Quaternary displacements are documented for the Maacama fault zone (McLaughlin, 1981), a fault that is considered by Herd (1979) to be an extension of the active Hayward fault zone located east and southeast of San Francisco Bay.

Studies of focal mechanisms of natural and induced seismicity in The Geysers area (Bufe et al., 1981; Oppenheimer, 1985) have shown that the pattern of deep faulting is predominantly strike-slip and normal, and that the vector of maximum compression in the present tectonic stress orientation is north-northeast to north-south. This stress orientation, along with many observed structural features, is compatible with northwest-trending, right-lateral wrench faulting, a concept developed from clay-cake models and shown to have wide-spread applicability (Wilcox et al., 1973; Sylvester, 1984). Structural features consistent with wrench faulting of this orientation include: en echelon north-to-north-northeasterly trending right-lateral faults of small offset; normal faults trending north to northeast; high angle reverse faults trending northeast to east-

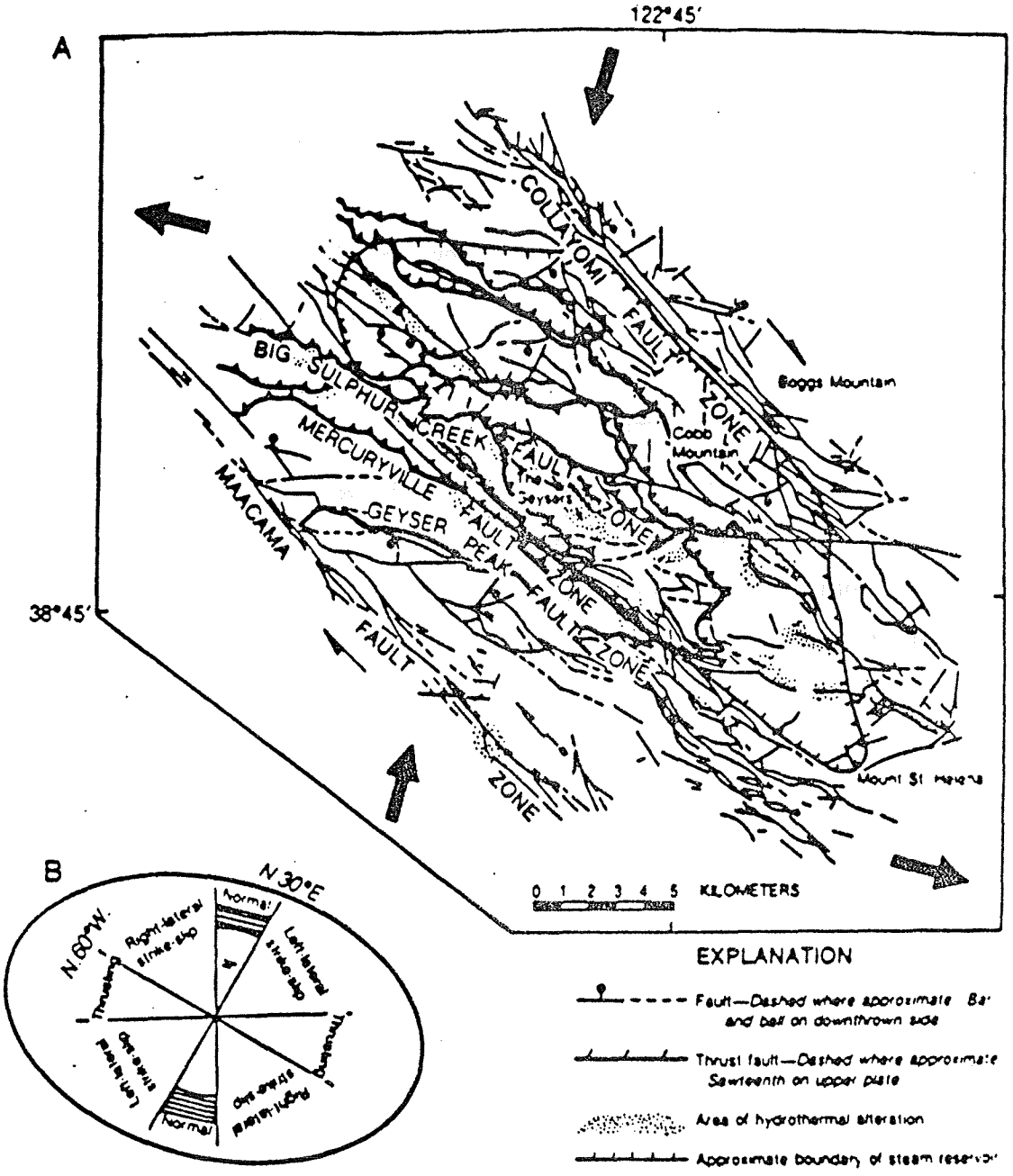

Figure 2-7. Faulting in the vicinity of the Geysers. (A) Small arrows shown dominant right-lateral sense of faulting along Maacama and Collayomi fault zones. Large arrows show approximate vectors of regional compression and extension. (B) Schematic combination of strain ellipse and structural pattern associated with right-lateral west-northwesterly wrench faulting. Sectors of ellipse show predicted displacements for vertical faults of various orientations (after McLaughlin, 1981 and Wilcox et al., 1973).

northeast; east-to-east-southeasterly trending folding; and increasing development over time of the main throughgoing right-lateral fault zone trending northwest parallel to the direction of shear (Figure 2-7). Similar features of approximately these orientations in The Geysers area have been described above, and they provide strong evidence for wrench fault mechanisms associated with the major fault zones, and with the Big Sulphur Creek fault zone in particular (Thomas, 1981).

The timing of Clear Lake and other Coast Range volcanism can be placed well within the setting of late Tertiary and Quaternary continental margin tectonics. As noted previously, a progressive decrease in age occurs along the line of Coast Range volcanic centers culminating at Clear Lake, and this progression and alignment correlates well with the direction and timing of the migration of the inter-plate triple junction (Figure 2-6). The initiation of volcanism in the Clear Lake field followed within 0.5 m.y. the passage of the triple junction and initiation of right-lateral transform faulting at that latitude (McLaughlin, 1977a), and similar correlations in timing have occurred at other volcanic centers (Pilger and Henyey, 1979). (Movement of the North American plate in a south-southeasterly direction over a stationary mantle hot spot, or a hot spot tied to the Pacific plate, have also been proposed (Hearn et al., 1981) to account for the migration of volcanism.)

Volcanic activity near the margin of the North American plate may be related to the subduction of thin, hot asthenosphere where the plate overrode a spreading zone boundary between the Pacific and Farallon plates (Pilger and Henyey, 1979). It may also have been facilitated by the presence of softened and splintered crust at the Pacific and North American plate margins (Crowell, 1974). The inception of strike-slip transform faulting after the cessation of subduction probably played an important role in allowing the rise of magmas to the surface, and several mechanisms for strike-slip-induced extension have been proposed. On a regional scale, westward rotation of the azimuth of transform shear within the past 10 m.y. may have contributed to an extensional regime within the San Andreas fault system (Blake and Jones, 1978; McLaughlin, 1981). Crowell (1974) describes the formation of pull-apart basins by strike-slip offset at releas-

ing bends along faults of the San Andreas system in southern California, and several basins in the northern Coast Ranges, including Clear Lake basin, have probably formed in this way (McLaughlin, 1981). On a more local scale, wrench tectonics provide a means for development of extensional features associated with strike-slip faults, and such features have been described in connection with the alignment of vents in the Clear Lake volcanic field (Hearn et al., 1981), and with the occurrence of igneous intrusive bodies at The Geysers (Thomas, 1981).

2.2.2. Geology of the Geothermal System

Geological and Structural Setting

The geothermal system at The Geysers is situated within the northeast limb of the southeast-plunging Mayacmas antiform. The steam reservoir appears to be bounded to the northeast by the Collayomi fault zone, and to the southwest by the Mercuryville fault zone (Figure 2-7) (McLaughlin, 1981; Hebein, 1983), but its boundaries to the northwest and southeast have not been clearly defined. McLaughlin (1981) estimated the reservoir depth at ≥ 2 mi (3 km); Hebein (1986) estimated the depth at 2.5 - 4 mi (4-6 km). The reservoir is characterized by nearly constant temperatures and pressures, both increasing somewhat with depth.

Surface manifestations of the steam reservoir include hot springs, fumaroles, and altered ground. Hydrothermal activity is most intense along and adjacent to the Big Sulphur Creek fault zone (Figure 2-7). Hydrothermal alteration is common along other faults as well, and is particularly extensive along the trend of the Mercuryville fault zone, suggesting that it may have been an earlier locus of hydrothermal discharge (McLaughlin, 1981). Hot spring discharges in the present system are predominantly sulfate-rich, low-chloride acidic waters characteristic of steam condensate from vapor-dominated systems (White et al., 1971; Goff et al., 1977). Total natural discharge from the system is small, and a portion of that discharge results from heating of perched ground water contained within landslide debris (Vantine, 1985). Mercury occurs in vapor from the steam field, and mercury mineralization has taken place on the periphery of the field (White et al., 1971). Northeast of the Collayomi fault zone, chloride-rich, low-sulphate waters discharge from a hot-water system underlying rocks of the Clear Lake volcanic field (Goff et al.,

1977; Sternfeld et al., 1983).

The general structure of the subsurface at The Geysers consists of a complex stacking of tectonic slabs and wedges, dipping steeply to the north and northeast, superimposed over an earlier, north-to-east-dipping, low-angle imbrication (Figure 2-8) in rocks of the central belt, and to a lesser extent the eastern and coastal belts, of the Franciscan assemblage (see Section 2.2.1). This structure is further deformed by major northwest-trending, high-angle strike-slip faults, and by southeast-plunging folds (McLaughlin, 1981; Thomas, 1981). Steam production occurs mainly from fractured zones in graywacke, which has low matrix permeability but is very brittle and able to maintain open fractures (McLaughlin, 1981), and in underlying felsic intrusive rocks (Hebein, 1986). Fluids flow through open fracture networks, and the maintenance of open fractures and the reopening of sealed fractures are key factors in the behavior of the reservoir. In the present regional stress regime, extension is most likely to occur along steeply dipping north-to-northeasterly trending faults (McLaughlin, 1981), but since few faults of this orientation have been mapped in most regions of The Geysers (Figure 2-7) the role of such faults in the occurrence and movement of steam may be minor (Thomas, 1986). Other structural features which may be important to the behavior of the reservoir include rotated blocks and pull-apart wedges associated with wrench faulting in the productive zones of shallow steam along the Big Sulphur Creek fault zone (Thomas, 1981), and the axial regions of folds and horsts, in which extensional fractures of sub-horizontal and other orientations may develop (McLaughlin, 1981).

Heat Source

Although there is a close spatial association between The Geysers and Quaternary volcanic eruptions, it is difficult to draw a direct link between the present steam reservoir and the main episodes of Clear Lake volcanism. The major portion of the volcanics, including all eruptions younger than 1 m.y.b.p., occur northeast of the Collayomi fault zone (Figure 2-4), and the youngest eruptions are in the vicinity of Clear Lake, well to the north of the steam reservoir.

Nonetheless, felsic intrusive rocks have been intersected in numerous drill holes in the steam field, and they indicate that igneous intrusions have provided the heat source for the

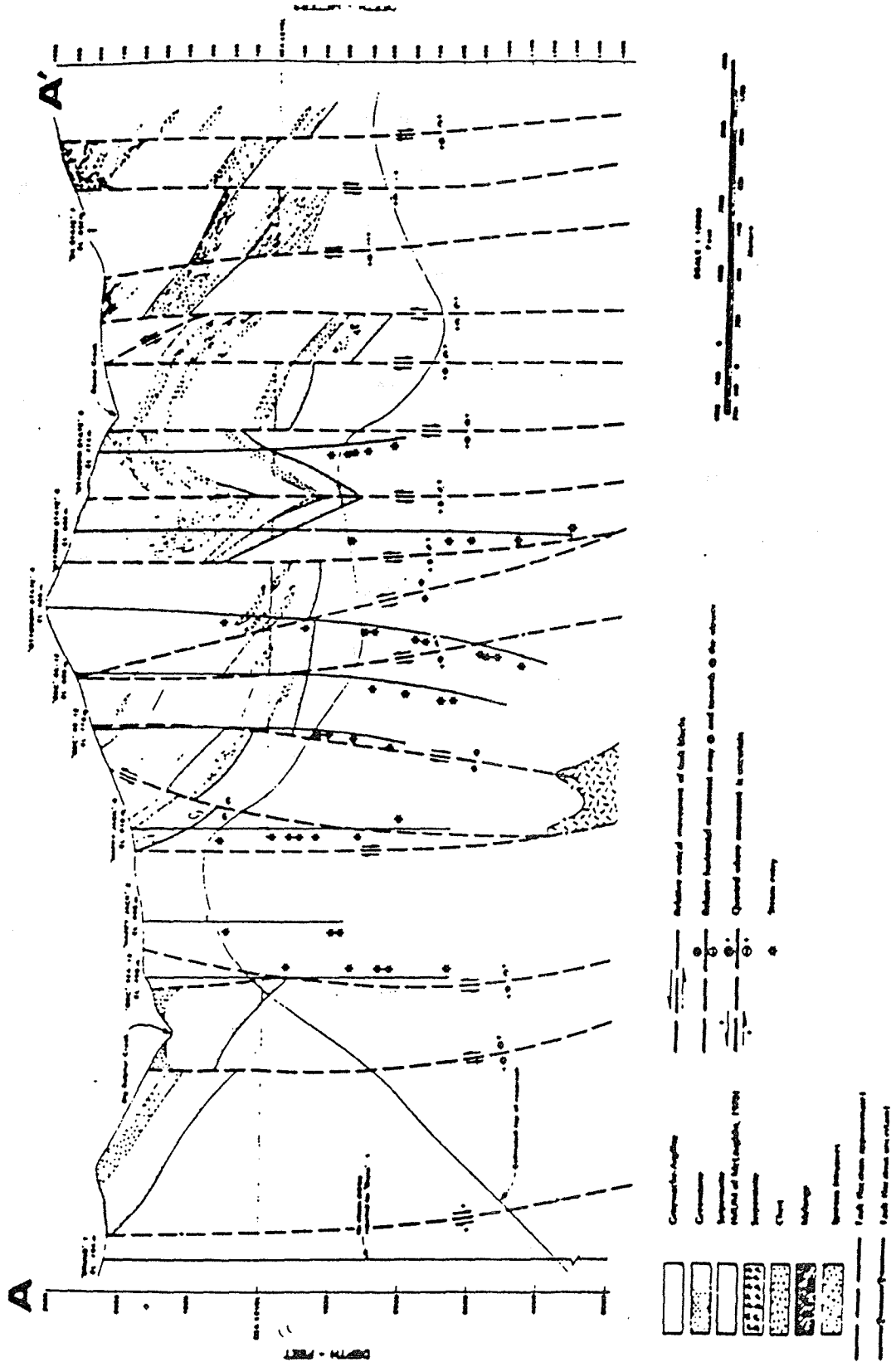

Figure 2-8. Geologic cross-section of The Geysers steam reservoir, showing wells and steam entries. Location of section line A-A' is shown in Figure 2-5 (after Thomas, 1981).

geothermal system. Large volumes of rhyolitic intrusive rocks found in drill cores and cuttings at depths as shallow as 4 mi (2.5 km) have been reported by Schriener and Suemnich (1980), which on the basis of their compositions and ages (1.6 to 2.7 m.y.b.p.) are probably correlative with Clear Lake volcanic extrusions. Hebein (1983, 1985b, 1986) believes that felsic igneous rocks representing successive intrusive pulses comprise large portions of the steam reservoir. Thomas (1981) also notes felsic intrusive rocks associated with shallow steam anomalies along and adjacent to the Big Sulphur Creek fault zone; these anomalies correlate with wrench fault extensional structures, which Thomas suggests may serve as steam conduits from deep sources. (The association of magmatic ascent with wrench fault structures has also been discussed by Hearn et al. (1981), with respect to vent patterns in the Clear Lake volcanics.)

The presence of magmatic intrusions may also be inferred from the occurrence of high-temperature alteration zones, particularly in deeper parts of the steam field, as described by Hebein (1985b) and McLaughlin et al. (1983). Sternfeld et al. (1983) describe similar alteration north of the steam field, where a liquid-dominated system appears to be present (Goff et al., 1977). The presence of tourmaline in these zones (associated with actinolite, biotite, garnet, or axinite) is suggestive of contact aureole alteration, as it may imply introduction of boron into the host rock from a deeper magma source.

Despite the common occurrence of felsic intrusive rocks, no magma body has been shown conclusively to exist beneath or adjacent to the steam reservoir. A large negative gravity anomaly, a resistivity anomaly, and a zone of teleseismic P-wave delays are centered north of the Collayomi fault zone in the vicinity of Mount Hannah (Figure 2-4) (Isherwood, 1976c; Stanley et al., 1973; Iyer et al., 1981), and these have been interpreted as indicating the presence of a large silicic magma chamber (Hearn et al., 1981; Goff et al., 1977). However, other geophysical techniques have not confirmed this interpretation, and other factors, including subsurface hydrothermal alteration and the presence of low-density rocks of the Great Valley sequence, may contribute to the gravity and seismic anomalies (Keller and Jacobson, 1983; Goldstein and Flexser, 1984). Analysis of non-condensible gases in steam wells has also provided no evidence of

derivation from a magmatic source (Brook, 1981; Nehring, 1981).

Large magma chambers have probably played a role in past episodes of Clear Lake volcanism, as suggested by structural, chemical, and isotopic evidence (Hearn et al., 1981; Bowman et al., 1973; Goldstein and Flexser, 1984). However, their overall importance in the eruptive history of the volcanic field has not been major, as there have been few pyroclastic eruptions. Faulting may have caused repeated tapping of magma bodies, inhibiting their growth as well as the buildup of volatiles necessary for large ash-flow eruptions. It is plausible that instead of large-scale upper-level chambers, magma has been and perhaps still is present in the crust in the Geysers-Clear Lake area in the form of relatively small, deep bodies.

Hydrothermal Alteration and the Evolution of the Geothermal System

Several distinct stages in the evolution of The Geysers geothermal system are recorded in alteration mineral assemblages. McLaughlin et al. (1983) describe three assemblages, the earlier two associated with hot water circulation, the last possibly with a change to a vapor-dominated system. The first stage of alteration consists of a propyllitic mineral suite, including epidote, amphibole, and adularia; the second stage includes sericite (or illite) and adularia; and the third includes calcite, sulfides of lead, zinc, and mercury, and the borosilicate datolite. Dating of adularia of the second stage indicates that the hot-water system has been active for at least 0.7 m.y.

Hebein (1983, 1985a, 1985b) also describes a generalized sequence of hydrothermal alteration that reflects evolution from a liquid-dominated to a vapor-dominated system. He interprets observed phyllic (illite as the characteristic mineral) and propyllitic (epidote, albite, and actinolite characteristic) alteration as sealings along the lateral boundaries, and along near-vertical, hydrothermally brecciated fractures and channels, of an ancestral liquid-dominated system. He considers phyllic alteration also to be characteristic of a condensation zone in the present vapor-dominated system, and in contrast to McLaughlin et al. (1983), he interprets the presence of adularia as indicative of boildown from a liquid-dominated to a vapor-dominated state.

The development of the steam reservoir from an earlier liquid-dominated system, docu-

mented in hydrothermal mineral suites, is seen as the normal sequence in the evolution of vapor-dominated systems, and the pivotal element in that sequence would be a change in the relative rates of recharge and discharge. The changeover to vapor domination takes place when net discharge begins to exceed recharge (White et al., 1971); in The Geysers system a decrease in the rate of recharge was probably the major cause of the changeover. An increase in heat input to the system, which would be compatible with the latest, high-temperature alteration suite of McLaughlin et al. (1983), could also have been a factor. And an increase in the discharge rate, perhaps resulting from enhanced erosion in areas of intense hydrothermal alteration and consequent rapid down-cutting into deeper parts of the system, could also have played a role (Thomas, 1986).

Recharge to The Geysers reservoir, which derives predominantly from meteoric water (White et al., 1971), is limited by the low permeability of the near-surface Franciscan rocks, and has probably been further reduced by hydrothermal alteration sealing resulting from prior episodes of hot-water circulation. The main areas of recharge are probably through vents which fed eruptions of the Clear Lake volcanics, as suggested by Goff et al. (1977). Vents beneath the silicic dome of Cobb Mountain, which is a major lava body, and beneath several smaller intrusions and extrusions, occur within or adjacent to the boundaries of the steam field (Figure 2-4). The porous silicic rocks of Cobb Mountain in particular could transmit large volumes of water to the system. Cobb Mountain also overlies an area of anomalously low heat flow, consistent with downflow of meteoric water (Thomas, 1985). Northeast of the Collayomi fault zone, there is an abundance of vents, probably fractured and brecciated, of the Clear Lake eruptions, and these permeable conduits should provide sufficient recharge to maintain the hot water-dominated system present there (Goff et al., 1977; Sternfeld et al., 1983).

Fractures and Flow in the Reservoir

Conceptual models of the internal configuration and flow regime of the steam reservoir have been developed by several authors, and many aspects remain speculative and controversial. But there is general agreement on the location of the major portion of the steam reservoir within

a thick body of graywacke known as the "main graywacke." The top of this body, which intersects the surface in outcrops near The Geysers resort, is encountered through much of the steam field at depths ranging from 3000 to ≥ 6000 ft below the surface (Figure 2-8) (Thomas, 1981; Hebein, 1983). Rocks overlying the main graywacke are characterized by conductive heat flow (Thomas, 1985), and in some parts of the field, a condensation zone occurs between those rocks and the main graywacke below. The main graywacke is probably underlain completely or in part by felsic intrusive rocks, which comprise the lower portion of the reservoir.

Considerable disagreement exists on many aspects of steam distribution and flow, particularly with respect to structural control and lateral continuity. The concept of a caprock lithologically distinct from the underlying main graywacke, and composed of more plastic Franciscan rocks, largely greenstone, serpentinite, and melange, and less suited for maintaining open fractures, has been mentioned by McLaughlin (1981) and Hebein (1983). But Thomas (1981) cites problems with this concept of a caprock, and believes that the upper boundary of the reservoir is defined more by fault and fracture orientation than by lithologic differences (Thomas, 1986). Within the reservoir, McLaughlin (1981) assigns the major role in controlling steam flow to the faults and fractures associated with the low-angle imbricate slab structure of the Franciscan rocks, and he envisions steam moving upstructure along these faults and fractures from a basal brine. This contrasts with the model of Thomas (1981), in which the low-angle imbricate structure of the reservoir rocks plays a more limited role, while the major factors in the upflow of steam are vertical zones produced by fracturing and faulting associated with wrench tectonics, which are in turn associated at depth with igneous intrusions. In this model, lateral networks of open fractures also play a role in controlling the flow of steam, but only after it has reached the crests of the vertical conduits. The lateral networks occur within and adjacent to the low-angle imbricate thrusts in the main graywacke (Figure 2-8), where permeability has been enhanced and maintained by water flow and dissolution of mineral phases (Thomas, 1986). The high-angle series of reverse faults (Figure 2-8), according to Thomas, appears to be filled and to play little or no role in fluid flow.

A model proposed by Hebein (1983, 1985a, 1985b) also stresses the importance of vertical steam conduits and wrench fault structural control, but differs markedly from Thomas' model in denying virtually any role in fluid flow to either the low-angle or high-angle imbricate fault structures, and in assigning a very minor role to lateral permeability. The dominant features in Hebein's model are numerous, discrete, vertical steam convection cells or sub-reservoirs, largely sealed above and to the sides by sericitic alteration, which developed from and are superimposed over earlier zones of hydrothermal alteration and brecciation. However, this conception of laterally discontinuous steam cells may be difficult to reconcile with well data relating to drawdown and steam entries. Steam entry zones often occur at similar intervals in widely separated wells (Thomas, 1981), and this observation, as well as reservoir pressure decline maps of Lipman et al. (1978), suggests that significant lateral communication exists between producing fracture networks.

2.3. GEOPHYSICS

Since 1960, when commercial steam production began at The Geysers, there have been many geophysical surveys performed over the field area by various organizations, including private industry, government agencies and universities. Little of the work done by private industry has been released to the public. Chapman (1981) and McLaughlin and Donnelly-Nolan (1981) have reviewed most of the work done with public funds. This section draws heavily from these two reviews, but where possible, the results of more recent investigations are included. The main body of published geophysical data for the area, including gravity, aeromagnetics, reconnaissance electrical resistivity and some seismic refraction, was collected by the U. S. Geological Survey as part of their Geothermal Assessment Program. Supplementary data were also collected by the California Division of Oil and Gas (DOG) and by other research and academic institutions.

The geophysical studies have dealt with the following aspects of The Geysers resource:

(a) location and nature of the heat source

(b) reservoir dimensions and boundaries

(c) physical parameters of the reservoir and caprock

(d) monitoring of net mass depletion, subsidence and seismicity

(e) the relation between induced seismicity, the regional stress-strain field, production rates and reservoir processes.

2.3.1. Gravity

Interpretations of the gravity data taken over The Geysers region have resulted in a better understanding of the reservoir but have also stimulated unresolved controversies. The main features in the terrain-corrected Bouguer gravity contour maps (Chapman, 1966, 1975; Isherwood, 1975, 1976a,b,c) are two major lows: one centered roughly over Mt. Hannah and the south end of the Clear Lake volcanic field, the second roughly coincident with the known steam field and commonly referred to as the "production low." Viewed separately, each low has its long direction oriented northwest-southeast, similar to the structural grain given by the strike of the major fault zones. Viewed together, the two lows seem to comprise a nearly circular gravity feature 15 mi (25 km) in diameter and extending from Mt. Konocti on the north to Middletown on the south (Figure 2-9). In simplest terms this feature may be related to a large intrusive-extrusive complex of felsic rocks.

The larger of the two lows is the Mt. Hannah low (–25 mGal) which has been argued to represent a partially molten intrusive mass whose depth is 3 - 6 mi (5 - 10 km), depending on the interpretation used (Chapman, 1975, 1978; Isherwood, 1975). The melt source is supported by the occurrence of rhyolitic dikes intersected by production wells at depths of about 1.5 mi (2.5 km) (Schriener and Suemnicht, 1980), and by the occurrence of abnormal P-wave velocities of earthquake-generated waves passing beneath the geothermal field (Iyer et al., 1979). If the melt hypothesis were correct, The Geysers geothermal field would be resupplied by a nearly inexhaustible supply of thermal energy. However, holes drilled to 10,000 feet (3,000 m) and more in the Mt. Hannah area (well Jorgenson 1) have encountered a large thickness of Great Valley sequence

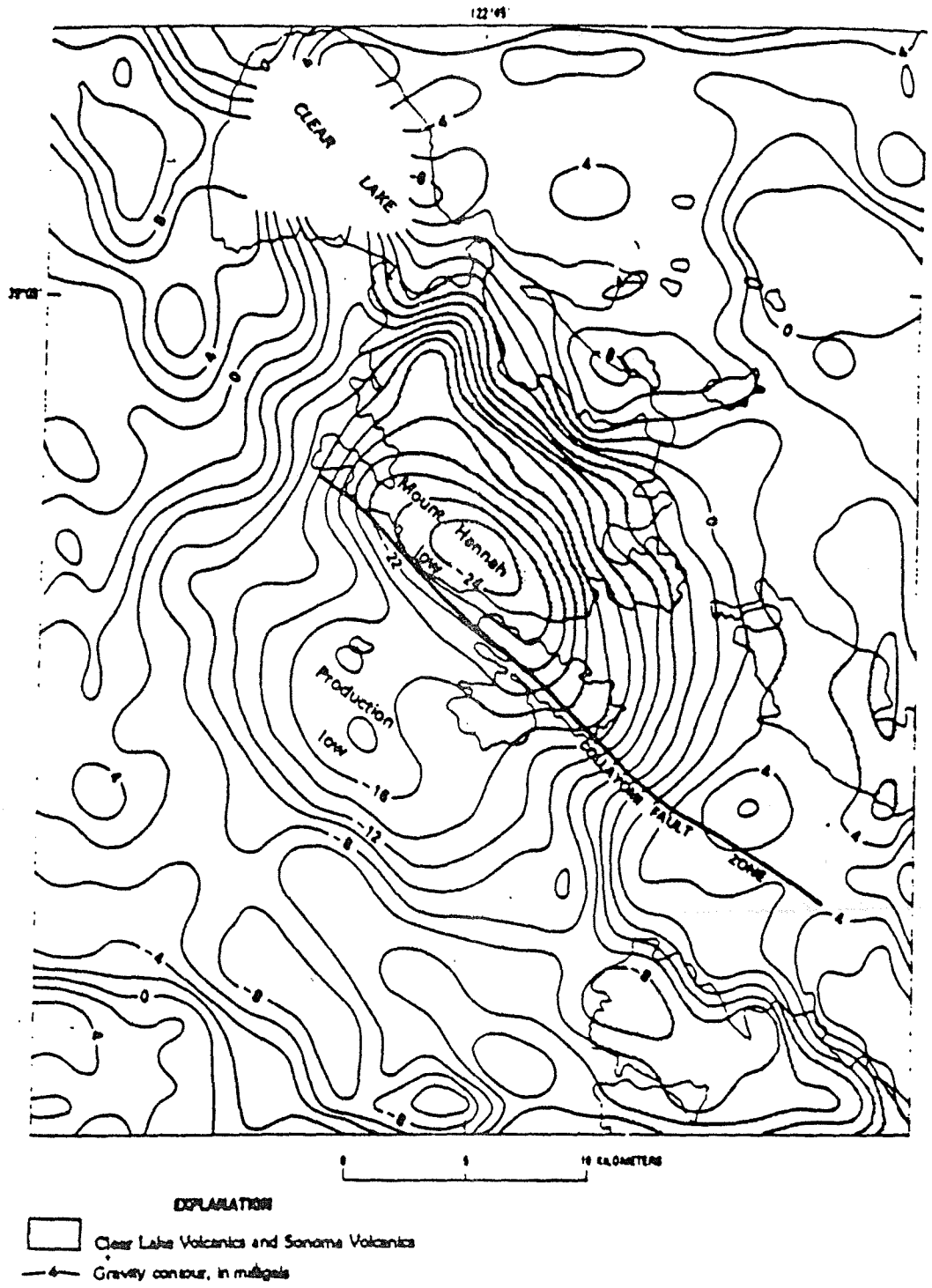

Figure 2-9. The Geysers area, California, showing residual gravity based on reduction densities of 172 lbs/ft^3 (2760 kg/m^3). Contour interval is 2 mGal (from Isherwood, 1975). The shaded areas are the Clear Lake volcanics.

sediments. This fact, plus the interpreted results from deep electromagnetic soundings, have led a number of geologists and geophysicists to alter their view of the partial melt hypothesis (A. Schriener, 1986, personal communication). The low-density sediments beneath the Clear Lake volcanics could explain the gravity low.

The production low, a residual gravity low of –3 to –5 mGal after the effect of the Mt. Hannah low is removed from the data (Denlinger, 1979; Denlinger and Kovach, 1984), conforms rather closely to the outline of The Geysers geothermal field and to the heat flow and temperature gradient anomalies associated with the field (Thomas, 1985). The gravity low is sandwiched between the Mercuryville thrust fault on the west and the Collayomi fault zone on the east; these faults are believed to act as boundaries to the steam field. The match between the gravity low and the thermal high are not exact everywhere, but the match was sufficient to prompt Denlinger (1979; see also Denlinger and Kovach, 1984), to derive a reservoir model on the basis of the gravity data. Denlinger calculated a reservoir volume of 25 mi^3 (100 km^3) consisting of rocks with steam-filled pores and fractures with a density contrast of -40 to -60 kg/m^3 with respect to the surrounding rock. If a deeper, low-density source is also included in the model, the shallow density contrast cannot be less than -40 kg/m^3. The model with the deep source fits the seismic P-wave delay data better. Chapman (1981) pointed out that the estimate of the reservoir volume computed from gravity data is very speculative due to the uncertainties involved in extracting the production low anomaly from the regional gradient and other interfering gravity anomalies. Furthermore, the anomaly in question is not due to so simple a geometric body as used in the calculations. The rocks are in fact a combination of less dense melange (mainly sandstones, shales, and blueschist facies rocks) with zones of denser serpentinite, greenstone and rhyolitic dikes. Chapman (1981) also argued that one can not use the gravity data to estimate reservoir volume because the "gravity low extends to the northwest well beyond the known (or likely) boundary of the geothermal field." However, recent drilling in the northwest Geysers area by GEO Corporation has extended the field an additional 3 mi (5 km) to the northwest without encountering a boundary (W. Randall, 1986, personal communication).

One of the more fascinating aspects of gravity surveys over geothermal reservoirs has been the use of repetitive, high-precision gravity and leveling surveys to determine the magnitude of the net mass change due to fluid extraction. Isherwood (1977) made such measurements during the 1974-1977 period, and found a broad decrease (–120 μGal) in gravity coincident with the steam production area. His analysis of the decrease showed that the gravity change was too large to be caused by the lowering of a deep water table below the producing zone intersected by the wells. Analyzing the gravity change in terms of a mass loss, Isherwood found that the predicted mass deficiency was nearly equal to the mass of the fluid produced during the 1974-1977 period. As only a small fraction of the produced mass was reinjected during this period, the gravity results suggest that there was negligible vertical recharge from meteoric water or lateral recharge of cooler connate waters from outside the steam field. The rate of gravity change (–40 μGal/y) was later confirmed in a separate experiment in which a cryogenic gravity meter recorded the short-term effects over a 38-day period (Olson and Warburton, 1979). The absence of natural recharge of water into the steam field is consistent with the underpressured nature of the field (Ramey, 1970a). A steam pressure decline since 1966 (Lipman et al., 1978), and ground subsidence of over 4 in (10 cm) since 1973 (Lofgren, 1981) are consistent with the mass depletion picture (Eberhart-Phillips and Oppenheimer, 1984).

2.3.2. Magnetics

Aeromagnetic data have been collected over The Geysers and published by CDOG (Chapman, 1975) and by the U. S. Geological Survey (1973). Of the two data sets, the one by the USGS is more useful because of the closer line separation (1 mi; 1.6 km), the lower flight elevation (0.86 mi; 1.37 km), and the larger scale of the map (1:62,500). The contours show a strong northwest-southeast trend, parallel to the dominant structural grain of the region. The grain seems to be related to a fault pattern that consists of at least two major components (McLaughlin and Stanley, 1975):

(1) imbricate high- to low-angle thrust faults that separate slabs in the Franciscan assemblage

(2) steeply-dipping faults with both normal and strike-slip displacements that overprint the earlier thrust faults.

A number of discrete highs (and corresponding polarization lows) exist that have been attributed to outcropping serpentinized ultramafics in slabs of the Franciscan assemblage, and to a lesser extent, the Clear Lake volcanics and topography. The early Pleistocene rhyolite and dacite forming Cobb Mountain appears to have a component of reverse magnetization.

Chapman (1981) reported that the geothermal field is situated within a northwest trending magnetic low, and there is no evidence for a "unique" magnetic anomaly in association with the field. Upon close examination of the USGS (1983) aeromagnetic map, it appears that within the DOG Administrative Boundary of the field there essentially exists only a narrow elongate magnetic high (Figure 3-10). This high of 40 to 100 nT extends from just north of The Geysers Resort southeastward into Township 10N., Range 8W. The high is flanked on its north and northeast sides by lows which seem to be the normal polarization effects. The high shows a weak but definite correlation to a high in the Bouguer gravity map, but more importantly it shows a definite correlation to a narrow band of serpentinite mapped at the surface. The serpentinite is considered to be a caprock overlying the fractured graywacke reservoir rocks (McLaughlin and Donnelly-Nolan, 1981).

2.3.3. Electrical Resistivity

Reconnaissance electrical resistivity surveys have been performed over The Geysers area by the U. S. Geological Survey and other institutions. Stanley et al. (1973) performed a dc bipole-dipole survey using five, 0.6 mi long (2 km long) source bipoles. They supplemented this work with a number of Schlumberger dc resistivity vertical electrical soundings (VES) with stations following a west-to-east line beginning near the Bottle Rock Road, past Mount Hannah and ending near Lower Lake. These two techniques were concentrated northeast of the geothermal field and over the Mt. Hannah-Boggs Mountain area. The bipole-dipole results show a large resistivity low (2 to 5 ohm-m) centered conformably over the Mt. Hannah gravity low discussed in an earlier section (Figure 2-11). The VES cross-section indicates a relatively thin (1000 -

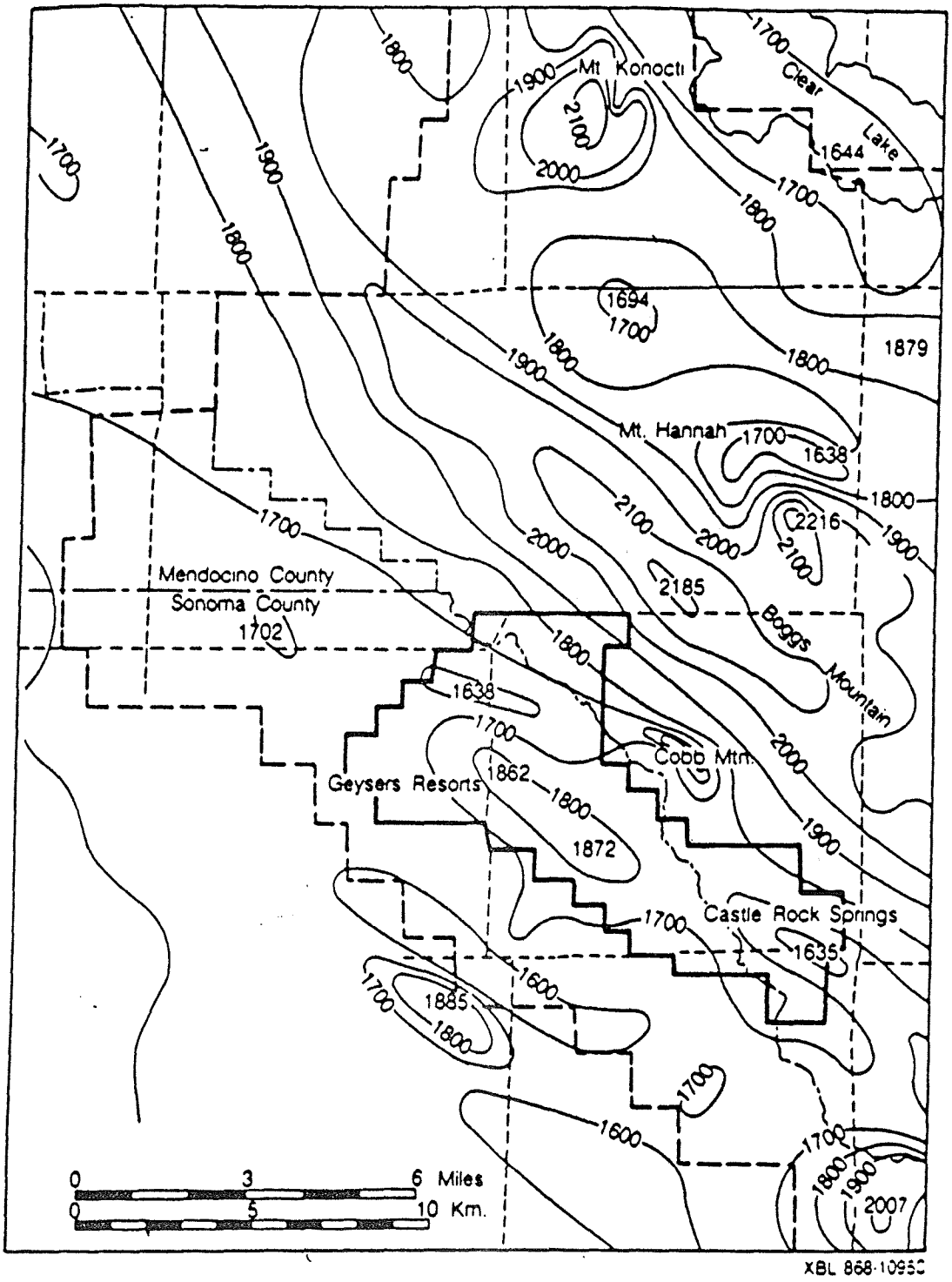

Figure 2-10. Aeromagnetic contour map of The Geysers geothermal area, adapted from USGS (1973). The contour interval is 100 nT.

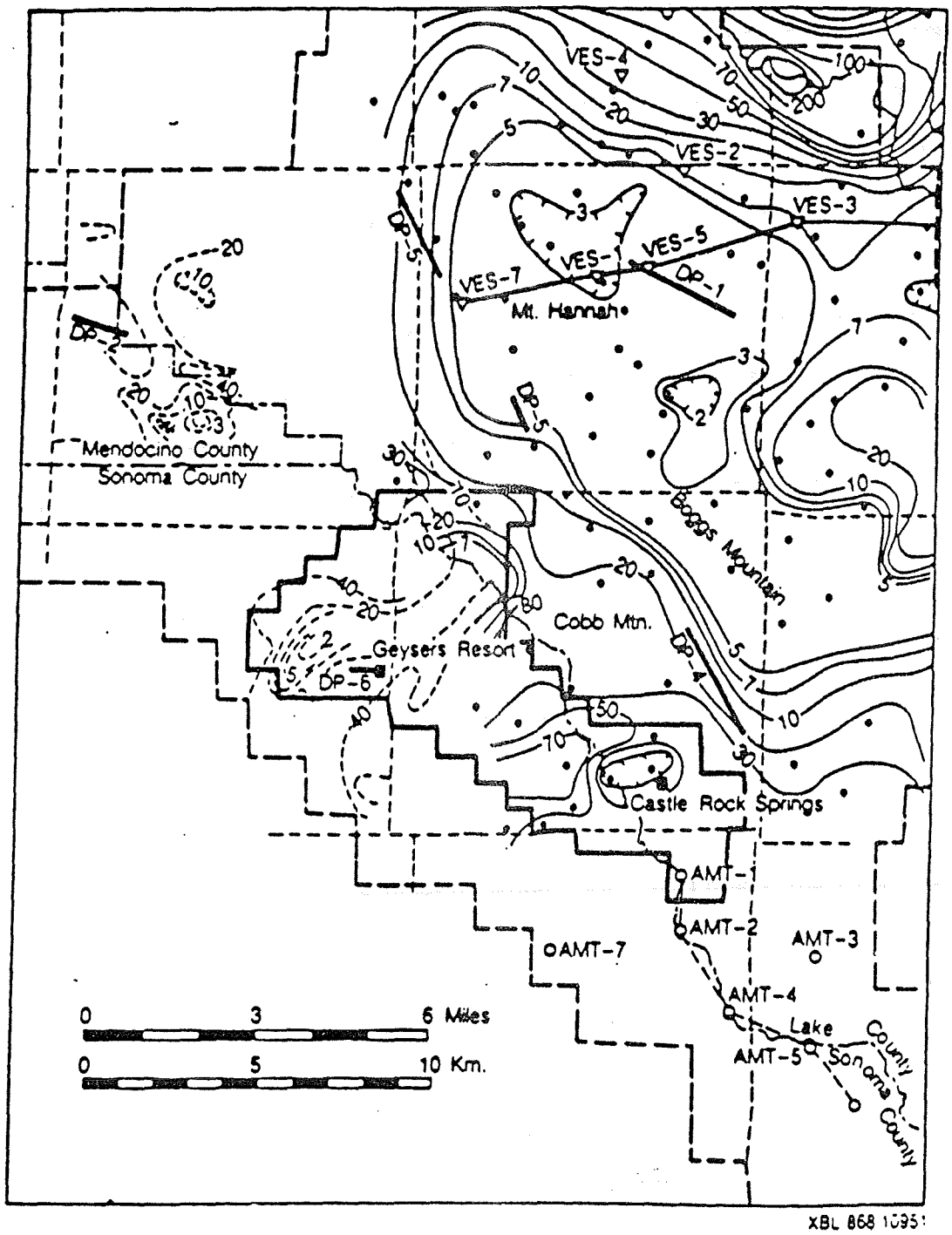

Figure 2-11. Reconnaissance bipole-dipole apparent resistivity contours (after Stanley et al., 1973).

2000 ft; 300 - 600 m) layer of Clear Lake volcanics overlying a low resistivity (2 to 3 ohm-m) region with a very large thickness (≈ 3 mi; 5 km).

Within the production area there are insufficient electrical resistivity data to form the basis for an interpretation or judgment on the value of electrical/electromagnetic surveys for well targeting. This may be due in part to the practical difficulty of making electrical/electromagnetic surveys in the area because of the steep, brush-covered hills and man-made noise. The reconnaissance bipole-dipole data indicate two areas of resistivity lows, both close to local gravity lows; one is northwest of the Geysers Resort; the other near Castle Rock Springs (Figure 2-11). The precise geological reasons for these correlations are not definitely known, but Chapman (1981) thinks they are related to regions of hydrothermally altered rock or near-surface hot water.

The second published U. S. Geological Survey resistivity reconnaissance consisted of a group of audio-magnetotelluric (AMT) soundings that extended from south of Castle Rock Springs and followed the Lake County-Sonoma County boundary toward Mount St. Helena (Long and Senterfit, 1976). These data were never properly interpreted; therefore, the results cannot be integrated into the overall geophysical model for the area.

The Colorado School of Mines operated its "Megasource" time-domain EM system (TDEM) in the area around Clear Lake, northeast of the producing area, and obtained 245 soundings (Keller and Jacobson, 1983; Keller et al., 1984). The single source, a 0.6 mi (1 km) length of AWG 4-0 wire, was located in a marshy area at the southeast corner of Clear Lake. South of the source, in the area of Boggs Mountain, the electric section appears to indicate three layers:

(1) a surface layer, to a depth of about one km, which is resistive (~ 40 ohm-m) and probably of Clear Lake volcanics;

(2) a second layer, with a thickness of about two km, which is more conductive (< 10 ohm-m), and known from drilling to be the Great Valley sequence;

(3) a third layer, which is poorly resolved by the soundings and presumed to be Franciscan assemblage.

Figure 2-12 from Keller et al. (1984) compares the TDEM soundings near the Boggs 2 well to an induction electric log from that well. The TDEM sounding results are quantitatively similar to those from the VES dc electric work near Mount Hannah (Stanley et al., 1973). Together, the TDEM and dc electric surveys give us a reasonably good picture of the geology northeast of the field. There are no published TDEM results for the production area.

2.3.4. Temperature Gradient and Heat Flow

Thomas (1985) presented the first comprehensive set of temperature gradient and heat flow contour maps issued for The Geysers area. The data cover a 100 mi^2 (260 km^2) study area. Temperature-depth data from 70 of 187 gradient holes were selectively terrain-corrected, compiled and plotted. Mean thermal conductivities were determined for the three main rock types encountered in the area: graywacke, serpentinized ultramafic rock and greenstone. Thomas confirmed the earlier conclusion by Urban et al. (1976) that the natural heat loss from the system is mainly by conduction, and that the temperature gradient is nearly linear down to the first steam entry. Thomas could not use the thermal data to accurately determine the extent of the field because the data set is limited by the locations of wells with usable information. For example, he could not use many wells that had not reached thermal equilibrium or which were too shallow to give reliable temperature gradients. Nevertheless, the general outline of the area of highest heat flow ($\geq$ 350 mW/m^2) and highest gradient ($\geq$ 350°F/mi; 120°C/km) conforms roughly with the area of the gravity low referred to as the "production low." Within the narrow northwest-trending zone, which extends about 20 km in length, there seem to be two thermal "highs;" one centered near sec. 11, T. 11N., R. 9W. (near The Geysers Resort) and the other centered near sec. 35, T. 11N., R. 8W. (near Castle Rock Springs). Both of these areas are closely related to local resistivity lows. A more complete discussion of thermal data is given in Section 6.2.3 of this report.

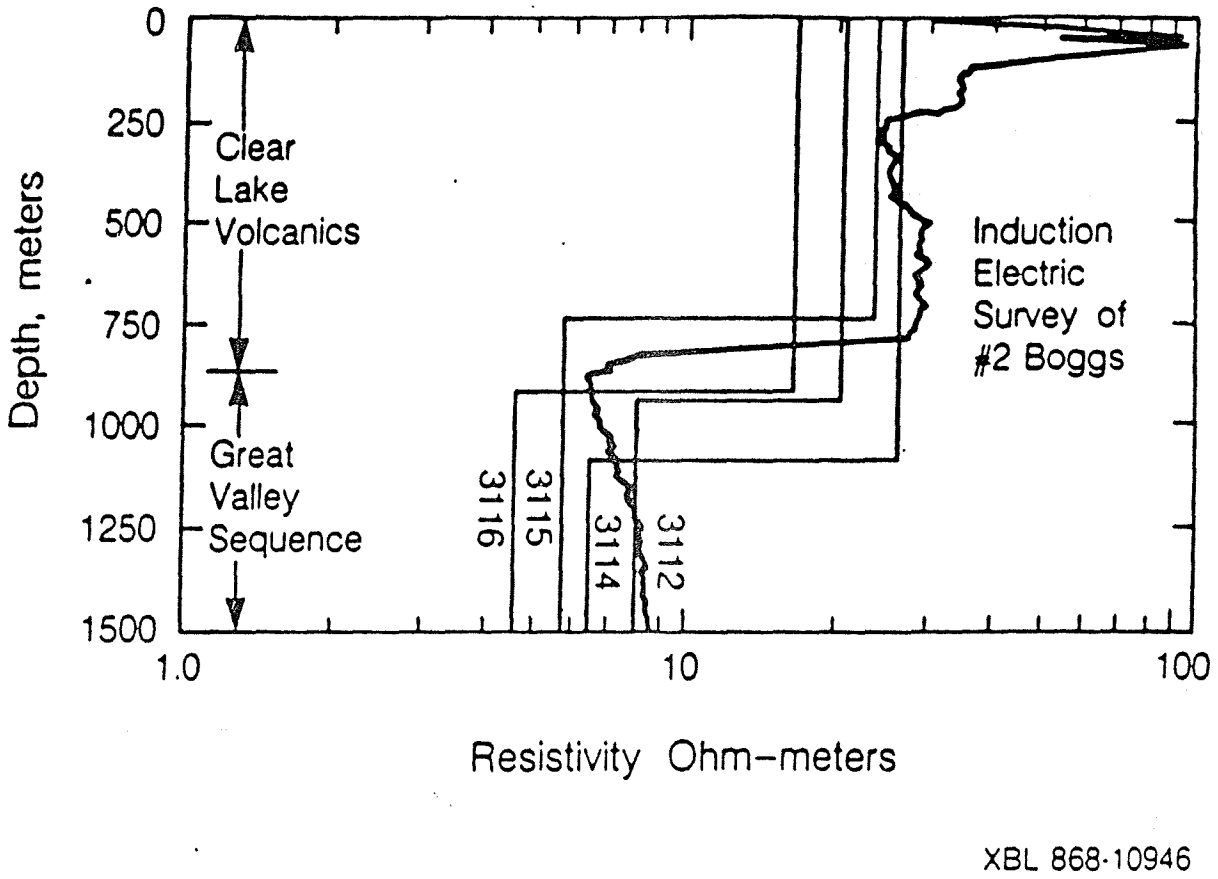

Figure 2-12. Comparison of inverted TDEM soundings collected near the Boggs 2 well with the induction electric log from that well (after Keller et al., 1984). The Great Valley sequence may be up to 1.2 mi (2 km) thick and is underlain by a more resistive third layer, presumed to be Franciscan assemblage.

2.3.5. Seismological Studies

Passive Seismic

Iyer et al. (1981) conducted a teleseismic P-wave delay study in The Geysers-Clear Lake area using 26 telemetered and 12 portable seismic stations. They found a large teleseismic delay which they subdivided into three spatial components:

(1) a general delay of 0.5 s centered on Mount Hannah and extending southwesterly into the steam field

(2) peak delays of 1 s near Mount Hannah

(3) peak delays of 1 s at one station (GBO) in the steam production area.

Iyer et al. (1981) numerically modeled the low velocity zone using ray-tracing techniques. Taking into consideration that Majer and McEvilly (1979) had found high velocities over the production area to depths of 2 mi (3 km), they assumed a flat-topped "body" with an upper surface 2.4 mi (4 km) deep, the depth of the seismogenic zone. They found that the delays could be explained by a broad zone of 15-percent velocity decrease surrounding a central zone of 25-percent velocity decrease (Figure 2-13). The low-velocity zones extend to depths of about 20 mi (30 km).

In spite of their modeling limitations, Iyer et al. (1981) concluded that their results supported the gravity model of a partial melt zone. They could not determine from the seismic data alone, however, if part of the delay from below the production area is due to the extension of the Mount Hannah magma chamber beneath a fractured, steam-filled reservoir. This study, together with the absence of earthquake foci deeper than 2.4 - 3 mi (4 - 5 km; Bufe et al., 1981) in the Geysers-Clear Lake area and the 10 mi (15 km) wide, low-Q (high elastic wave attenuation) anomaly (Young and Ward, 1981) running through the area, refueled the magma model controversy, but has shed little light on the question of reservoir geometry.

In a more recent study, Eberhart-Phillips (1986) analyzed 170 local earthquakes to determine the crustal velocities in a large area around The Geysers using a three-dimensional inver-

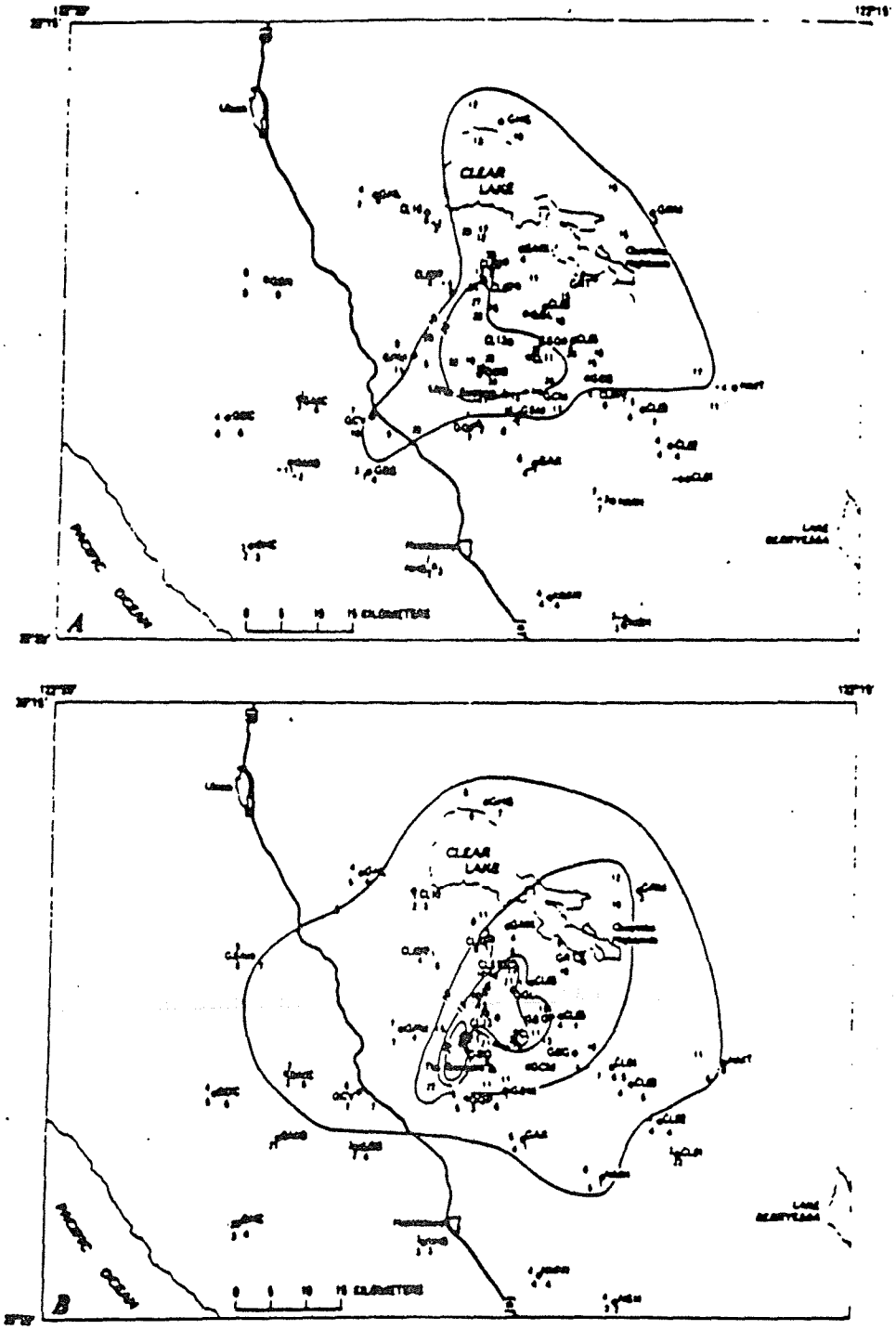

Figure 2-13. Calculated depth to bottom of anomalous body required to account for observed delays. Top of body is considered flat and assumed to be at a depth of 2.4 mi (4 km). Numbers near station locations indicated depth in kilometers to bottom (+) or top (-)d of body. Normal seismic velocity outside body is 4 mi/s (6 km/s). (A) 15% velocity decrease; contour interval is 6 mi (10 cm). (B) 26% velocity decrease; contour interval is 3 mi (5 km) (from Iyer et al., 1981).

sion of P-wave travel-time residuals. She found only weak evidence for a velocity anomaly related to the steam reservoir and no evidence for a low-velocity region shallower than 4.5 mi (7 km) below Mount Hannah. Her analysis did, however, reveal several other interesting features: (1) anomalously low velocities to at least 4 mi (6 km) depth along the Maacama and the Healdsburg-Rogers Creek (HRC) fault zones; (2) low velocities 0 - 2 mi (0 - 3 km) in depth, associated with the Clear Lake basin, where there is a thick sequence of young volcanics overlying sediments; and (3) a high-velocity body approximately 12 mi (20 km) long and 6 mi (10 km) wide, below 2 mi (3 km), located southeast of The Geysers and between the Maacama and Collayomi fault zones.

Direct or indirect evidence for the high-velocity zone (3) is not apparent in any of the other geophysical data sets, but the zone may be related to either an extensive region of high-grade metamorphic rock or granitic igneous intrusives with seismic velocities of around 4 mi/s (6.3 km/s; Eberhart-Phillips, 1986).

The distribution of microearthquakes was initially believed to be a characteristic of geothermal areas, and early microearthquake studies such as those done by Lange and Westphal (1969) and Hamilton and Muffler (1972) over The Geysers field were viewed initially as useful for geothermal exploration. Later surveys of this type at The Geysers and elsewhere produced inconsistent results and have led seismologists to re-evaluate the premise that high microearthquake activity is associated with geothermal reservoirs in their natural state. Most seismic studies at The Geysers have been done since production began. Bufe et al. (1981) found a steady occurrence of small, shallow earthquakes in the production area during the 1975-1979 period. The location and nature of the seismicity led Bufe et al. to conclude that most of the seismicity was induced by a combination of fluid withdrawal from the already underpressured reservoir coupled with massive injection of relatively cool condensate.

In contrast to the results of Bufe et al., Majer and McEvilly (1979) found only weak and diffuse microseismic activity with a general absence of microearthquakes within the production area and along the known fault structures. The lack of measured seismicity is believed to be due

to the high threshold level chosen as a detection criterion. They tentatively concluded that the microearthquakes may be related to large pressure or temperature gradients or to volume changes due to fluid removal. If so, they reasoned, the distribution may be useful for delineating the reservoir boundary. However, they cautioned that the boundary may be dynamic, driven by the exploitation of the field. The continuous monitoring of seismicity would therefore offer the hope of being able to monitor the steam zone configuration. Used in combination with production-injection rates and cumulative mass extraction, seismicity might also show some interesting features related to depletion.

There is ample evidence now that local seismicity (the amplitudes, occurrence rate and depths) is indeed related to production and not to injection. Marks et al. (1978) found that an increase in $M \geq 2$ activity during 1975-1977 was about twice as high as the 1962-1963 level prior to production. Eberhart-Phillips and Oppenheimer (1984) studied over 7000 events recorded in the 1975-1982 period, and also inferred from the spatial and temporal pattern of seismicity that seismicity is related to production as evidenced by the spread of seismicity into new areas as new wells come on-line. They found no correlation between seismicity and injection wells or production wells in use more than seven years. They also reported an increase in seismicity to the northwest, beyond the Big Geysers area, where there were no production wells during the observation period.

Presently, the seismic activity is considered to be benign, but it is not well understood. Eberhart-Phillips and Oppenheimer (1984) find only two plausible mechanisms to explain the microearthquake activity. There may be a volumetric contraction due to fluid extraction which perturbs the stress field enough to cause faulting of rocks already close to brittle failure in the regional stress field (Majer and McEvilly, 1979). Alternatively, fluid extraction might increase the coefficient of friction along fault traces so that rocks deforming aseismically might begin to deform by a stick-slip (seismic) process (Allis, 1982). In a more recent study to understand the mechanisms for seismicity within The Geysers geothermal field, Oppenheimer (1986) analyzed 210 local earthquakes and compared the seismicity to annual fluid production. He also confirmed

that most of the seismicity is induced, and he attempted to determine the inducing mechanism on the basis of the orientations and relative magnitudes of the principal components of the stress field from fault plane solutions and correlations with geodetic data. He concluded that The Geysers is undergoing uniaxial extension below 0.6 mi (1 km) with the minimum stress component (σ_3) oriented horizontally at approximately N 75°W. The good agreement between the stress field within the geothermal reservoir region and the regional strain-rate axes demonstrates that any stress perturbations due to reservoir rock contraction must be small in comparison to the regional tectonic stress field. On this basis, then, Oppenheimer's (1986) fault plane study would support the hypothesis that the induced seismicity results from the conversion of aseismic to stick-slip deformation due to the increase in the coefficient of friction on fracture surfaces as steam is withdrawn. Both the dewatering of clays and the precipitation of dissolved silica on fracture surfaces as a result of pressure-temperature changes caused by production have been mentioned as contributing factors for the increase in friction (Allis, 1982). However, neither reaction is physically realistic at The Geysers, and therefore seismicity induced by a volume contraction remain a very likely explanation. Reservoir contraction is indicated by measured subsidence of up to 1 in/yr (2 cm/yr) between the Mercuryville and Collayami fault zones and over 1.5 in/yr (3 cm/y) directly over the Big Geysers production area (Lofgren, 1981).

Oppenheimer (1986) also has tried to explain the cause of induced seismicity at depths of up to 4 mi (6 km), about 2 mi (3 km) deeper than the bottoms of the deepest production wells. Such seismicity may indicate that steam is being produced from increasingly deeper and deeper parts of the reservoir as time goes on, and that an extensive network of pre-existing near-vertical fractures must therefore be present (Figure 2-14). The data at hand were not sufficient for Oppenheimer to determine whether the downward propagation of seismicity is related to local vertical gradient in the effective principal stress σ_3.

O'Connell (1986) examined microearthquakes detected by means of a 9 station array of 3-component geophones over the production area. The variable V_p/V_s structure determined by means of inversion (Figure 2-15) can be explained strictly on the basis of liquid saturation

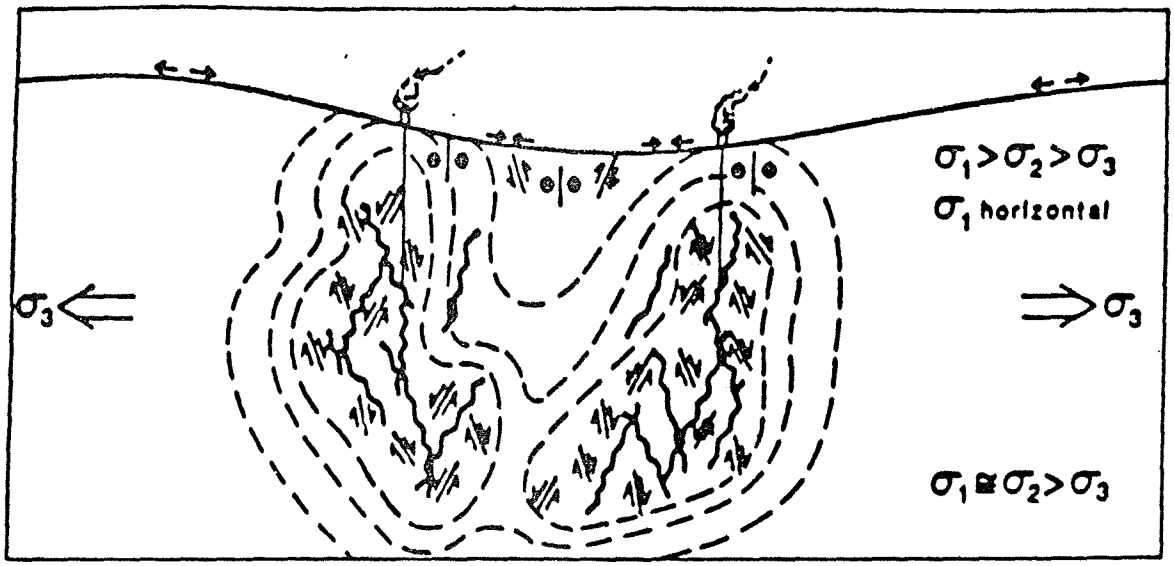

Figure 2-14. Schematic of induced strains within The Geysers geothermal field (after Oppenheimer, 1986). The dashed curves represent contours of equal strain. The wavy solid lines represent the fractures supplying steam to the wells. The short straight lines and adjacent arrows represent the sense of slip from the regional shear stresses. Induced seismicity at depths up to 2 mi (3 km) below the deepest production wells indicate that steam is being produced from a deep zone via an extensive network of near-vertical fractures.

(Toksög, et al., 1976). The peak V_p/V_s at a model depth of 1.0 km (0.37 mi or 0.6 km below sea level) corresponds to the saturated condensation zone. The minimum in V_p/V_s at depths of 0.37 to 1.3 mi (0.6 to 2.1 km) below sea level can be explained by the depletion of pore fluids and vapor static conditions in the production zone. Fracturing, as it is known to be at The Geysers, cannot explain the observed V_p/V_s structure.

O'Connell (1986) also found that earthquake foci are confined to two distinct depth intervals. Shallow seismicity is associated with production from the main reservoir graywacke. Deeper seismicity, as Oppenheimer (1986) had also noticed, was clearly discerned. O'Connell (1986) speculated that the deep seismicity is caused by the upward migration of water along a vertical fracture system from a deeper reservoir. This is a different model than that proposed by Oppenheimer (1986), but similar to one proposed earlier by White et al. (1971).

Active Seismic

Reflection seismology is widely used in petroleum exploration, and has also been used in geothermal exploration to resolve subsurface structures and to map faults and zones of fracturing or hydrothermal alteration. Only limited attempts have been made to use reflection techniques at The Geysers, possibly because of practical problems typical of many geothermal areas, such as:

(1) a limited number of winding roads through a topographically rough area;

(2) the difficulty of getting energy into the ground in areas of volcanic cover.

Denlinger (1979) and Denlinger and Kovach (1981) reported on an experiment in the Castle Rock Springs area intended to determine if standard reflection techniques, supplemented by state-of-the-art data processing, are useful for geothermal prospecting in geologically complex areas. Interpretable data were obtained along two short, crossed lines along winding gravel roads. A commercial contractor, using four Vibroseis® trucks applying four 16-s downsweeps over the frequency range of 58 - 12 Hz, was employed. The geophone lines were a split-spread, 12-fold, with a 110 ft (33 m) group interval and a cable length of 3,000 ft (880 m). The short survey lines helped improve signal-to-noise at depths of 0.6 - 1.8 mi (1 - 3 km), and allowed the

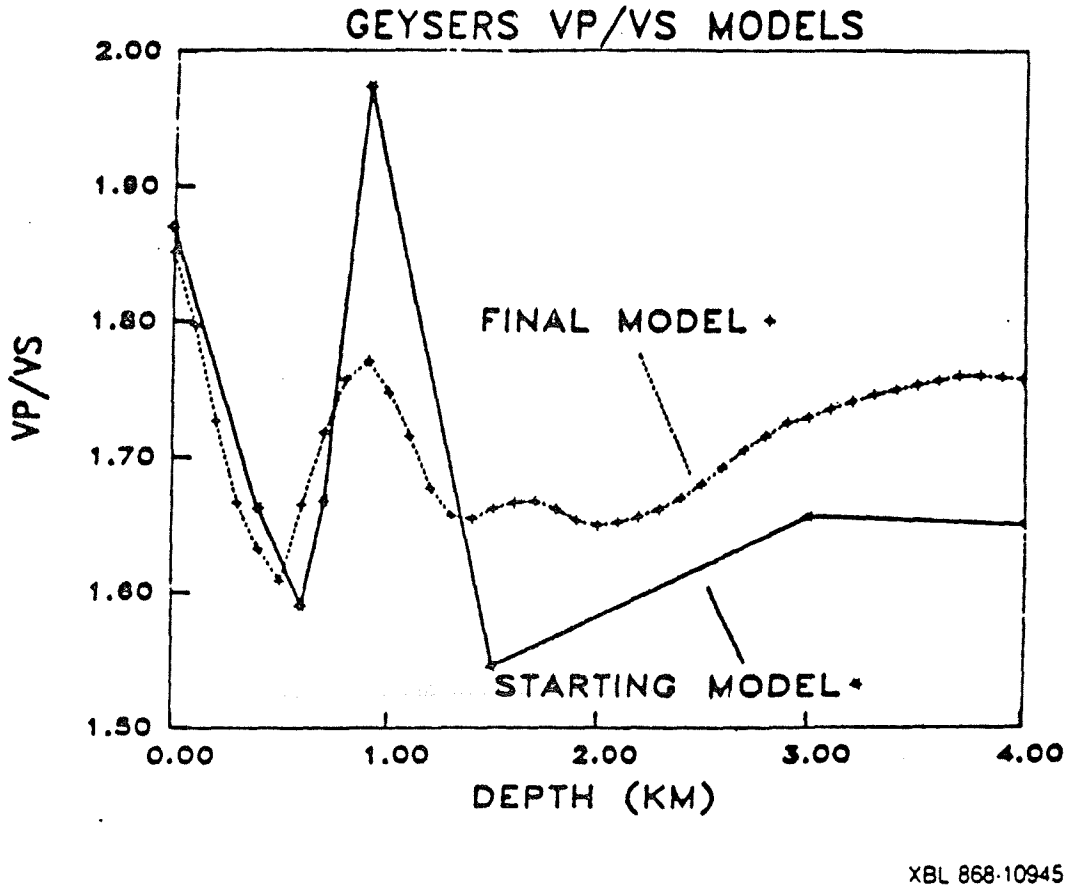

Figure 2-15. Calculated V_p/V_s ratio for the section at The Geysers geothermal field. The layered model was determined from an inversion of microearthquakes occurring at depths of up to 2.5 mi (4 km) (from O'Connell, 1986).

researchers to pick up an anticlinal structure, a dipping layered structure and fracture-related features near the crest of the anticline, all of which were confirmed by well data. Among the reservoir characteristics resolved by the reflection survey was an indication that the greenstone acts as an impermeable cap over portions of the fractured graywacke reservoir rocks. This is the pattern reported for steam occurrences in other parts of the field (McLaughlin and Stanley, 1975).

A reflection seismic experiment using both compressional- and shear-wave sources was conducted by Rossow et al. (1983) to obtain information on the characteristics of subsurface rocks under high-temperature conditions. Little is known about this work because only an abstract was published. However, the authors reported Poisson's ratios of less than 0.25 northeast of the production area and at depths of between 3 - 7 mi (5 - 11 km). The reported result is perplexing in view of the normal Poisson's ratio found by O'Connell (1986) beneath the production area. It is also interesting that Rossow et al. (1983) found no evidence for the abnormally high Poisson's ratio that one would associate with a partial melt in the region of the postulated magma.

2.4. GEOCHEMISTRY

The Geysers is one of the two largest vapor-dominated geothermal systems known (the other is Larderello in Tuscany, Italy). These systems produce only steam from drill holes but the presence of liquid water in the reservoir is well established. The role of geochemistry in understanding the origin and reservoir mechanics of these systems has been significant, in part because the physical chemistry of water and gas is critical and in part because the pioneering researchers were geochemists. Although much of our knowledge of vapor-dominated systems has come from Larderello, Italy, where exploitation started much earlier and where most important information has been available to the public, there is substantial literature on the geochemistry of fluids, rocks, and alteration minerals at The Geysers.

2.4.1. Early Studies

The first major scientific study of The Geysers was made in 1924-1926 by E. T. Allen and

A. L. Day of the Carnegie Institute (Allen and Day, 1927). They studied the natural fumaroles and hot springs and their associated alteration along with chemical and physical characteristics of fluid from the eight shallow steam wells drilled in 1921-1925. These workers also studied Lassen and Yellowstone, where they explored the relationship between of geothermal activity and magmatism. The causative connection of magmatic activity with high-temperature geothermal heat was clear to Allen and Day and remains so now, but the magmatic origin of gases and dissolved salts advocated by Allen and Day for The Geysers and elsewhere remains controversial.

Allen and Day made a careful study of the natural activity, which was much more intense then than it is now although major decline did not occur until the 1970s. They distinguished relatively concentrated, low-flow, acid-sulfate hot-spring waters formed by condensation of steam, surface oxidation of H_2S to sulfuric acid, and rock leaching, from dilute neutral bicarbonate hot-spring waters formed by adsorption of steam and CO_2 into meteoric ground water and subsurface reaction with rock. They noted the near absence of chloride in surface manifestations, an observation crucial to the model of vapor-dominated systems proposed by White et al. (1971). Other important observations included the production of saturated steam without liquid from wells; small total flow of the springs and fumaroles (<100 lpm) and the association of alteration, fumaroles and hot springs, and mercury deposits. Gases in steam from fumaroles and the few shallow (<600 ft; 200 m) wells, drilled in the 1920s, were found to be rich in hydrocarbons and hydrogen compared with steam from Lassen and Yellowstone.

After Allen and Day there was no specifically geochemical study of The Geysers until the early 1970s, when D. E. White and his coworkers proposed their model of vapor-dominated systems that is now almost universally accepted among workers on The Geysers (White et al., 1971). This model was expanded by Truesdell and White (1973) and D'Amore and Truesdell (1979), who also based their interpretation on the chemical and physical characteristics of steam from The Geysers and Larderello and on the thermodynamics of water and gases. This model has provided the conceptual basis for mathematical studies of the origin of vapor-dominated sys-

tems and their response to exploitation. Later geochemical studies have used this framework and emphasized the estimation of original and exploited temperatures and vapor-liquid ratios and the response of these systems to exploitation and reinjection of steam condensate.

2.4.2. The Vapor-Dominated-System Model of White and Others

The White et al. model for vapor-dominated systems considered a reservoir consisting of fractured rock with low-permeability boundaries containing a mixture of water and steam. The reservoir is capped with a condensate-saturated zone of lower permeability and bottoms in a brine(?)-saturated zone (Figure 2-16). Boiling in the brine produces steam that flows upward along large fractures and condenses in the condensate zone. Condensate flows downward along rock surfaces and small pores to join the deep brine and boil again. The large differences in density, viscosity, and specific enthalpy of steam and water produce an efficient "heat pipe" that transfers heat upward with little or no mass transfer and small temperature (and pressure) gradients. The pressure gradient is close to vaporstatic, controlled by the density of vapor, which occupies interconnected large voids and fractures and is the continuous phase. The term "vapor-dominated" refers to the dominance of vapor in controlling pressure within the two-phase liquid-vapor reservoir and in determining the chemistry of fluids within and above the reservoir. It should be understood that the reservoir fluid may be mostly liquid by mass.

White et al. (1971), and in more detail Truesdell and White (1973), suggest that the large volumes of saturated to slightly superheated steam produced by these systems result from boiling in place of essentially immobile liquid water with heat transferred from reservoir rocks. This boiling results from the decrease in reservoir pressures caused by production. Although in the natural state some part of the liquid water in the reservoir is mobile enough to flow downward to balance the mass of upward flowing steam, all liquid water appears effectively immobile during production except very-near-well water produced from some wells soon after drilling.

The observations on which this model were based include (1) the lack of chloride in surface discharges; (2) the small rate of surface fluid flow relative to the large size of the reservoir and the amount of surface heat flow (this is more true of The Geysers than Larderello); (3) the

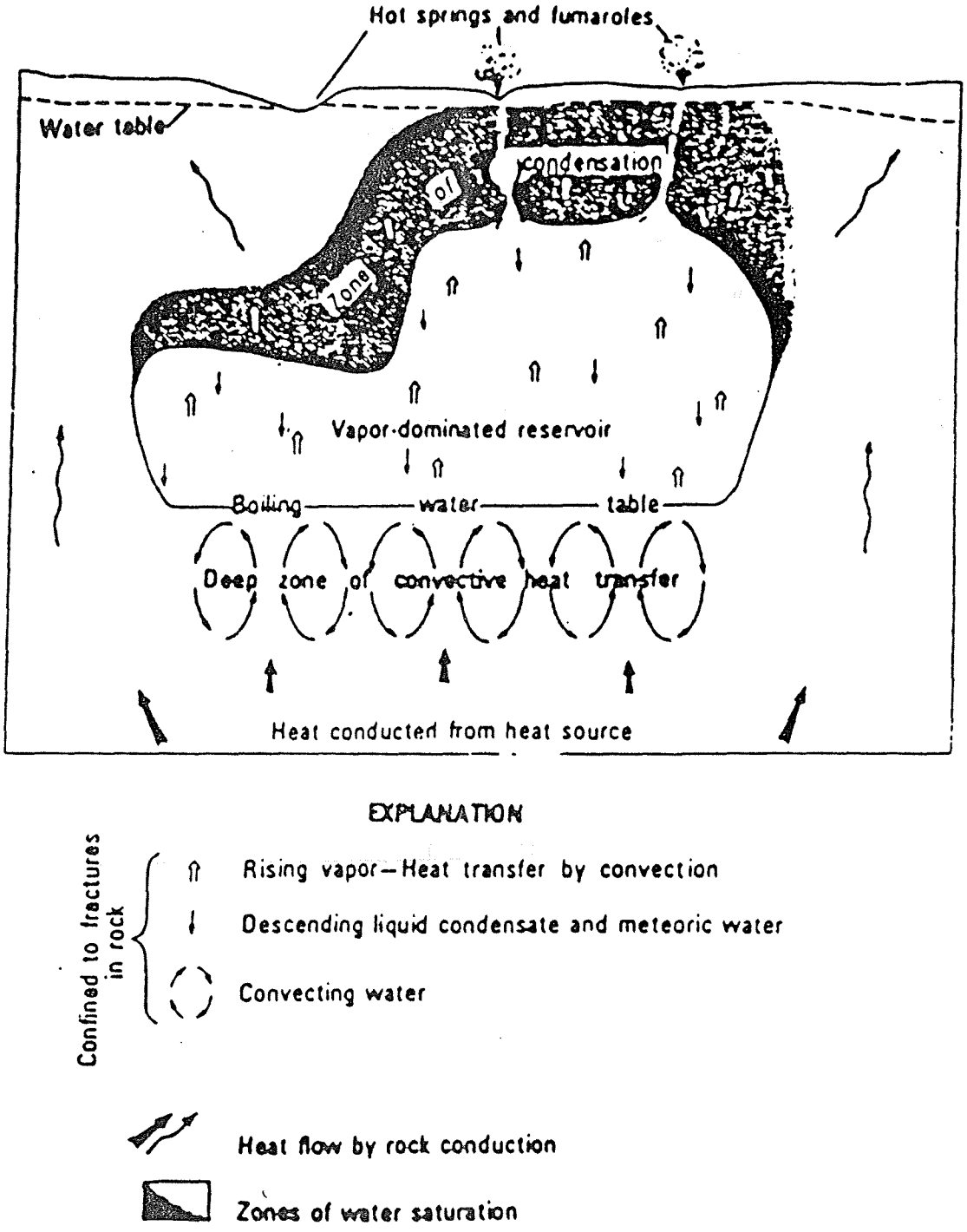

Figure 2-16. Conceptual model of a vapor-dominated system (after White et al., 1971).

production from wells of saturated or superheated steam alone rather than the steam-water mixture produced from most geothermal reservoirs; and (4) the enormous total production of steam, far more than could have been contained as vapor in a reservoir of reasonable volume. Essentially all of these observations except the last were made by Allen and Day, but subsequent scientific studies and expanded exploitation of both The Geysers and Larderello provided much additional data for the White et al. model.

2.4.3. Later Models of Vapor-Dominated Systems

The White et al. model has provided a conceptual basis for many later papers involving geology and geochemistry as well as experimental and mathematical simulations. An extension of the model to include lateral steam movement and condensation was made by D'Amore and Truesdell (1979) on the basis of regular variations of steam composition with location at Larderello and The Geysers. These chemical variations were suggested to result from lateral steam flow away from central areas of boiling (and upflow) with progressive condensation during lateral flow due to conductive heat loss to the surface. The condensate migrates down to a deep water table and flows back to the central boiling zone. Since gases and volatile salts distribute themselves between steam and condensate according to their solubilities, gas concentrations will increase and salt concentrations decrease in residual steam as condensation progresses. This was modeled by D'Amore and Truesdell as a Rayleigh process, which is similar to precipitation forming from water vapor in clouds. This model also provides a mechanism for the enlargement of vapor-dominated systems through rock solution by CO_2-charged steam condensate formed along and at the distal ends of steam-flow paths. The continued solution should increase permeability to steam wherever condensation occurs (the condensate forms along steam-flow channels wherever cooling occurs) and extend the system into new rock. In the same paper, D'Amore and Truesdell reported changes of Larderello steam composition, temperature, and flow with time that supported the White et al. division of the reservoir into condensate, vapor-dominated, and brine layers.

The White et al. model provides the conceptual basis for most of the numerical and experimental simulations of the origin and reservoir processes in vapor-dominated systems as well as the theory of well testing in these systems. These studies are outside the scope of this review and are discussed in a companion paper.

2.4.4. Geochemical Methods of Estimating Temperature and Steam Saturation

Most geothermometer methods are based on analyses of liquid from hot springs or geothermal wells and cannot be applied to steam samples. Thus geothermometers for vapor-dominated systems must be based on the chemical and isotopic composition of gases including water vapor. Several isotopic geothermometers have been tested at Larderello and The Geysers but appear to equilibrate either too rapidly (CO_2–H_20) or too slowly (CO_2–CH_4) and therefore yield either temperatures of sample collection or temperatures deep in the system below the exploited reservoir (Truesdell and Hulston, 1980).

The application of chemical gas geothermometers to vapor-dominated systems was not very successful initially, although some empirical gas geothermometers have been useful at Larderello and to a lesser extent at The Geysers (D'Amore and Truesdell, 1980). The problem with earlier attempts to use gas geothermometry on vapor-dominated systems was shown by D'Amore et al. (1982) to result from the mixed origin of produced steam that comes in part from reservoir vapor and in part from vaporized reservoir liquid. When gases are in equilibrium in both liquid and vapor, each gas will have the same partial pressure in both phases, but gas concentrations will not be the same and a mixture of vapor and vaporized liquid will have gas concentrations apparently out of equilibrium. Using a method that Giggenbach (1980) developed for hot-water systems, D'Amore et al. (1982) and D'Amore and Celati (1983) showed that by combining two gas equilibria with gas solubility data, both the reservoir temperature and the effective reservoir vapor saturation could be calculated. The latter quantity, called "y," is potentially very important in estimating reserves of vapor-dominated systems because liquid in the reservoir constitutes most of the reserves and should be proportional to the fraction of vaporized water in produced steam. This method was applied to parts of The Geysers reservoir by D'Amore and Truesdell

(1985). The study showed that different areas varied greatly in y but showed very similar temperatures (Figure 2-17). Part of the Southeast Geysers showed y values of 0.005 to 0.1, indicating large contributions from vaporized liquid. Wells further to the north showed y values from 0.1 to 1.0, indicating little vaporizing liquid in the reservoir. Both areas have indicated temperatures near 440°F (225°C), with the southeastern area slightly higher and the northern area slightly lower. A study combining these chemical methods with more traditional methods of resource assessment should be made to test the method.

2.4.5. Petrologic Studies

Petrologic studies of The Geysers reservoir are difficult because the rock is metamorphosed, lithologically complex, and tectonically disturbed. In addition, core is rare, and finely powdered air-drilled cuttings are difficult to study. Despite these problems there have been several very informative petrologic studies of The Geysers rocks.

The most ambitious study was that of Lambert (1977), who analyzed the isotopic compositions of mineral separates from different depths in seven Geysers wells (with as many as 100 samples from a single well). A later study by Sternfeld (1981) also used isotope methods along with fluid inclusions and more detailed petrology to study samples from two wells. More limited mineralogical studies were made by Steiner (1958) and Moore (1980). These studies were descriptive and did not discuss mineral origins.

Lambert and Sternfeld studied materials from the central part of The Geysers operated by the Union Oil Co. (now Unocal). They came to very similar conclusions, and the following is based on both studies (unfortunately, still available only as unpublished dissertations).

The Franciscan Event

The Franciscan host rocks of The Geysers were deposited in a marine environment with clastic (graywacke) volcanogenic (greenstone), chemical (chert), and igneous (serpentinite) units. During and soon after deposition these rocks were deeply buried in a normal geothermal gradient to produce low-grade greenstone metamorphism, referred to by Sternfeld as the

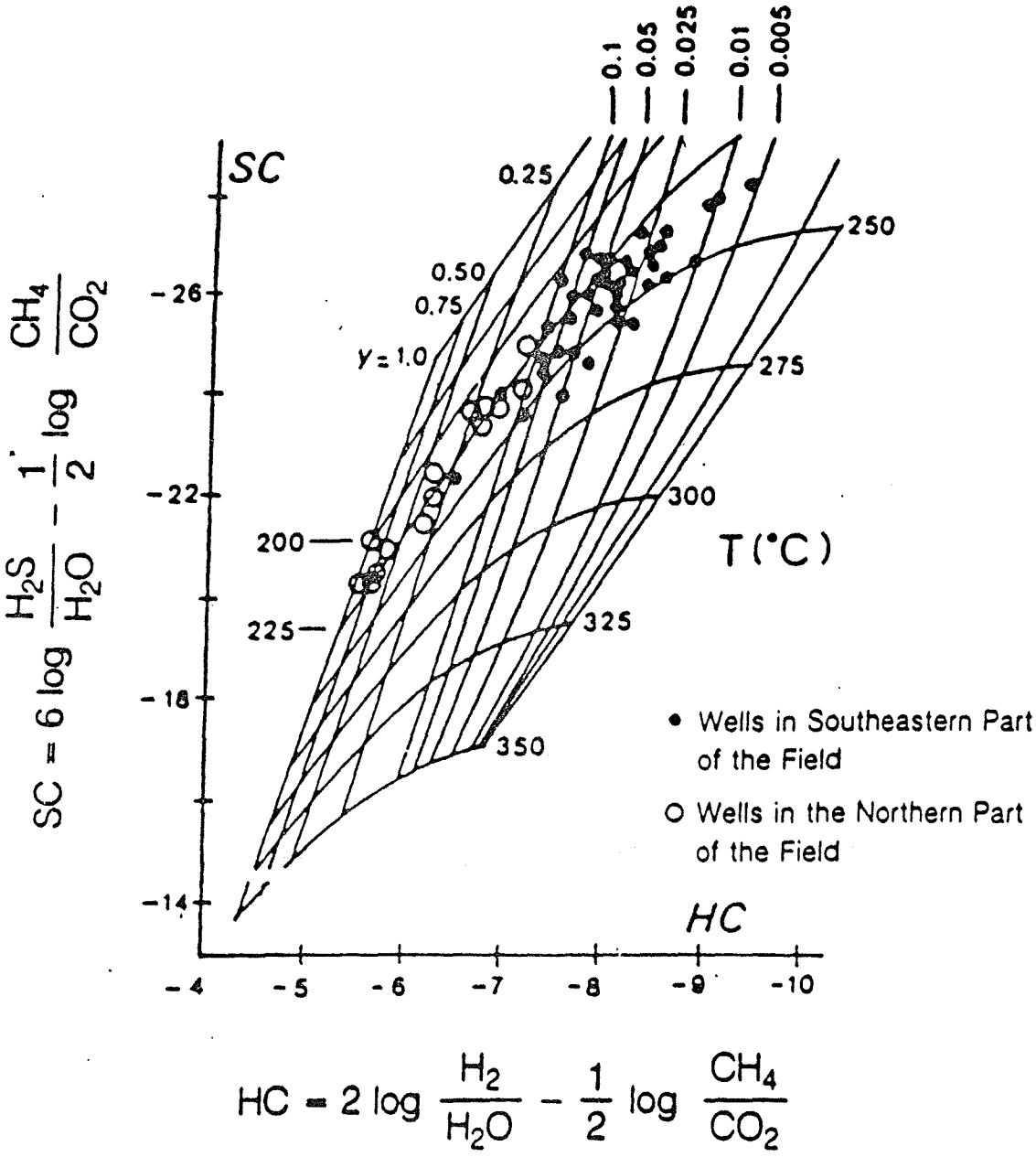

Figure 2-17. HC versus SC for The Geysers field (after D'Amore and Truesdell, 1985).

"Franciscan" event. Temperatures reached 340 - 400°F (170 - 200°C) and the rock was saturated with connate sea water with a $\delta^{18}O$ composition altered to +5 to +7 0/∞ by oxygen isotope shift. The record of this event was mainly preserved in the shallow parts of wells above the steam reservoir. The wide range in $\delta^{13}C$ of abundant calcite in these rocks suggests little fluid circulation, local origin of carbon, and (along with the shifted water ^{18}O) low water/rock ratios.

The Geysers Event(s)

After the Franciscan hydrothermal event The Geysers area was subjected to volcanic activity from Pliocene to recent time, with the activity shifting northward with time from Sonoma (2.9 to 5.3 m.y.) to Clear Lake (0.01 to 2.1 m.y.) adjacent to The Geysers (McLaughlin, 1981). In the present Geysers reservoir these events were accompanied by increasing temperature and a replacement of the connate reservoir fluid with one derived from meteoric water. This higher-temperature hydrothermal reservoir was liquid-dominated, as indicated by deposition of minerals such as adularia, epidote, diopside, tremolite, and garnet, characteristic of hot-water systems with moderate to high salinity and temperatures from 212 - 620°F (100 - 325°C). Isotopic and fluid inclusion data suggest temperatures from 430 - 610°F (220 - 320°C) and fluids with $\delta^{18}O$ of -2.5 to -0.5. Some evidence suggests that high temperatures (> 620°F; >325°C) extended to shallow depths (1800 - 2400 ft; 600 - 800 m) as a result of geopressured conditions. Release of this pressure may have been important in the later transitions to vapor domination. The fluid in this hot-water reservoir appears to have been isotopically lighter in the south-central Geysers (Lambert's data) than in the north-central Geysers (Sternfeld's data), suggesting either a lower water/rock ratio (more oxygen isotope shift) or less complete flushing of connate waters in the north.

When this hot-water system was well established, either recharge diminished or heat input increased, and steam vented to the surface faster than it was replaced by recharge, initiating the formation of a vapor-dominated reservoir (the second Geysers event). These processes resulted in an increase of steam saturation to form a two-fluid-phase, vapor-dominated zone that started at a depth of about 1200 ft (400 m) and extended downward through the entire present vapor-dominated reservoir. The boil-down started at 455°F (235°C) because at this temperature

saturated steam has its maximum enthalpy and can accumulate stably without adiabatic segregation into liquid and vapor. Boiling at high temperatures deeper in the system was accompanied by gravity separation of liquid that remained at that level and vapor that rose to lower-pressure zones and again separated adiabatically into more liquid and steam of higher enthalpy until maximum enthalpy steam was formed.

The fluids in the now vapor-dominated reservoir were out of equilibrium with minerals deposited by the earlier system since they were cooler [465°F (240°C) instead of 610°F (320°C)], much less saline (consisting now of steam condensate), and probably more acid. This last condition resulted from the removal (in descending condensate) of bicarbonate formed by fluid-rock reactions and its replacement by CO_2 in ascending steam. CO_2-charged condensate probably dissolved many of the previously formed alteration minerals where they were not sealed from fluid contact and attacked fresh country rock to extend and enlarge conduits. In particular, calcite was strongly leached and is nearly absent from the steam zone, although it is very common at shallow depths.

The indications of higher water/rock ratios of more meteoric water flushing is in agreement with the limited data available on fieldwide patterns of chemical and isotopic compositions of steam at The Geysers. Rapid flow of steam, both upward and laterally, with condensate flow downward and back to centers of boiling, allowed the system to spread laterally and lose heat by conduction at the top and sides so that heat flow through the system was nearly constant despite lower reservoir temperatures.

2.4.6. Fieldwide Steam Composition Patterns

Although isolated steam analyses have been quoted (e.g., in White et al., 1971) and samples of drill core and cuttings from a few wells have been studied, very few data on fieldwide variations in steam (or rock) compositions are available. Although presenting data for only part of the field, Haizlip (1985) described oxygen isotope variation from $\delta^{18}O$ values of -7 in the southeast to nearly +3 in the northwest. This extreme range is from near meteoric water composition to close to that of the isotope-shifted connate water that occupied the Jurassic-Cretaceous Geysers

reservoir (>+5). This observed range in steam isotopes agrees with suggestions from isotope analyses of minerals that there was a lower water/rock ratio or more residual connate water in the northern part of the field during the Pliocene(?)-recent hot-water event (Sternfeld, 1981). Data on steam compositions at the power plants suggests higher total gas and H_2O to the northwest (see Section 6.2.6). This could also (along with increasing ^{18}O) result from a lower water/rock ratio or more residual connate water, either during the past hot-water event or at present below the steam reservoir.

2.4.7. Summary

The Geysers is a large, complex geothermal field whose origin, fluid compositions, host-rock properties, and reservoir processes are still imperfectly known, despite the drilling of numerous wells and a relatively long period of production. Part of this lack of understanding is due to the reticence of the steam producers to share information or encourage outside research. The situation is also a result of the complexity of the reservoir, the difficulty of sampling uncontaminated fluids from specific depths in the system, and the required sophistication of studies of the reservoir rock. Despite these problems, the properties of The Geysers as a vapor-dominated system are becoming clearer. The "heat-pipe" model of convection in these systems, first described by White et al. (1971), has reached near-universal acceptance and explains qualitatively most of their important characteristics, including high productivity, uniform pressures and temperatures and, through later extensions (D'Amore and Truesdell, 1979; Thomas, 1981), the large reservoir size and local variations in steam chemistry.

There are encouraging indications of advancement in geochemical studies and knowledge of The Geysers. Sophisticated models for gas equilibria and phase distribution hold promise for estimation of reservoir liquid reserves (D'Amore et al., 1982). Greater cooperation between steam producers along with compilation of public but scattered data (as in this volume) will encourage fieldwide studies of fluid and rock geochemistry.

2.5. RESERVOIR ENGINEERING

Over 500 wells have been completed at The Geysers since drilling commenced in the 1920s. Large amounts of reservoir engineering data have been collected from the wells, especially since the late 1960s, when large-scale power production began. These data include temperature/pressure surveys, rig test data, wellhead data, production and injection histories and pressure transient test data. Many of the wells have been producing for over a decade, yielding flow rate histories that reflect changes in reservoir conditions. Unfortunately, much of the reservoir engineering data from The Geysers field are proprietary and not available in the open literature. However, papers and reports have been published that describe in general terms the reservoir behavior prior to and during exploitation. The most comprehensive reviews include those of Ramey (1968), Lipman et al. (1977) and Dykstra (1981). Allan and Day (1927) give a very detailed description of the characteristics and behavior of the early wells drilled in The Geysers area. The present review is primarily based upon information given in those references, but also includes recently published information.

2.5.1. Reservoir Rocks

The main reservoir formation at The Geysers is the Franciscan graywacke, which is a metamorphosed sandstone containing considerable amounts of clay (Ramey, 1970a). The graywacke is extensively fractured, but also contains large blocks of rock with few or no major fractures. Many of the productive fractures (steam entries) in the northern and central part of the field can be correlated between wells, and indicate near-horizontal trends (Thomas, 1981). Much less is known about the fracture characteristics of the southern part of the field (T. Box, personal communication, 1987). Some steam-filled fractures are also found in some of the other lithologic units such as the greenstone. The caprock does not appear to correlate with lithologic units (Thomas, 1981), but is probably created by crystalline deposits forming hydrologic seals in various rocks.

Well test data collected at The Geysers show that the overall reservoir permeability is fairly high due to high-conductivity fractures and faults. Capuano (1979) estimates that the fracture

porosity in The Geysers reservoir is in the range of 1 - 3%. Little is known about the hydrological properties of the rock matrix. Limited core studies indicate a matrix porosity of 3 - 7% and permeability of less than 1 md (Lipman et al., 1977; Dykstra, 1981). Pruess and Narasimhan (1982) concluded from a modeling study that if substantial fluid reserves exist in liquid form in the matrix, the matrix permeability must be very low (microdarcies), for only steam to recharge the fracture system.

In many areas of The Geysers a condensation zone with liquid-filled fractures and matrix exists above the vapor-dominated zone (Ramey, 1970a; Hebein, 1982). Schubert and Straus (1980) have shown that for such a liquid zone to be stable the permeability connecting it to the vapor-dominated zone must be less than 0.04 md.

2.5.2. Thermodynamic State

The Geysers is the largest known vapor-dominated reservoir in the world. The distinctive feature of this type of geothermal system is that vapor is the pressure-controlling phase. Vertical pressure gradients are small, on the order of vapor-static (Truesdell and White, 1973; Celati et al., 1975; Lipman et al., 1977). Undisturbed reservoir temperatures are usually close to saturated values at given pressures, and are near 465°F (240°C) at the top of the reservoir (Truesdell and White, 1973). Substantially higher temperatures, in excess of 570°F (300°C), have been observed at greater depth (Drenick, 1986). In the early literature there was considerable controversy over the fluid and heat-flow conditions in vapor-dominated systems (Facca and Tonani, 1964; Elder, 1965; Ramey, 1970a; Facca, 1973). Much of the disagreement was concerned with the presence of liquid water, and its distribution in vapor-dominated reservoirs. White, Muffler, and Truesdell (1971) proposed a comprehensive conceptual model for these systems, which has found general acceptance in the technical community. The essential elements of the White et al. model are (1) the recognition that vapor-dominated reservoirs are two-phase (vapor-liquid) systems, even though liquid may never appear in well discharges; and (2) the explanation of vertical heat transfer in these systems by means of a vapor-liquid counterflow mechanism known as "heat pipe" (see Figure 3-16). Heat pipe systems can form when a permeable medium containing a

volatile fluid is subjected to an imposed heat flux (Eastman, 1968). They can transport large heat fluxes over regions of small temperature gradients by means of a vapor-liquid counterflow mechanism: liquid is vaporized at the "hot" end, and the vapor flows towards the cold end where it condenses, releasing its large latent heat of vaporization. The liquid condensate then flows back towards the heat source. In engineered heat pipes the backflow of liquid is generated by capillary forces, whereas in vapor-dominated reservoirs the counterflow is due to gravity. The heat pipe model explains the main heat transfer mechanisms in vapor- dominated reservoirs. It does not describe the distribution of liquid water, nor does it address the question of how vapor-dominated conditions can evolve naturally.

2.5.3. Phase Composition

From the large cumulative production obtained from The Geysers reservoir, it has been concluded that most of the fluid reserves were originally in liquid form, because the large produced mass, if present in vapor form, would require an unreasonably large reservoir thickness (James, 1968; Nathenson, 1975; Weres et al., 1977). The amount of liquid present, and its distribution throughout the reservoir, have not been established. From a consideration of vaporization processes and production enthalpies, Truesdell and White (1973) have suggested that the saturation of distributed liquid is in the range of 20 - 50%. Additional liquid is supposed to be present in a "deep water table" (White et al., 1971; D'Amore and Truesdell, 1979). Most investigators have held that distributed water-saturation in vapor-dominated systems is near the irreducible limit of perhaps 30%, and have considered that higher water saturations are incompatible with the small vertical pressure gradients (e.g., Grant 1979; Straus and Schubert, 1981). More recently it was suggested by Pruess and Narasimhan (1982) that vapor-dominated reservoirs could be nearly fully water saturated, the small vertical pressure gradient being consistent with the presence of mobile water in a fractured porous medium with small permeability of the unfractured rock (the "cracked sponge" model of Weres et al., 1977). The hypothesis of large water saturation has recently obtained independent support from geochemical observations. From an analysis of non-condensible gases it was concluded by D'Amore et al. (1982) that a very large fraction of

fluids produced at The Geysers (up to 99%) originated from boiling of liquid phase in the reservoir. Additional support for the hypothesis of nearly full water-saturation is obtained from considerations of the natural evolution of vapor-dominated systems (see below).

2.5.4. Natural Evolution

It is now well established that vapor-dominated reservoirs have evolved from liquid-dominated precursors with significantly higher temperatures at depth (Sternfeld and Elders, 1982; Hebein, 1983, 1985b). The nature of the events which triggered the evolution towards a vapor-dominated state, and the role of geochemical and geomechanical processes in this evolution, are highly speculative at the present time. Noting that all known vapor-dominated reservoirs occur in a fractured-porous hydrologic setting, Pruess (1985) suggested that a combination of fracture and matrix permeability is a prerequisite for the evolution of a vapor-dominated state. Using numerical simulation he demonstrated that a limited-discharge event can cause a liquid-dominated system in fractured rock to evolve vapor-dominated conditions with very large liquid saturation (on the order of 90%). White et al. (1971) had suggested that chemical self-sealing would be an important part of the processes leading up to a vapor-dominated system. This suggestion was recently taken up by Ingebritsen (1986), whose simulation studies confirmed that permeability decline with time in recharge zones, such as would be expected from mineral redistribution, can in fact cause vapor-dominated conditions to evolve. A very significant feature of vapor-dominated systems is that the undisturbed temperatures near the top of the reservoir are invariably close to 570°F (240°C). Noting that this temperature is near the point of maximum of saturated steam (450°F; 235°C), James (1968) and others proposed 450°F; 235°C), James (1968) and others proposed a mechanism by which decompression of hotter steam rising from depth would eventually lead to accumulation of steam in maximum enthalpy conditions at the reservoir top. Ingebritsen (1986) noted that his simulations failed to converge toward the temperature of maximum enthalpy steam, even though the relevant thermodynamic features of water and steam were adequately represented in the simulator he was using. He suggested that some alternative mechanism would be needed to explain the observed temperatures. Ingebritsen's findings are

consistent with unpublished work of one of the authors (Pruess). In our simulations we noted that the rate of steam condensation from decompression at conditions above the maximum enthalpy point is negligibly small in comparison to condensation from conductive heat loss to the caprock (Pruess, to be published).

2.5.5. Well Testing

The standard practice at The Geysers is to flow a new well soon after drilling is completed to investigate its flow capability. After the flow period pressure buildup data are collected and used to compute the permeability-thickness product (kh), the skin value of the well and the reservoir pressure. Pressure buildup tests are also performed on selective wells periodically to monitor the pressure decline in the reservoir and to investigate if changes have occurred in the skin factor or the kh product. It is estimated that around 50 pressure buildup tests are conducted annually at The Geysers.

Unfortunately, only few pressure buildup data have been published in the literature. Furthermore, for many of the buildup tests published, the corresponding wells are not identified with their proper names. Thus, from the published data one can at best obtain some representative values on kh and skin for The Geysers field. Pressure buildup data from Geysers wells have been published by Ramey (1970b, 1976), Ramey and Gringarten (1976), Strobel (1976, 1978), Economides and Fehlberg (1979) and Economides et al. (1980).

The pressure buildup tests analyzed by these investigators indicate that many of the tests show wellbore storage effects (unit slope on log-log plots). Some of the buildup test data show fracture effects, illustrated by 1/2 slope on log-log plots (Ramey and Gringarten, 1976; Economides and Fehlberg, 1979). However, the most characteristic feature of pressure buildup tests at The Geysers is the apparent constant pressure conditions close to the wells (Ramey, 1970a; Strobel, 1976; Lipman et al. 1977). The exact cause for this behavior does not appear to be known at present. Possible explanations include strong vertical recharge from depth or pressure stabilization due to boiling in the vicinity of the wells. Some of the pressure buildup tests also exhibit linear flow effects (Economides et al., 1980).

The results of the analysis of available buildup tests indicate that the kh of the reservoir ranges from 6,000 to 100,000 md·ft (2 - 30 Dm). Repeat measurements of kh for a given well give remarkably consistent results (Strobel, 1976). Most of the wells have negative skin, indicating strong fracture effects close to the wellbore. In general, one would not expect positive skin at The Geysers because the wells are drilled with air. Typically the skin values reported in the literature range from -1 to -3. The flow rates reported for the wells range from 100,000 to 200,000 lbs/hr (12 - 24 kg/s).

The major problem with analyzing pressure buildup tests at The Geysers is steam condensation in the wellbore (Strobel, 1976). Condensation effects may mask any portion of the buildup data depending upon the well and formation characteristics. Other problems arise when only wellhead data are measured, as the downhole pressure must be computed for a given datum which is often arbitrarily selected as the mid-point between the first steam entry and the deepest one.

Some interference tests have been conducted at The Geysers as reported by Economides et al. (1980) and Mogen et al. (1985). Perhaps the first "interference test" reported on Geysers wells is that described by Allen and Day (1927). They reported that "notwithstanding that the wells were close together, the pressure of neither seemed to be affected by the discharge of the other. Also, when either well was allowed to discharge continuously for months and then closed again the pressure soon attained the same value as before." This indicates good permeability and strong recharge, which agrees well with the results of Mogen et al. (1985) for interference testing of the Thermal Shallow reservoir. They found permeabilities ranging from 100,000 to 2,000,000 md·ft (30 to 700 Dm) for this shallow anomaly (Figure 2-18); these values are much higher than those obtained for the underlying reservoir (Ramey, 1970a; Mogen et al., 1985). Mogen et al. (1985) also performed analysis of enthalpy and tracer data and developed the conceptual model of the Thermal Shallow reservoir shown in Figure 2-18. The model shows upflow of steam from the main Geysers reservoir and lateral flow from the core of the shallow anomaly to the margins. Between the shallow reservoir and the underlying main reservoir there is a con-

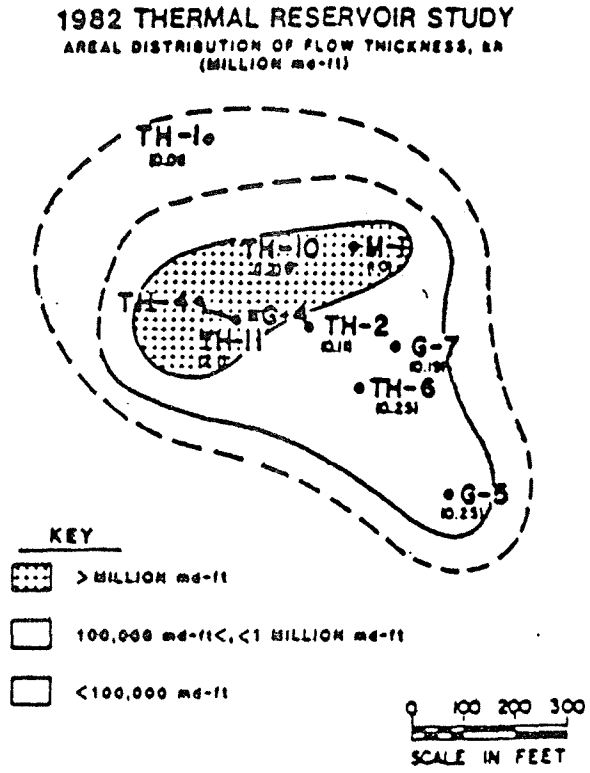

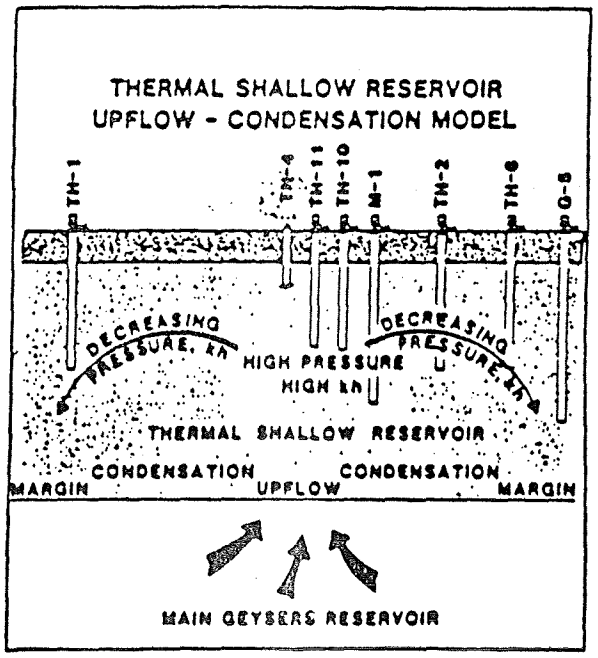

Figure 2-18. The Thermal Shallow reservoir - a conceptual model and the permeability distribution (Mogen et al., 1985).

densation layer, as reported earlier by Ramey (1970a). More detailed discussion of the available well test data from The Geysers is given in Section 8.0.

2.5.6. Production and Pressure Decline

As illustrated in Figure 2-1, it is estimated that over 200 billion lbs (100 billion kg) of steam have been produced at The Geysers since 1968. Although initially it was believed that steam production would remain fairly constant with time and no significant pressure decline would occur at The Geysers, it is now well established that the wells decline in productivity with time and that significant pressure decline has occurred (Ramey, 1970a; Lipman et al., 1977; Dykstra, 1981). The flow rate decline from the wells is offset by infill drilling or expansion of the wellfield feeding a given power plant. Lipman et al. (1977) state that on the average one (1) make-up well per year must be drilled for each 100 MW_e unit.

Well productivity varies greatly from one well to another, which is to be expected given the heterogeneous, fractured nature of the resource. An average well produces some 150,000 lbs/hr (20 kg/s), but the productivity is highly dependent upon the formation permeability and the diameter and overall completion of the well (Budd, 1972; Sutter, 1980). Experience at The Geysers has shown that large-diameter wells are more economical because of the higher flow rates achieved (Drenick, personal communication, 1985). Steam rates in excess of 300,000 lbs/hr (38 kg/s) have been obtained for some of the best producers at The Geysers. Wells at The Geysers show flow rate decline with time, which is caused by pressure decline in the reservoir due to fluid extraction (Budd, 1972). Ramey (1970a) noted that all of the wells available in 1968 showed measureable pressure decline.

The rate of production decline varies greatly between wells and also from region to region within The Geysers area. Budd (1972) published decline curves for various well spacings based upon a theoretical model and estimated that a 50% flow rate decline would occur in 5, 15 and 25 years for well spacings of 5, 20 and 45 acres, respectively (see Figure 2-19). Dykstra (1981) used actual flow histories from 18 wells at The Geysers and concluded that, on the average, a 50% decline in flow rate occurs after about 8 years of production. He also concluded that a

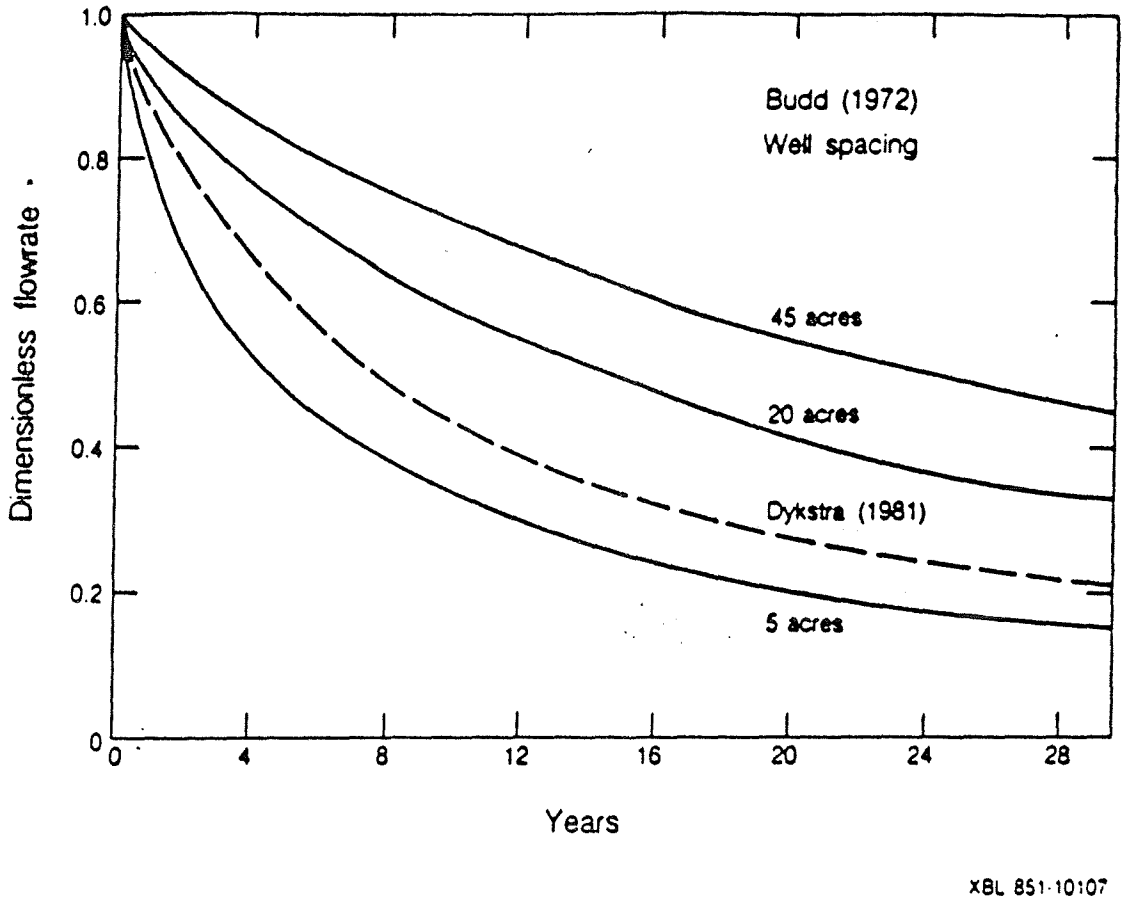

Figure 2-19. Flow rate decline curves for steam wells based on model studies (Budd, 1972) and limited production data (Dykstra, 1981).

harmonic-type model (Fetkovich, 1973) with b = 1 best represented the flow rate decline. However, one must be aware that the wells used by Dykstra (1981) were completed in areas with well spacings varying from 40 acres to about 5 acres.

In addition to well spacing, many other factors affect the flow rate decline. Using a fracture model proposed by Pruess and Narasimhan (1982) that assumes significant fluid reserves in the rock matrix, Bodvarsson and Witherspoon (1985) evaluated the effects of various parameters on the flow rate decline. They concluded that the main parameter controlling the flow rate decline is k_m/D^2, where k_m is the matrix permeability and D is the average fracture spacing. Brigham and Dee (1985), on the other hand, used a model that assumes that the fluid reserves are primarily associated with a deep water table. They found that the long term flow rate decline depends primarily on the flow resistance in the primary pathways from the steam entries to the deep water table, hence, the fracture permeabilities.

Information on the pressure decline at The Geysers is given by Ramey (1970) and Lipman et al. (1979). Ramey (1970a) concluded that the pressures in the Thermal Shallow reservoir had declined from 200 - 270 psi in 1926 to about 130 psi in 1966; during this time an estimated 46.9 billion lbs (22 billion kg) of steam were produced. With further development the pressure decline spread both areally and into the deeper parts of the reservoir. Lipman et al. (1977) published a contour map of the pressure conditions in 1977; this map is reproduced in Figure 3-20. In 1977, Units 1 through 11 were on-line; all of these units are located in the Sulphur Banks area (Units 1 through 6) or in state lease PRC 4596 (Units 7, 8 and 11), with the exception of Units 9 and 10, which are located in state lease PRC 4597, some 2 to 3 mi (3 - 5 km) south of Sulphur Banks. Figure 3-20 shows that in 1977 the pressure had declined by 150 - 200 psi (10 - 13 bars) in those areas where most production had occurred (Sulphur Banks and Happy Jack). The pressure contours as drawn by Lipman et al. (1977) also suggest that the fracture system at The Geysers is interconnected over large areas, as the pressure sinks for the various units seem to grow together. A possible exception is the area to the southwest (Units 9 - 10), but in 1977 these units had only been on production for 3 to 4 years. No information has been published on the

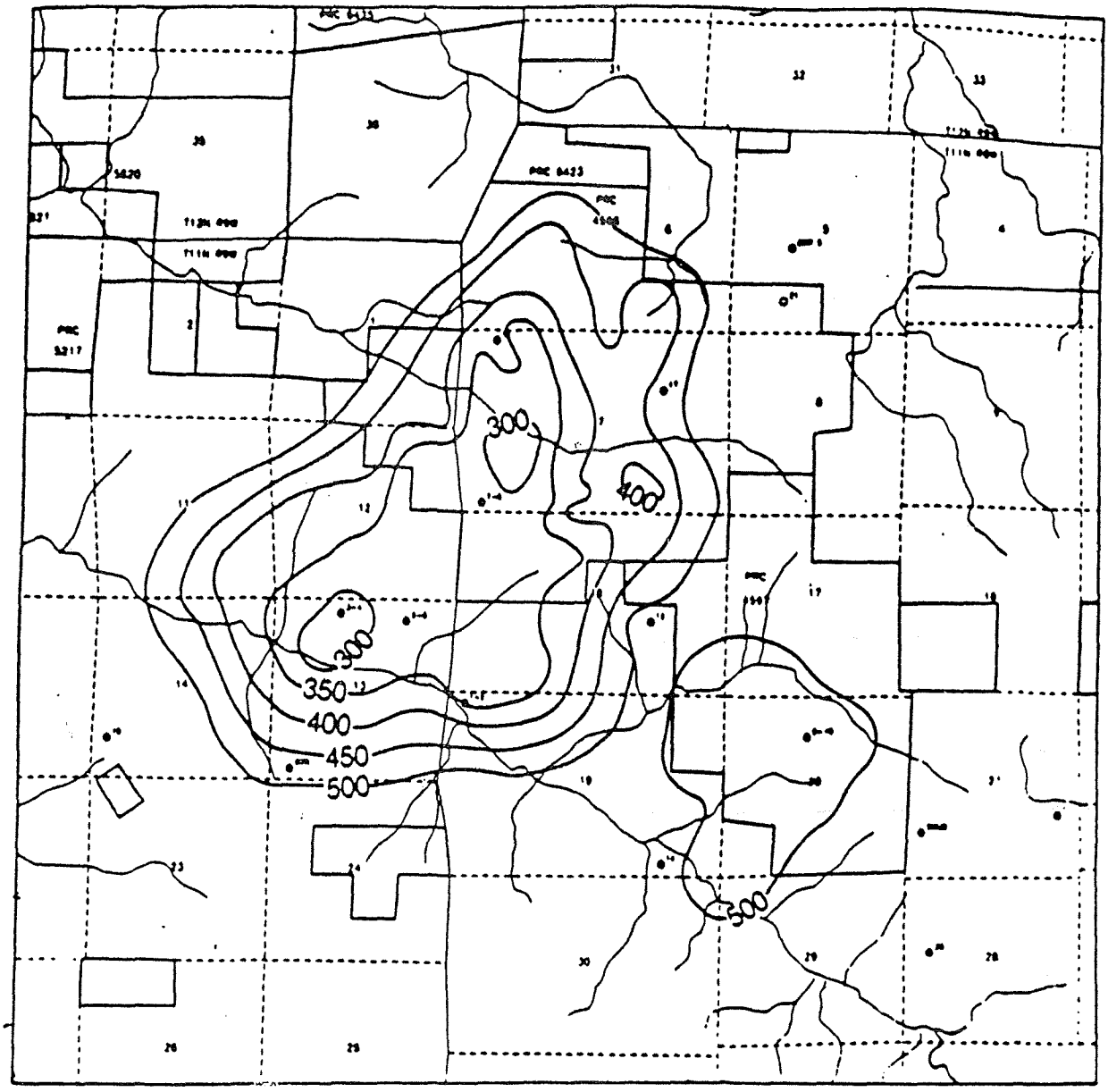

Figure 2.20. Pressure conditions (in psi) in The Geysers reservoir in 1977 (after Lippmann et al., 1977).

pressure decline in the reservoir since 1977.

2.5.7. Reserves

Evaluation of fluid reserves is much more difficult for vapor-dominated systems than for hot water or two-phase liquid-dominated reservoirs. The main problem is in evaluating the distribution and amount of liquid water, as it is well established that most of the steam produced originates as liquid water in the reservoir (D'Amore et al., 1982). It is currently not known whether the bulk of the steam produced comes from boiling of a deep water body or from boiling of liquid reserves originating in the tight matrix blocks.

Reserve estimates for parts of The Geysers reservoir have been made using the so-called P/z method developed for gas reservoirs (Craft and Hawkins, 1959). Ramey (1970a) argued that this method could be applied to vapor-dominated systems, since they must be confined laterally, because of the low reservoir pressures. Bodvarsson and Witherspoon (1985) performed model calculations and found that the P/z method generally gave reserve estimates which were accurate within a factor of two, although the theoretical basis of this method for boiling systems is questionable (Pruess et al. 1979). Ramey (1970a) estimated the steam reserves of the Shallow Thermal reservoir to be 88.1 billion lbs (40 billion kg) using the P/z method; it was later found that most of the steam recharging this reservoir comes from depth (Lipman et al., 1977).

Another approach that has been applied to The Geysers field is reserve estimation by volumetric means. Dykstra (1981) estimated the areal extent of the reservoir by using data on first steam entries. Assuming that the reservoir extended to a depth of 15,000 ft (4570 m) below sea level, he obtained a reservoir volume of 9×10^{12} cubic feet (3×10^{11} m^3). Furthermore, he assumed a reservoir porosity of 8% and initial liquid saturation of 50%, yielding a total heat content of 9×10^{15} Btu (1×10^{18} Joules), and total fluid content of 2×10^{19} lbs (1×10^{19} kg). By assuming heat recovery of 20% the estimated generating capacity is 120,000 MW-years, or 2000 MW_e for 60 years.

2.5.8. Injection

Water injection started in 1969 in the Sulphur Banks area, with Well SB-1 being converted from a producer to an injector (Dykstra, 1981). In the beginning the primary objective of the injection was to dispose of the condensate (Gulati et al., 1978). The injection wells were located far from existing producers and the injection interval was deeper than the producing interval of nearby producers (Chasteen, 1976). With increasing steam production in the early 1970s new injectors were put on-line; in 1975 five wells were used for injection, all of which were drilled as potential producers.

As more experience with injection was gained the beneficial effects became apparent. Gulati et al. (1978) describe a tritium tracer experiment performed in Sulphur Bank 1 in 1975. The results of the experiment showed that at least some of the injected water was vaporized and produced as steam. The tracer test also showed that the injected fluids dispersed widely in the reservoir, as the tritium was produced in 20 different wells. In 1979, Unocal started supplementing the condensate by injecting water from the Big Sulphur Creek. Also, some of the recent injection wells have been drilled near the center of the field in an attempt to reduce the rate of pressure decline (Dykstra, 1981). Figure 2-1 shows that at the end of 1985, about 60 billion lbs (30 billion kg) of water had been injected; this amounts to about 25% of the total steam produced.

In general, the problems encountered with injection have been rather small. The injection wells are generally located at topographic lows to take advantage of gravity drainage (Drenick, 1985). However, there have been problems with injectivity decline of some wells, believed to be due to plugging of fractures with elemental sulphur, which is readily remedied by shutting-in the well and letting it heat up (Chasteen, 1976). In some wells, water breakthrough has been observed, which has been overcome by reducing the injection rate of selected injectors or by deepening the injection interval.

In the future one expects that injection on a much larger scale will be implemented at The Geysers. Experience with injection at the vapor-dominated system at Larderello, Italy has

indicated high return of the vaporized water, with no measurable changes in wellhead temperatures of producing wells (Bertrami et al., 1985). Presently, some field operators at The Geysers are considering bringing in water from other areas to supplement the water already being injected.

2.5.9. Summary

Large amounts of reservoir engineering data have been collected at The Geysers, only a fraction of which is available to the public. Over 500 wells have been drilled at The Geysers, indicating the enormous size of the reservoir. The wells have given information regarding the thermodynamic conditions of the reservoir, the geological characteristics, formation properties and production histories. This has allowed the development of a conceptual model that explains some of the essential heat transfer processes occurring in vapor-dominated systems (White et al., 1971).

However, many questions still remain, especially regarding the amount and distribution of liquid water, the fracture characteristics of the formation and long-term effects of injection. The lack of understanding of the fracture system reduces the success of drilling productive wells, and limits the understanding of steam migration within the reservoir. The importance of injection seems to be recognized and should be investigated thoroughly in the years to come. Other questions that need to be addressed include the prevalence of temperatures of 465°F (240°C) at the top of vapor-dominated systems, and the fluid and heat flow processes at the "deep end" of these systems, where substantially higher temperatures have been encountered.

3.0. THE GEYSERS DATABASE

3.1. GENERAL DESCRIPTION

The Geysers database consists of well locations, elevations, directional surveys, lithologic data, steam entries, production and injection data, pressure and temperature data, and geochemical data. The data come from several sources, but primarily from the California Division of Oil and Gas (DOG), and from the Sacramento office of the California State Lands Commission. The DOG data were sent to us on tape, but most of the State Lands data had to be obtained by visiting the SLC office in Sacramento, and copying most of the files. The database is by no means complete, and efforts are being made to obtain the missing data.

The data are stored in tables within an INGRES database called "GEYSERS." Wells are identified by an American Petroleum Institute (API) number, which is a unique number assigned by DOG, and by a lease name followed by an operator number. The API number is an 8 digit number, containing a county code in the second and third digits (11 = Colusa, 33 = Lake, 45 = Mendocino, 55 = Napa, and 97 = Sonoma). Most of the wells are located in Sonoma County and for these wells the API number starts with 097. The lease name and operator number are not always consistent from the various data sources. In most cases, the lease names have been assigned to match the DOG records.

Table 3-1 lists the tables contained in the database. Data from the tables can be retrieved and manipulated based on ai numbers, well names or data parameters.

3.2. AVAILABLE DATA

3.2.1. Location Data

Location data contained in the Geysers database are from several sources. Because of the different sources, the data are contained in separate tables. The primary source is a tape from

Table 3-1. List of tables contained in the INGRES DBMS for The Geysers

Table Name	Available Data	Data Source	Number of Wells
DOG	Monthly production and pressures	DOG tape (Sacramento)	310
KBLOC	Well locations in California Lambert coordinates; Kelly bushing elevations	Tables UNLOC and GSLOC, with additions from digitized map	491
UNLOC	Well locations in California Lambert coordinates	Unocal tape	340
GSLOC	Well locations in California Lambert coordinates	USGS Open File Report	229
GRC	Well locations in meters from section corners, elevations, completion dates	GRC Special Report	336
DS	Directional surveys	SLC files (Sacramento) DOG files (Santa Rose)	172
DSST	Directional surveys for sidetracks and redrills	SLC files (Sacramento) DOG files (Santa Rosa)	
CASE	Well casing diameters and lengths	SLC files (drilling summaries)	217
ENTRY	Steam entries	SLC files and DOG files	197
LITH	Lithologic summaries	SLC files and DOG files	211
HEATFLO	Temperature data	Dick Thomas	165
SHPRESS	Shut-in pressures	SLC files	63
RIGTEST	Flowing pressures	SLC files	71
GAS	Noncondensible gas to steam ratios	Sonoma County Air Quality District	6 power plants
LEASELIST	Lease names, operator numbers, section, township, range, completion data	From other tables	477
BUILDUP	Pressure buildup data	SLC files, Unocal	22

Unocal, supplied by DOG; the data are contained in the table UNLOC. These are the results of surveys of all of Union's 350 wells as of February 1986. These data are believed to be the most accurate information on the locations for wells at The Geysers. In addition to these location data, we have used well locations from USGS Open File Report 82-410 (Reed, 1982b). This report contains surface locations of 229 wells in The Geysers geothermal field. These are contained in the table GSLOC. Both the Union and USGS well locations are given in feet, referenced to California Lambert coordinates. These two data sources (UNLOC and GSLOC) were combined in a table called COMLOC, which contains best available well locations considering both data sets. Additional well locations were obtained from a map supplied by SLC, which we have digitized. In total we have well locations for 491 wells at The Geysers.

In addition to California Lambert coordinates, we also have well locations from a Geothermal Resources Council Special Report (Reed, 1982a). These locations are given in distance from the section corners, in meters, and are contained in a table called GRC. This table contains locations for 336 wells. Additional data for distance from section corners are contained in well summary reports.

Another helpful table containing locations is called LEASELIST. This table contains, in addition to locations, the lease name, operator number, API number, section, township, range, and completion date for all 491 wells in the database.

3.2.2. Elevation Data

Elevations for the wells, as well as the elevation of the kelly bushing, from which most data is referenced, are given in the GRC report (Reed, 1982b), and have been incorporated into the GRC table. In addition, the kelly bushing elevations, in feet, along with the California Lambert coordinates, are given in the table called KBLOC. These are used for plotting purposes. If the elevation is not known, a value of 1999 appears in the column "kb". This value represents a typical elevation at The Geysers. These will be converted to true elevations as these data become available.

3.2.3. Directional Surveys

Directional Surveys for 172 wells were obtained from SLC files in Sacramento, and from DOG files in Santa Rosa (courtesy of Ken Stelling). The bottomhole locations of these wells are shown in Figure 3-1. Directional surveys are needed to obtain the true path of the well. It is typical at The Geysers for several wells to be drilled from the same drillpad in divergent directions. The final bottomhole locations may be several thousand feet from the surface location. A typical survey contains 40 or 50 survey points, giving the measured depth, the drift and azimuth of the deviation, the coordinates, and the true vertical depth. This information was typed into the database, and checked for accuracy. In some cases only the raw data were given, and the downhole coordinates had to be calculated. This was done with a program written by R. Terrebonne at SLC.

The tables containing the data are called DS and DSST. DS contains the surveys of wells without redrills or sidetracks. DSST contains surveys for wells with redrills and/or sidetracks. The two tables are kept separate for ease in plotting. The column headings in these two tables are lease name (lease), operator number (opern), API number (api), station number (sta), measured depth in feet (mdft), vertical depth in feet (vdft), direction angle (drang), direction bearing (drbng), north coordinate in feet from origin(ccn), east coordinate in feet from origin (cce), year, month, day, weighting factor (wf), and projected azimuth (pro).

3.2.4. Casing Data

Casing data, obtained primarily from well summaries, are included in a table called CASE, which gives the diameter and length of casings in 217 wells. The column headings for this table are lease name (lease), operator number (opern), API number (api), redrill number (rd), sidetrack number (st), top of the casing in feet (topft), bottom of the casing in feet (botft), and diameter of the casing in inches (diamin).

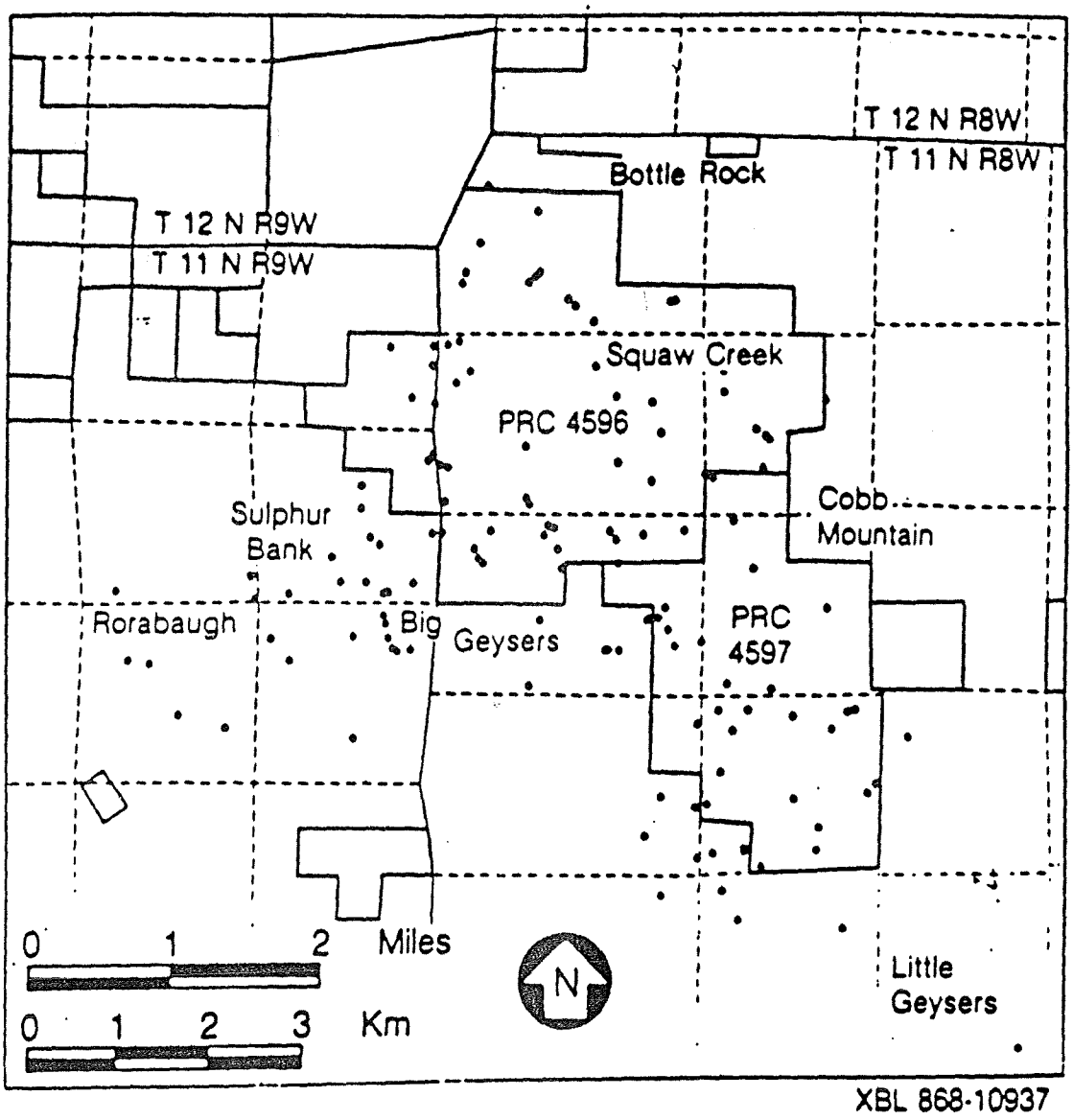

Figure 3-1. Map of The Geysers geothermal field, showing the bottomhole locations for wells in the database. Note that only wells with directional surveys are shown.

3.2.5. Lithologic Data

The lithologic data come from SLC files in Sacramento, and from DOG files in Santa Rosa. At this time we have detailed lithologic logs for over 200 wells; these wells are shown in Figure 3-2. The data were entered into a table called LITH. The column headings for this table are lease name (lease), operator number (opern), API number (api), redrill number (rd), sidetrack number (st), top of unit in feet (top ft), bottom of unit in feet (botft), thickness of unit or interval in feet (thickft), drilled or cored (dc), rock type (rock), and code.

3.2.6. Steam Entries

Steam entries were obtained from SLC files. These data were taken mostly from well histories supplied to SLC by field operators. The records usually consist of a depth, pressure, and occasionally flow rates and temperatures. Some steam entries were obtained from mud logs. The data were entered into a table called ENTRY, and represent 197 wells. These wells are shown in Figure 3-3. Water entries are designated with a W under Type. The column headings are lease name (lease), operator number (oper), API number (api), redrill number (rd), sidetrack number (st), year, month, day, depth in feet (feet), depth in meters (m), type, pressure increase in psi (psig), pressure increase in bars (bar).

3.2.7. Pressure Data

There are 3 tables containing pressure data, in addition to the DOG tape. The table SHPRESS contains shut-in pressures reported in SLC files for 63 wells. This information is more detailed than the shut-in pressure data supplied in the DOG tape. The table RIGTEST contains flowing pressure tests data for 71 wells, obtained from files at the SLC offices in Sacramento. The table BUILDUP contains pressure buildup tests for 322 wells obtained from SLC files and Unocal. The column headings for SHPRESS are lease name (lease), operator number (opern), API number (api), year, month, hours, and pressure (psig). The column headings for RIGTEST are lease name (lease), operator number (opern), API number (api), pressure (psi), depth in feet (depthft), month, day and year. The column headings for BUILDUP are

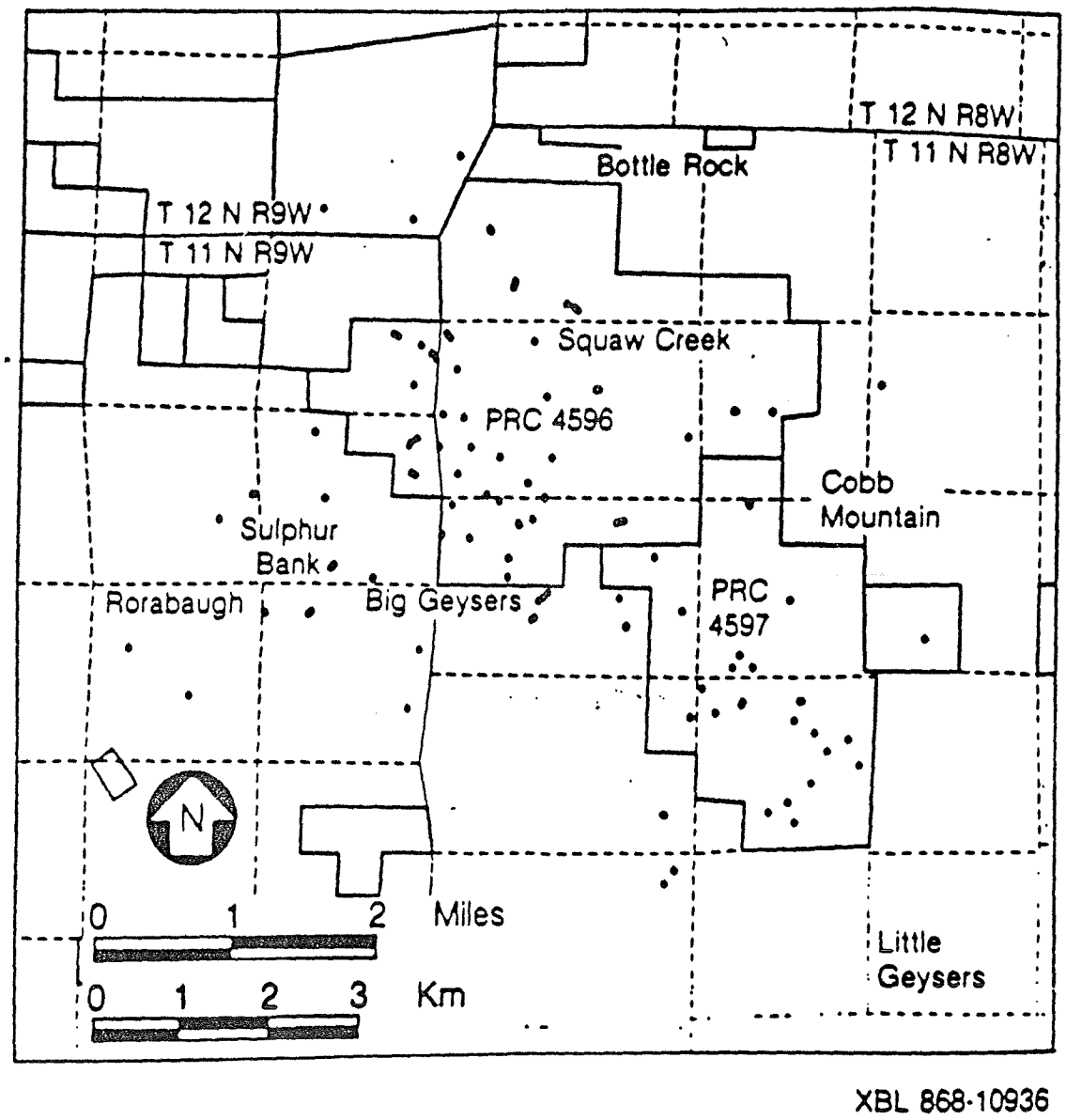

Figure 3-2. Map of The Geysers geothermal field, showing the surface locations of wells with lithologic data.

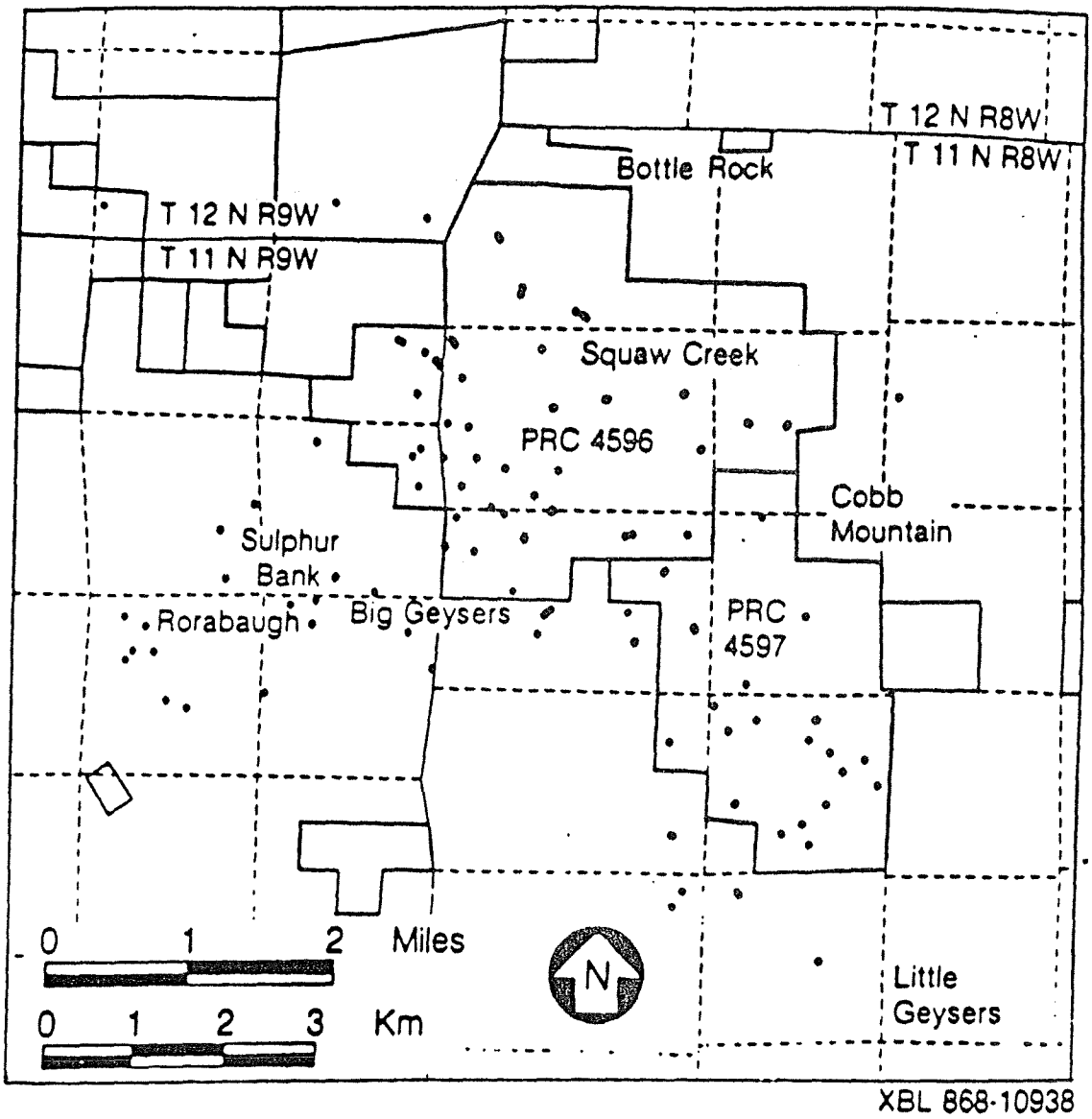

Figure 3.3. Map of The Geysers geothermal field, showing the surface locations of wells with steam entry data.

lease name (lease), operator number (opern), API number (api), seconds (sec), wellhead pressure (psiwh), bottomhole pressure (psib), year, month, and day.

3.2.8. Heat Flow Data

The table HEATFLO contains data from 165 shallow temperature-gradient wells, furnished to LBL by R. P. Thomas. The data include well identification and location information (column headings "well," "opno," "ewlamb," and "nslamb"). The location data were supplied as latitudes and longitudes, in degrees, minutes and seconds, and converted to California Lambert coordinates using conversion coordinates supplied by the USGS.

The table also contains the surface elevations of the wells, both in feet and meters relative to sea level, the total depths of the wells, in feet, and location of interval for which the temperature gradient was measured, in feet. These columns are labeled "elevft," "elevm," "tdft," "topft," and "botft," respectively.

For each well, there is a subjective evaluation, in the form of a "letter grade" (A, B, C, etc.), of the quality of the data for each well. This column is labeled "qual." The time in days between the time the hole was completed and the time the temperature was logged is called "lagdays". The temperature gradient (in °C/km) both corrected and uncorrected for terrain effects are labeled "tgcckm" and "tguckm", respectively.

The type of terrain correction employed is labeled "tercor." In this column, standard Birch terrain correction is indicated by BTC, and values estimated by interpolation, by EST. The thermal conductivity of the surface lithology, based on laboratory measurements on the principal rock types, is also included in watts/meter-K. The latter column is labeled "conwmk".

3.2.9. Geochemical Data

The table GAS contains data on total non-condensible gas content of steam from various geothermal plants in The Geysers field. Data from 6 different plants (Units 3, 11, 12, 14, 17 and 20) were made available by the Sonoma County Air Quality Management District.

Included in the table are the date of the measurement (year, month and day), the plant number, and the gas/steam ratio. The gas contents are expressed in parts per million (ppm) by volume in steam.

The data initially furnished to The Geysers project consisted of several different types of analyses, which included information on the amounts of a number of individual gas species contained in the steam. However, as the analytical techniques were not well-documented, and there was frequent ambiguity as to whether the subspecies were measured as fraction of the steam as opposed to fraction of the total noncondensibles, it was considered inadvisable to tabulate individual gas data at this time. Some data are also available from Rorabaugh 1, 2 and 3 and Prati State 10 and 31. Several different varieties of data on total noncondensibles are included for these wells, including data from tests during drilling and from flow tests performed during production. Some of these data are broken down by individual gases as well.

3.2.10. Production/Injection Data

The production data come primarily from a tape provided by DOG, which represents the monthly production data supplied by the operators. This information includes gross steam and water production, production and injection rates, pressures and temperatures, power plants where steam is delivered and total noncondensibles. DOG sent us a tape of all open file information, as well as all information on SLC leases. A description of the column headings for the table called DOG is shown in Table 3-2. This table is updated about every six months, as LBL receives new tapes from DOG. Data for 310 wells are available in the database. Plots of steam flowrates and cumulative mass flow for every open file well are provided in Appendix A.

4.0. REFERENCES

Allen E. T. and A. L. Day, Steam wells and other thermal activity at "The Geysers", California, Carnegie Inst. Washington Publication, No. 378, pp. 105, 1927.

Allis, R. G., Mechanism of induced seismicity at The Geysers geothermal reservoir, California, *Geophys. Res. Letters*, Vol. 9, No. 6, pp. 629-632, 1982.

Anderson, D. N., B. C. McCabe and Magma Power Company, *Bulletin Geothermal Resources Council*, Vol. 15, No. 6, p. 3-5, 1986.

Arps, J., Analysis of decline curves, *Trans. AIME*, 1945.

Atkinson, P., A. Barelli, W. Brigham, R. Celati, G. Maneth, F. G. Miller, G. Neri, and H. J. Ramey, Jr., Well-testing in Travale-Radicondoli Field, *Geothermics*, Vol. 7, pp. 145-184, Pergamon Press, Ltd., Great Britain, 1978.

Atwater, T., Implications of late tectonics for the Cenozoic tectonic evolution of western North America, *Geological Society of America Bulletin*, Vol. 81, pp. 3513-3536, 1970.

Atwater, T. and P. Molnar, Relative motion of the Pacific and North American plates deduced from sea floor spreading in the Atlantic, Indian, and south Pacific Oceans, in *Proceedings of the Conference on Tectonic Problems of the San Andreas Fault System*, R. L. Kovach and A. Nur (eds.) Stanford University, Publications in the Geological Sciences, Vol. 13, pp. 136-148, 1973.

Bailey, E. H., J. C. Blake, Jr., and D. L. Jones, On-Land Mesozoic oceanic crust in the California Coast Ranges, U. S. Geological Survey *Prof. Paper 700c*, pp. c70-c81, 1970.

Berkland, J. O., L. A. Raymond, J. C. Kramer, E. M. Moores and Michael O'Day, What is Franciscan?, *American Association of Petrol. Geologists Bulletin*,

Bertrami, R., C. Calore, G. Cappetti, R. Celati, and F. D'Amore, A three-year recharge test by reinjection in the central area of Larderello field: Analysis of production data, 1985, International Symposium on Geothermal Energy, *Geothermal Resources Council Transactions*, Vol. 9, pp. 293-298, 1985.

Birch, Francis, Flow of heat in the Front Range, Colorado *Geol. Soc. Amer. Bull.* Vol. 61, pp. 567-630, 1950.

Blake, M. C., Jr. and W. P. Irwin and R. G. Coleman, Upside-down metamorphic zonation, blue schist facies, along a regional thrust in California and Oregon, U. S. Geological Survey *Prof. Paper 575c*, pp. c1-c9, 1967.

Blake, M. C., Jr., D. L. Jones, Allochthonous terranes in northern California --A reinterpretation, in *Mesozoic paleogeography of the western United States:* Society of Economic Paleontologists and Mineralogists, Pacific Section, Pacific Coast Paleogeography Symposium, April 1978, Proceedings, pp. 397-400, 1978.

Bodvarsson, G. S. and P. A. Witherspoon, Flow rate decline of steam wells in fractured geothermal reservoirs, *Proceedings Tenth Workshop on Geothermal Reservoir Engineering,* Stanford University, p. 105, January 22-24, 1985.

Bowman, H. R., F. Asaro and I. Perlman, On uniformity of composition in obsidians, and evidence for magmatic mixing, *Journal Petr.*, Vol. 81, pp. 312-327, 1973.

Brook, C. A., Variability and sources of hydrogen sulfide and other gases in steam at The Geysers, in *Research in The Geysers-Clear Lake area, Northern California,* R. J. McLaughlin and J. M. Donnelly-Nolan (eds.) U. S. Geological Survey *Prof. Paper 1141,* pp. 205-210, 1981.

Budd, C. F., Jr., Producing geothermal steam at The Geysers field, SPE paper 4178, Bakersfield, California, November 8-10, 1972.

Brigham, W. E. and W. B. Morrow, P/z behavior for geothermal steam reservoirs, *Soc. Pet. Engr. Jour.*, Vol. 17, No. 6, pp. 407-412, Dec. 1977.

Bufe, C. G., S. M. Marks, F. W. Lester, R. S. Ludwin and M. C. Stickney, Seismicity of the Geysers-Clear Lake region, in *Research in The Geysers-Clear Lake area, Northern California,* R. J. McLaughlin and J. M. Donnelly-Nolan (eds.) U.S. Geological Survey *Prof. Paper 1141,* pp. 129-138.

Capuano, L. E., Jr., How Geysers steam wells are drilled and equipped, *World Oil,* Vol. 188, No. 2, pp. 69-72, 1979.

Celati, R. P. Squarci, L. Taffi, and G. Stefani, Analysis of water levels and reservoir pressure measurements in geothermal wells, *Proceedings Second United Nations Symposium on the Development and Use of Geothermal Resources,* San Francisco, California, Vol. II, pp. 1883-1590, May 1975.

Chapman, R. H., Gravity map of The Geysers area, California, California Division of Mines and Geology, Mineral Information Service, Vol. 19, pp. 148-149, 1966.

Chapman, R. H., Geophysical study of the Clear Lake region, California, California Division of Mines and Geology, *Special Report 116,* p. 23, 1975.

Chapman, R. H., Gravity anomalies in The Geysers-Clear Lake Area, Northern California, *Field Trip Guidebook 45, Castle Steam Field, Great Valley Sequence,* 53rd Annual Meeting Pacific Section American Association of Petroleum Geologists, Society of Economic Paleontologists and Mineralogists, and Society of Exploration Geophysicists, Sacramento, California, pp. 89-98, April 26-29, 1978.

Chapman, R. H., R. P. Thomas, H. Dykstra, and L. D. Stockton, A reservoir assessment of The Geysers Geothermal Field, California Division of Oil and Gas, *Publication TR 27*, pp. 21-33, 1981.

Chapman, R. G., et al., Bouguer gravity map of California Ukiah Sheet, California Division of Mines and Geology, 1975. Map and 6 p. text, scaler 1:250,000.

Chasteen, A. J., Geothermal condensate steam reinjection, *Proceedings Symposium of the Development and Use of Geothermal Resources*, Vol. 2, pp. 1335-1336, San Francisco, California, 1976.

Craft, B. C. and M. F. Hawkins, *Applied Petroleum Reservoir Engineering*, Prentice Hall, Inc., 1959.

Crowell, J. C., Origin of late Cenozoic basins in southern California, in tectonics and sedimentation, Society of Economic Paleontologists and Mineralogists, *Special Publication 22*, pp. 190-203, 1974.

D'Amore, F. and A. H. Truesdell, Models for steam chemistry at Larderello and The Geysers, *Proceedings Fifth Workshop Geothermal Reservoir Engineering*, Stanford University, pp. 283-297, December 11-14, 1979.

D'Amore, F. and A. H. Truesdell, Gas geothermometry for drill hole fluids from vapor-dominated and hot-water geothermal fields, *Proceedings Sixth Workshop on Geothermal Reservoir Engineering*, Stanford University, Stanford Report SGP-TR-50, pp. 351-360, 1980.

D'Amore F. and A. H. Truesdell, Calculation of geothermal reservoir temperatures and steam fraction from gas compositions, 1985 International Symposium on Geothermal Energy, *Geothermal Resources Council Transactions*, Vol. 9, No. 1, pp. 305-310, 1985.

D'Amore, F. and R. Celati, Methodology for calculating steam quality in geothermal reservoirs: *Geothermics*, Vol. 12, No. 2-3, pp. 129-140, 1983.

D'Amore, F., R. Celati, C. Calore, Fluid geochemistry applications in reservoir engineering (vapor-dominated systems), *Proceedings Eighth Workshop on Geothermal Reservoir Engineering*, Stanford University, pp. 295-308, December 14-16, 1982.

Dee, J. F. and W. E. Brigham, A reservoir engineering analysis of a vapor-dominated geothermal field, *Geothermal Resources Council Transactions*, Vol. 9, No. 2, pp. 299-306, August 1985.

Denlinger, R. P., Geophysics of The Geysers Geothermal field, Northern California: Ph.D. thesis, Stanford University, Stanford, California, 87 pp., 1979.

Denlinger, R. P. and R. L. Kovach, Seismic-reflection investigations at Castle Rock Springs in The Geysers Geothermal area, Northern California, U. S. Geological Survey *Prof. Paper 1141*, pp. 117-128, 1981.

Denlinger, R. P., and Kovach, R. L., Three-dimensional gravity modeling of the Geysers hydrothermal system and vicinity, northern California: *Geol. Soc. Am. Bull.*, Part 1, Vol. 92, pp. 404-410, 1984.

Dickinson, W. R., Clastic sedimentary sequences deposited in shelf, slope, and trough settings between magmatic area and associated trenches, *Pacific Geology*, Vol. 3, pp. 15-30, 1970.

Di Pippo, R., Geothermal electric power, the state of the world, 1985, International Symposium on Geothermal Energy, *Geothermal Resources Council Transactions, International Vol.*, pp. 3-18, 1985.

Donnelly, M. J., B. C. Hearn, Jr. and F. E. Goff, The Clear Lakes Volcanics, California: Geology and field trip guide, in *Field Trip Guide to The Geysers-Clear Lake Area*, Geological Society of America, Cordilleron Section, pp. 25-56, April 1977.

Donnelly, J. M., R. J. McLaughlin, R. E. Goff, and B. C. Hearn, Jr., Active faulting in The Geysers-Clear Lake area, Northern California, *Geological Society of America Abstracts with Programs*, Vol. 8, pp. 369-370, 1976.

Donnelly-Nolan, J. M., B. C. Hearn, Jr., G. H. Curtis, and R. E. Drake, Geochronology and evolution of the Clear Lake Volcanics, in *Research in The Geysers-Clear Lake area, Northern California*, R. J. McLaughlin and J. M. Donnelly-Nolan (eds.) U. S. Geological Survey *Prof. Paper 1141*, pp. 47-60, 1981.

Drenick, A., Reservoir development strategy for vapor-dominated geothermal resources, lecture notes prepared for Geothermal Resources Council, 1985.

Drenick, A., Pressure-temperature-spinner surveys in wells at The Geysers, *Proceedings Eleventh Workshop on Geothermal Reservoir Engineering*, Stanford University, in press, 1986.

Dykstra, H., Production history of The Geysers steam field, *Proceedings Sixth Workshop on Geothermal Reservoir Engineering*, Stanford University, pp. 13-20, 1980.

Dykstra, H., Reservoir assessment, in *A Reservoir Assessment of The Geysers Geothermal Field*, A. D. Stockton, Principal Investigator, California Div. Oil and Gas., Sacramento, California, 1981.

Earlougher, R. C., Jr., Advances in well test analysis, *Society of Petroleum Engineers of AIME*, New York, 1977.

Eastman, G. Y., The heat pipe, *Scientific American*, Vol. 218, No. 5, pp. 38-46, May 1968.

Eberhart-Phillips, D., Three-dimensional velocity structure in northern California Coast Ranges from inversion of local earthquakes, *Bull. Seism. Soc. Am.*, in press, 1986.

Eberhart-Phillips, D. and D. H. Oppenheimer, Induced seismicity in The Geysers geothermal area, California, *Journal of Geophysical Research*, Vol. 89, No. B2, pp. 1191-1207, 1984.

Economides, M. J., Shut-in and flowing bottomhole pressure calculations for geothermal steam wells, *Proceedings Fifth Geothermal Reservoir Engineering Workshop*, Stanford University, pp. 139-151, 1979.

Economides, M. J. and E. L. Fehlberg, Two short-time buildup test analyses for Shell's Geysers Well D-6, a year apart, *Proceedings Fifth Workshop Geothermal Reservoir Engineering*, Stanford University, 1979.

Economides, M. J., D. O. Ogbe, F. G. Miller and H. J. Ramey, Geothermal steam well testing: State-of-the-art, paper SPE 9272 presented at the 55th Annual Meeting of Society of Petroleum Engineers, Dallas, Texas, Sept 21-24, 1980.

Elder, J. W., Physical processes in geothermal area, American Geophysical Union, *Geophys.*, Vol. 8, University of California, San Diego, 1965.

Evitt, W. R. and S. T. Pierce, Early Tertiary ages from the coastal belt of the Franciscan complex, northern California, *Geology*, pp. 437-436, August 1975.

Facca, G., The structure and behavior of geothermal fields, in UNESCO (ed.), *Geothermal Energy*, pp. 61-69, 1973.

Facca, G., and F. Tonani, Theory and technology of a geothermal field, *Bull. Volcan.*, Vol. 27, pp. 143-189, 1964.

Fetkovich, M. J., Decline curve analysis using type curves, *J. of Pet. Tech.*, pp. 1065-1077, June 1980

Fuller, P. D. and M. Ripperda, User's guide to the program GRAPH, in preparation, 1986.

Fuller, P. D. and M. Ripperda, User's Guide to the programs GRID and CON1D, in preparation, 1986.

Fuller, P. D., D. Nguyen, and B. L. Cox, User's guide to the program PLOT, in preparation, 1986.

Futa, K., C. E. Hedge, B. C. Heam, Jr., and J. M. Donnelly-Nolan, Strontium isotopes in the Clear Lake Volcanics, in *Research in The Geysers-Clear Lake area, Northern California*, R. J. McLaughlin and J. M. Donnelly-Nolan (eds.) U. S. Geological Survey *Prof. Paper 1141*, pp. 193-204, 1981.

Garcia-Rivera, J., and R. Raghaven, Analysis of short-time pressure data dominated by wellbore storage and skin, Pressure transient testing methods, Society of Petroleum Engineers, *SPE reprint Report*, No. 14, pp. 106-114, 1980.

Garrison, L. E., Geothermal steam in The Geysers-Clear Lake Region, California, *Geological Society of America Bulletin*, Vol. 83, pp. 1449-1468, 1972.

Gentry, R. and A. McCray, The effect of reservoir and fluid properties on production decline curves, *J. of Pet. Tech.*, Sept. 1978.

Giggenbach, W. F., Geothermal gas equilibria, *Geochimica et Cosmochimica Acta*, Vol. 44, pp. 2021-2032, 1980.

Goff, F. E., J. M. Donnelly, J. M. Thompson, and B. C. Hearn, Jr., Geothermal prospecting in The Geysers-Clear Lake area, Northern California, *Geology*, Vol. 5, pp. 509-515, 1977.

Goldstein, N. E. and S. Flexser, Melt zones beneath five volcanic complexes in California: An assessment of shallow magma occurrences, Lawrence Berkeley Laboratory Report 18232, 134 pp., 1984.

Grant, M. A., Water content of the Kawah Kamojang Geothermal Reservoir, *Geothermics*, Vol. 8, pp. 21-30, 1979.

Gulati, M. S., S. C. Lipman and C. J. Strobel, Tritium tracer test at The Geysers, *Geothermal Resources Council Transactions*, Vol. 2, pp. 237-239, July 1978.

Haizlip, M. R., Stable, isotopic composition of steam from wells in the Northwest Geysers, The Geysers, Sonoma County, *Geothermal Resources Council Transactions*, Vol. 9, No. 1, August 1985.

Hamilton, R. M., and L. M. P. Muffler, Microearthquakes at The Geysers Geothermal area, California, *Journal of Geophysical Research*, Vol. 77, No. 11, pp. 2081-2086, 1972.

Hearn, B. C., Jr., J. M. Donnelly-Nolan and F. E. Goff, The Clear Lake volcanics: tectonic setting and magma sources in The Geysers-Clear Lake area, Northern California, U. S. Geological Survey *Prof. Paper 1141*, pp. 25-45, 1981.

Hebein, J. J., Exploration, drilling and development operations in the Bottle Rock area of The Geysers steam field with new geologic insights and models defining reservoir parameters, *Proceedings Ninth Workshop Geothermal Reservoir Engineering*, Stanford University, SGP-TR-74, pp. 135-144, December 1983.

Hebein, J. J., Discussions on a type of reservoir cell boundary in The Geysers steam field, *Proceedings Tenth Workshop Geothermal Reservoir Engineering*, Stanford University, SGP-TR-84, pp. 89-96, 1985a.

Hebein, J. J., Historical hydrothermal evolutionary facets revealed within the exploited Geysers steam field, *Geothermal Resources Council Bulletin*, Vol. 14, No. 6, pp. 13-16, June 1985b.

Hebein, J. J., Conceptual schematic geologic cross-sections of The Geysers steam field, *Proceedings Eleventh Workshop Geothermal Reservoir Engineering*, Stanford University, in press, 1986.

Herd, D. G., Neotectonic framework of Coastal California and its implications to microzonation of the San Francisco Bay region, in *Progress on Seismic Zonation in the San Francisco Bay Region*, E. E. Brabb (ed.), U. S. Geological Survey *Circular 807*, pp. 3-10, 1979.

Ingebritsen, S. E., The evolution and natural state of large-scale vapor-dominated zones, paper presented at Eleventh Workshop on Geothermal Reservoir Engineering, Stanford University, Stanford, California, 1986.

Isherwood, W. F., Gravity and magnetic studies of The Geysers-Clear Lake geothermal region, California, U. S. Geological Survey *Open-File Report 75-368*, 37 pp., 1975.

Isherwood, W. F., Complete Bouguer gravity map of The Geysers area, California, U. S. Geological Survey *Open File Report 76-357*, 1976a. Scale 1:62,500.

Isherwood, W. F., Residual gravity map of The Geysers area, California, U. S. Geological Survey *Open-File Report 76-356*, 1976b.

Isherwood, W. F., Gravity and magnetic studies of The Geysers-Clear Lake Geothermal Region, California, USA, in *Proceedings Second U. N. Symposium on the Development and Use of Geothermal Resources*, Vol. 2, pp. 1065-1073, San Francisco, 1976c.

Isherwood, W. F., Reservoir depletion at The Geysers, California, *Geothermal Resources Council Transactions*, Vol. 1, p. 149, 1977.

Iyer, H. M., D. H. Oppenheimer and Tim Hitchcock, Abnormal P-wave delays in The Geysers-Clear Lake geothermal area, *Science*, Vol. 204, pp. 495-497, 1979.

Iyer, H. M., D. H. Oppenheimer, T. Hitchcock, J. N. Roloff and J. M. Coakley, Large teleseismic P-wave delays in the Geysers-Clear Lake geothermal area, in *Research in The Geysers-Clear Lake Area, Northern California*, R. J. McLaughlin and J. M. Donnelly-Nolan (eds.) U. S. Geological Survey *Prof. Paper 1141*, pp. 97-116, 1981.

James, R., Wairakei and Lardarello geothermal power systems compared, *New Zealand Journal of Science and Technology*, II, pp. 706-719, 1968.

Jamieson, I. M., Heat flow in a geothermally active area: The Geysers, California, Ph.D. Thesis, University of California, Riverside, California, 143 pp., 1976.

Jones, D. L. M. C. Blake, Jr., E. H. Bailey and R. J. McLaughlin, Distribution and character of upper Mesozoic subduction complexes along the west coast of North America, *Tectonophysics*, Vol. 47, pp. 207-222, 1978.

Keller, G. V. and J. J. Jacobson, Deep electromagnetic soundings northeast of The Geysers steam field, *Geothermal Resources Council Transactions*, Vol. 7, pp. 497-603, 1983.

Keller, G. V., J. I. Pritchard, J. J. Jacobson, and N. Harthill, Megasource time-domain electromagnetic sounding methods: *Geophysics*, Vol. 49, pp. 993-1009. U. S. Geol. Survey *Open-File Report 76-700D*, 3 pp., 1984.

Lange, A. L., and W. H. Westphal, Microearthquakes near The Geysers, Sonoma County, California, *Journal of Geophysical Research*, Vol. 74, No. 17, pp. 4377-4378, 1969.

Lipman, S. C., C. J. Strobel and M. S. Gulati, Reservoir performance of The Geysers field, in *Proceedings of the Larderello Workshop on Geothermal Resource Assessment and Reservoir Engineering, Geothermics*, Vol. 7, pp. 209-219, 1977.

Lofgren, B. E., Monitoring crustal deformation in The Geysers-Clear Lake region, U. S. Geological Survey *Prof. Paper 1141*, pp. 139-148, 1981.

Long C. L. and R. M. Senterfit, Audio-magnetotelluric station location map, The Geysers-Calistoga known geothermal resource area, California, U. S. Geological Survey *Open-File Report 76-700D*, 3 pp. 1976.

Majer, E. L. and T. V. McEvilly, Seismological investigations at The Geysers geothermal field, *Geophysics*, Vol. 44, No. 2, pp. 246-269, 1979.

Mankinen, E. A., Paleomagnetism and potassium-argon ages of the Sonoma Volcanics, California, *Geological Society of America Bulletin*, Vol. 83, pp. 2063-2072, 1972.

Marks, S. M., R. S. Ludwin, K. B. Louie, and C. G. Bufe, Seismic monitoring The Geysers Geothermal field, California, U. S. Geological Survey *Open-file Report 78-798*, 26 pp., 1978.

Matthews, C. S. and D. G. Russell, Pressure buildup and flow tests in wells, *Soc. Petroleum Engineering of AIME*, Vol. 1, Dallas, Texas, 1967.

McLaughlin, R. J., Late Mesozoic-Quaternary plate tectonics and The Geysers-Clear Lake geothermal anomaly, northern Coast Ranges, California, *Geological Society of America Abstracts with Programs*, Vol. 9, No. 4, pp. 464, 1977a.

McLaughlin, R. J., The Franciscan assemblage and Great Valley sequence in The Geysers-Clear Lake region of northern California, Geological Society of America, Cordilleran Section, Field trip guide, pp. 3-24, April 1977b.

McLaughlin, R. J., Preliminary geologic map and structural sections of the central Mayacamas Mountains and The Geysers steam field, Sonoma, Lake and Mendocino Counties, U. S. Geological Survey *Open-File Report No. 78-389*, 1978.

McLaughlin, R. J., Tectonic setting of pre-Tertiary rocks and its relation to geothermal resources in The Geysers-Clear Lake Area, in *Research in The Geysers-Clear Lake Area, Northern California*, R. J. McLaughlin and J. M. Donnelly-Nolan (eds.) U. S. Geological Survey *Prof. Paper 1141*, pp. 3-23, 1981.

McLaughlin, R. J., and J. M. Donnelly-Nolan, eds., *Research in The Geysers-Clear Lake Geothermal Area, Northern California*, U. S. Geol. Survey *Prof. Paper 1141*, 259 pp., 1981.

McLaughlin, R. J., D. E. Moore, D. H. Sorg and E. H. McKee, Multiple episodes of hydrothermal circulation, thermal metamorphism and magma injection beneath The Geysers steam field, California (abstr.), *Geological Society America Abstracts and Programs*, Vol. 15, p. 417, 1983.

McLaughlin, R. J. and C. A. Pessagno, Significance of age relations above and below Upper Jurassic ophiolite in The Geysers-Clear Lake region, California, *U. S. Geological Survey Journal of Research*, Vol. 6, pp. 715-726, 1978.

McLaughlin, R. J. and W. D. Stanley, Pre-Tertiary geology and structural control of geothermal resources, The Geysers steam field, California, *Proceedings Second U. N. Symposium on the Development and Use of Geothermal Resources*, Vol. 1, pp. 475-485, San Francisco, California, 1976.

Moench, A. F. and W. N. Herkelrath, The effect of vapor pressure lowering upon pressure drawdown and buildup in geothermal steam wells, *Geothermal Resources Council, Transactions*, Vol. 2, pp. 465-468, July 1978.

Moench, A. F. and G. Neri, Analysis of Gabbro 1 steam pressure buildup test, *Proceedings Fifth Workshop Geothermal Reservoir Engineering*, Stanford University, pp. 99-104, 1979.

Mogen, P. and J. Maney, The thermal 15 relief well and production performance of the Thermal Shallow Reservoir, *Proceedings 10th Geothermal Reservoir Engineering Workshop*, Stanford University, pp. 141-144, 1985.

Mogen, P., L. Pittinger, and M. Magers, Thermal Shallow Reservoir testing, *Proceedings Tenth Workshop Reservoir Engineering*, Stanford University, pp. 133-140, 1985.

Moore, D., Hydrothermal alteration minerals at The Geysers steam field, California, and their potential use in exploration, *Proceedings Sixth Workshop on Geothermal Reservoir Engineering*, Stanford University, Report SGP-TR-50, pp. 361-366, 1980.

Nathenson, M., Some reservoir engineering calculations for the vapor-dominated system at Larderello, Italy, U.S. Geological Survey, *Open File Report 75-142*, April 1975.

Nehring, N. L., Gases from springs and wells in the Geysers-Clear Lake area, in *Research in The Geysers-Clear Lake Area, Northern California*, R. J. McLaughlin and J. M. Donnelly-Nolan (eds.) U. S. Geological Survey *Prof. Paper 1141*, pp. 193-204, 1981.

O'Connell, D.R., Seismic velocity structure and microearthquake source properties at The Geysers, California geothermal area, Ph.D. thesis, Dept. of Geology and Geophysics, University of California, Berkeley, Lawrence Berkeley Laboratory Report LBL-22280, 204 pp., 1986.

Olson, J. J. and R. J. Warburton, Continuous gravity observations at The Geysers, *Geothermal Resources Council Transactions*, Vol. 3, pp. 519-522, 1979. A preliminary report.

Oppenheimer, D., Induced seismicity mechanism at The Geysers, California, *Geothermal Resources Council Transactions*, Vol. 9, No. 2, August 1985.

Oppenheimeer, D. H., Extensional tectonics at The Geysers geothermal area: *Journal Geophysical Research*, Vol. 91, pp. 11463-11476, 1986.

Pilger, R. H., Jr. and T. L. Henyey, Pacific-North American plate interaction and Neogene volcanism in coastal California, *Tectonophysics*, Vol. 57, pp. 189-209, 1979.

Pruess, K., A quantitative model of vapor-dominated geothermal reservoirs as heat pipes in fractured porous rock, *Geothermal Resources Council Transactions*, Vol. 9, Part II, pp. 353-361, 1985.

Pruess, K., and T. N. Narasimhan, On fluid reserves and the production of superheated steam from fractured, vapor-dominated geothermal reservoirs, *Journal of Geophysical Research*, Vol., 87, No. B11, pp. 9329-9339, 1982.

Pruess, K., J. M. Zerzan, R. C. Schroeder, and P. A. Witherspoon, Description of the three-dimensional two-phase simulator SHAFT78 for use in geothermal reservoir studies, *Soc. Petr. Eng. AIME, Fifth Symposium Reservoir Simulation*, SPE-7699, 1979.

Raasch, G., Development of Thermal Shallow Reservoir, *Proceedings Tenth Workshop Geothermal Reservoir Engineering*, Stanford University, pp. 129-132, 1985.

Ramey, H. J., Jr., A reservoir engineering study of The Geysers geothermal field, Reich and Reich, Petitioners, vs. Commissioner of Internal Review, 1969 Tax Court of the United States, 52, T.C. No. 74, 1970.

Ramey, H. J., Jr., Short-time well test data interpretation in the presence of skin effect and wellbore storage, *Journal Pet. Tech.*, Vol. 22, pp. 97-104, 1970b.

Ramey, H. J., Jr., Pressure transient analysis for geothermal wells, *Proceedings Second U. N. Symposium on the Development and Utilization of Geothermal Resources*, Vol. 3, pp. 1749-1757, San Francisco, 1976.

Ramey, H. J., Jr. and A. C. Gringarten, Effect of high volume vertical fracture on geothermal steam well behavior, *Proceedings Second U. N. Symposium on the Development and Use of Geothermal Resources*, Vol. 3, pp. 1759-1762, San Francisco, 1976.

Ramsay, H. J., Jr. and E. T. Guerrero, The ability of rate-time decline curves to predict production rates, *J. of Pet. Tech.*, pp. 139-141, February 1969.

Reed, M. J., Data for geothermal well in The Geysers-Clear Lake area of California as November 1980, Special Report 11, Geothermal Resources Council, Davis, California, 1982a.

Reed, W. J., Latitude, longitude and California Lambert coordinates for 229 well in The Geysers team field, California, U.S. Geological Survey Open File Report 82-410, 10 pp. 1982b.

Rossow, J., J. K. Applegate, and G. V. Keller, An attempt to measure Poisson's ratio in the subsurface in The Geysers-Clear Lake geothermal areas of California: Expanded Abstracts of the Technical Program, Soc. Expl. Geophysicists, 53rd Annual International Meeting and Exposition, Las Vegas, Nevada, pp. 143-144, 1983.

Schriener, A., Jr. and G. A. Suemnich, Subsurface intrusive rocks at The Geysers Geothermal area, California, *Geological Society of America, Abstracts with Programs*, Vol. 12, No. 3, pp. 152, 1980.

Schubert, G. and J. M. Straus, Gravitational stability of water over steam in vapor-dominated geothermal systems, *Journal of Geophysical Research*, Vol. 85, pp. 6505-6512, 1980.

Stanley, W. D., D. B. Jackson and B. C. Hearn, Jr., Preliminary results of geoelectrical investigations near Clear Lake, California, U. S. Geological Survey *Open-File Report*, 20 pp., 1973.

Steiner, A., Occurrence of wairakeite at The Geysers, California, *American Mineralogist*, Vol. 43, pp. 781, 1958.

Sternfeld, J. N., The hydrothermal petrology and stable isotope geochemistry of two wells in The Geysers geothermal field, Sonoma county, California, University of California, Riverside Report UCR/IGPP 81/7, M. S. thesis, 202 pp., 1981.

Sternfeld, J. N., and W. A. Elders, Mineral zonation and stable isotope geochemistry of a production well in The Geysers geothermal field, California, *Geothermal Resources Council Transactions*, Vol. 6, pp. 51-54, October 1982.

Sternfeld, J., M. Keskinen and R. Blethen, Hydrothermal mineralization of a Clear Lake geothermal well, Lake County, California, *Geothermal Resources Council Transactions*, Vol. 7, pp. 193-197, 1983.

Straus, J. M., and G. Schubert, One-dimensional model of vapor-dominated geothermal systems, *Journal of Geophysical Research*, Vol. 86, No. B10, pp. 9433-9438, October 1981.

Strobel, C. J., Field case studies of pressure buildup behavior in Geysers steam wells, *Proceedings Second Workshop Geothermal Reservoir Engineering*, Stanford University, pp. 143-149, 1976.

Strobel, C. J., Formation plugging while testing a steam well at The Geysers, *Proceedings Fourth Geothermal Reservoir Engineering Workshop*, Stanford University, pp. 106-111, 1978.

Sutter, V. E., The application of petroleum engineering to geothermal development, *J. Geothermal Energy*, pp. 5-12, 1980.

Sylvester, A. G., ed., Wrench fault tectonics, American Association Petroleum Geologists Reprint Series, No. 28, Tulsa, Oklahoma, 374 pp., 1984.

Theis, C. V., The relationship between the lowering of piezometric surface and the rate and duration of discharge using groundwater storage, *Transactions American Geophysical Union*, Vol. 2, pp. 519-525, 1935.

Thomas, R. P., Subsurface geology, in *A Reservoir Assessment of The Geysers Geothermal Field*, Principal Investigator D. Stockton, California Division Oil and Gas, publication TR27, pp. 9-20, 1981.

Thomas, R. P., Summary of a heat flow mapping project at The Geysers geothermal field, California, *Geothermal Resources Council Transactions*, Vol. 9, Part 2, pp. 65-70, 1985.

Toksöz, M.N., C. H. Cheng, and A. Timur, Velocities of seismic waves in porous rocks: *Geophysics*, Vol. 41, pp. 621-645, 1976.

Truesdell, A. H. and A. H. Hulston, Isotopic evidence on environments of geothermal systems, in Fritz, P. and J. Fontes, eds., *Handbook of Environmental Isotope Geochemistry*, New York, Elsevier, pp. 179-226, 1980.

Truesdell, H. and D. White, Production of superheated steam from vapor dominated geothermal reservoirs, *Geothermics*, Vol. 2, pp. 159-173, 1973.

U. S. Geological Survey, Aeromagnetic map of the Clear Lake area, Lake, Sonoma, Napa and Mendocino Counties, California, U. S. Geological Survey *Open-File Report 73-299*, 1973, scale 1:62,500.

Urban, T. C., W. H. Diment, J. H. Sass, and I. M. Jamieson, Heat flow at The Geysers, California, *Proceedings Second U. N. Symposium on the Development and Use of Geothermal Resources*, Vol. 2, pp. 1241-1245, San Francisco, 1976.

Vantine, J. V., Hydrogeology of the Thermal landslide, *Proceedings Tenth Workshop Geothermal Research Engineering*, Stanford University, SGP-TR-84, pp. 123-128, 1985.

Wattenbarger, R. A. and H. J. Ramey, Jr., Gas well testing with turbulence, damage and wellbore storage, Pressure Transient Testing Methods, SPE Reprint Series No. 14, Society of Petroleum Engineers, pp. 322-332, 1980.

Weres, O., K. Tsao and B. Wood, Resource technology and environment at The Geysers, Lawrence Berkeley Laboratory, Report LBL-5231, 150 pp, 1977.

White, D. E., L. J. P. Muffler and A. H. Truesdell, Vapor-dominated hydrothermal systems compared with hot water systems, *Economic Geology*, Vol. 66, No. 1, pp. 75-97, 1971.

Wilcox, R. E., T. P. Harding and D. R. Seely, Basic wrench tectonics, *American Association of Petroleum Geologists Bulletin*, Vol. 57, pp. 74-96, 1973.

Young, C. -Y. and Ward, R. W., Attenuation of teleseismic P-waves in The Geysers-Clear Lake region, U. S. Geol. Survey *Prof. Paper 1141*, pp. 149-160, 1981.

Zais, E. J. and G. Bodvarsson, Analysis of production decline in geothermal reservoirs, *Geothermal Reservoir Engineering Management #4503010*, Sept. 1980.

LAWRENCE BERKELEY LABORATORY
UNIVERSITY OF CALIFORNIA
EARTH SCIENCES DIVISION

A DATABASE FOR THE GEYSERS GEOTHERMAL FIELD
VOLUME II
Appendix A: Steam Flowrates and Cumulative Mass Flows

G. S. Bodvarsson, B. L. Cox, P. Fuller, M. Ripperda
H. Tulinius, P. A. Witherspoon, N. Goldstein,
S. Flexser, K. Pruess, and A. Truesdell

28618 2/3

A DATABASE FOR THE GEYSERS GEOTHERMAL FIELD

Volume II

Appendix A: Steam Flowrates and Cumulative Mass Flows

Gudmundur S. Bodvarsson, B. Lea Cox, Peter Fuller, Mark Ripperda,
Helga Tulinius, Paul A. Witherspoon, Norman Goldstein,
Steve Flexser, Karsten Pruess and Alfred Truesdell*

Earth Sciences Division
Lawrence Berkeley Laboratory
University of California
Berkeley, California 94720

*U. S. Geological Survey
345 Middlefield Road
Menlo Park, California 94025

September 1989

This work was supported by the California State Lands Commission and by the U.S. Department of Energy under Contract No. DE-AC03-76SF00098.

APPENDIX A

Steam Flowrates and Cumulative Mass Flows

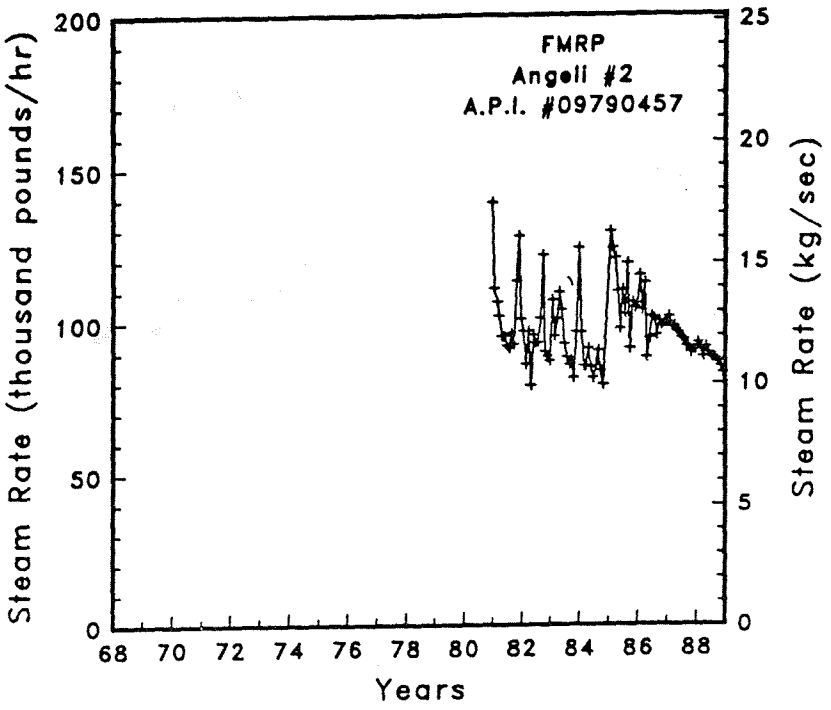

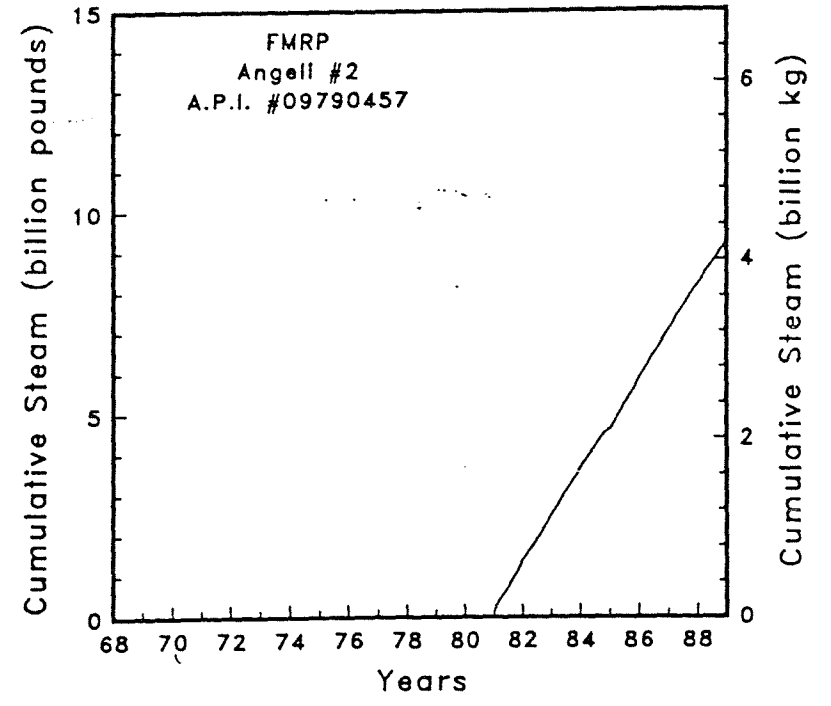

Figure A-2 Steam rate and cumulative mass flow for well Angeli #2

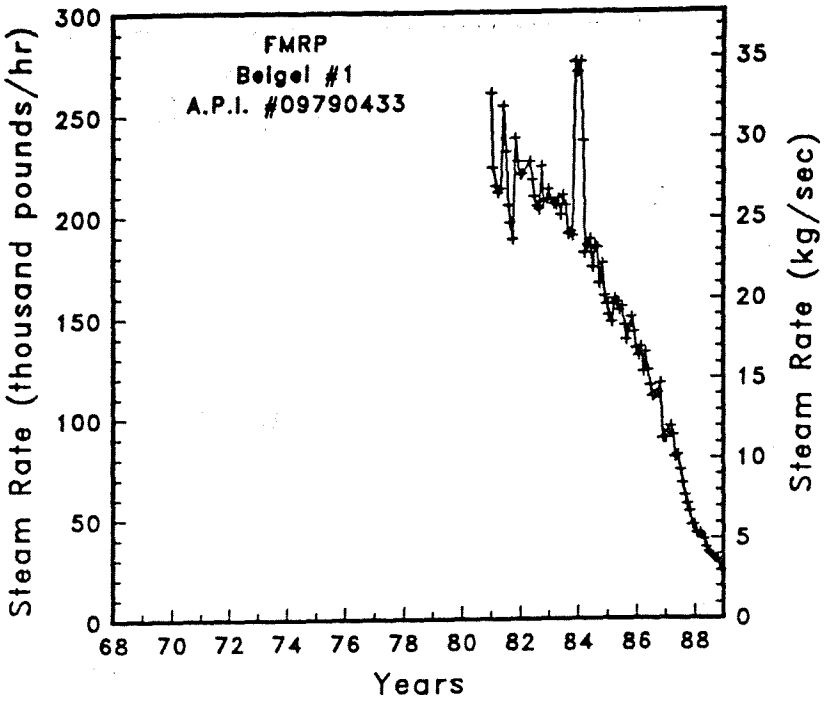

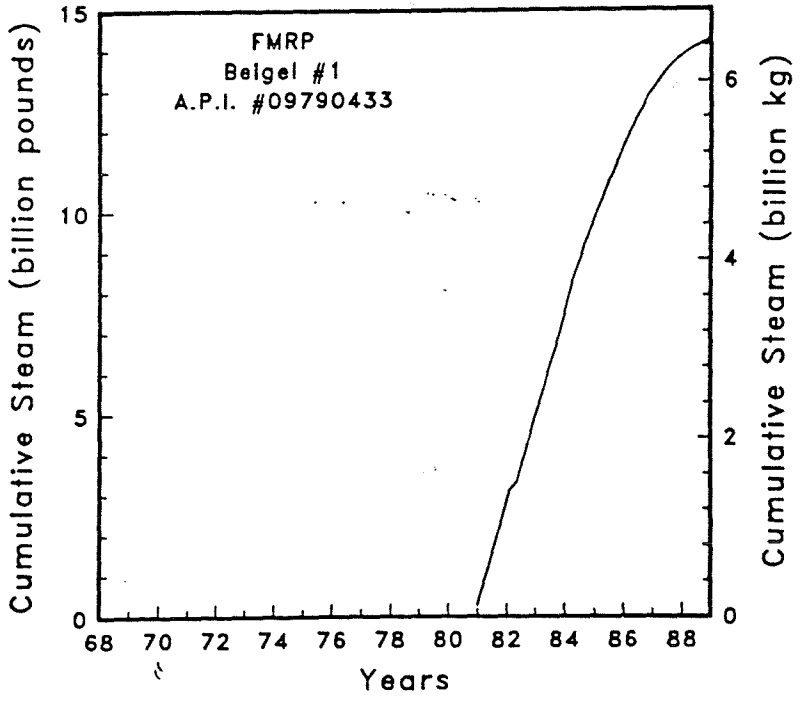

Figure A-3 Steam rate and cumulative mass flow for well Beigel #1

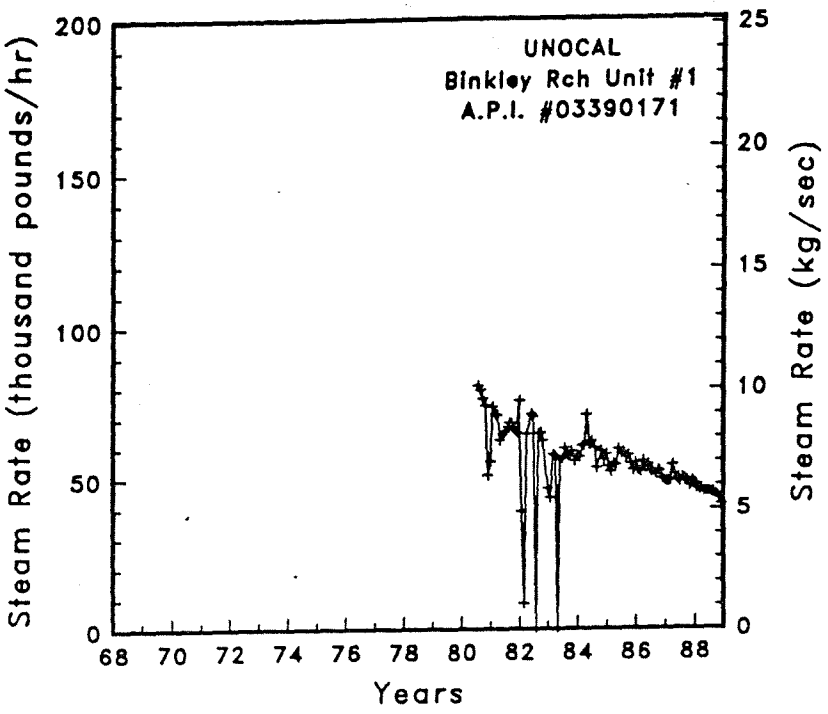

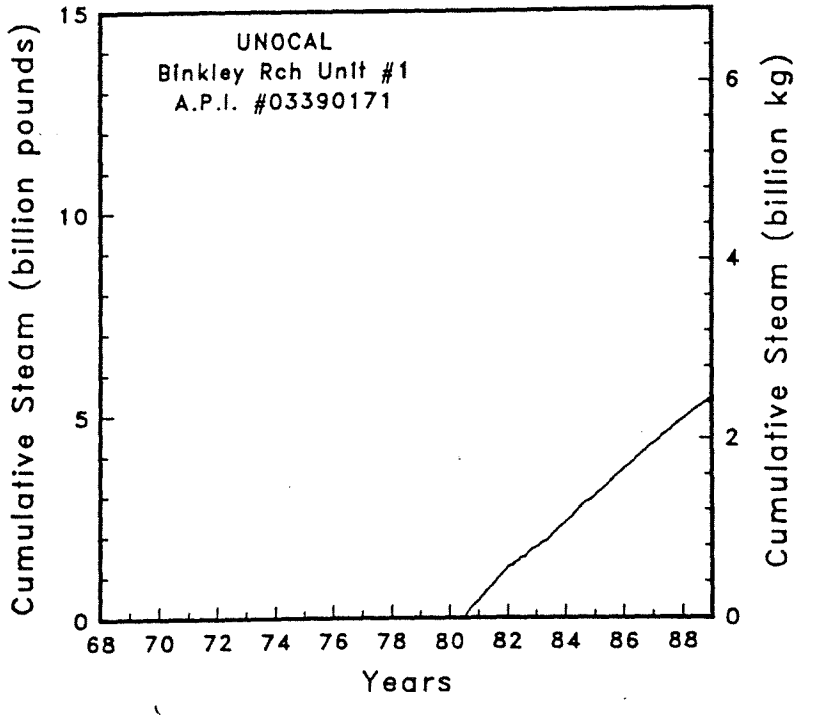

Figure A-4 Steam rate and cumulative mass flow for well Binkley Rch Unit #1

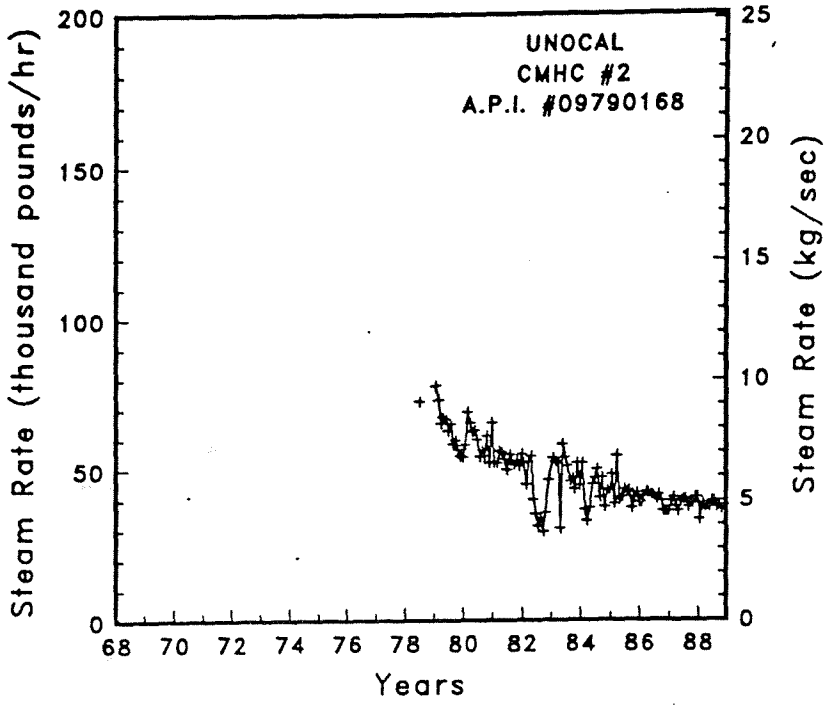

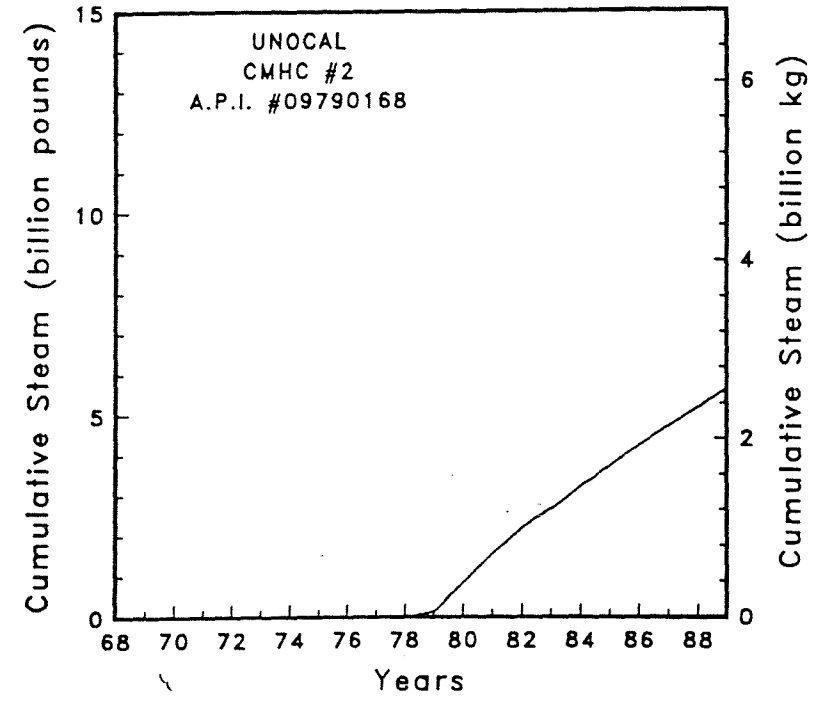

Figure A-5 Steam rate and cumulative mass flow for well CMHC #2

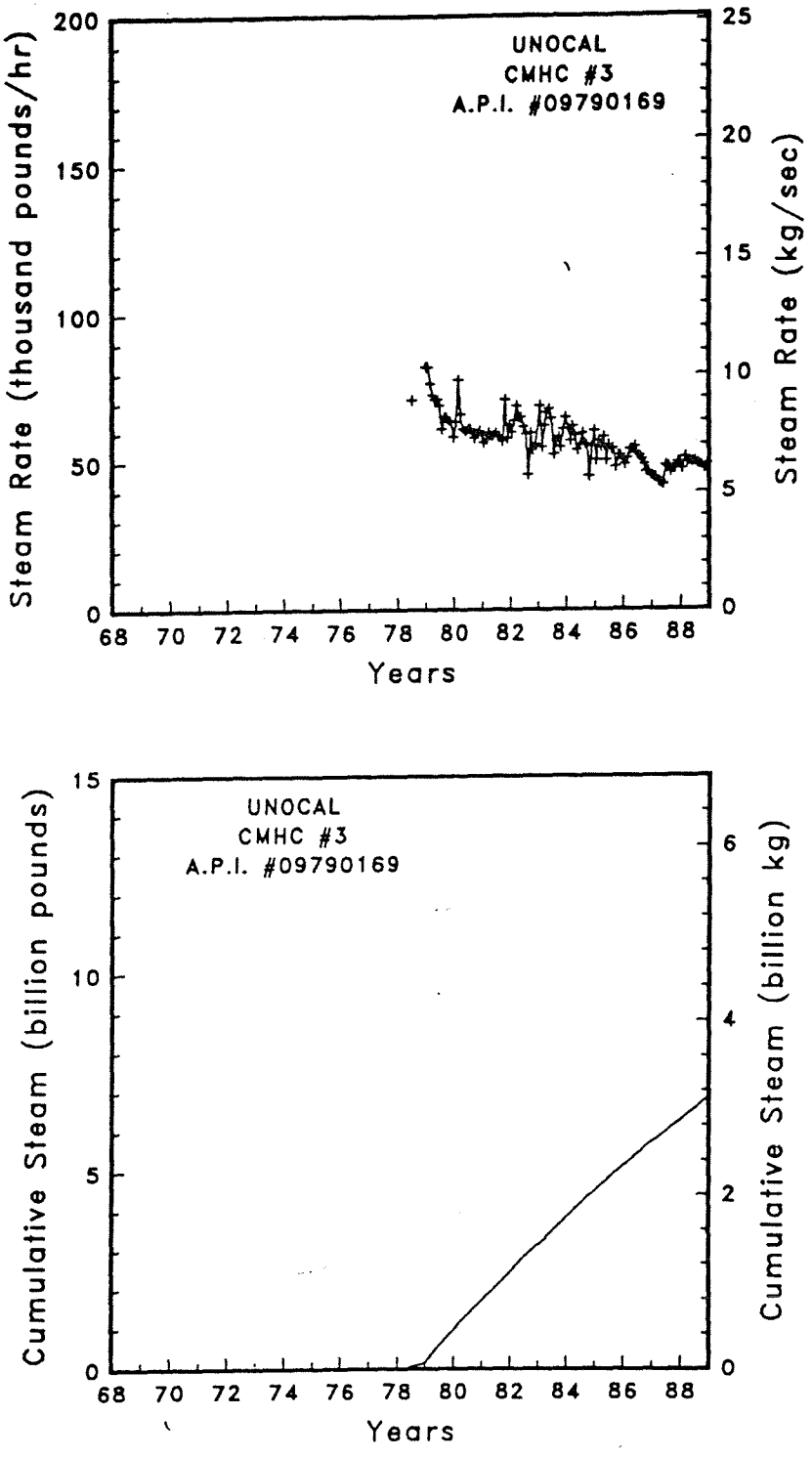

Figure A-6 Steam rate and cumulative mass flow for well CMHC #3

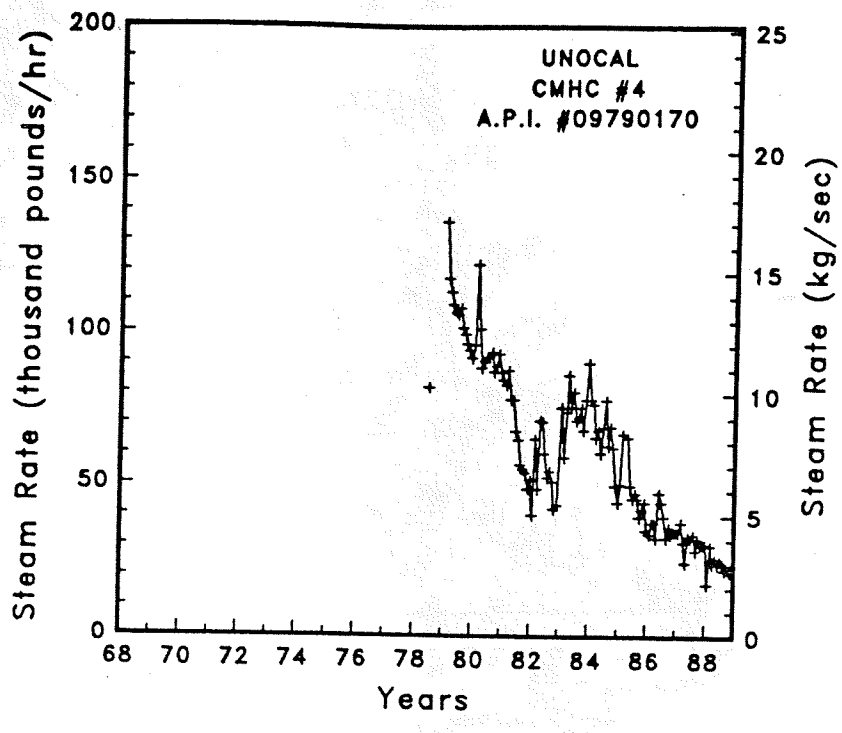

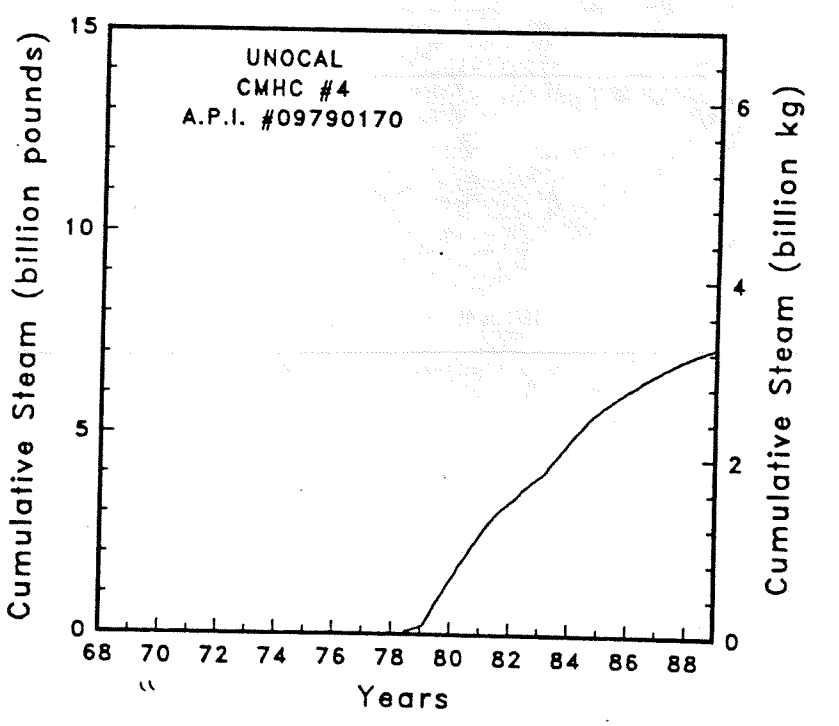

Figure A-7 Steam rate and cumulative mass flow for well CMHC #4

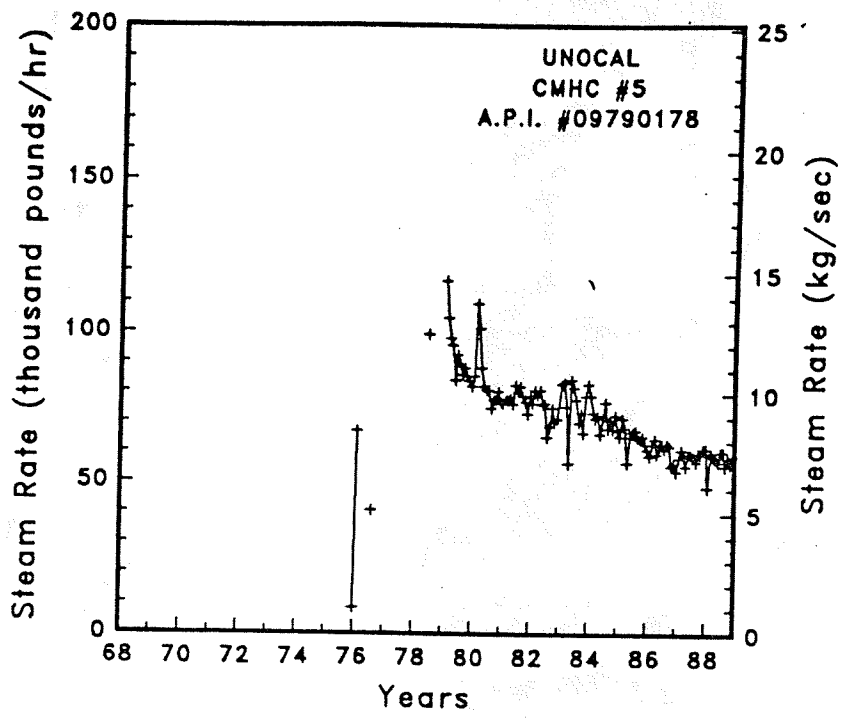

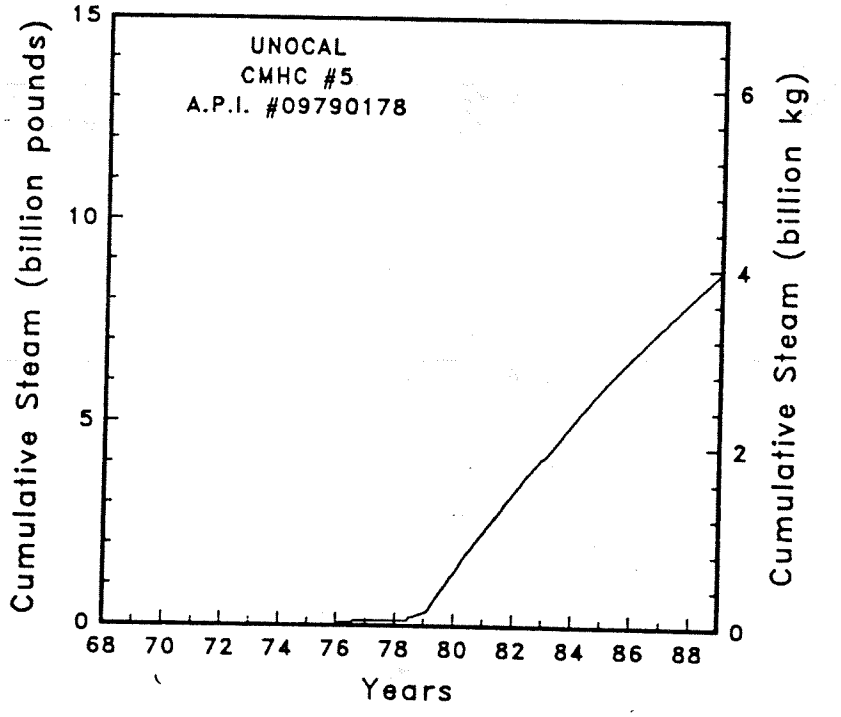

Figure A-8 Steam rate and cumulative mass flow for well CMHC #5

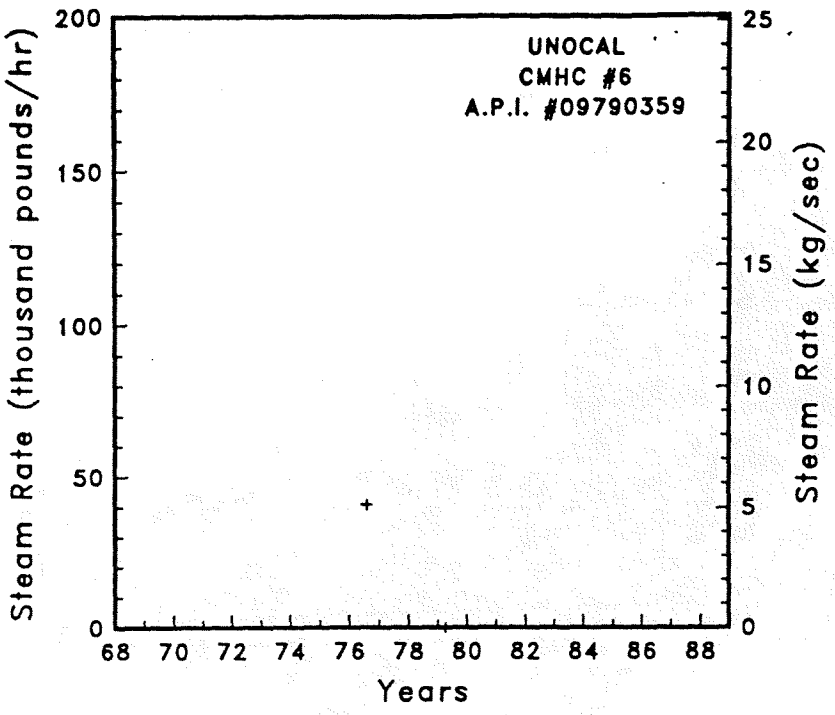

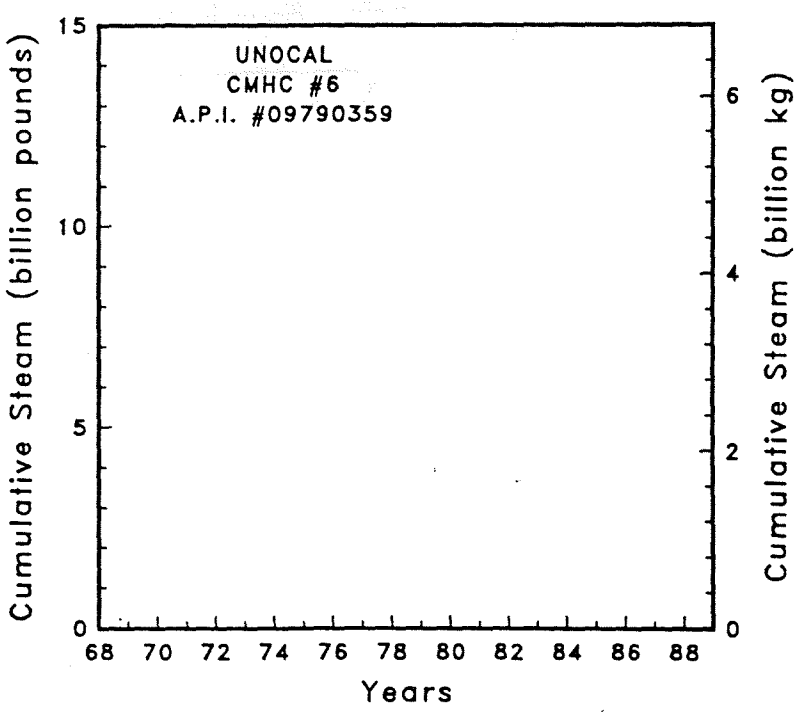

Figure A-9 Steam rate and cumulative mass flow for well CMHC #6

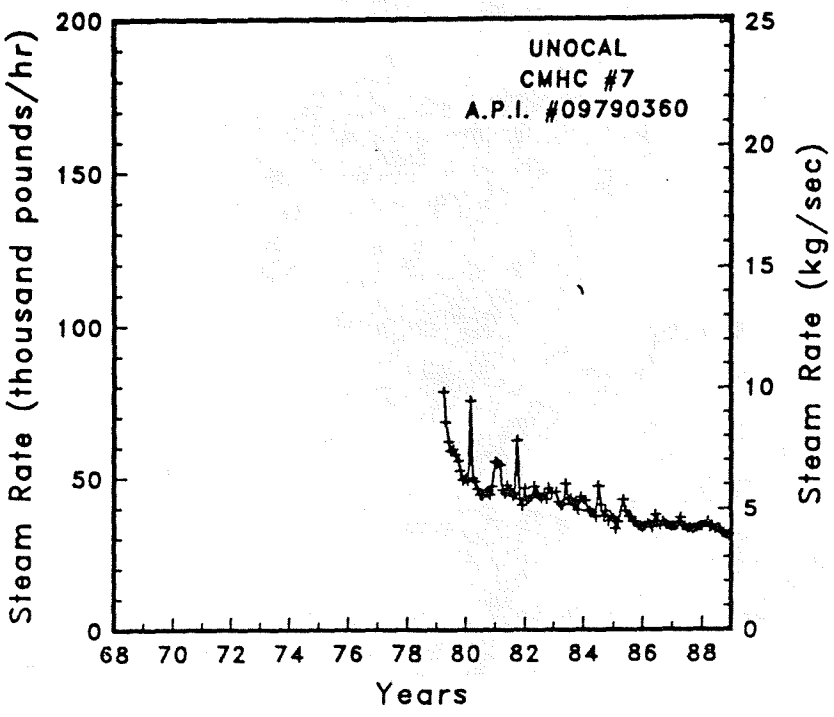

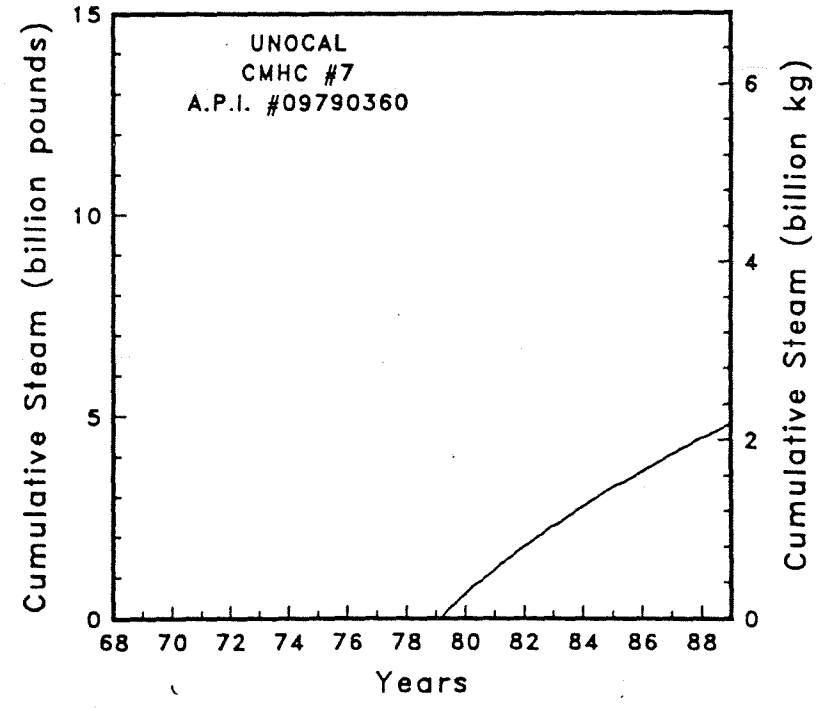

Figure A-10 Steam rate and cumulative mass flow for well CMHC #7

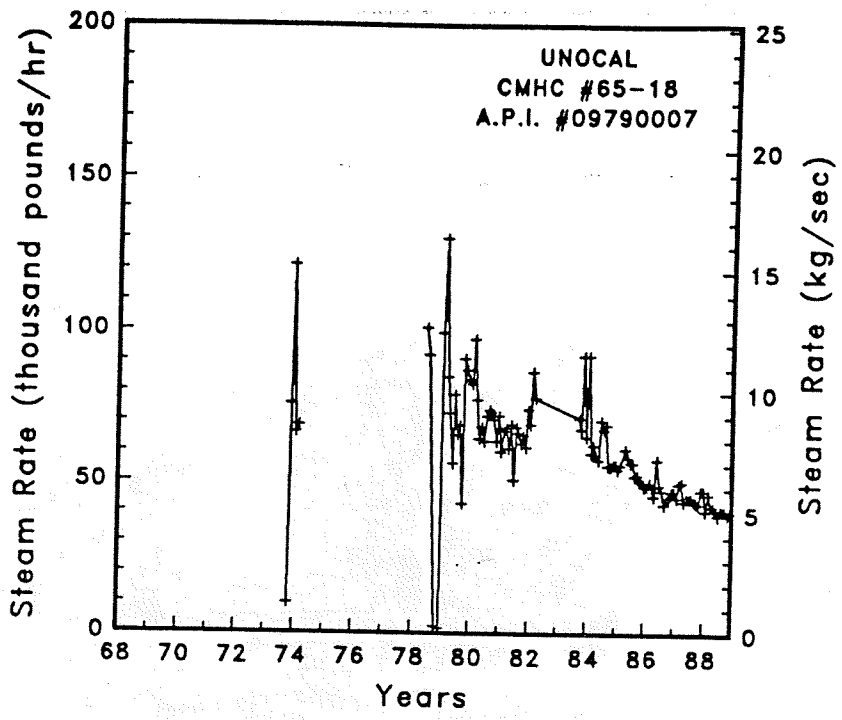

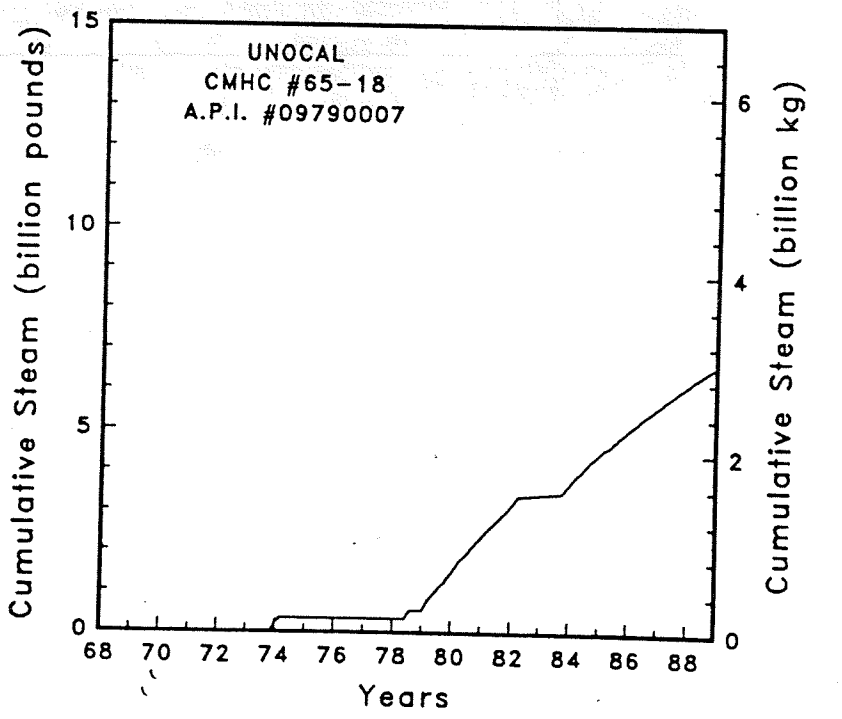

Figure A-11 Steam rate and cumulative mass flow for well CMHC #65-18

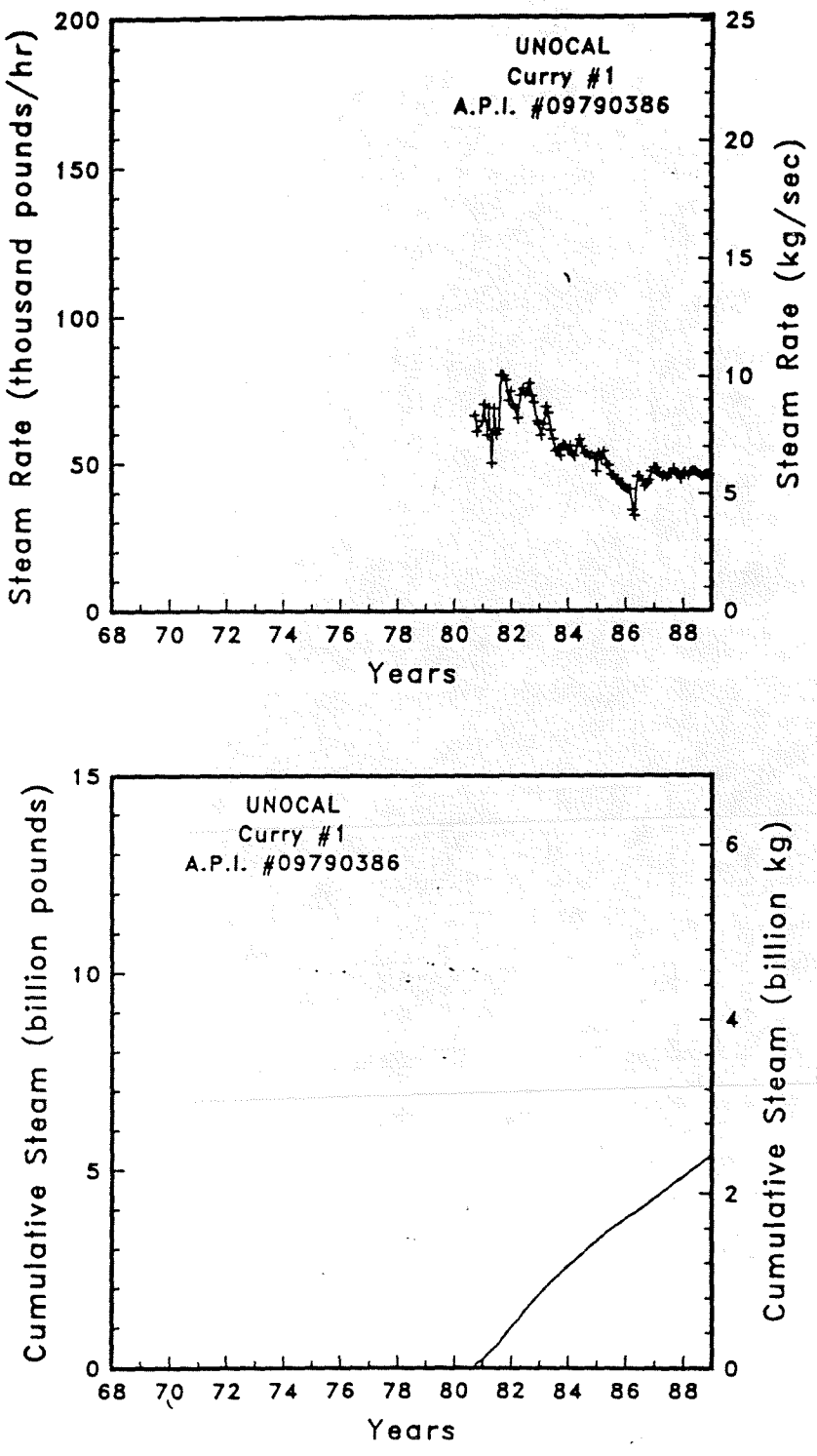

Figure A-12 Steam rate and cumulative mass flow for well Curry #1

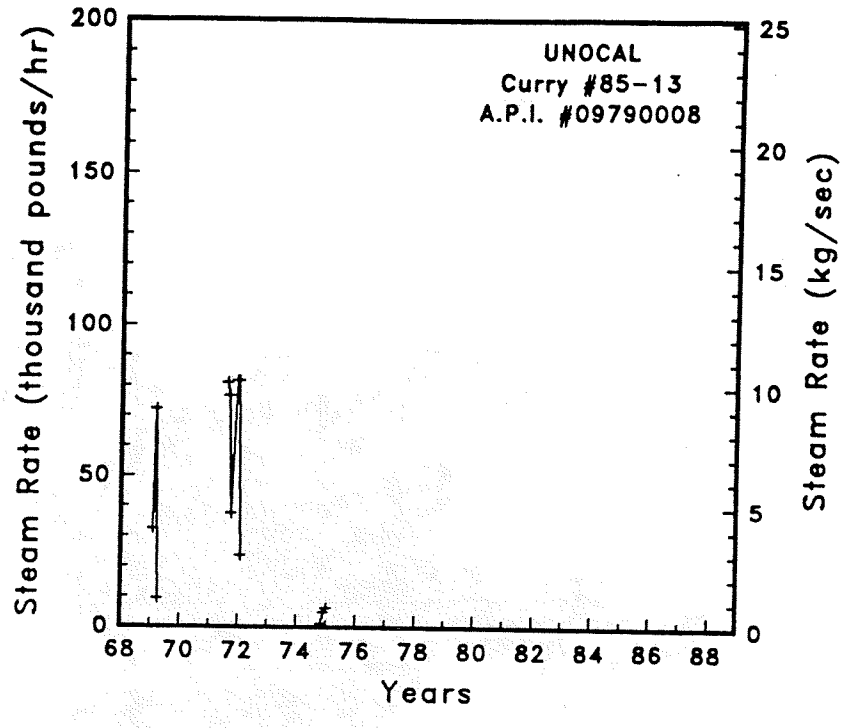

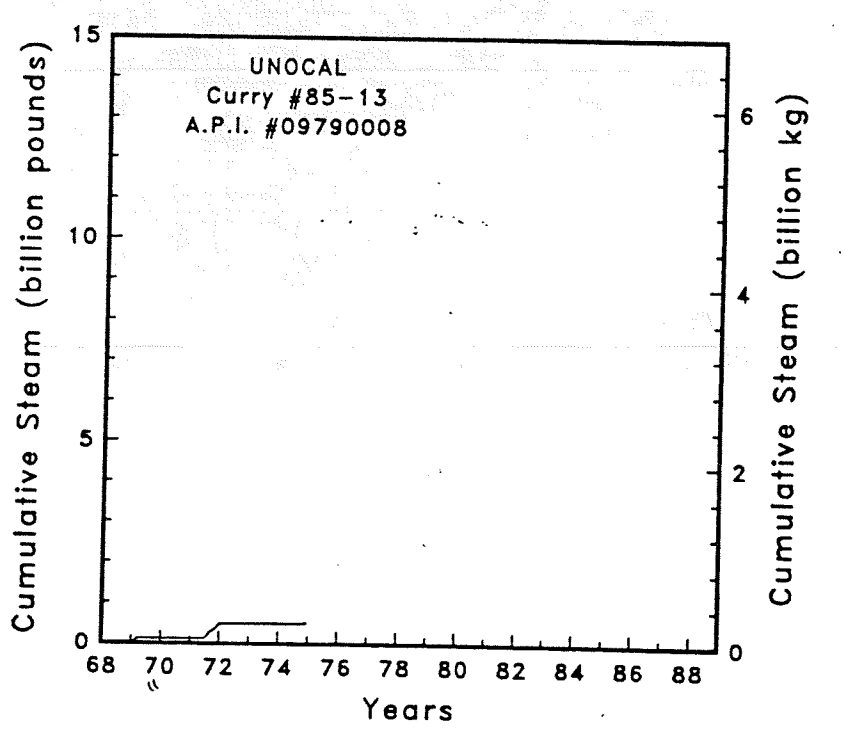

Figure A-13 Steam rate and cumulative mass flow for well Curry #85-13

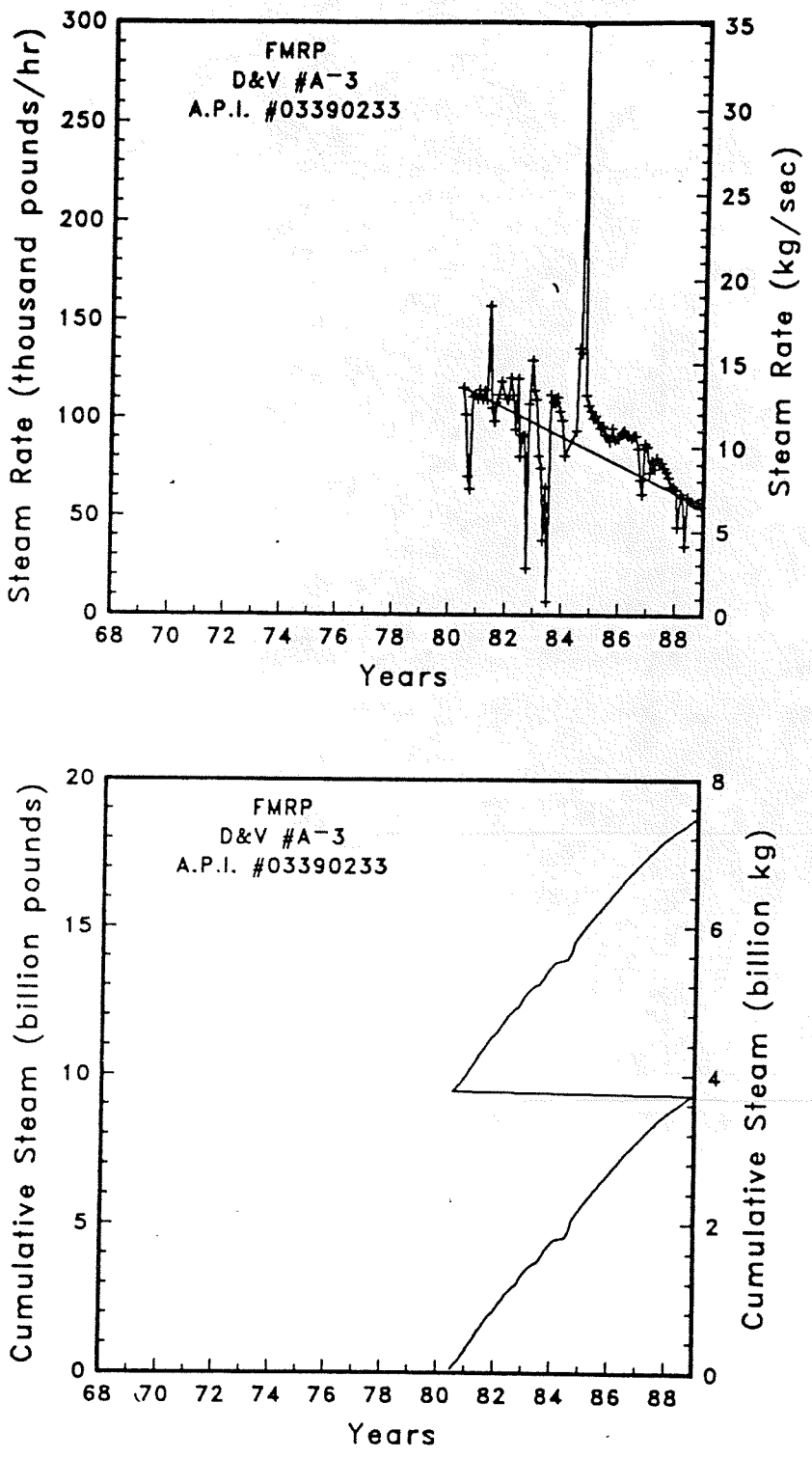

Figure A-14 Steam rate and cumulative mass flow for well D&V #A-3

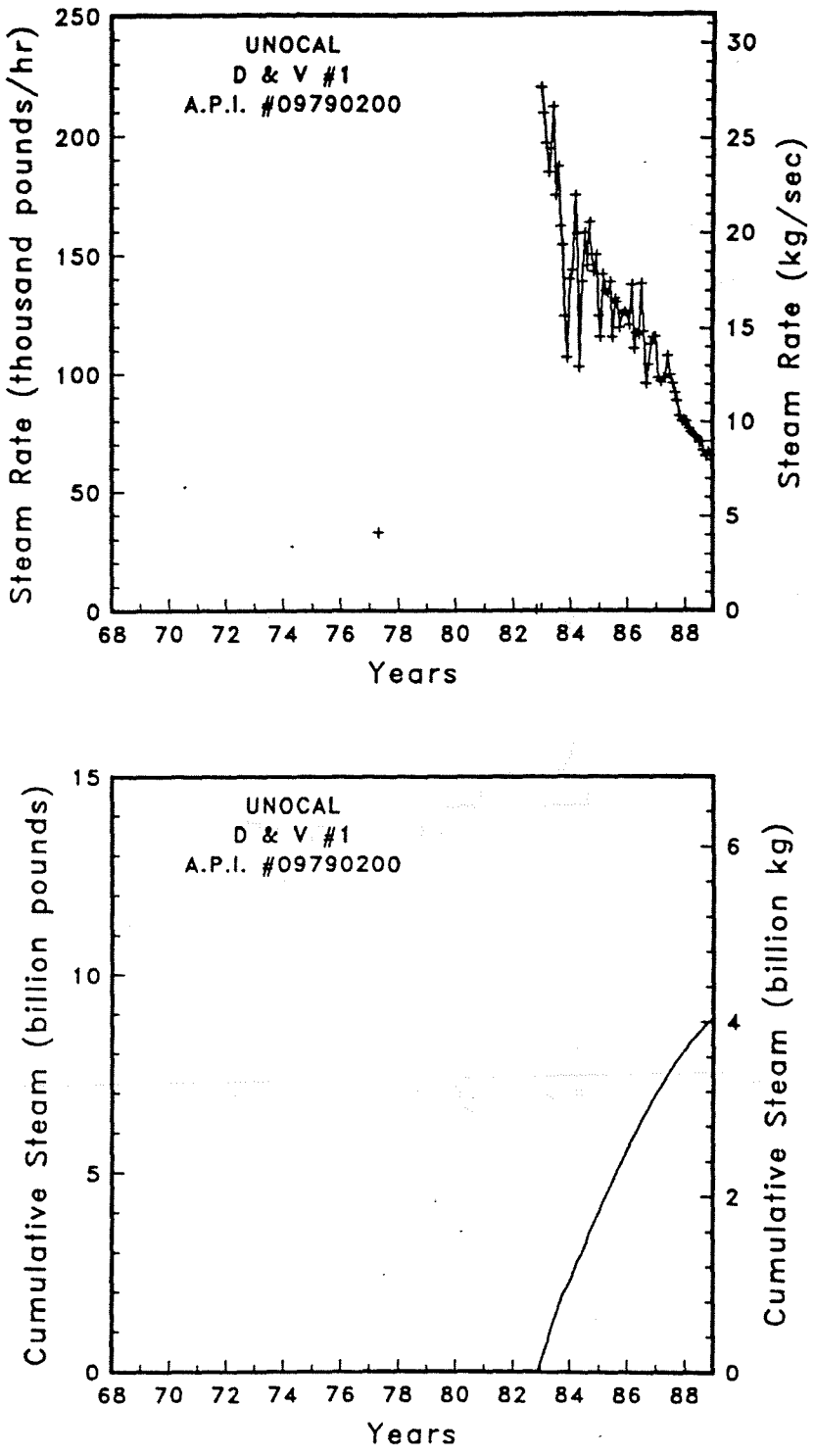

Figure A-15 Steam rate and cumulative mass flow for well D & V #1

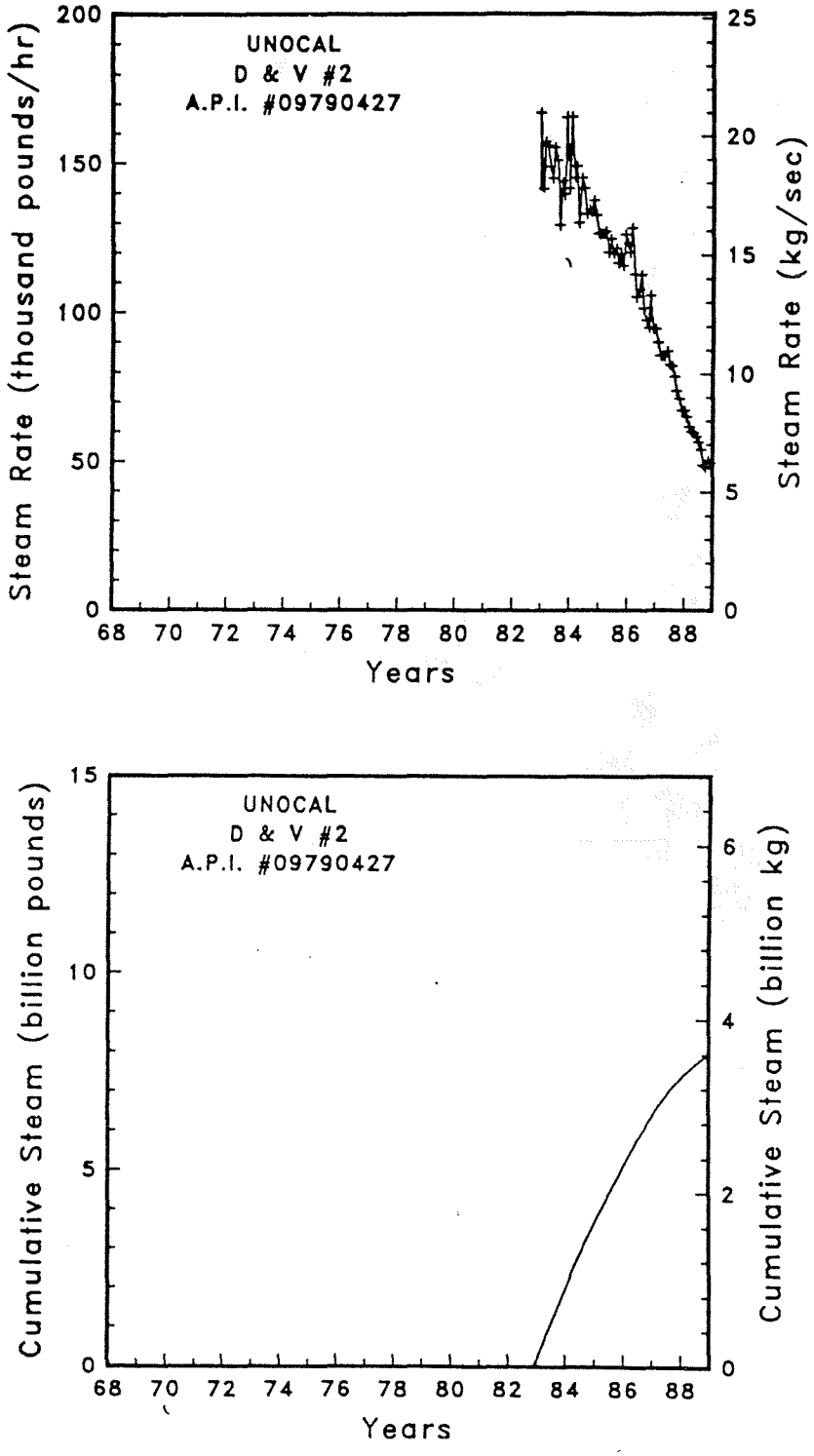

Figure A-16 Steam rate and cumulative mass flow for well D & V #2

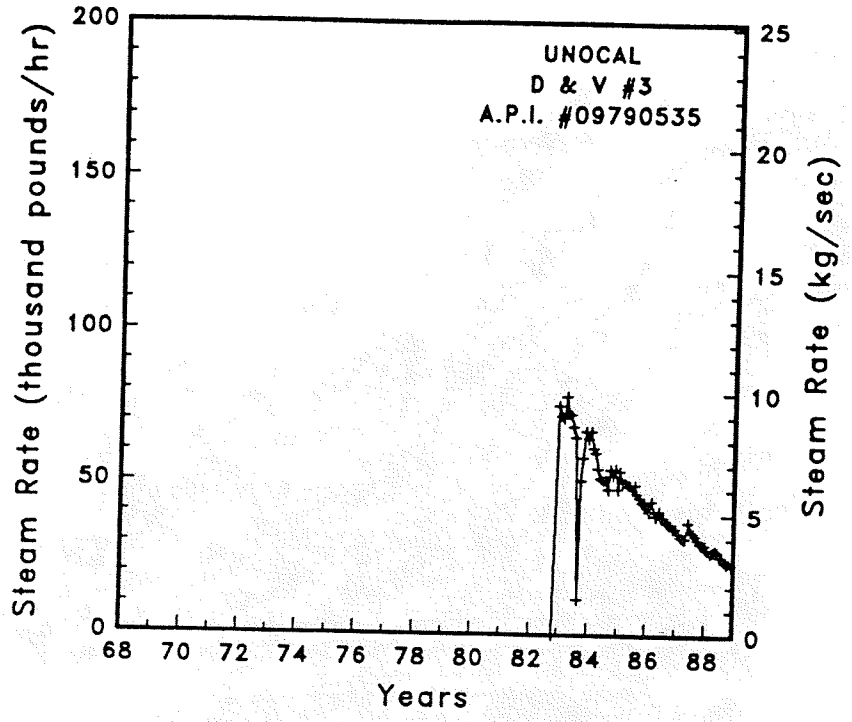

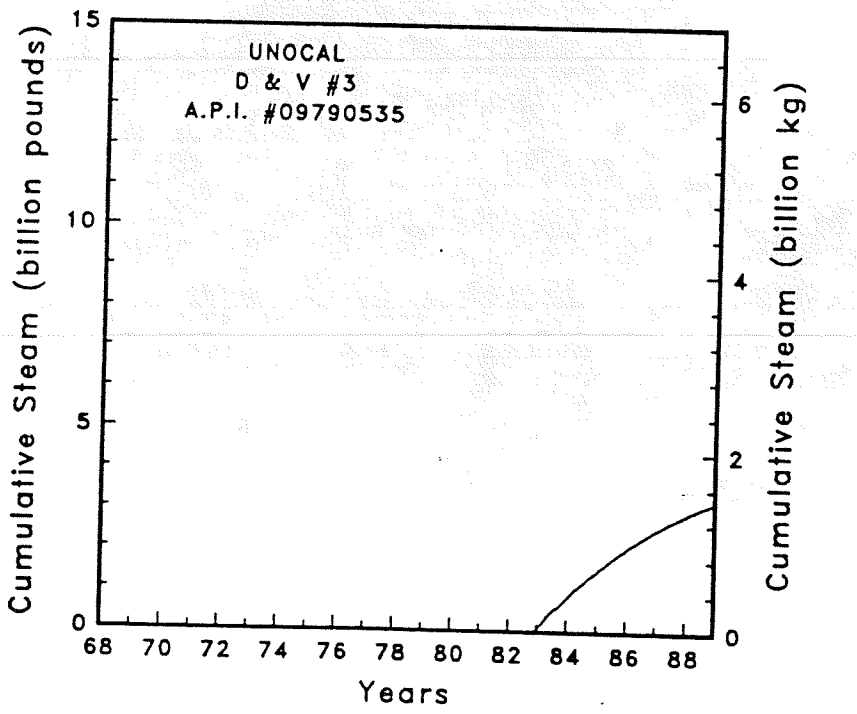

Figure A-17 Steam rate and cumulative mass flow for well D & V #3

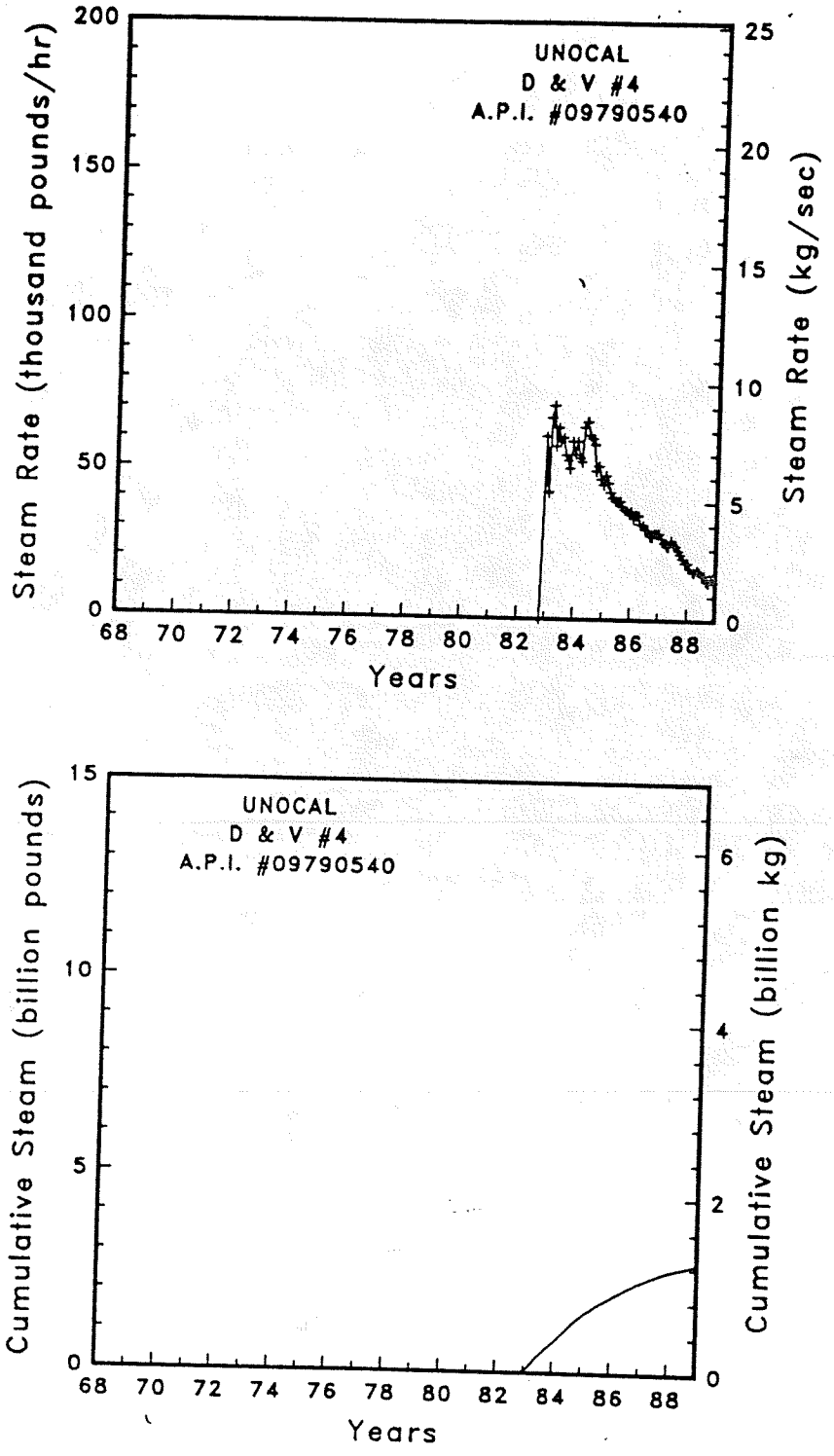

Figure A-18 Steam rate and cumulative mass flow for well D & V #4

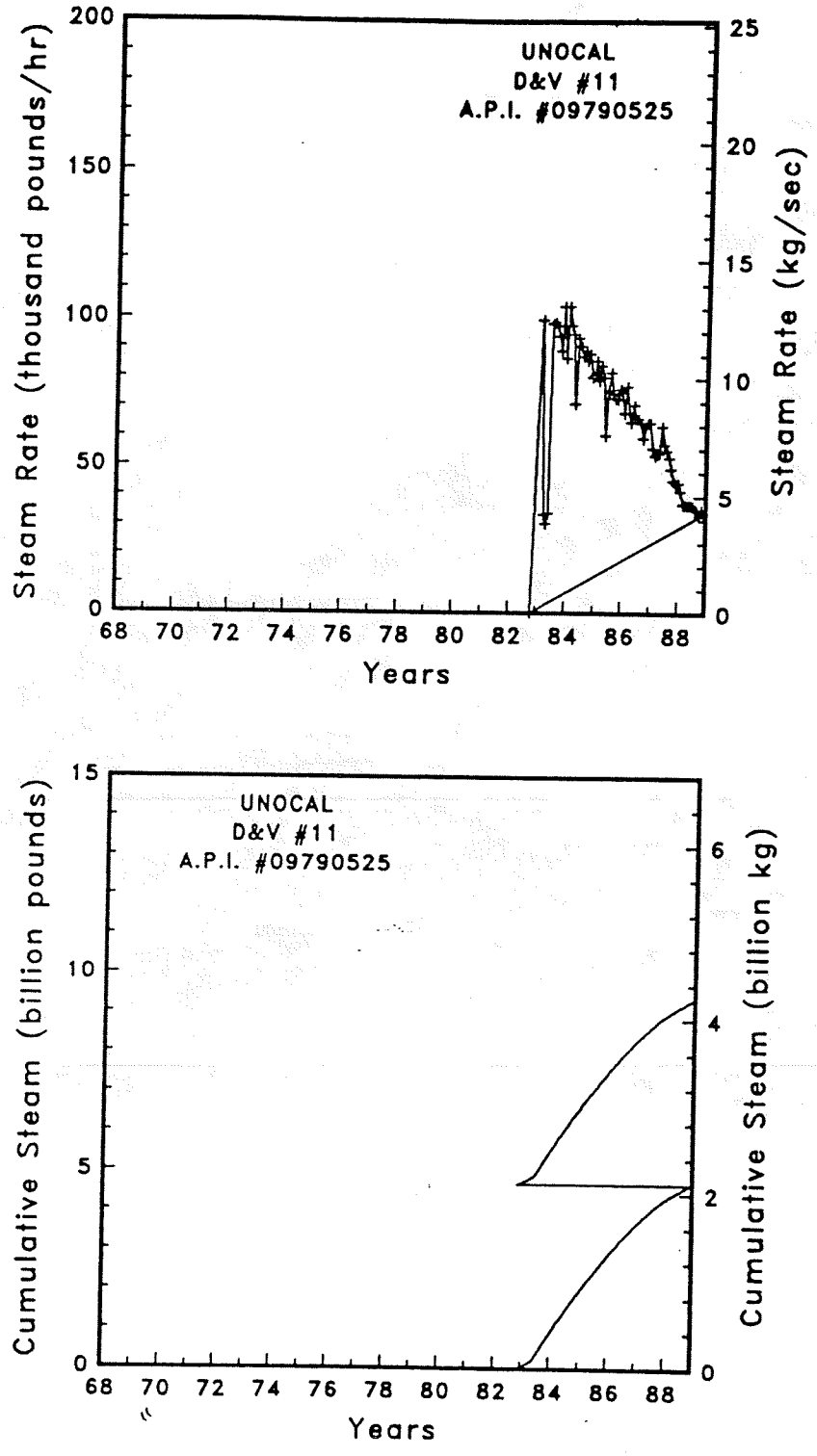

Figure A-19 Steam rate and cumulative mass flow for well D&V #11

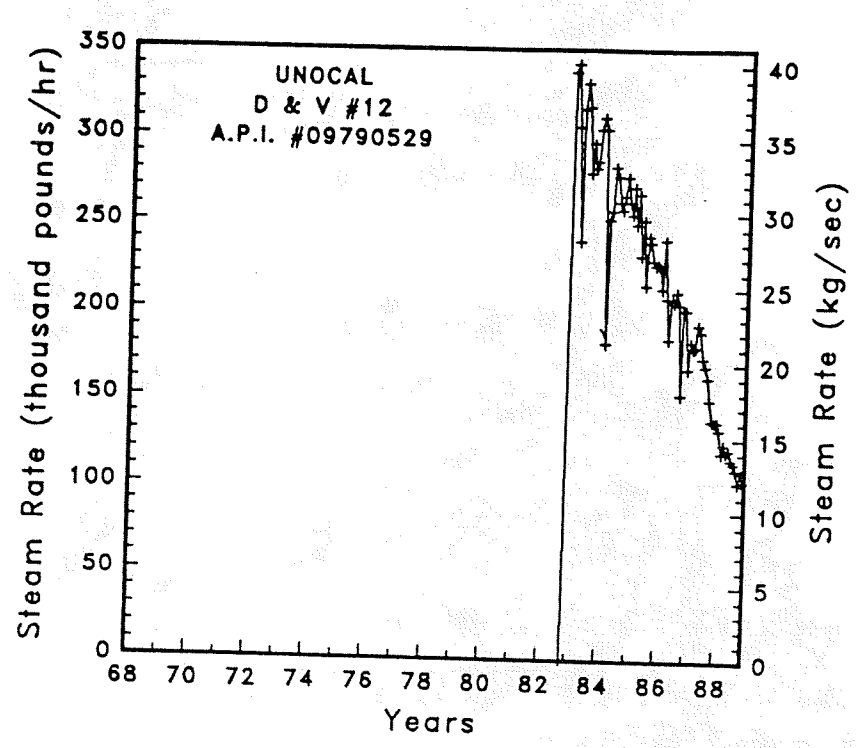

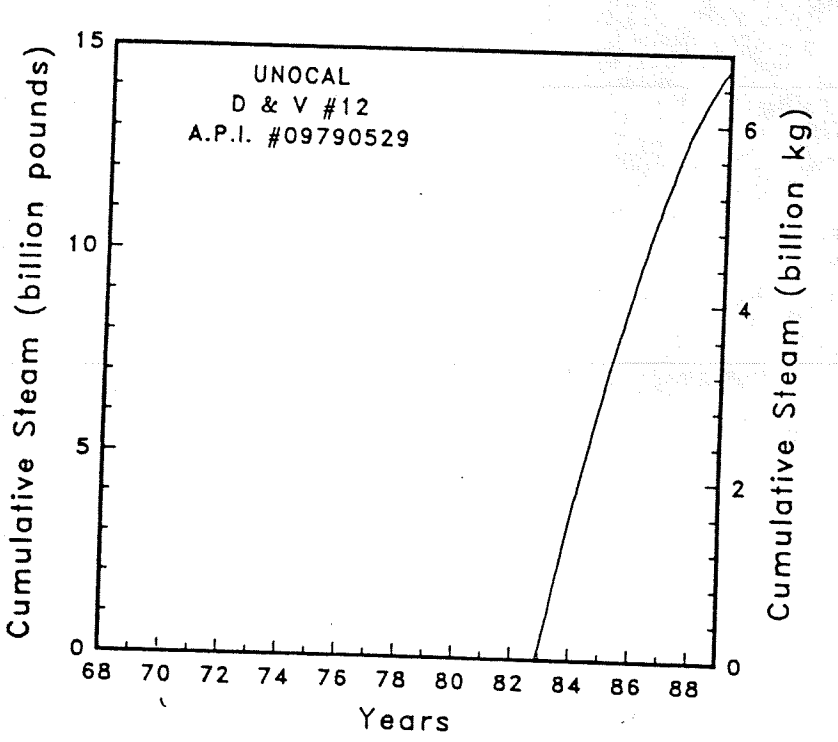

Figure A-20 Steam rate and cumulative mass flow for well D & V #12

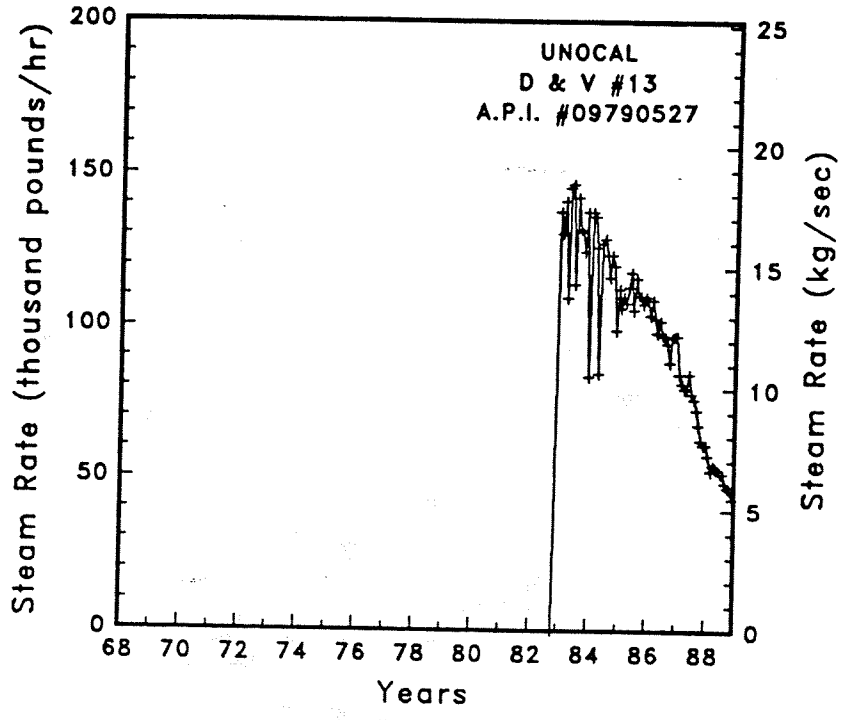

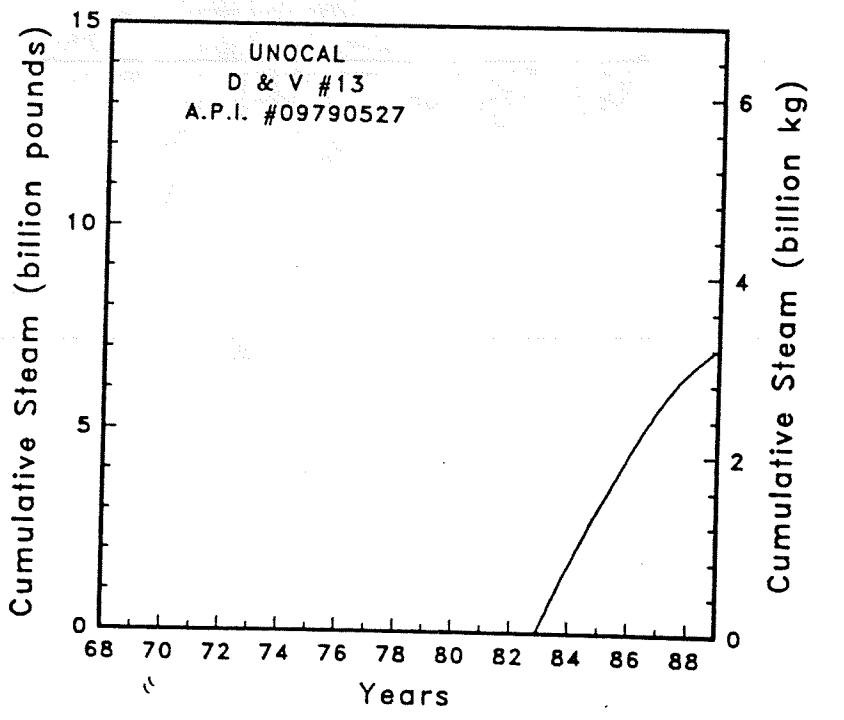

Figure A-21 Steam rate and cumulative mass flow for well D & V #13

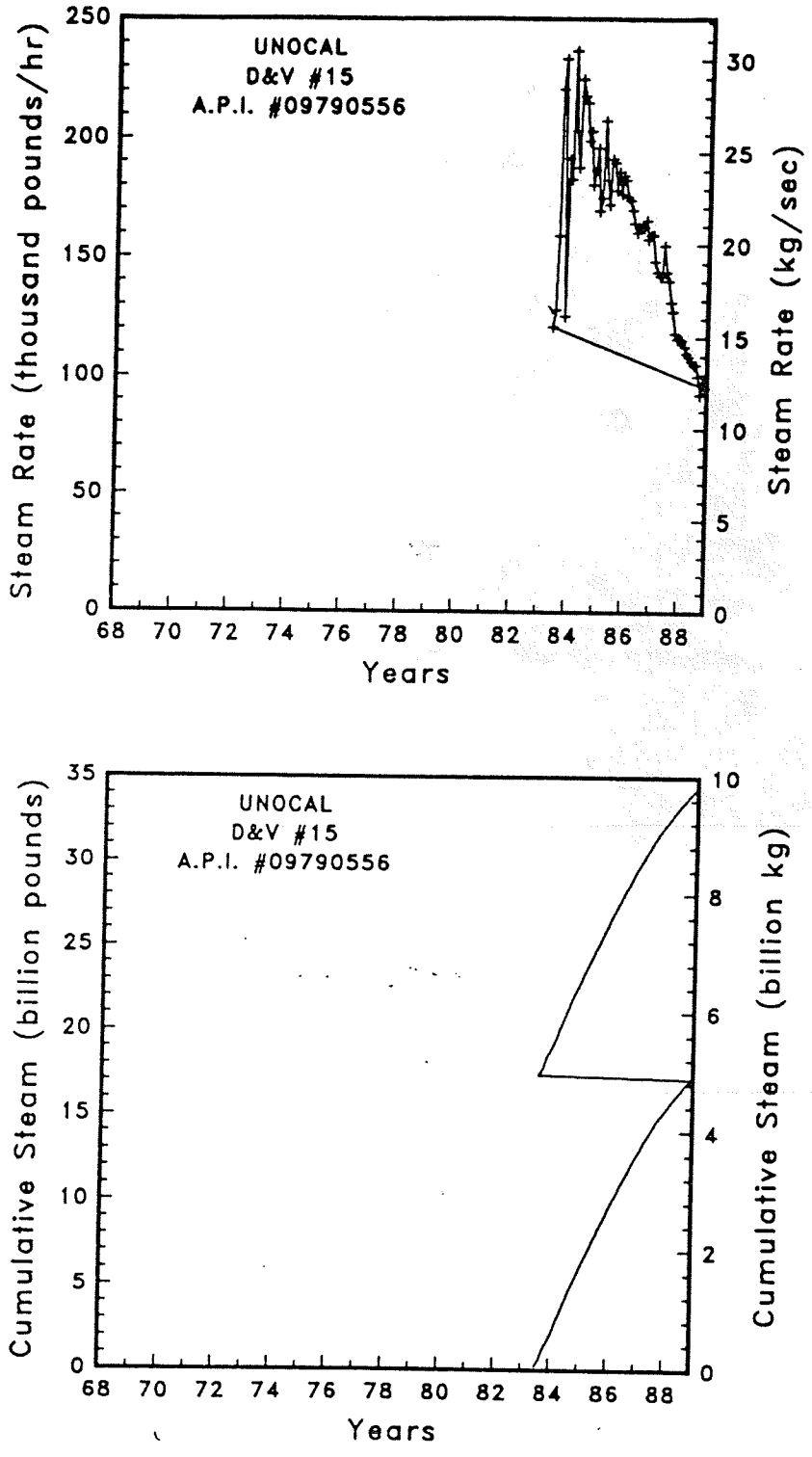

Figure A-22 Steam rate and cumulative mass flow for well D&V #15

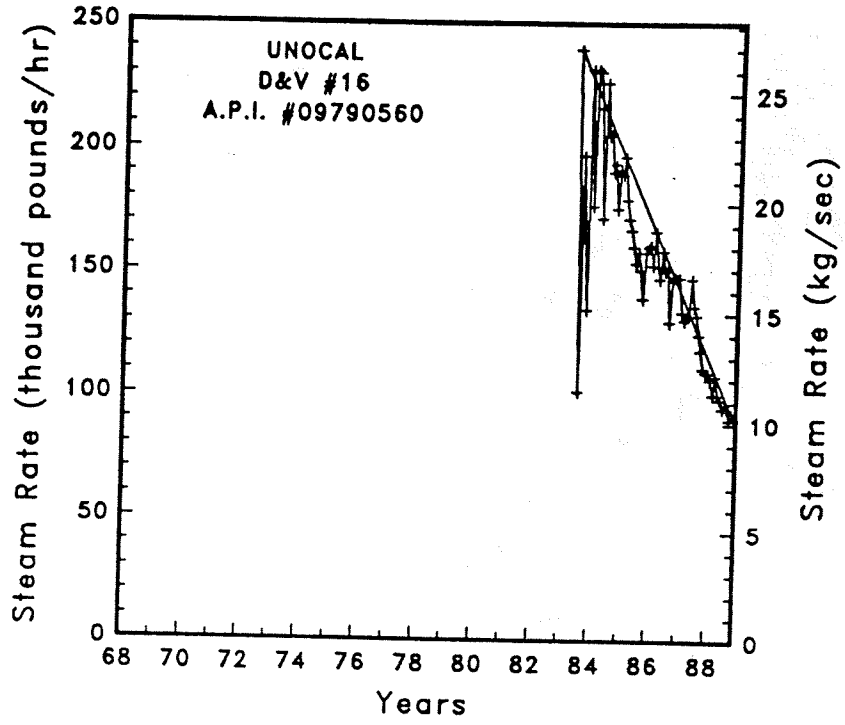

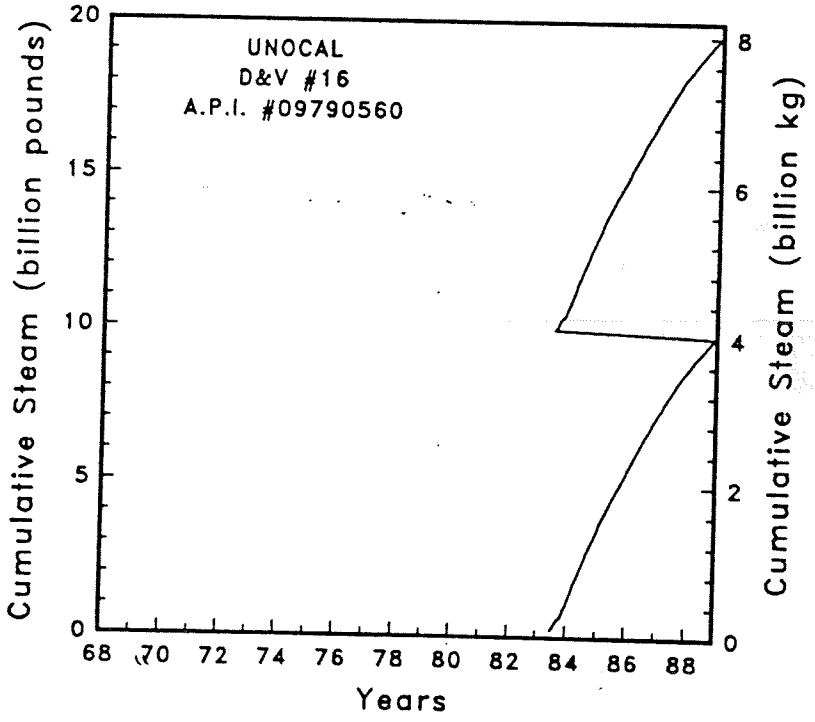

Figure A-23 Steam rate and cumulative mass flow for well D&V #16

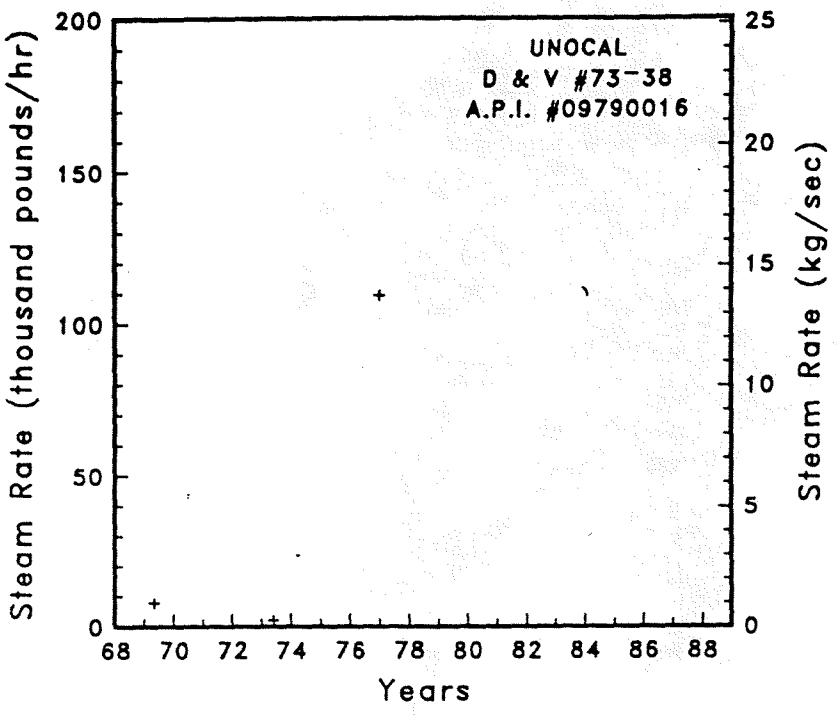

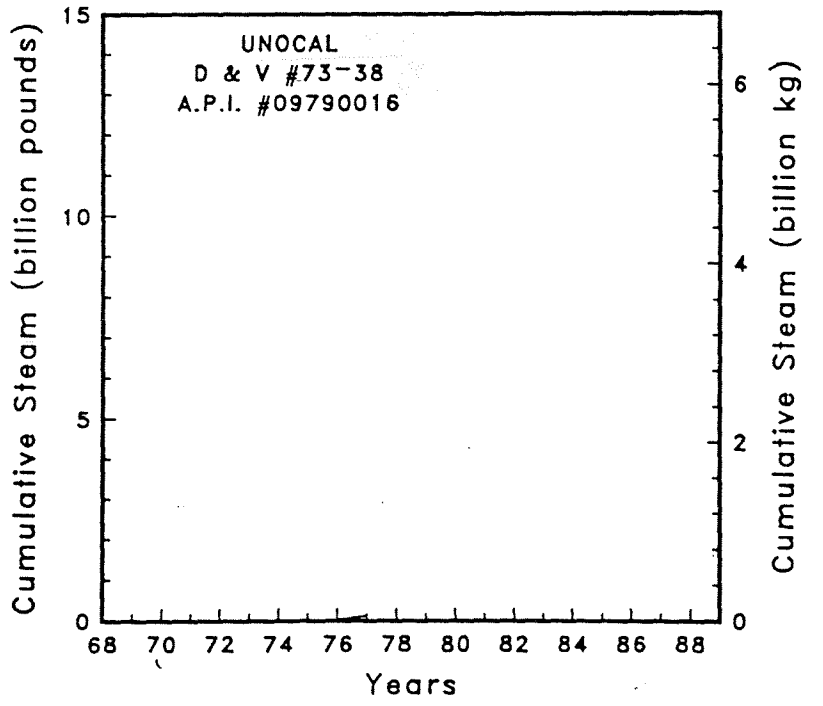

Figure A-24 Steam rate and cumulative mass flow for well D & V #73-38

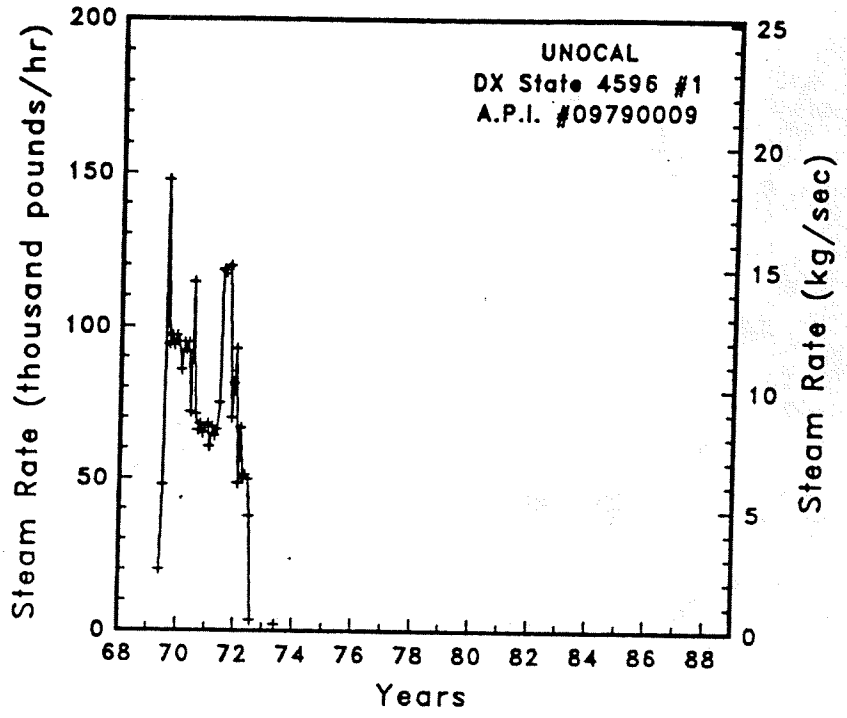

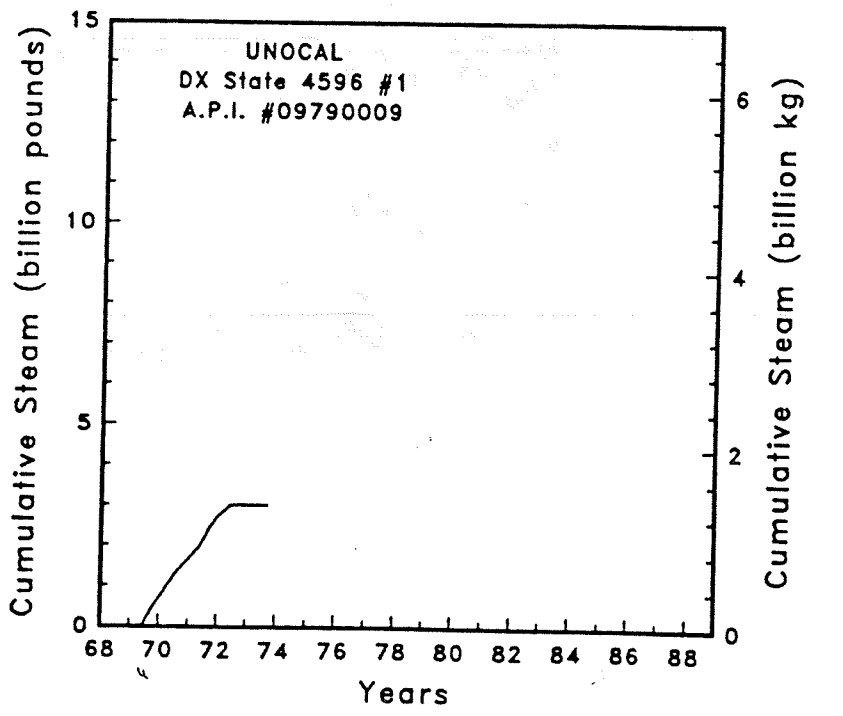

Figure A-25 Steam rate and cumulative mass flow for well DX State 4596 #1

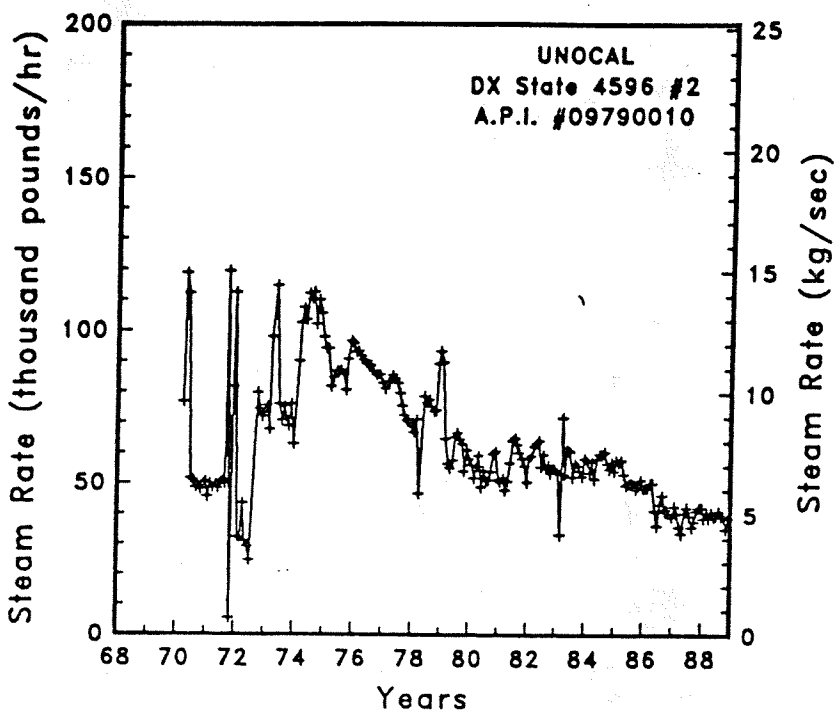

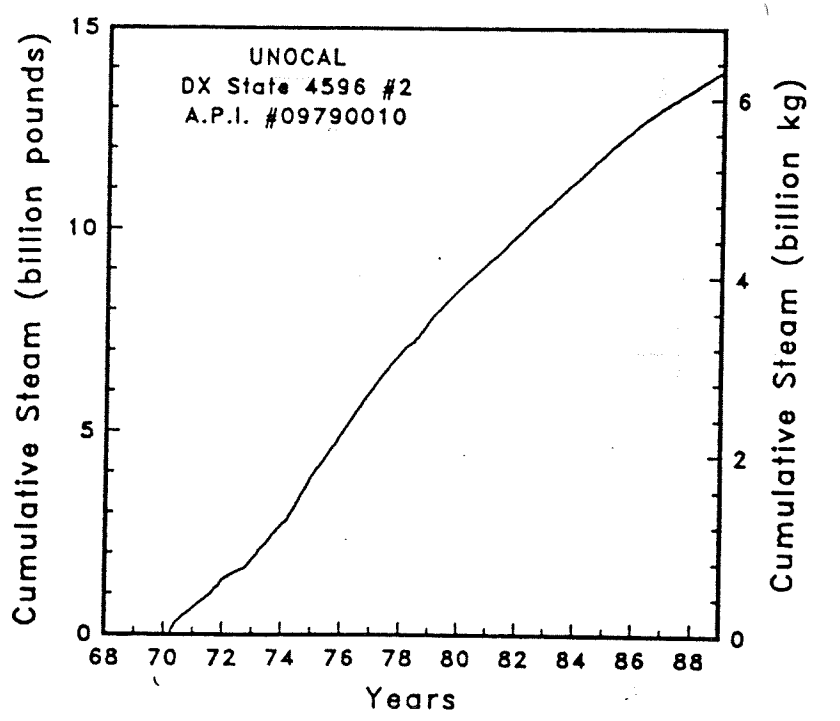

Figure A-26 Steam rate and cumulative mass flow for well DX State 4596 #2

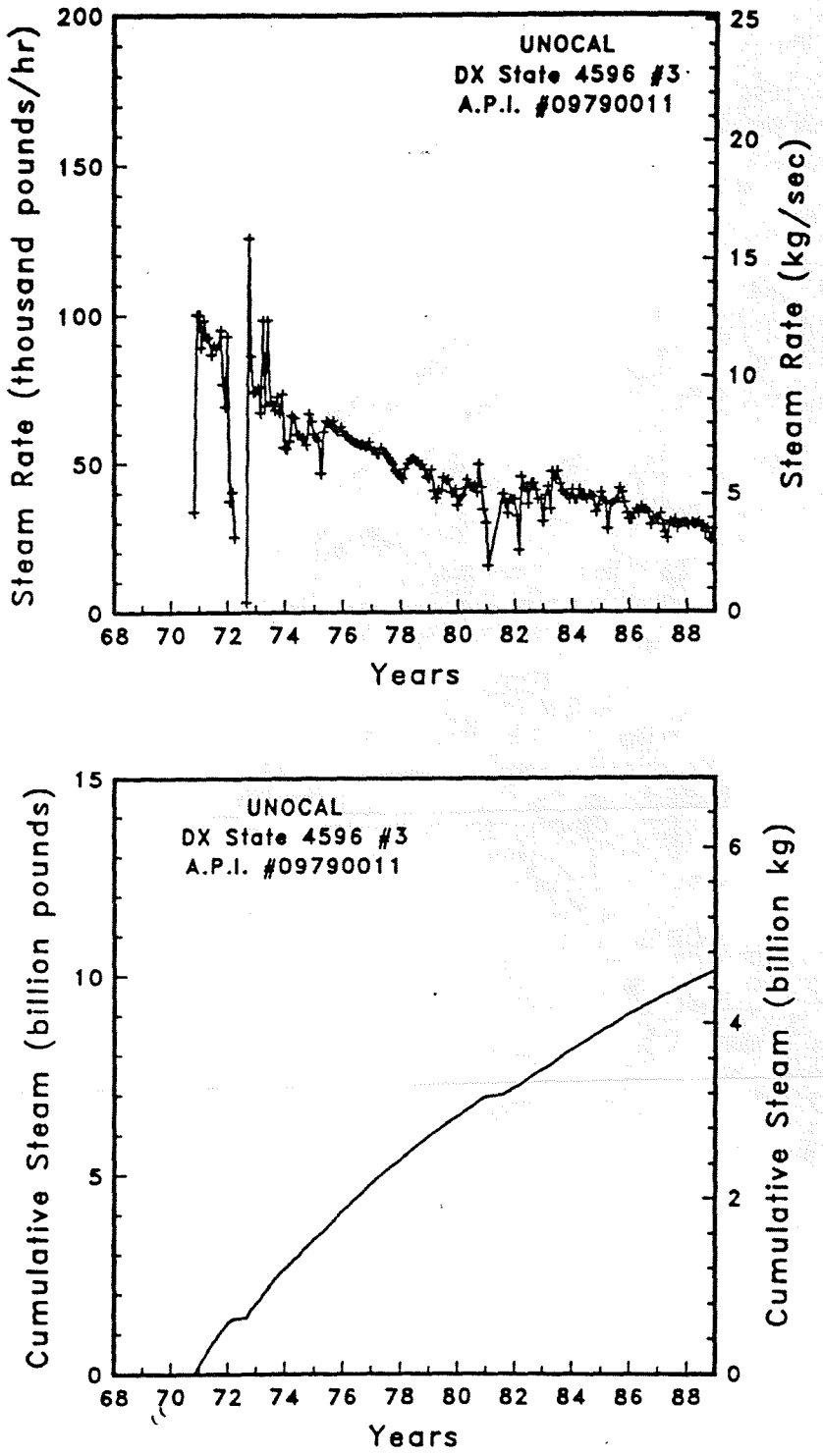

Figure A-27 Steam rate and cumulative mass flow for well DX State 4596 #3

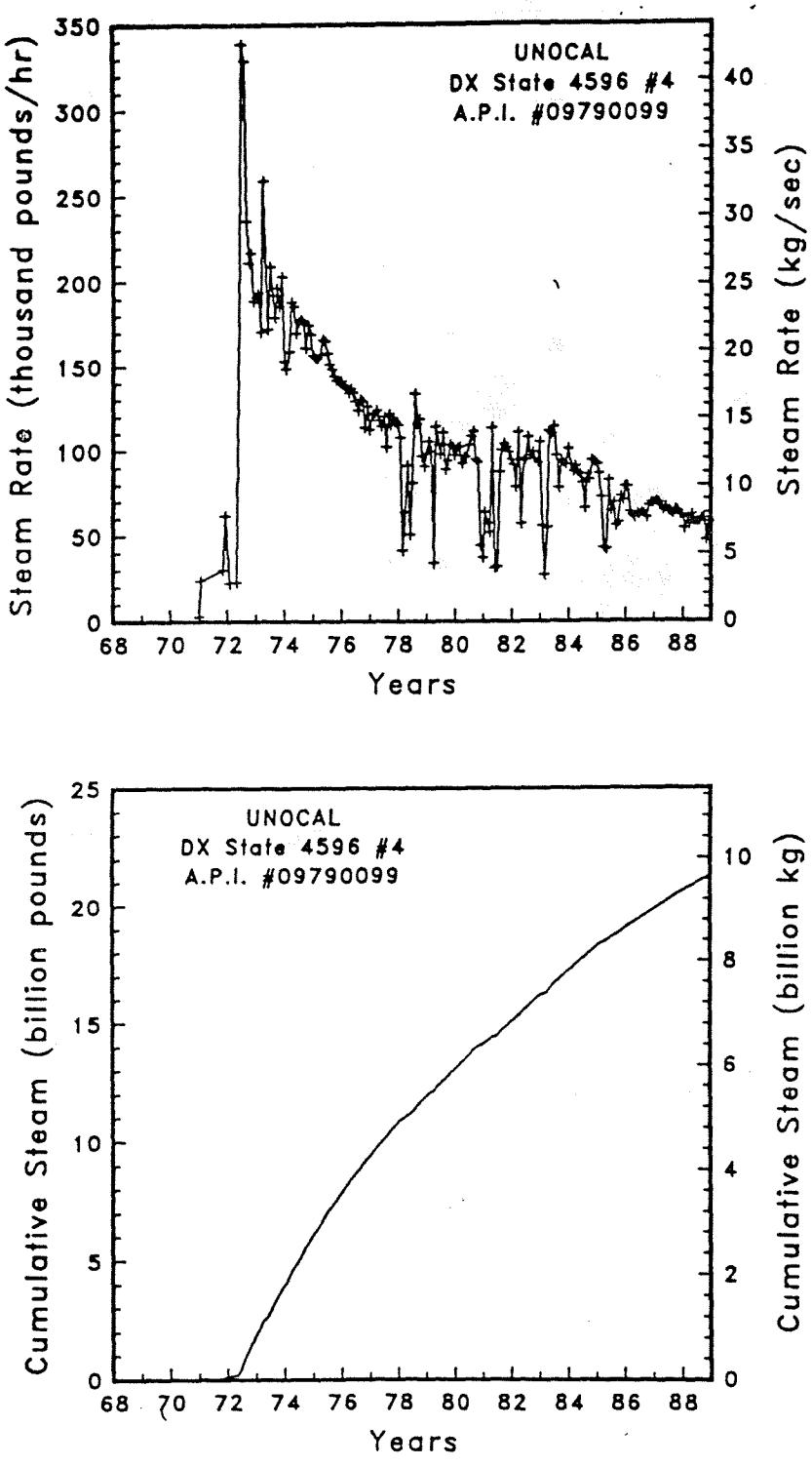

Figure A-28 Steam rate and cumulative mass flow for well DX State 4596 #4

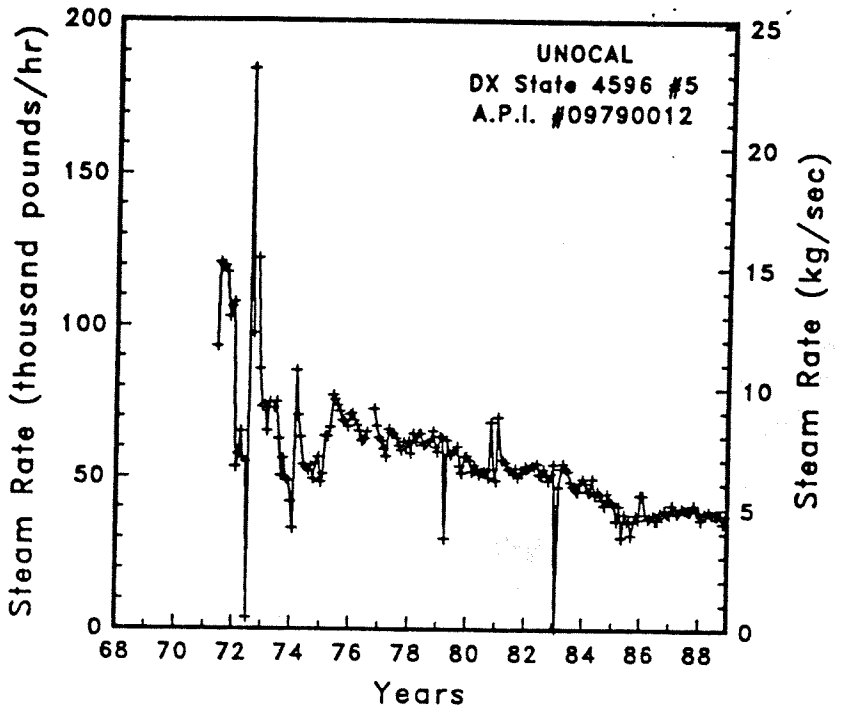

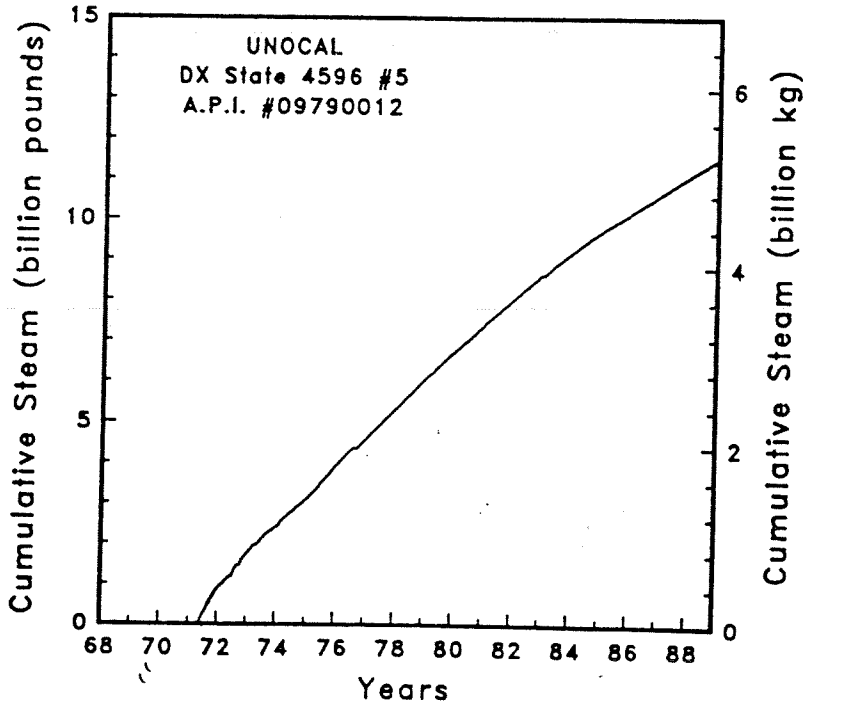

Figure A-29 Steam rate and cumulative mass flow for well DX State 4596 #5

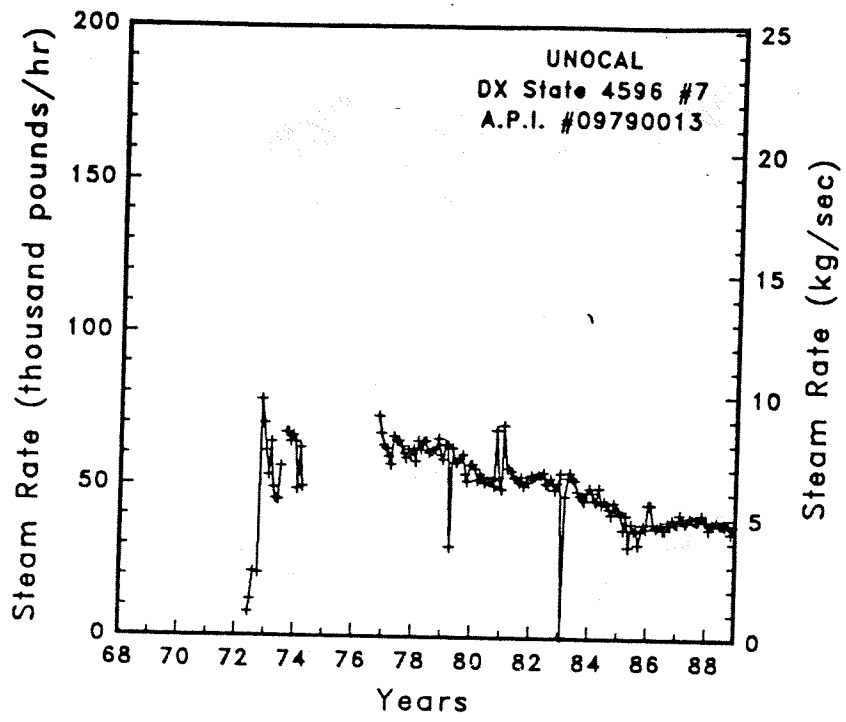

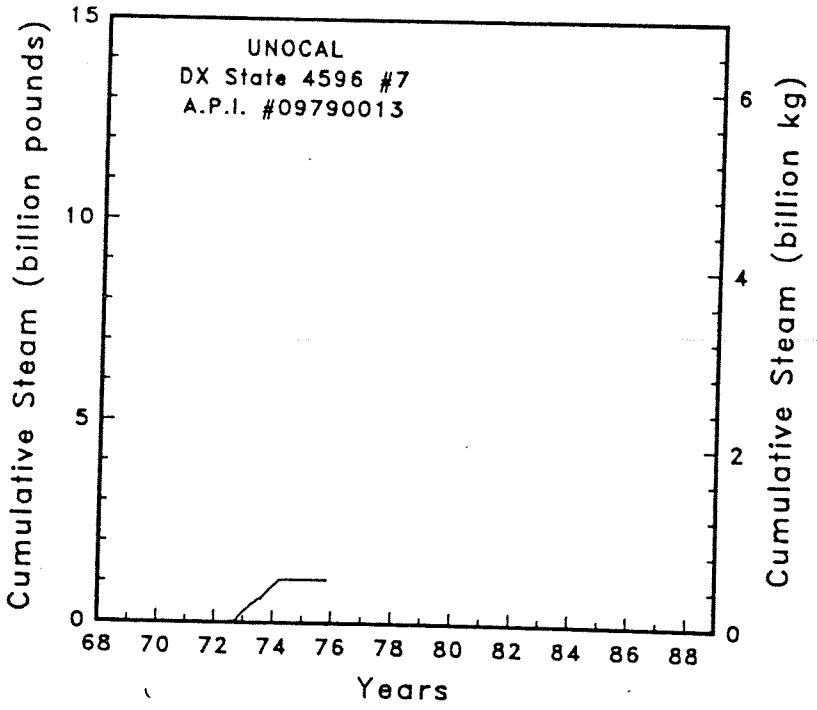

Figure A-30 Steam rate and cumulative mass flow for well DX State 4596 #7

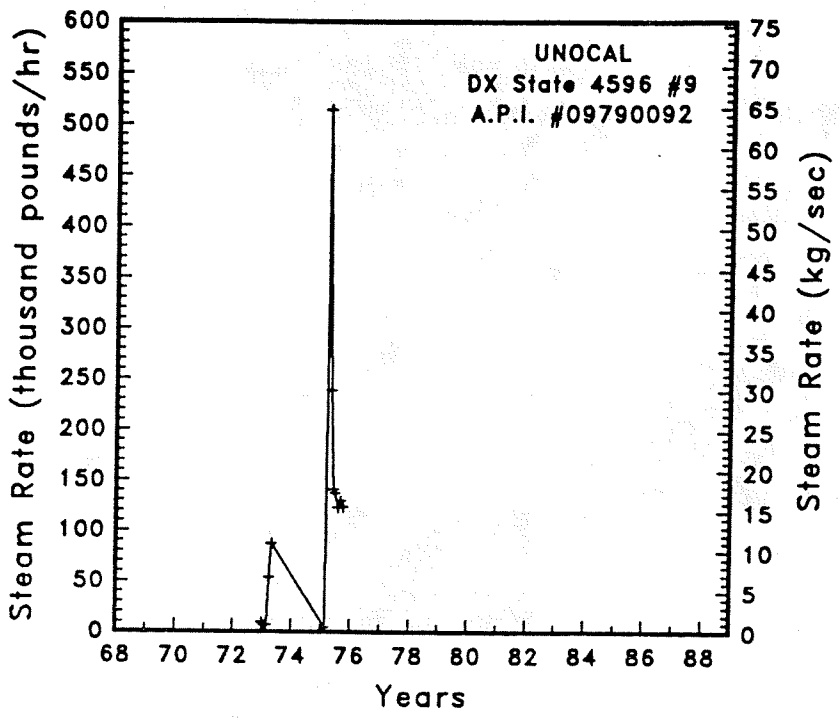

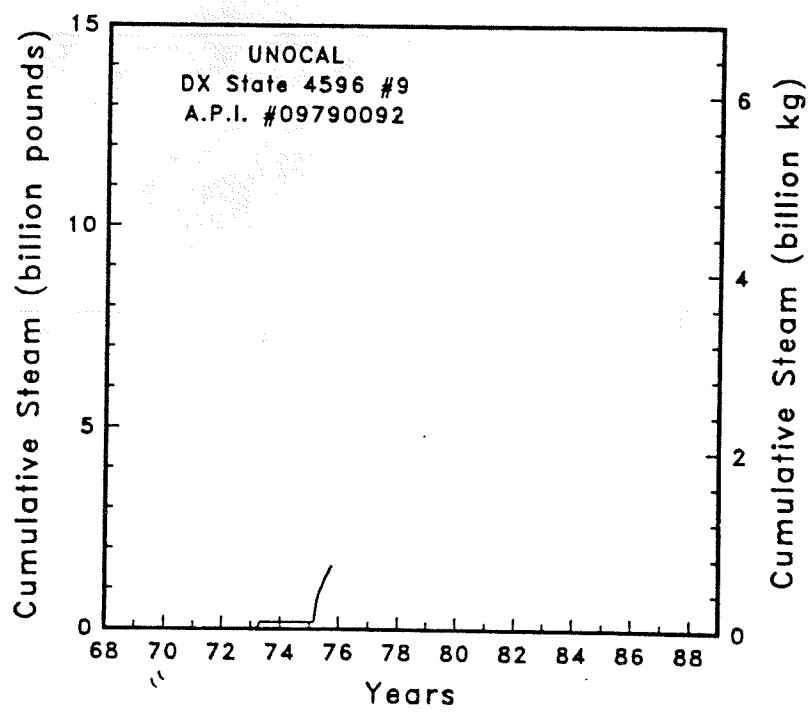

Figure A-31 Steam rate and cumulative mass flow for well DX State 4596 #9

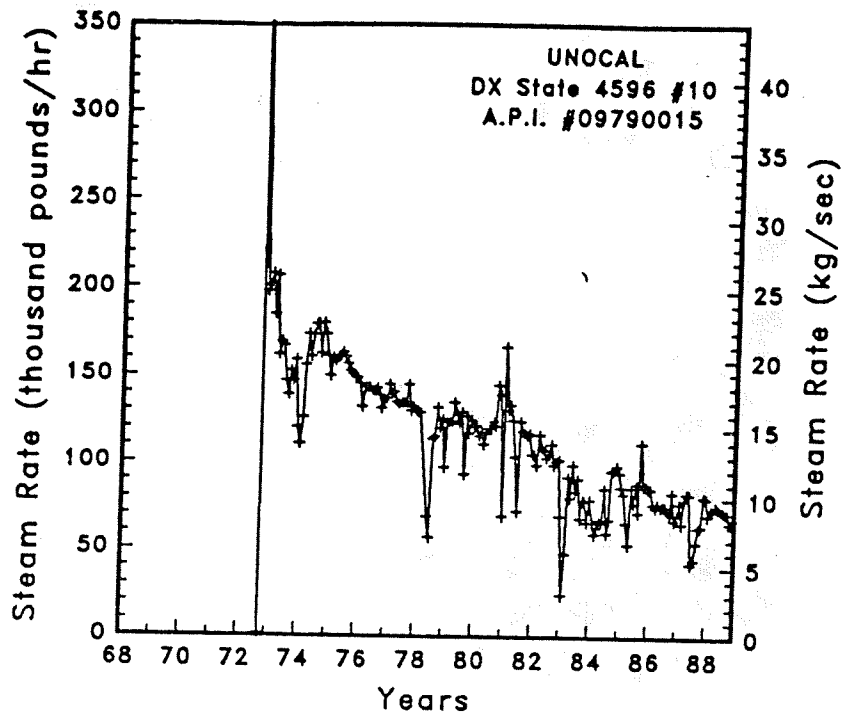

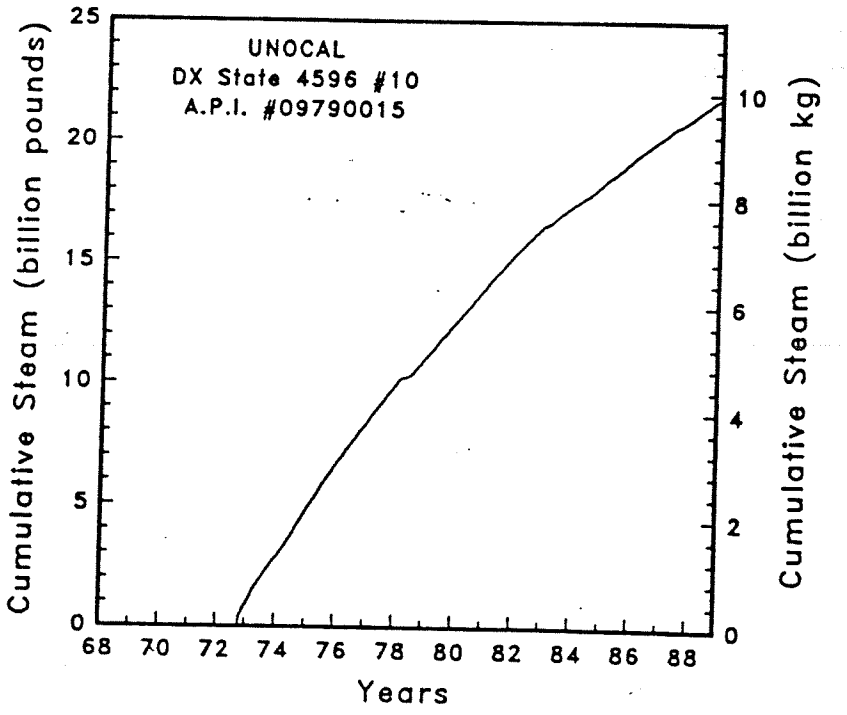

Figure A-32 Steam rate and cumulative mass flow for well DX State 4596 #10

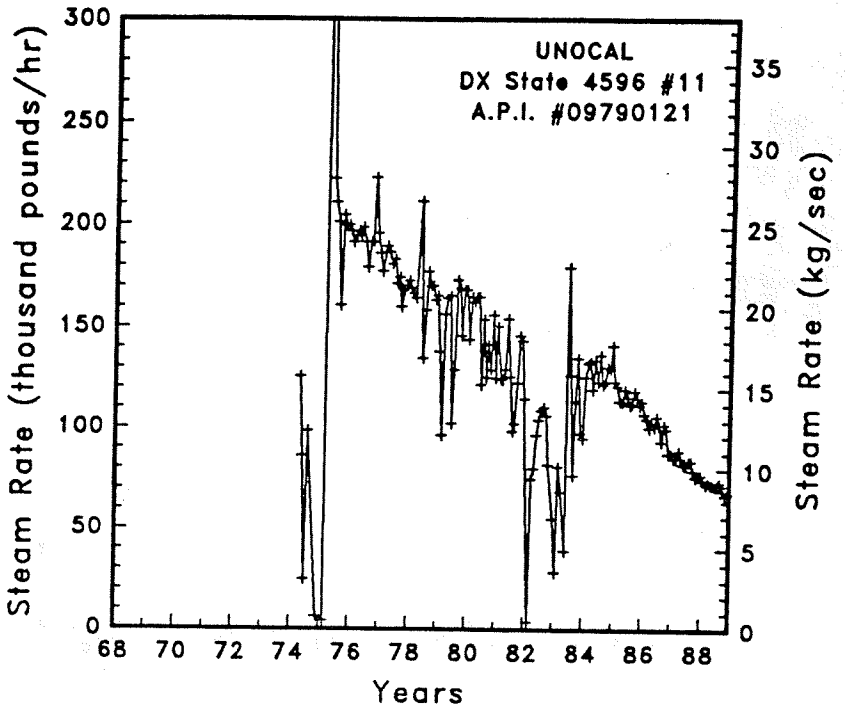

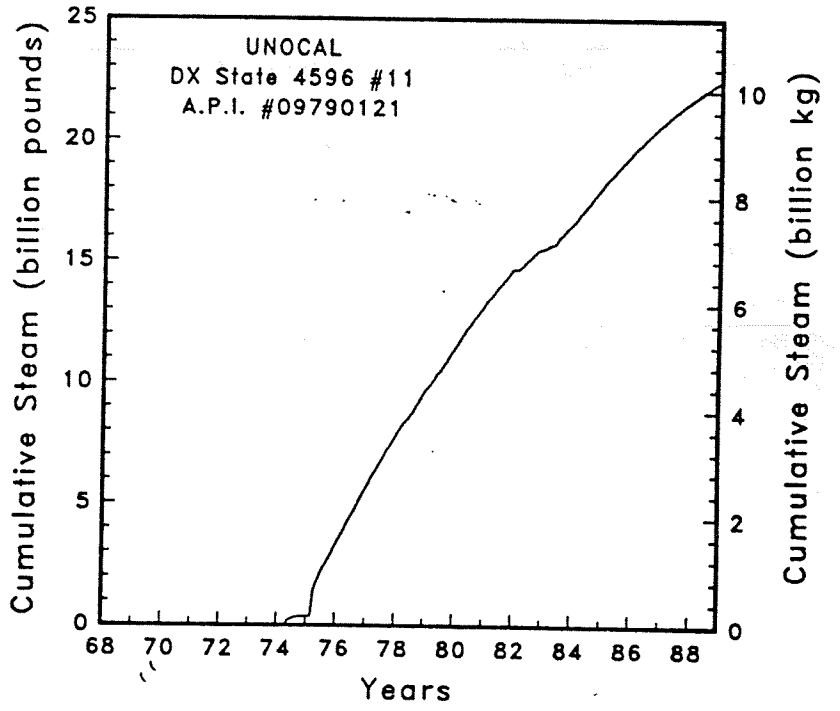

Figure A-33 Steam rate and cumulative mass flow for well DX State 4596 #11

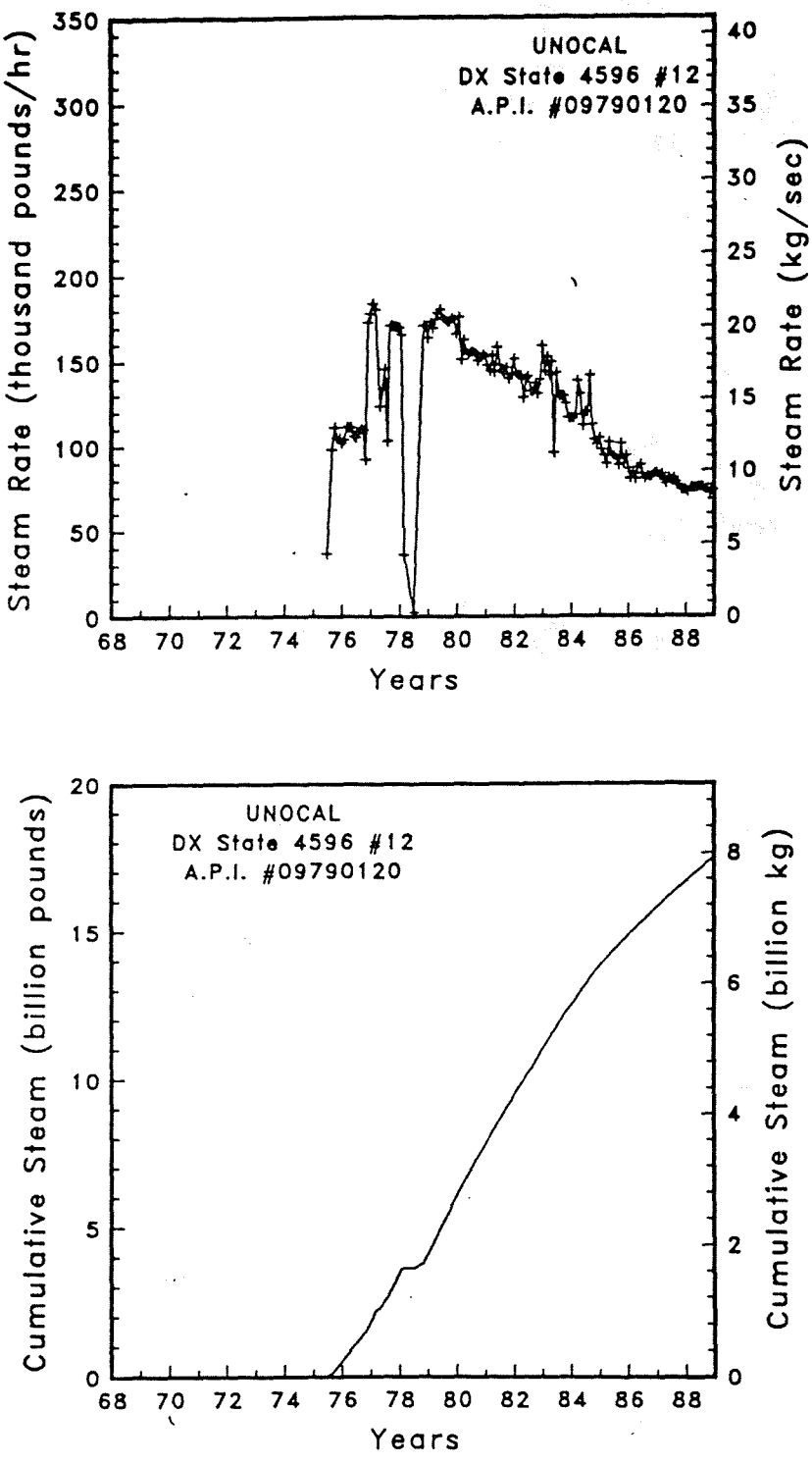

Figure A-34 Steam rate and cumulative mass flow for well DX State 4596 #12

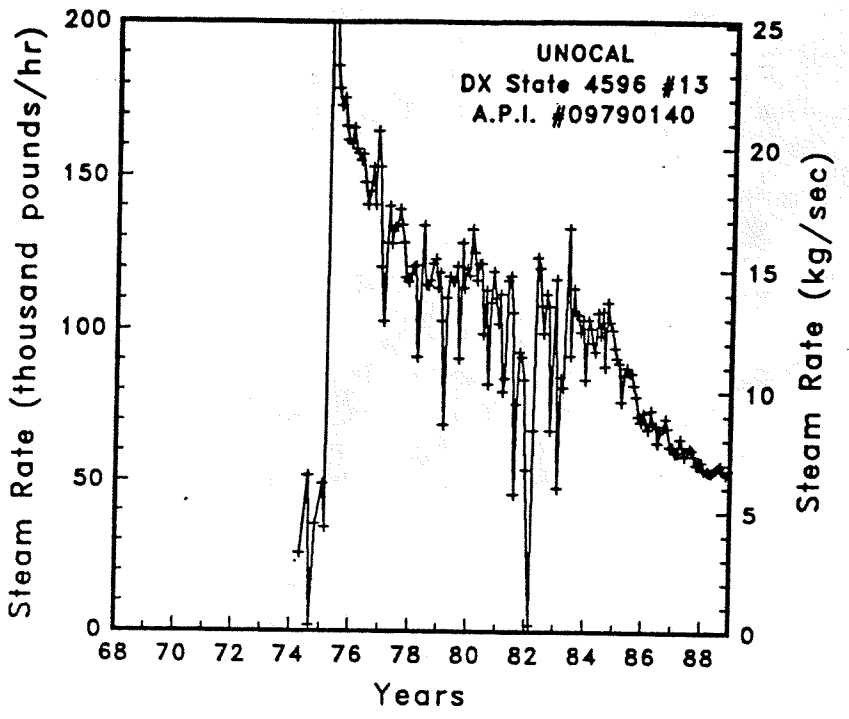

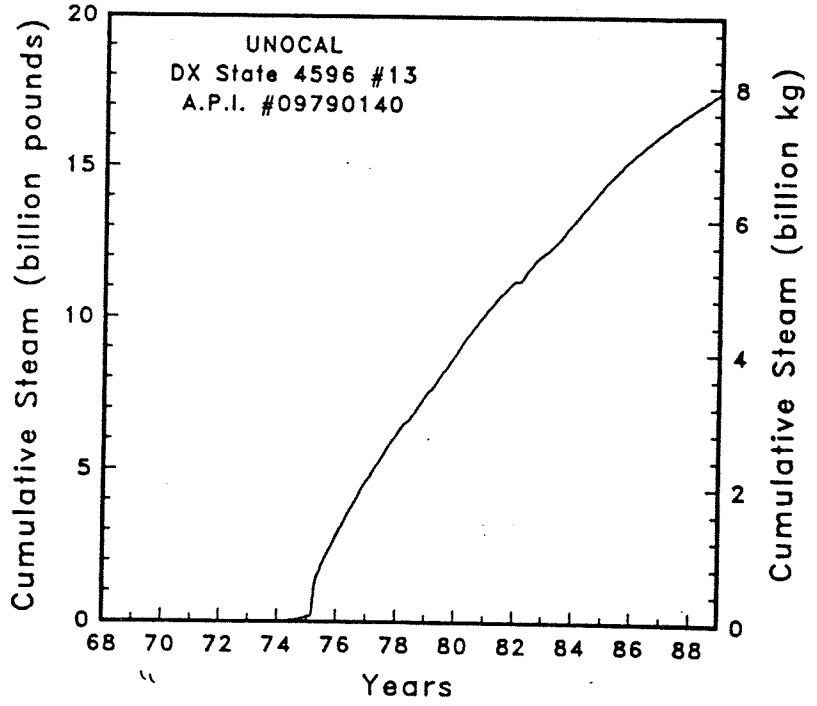

Figure A-35 Steam rate and cumulative mass flow for well DX State 4596 #13

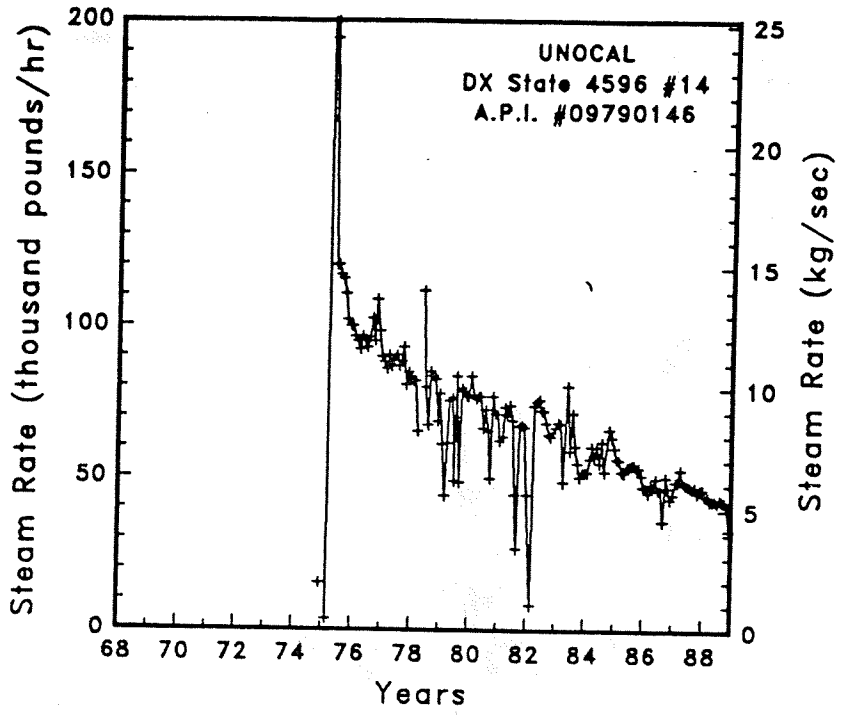

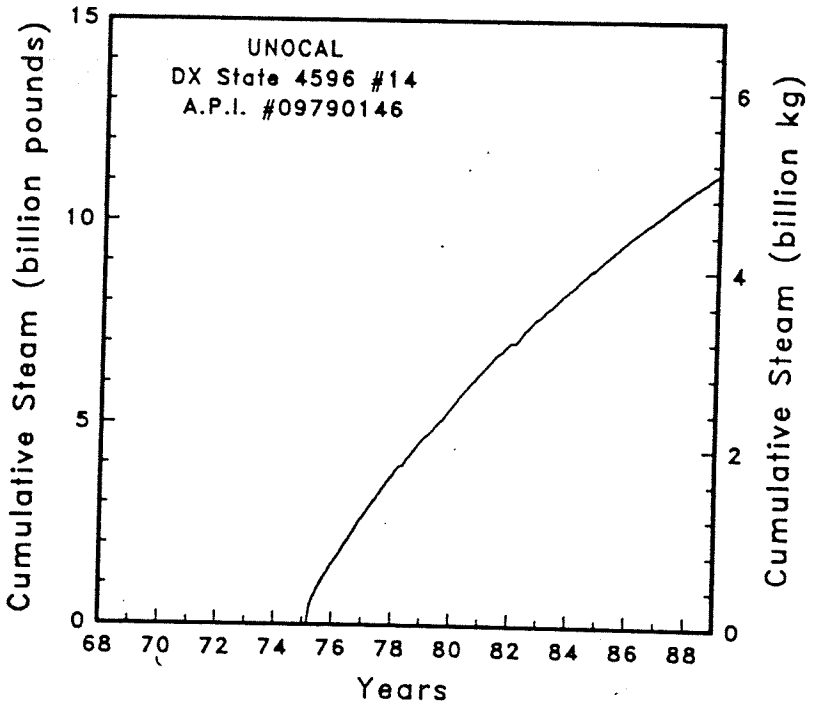

Figure A-36 Steam rate and cumulative mass flow for well DX State 4596 #14

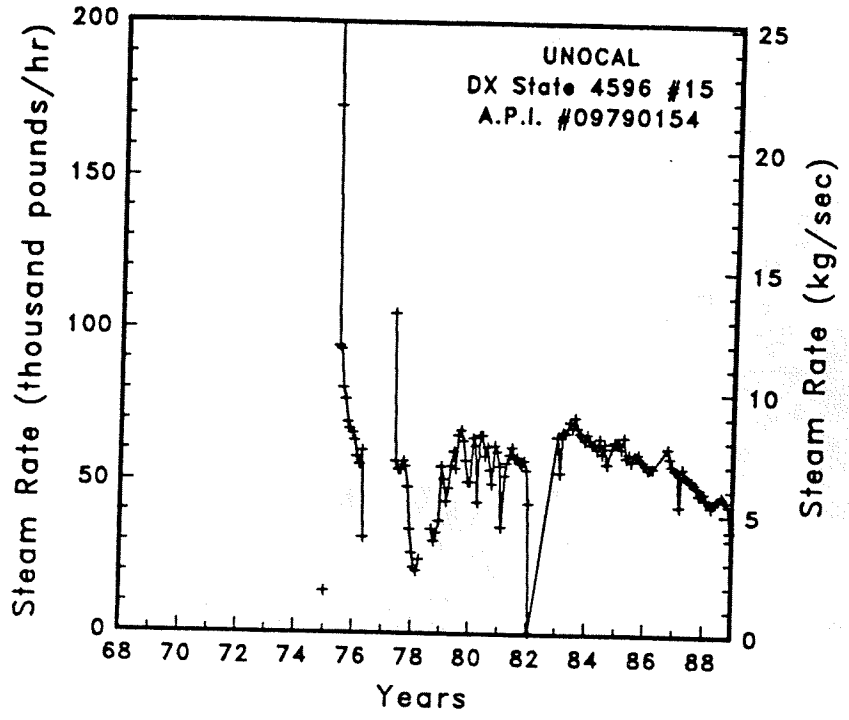

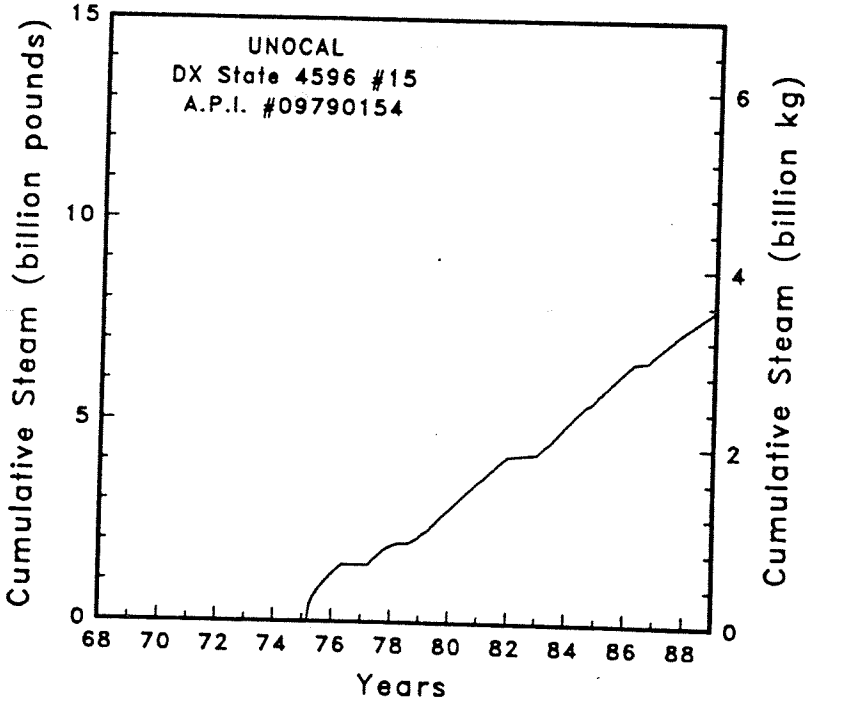

Figure A-37 Steam rate and cumulative mass flow for well DX State 4596 #15

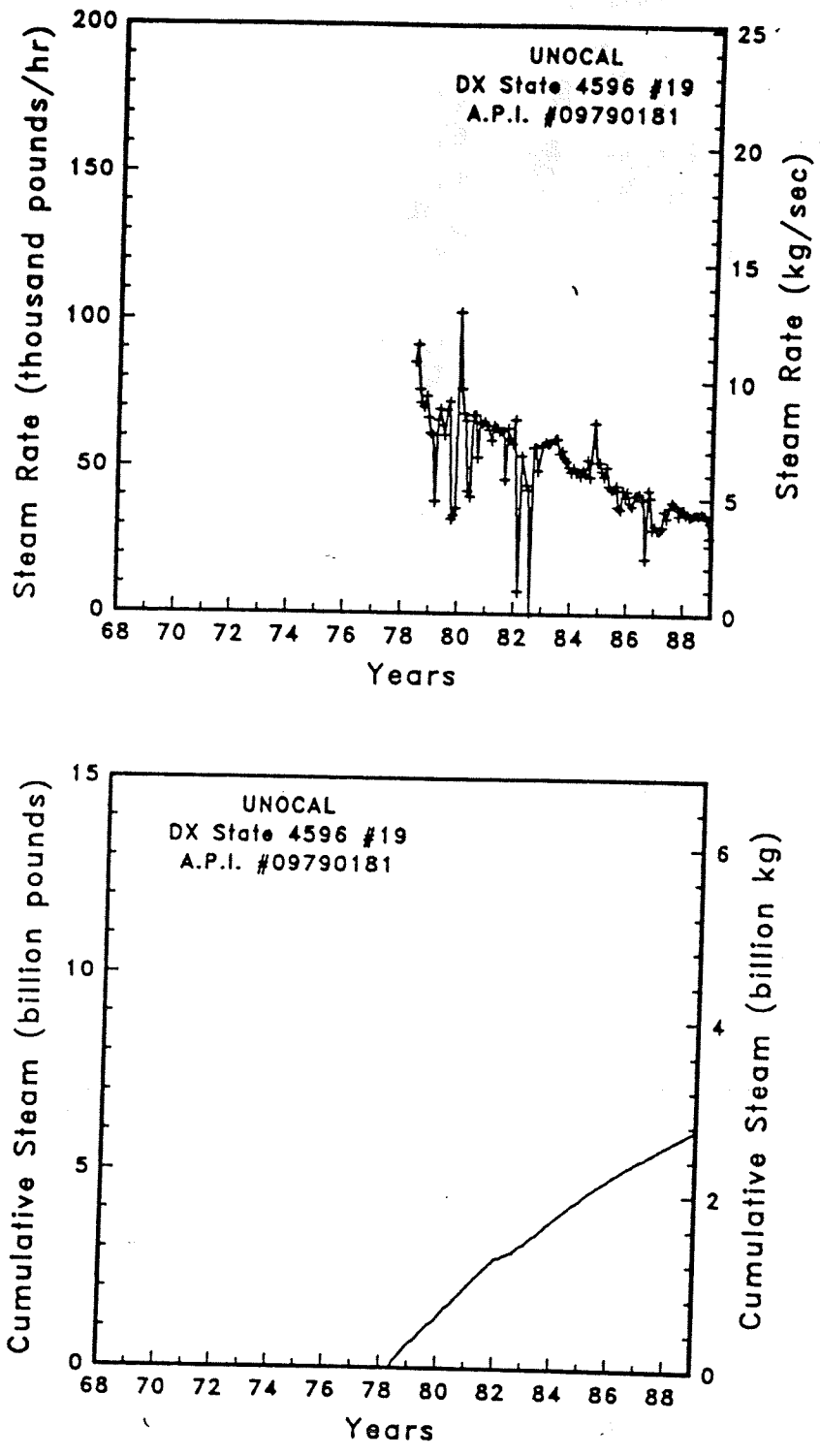

Figure A-38 Steam rate and cumulative mass flow for well DX State 4596 #19

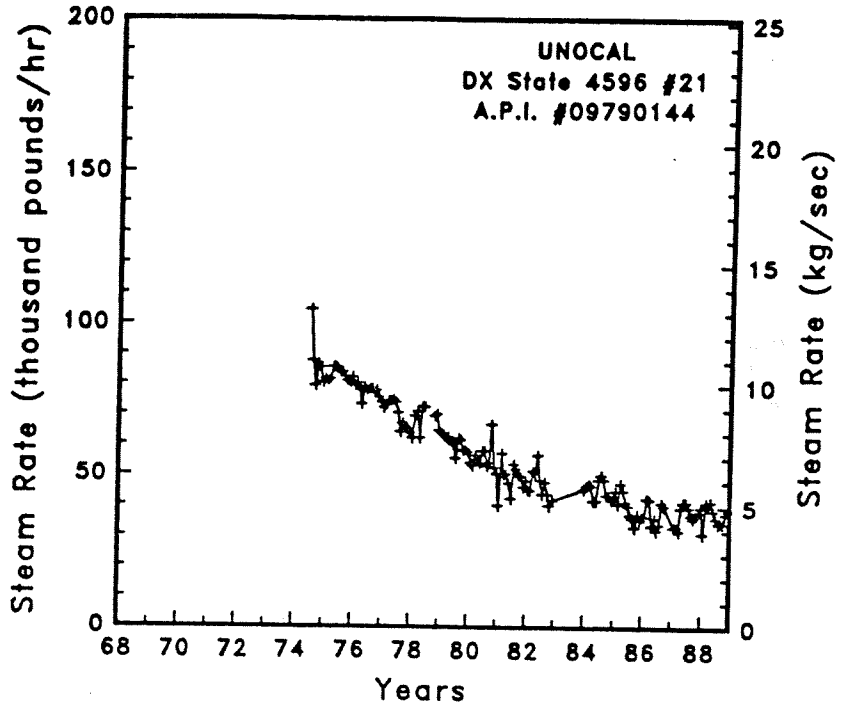

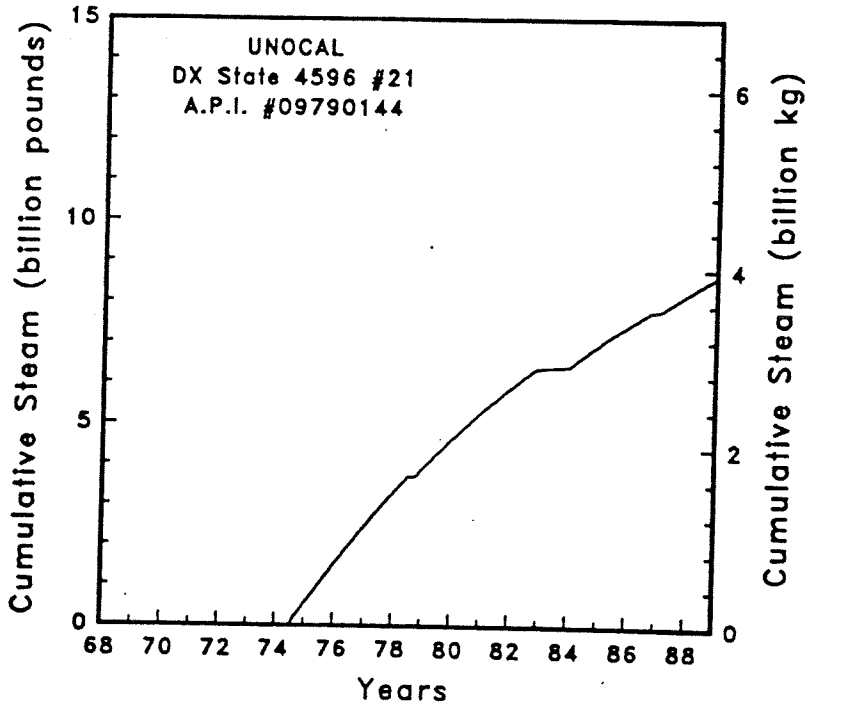

Figure A-39 Steam rate and cumulative mass flow for well DX State 4596 #21

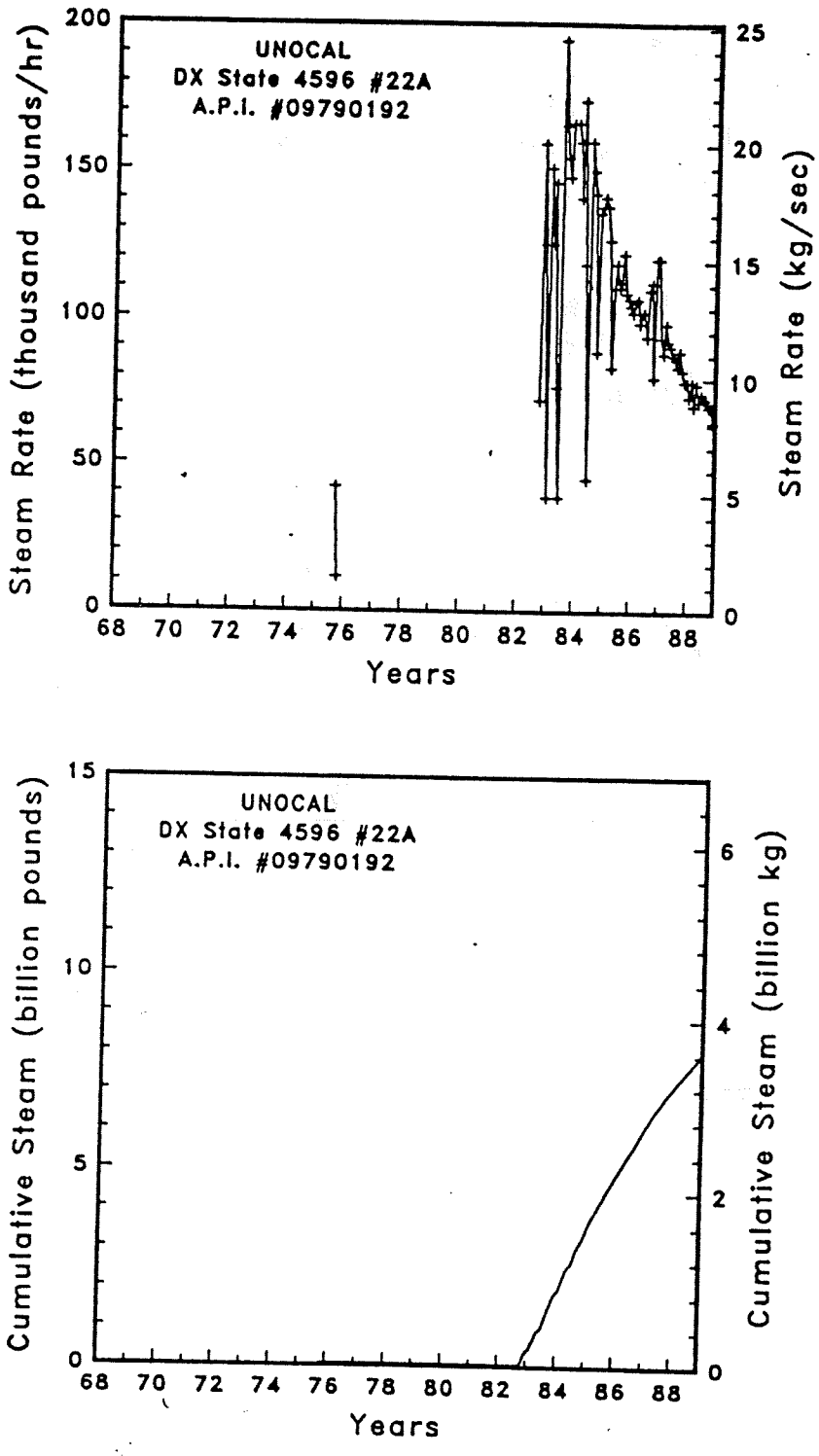

Figure A-40 Steam rate and cumulative mass flow for well DX State 4596 #22A

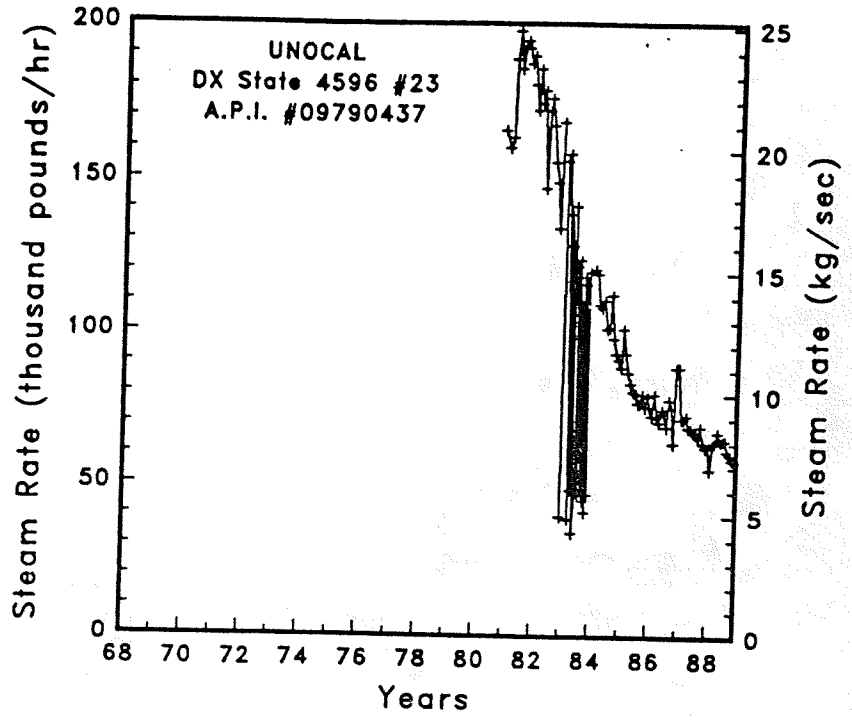

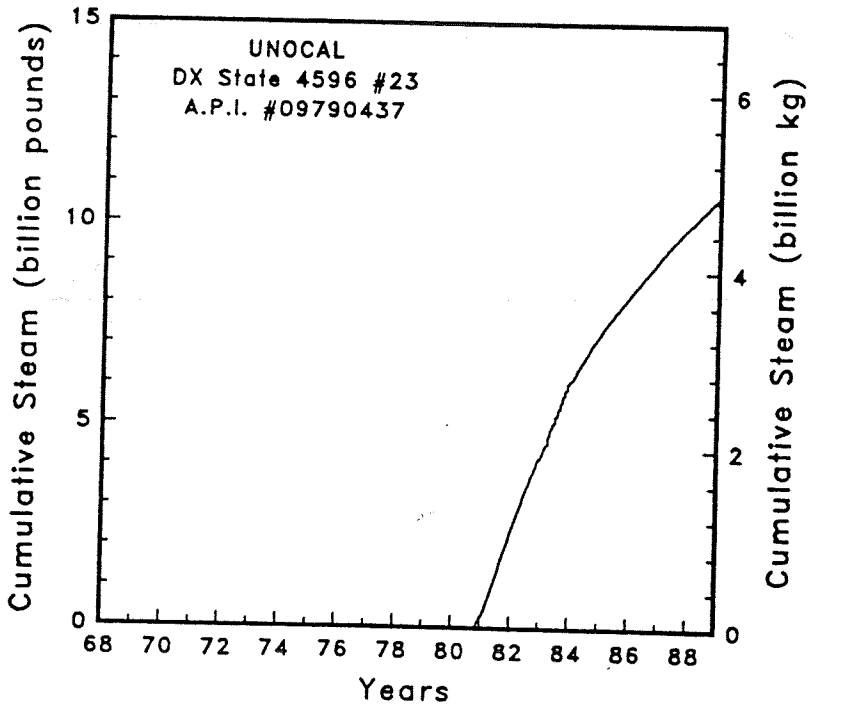

Figure A-41 Steam rate and cumulative mass flow for well DX State 4596 #23

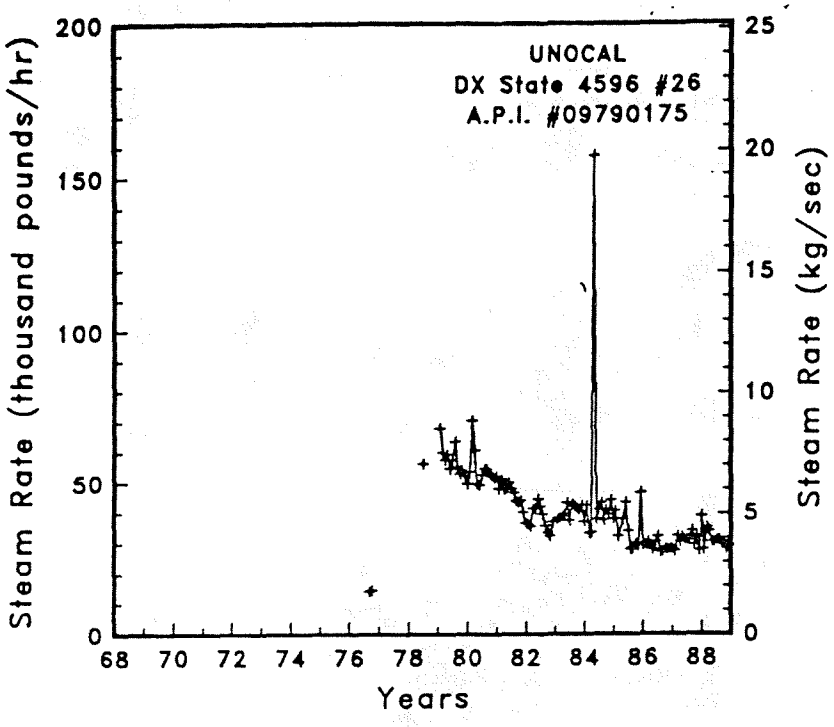

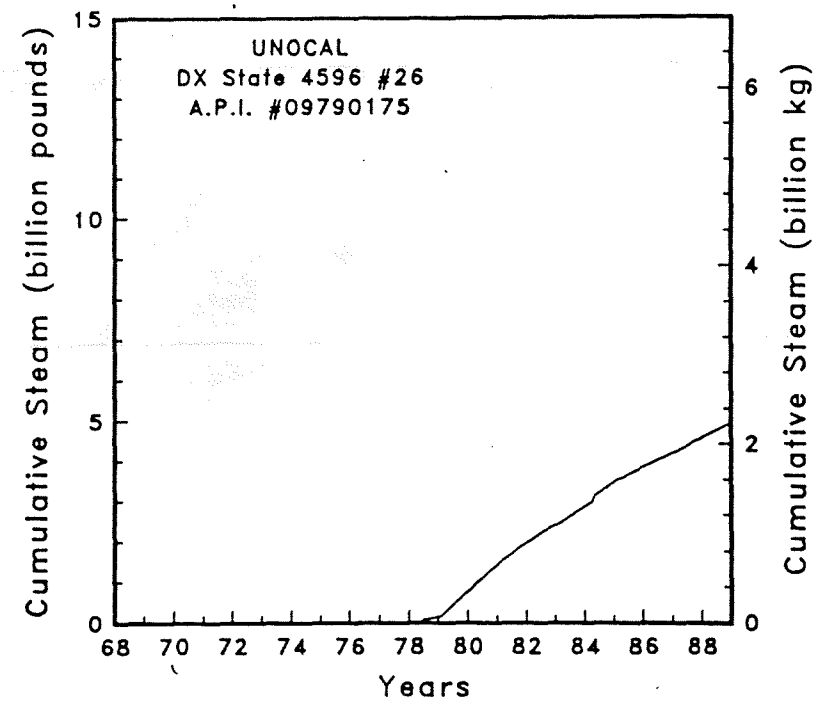

Figure A-44 Steam rate and cumulative mass flow for well DX State 4596 #26

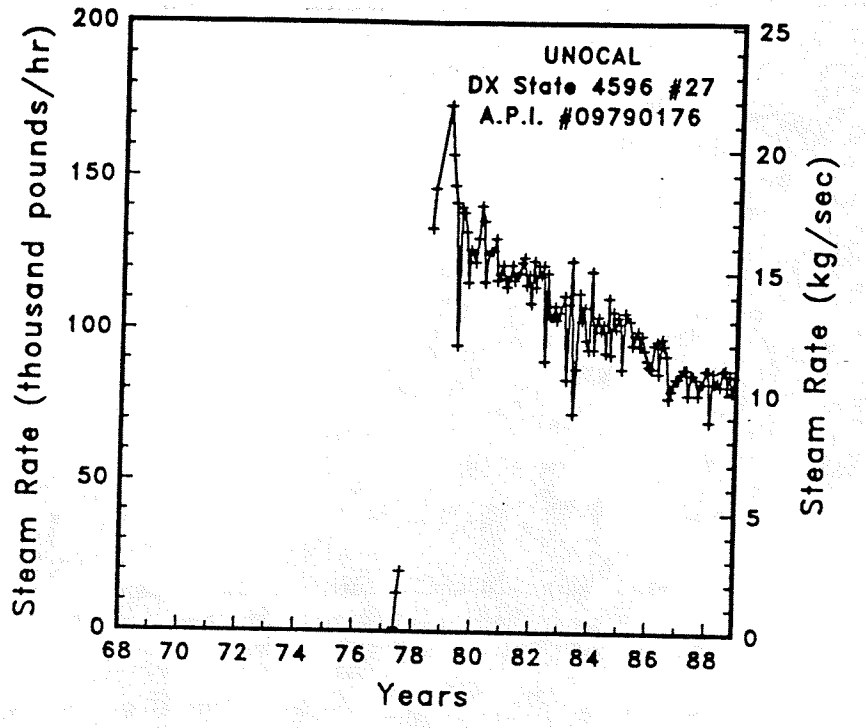

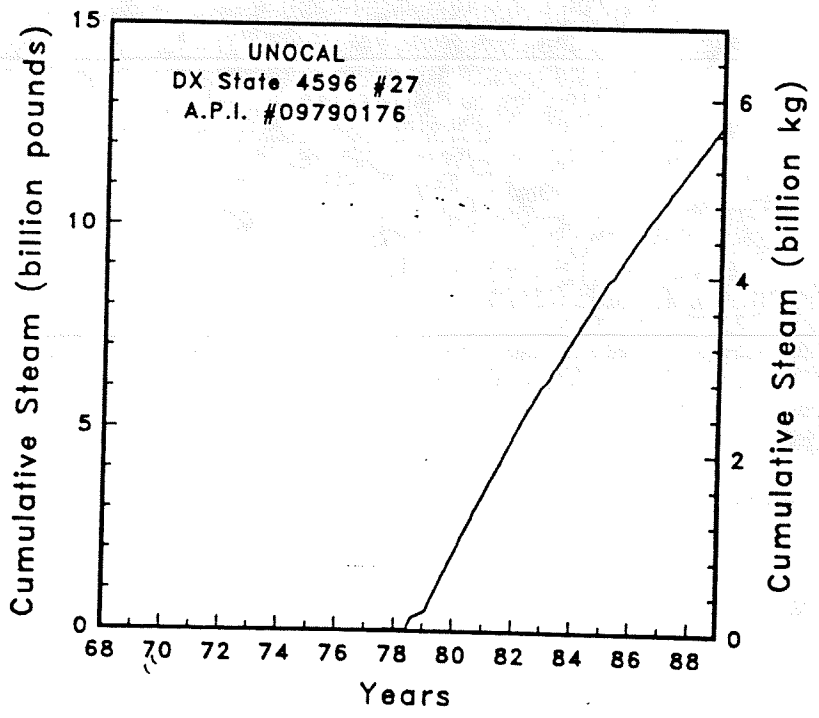

Figure A-45 Steam rate and cumulative mass flow for well DX State 4596 #27

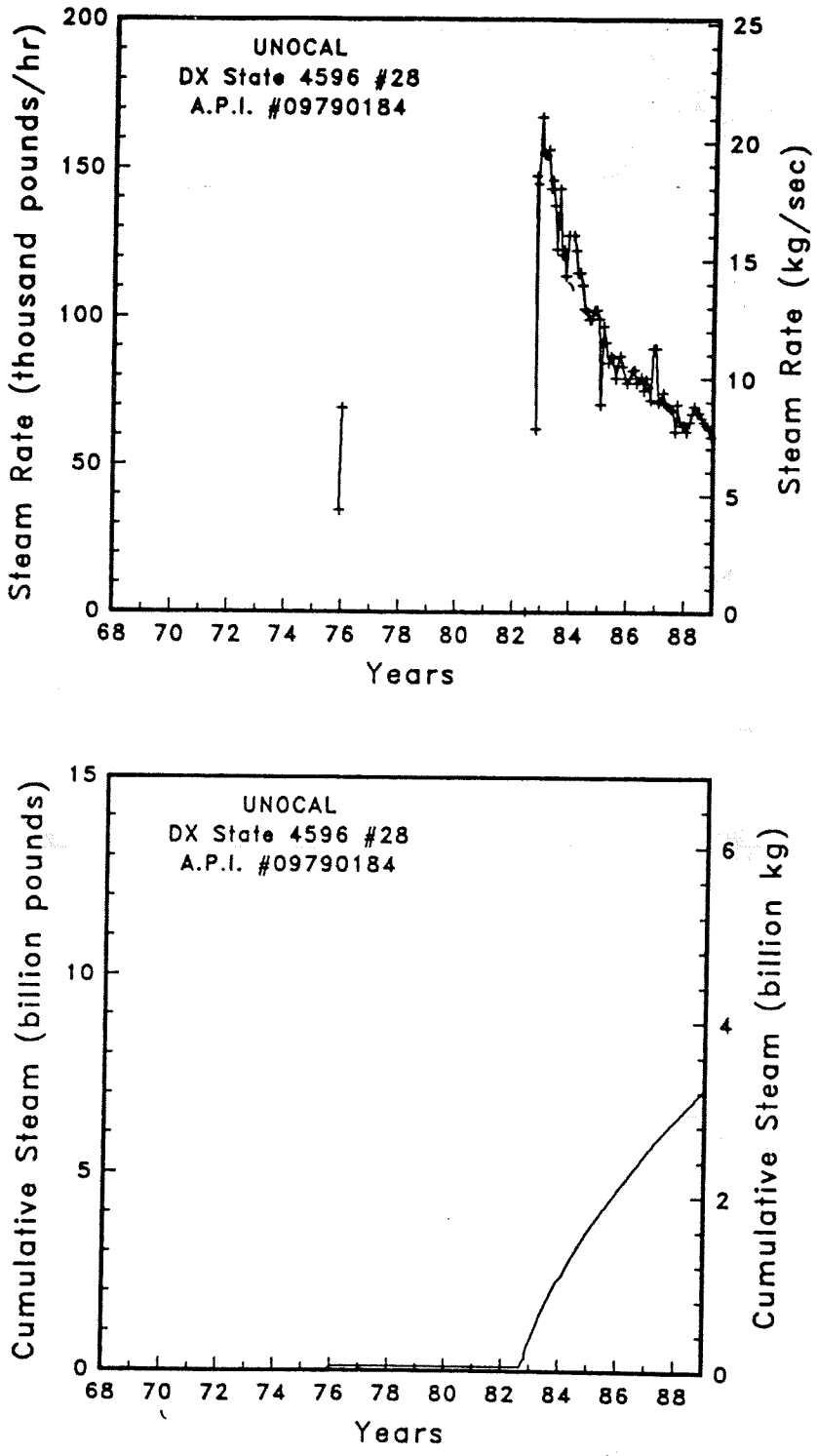

Figure A-46 Steam rate and cumulative mass flow for well DX State 4596 #28

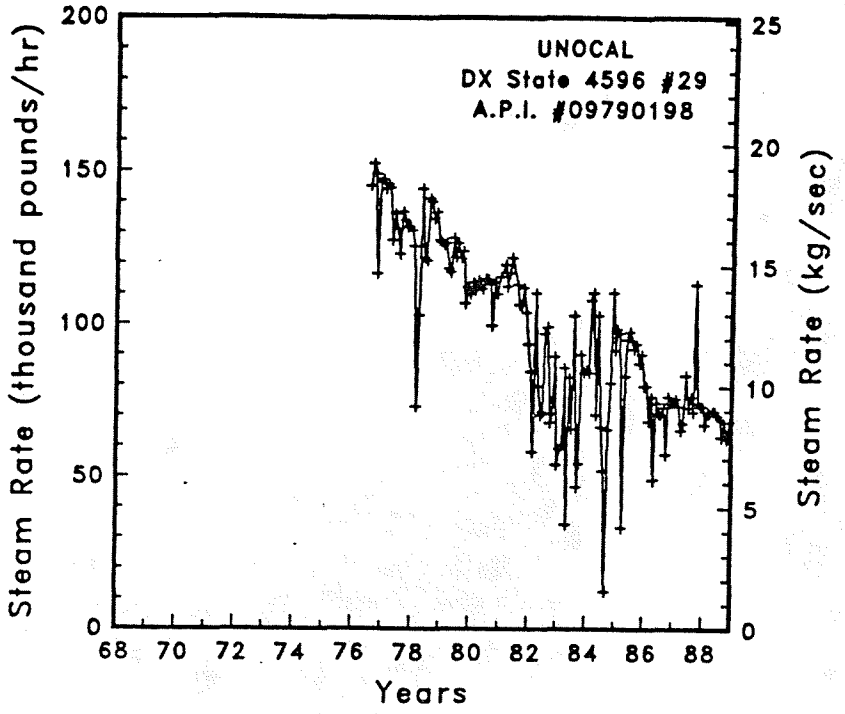

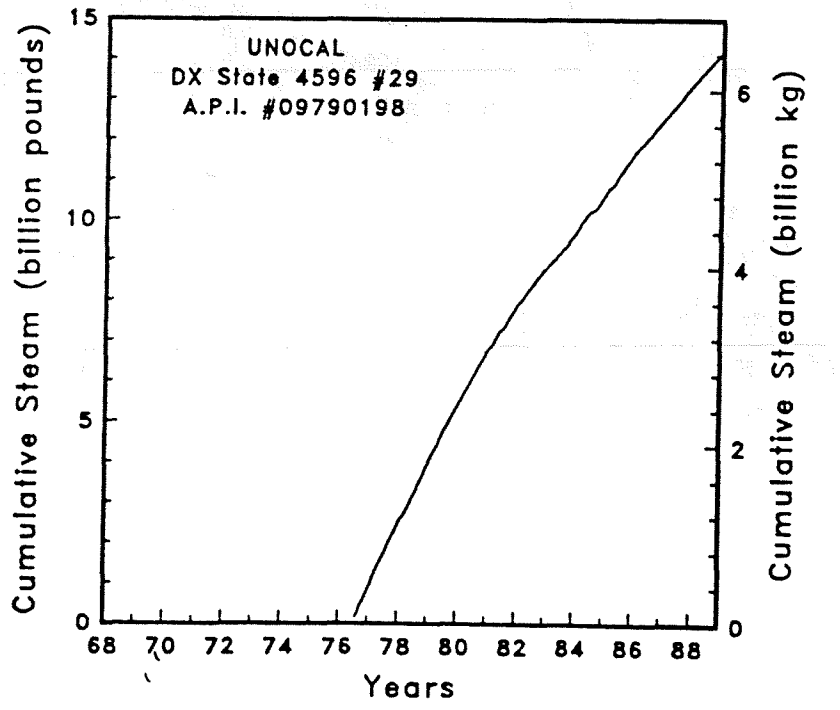

Figure A-47 Steam rate and cumulative mass flow for well DX State 4596 #29

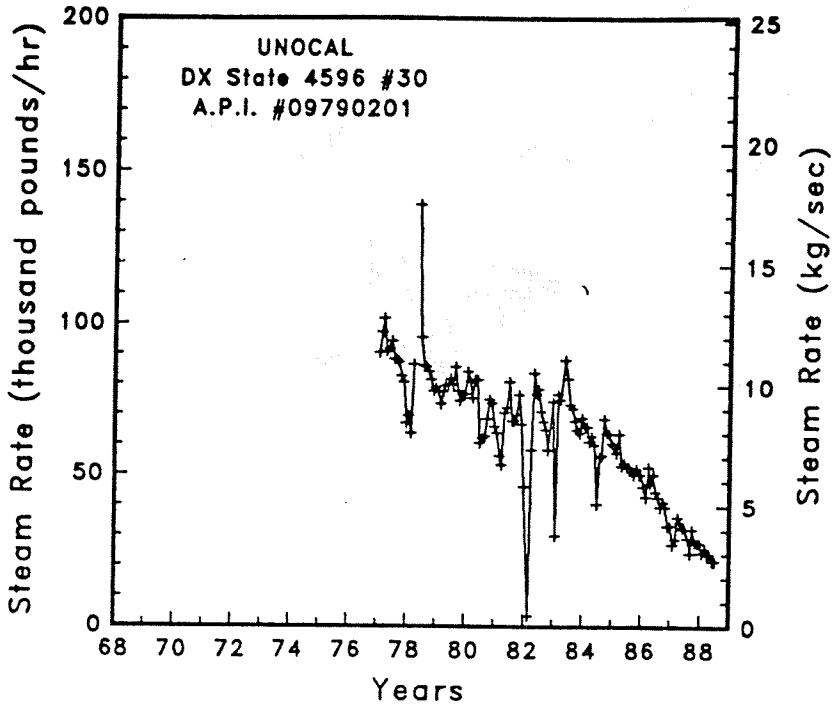

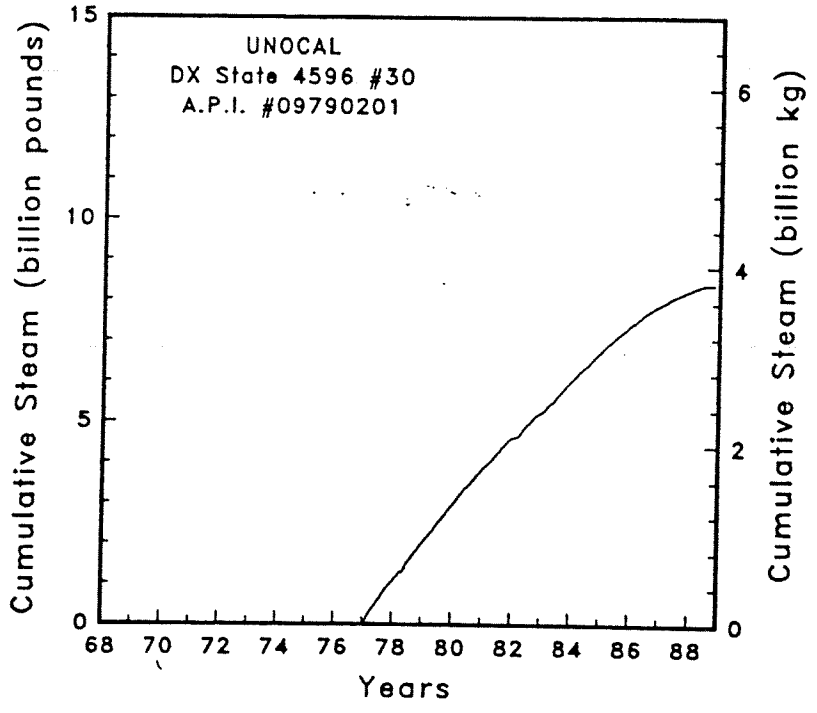

Figure A-48 Steam rate and cumulative mass flow for well DX State 4596 #30

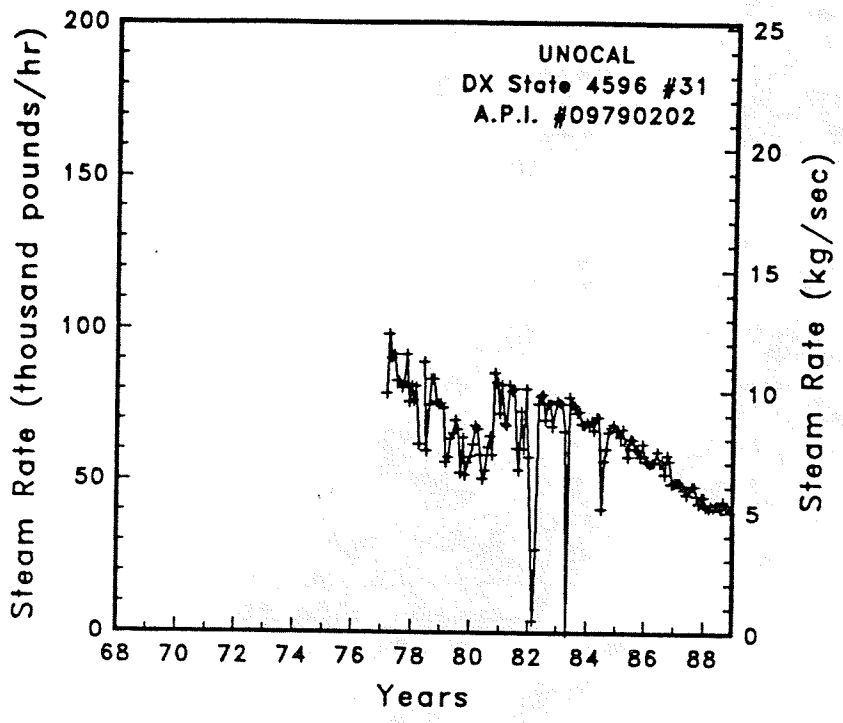

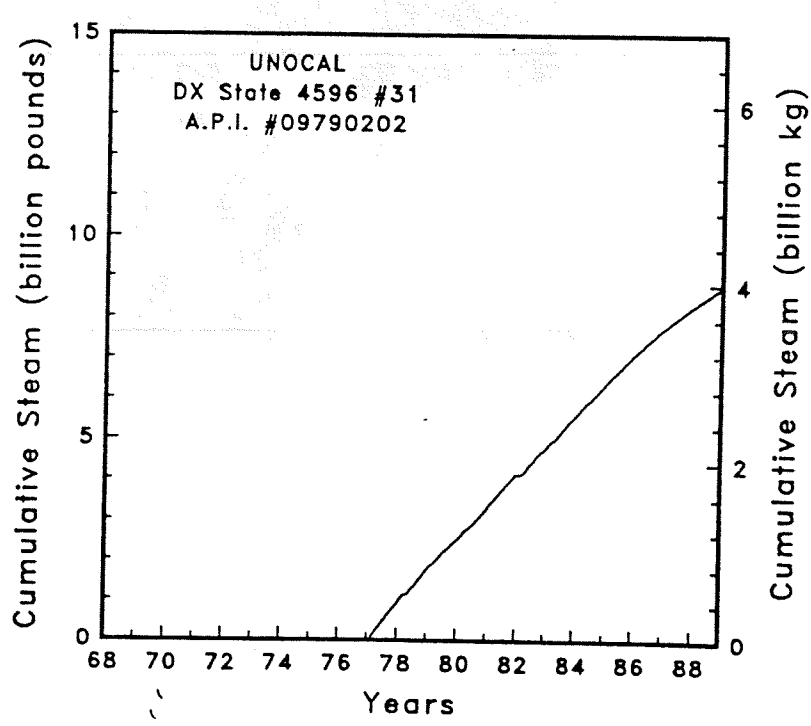

Figure A-49 Steam rate and cumulative mass flow for well DX State 4596 #31

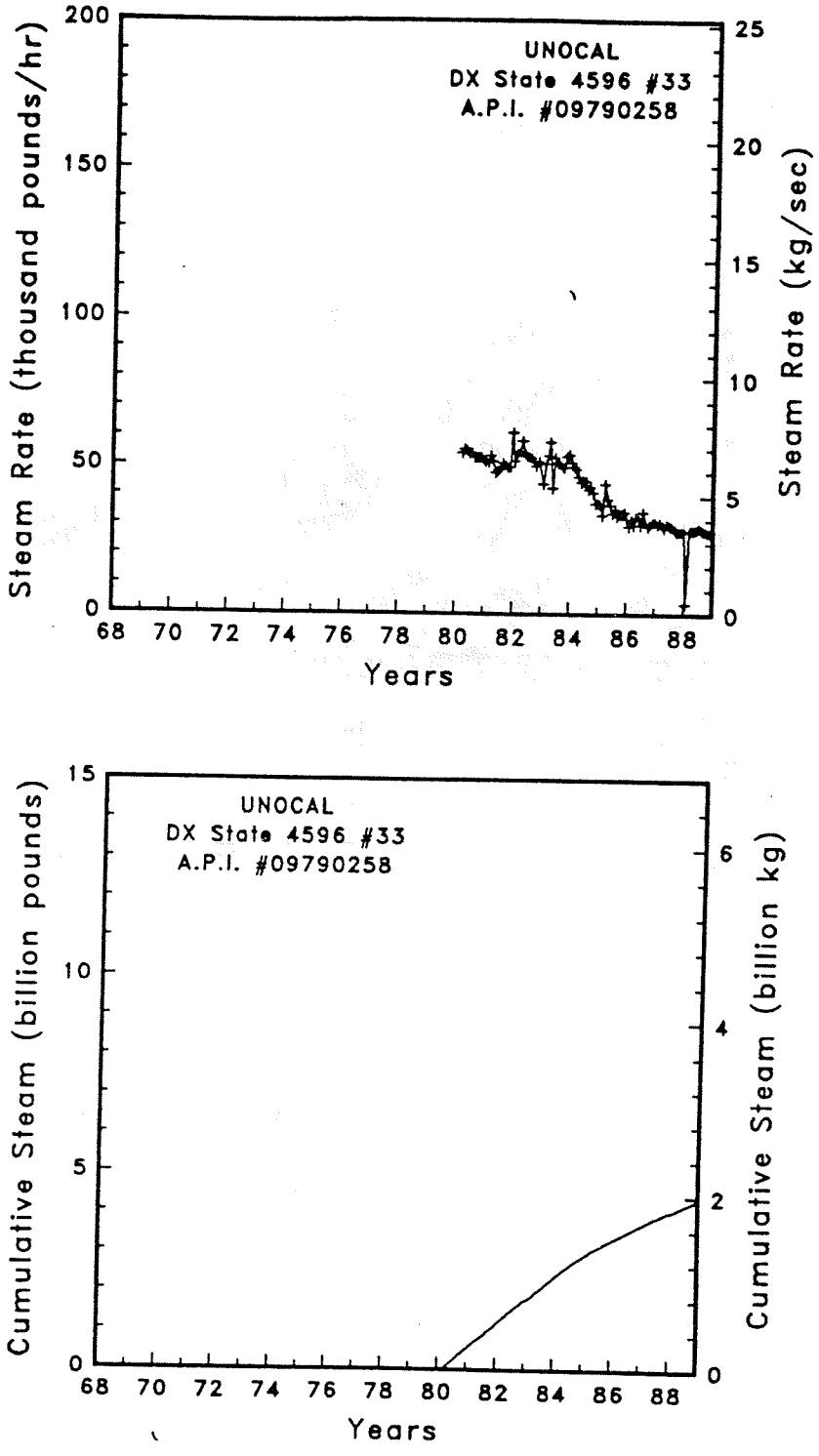

Figure A-50 Steam rate and cumulative mass flow for well DX State 4596 #33

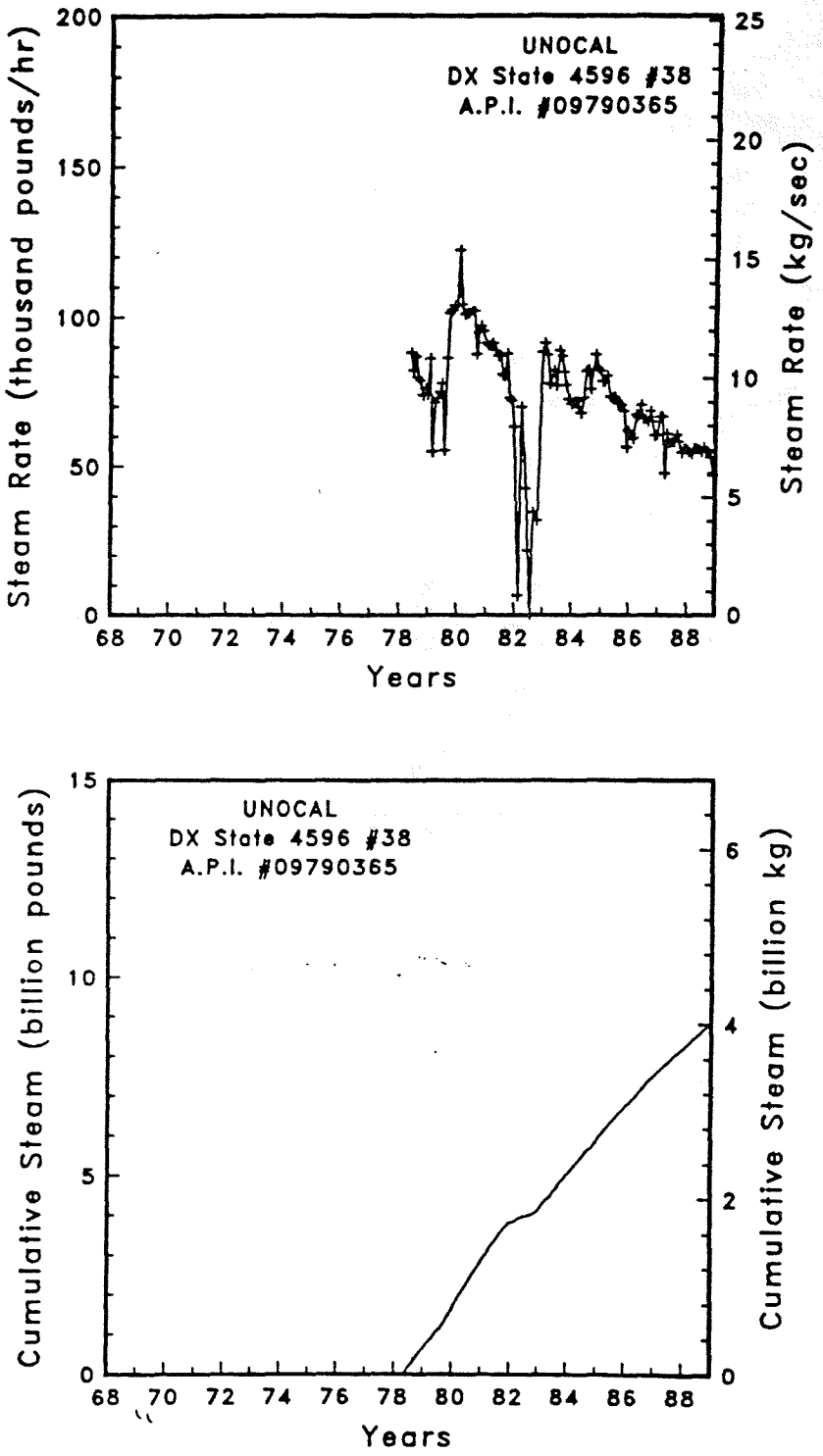

Figure A-51 Steam rate and cumulative mass flow for well DX State 4596 #38

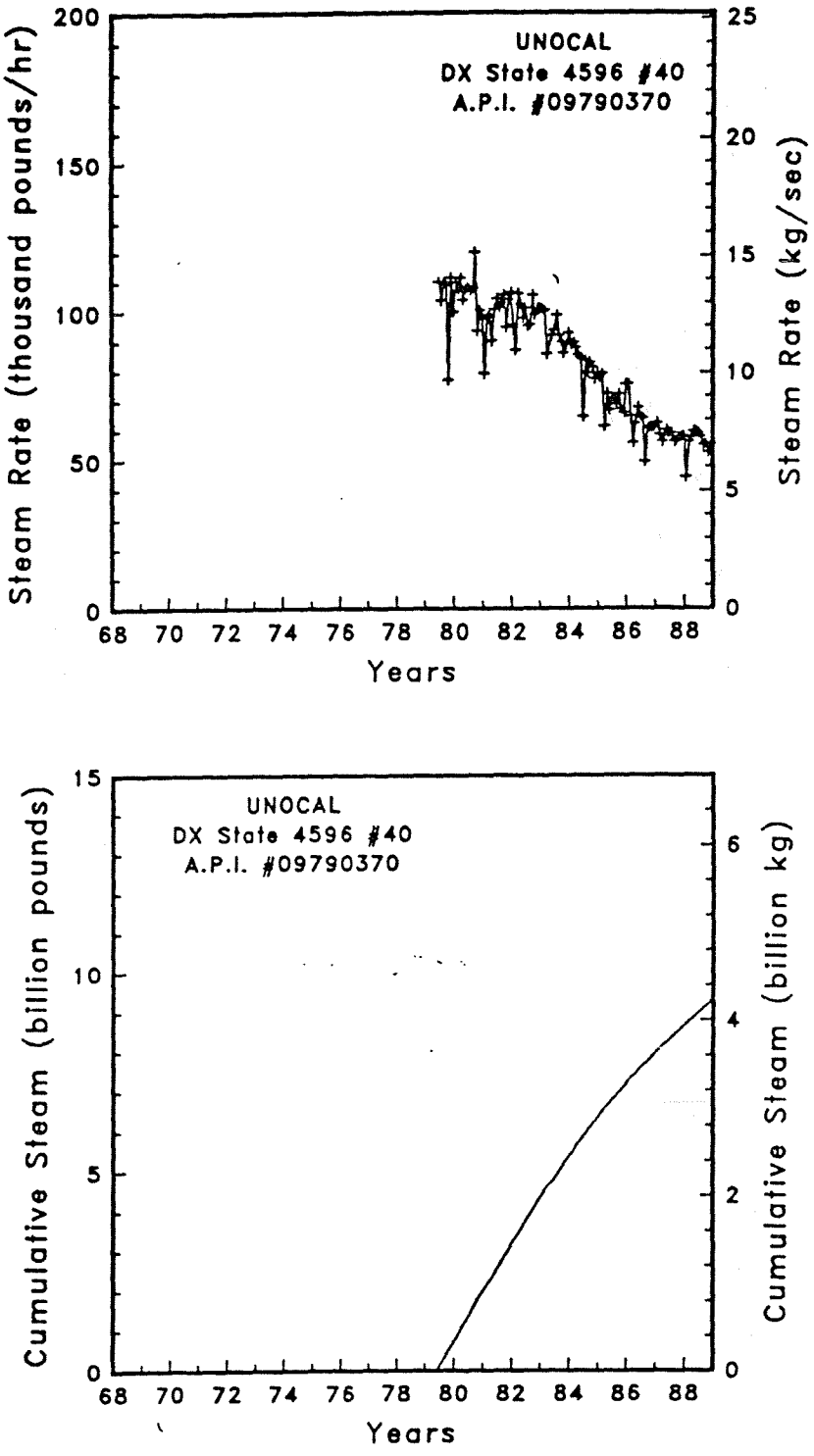

Figure A-52 Steam rate and cumulative mass flow for well DX State 4596 #40

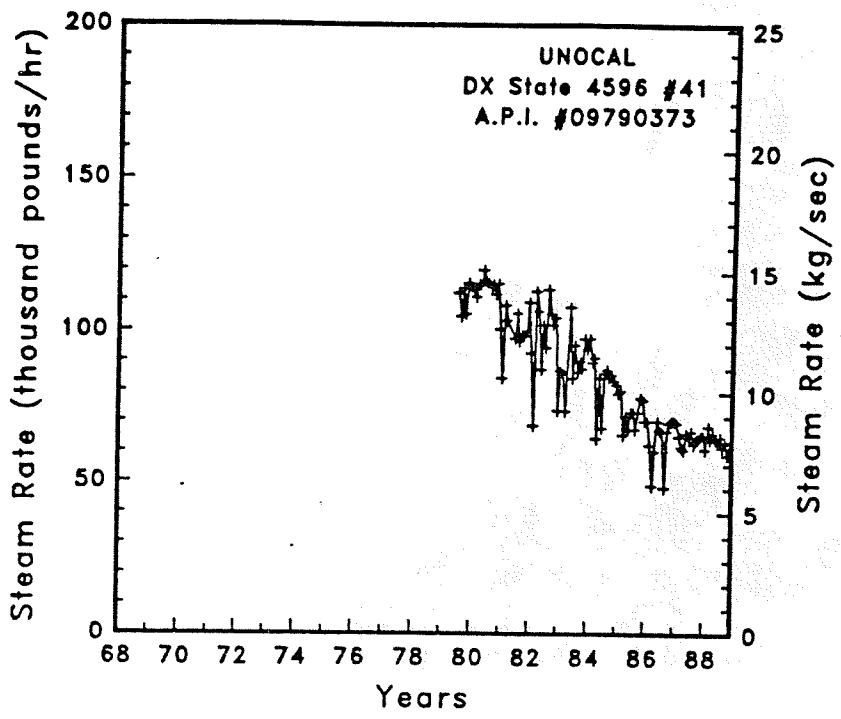

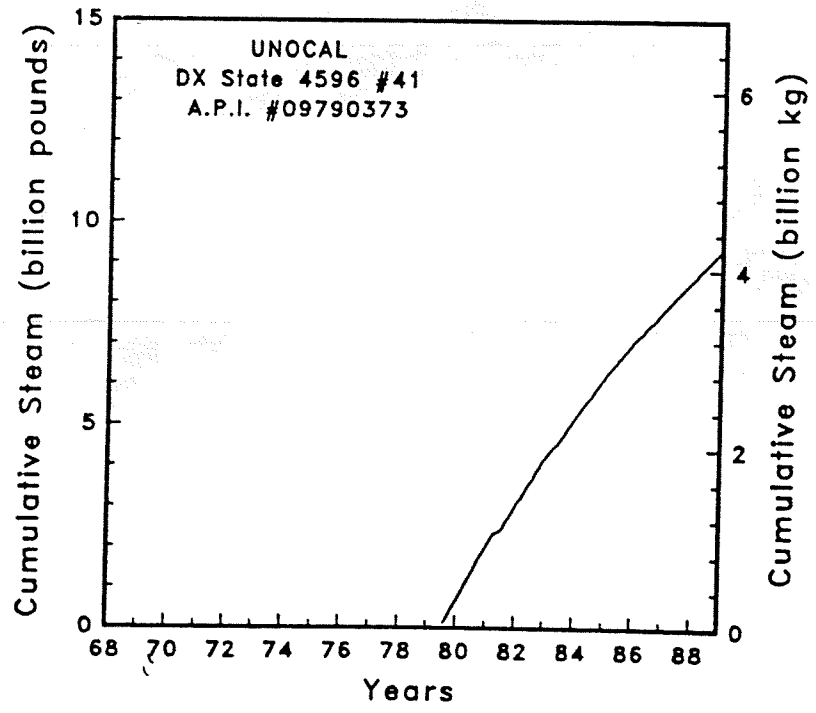

Figure A-53 Steam rate and cumulative mass flow for well DX State 4596 #41

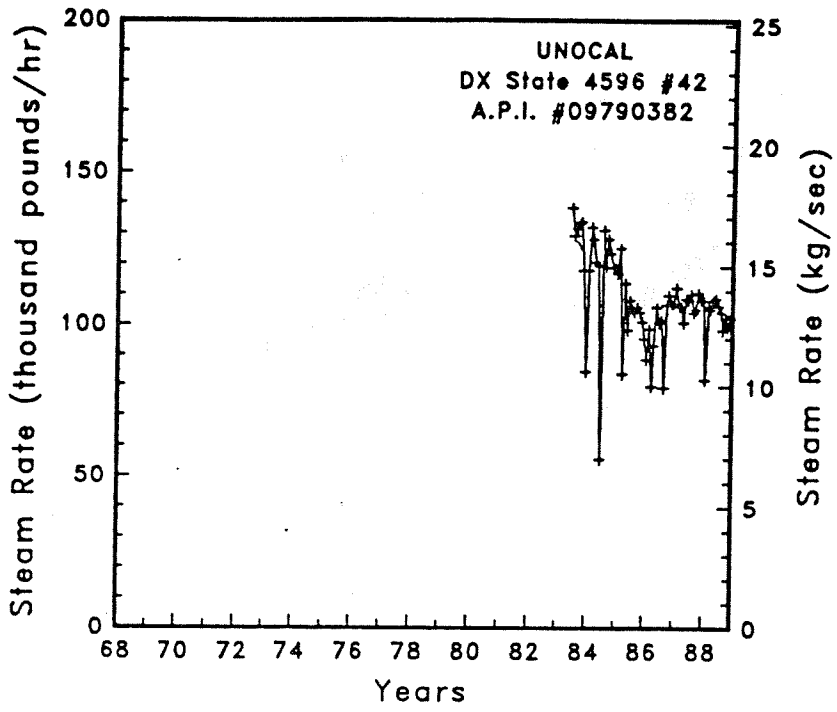

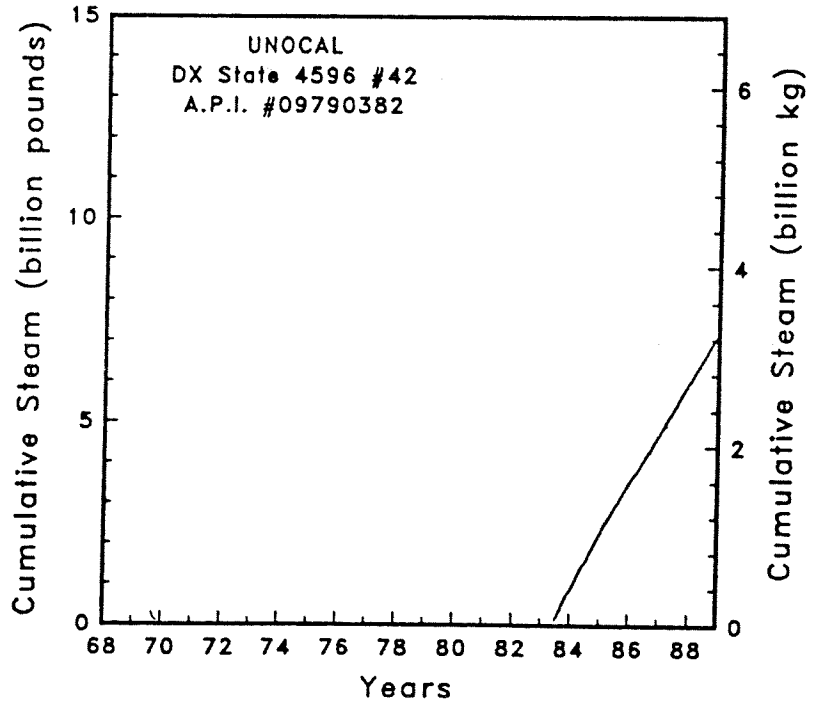

Figure A-54 Steam rate and cumulative mass flow for well DX State 4596 #42

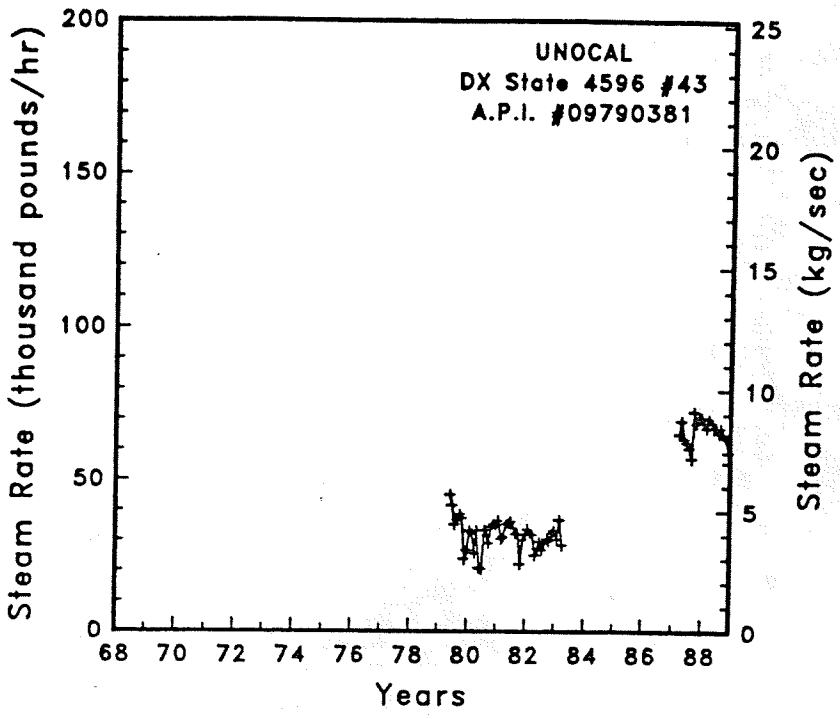

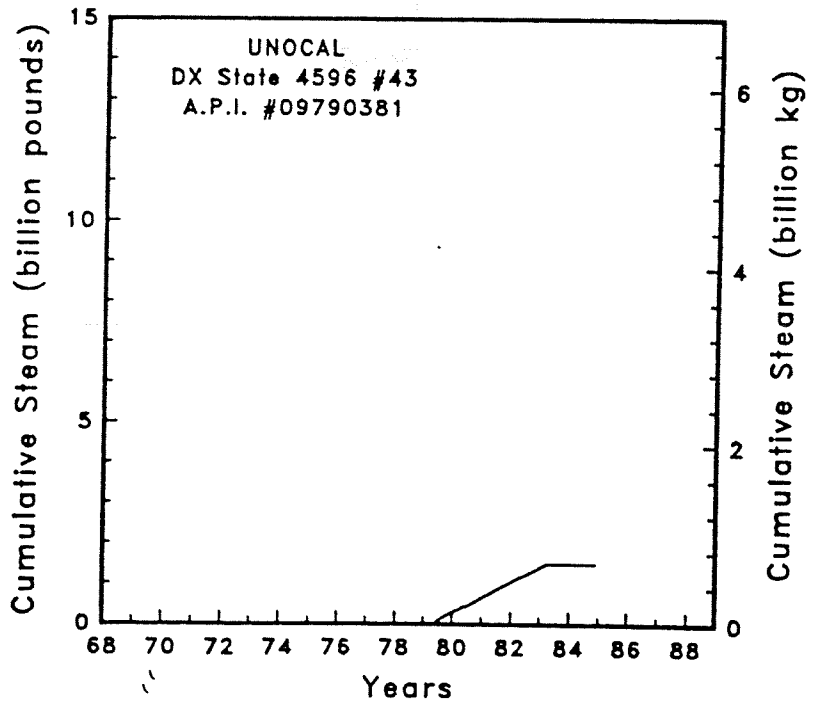

Figure A-55 Steam rate and cumulative mass flow for well DX State 4596 #43

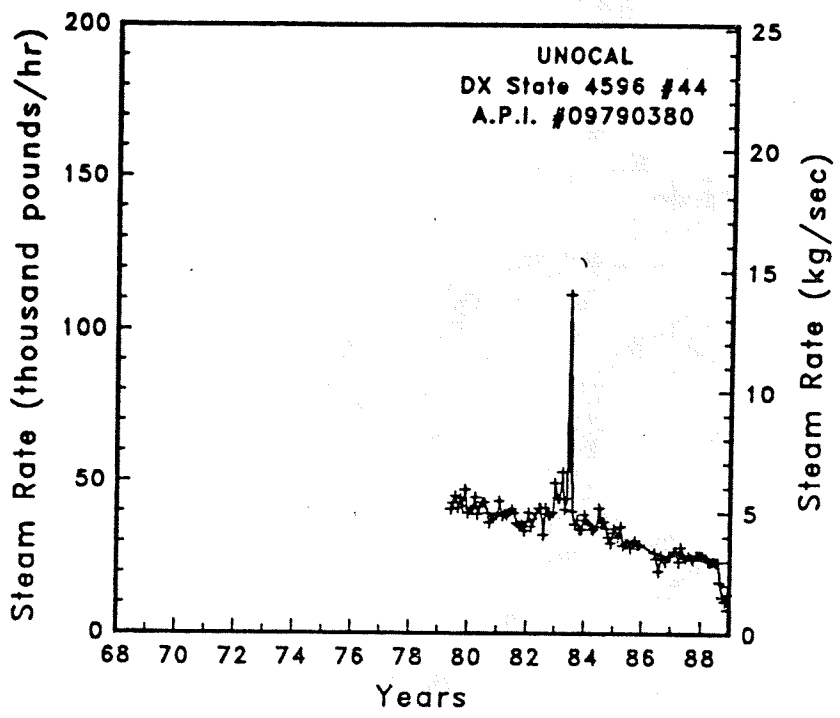

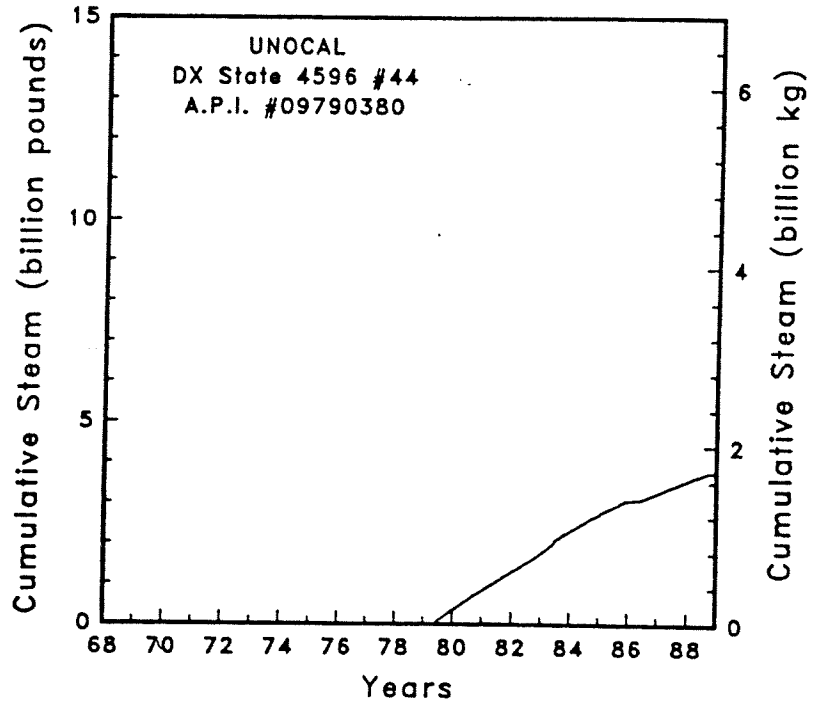

Figure A-56 Steam rate and cumulative mass flow for well DX State 4596 #44

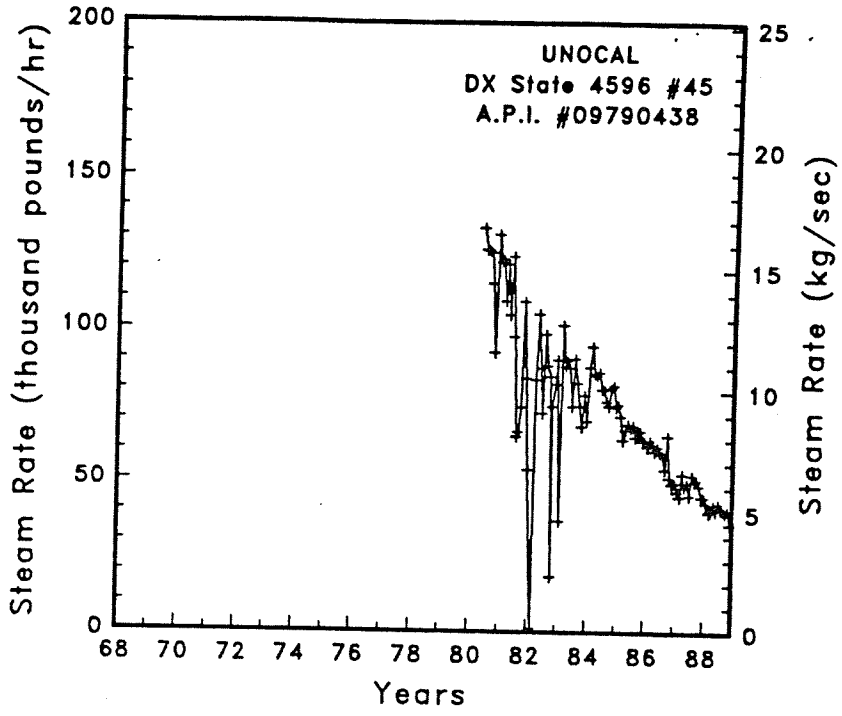

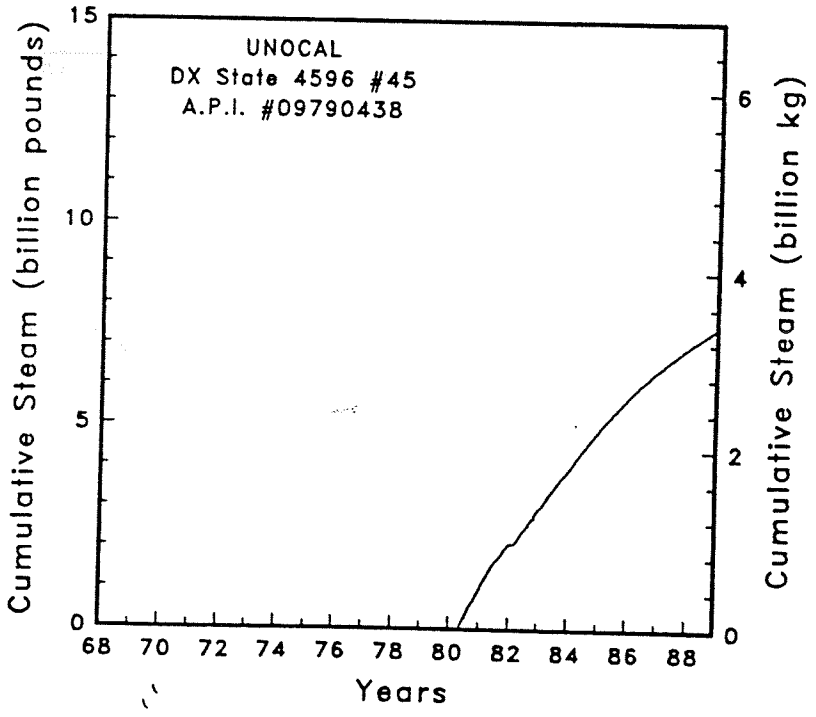

Figure A-57 Steam rate and cumulative mass flow for well DX State 4596 #45

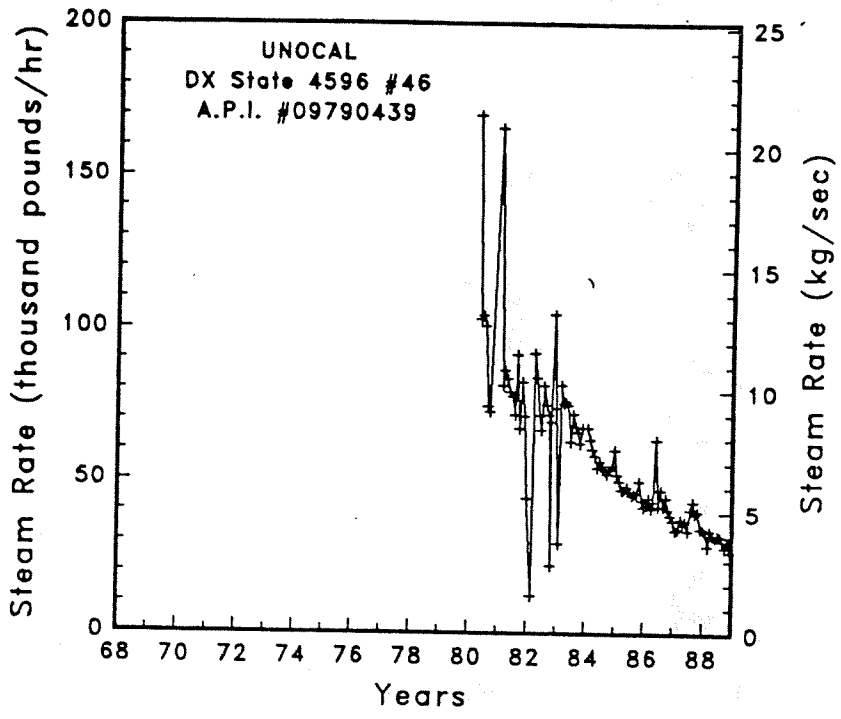

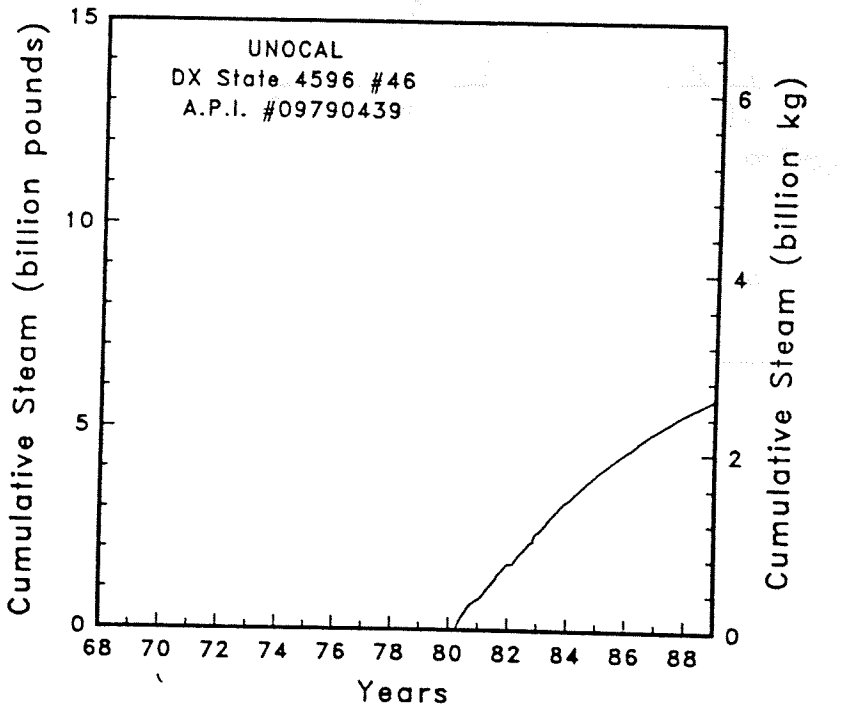

Figure A-58 Steam rate and cumulative mass flow for well DX State 4596 #46

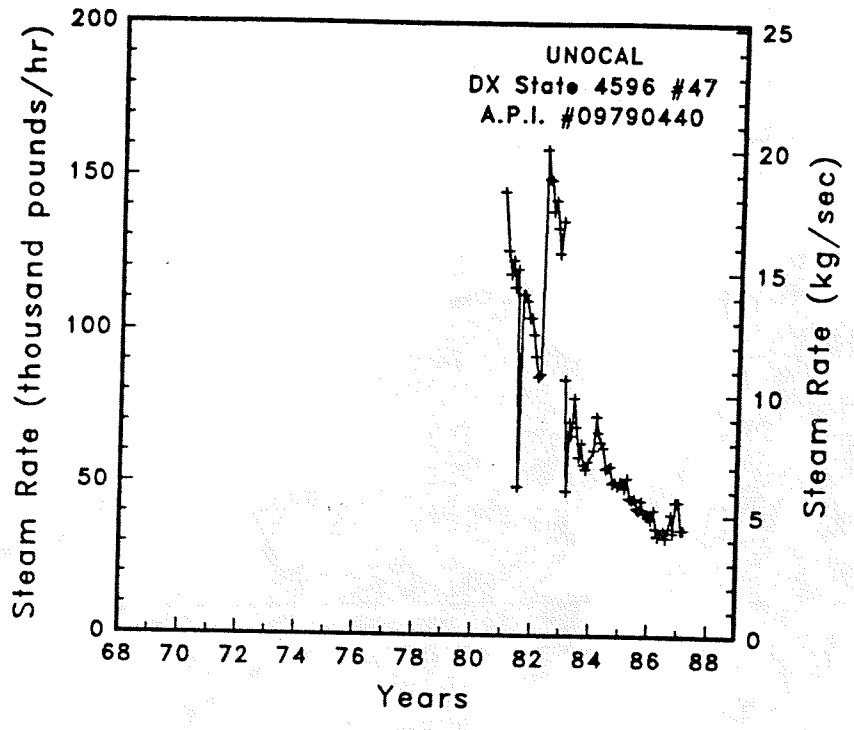

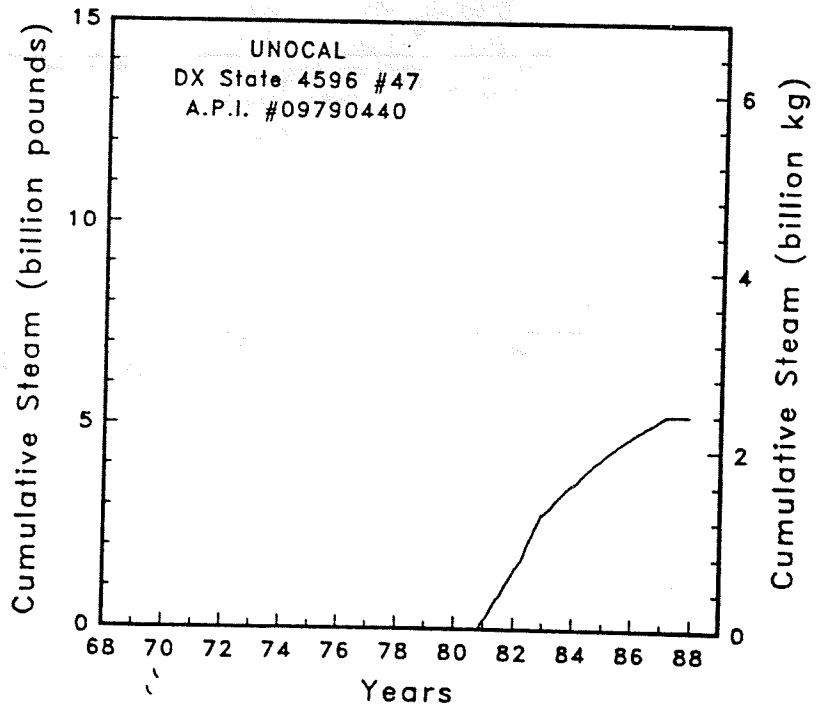

Figure A-59 Steam rate and cumulative mass flow for well DX State 4596 #47

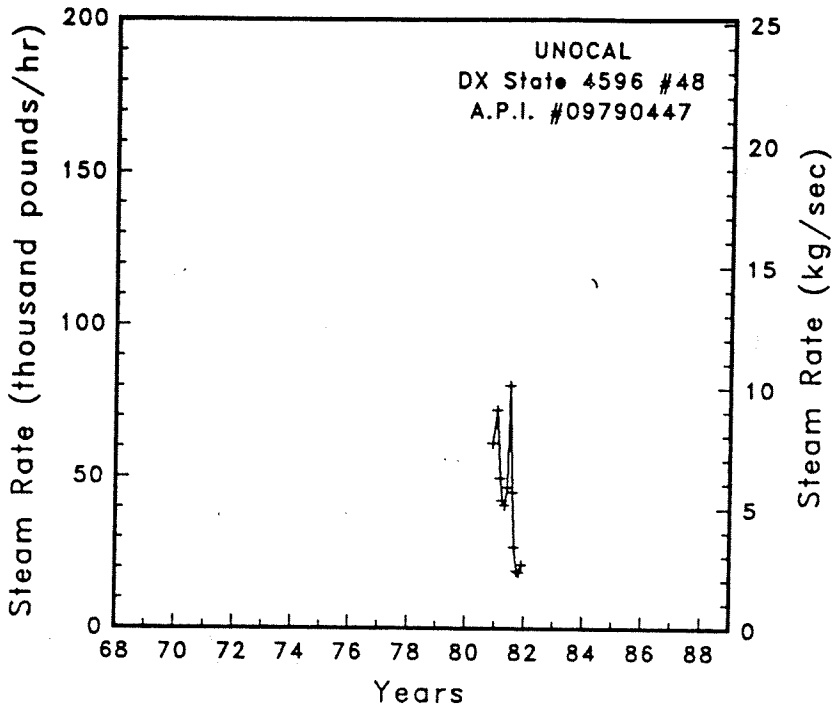

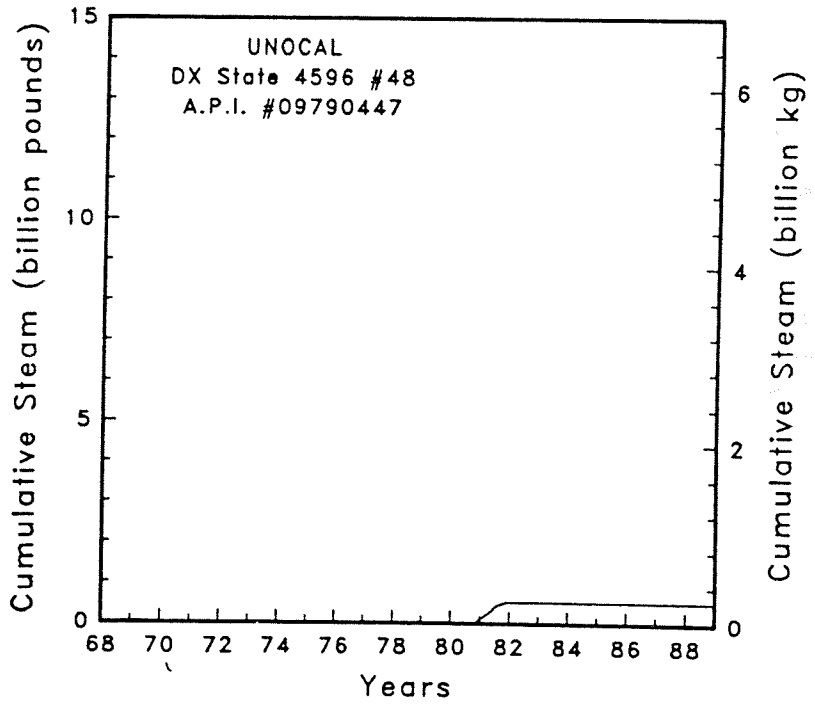

Figure A-60 Steam rate and cumulative mass flow for well DX State 4596 #48

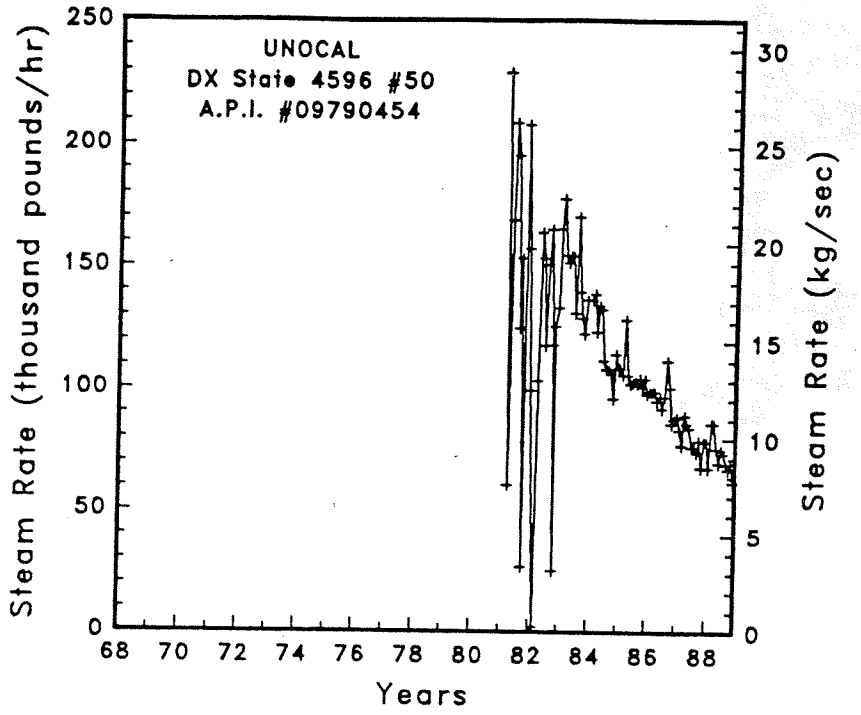

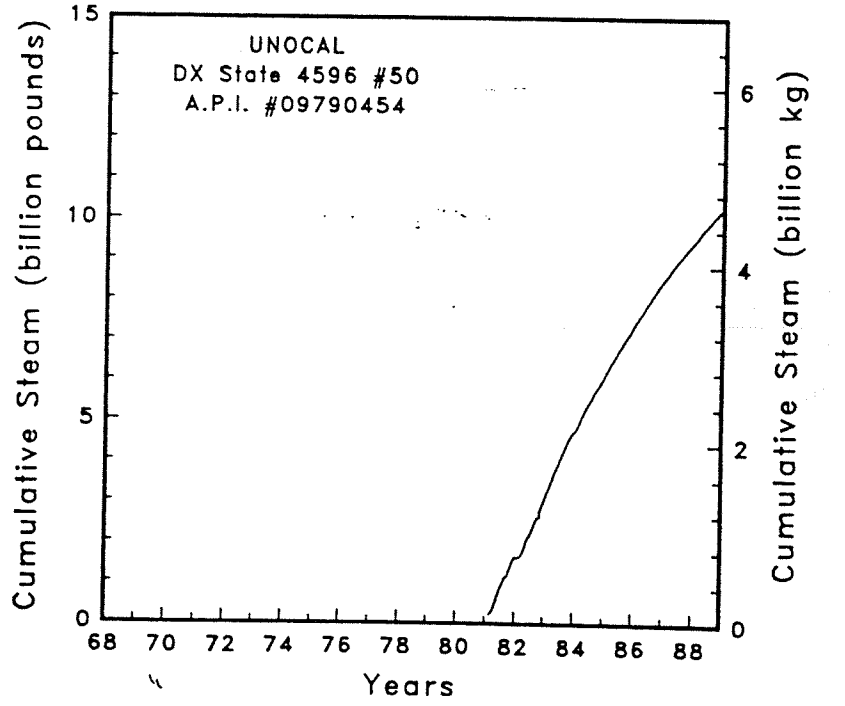

Figure A-61 Steam rate and cumulative mass flow for well DX State 4596 #50

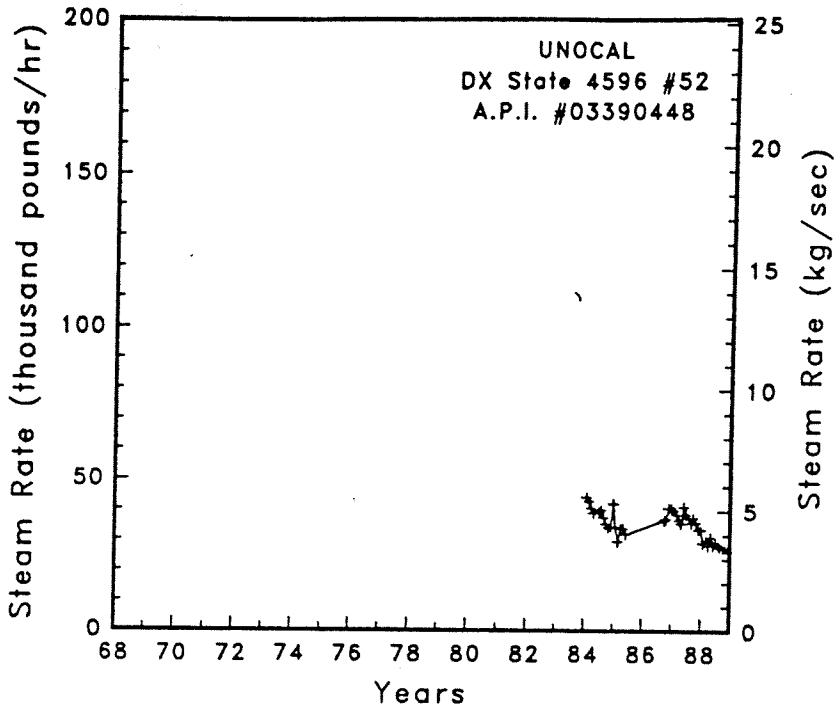

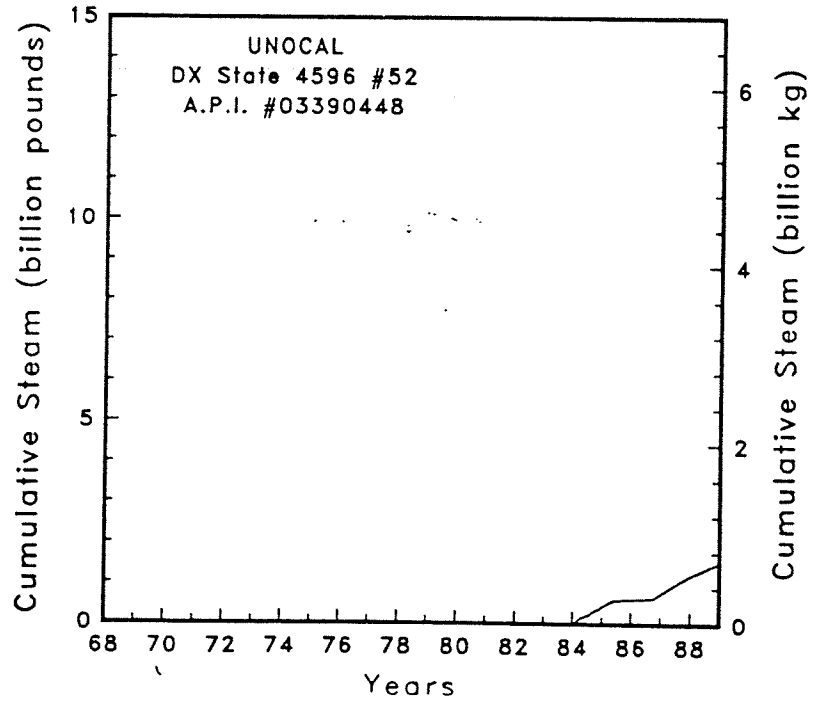

Figure A-62 Steam rate and cumulative mass flow for well DX State 4596 #52

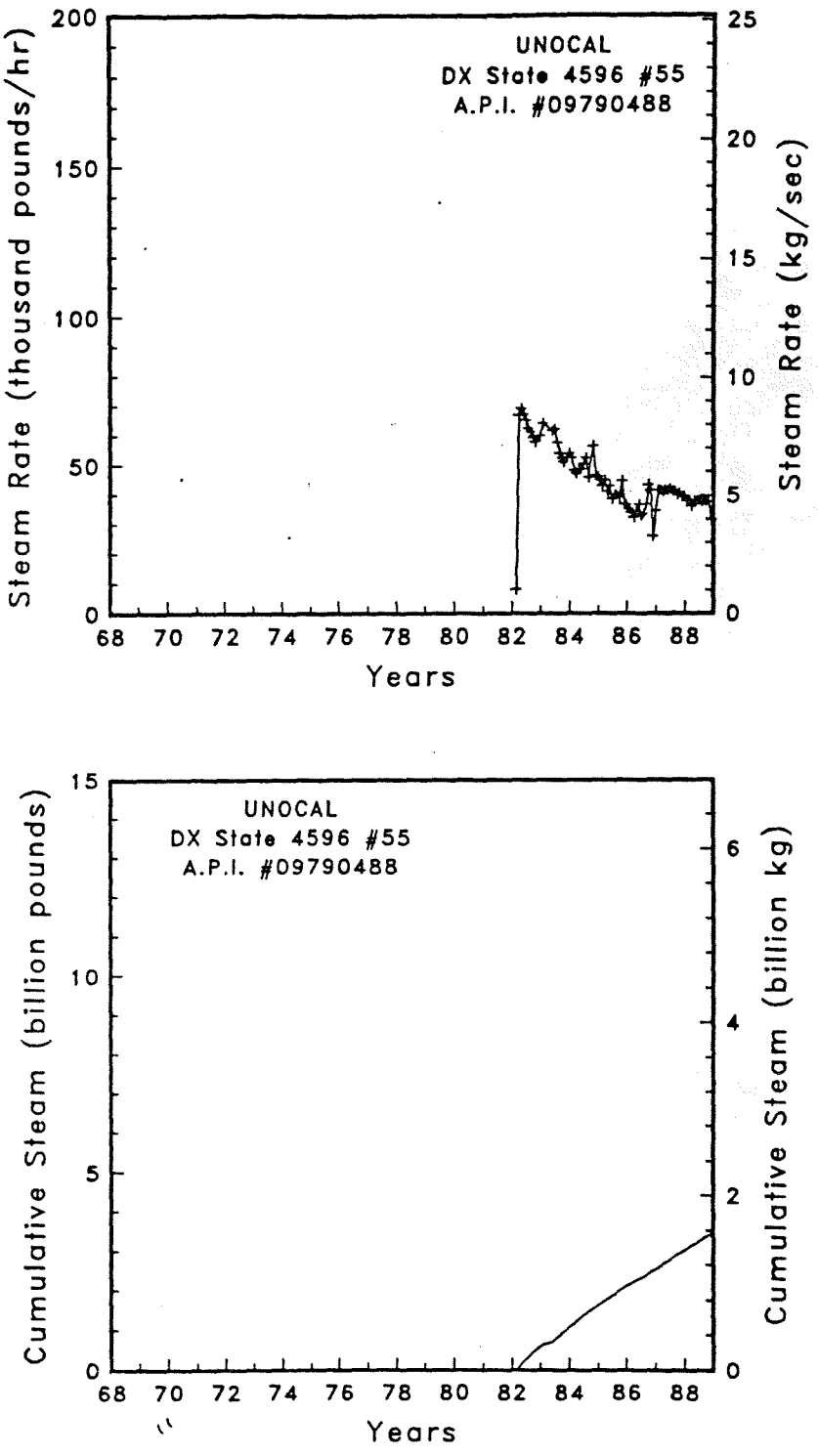

Figure A-63. Steam rate and cumulative mass flow for well DX State 4596 #55

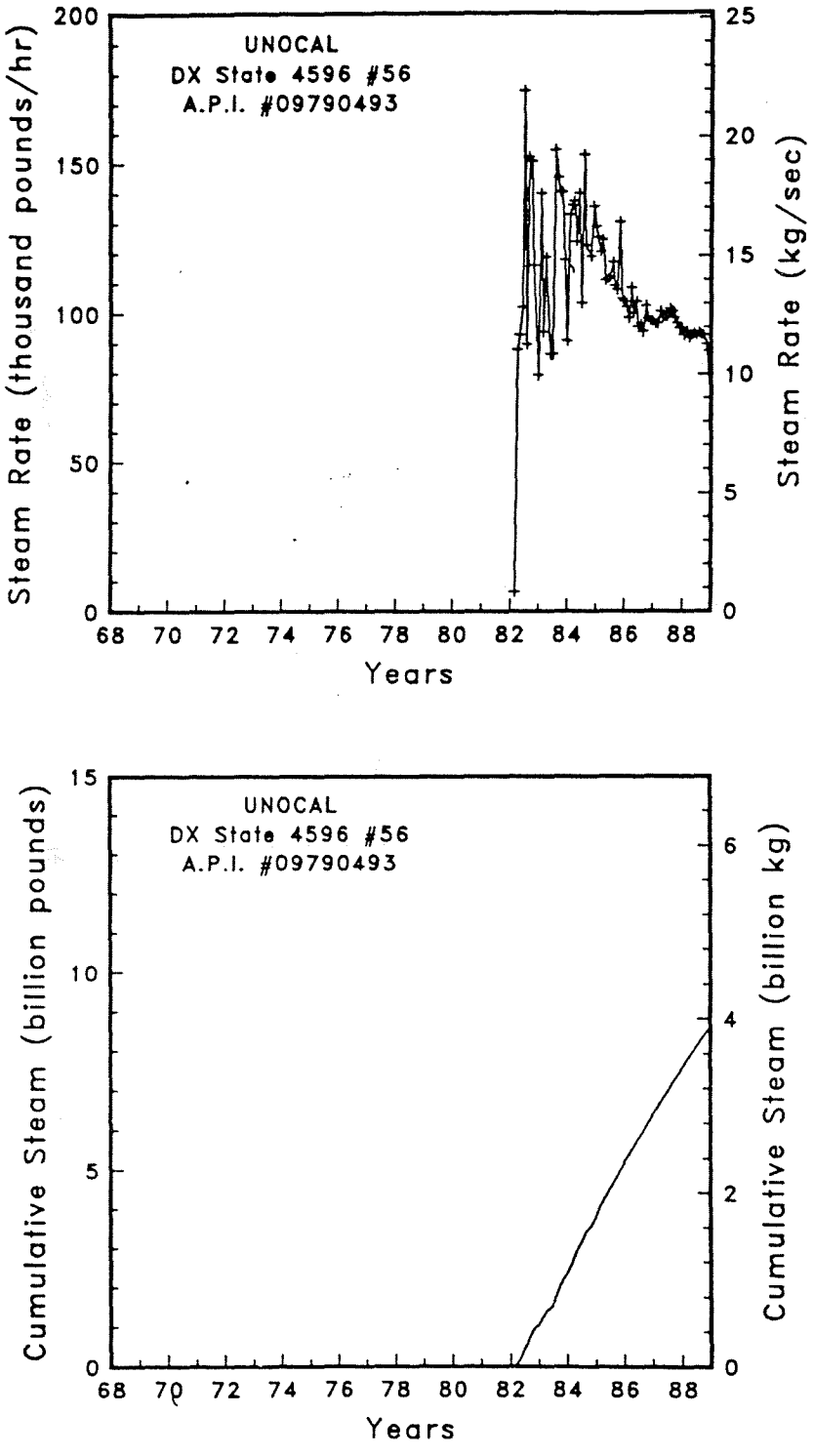

Figure A-64 Steam rate and cumulative mass flow for well DX State 4596 #56

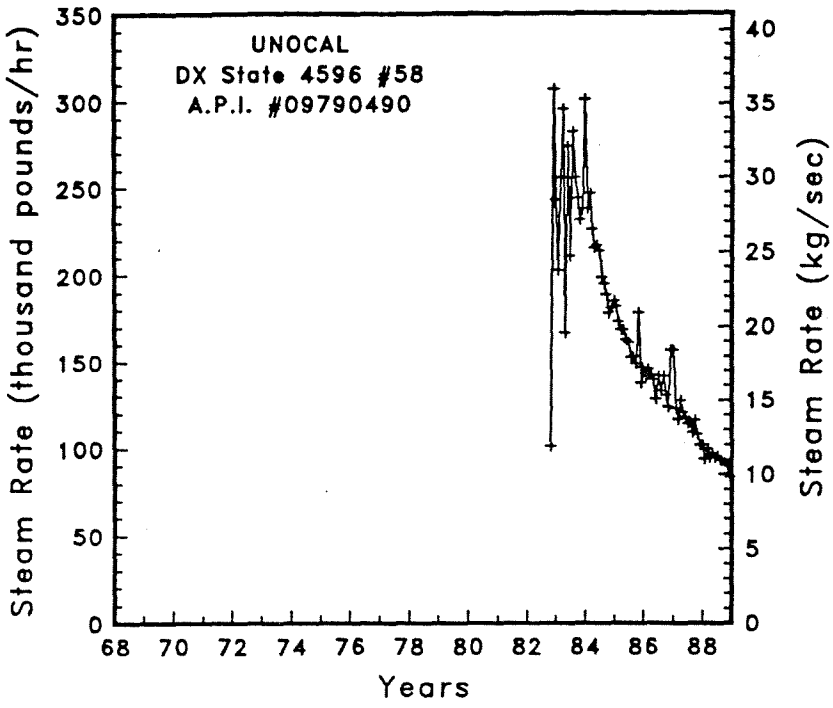

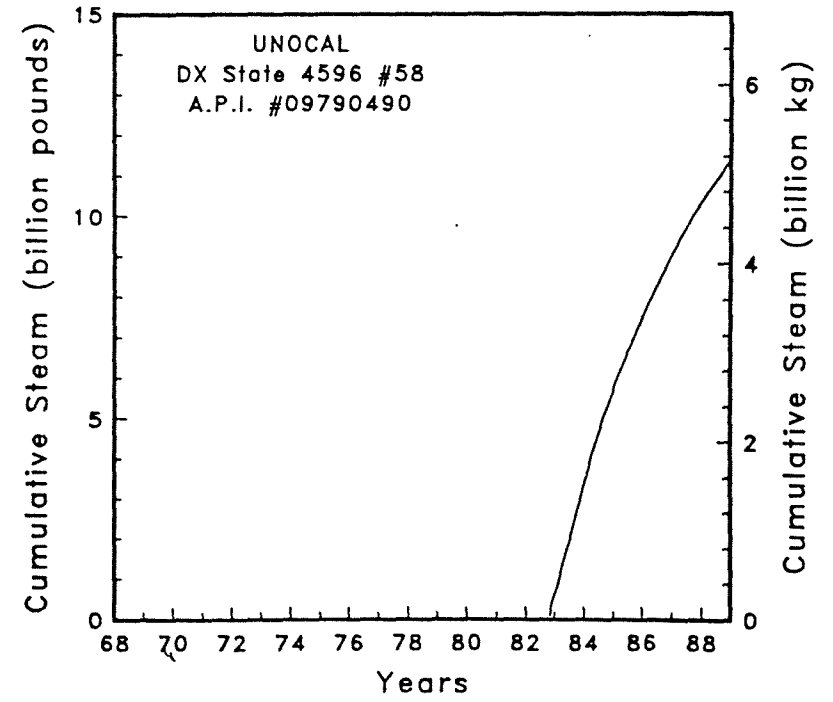

Figure A-65 Steam rate and cumulative mass flow for well DX State 4596 #58

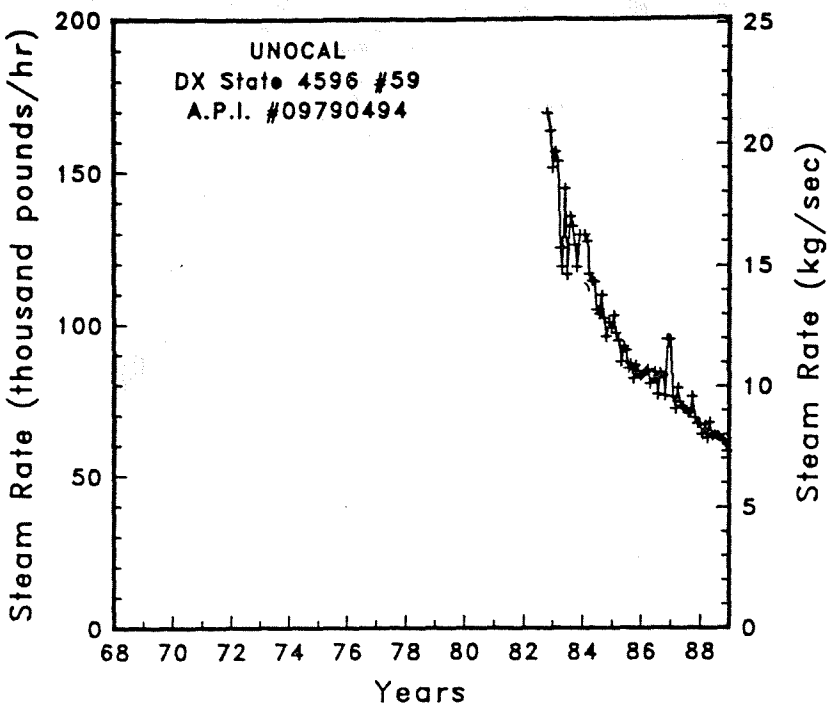

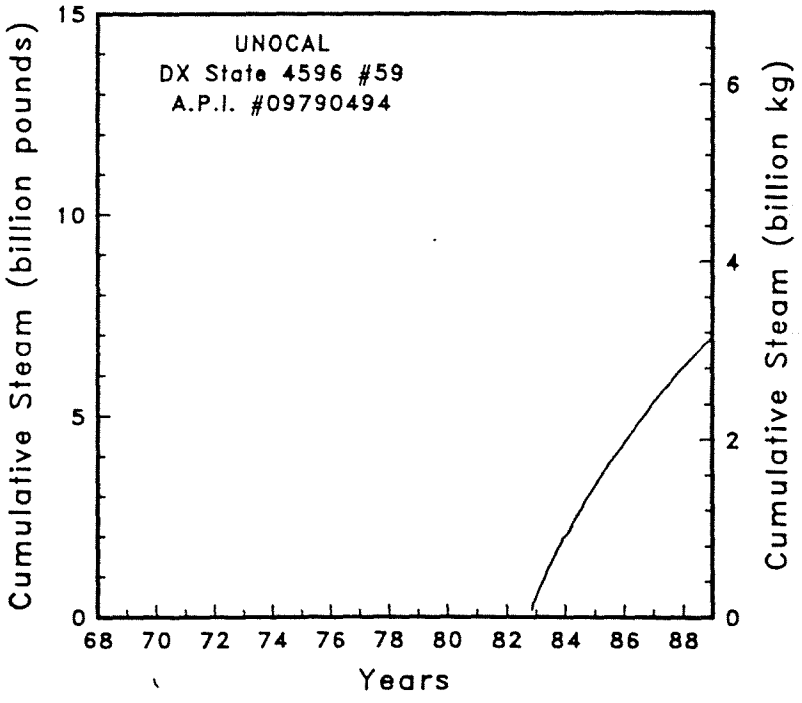

Figure A-66 Steam rate and cumulative mass flow for well DX State 4596 #59

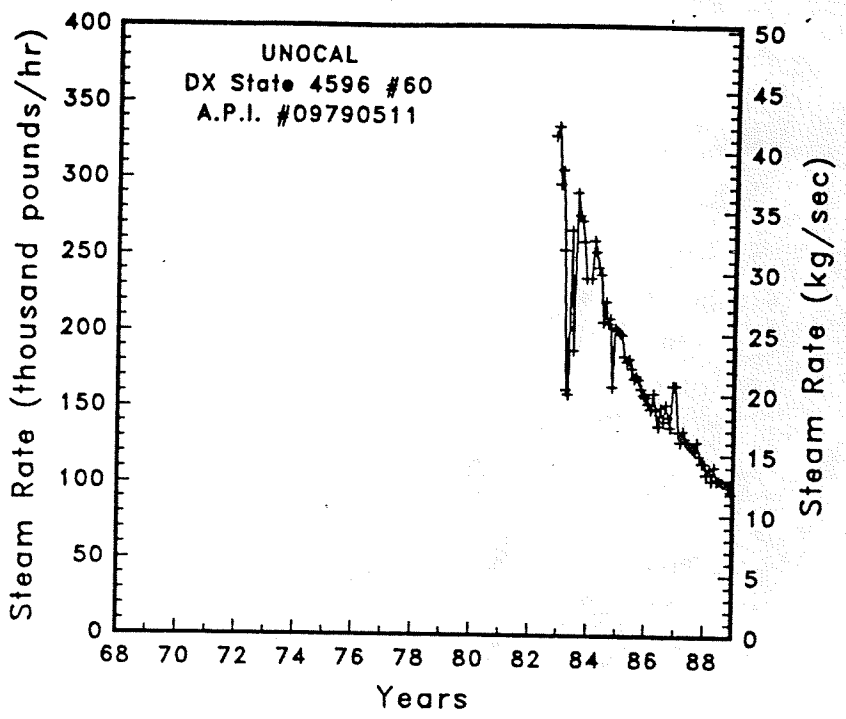

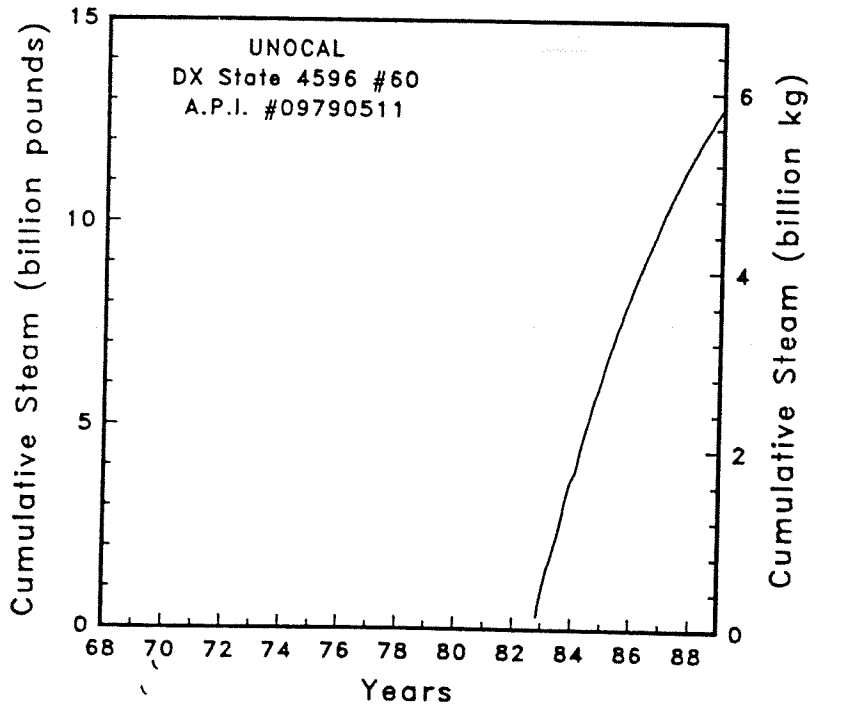

Figure A-67 Steam rate and cumulative mass flow for well DX State 4596 #60

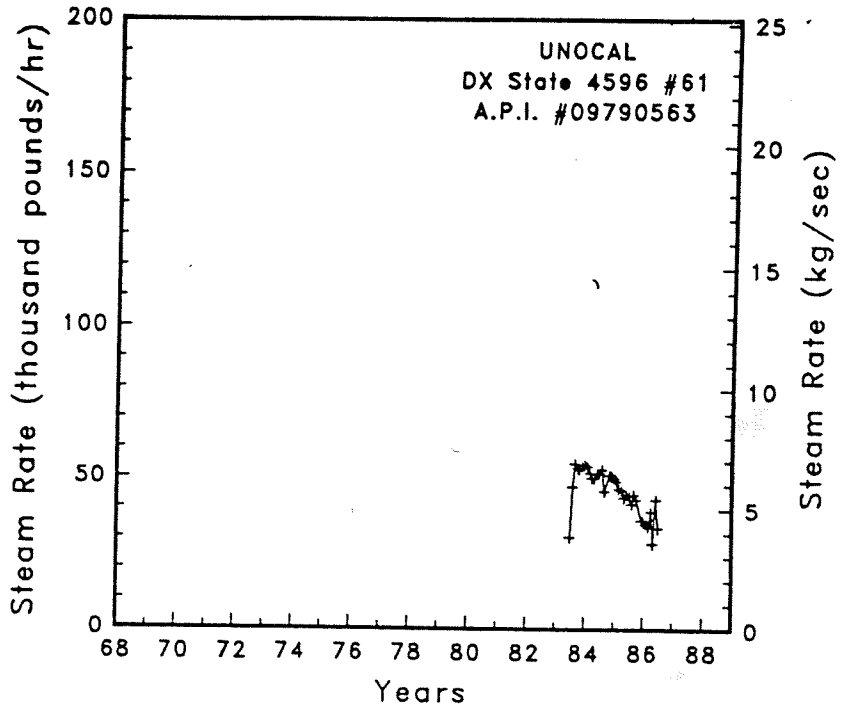

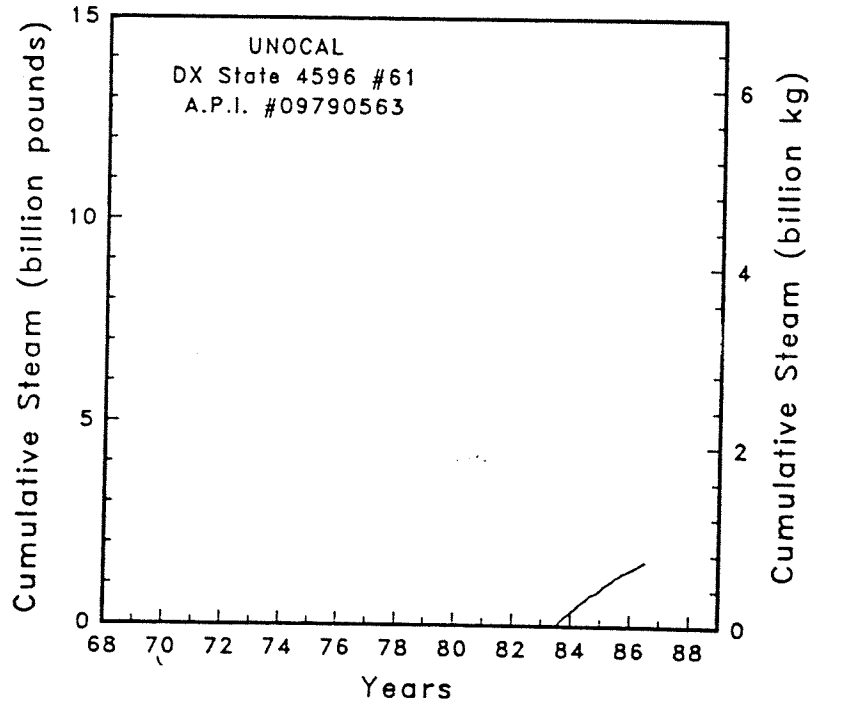

Figure A-68 Steam rate and cumulative mass flow for well DX State 4596 #61

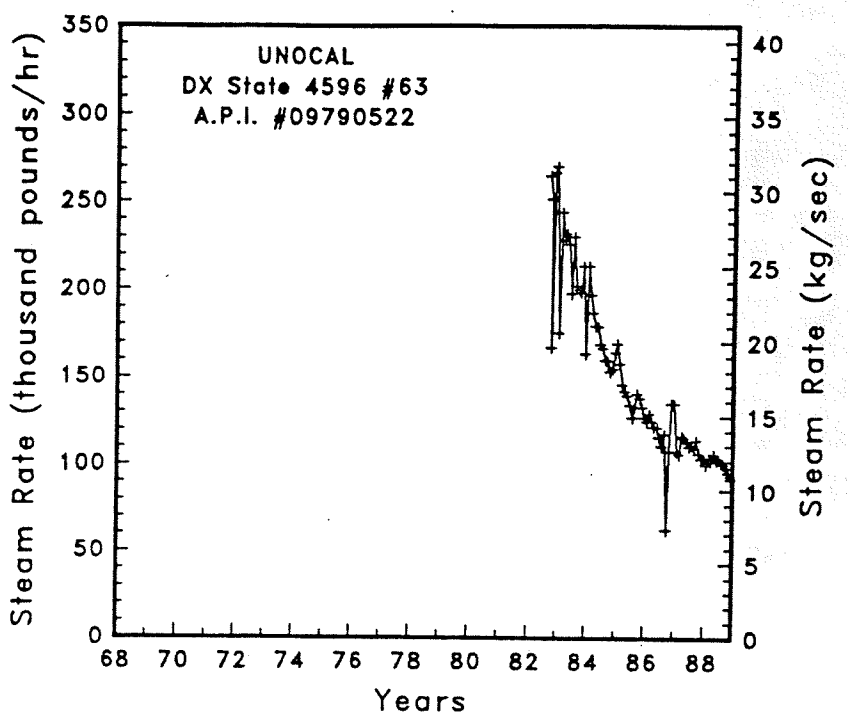

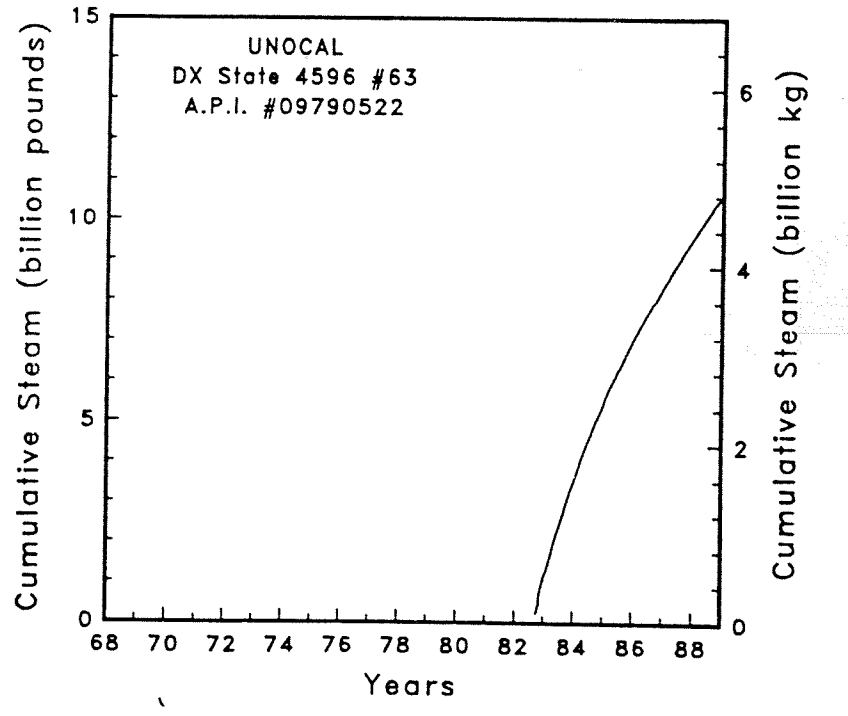

Figure A-69 Steam rate and cumulative mass flow for well DX State 4596 #63

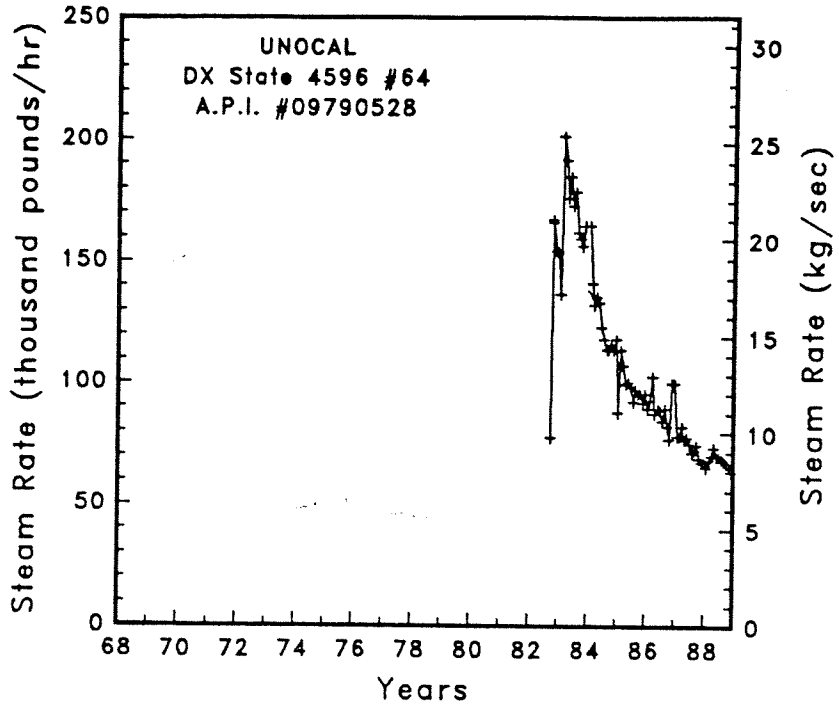

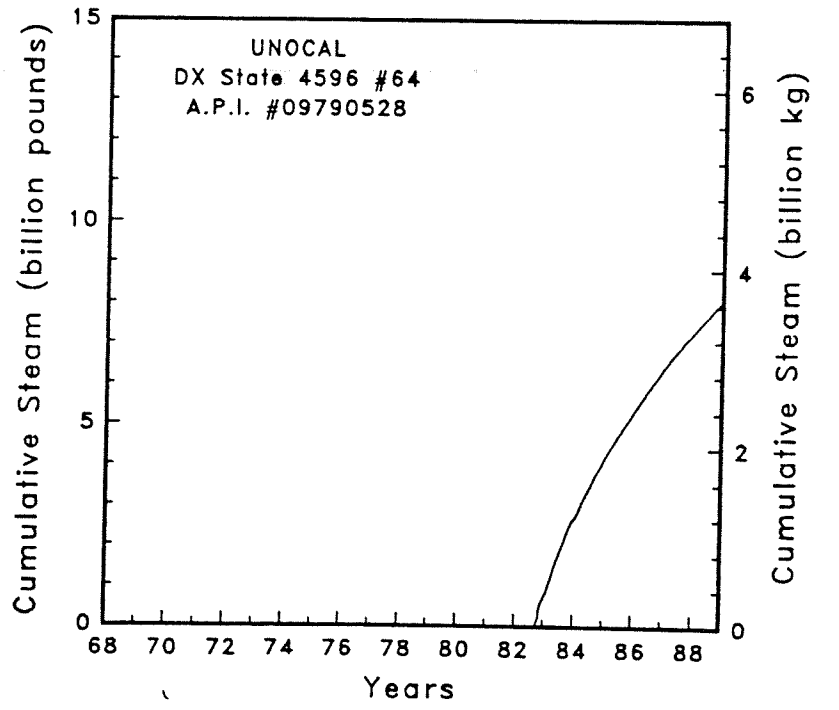

Figure A-70 Steam rate and cumulative mass flow for well DX State 4596 #64

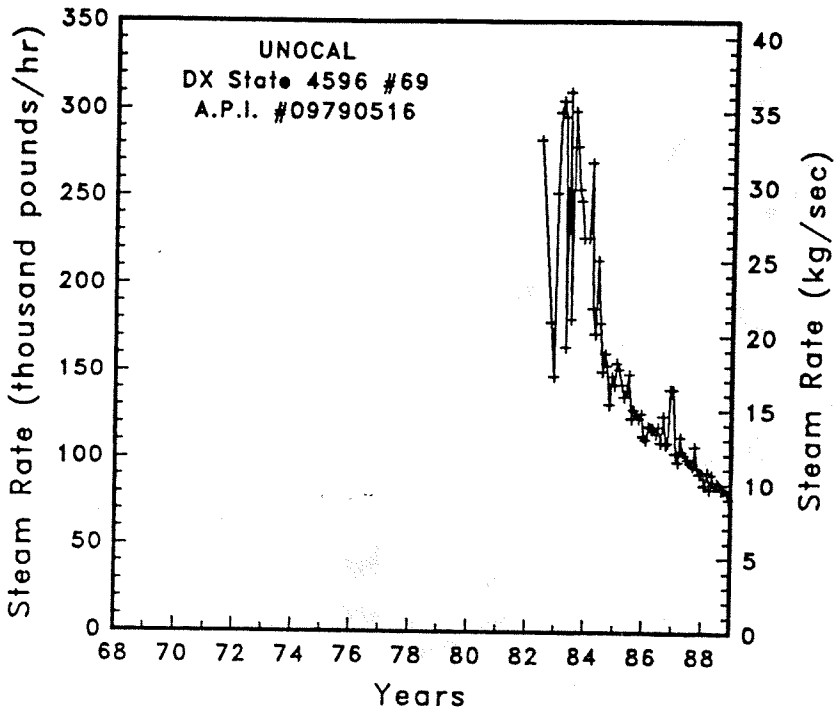

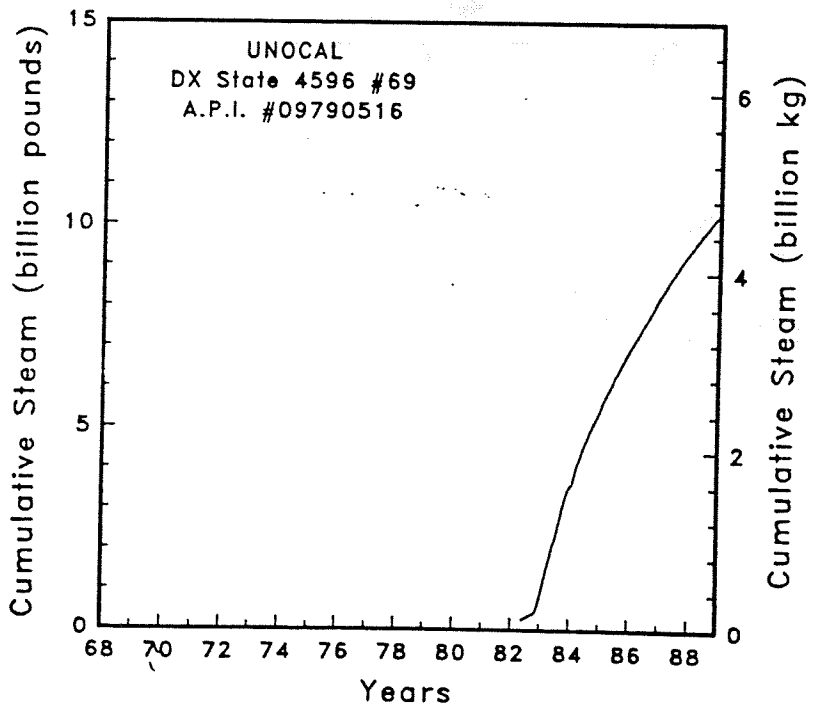

Figure A-71 Steam rate and cumulative mass flow for well DX State 4596 #69

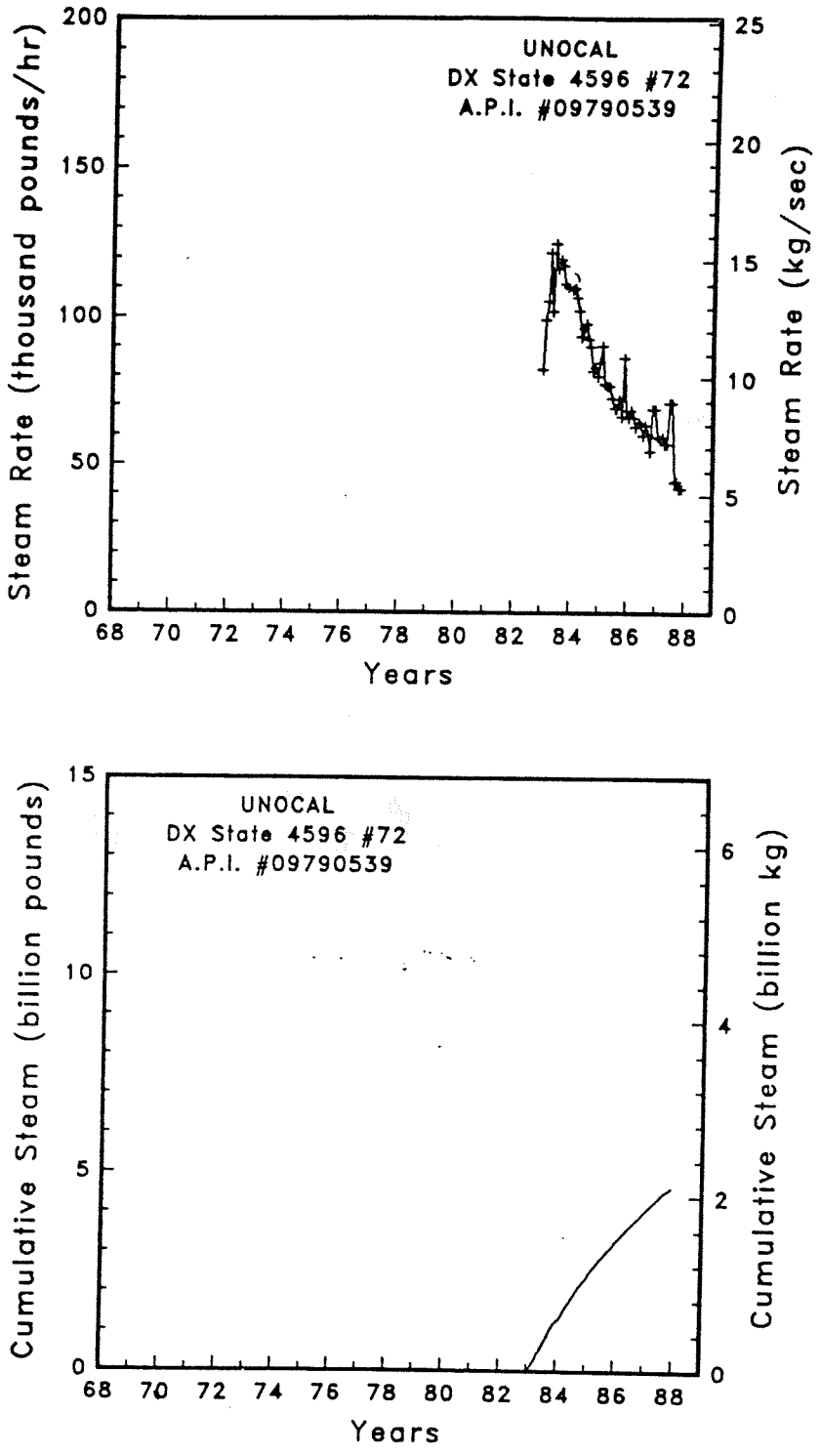

Figure A-72. Steam rate and cumulative mass flow for well DX State 4596 #72

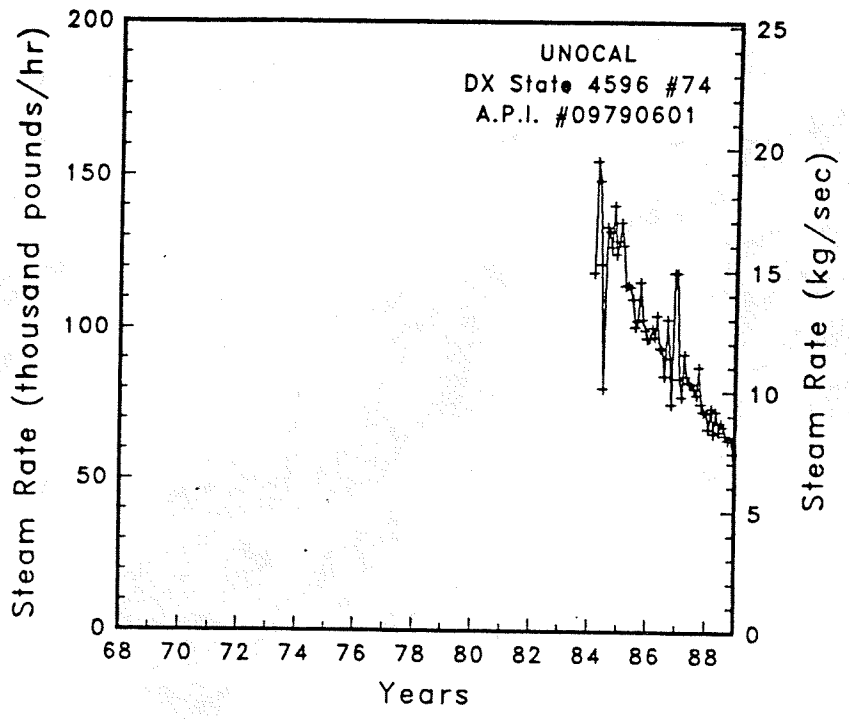

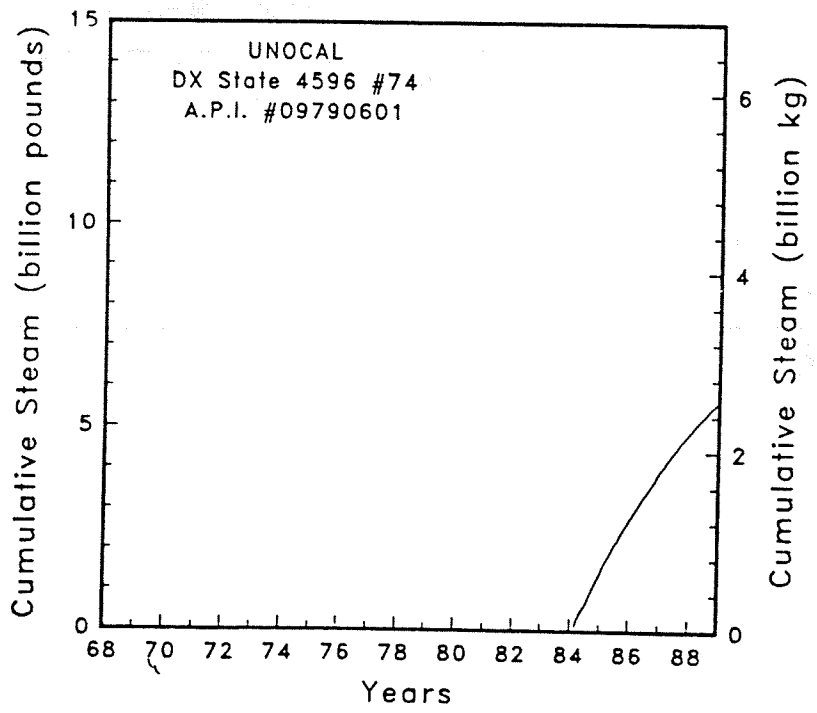

Figure A-73 Steam rate and cumulative mass flow for well DX State 4596 #74

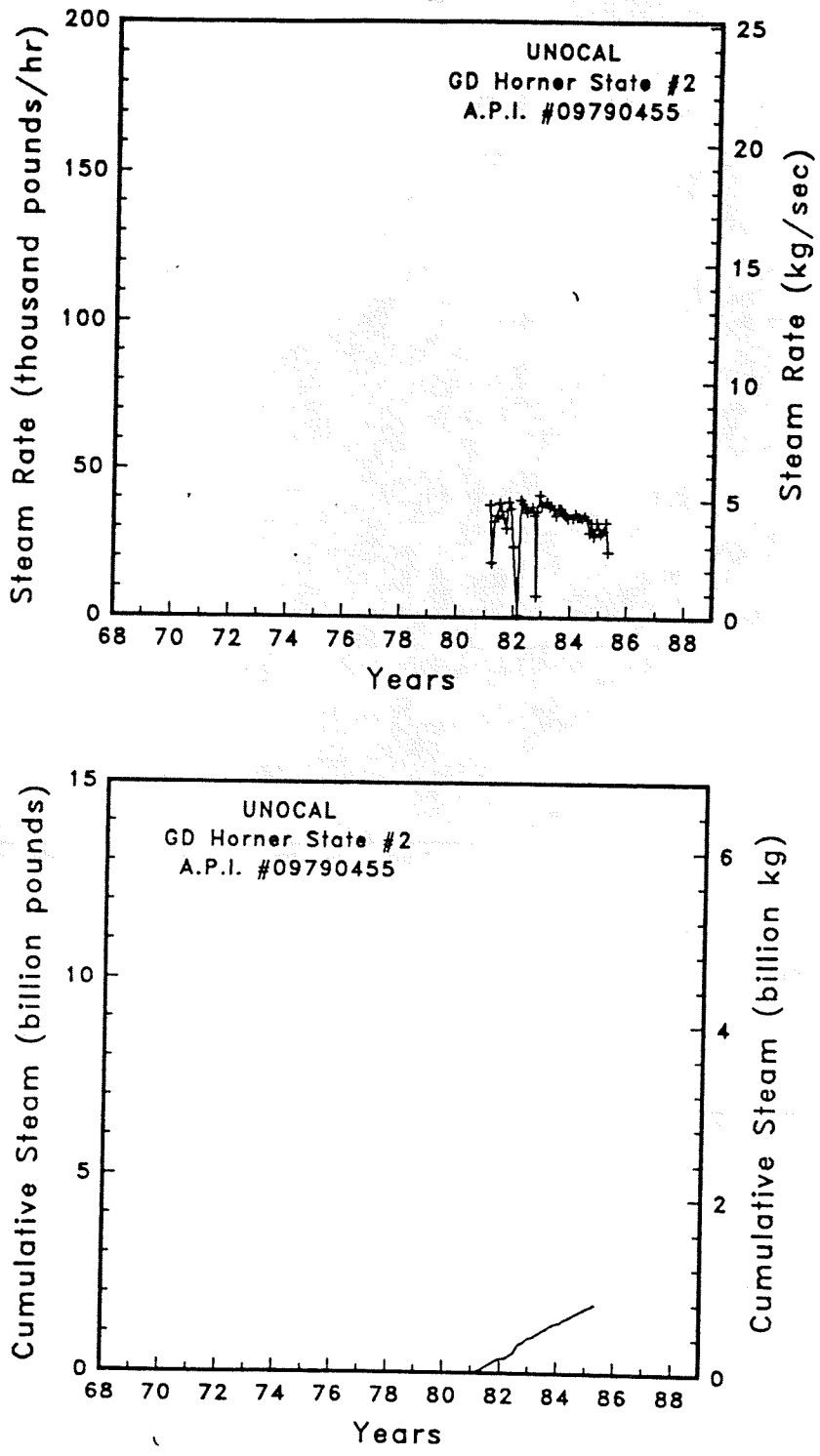

Figure A-74 Steam rate and cumulative mass flow for well GD Horner State #2

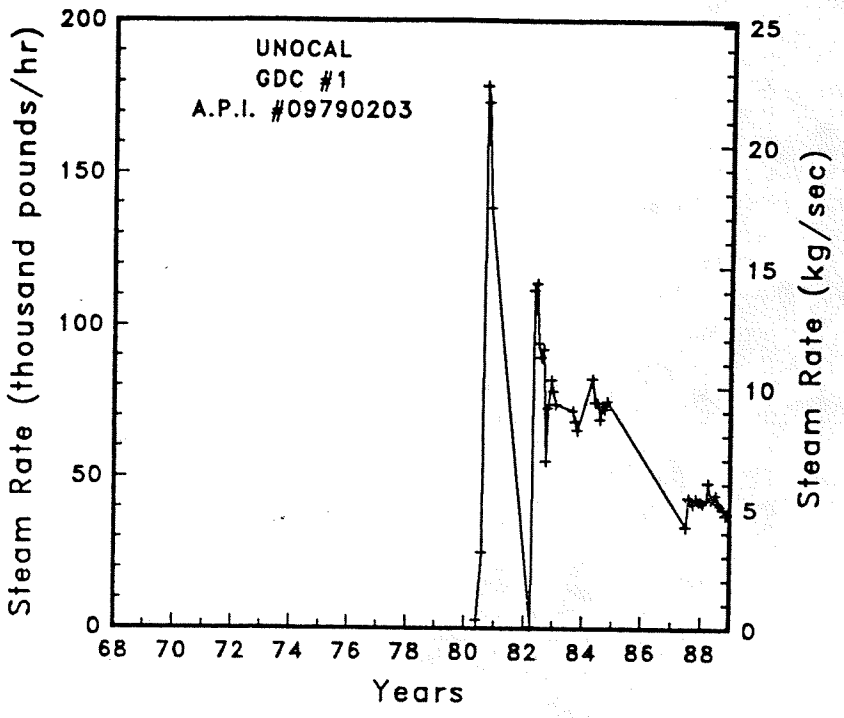

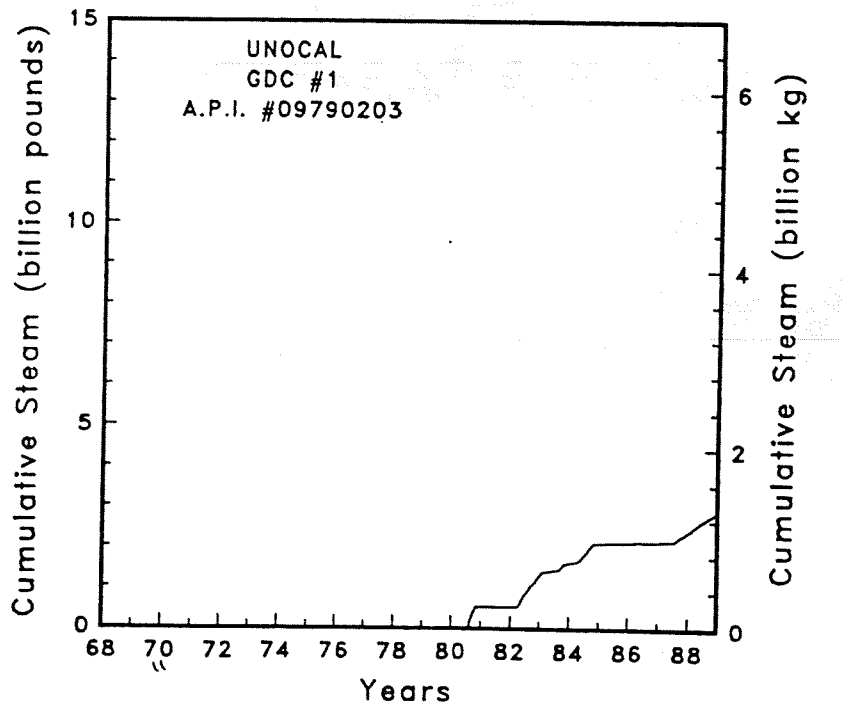

Figure A-75 Steam rate and cumulative mass flow for well GDC #1

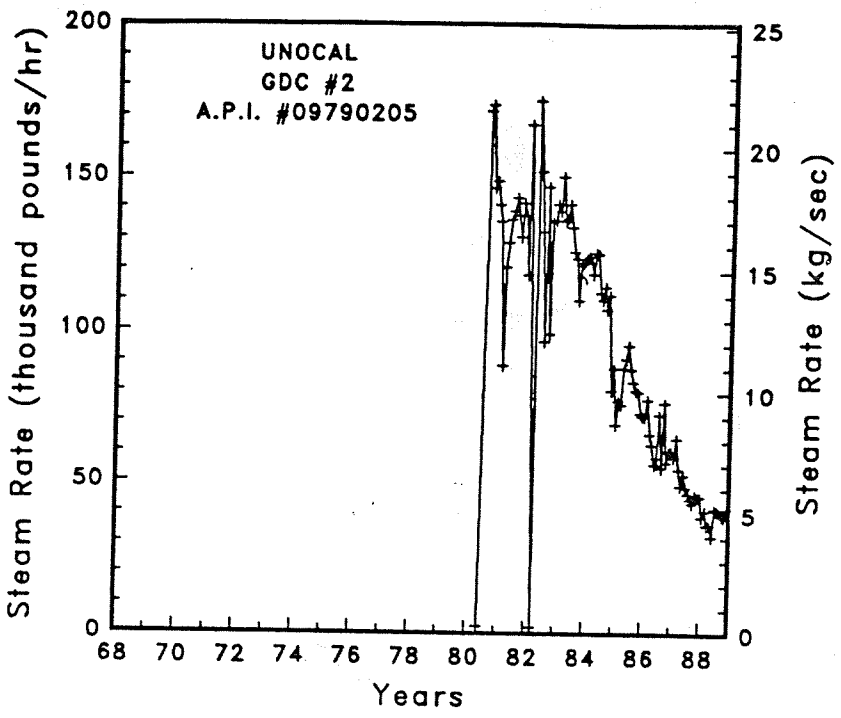

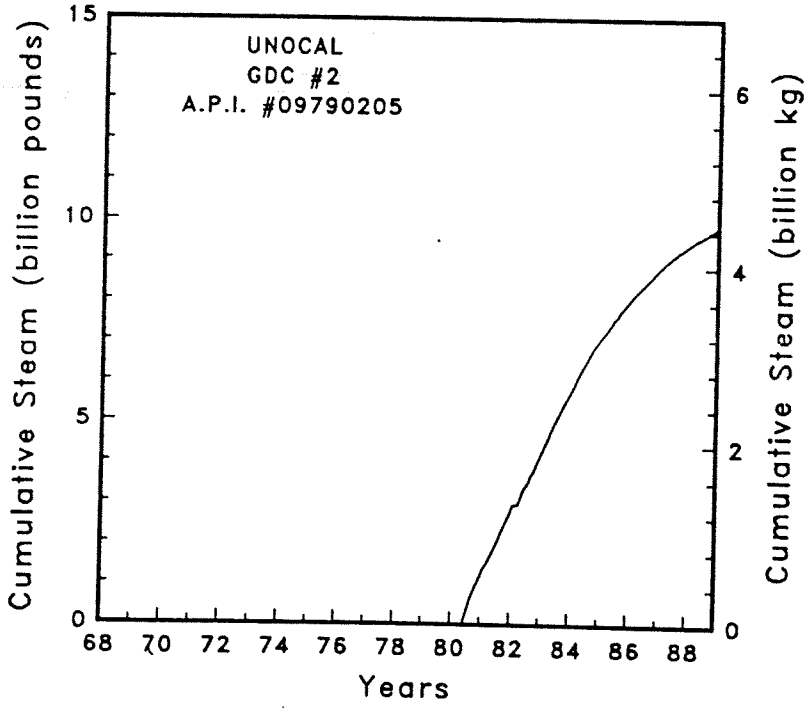

Figure A-76 Steam rate and cumulative mass flow for well GDC #2

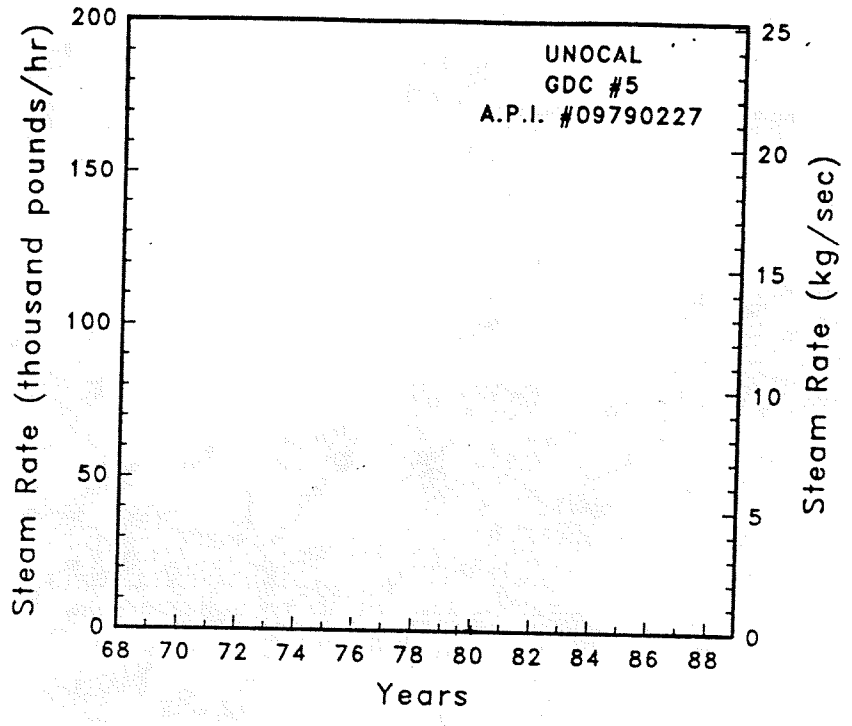

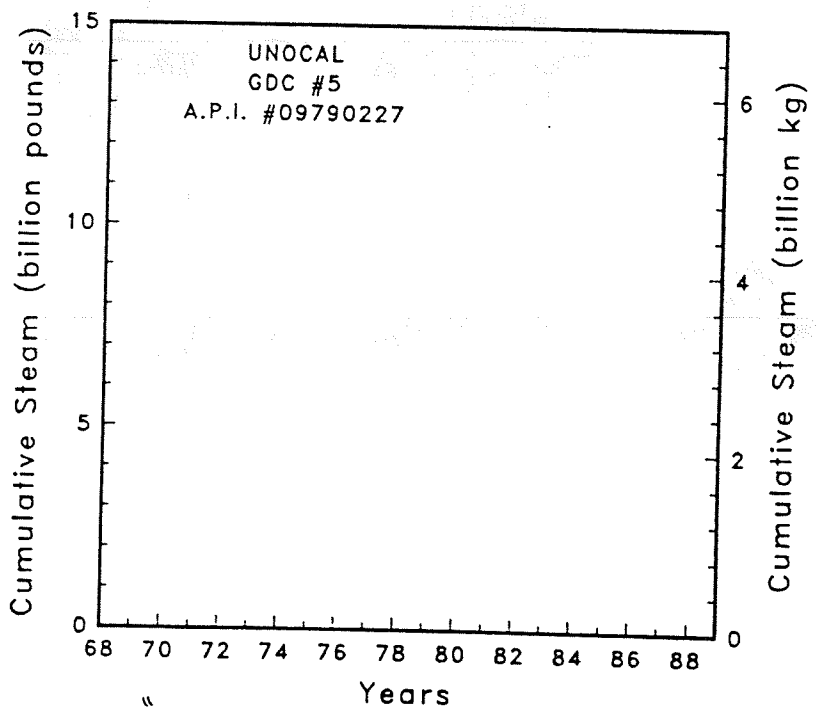

Figure A-77 Steam rate and cumulative mass flow for well GDC #5

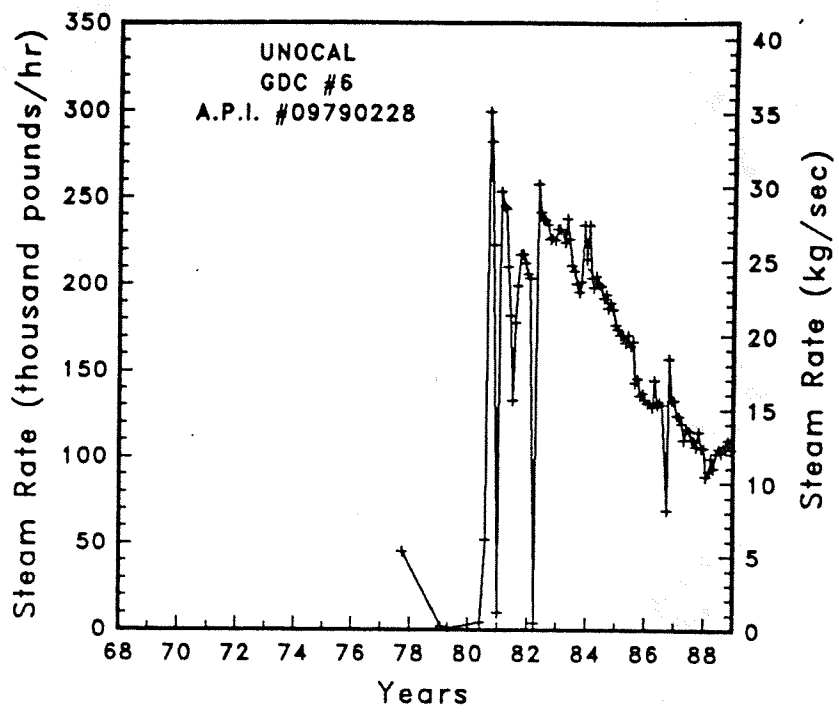

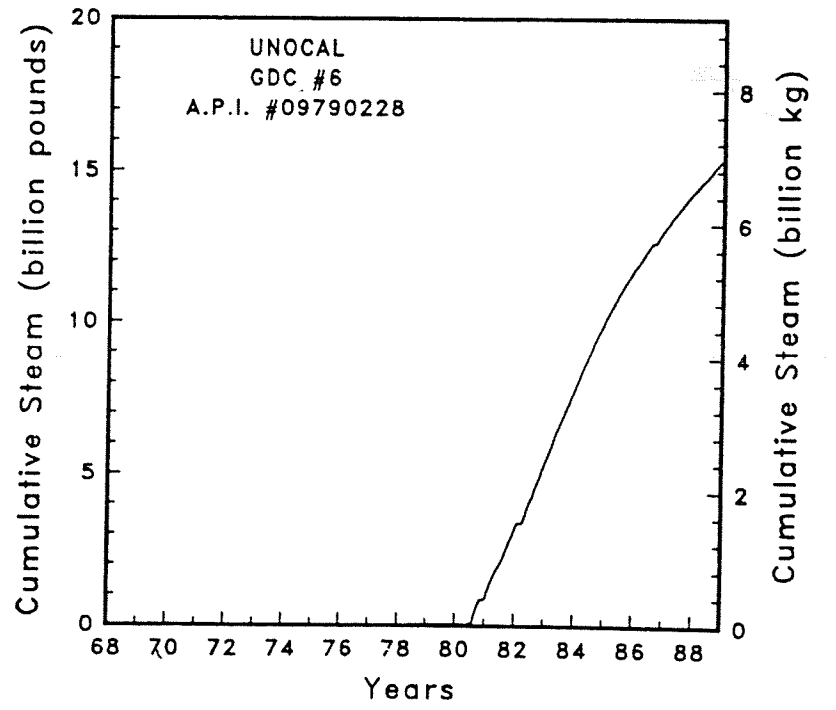

Figure A-78 Steam rate and cumulative mass flow for well GDC #6

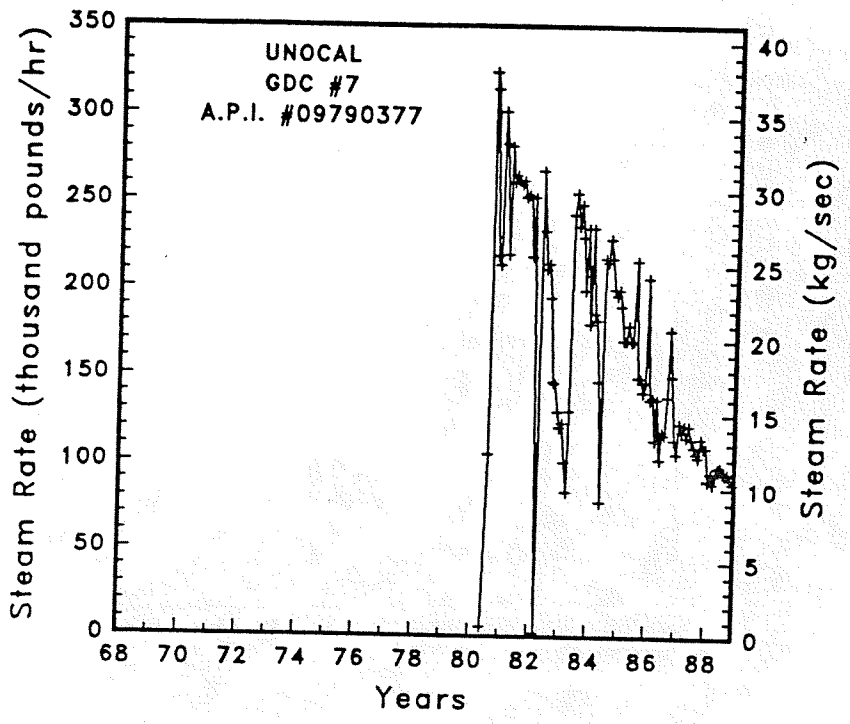

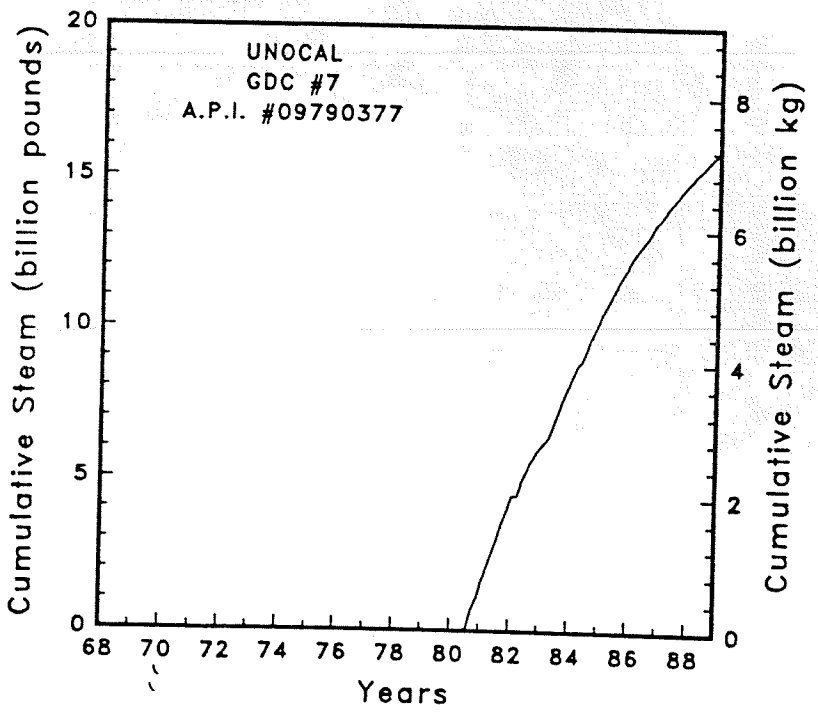

Figure A-79 Steam rate and cumulative mass flow for well GDC #7

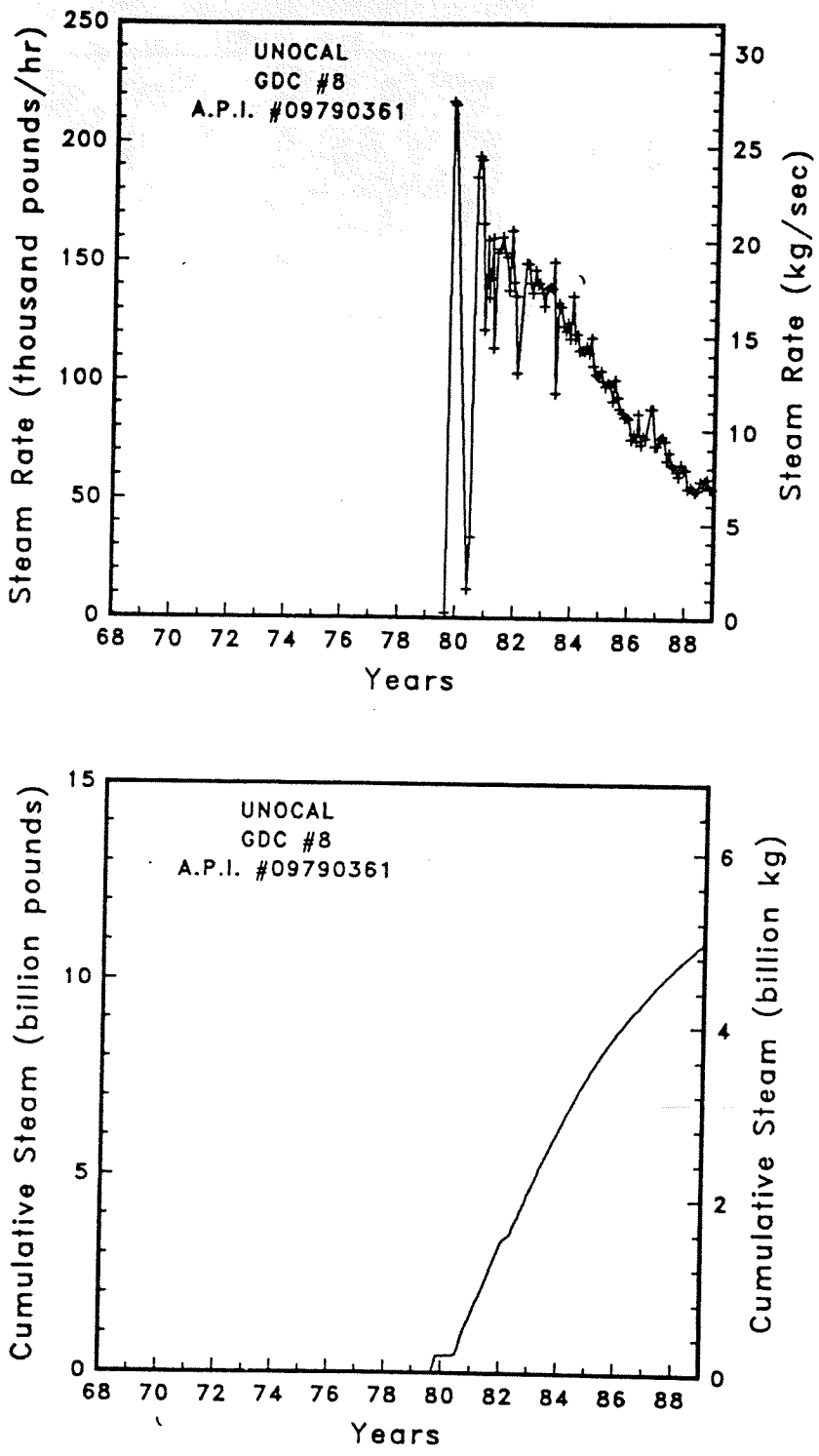

Figure A-80 Steam rate and cumulative mass flow for well GDC #8

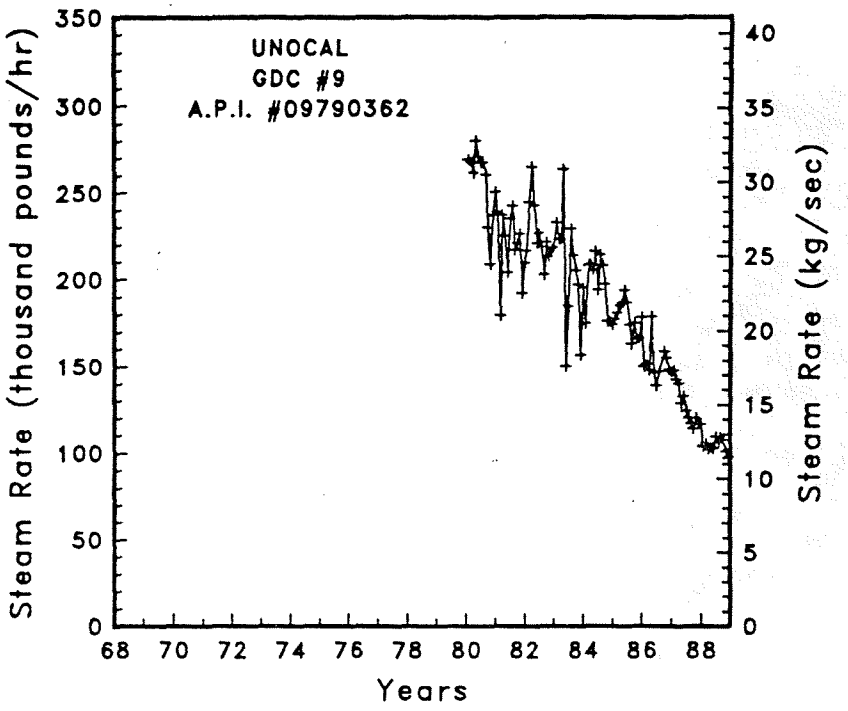

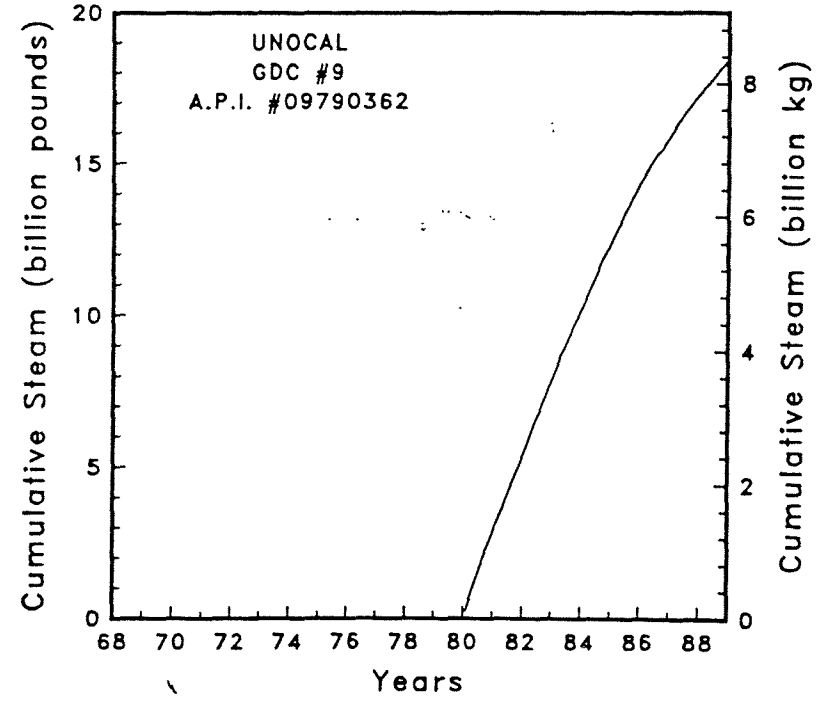

Figure A-81 Steam rate and cumulative mass flow for well GDC #9

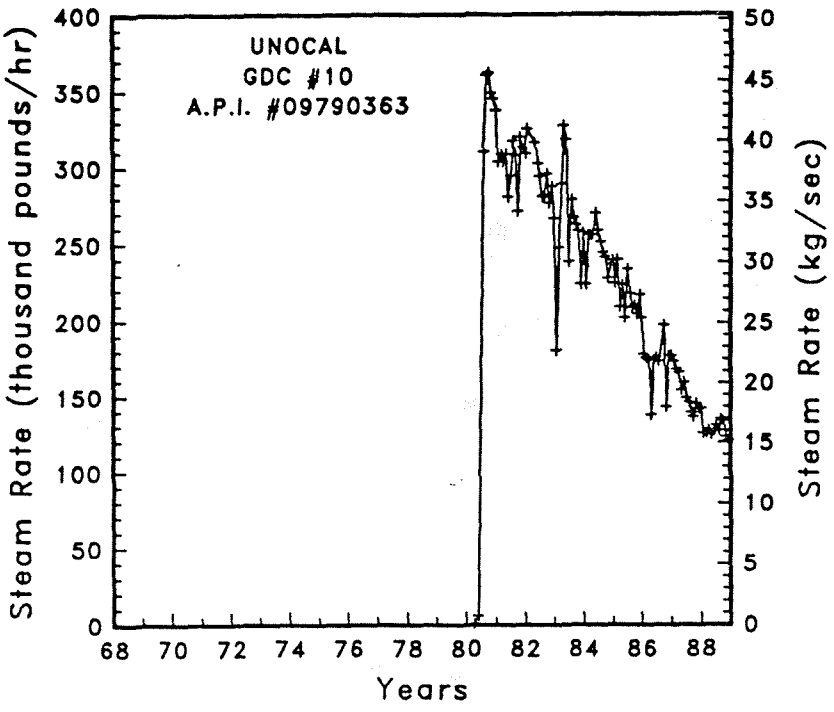

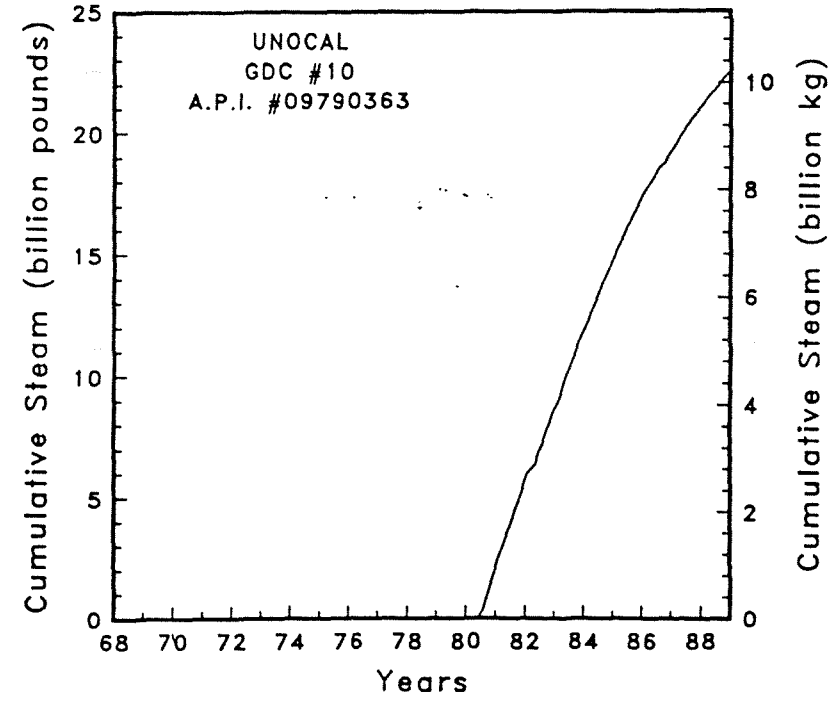

Figure A-82 Steam rate and cumulative mass flow for well GDC #10

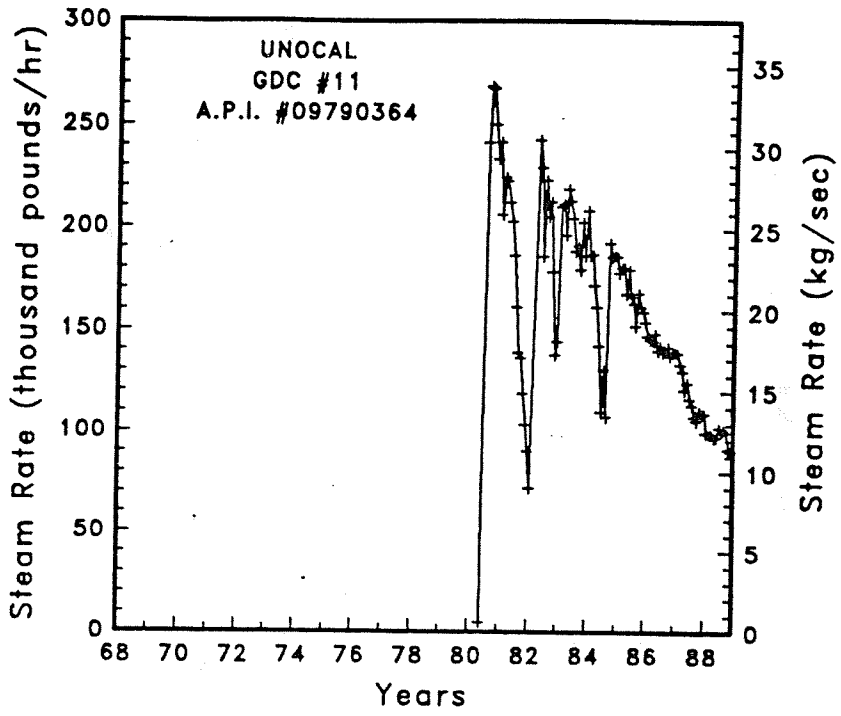

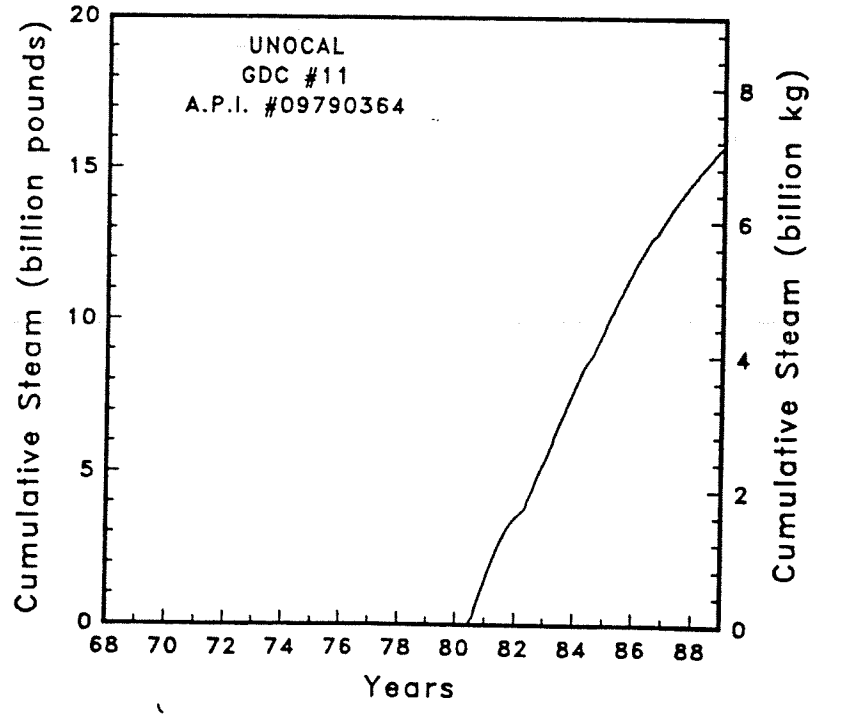

Figure A-83: Steam rate and cumulative mass flow for well GDC #11

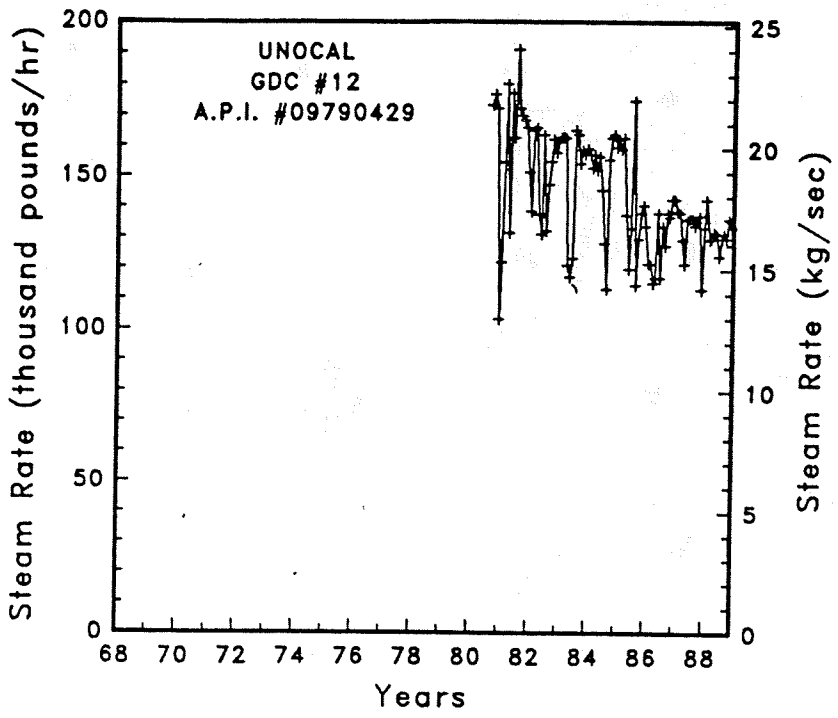

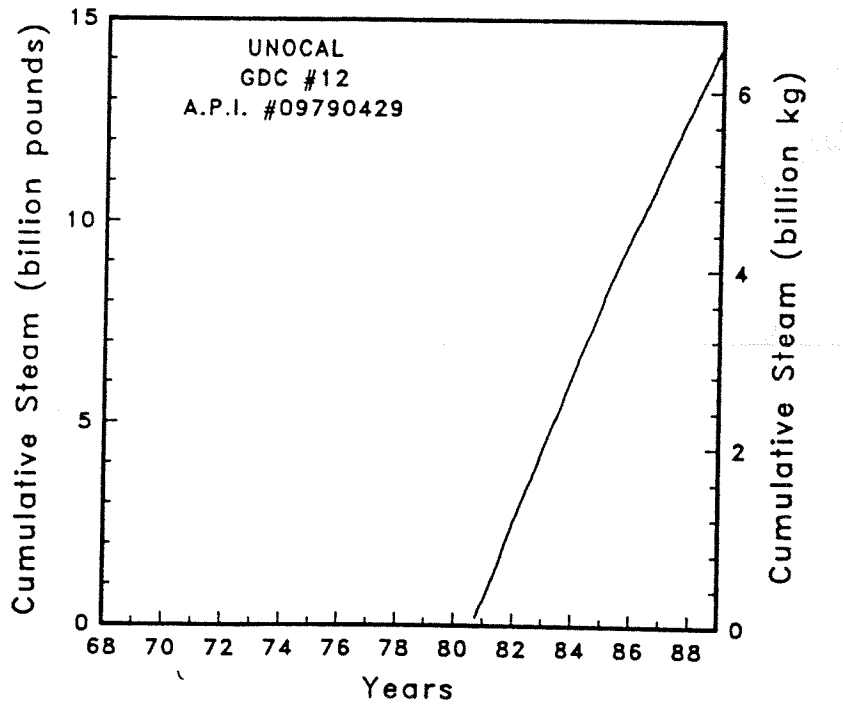

Figure A-84 Steam rate and cumulative mass flow for well GDC #12

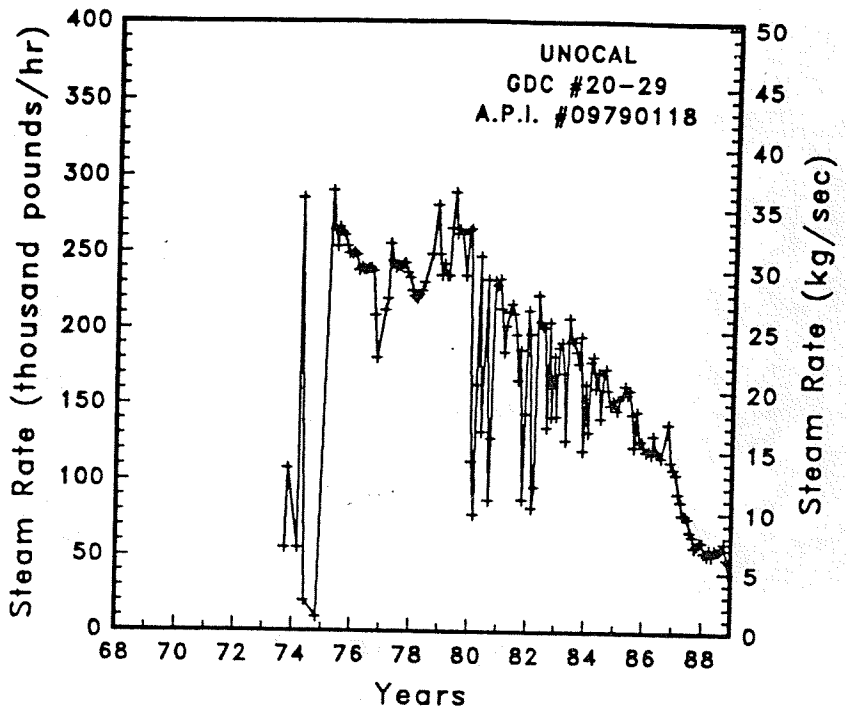

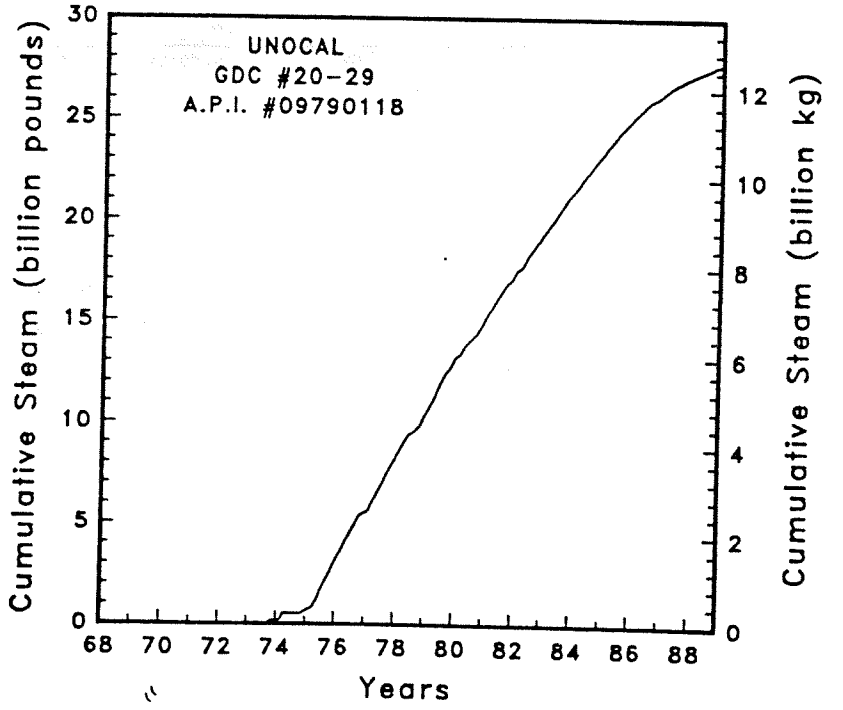

Figure A-85 Steam rate and cumulative mass flow for well GDC #20-29

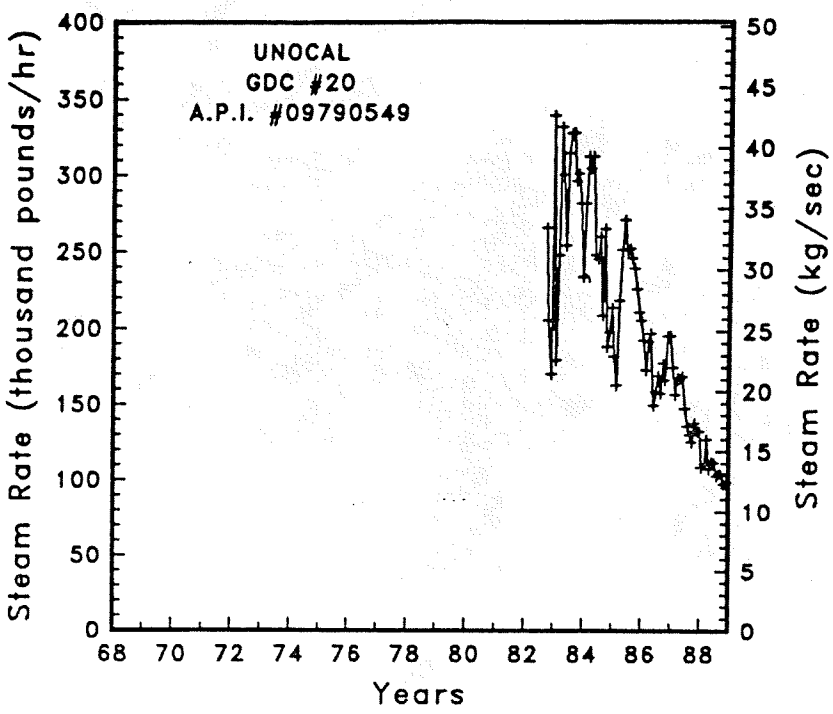

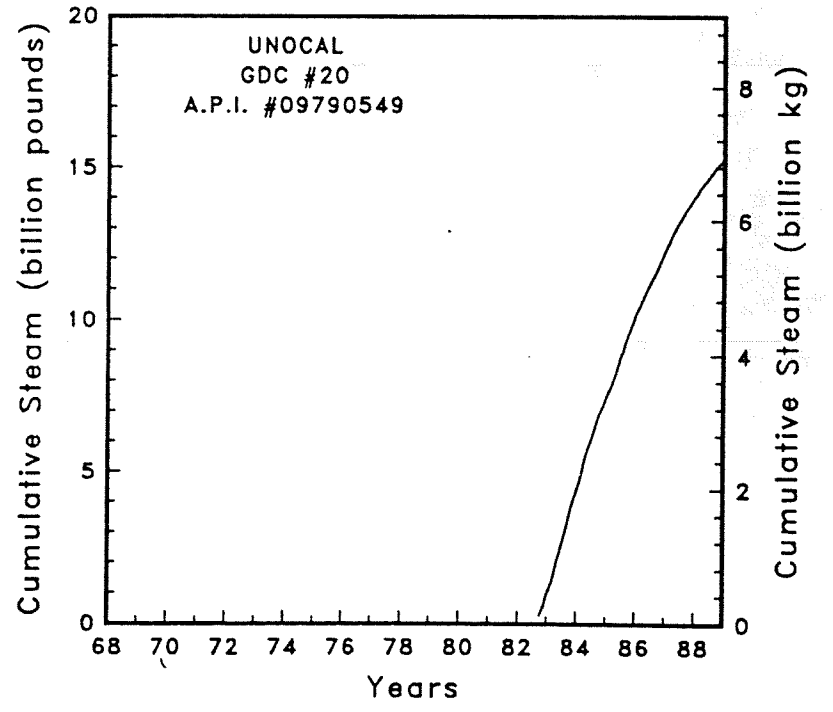

Figure A-86 Steam rate and cumulative mass flow for well GDC #20

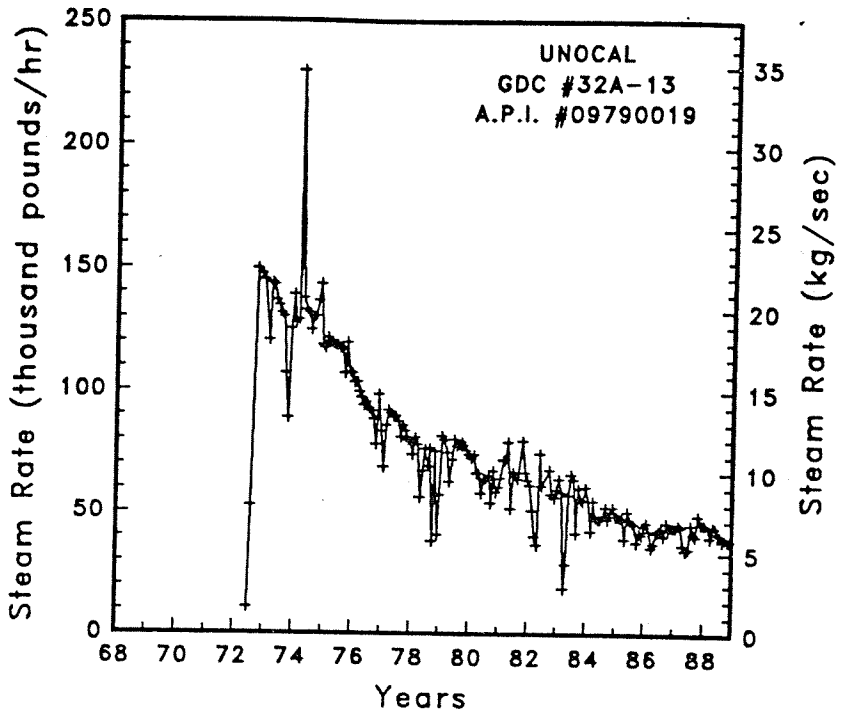

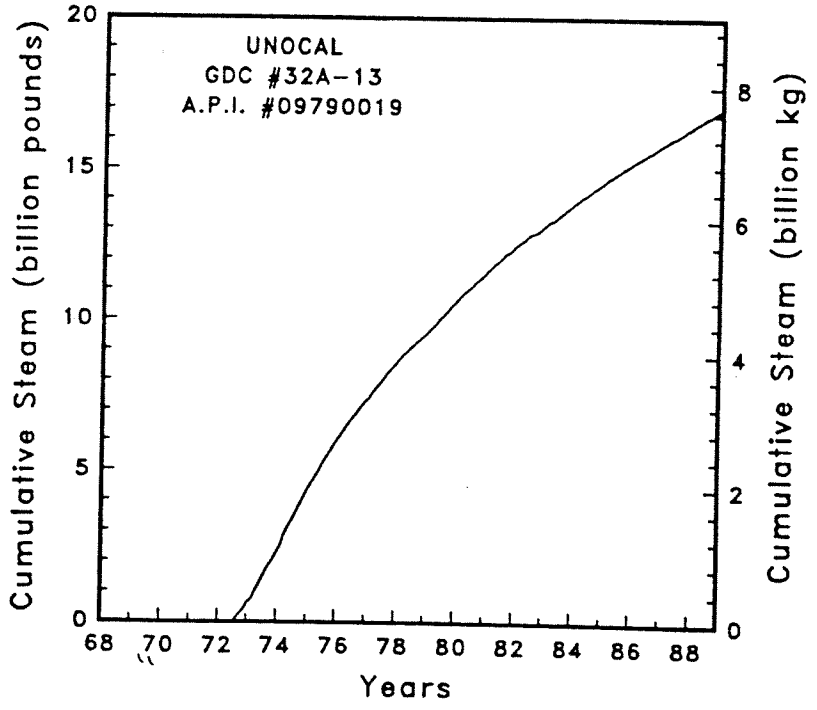

Figure A-87 Steam rate and cumulative mass flow for well GDC #32A-13

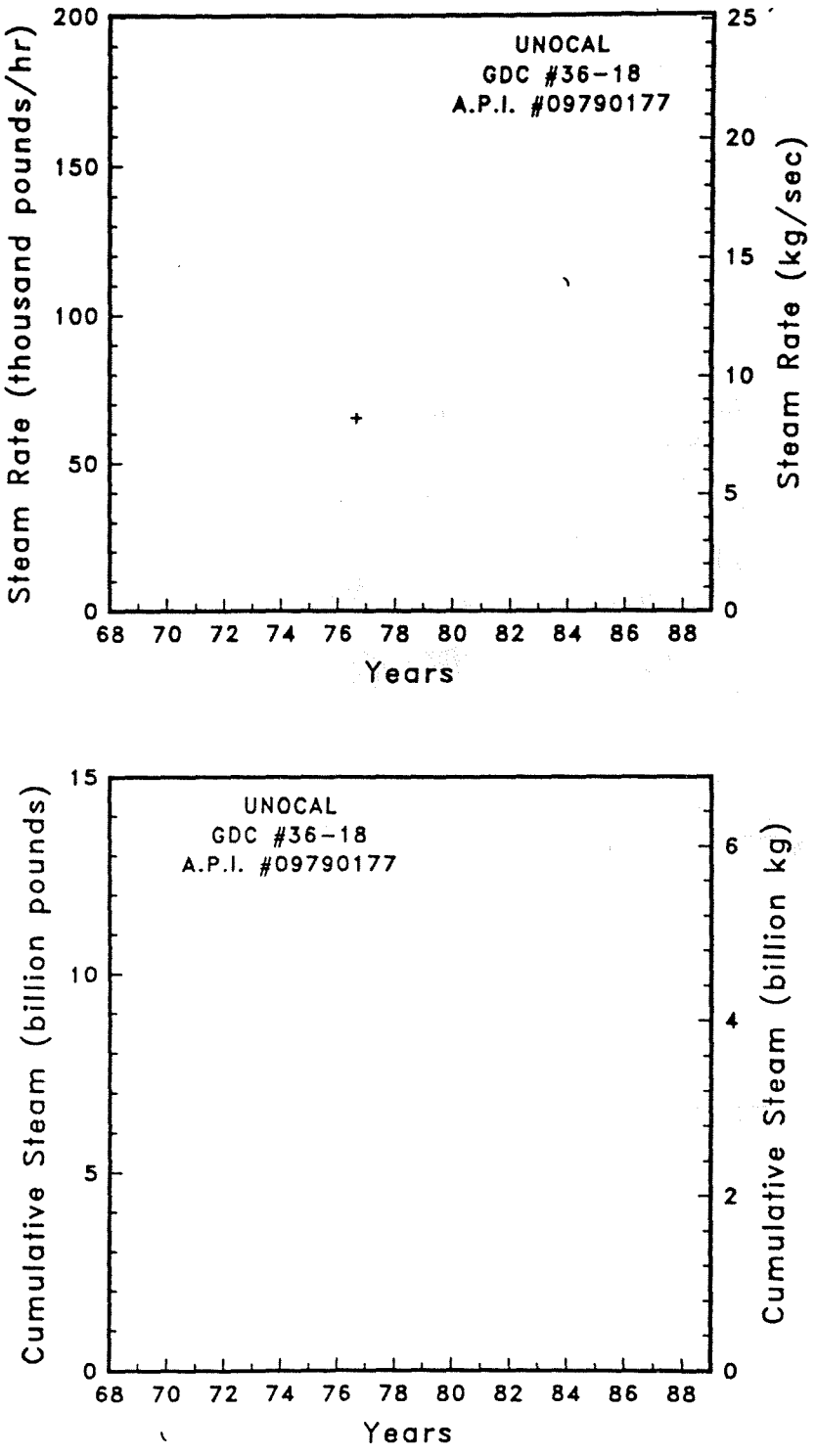

Figure A-88 Steam rate and cumulative mass flow for well GDC #36-18

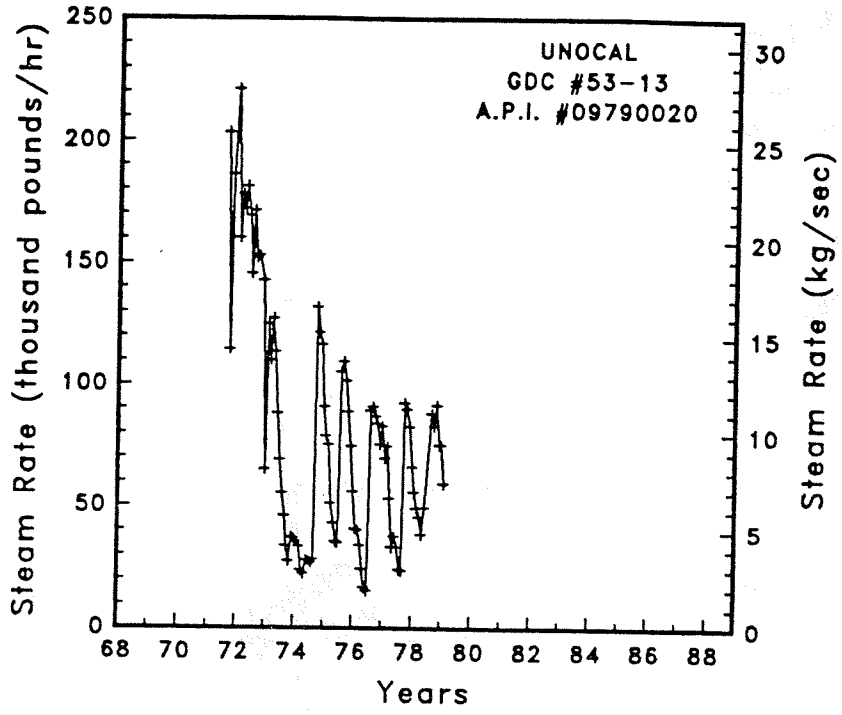

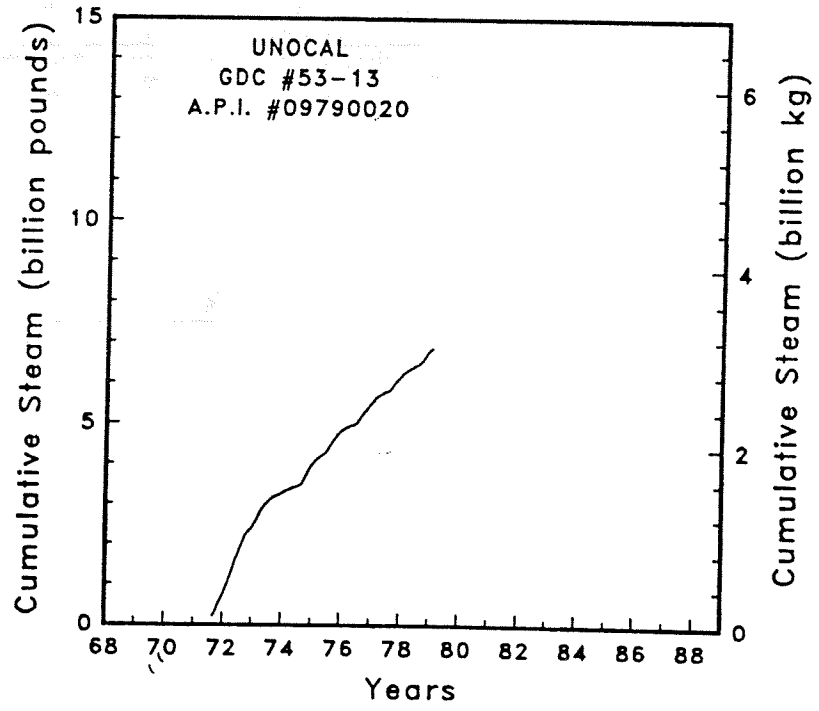

Figure A-89 Steam rate and cumulative mass flow for well GDC #53-13

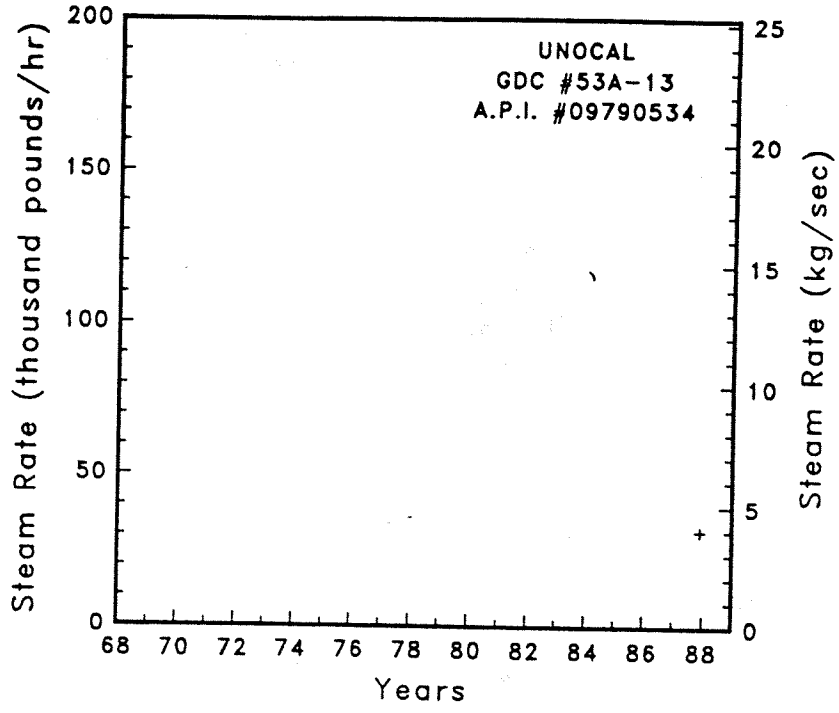

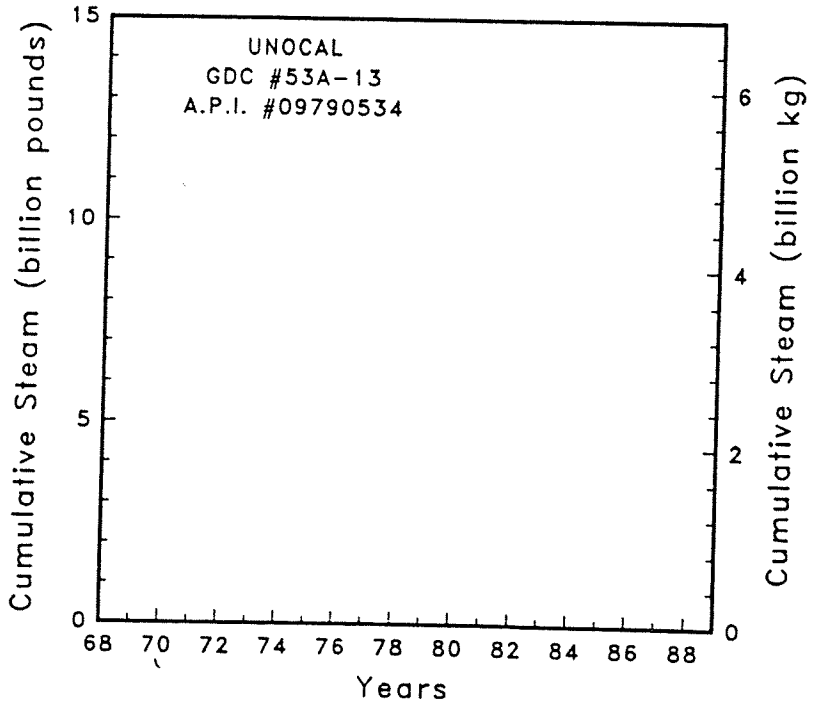

Figure A-90 Steam rate and cumulative mass flow for well GDC #53A-13

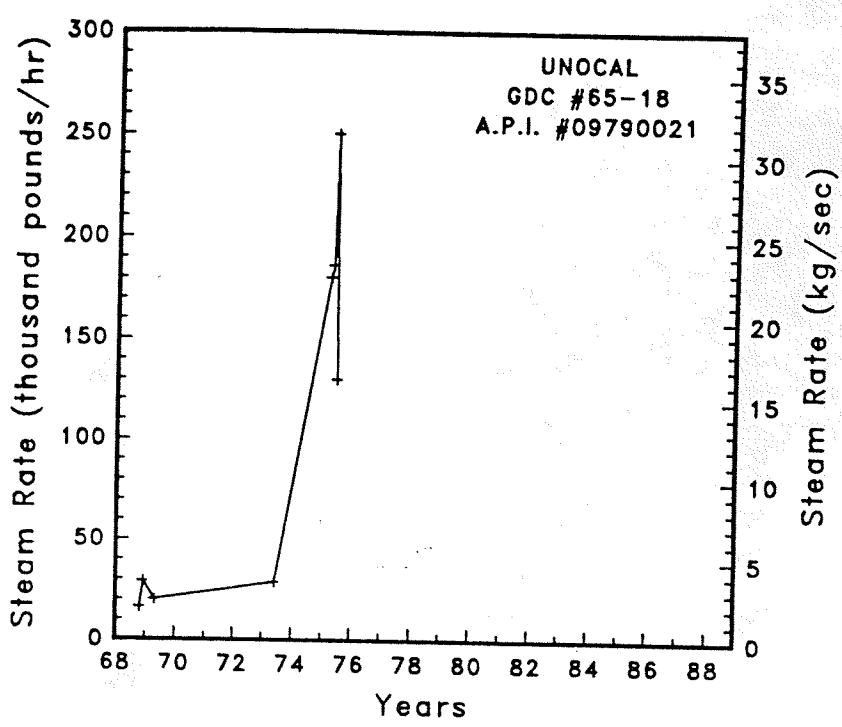

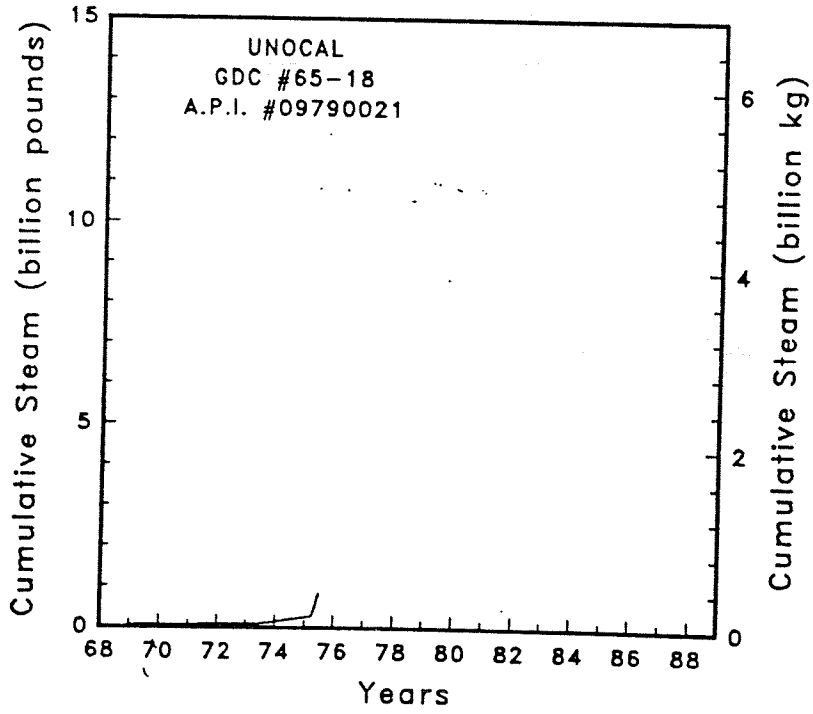

Figure A-91 Steam rate and cumulative mass flow for well GDC #65-18

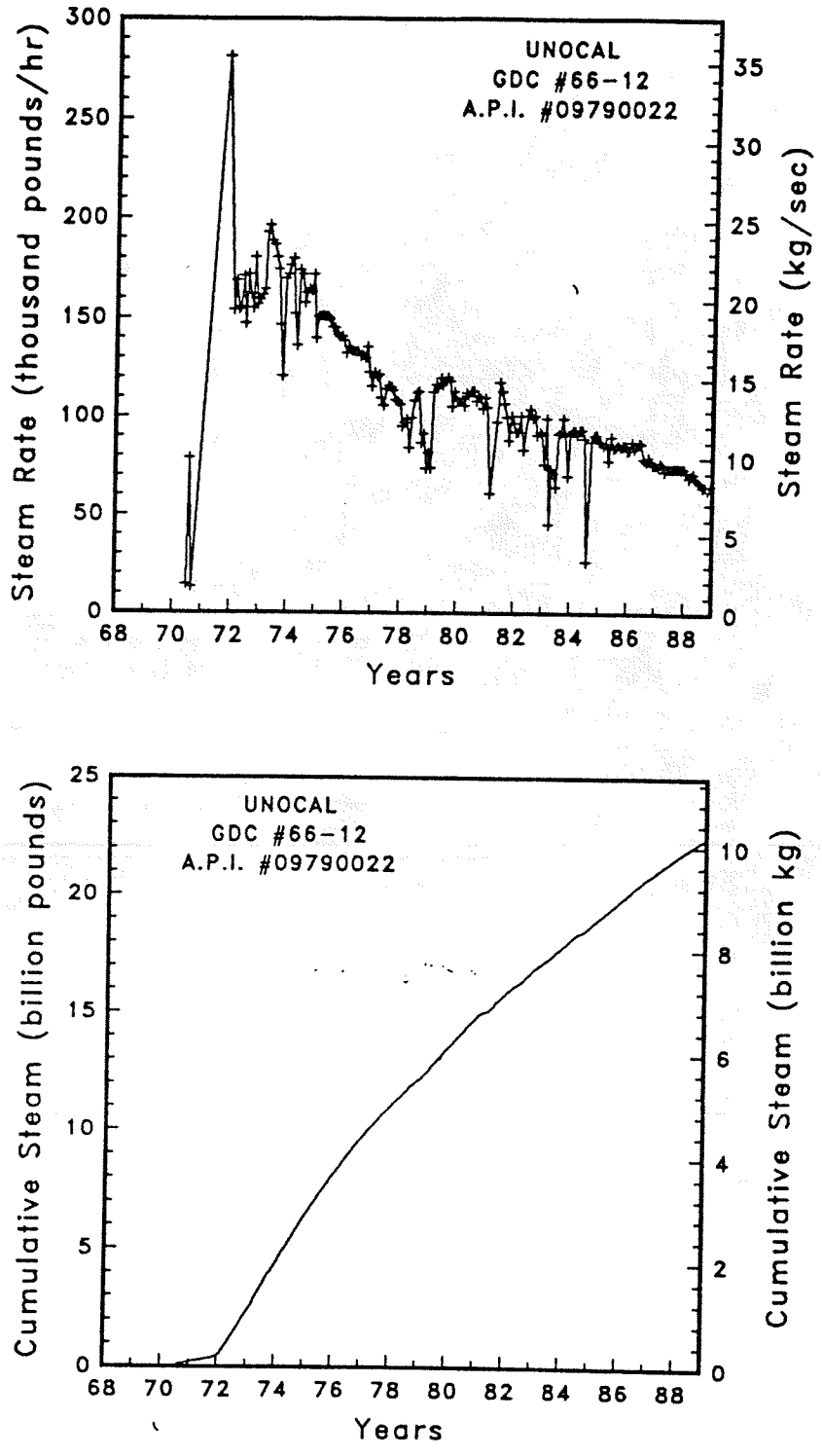

Figure A-92 Steam rate and cumulative mass flow for well GDC #66-12

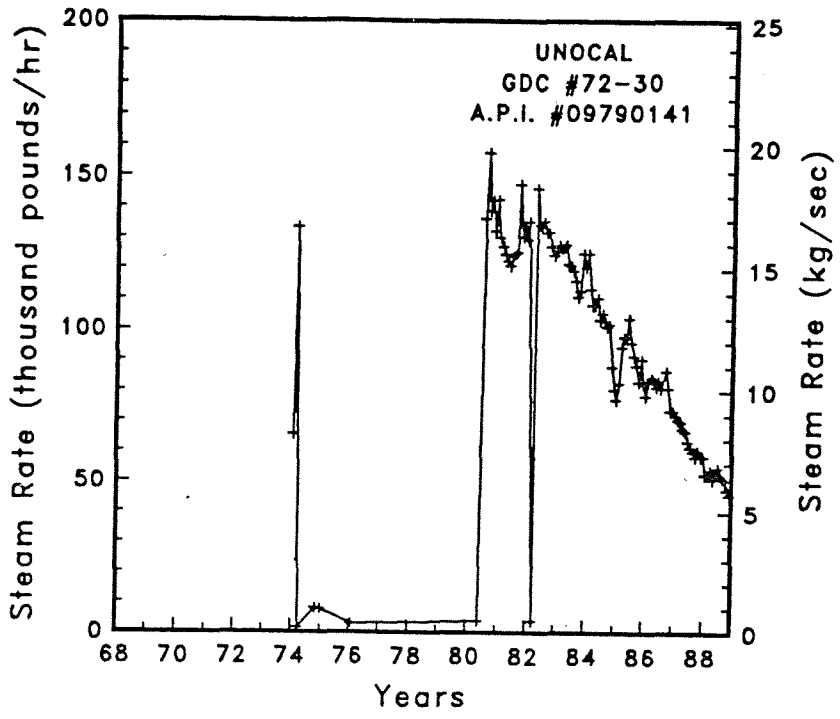

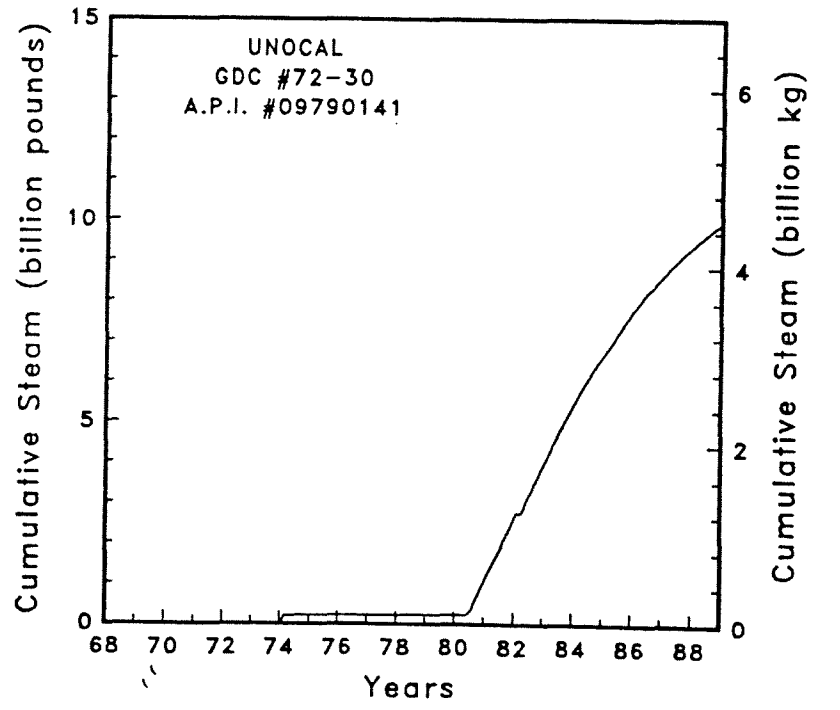

Figure A-93 Steam rate and cumulative mass flow for well GDC #72-30

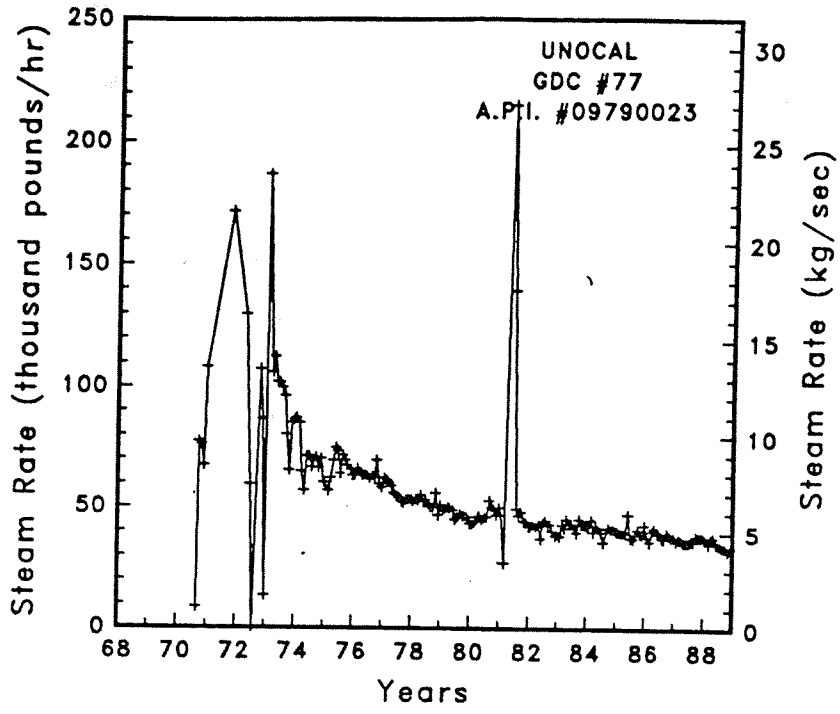

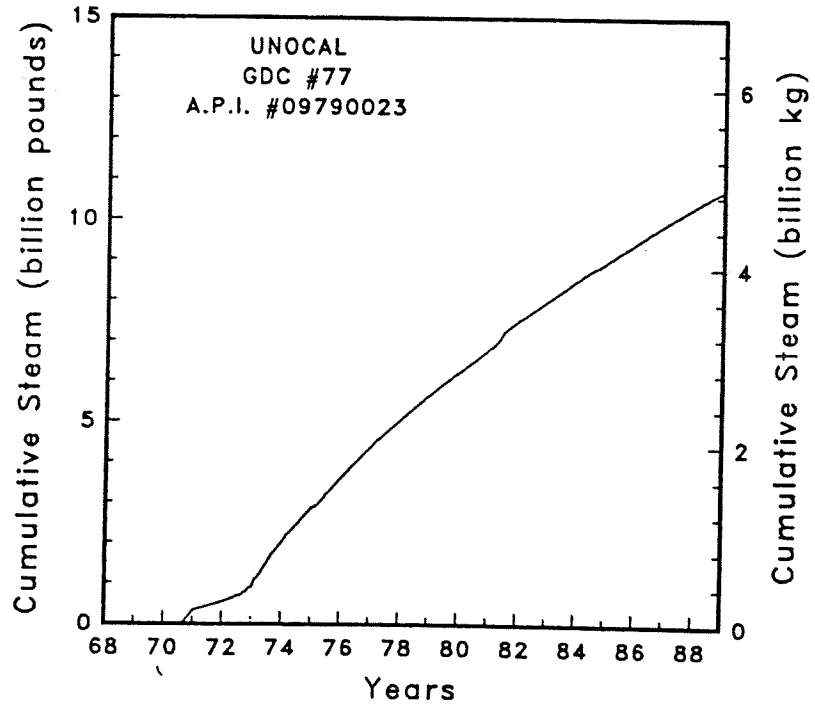

Figure A-94 Steam rate and cumulative mass flow for well GDC #77

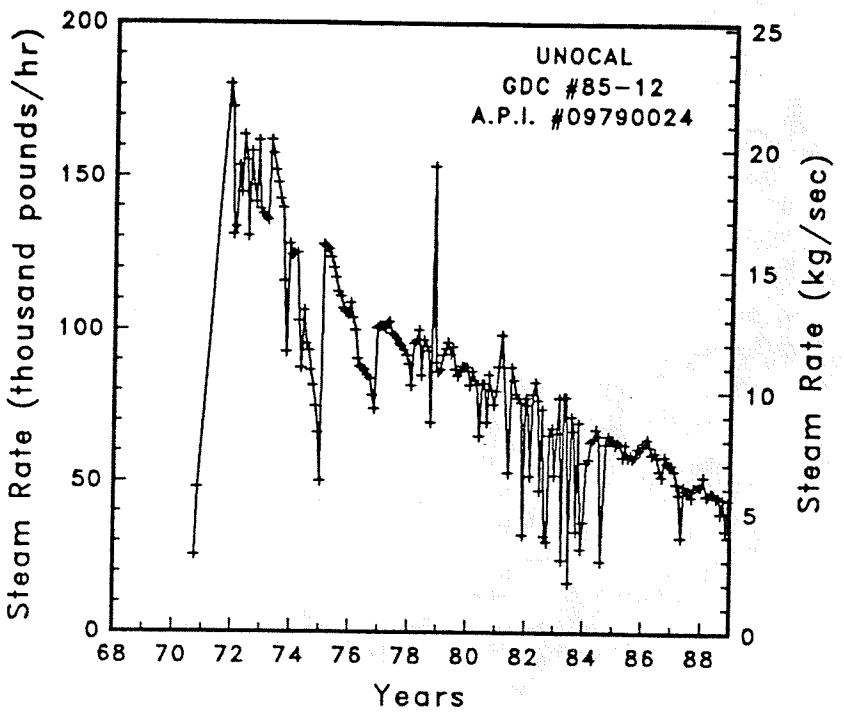

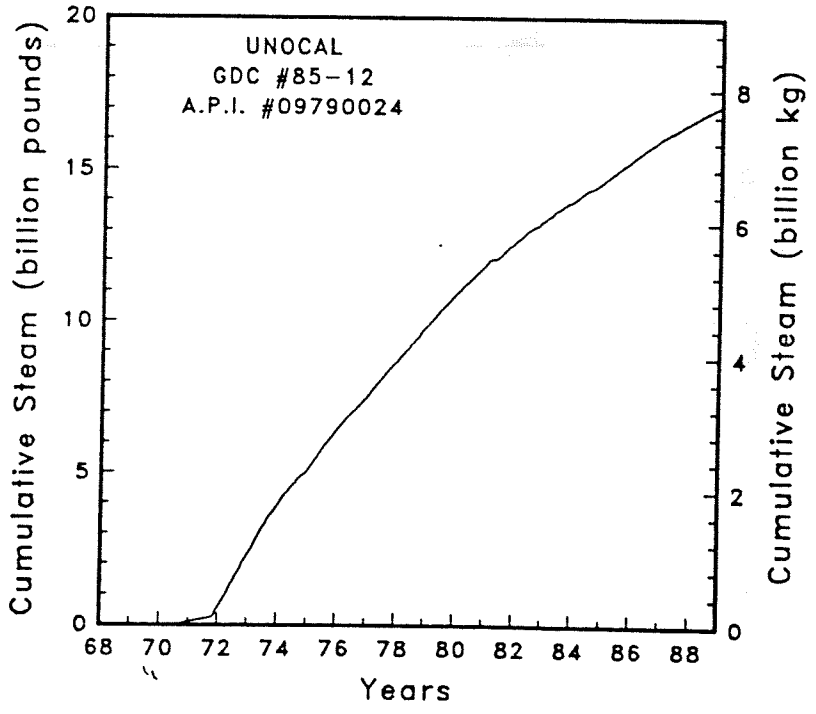

Figure A-95 Steam rate and cumulative mass flow for well GDC #85-12

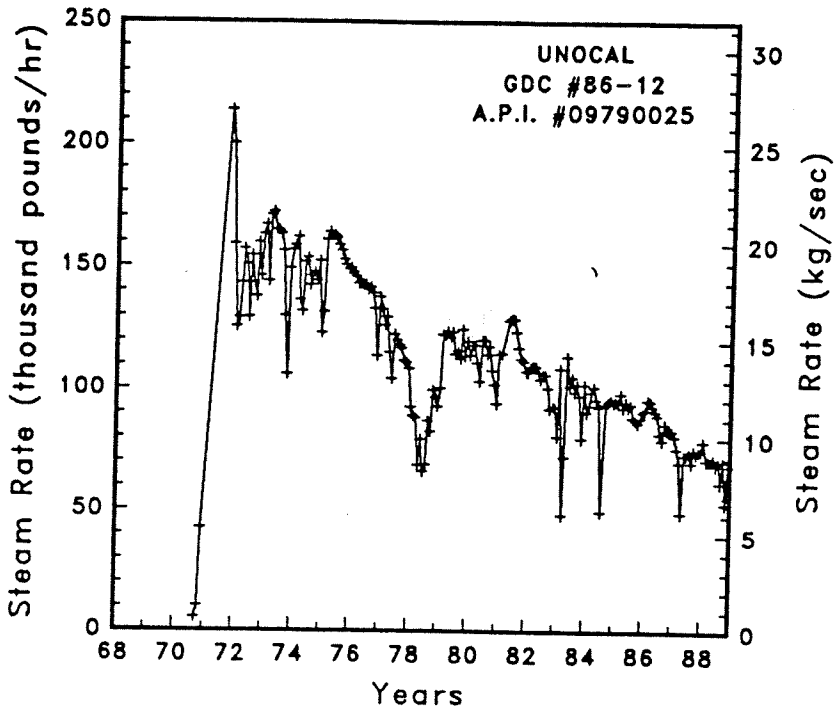

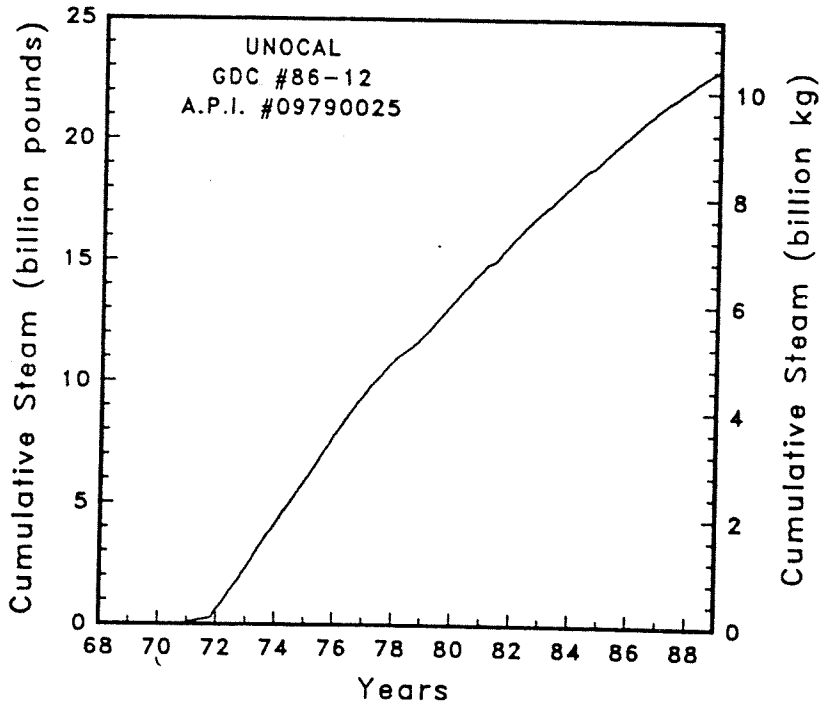

Figure A-96 Steam rate and cumulative mass flow for well GDC #86-12

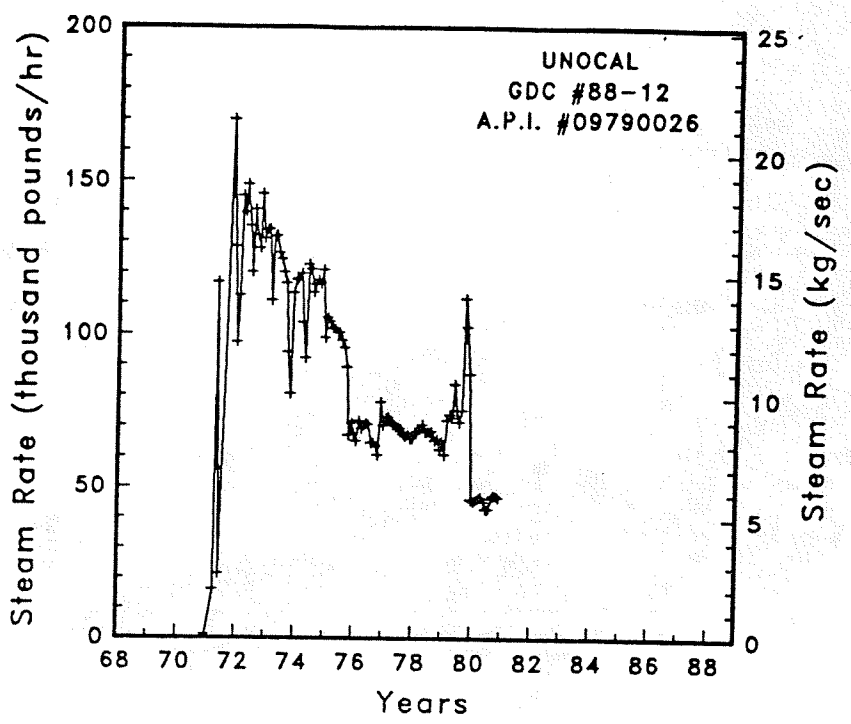

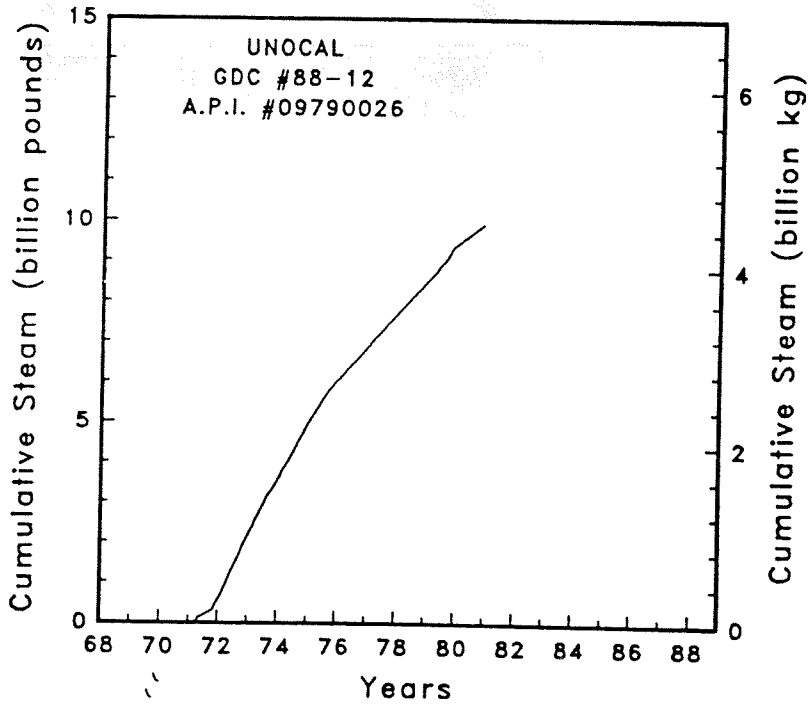

Figure A-97 Steam rate and cumulative mass flow for well GDC #88-12

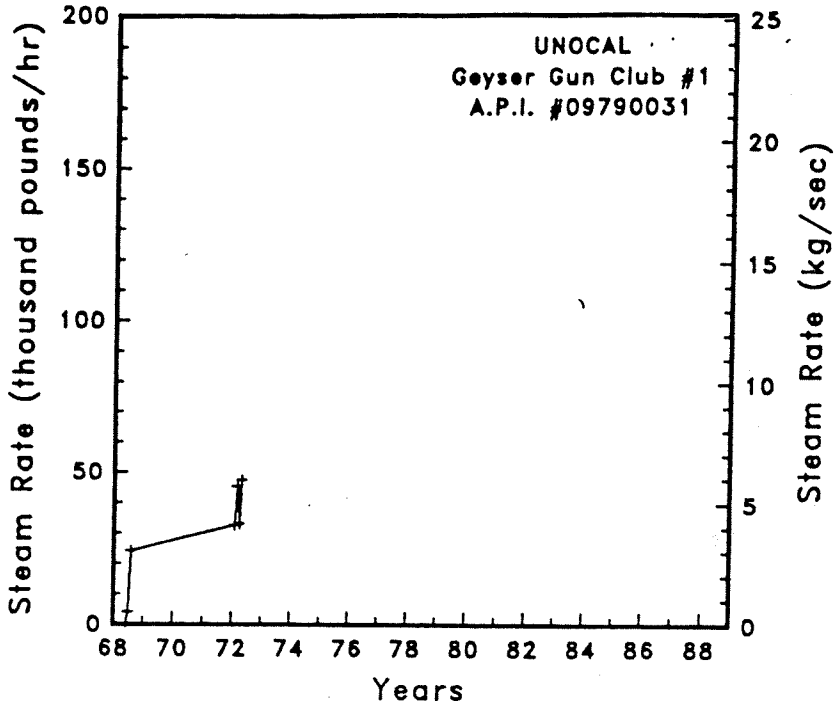

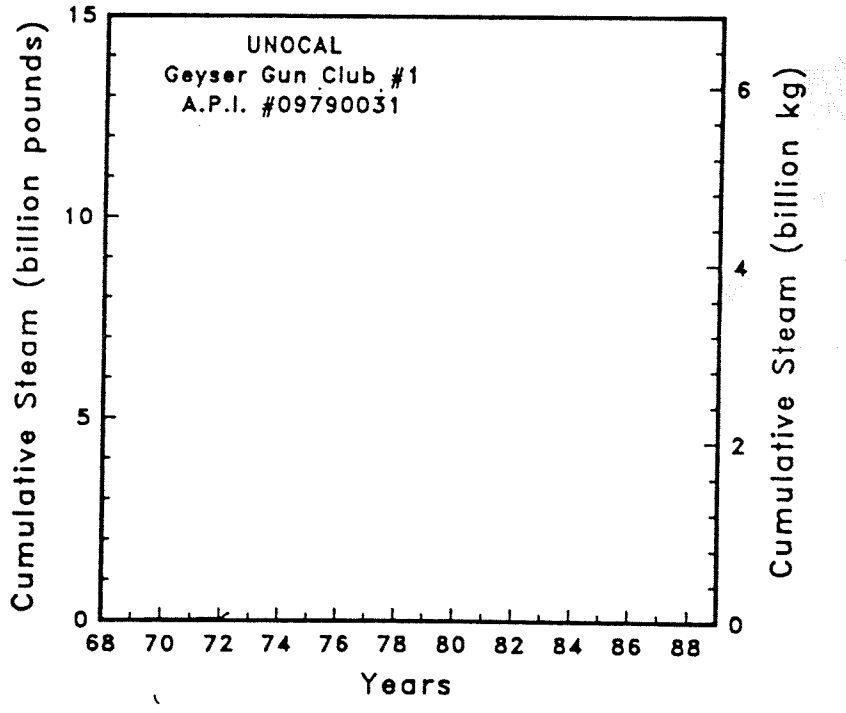

Figure A-98 Steam rate and cumulative mass flow for well Geyser Gun Club #1

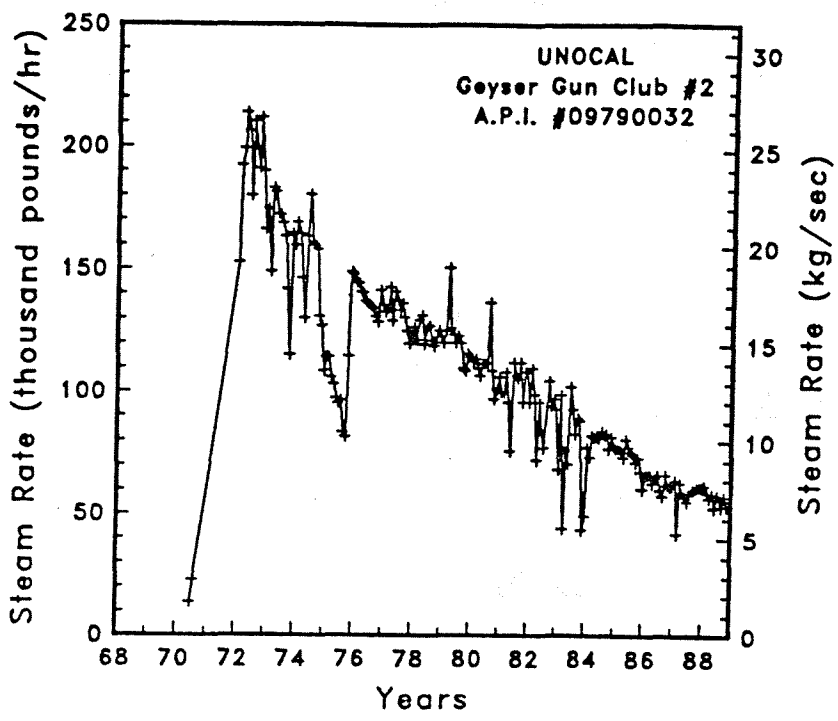

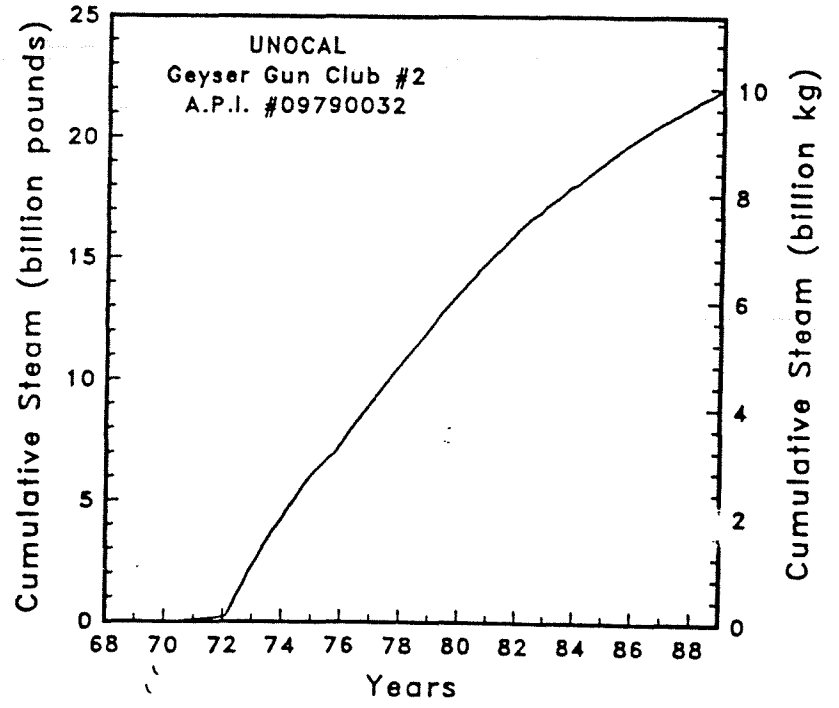

Figure A-99 Steam rate and cumulative mass flow for well Geyser Gun Club #2

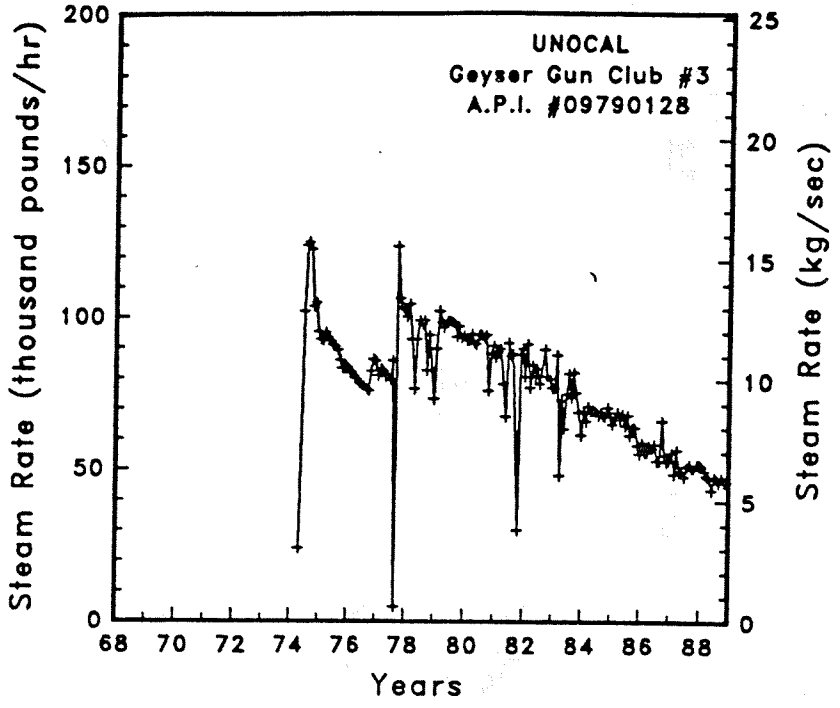

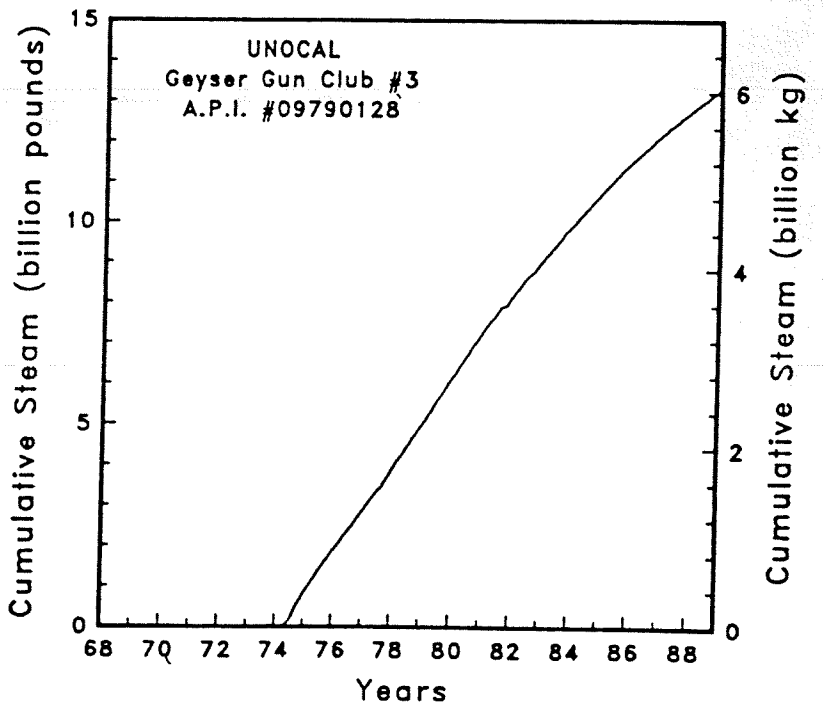

Figure A-100 Steam rate and cumulative mass flow for well Geyser Gun Club #3

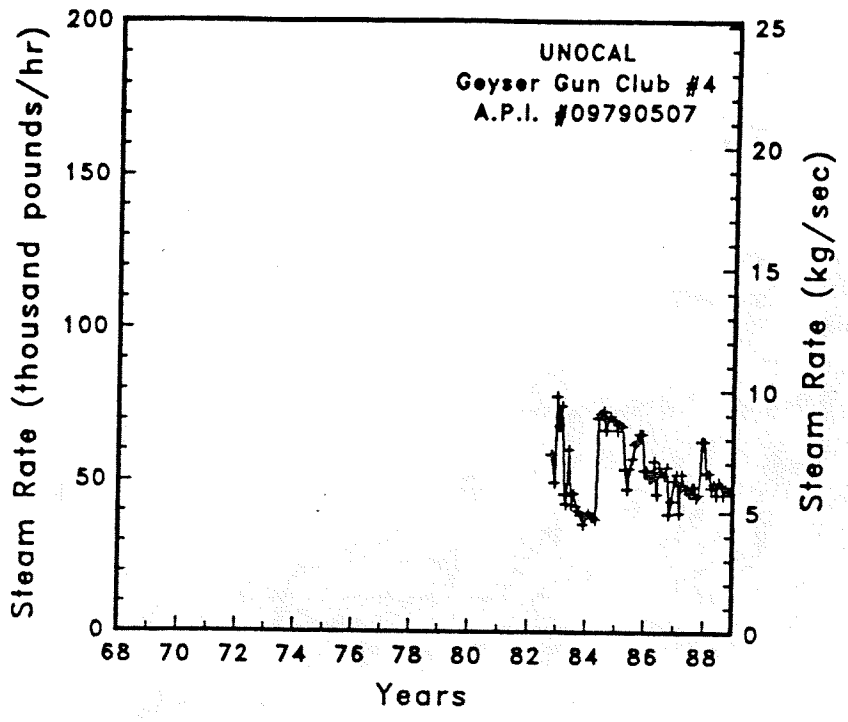

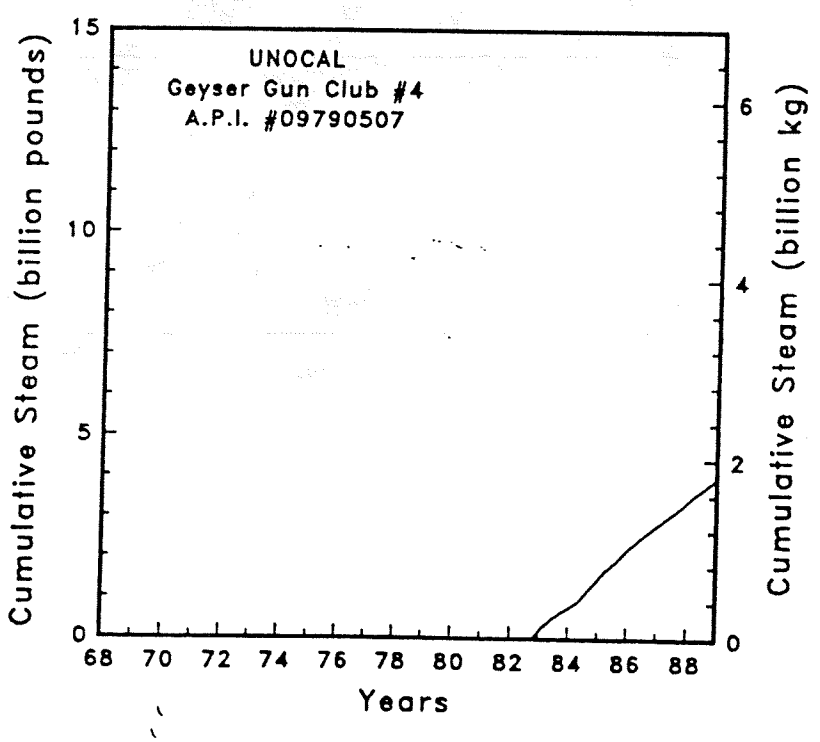

Figure A-101 Steam rate and cumulative mass flow for well Geyser Gun Club #4

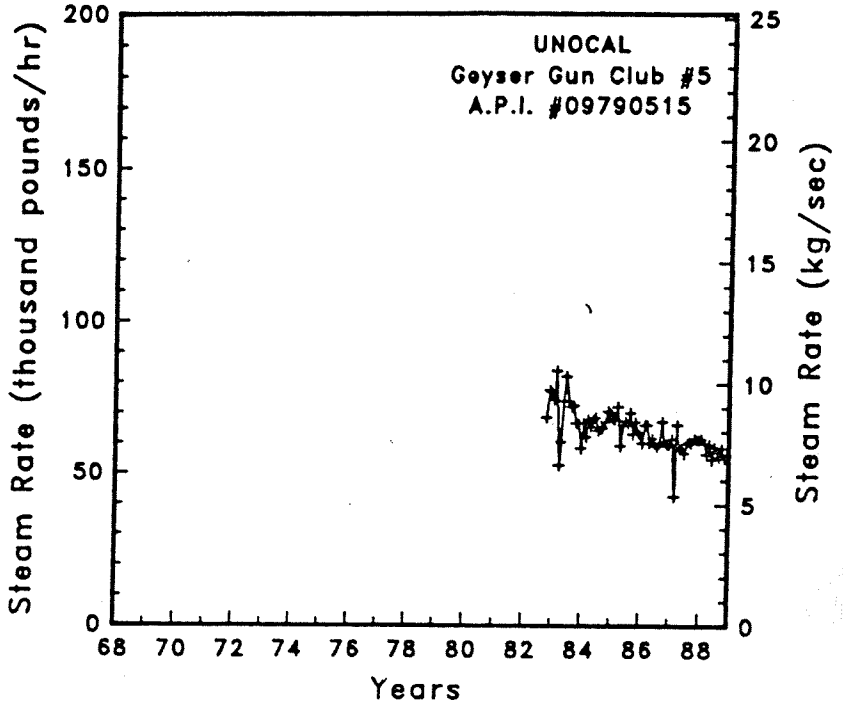

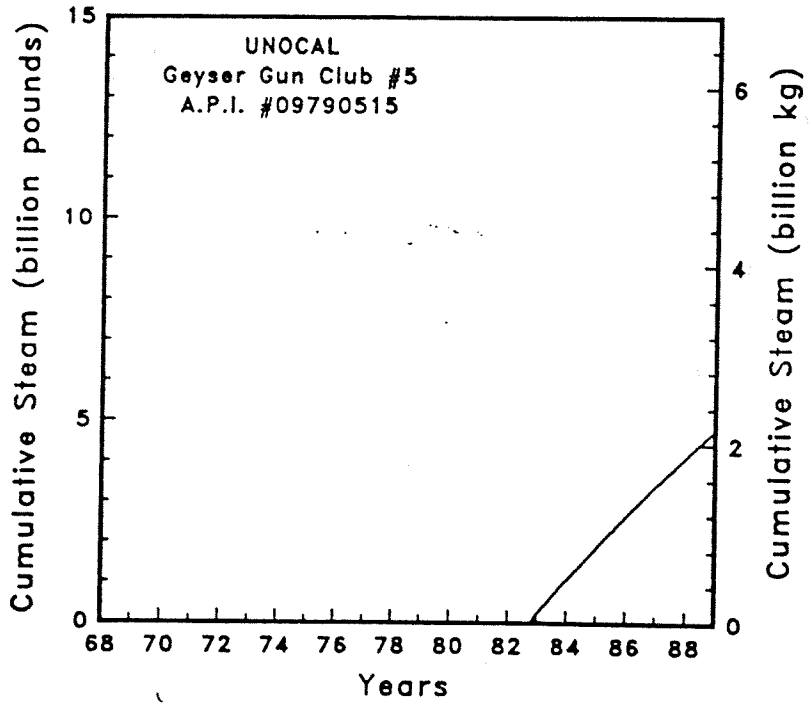

Figure A-102 Steam rate and cumulative mass flow for well Geyser Gun Club #5

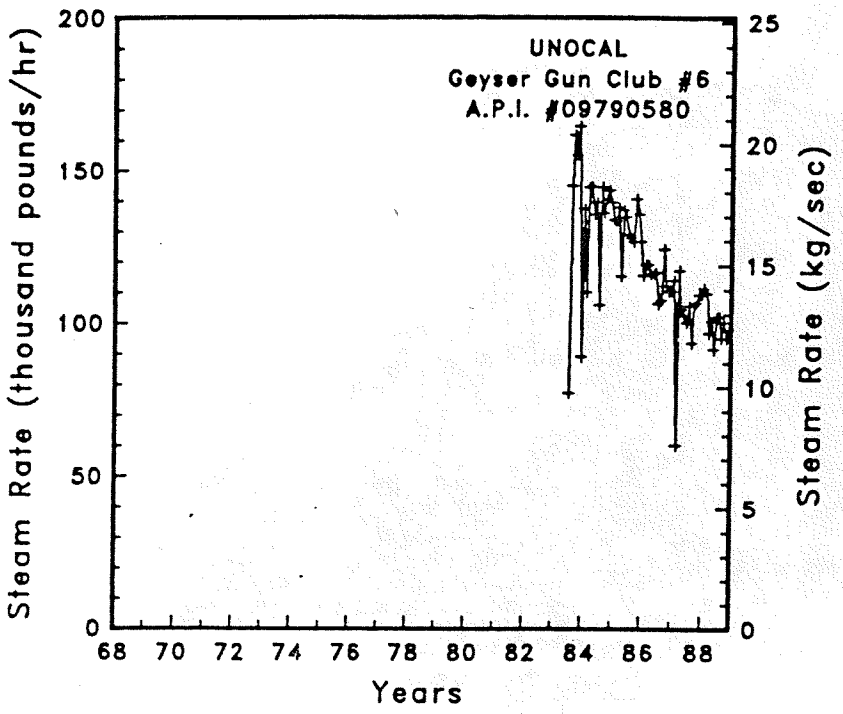

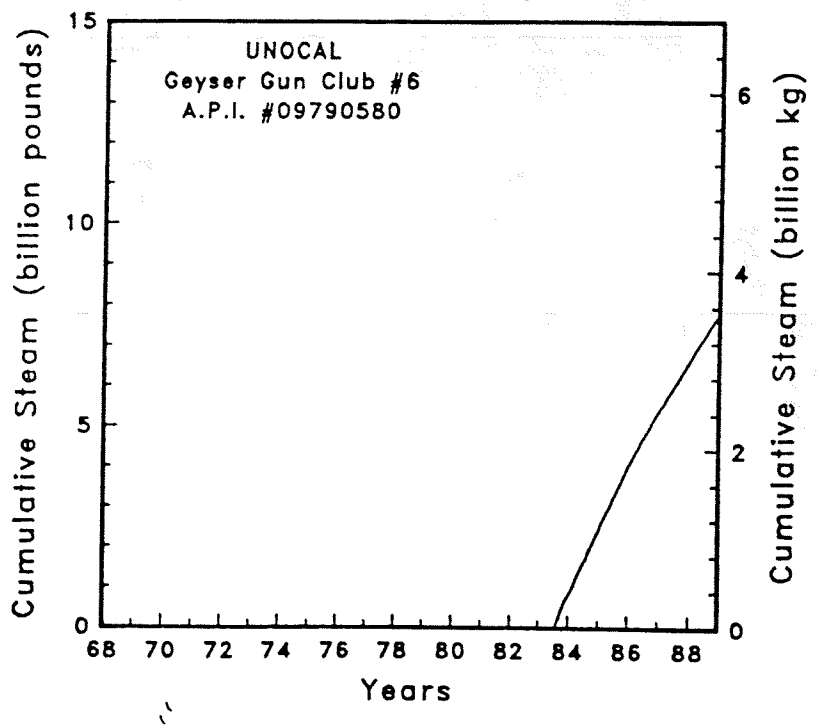

Figure A-103 Steam rate and cumulative mass flow for well Geyser Gun Club #6

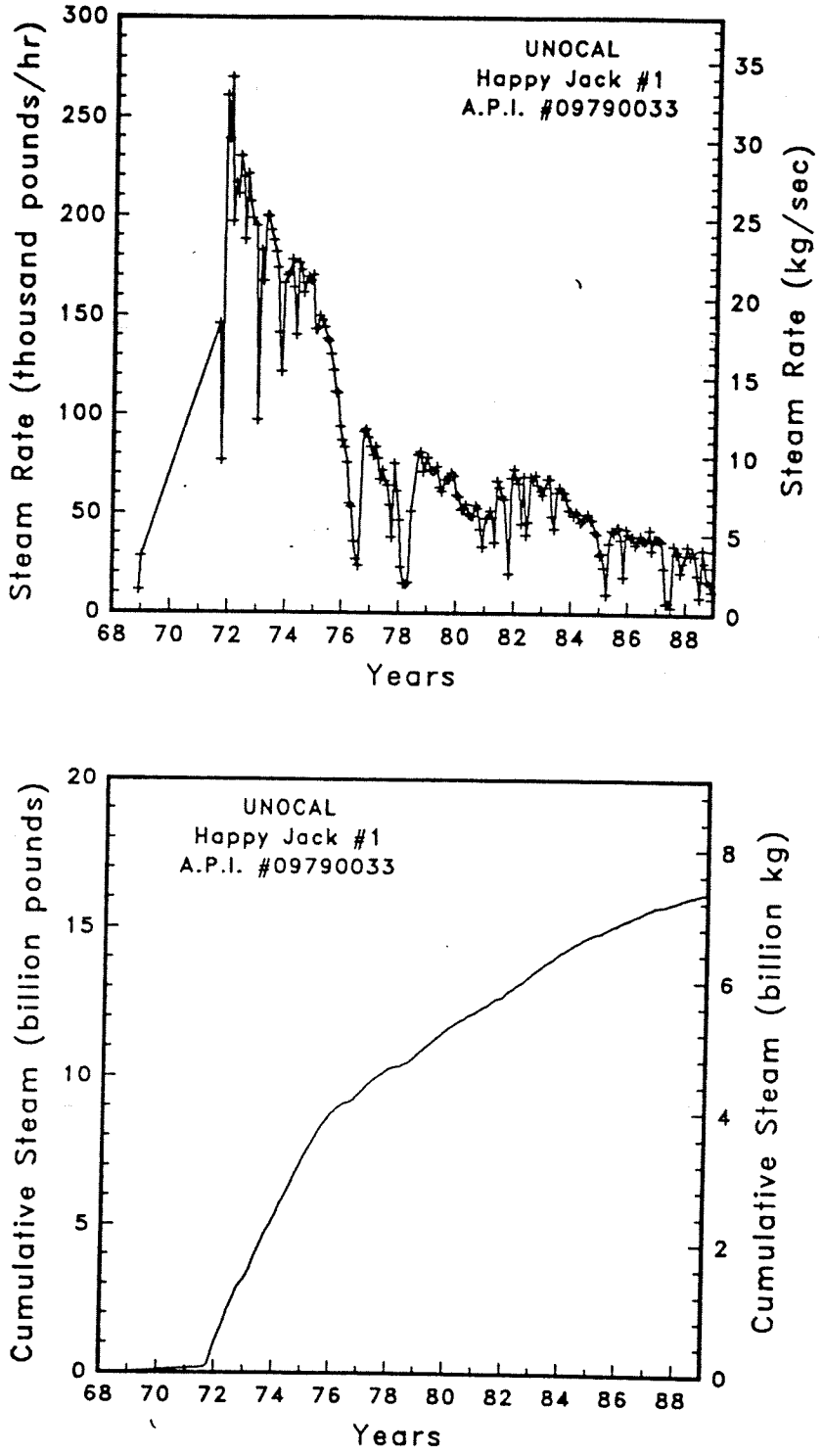

Figure A-104 Steam rate and cumulative mass flow for well Happy Jack #1

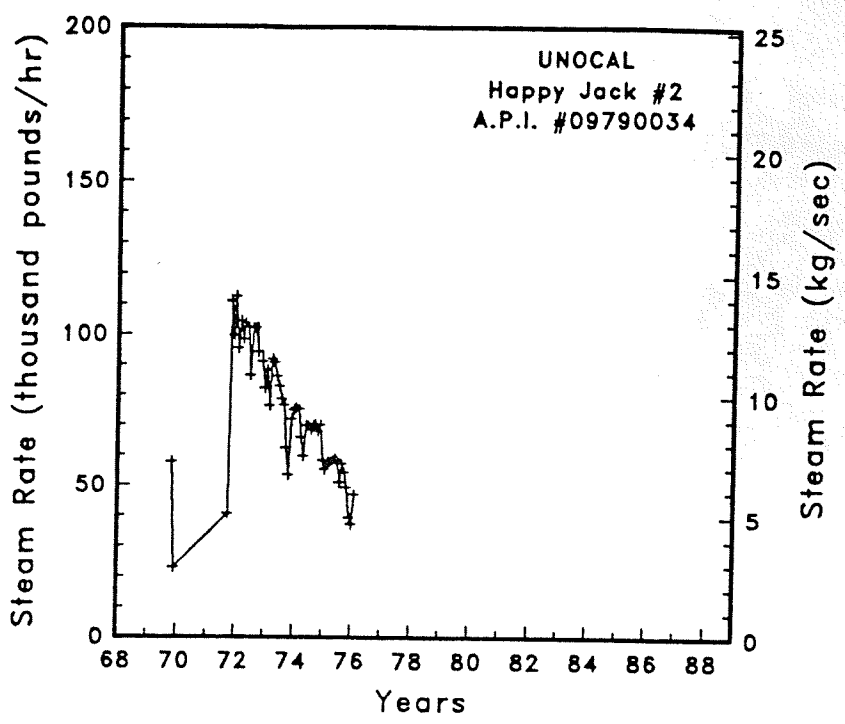

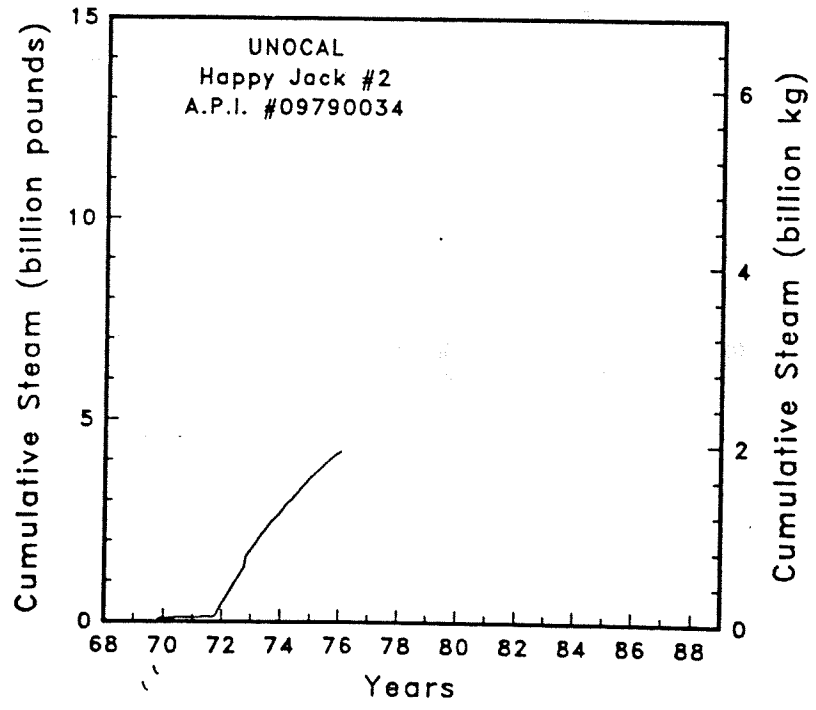

Figure A-105 Steam rate and cumulative mass flow for well Happy Jack #2

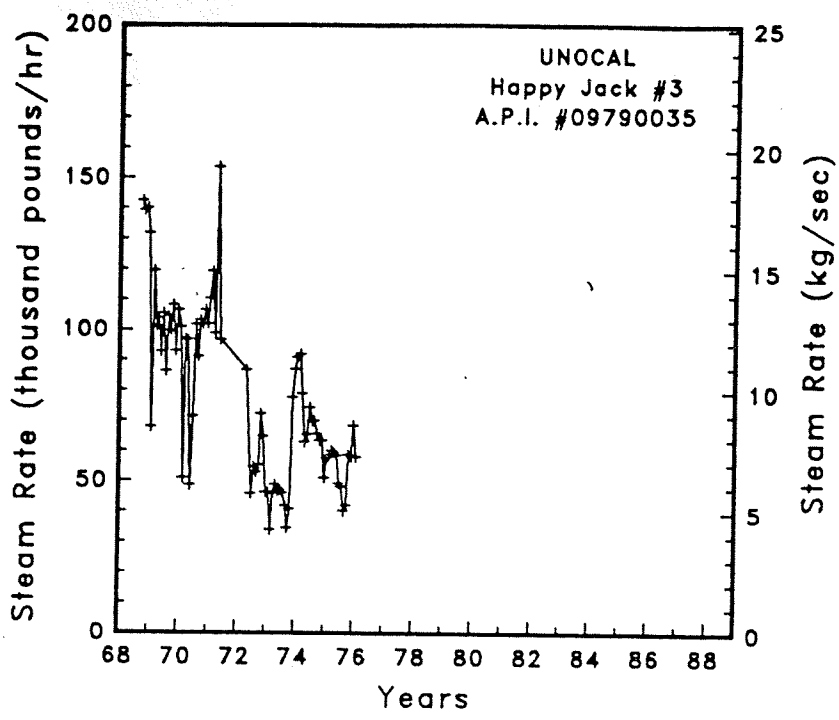

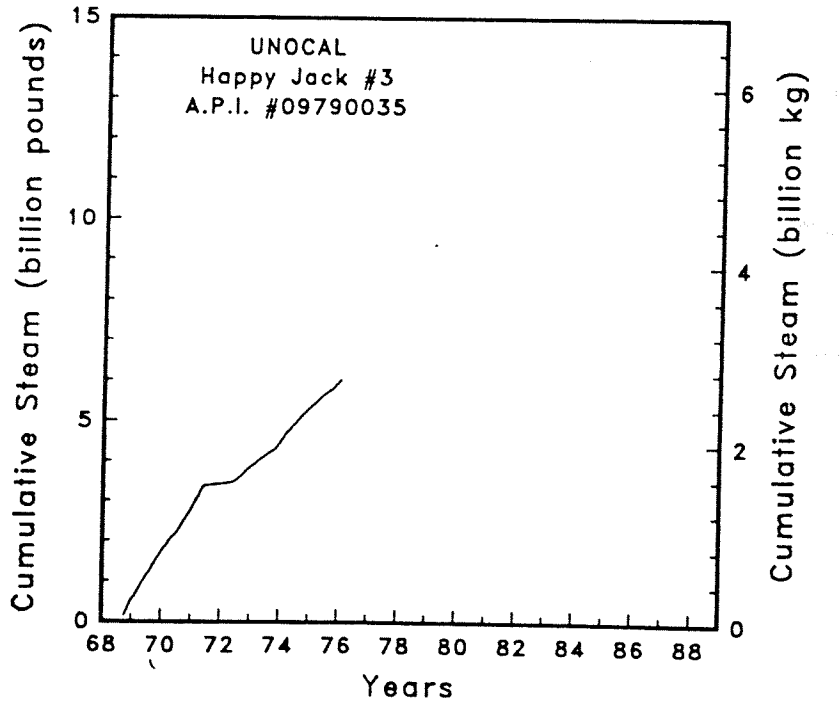

Figure A-106 Steam rate and cumulative mass flow for well Happy Jack #3

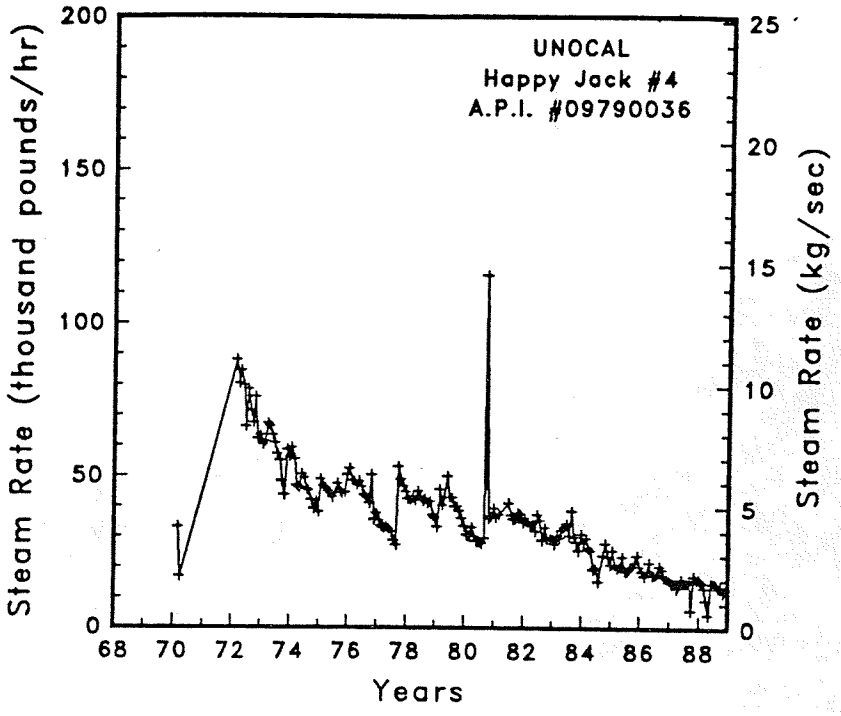

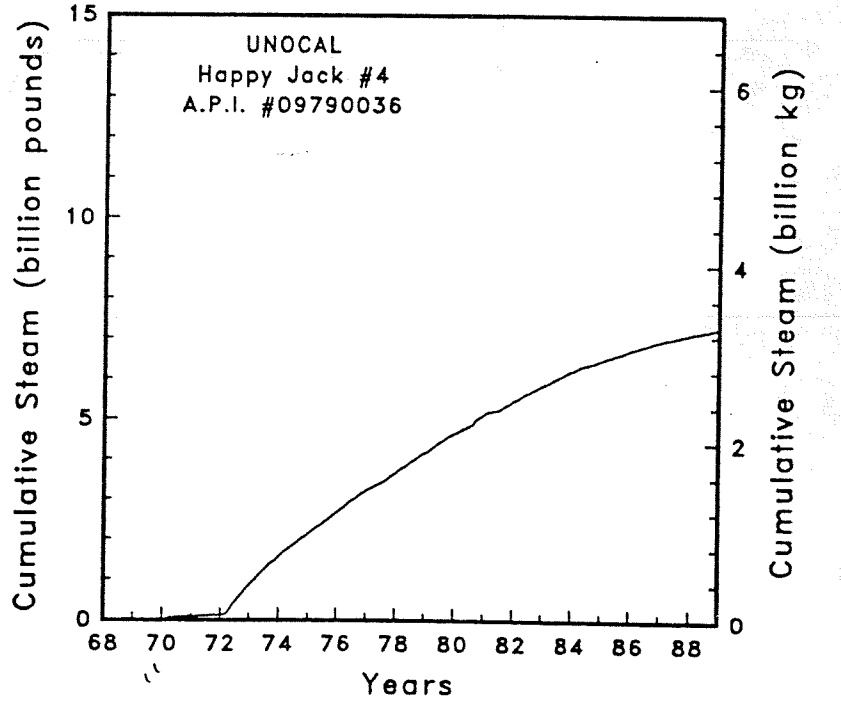

Figure A-107 Steam rate and cumulative mass flow for well Happy Jack #4

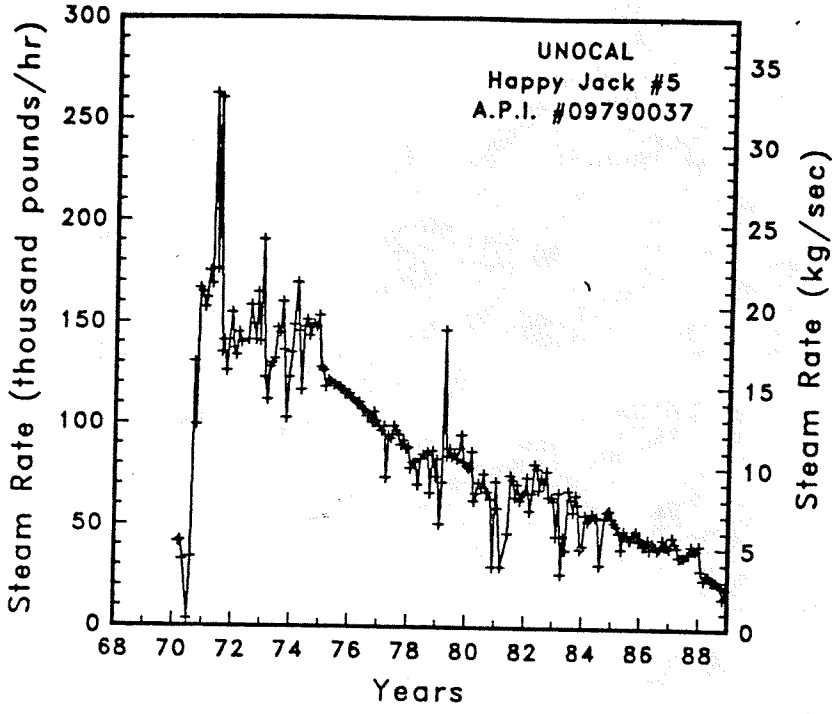

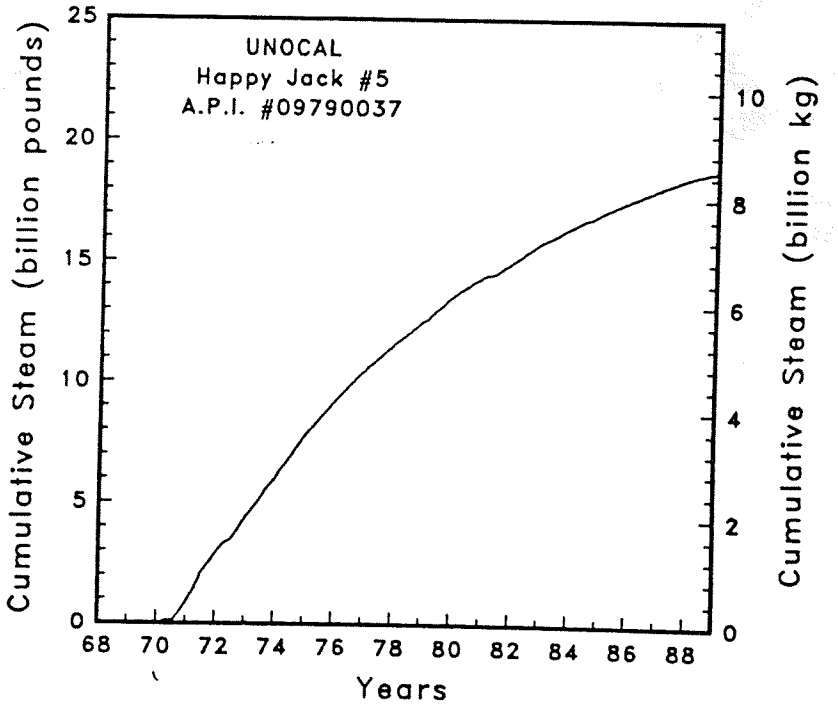

Figure A-108 Steam rate and cumulative mass flow for well Happy Jack #5

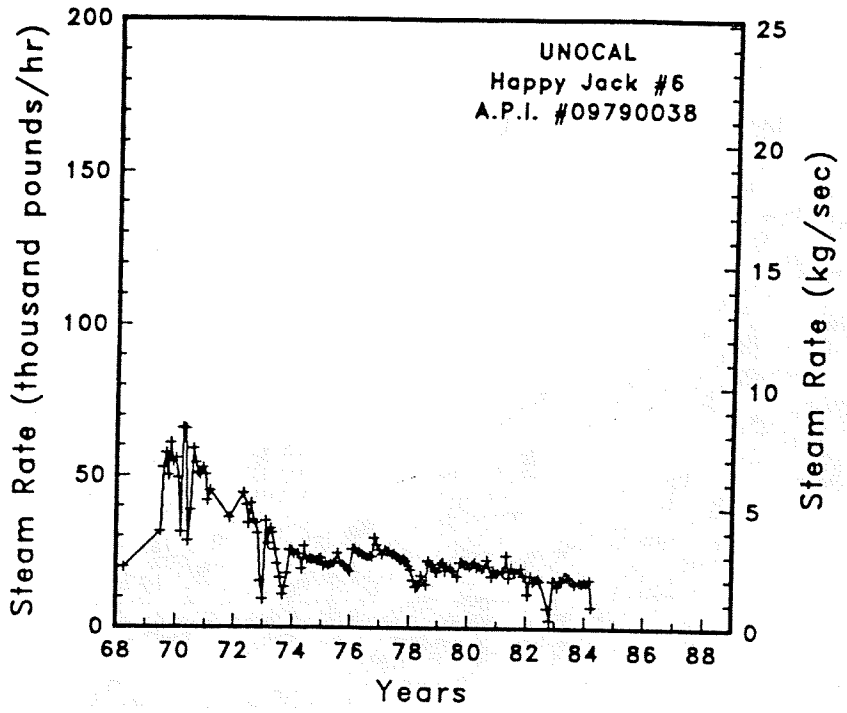

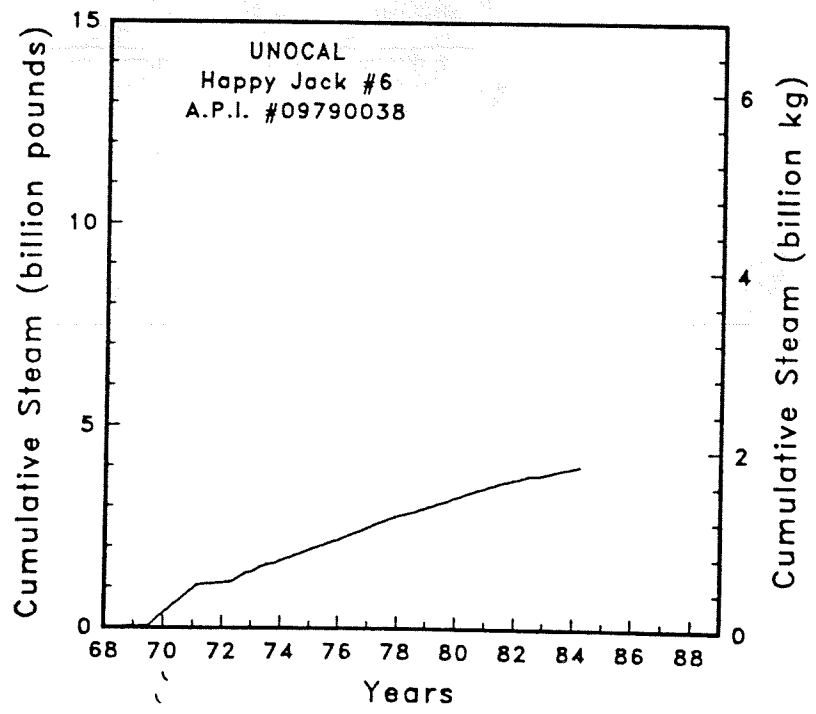

Figure A-109 Steam rate and cumulative mass flow for well Happy Jack #6

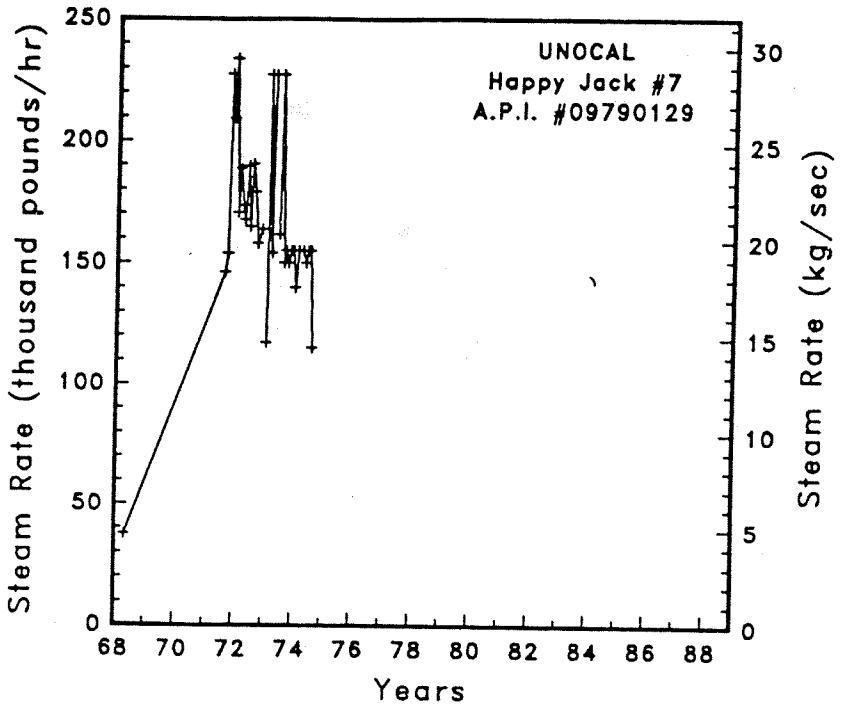

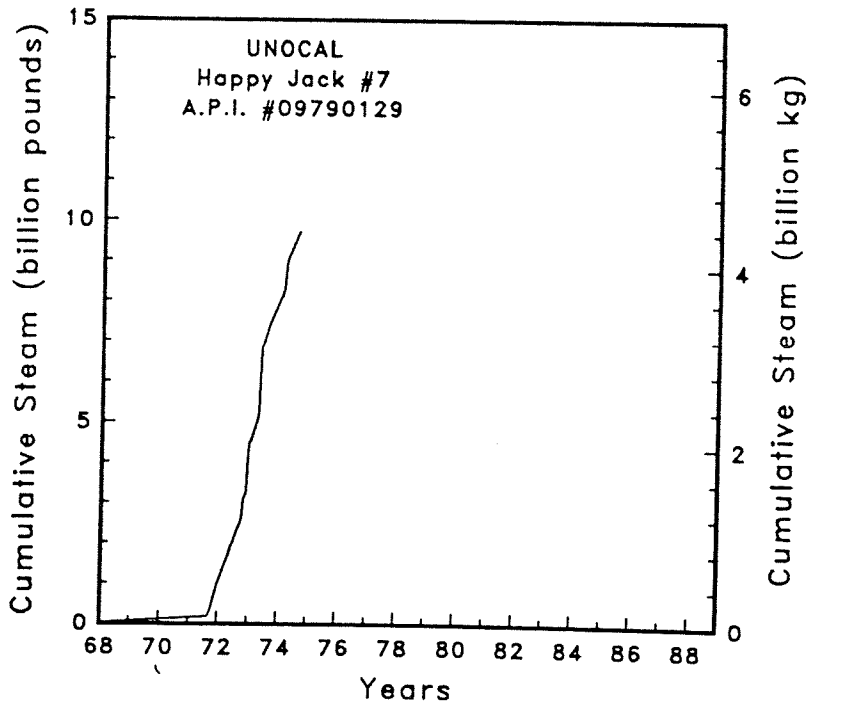

Figure A-110 Steam rate and cumulative mass flow for well Happy Jack #7

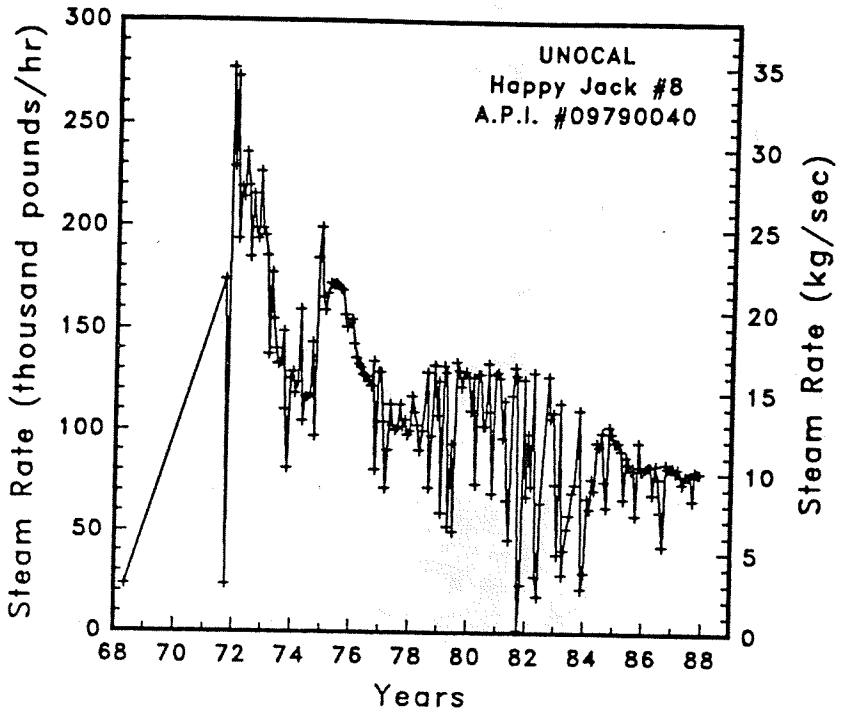

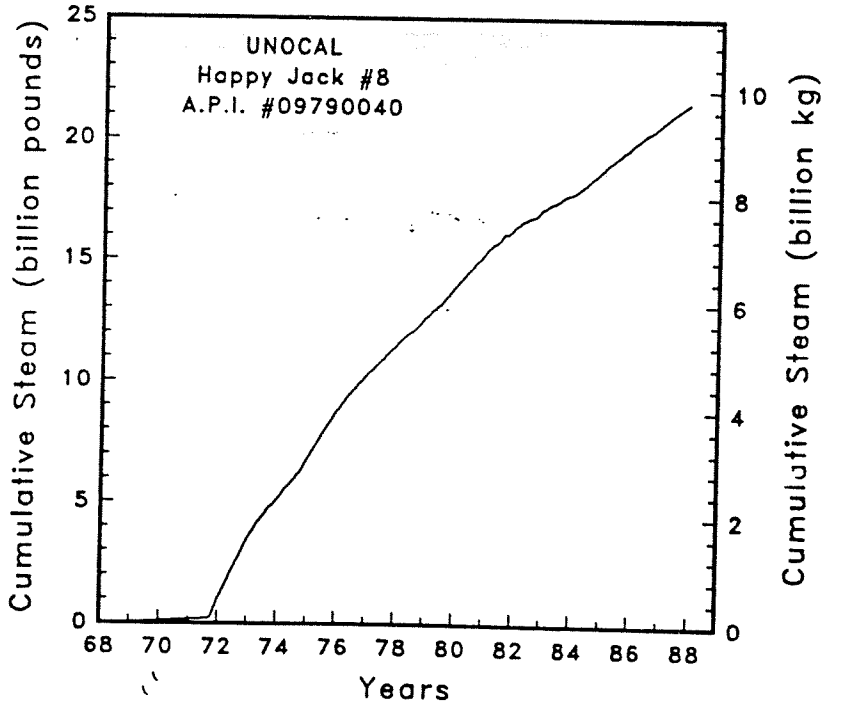

Figure A-111 Steam rate and cumulative mass flow for well Happy Jack #8

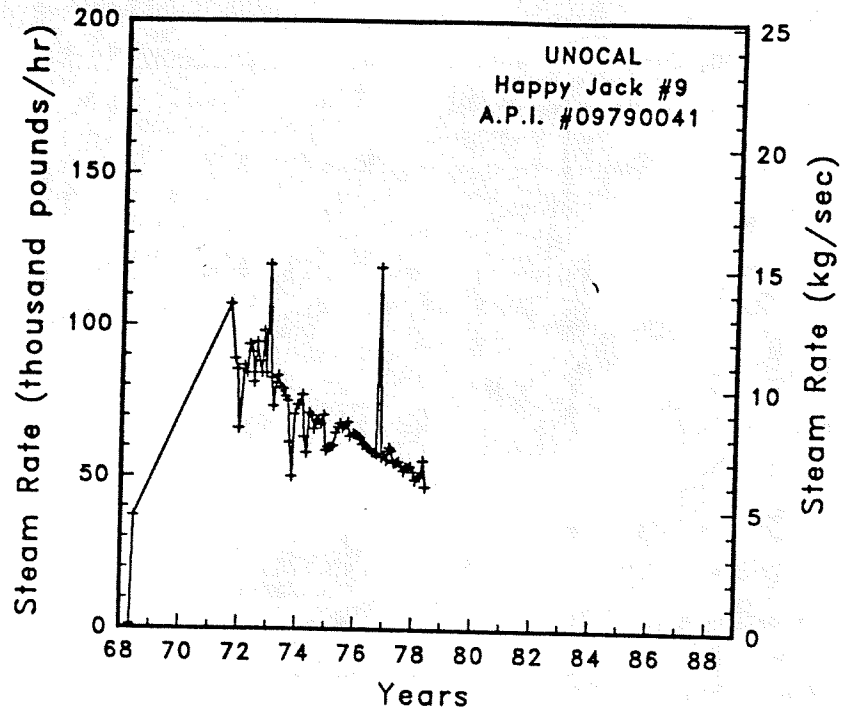

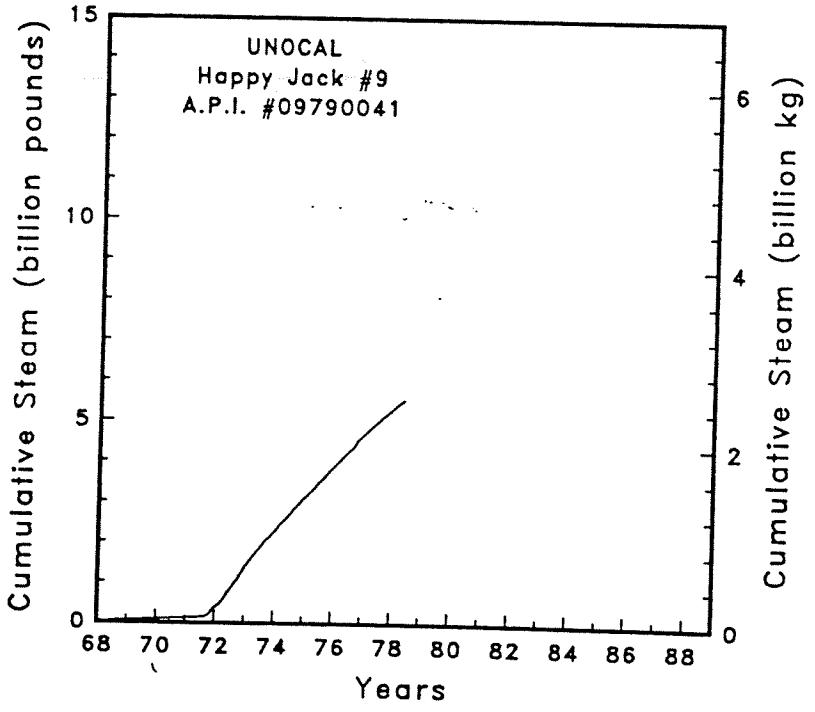

Figure A-112 Steam rate and cumulative mass flow for well Happy Jack #9

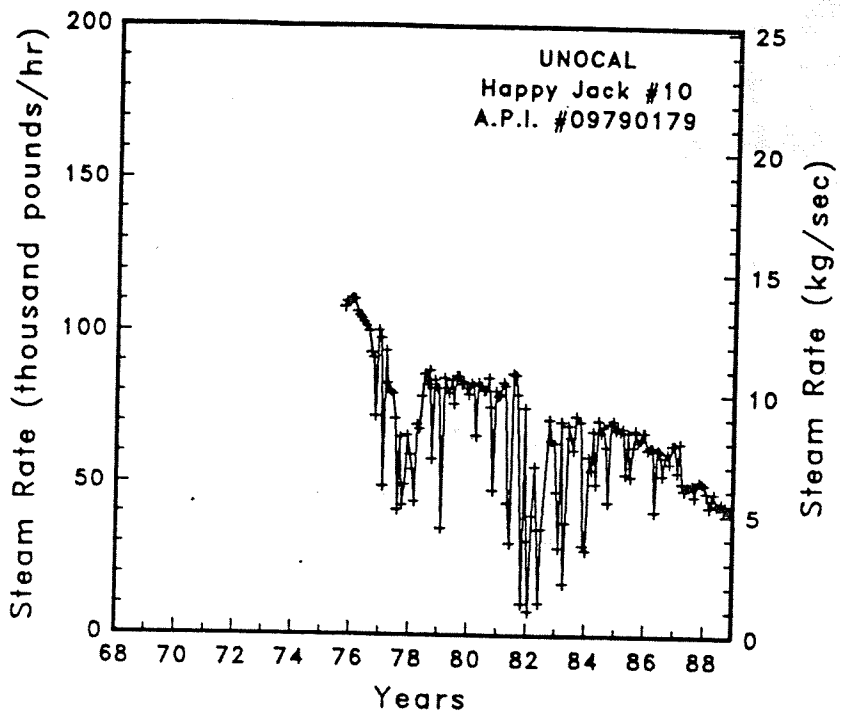

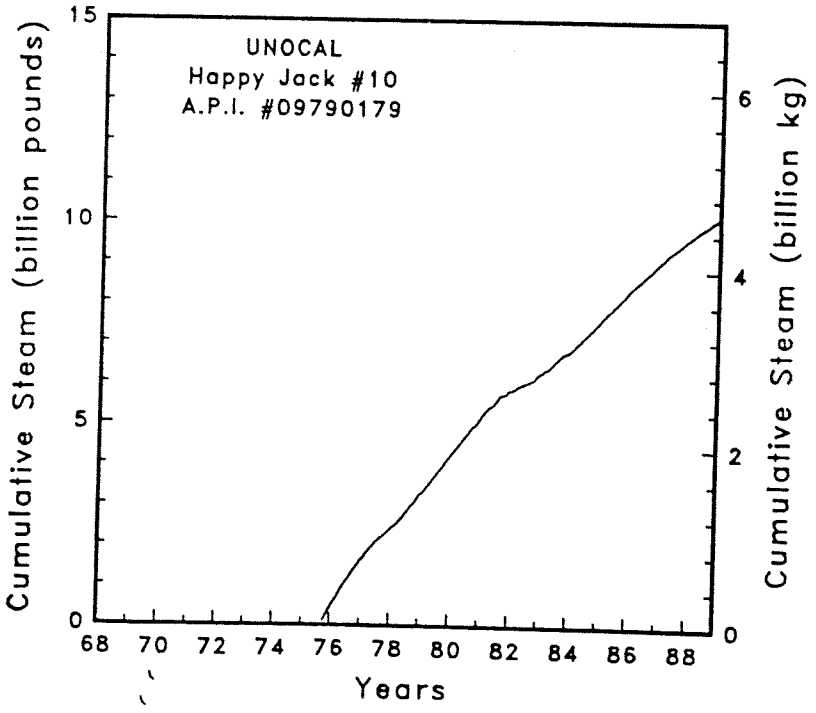

Figure A-113 Steam rate and cumulative mass flow for well Happy Jack #10

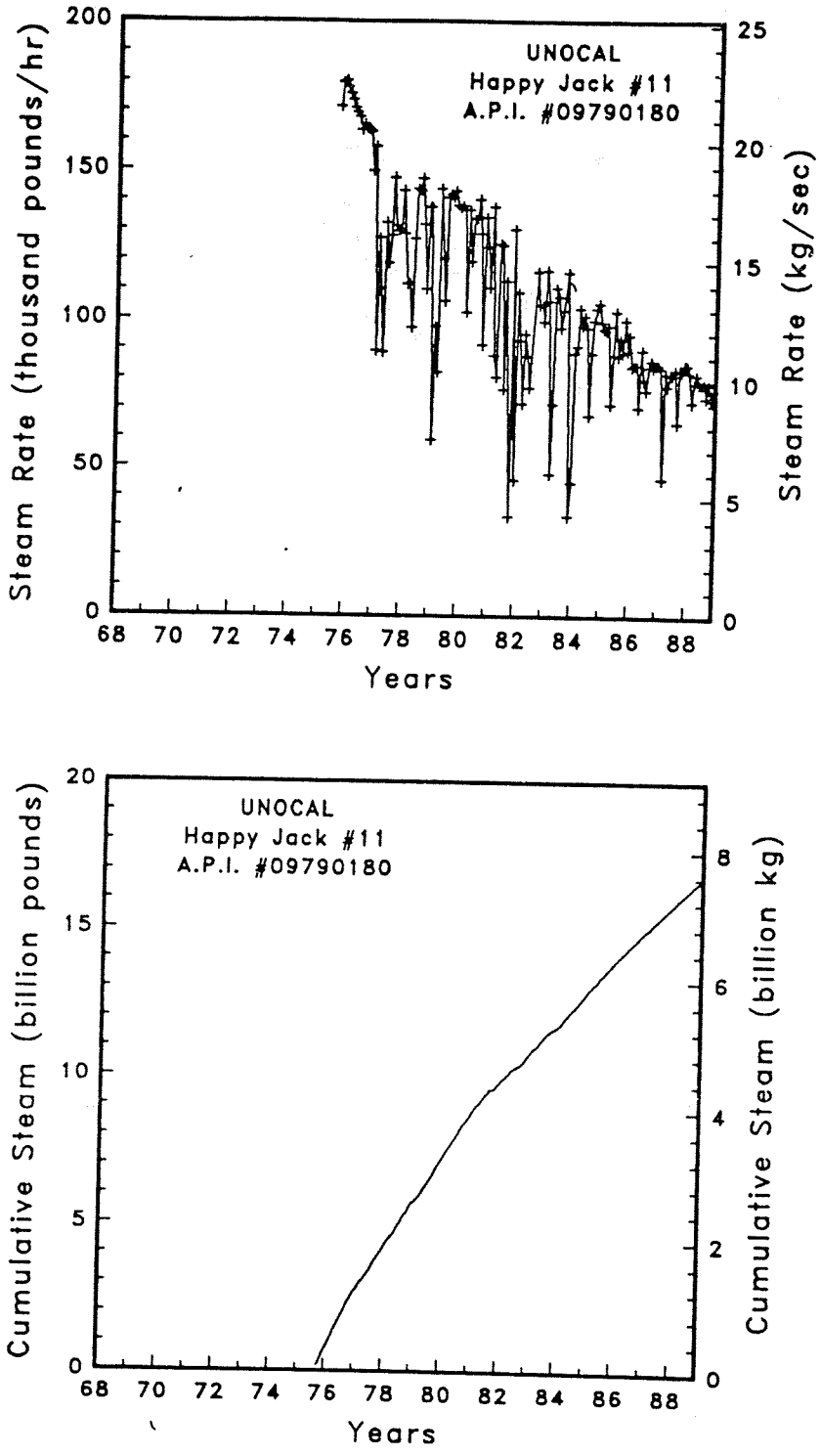

Figure A-114 Steam rate and cumulative mass flow for well Happy Jack #11

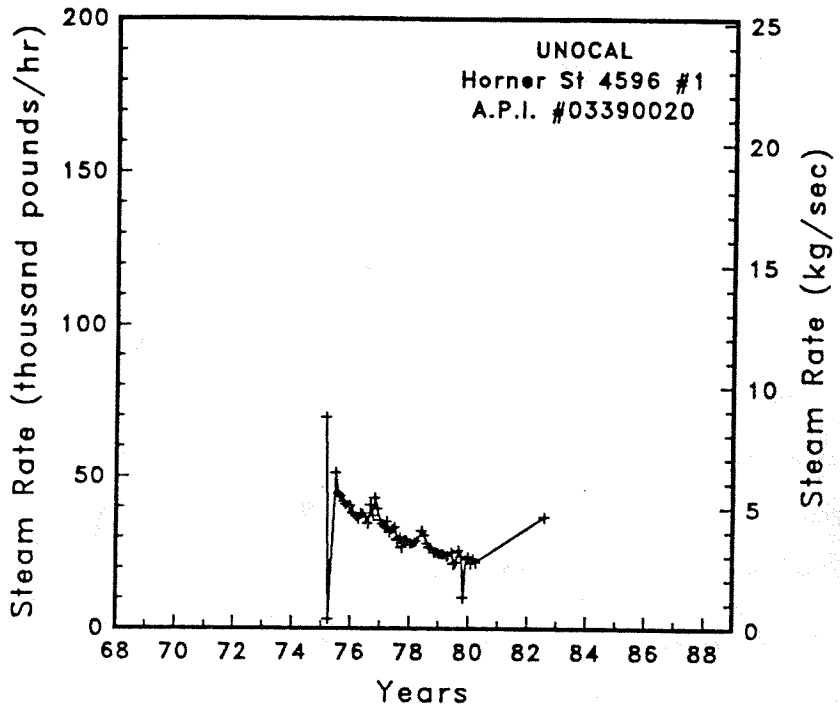

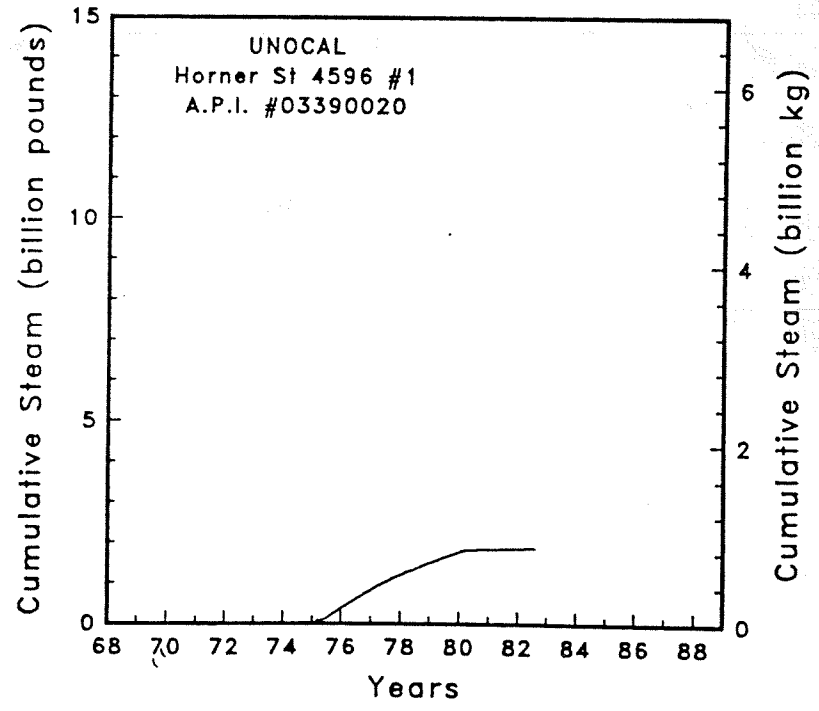

Figure A-115 Steam rate and cumulative mass flow for well Horner St 4596 #1

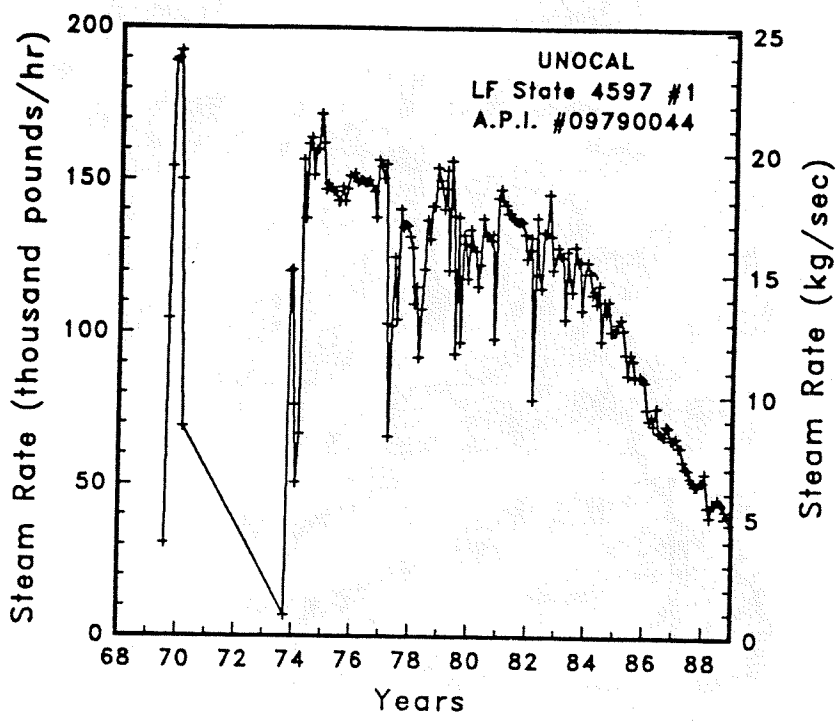

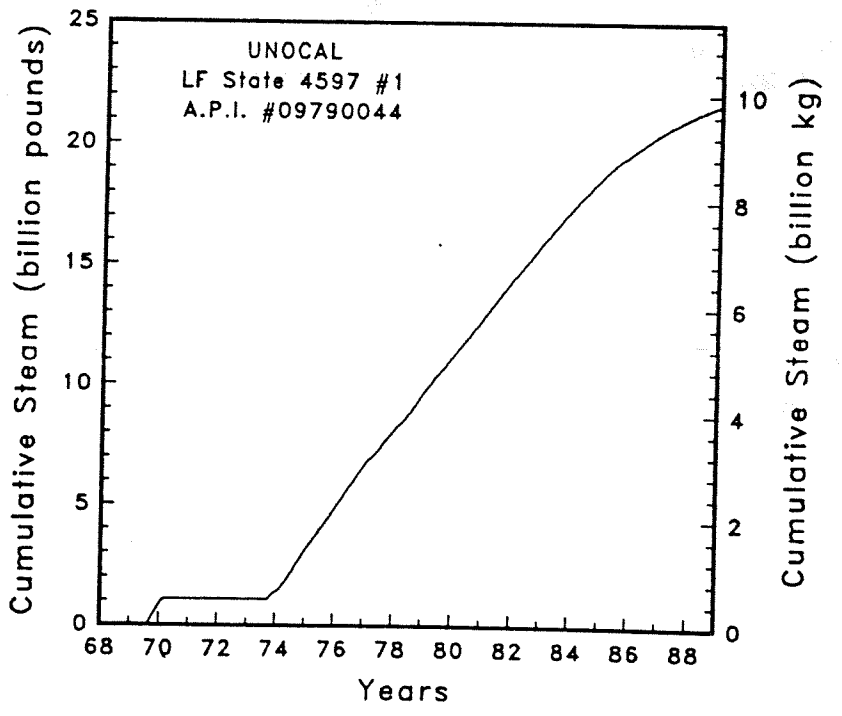

Figure A-116 Steam rate and cumulative mass flow for well LF State 4597 #1

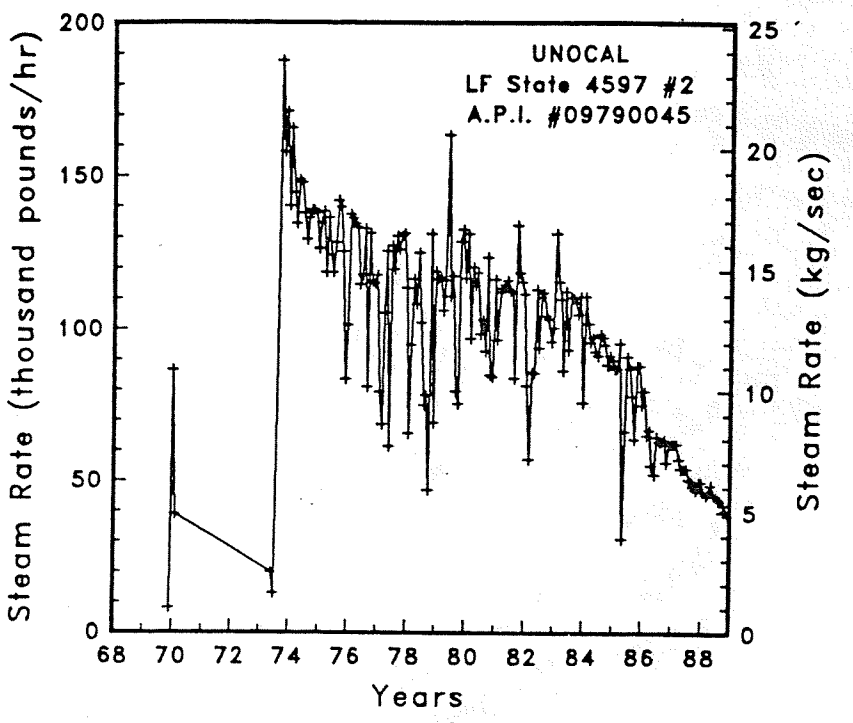

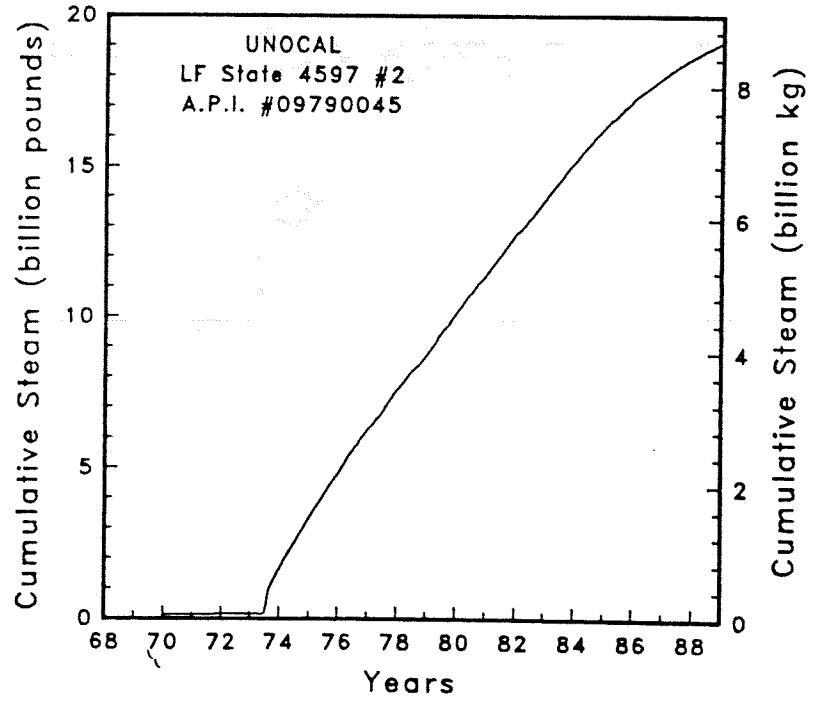

Figure A-117 Steam rate and cumulative mass flow for well LF State 4597 #2

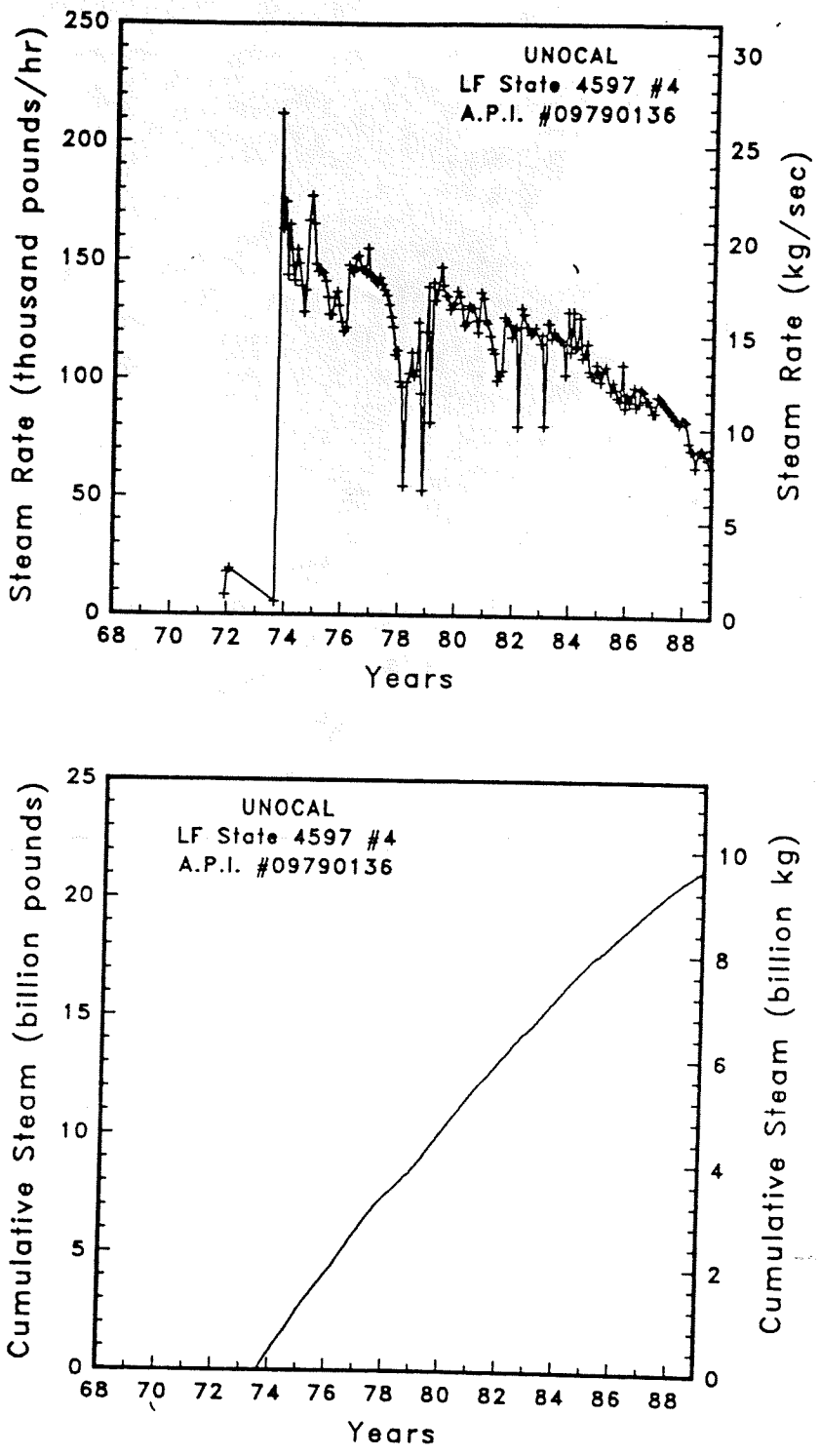

Figure A-118 Steam rate and cumulative mass flow for well LF State 4597 #4

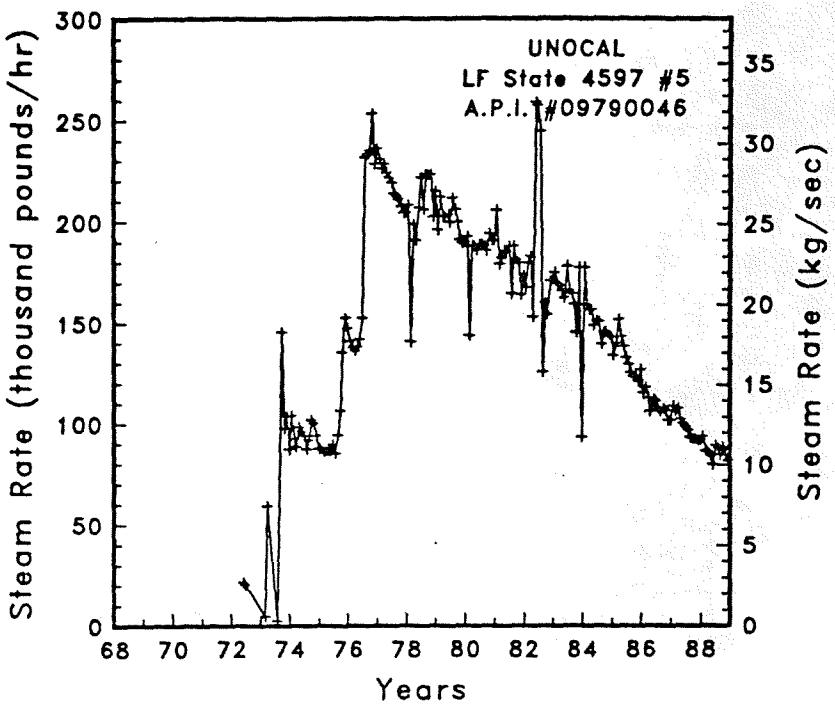

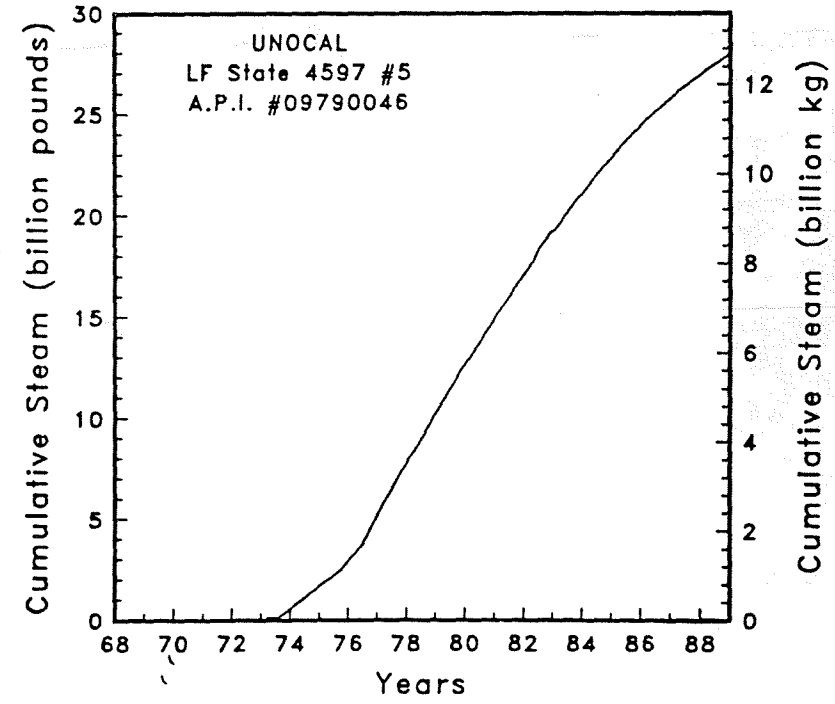

Figure A-119 Steam rate and cumulative mass flow for well LF State 4597 #5

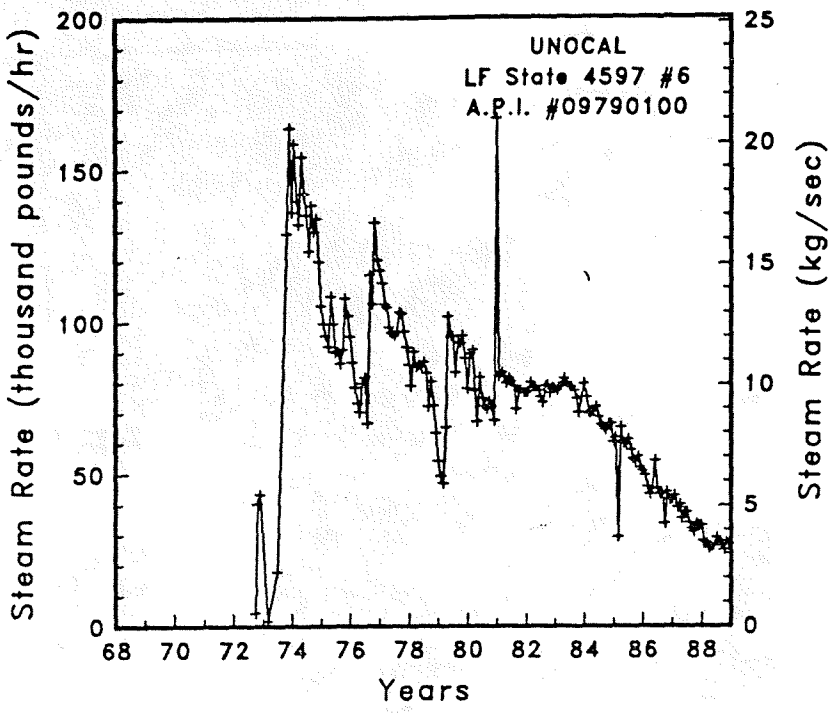

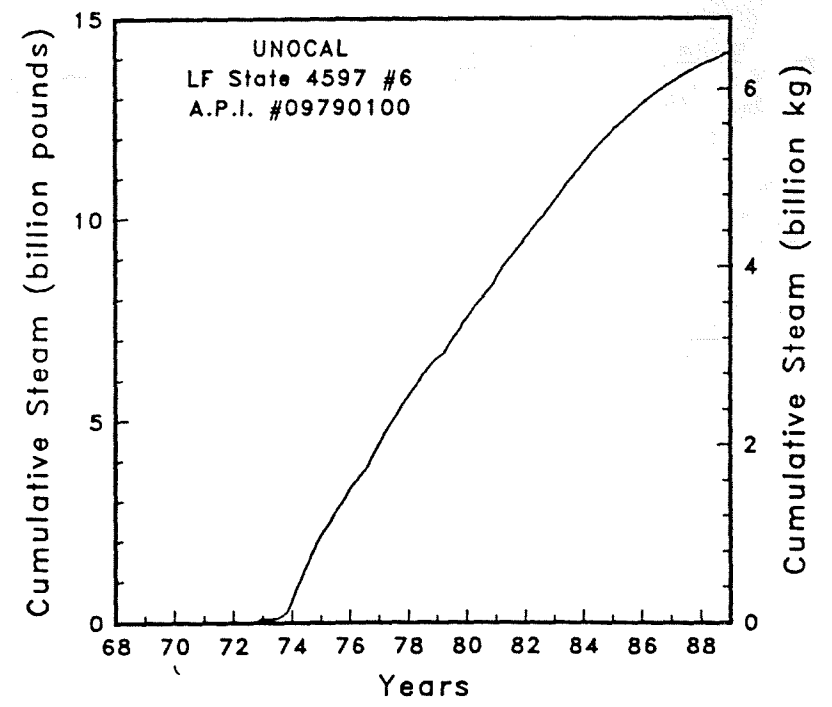

Figure A-120 Steam rate and cumulative mass flow for well LF State 4597 #6

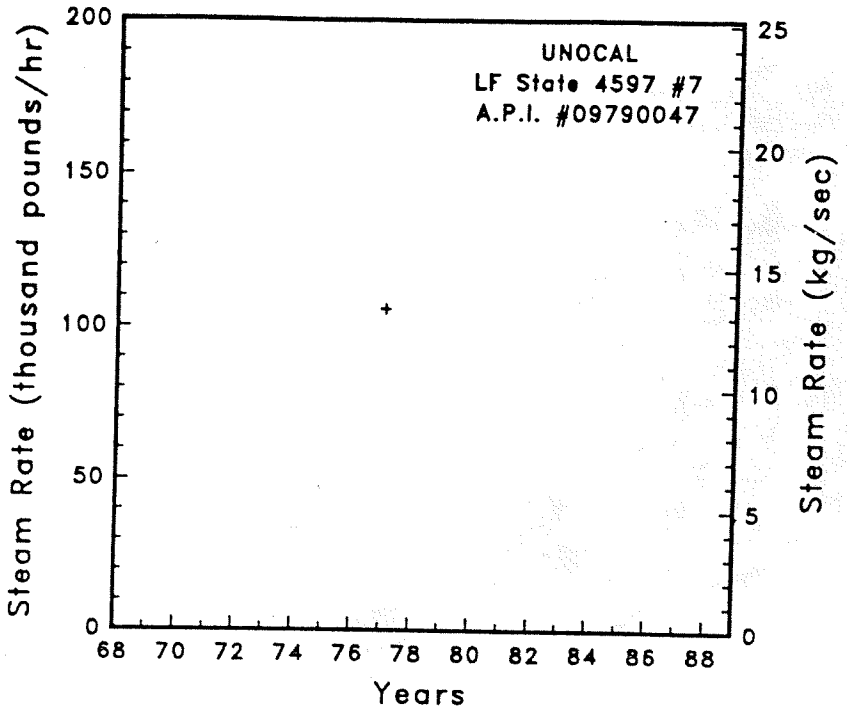

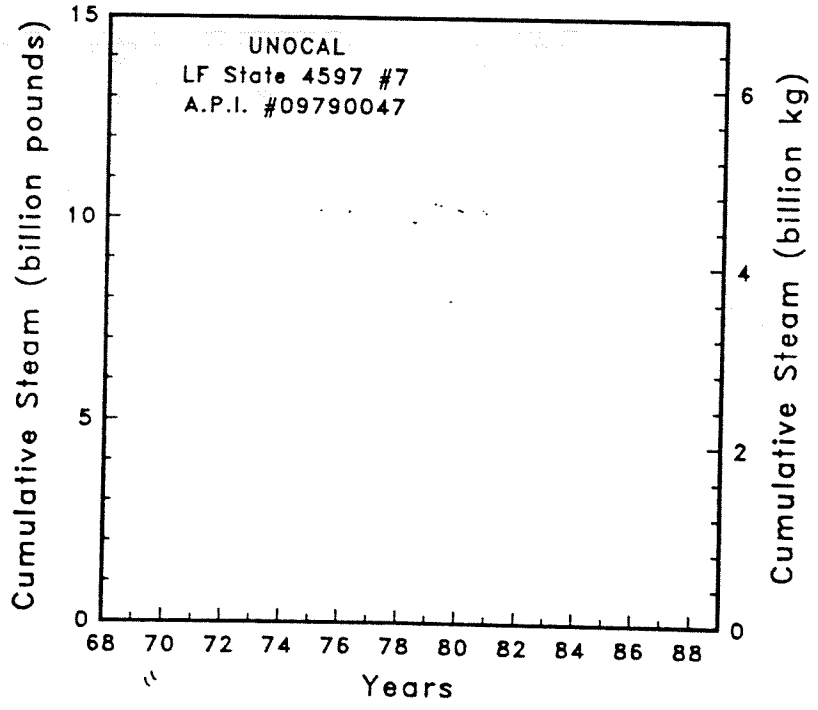

Figure A-121 Steam rate and cumulative mass flow for well LF State 4597 #7

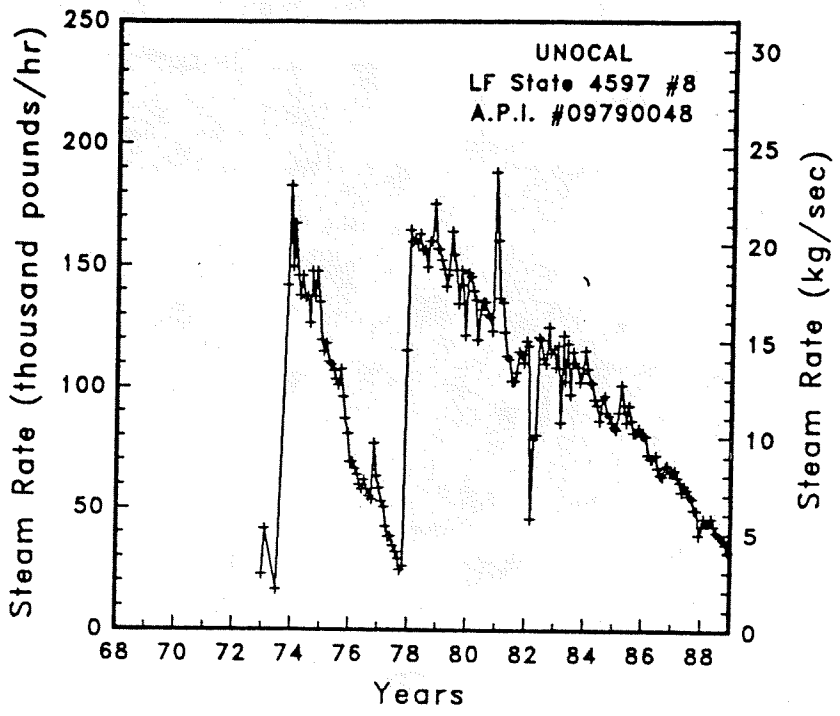

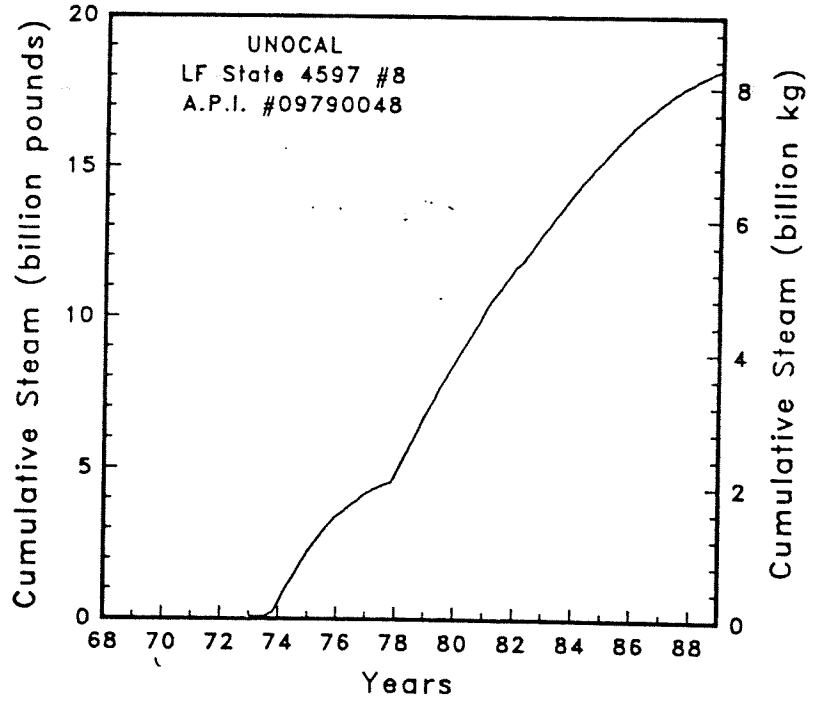

Figure A-122 Steam rate and cumulative mass flow for well LF State 4597 #8

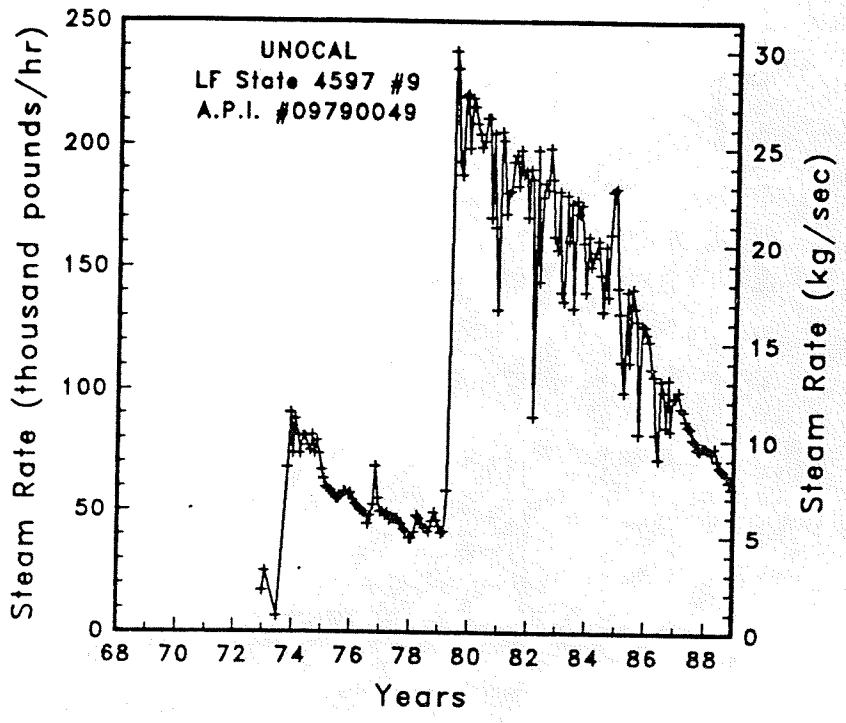

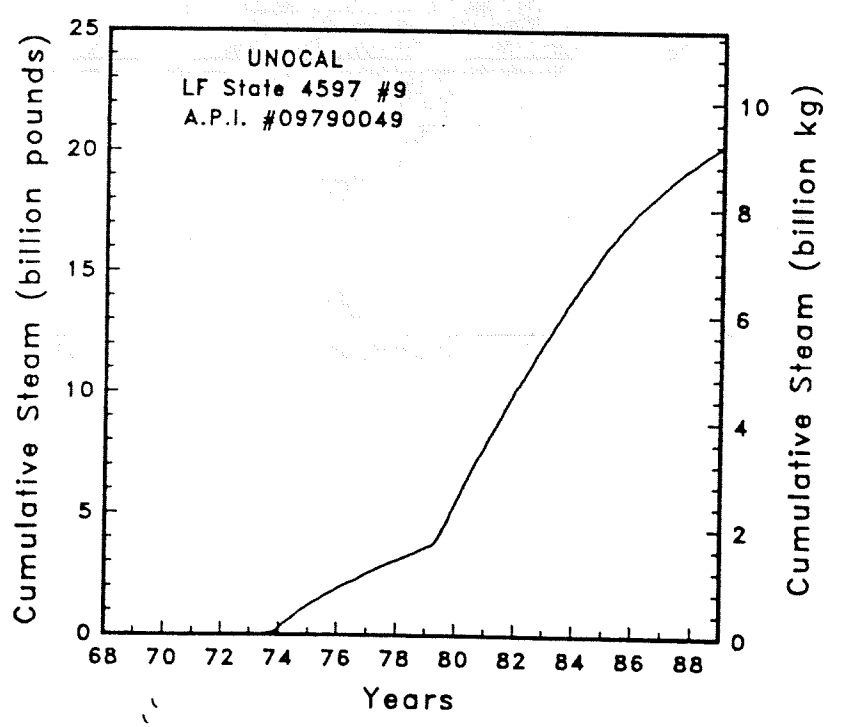

Figure A-123 Steam rate and cumulative mass flow for well LF State 4597 #9

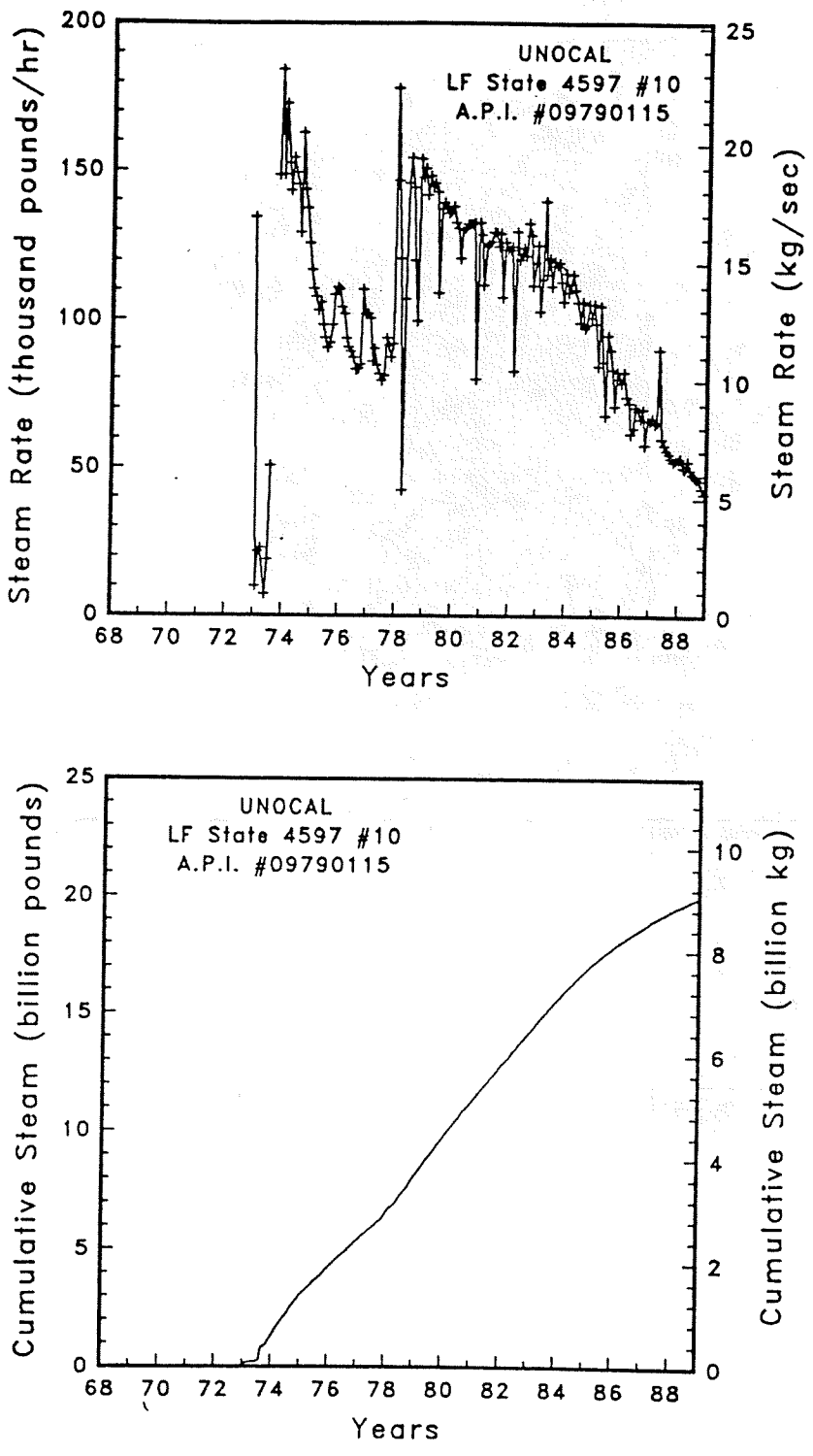

Figure A-124 Steam rate and cumulative mass flow for well LF State 4597 #10

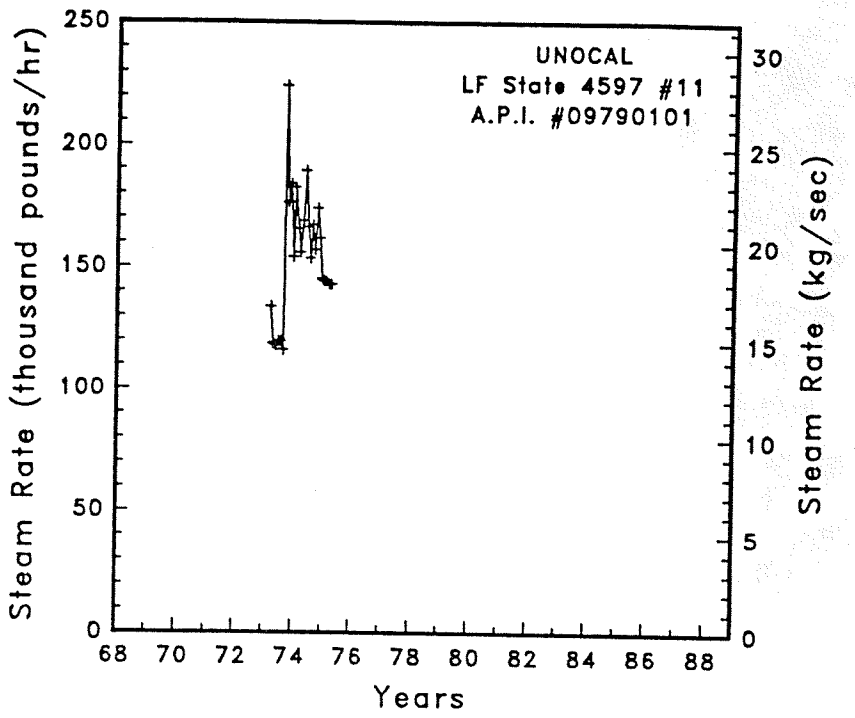

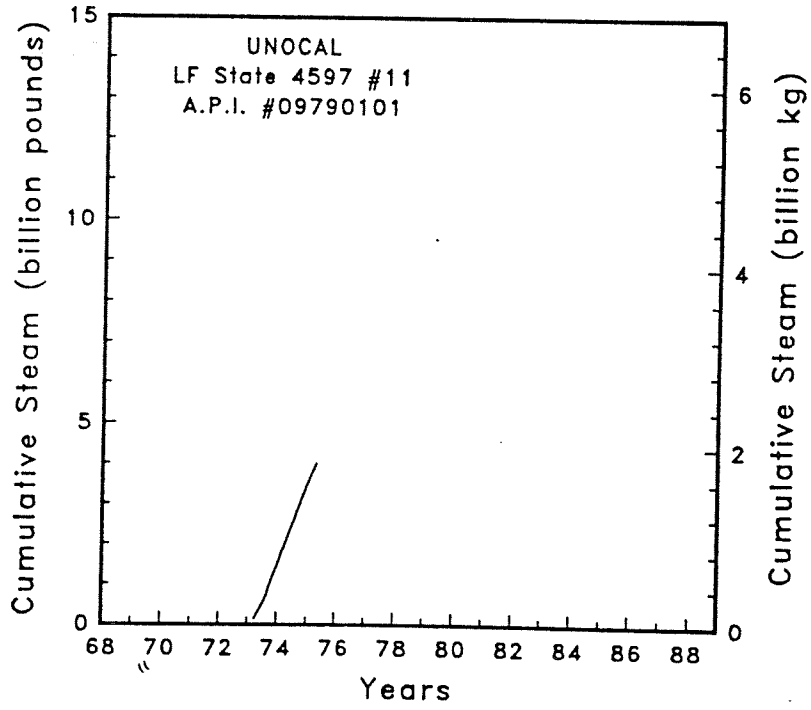

Figure A-125 Steam rate and cumulative mass flow for well LF State 4597 #11

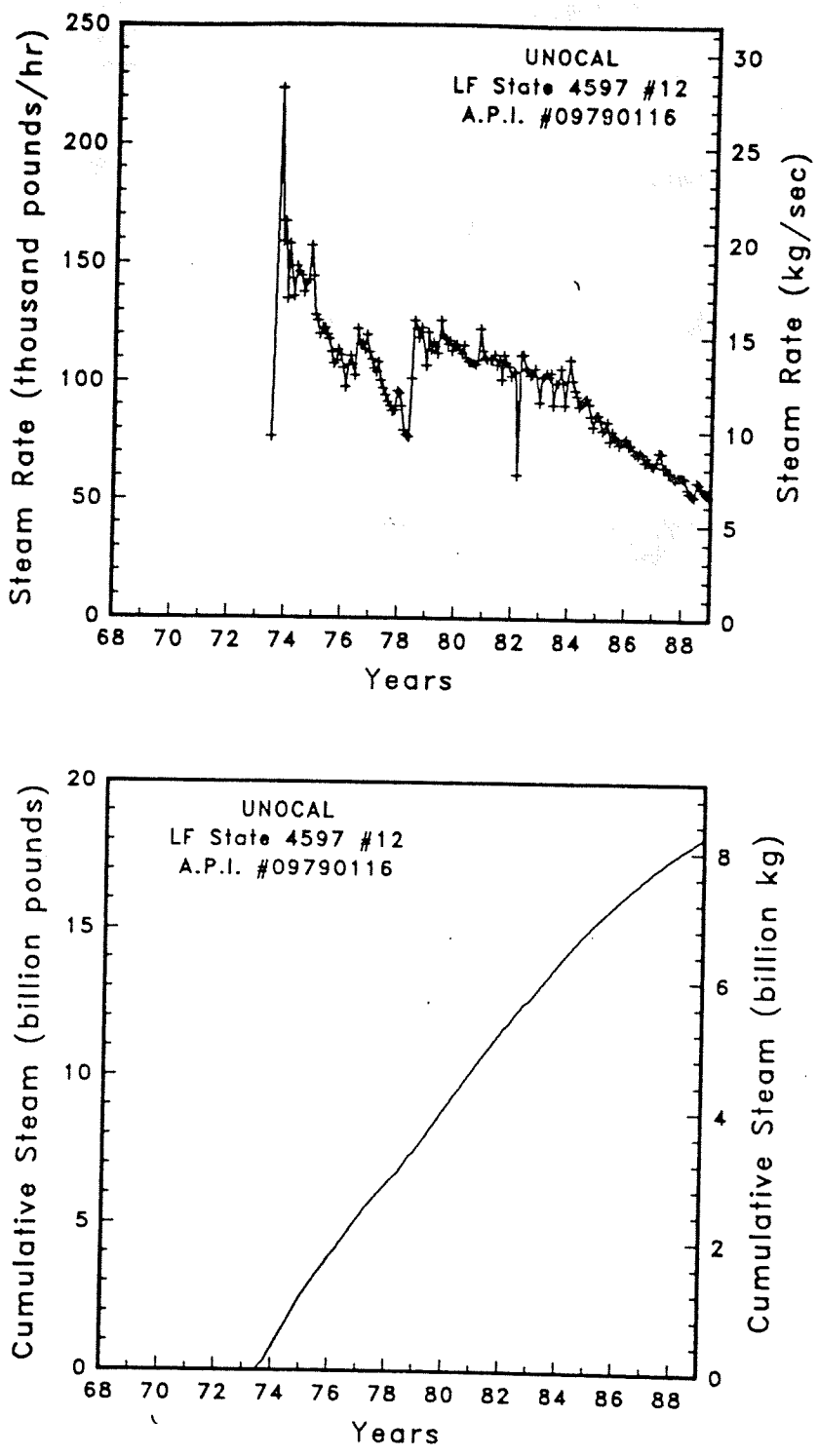

Figure A-126 Steam rate and cumulative mass flow for well LF State 4597 #12

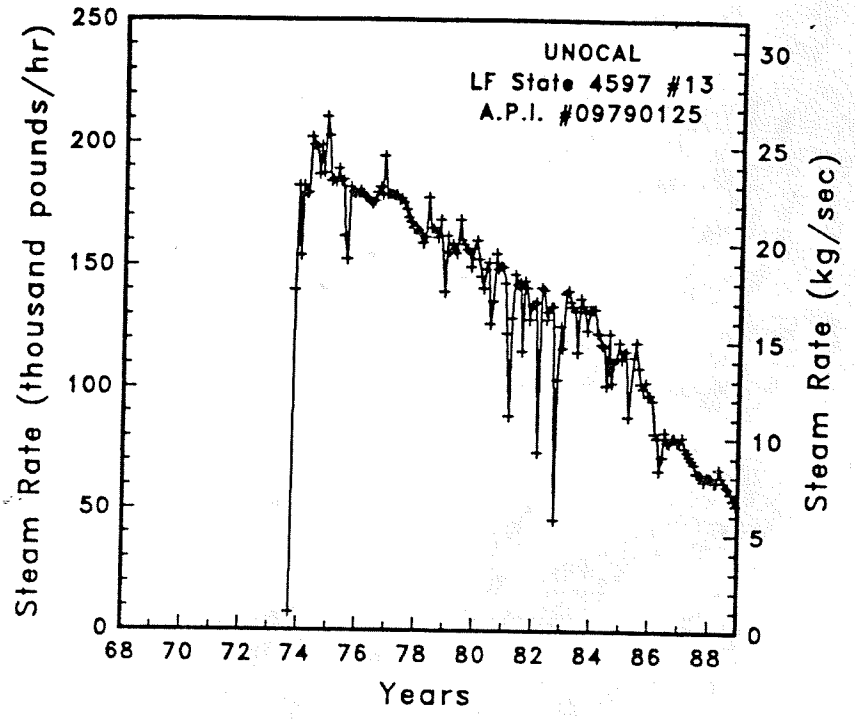

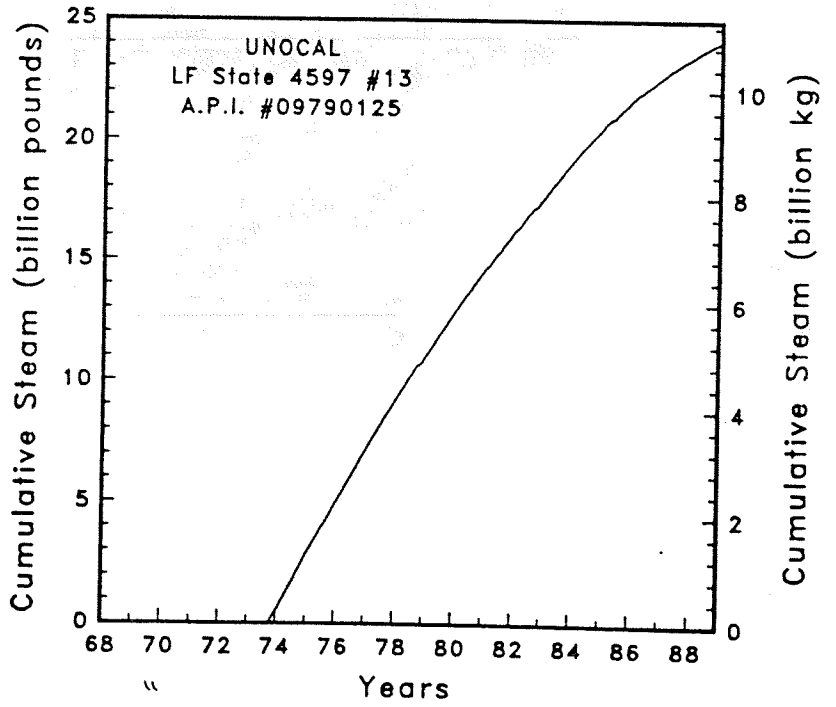

Figure A-127 Steam rate and cumulative mass flow for well LF State 4597 #13

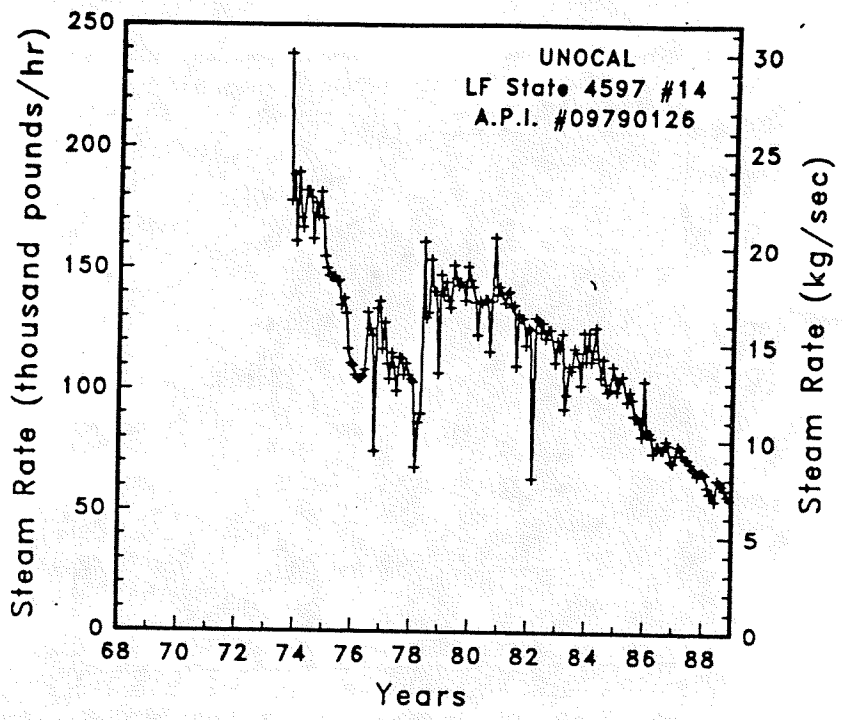

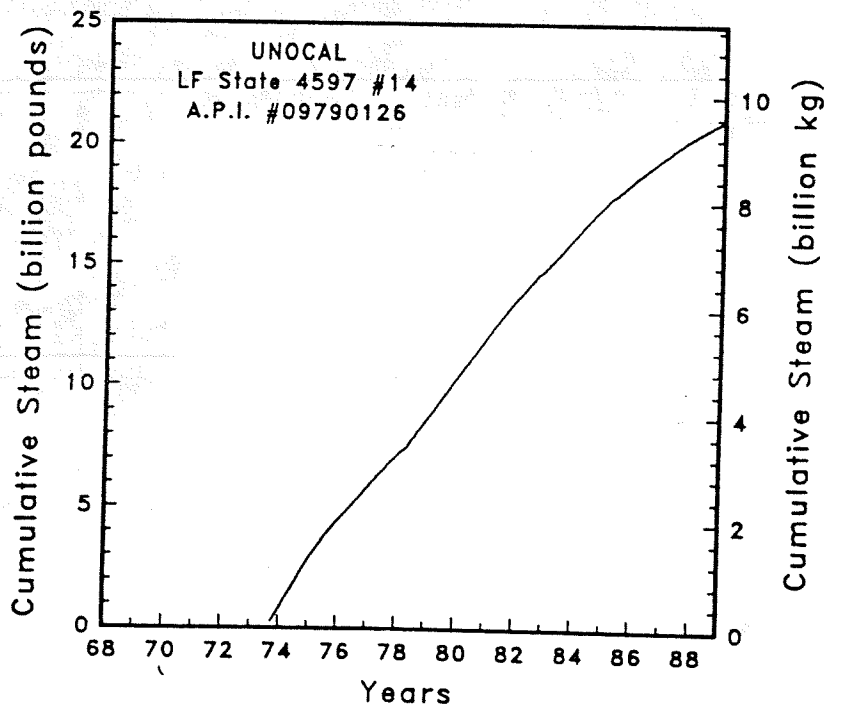

Figure A-128 Steam rate and cumulative mass flow for well LF State 4597 #14

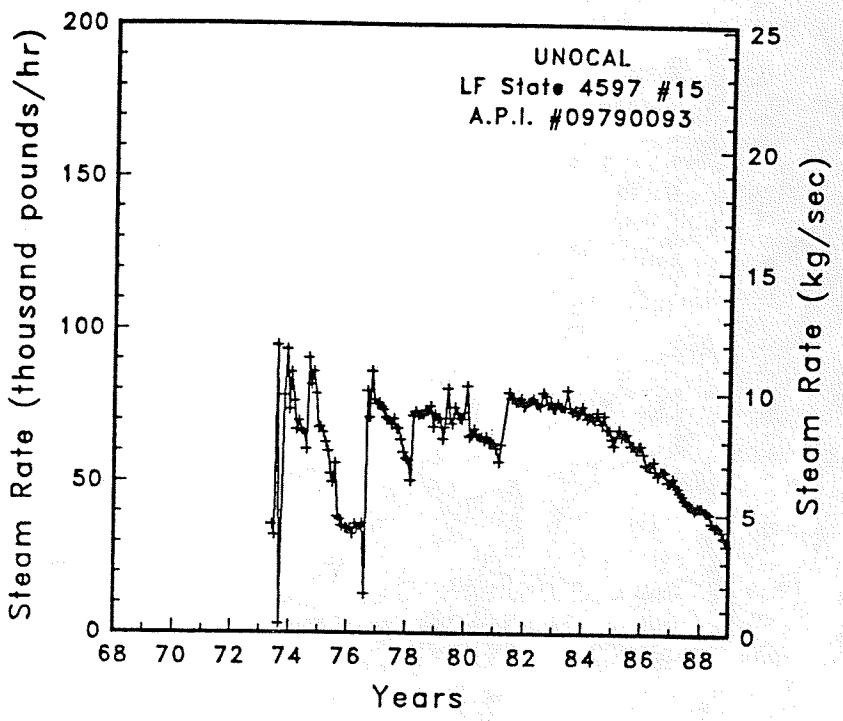

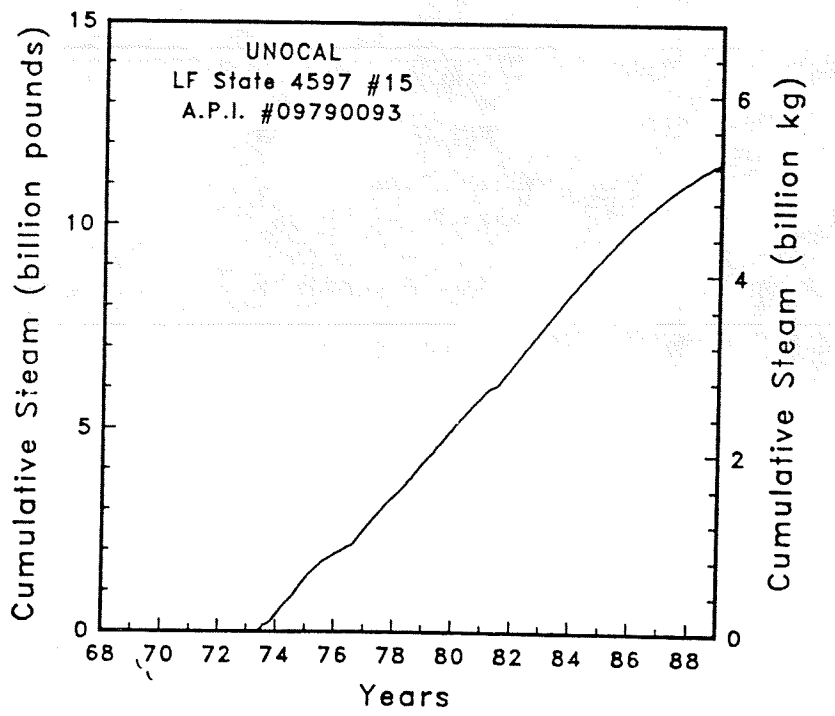

Figure A-129 Steam rate and cumulative mass flow for well LF State 4597 #15

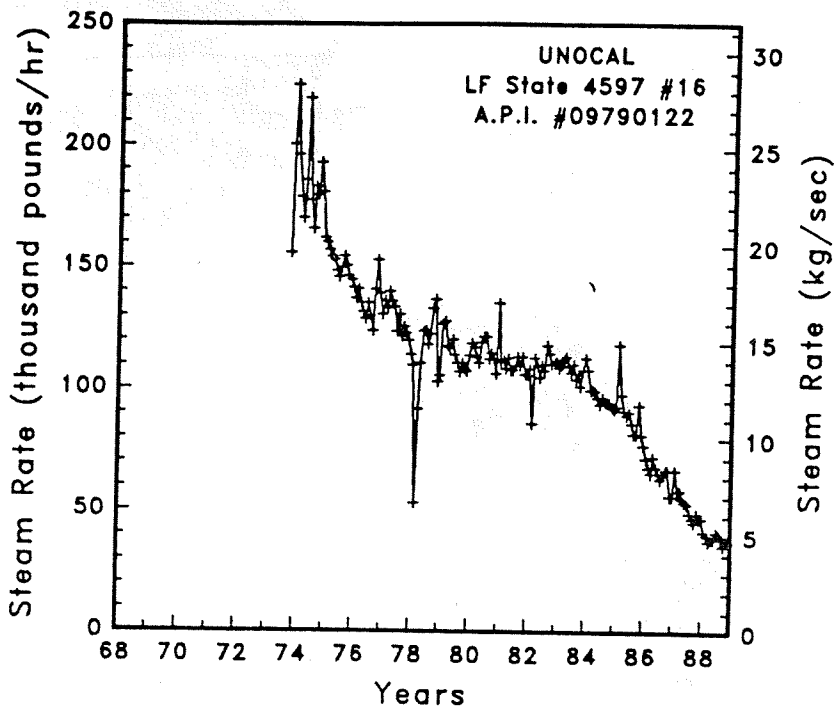

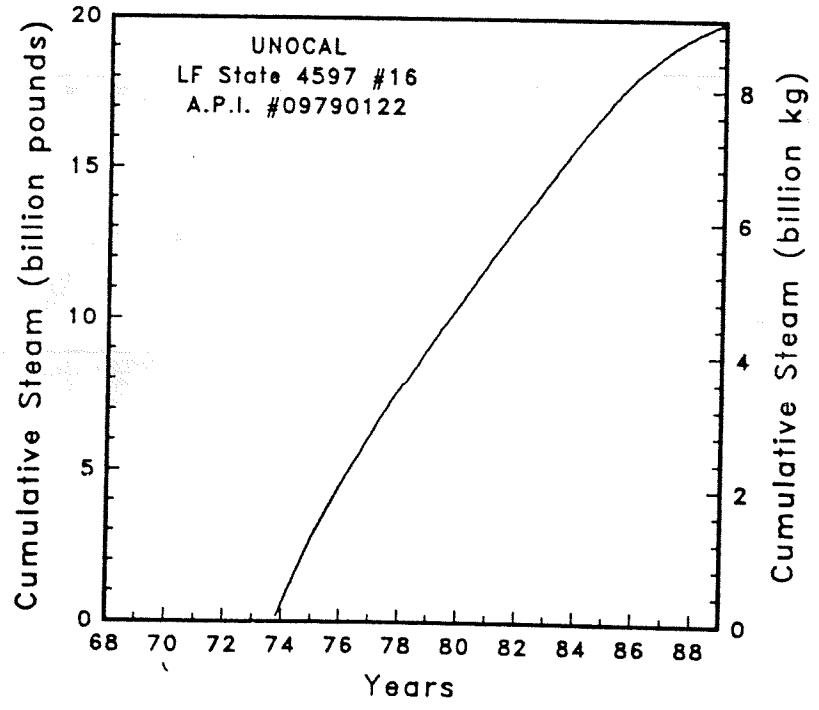

Figure A-130 Steam rate and cumulative mass flow for well LF State 4597 #16

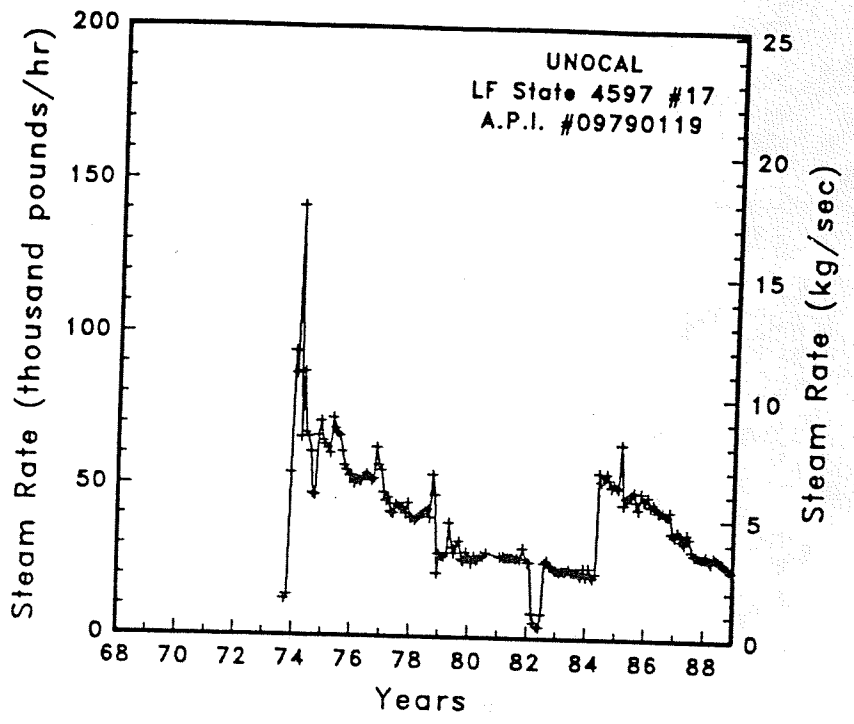

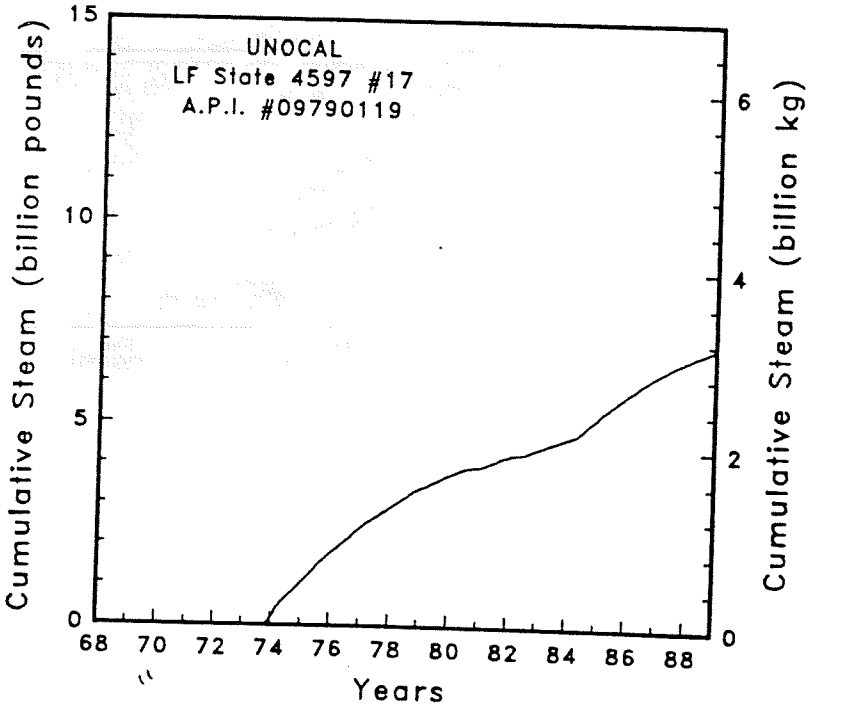

Figure A-131 Steam rate and cumulative mass flow for well LF State 4597 #17

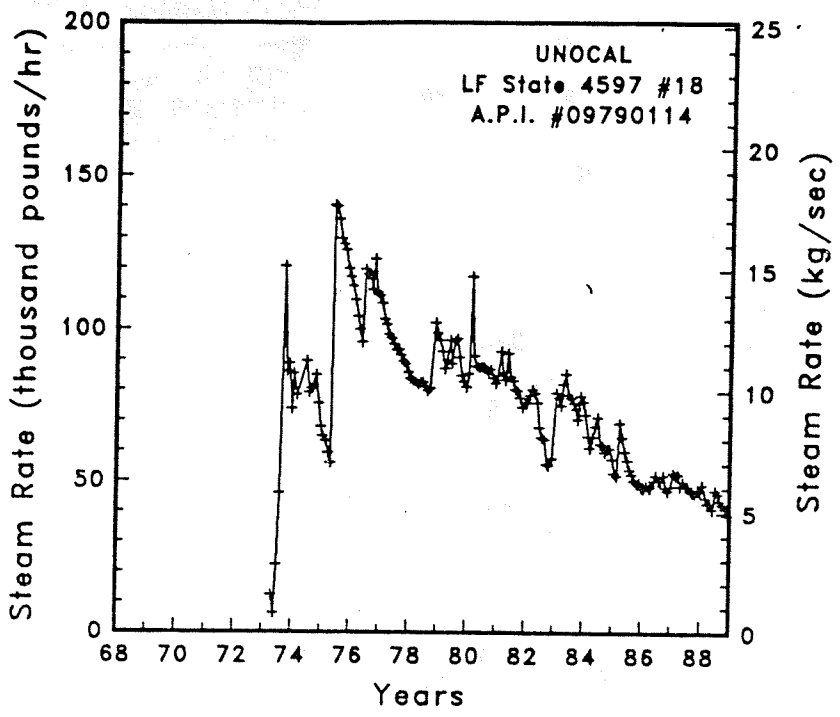

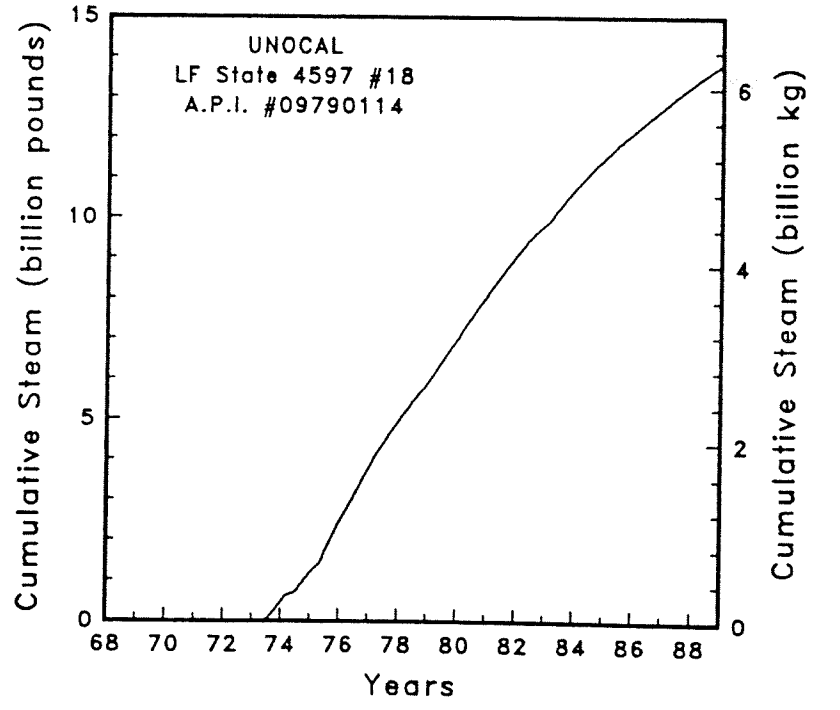

Figure A-132 Steam rate and cumulative mass flow for well LF State 4597 #18

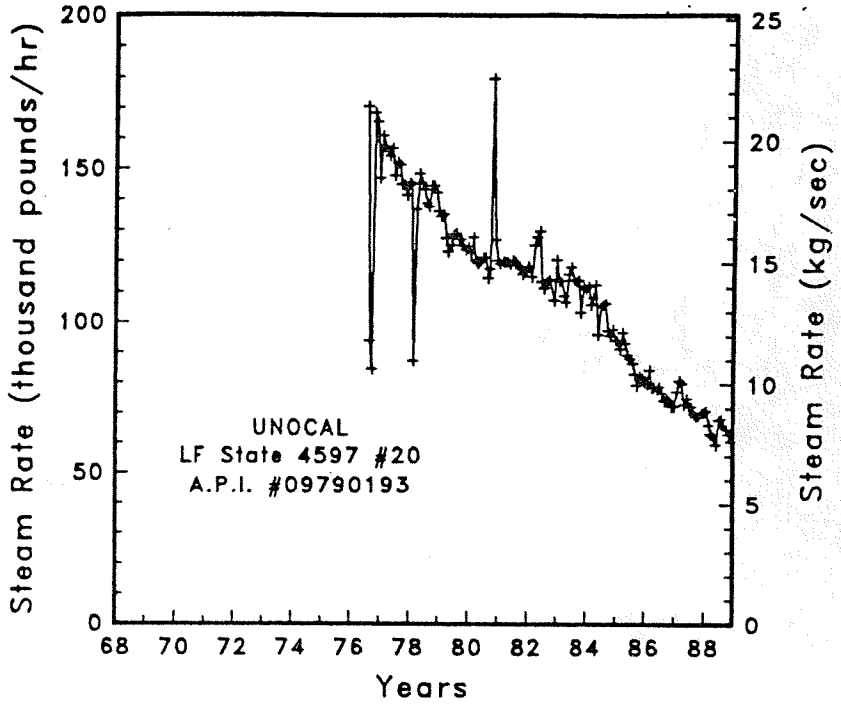

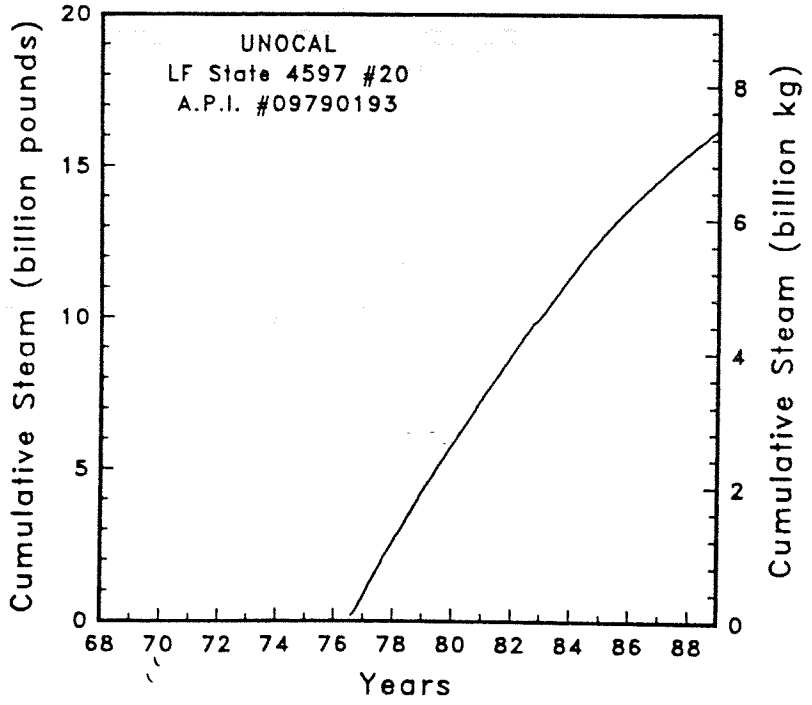

Figure A-133 Steam rate and cumulative mass flow for well LF State 4597 #20

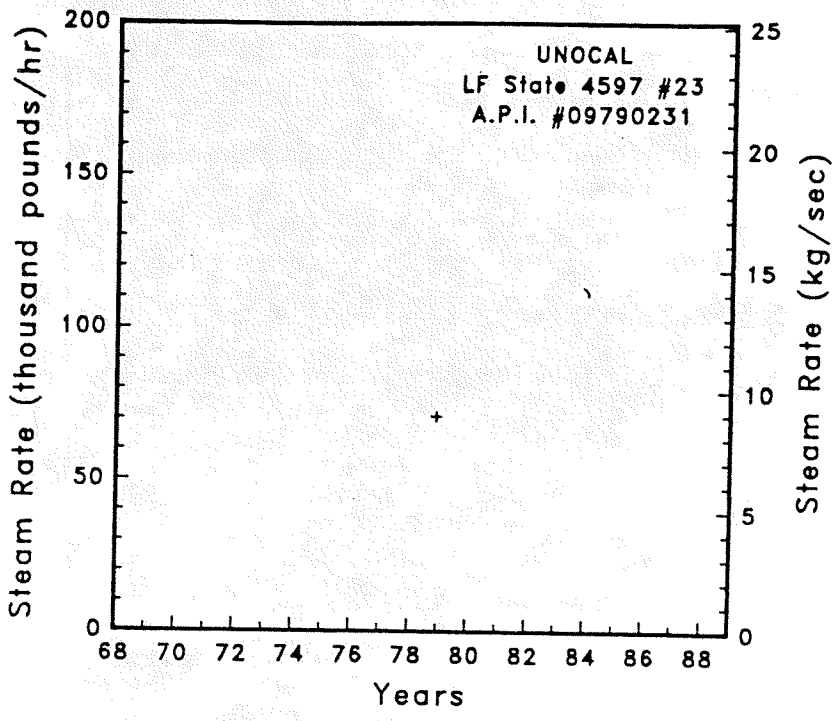

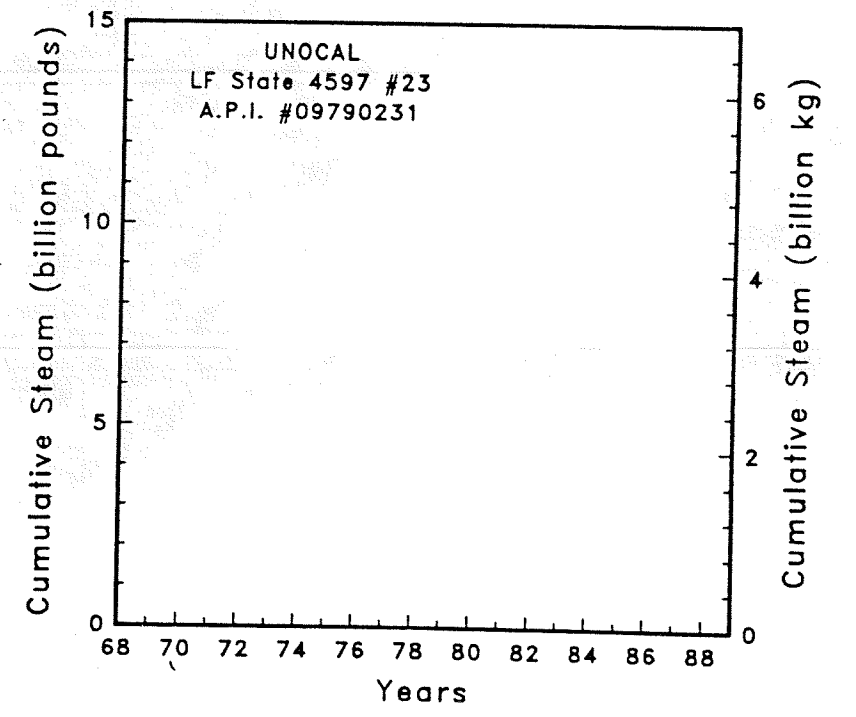

Figure A-134 Steam rate and cumulative mass flow for well LF State 4597 #23

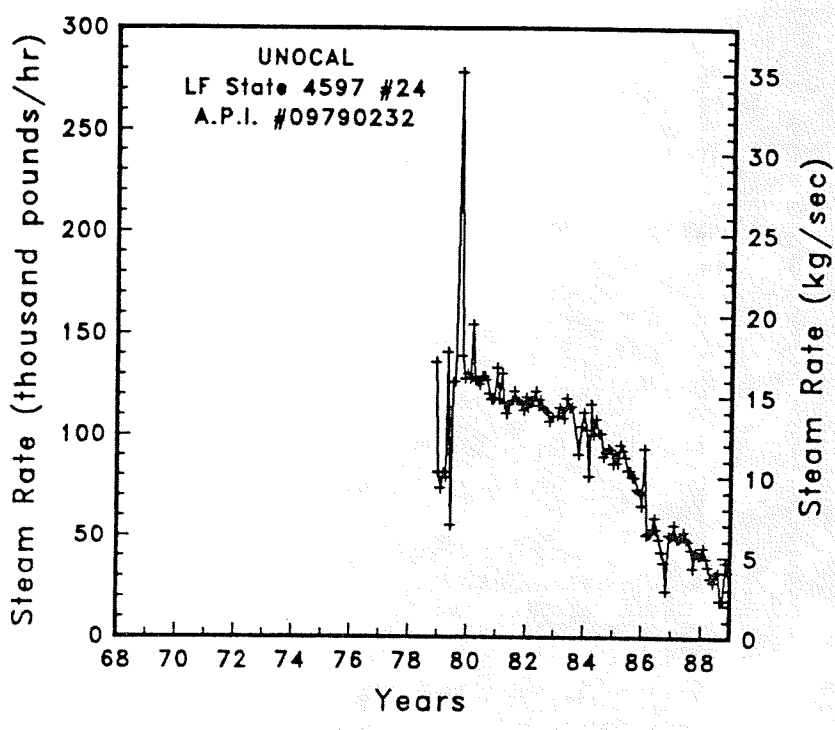

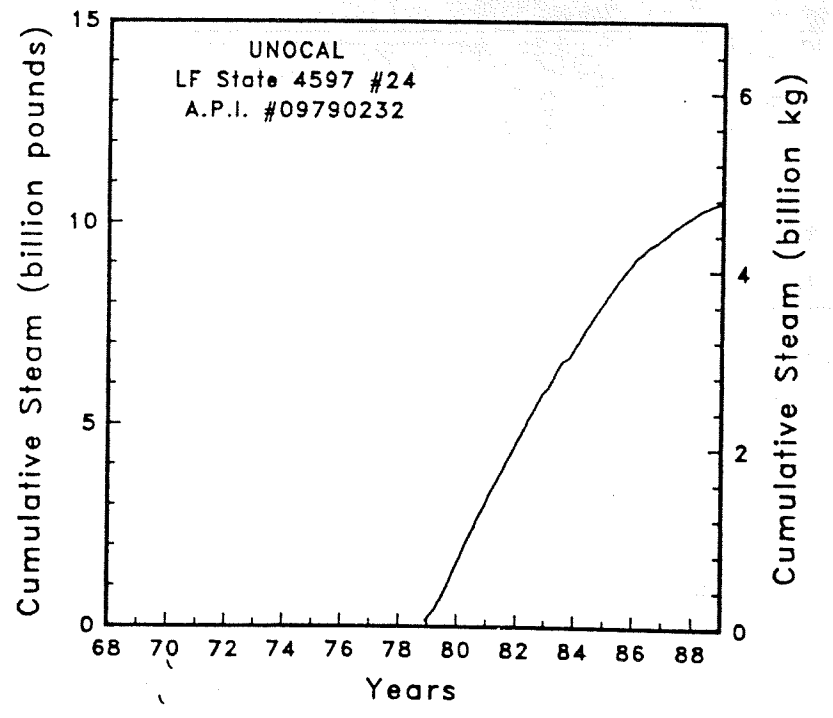

Figure A-135 Steam rate and cumulative mass flow for well LF State 4597 #24

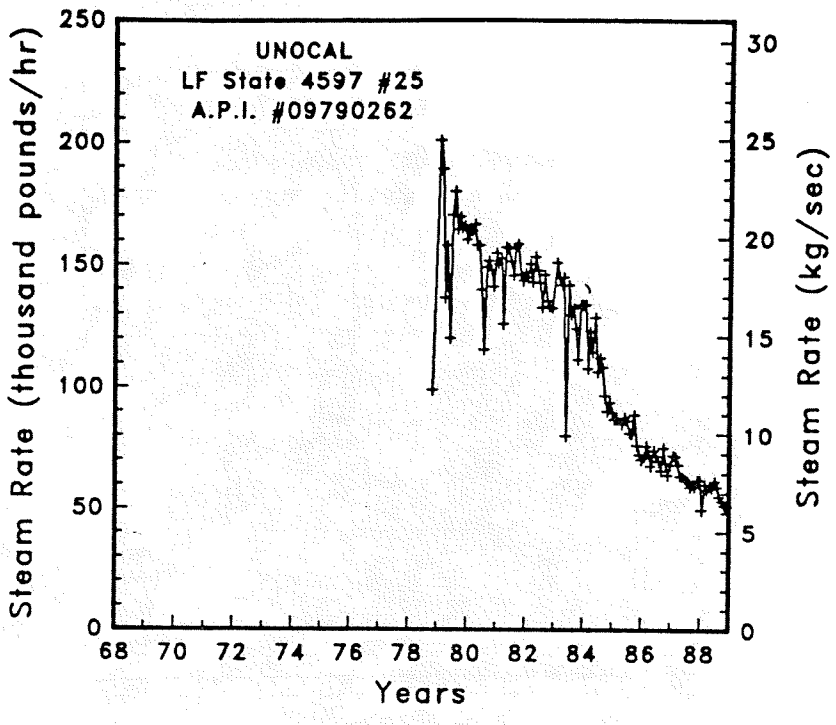

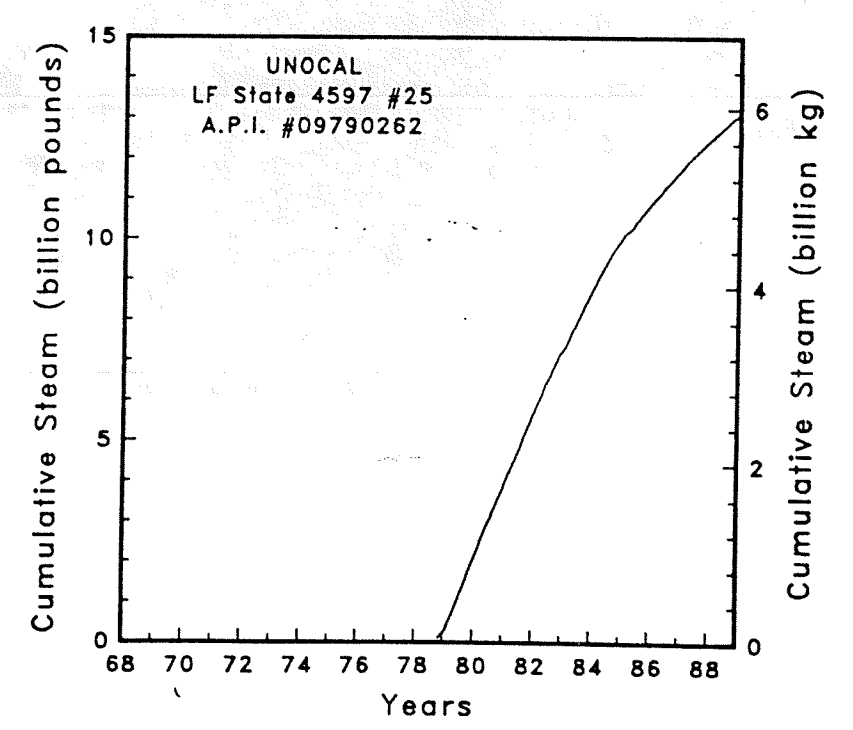

Figure A-136 Steam rate and cumulative mass flow for well LF State 4597 #25

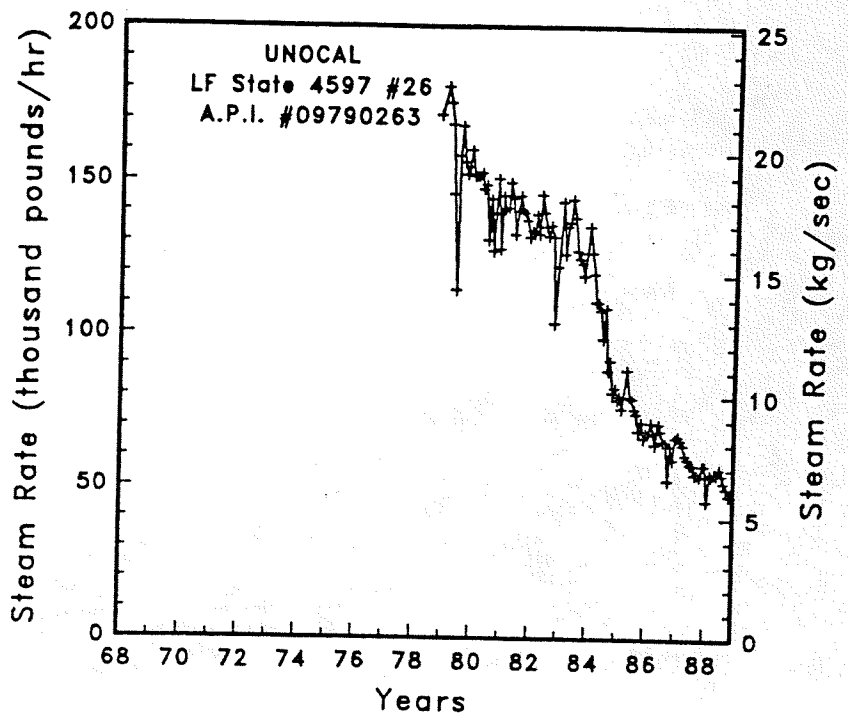

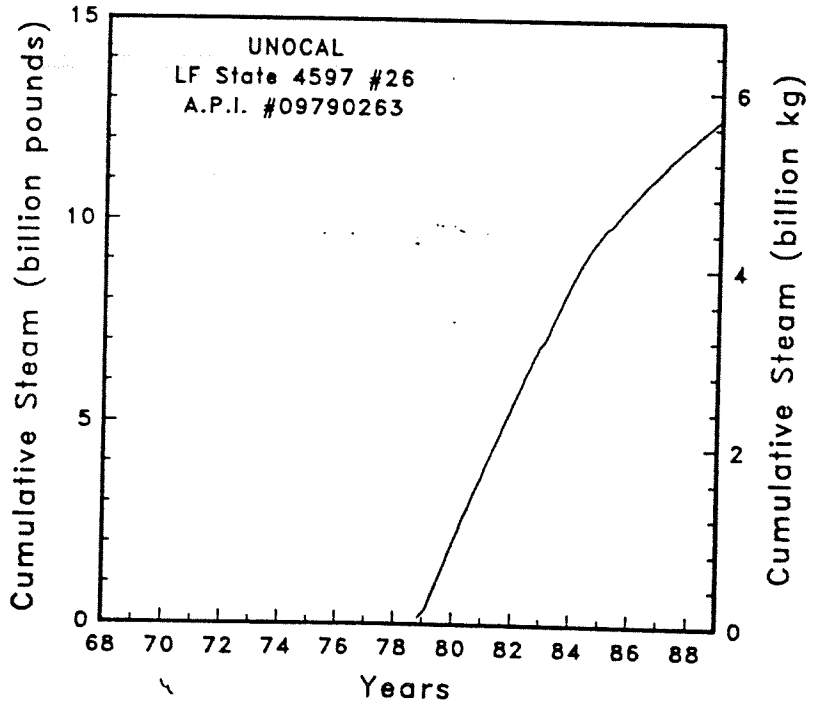

Figure A-137 Steam rate and cumulative mass flow for well LF State 4597 #26

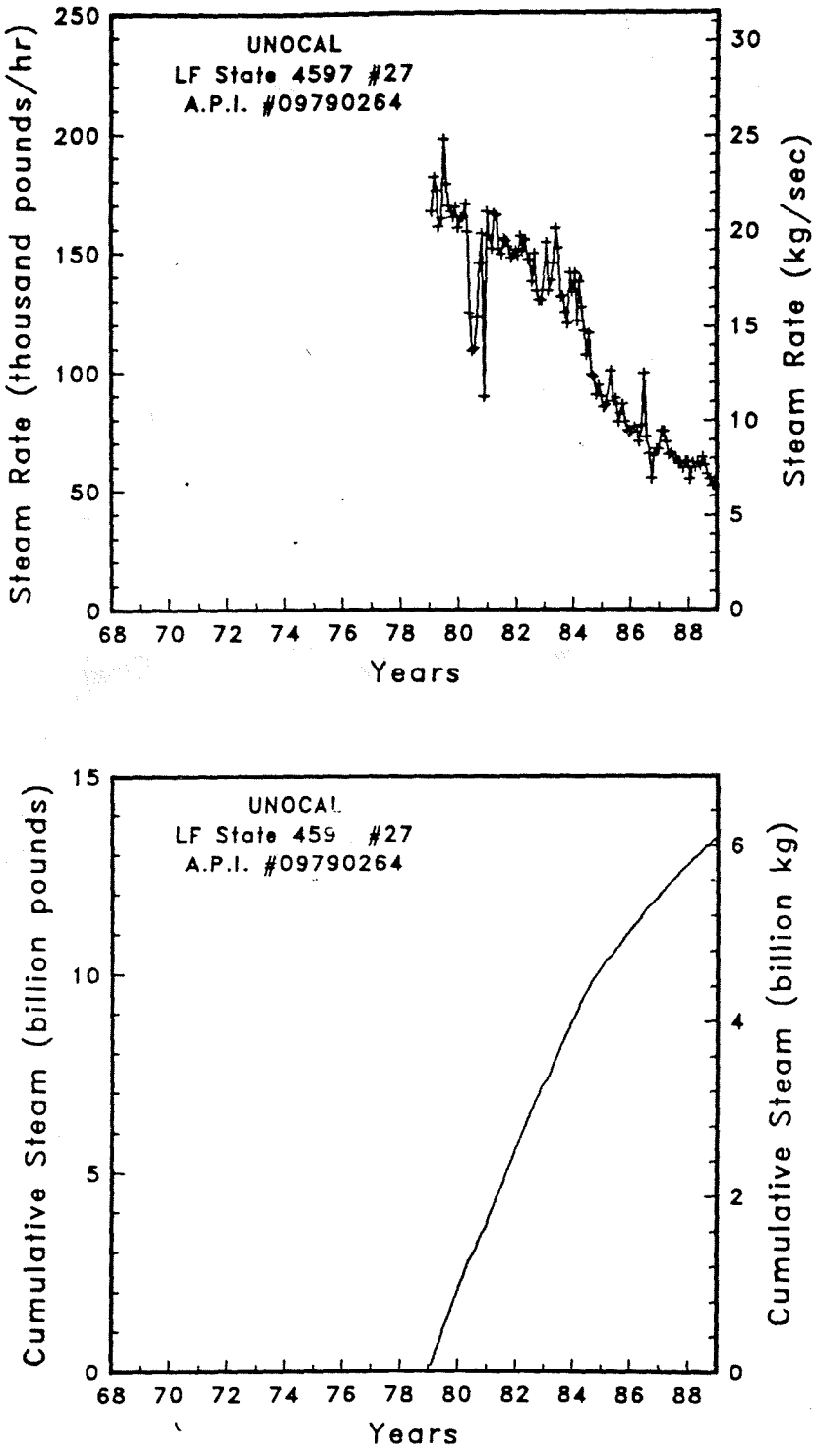

Figure A-138 Steam rate and cumulative mass flow for well LF State 4597 #27

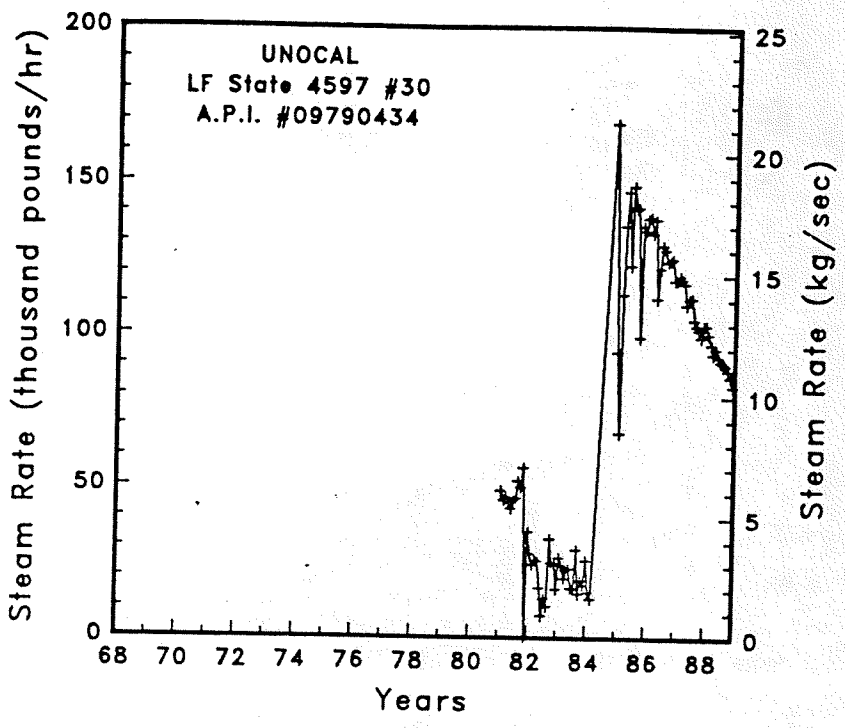

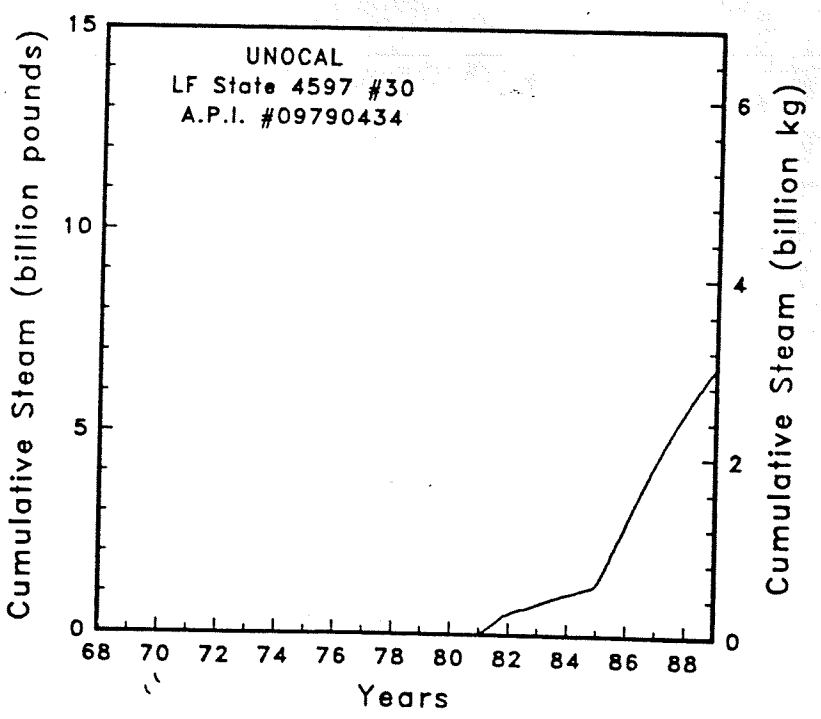

Figure A-139 Steam rate and cumulative mass flow for well LF State 4597 #30

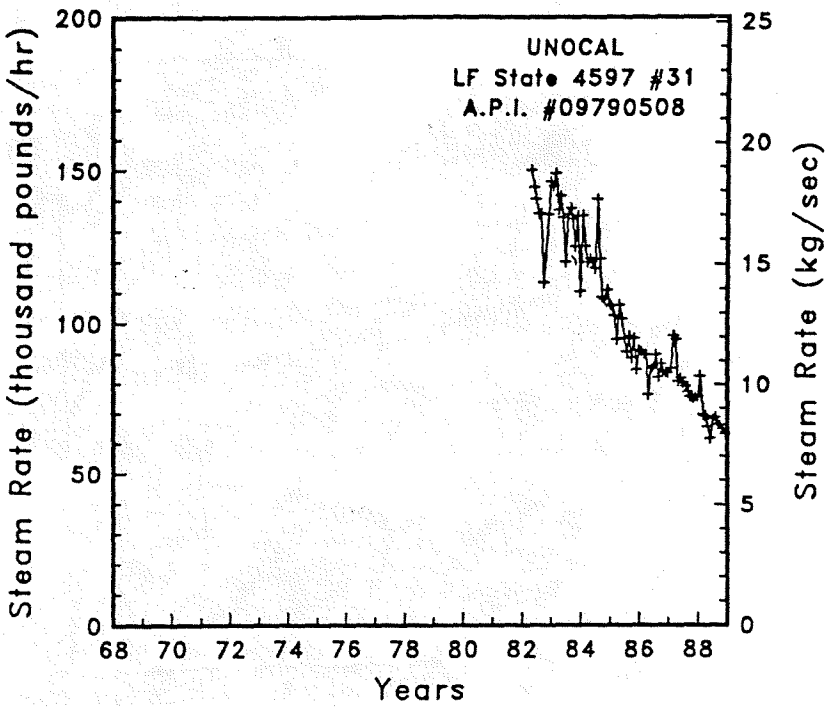

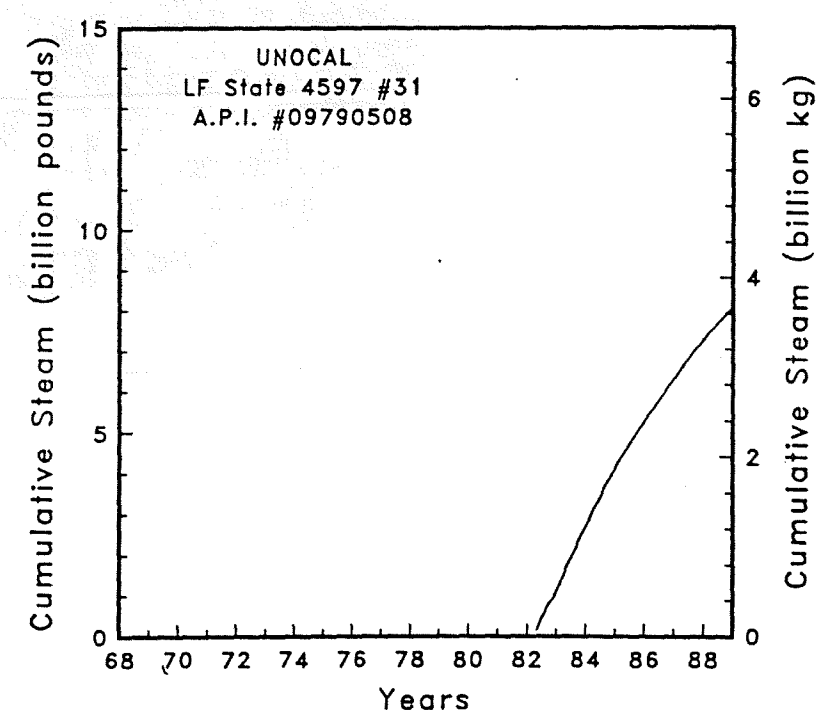

Figure A-140 Steam rate and cumulative mass flow for well LF State 4597 #31

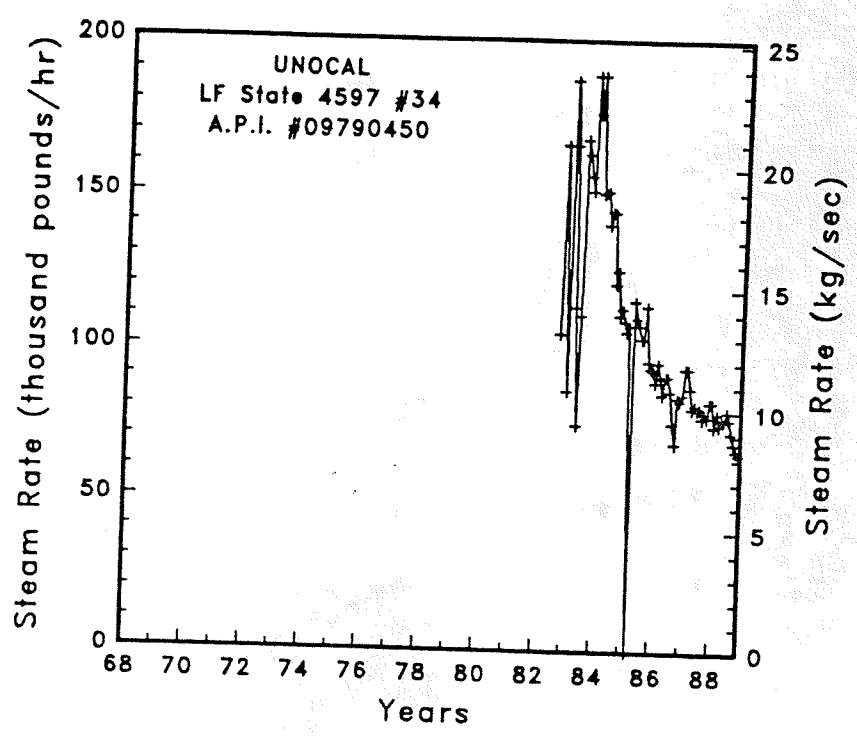

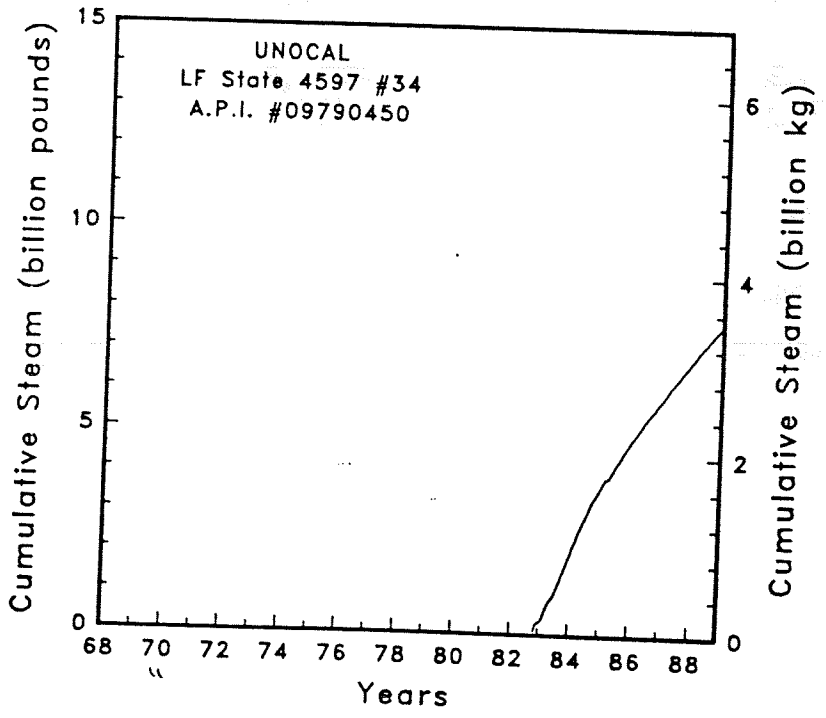

Figure A-141 Steam rate and cumulative mass flow for well LF State 4597 #34

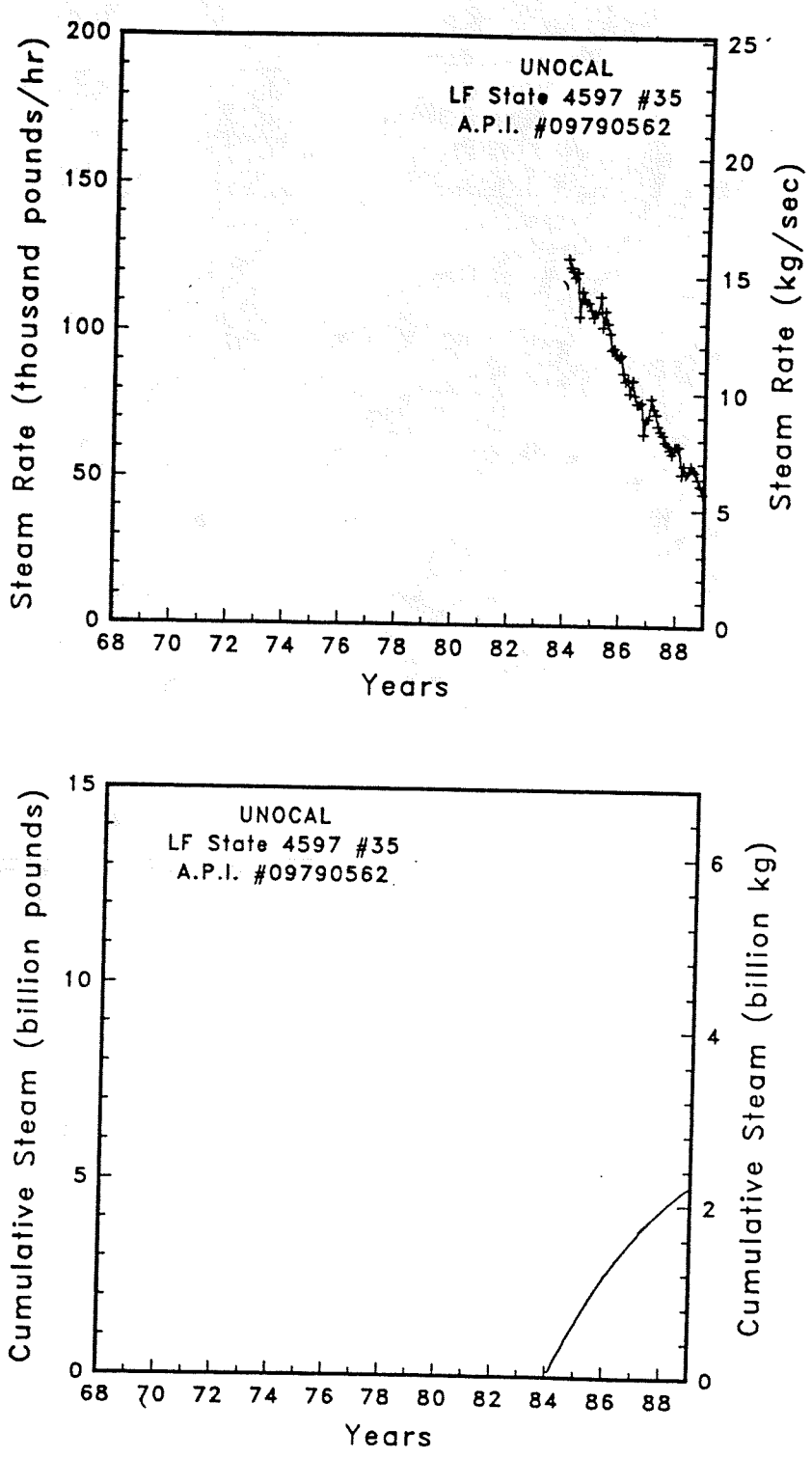

Figure A-142 Steam rate and cumulative mass flow for well LF State 4597 #35

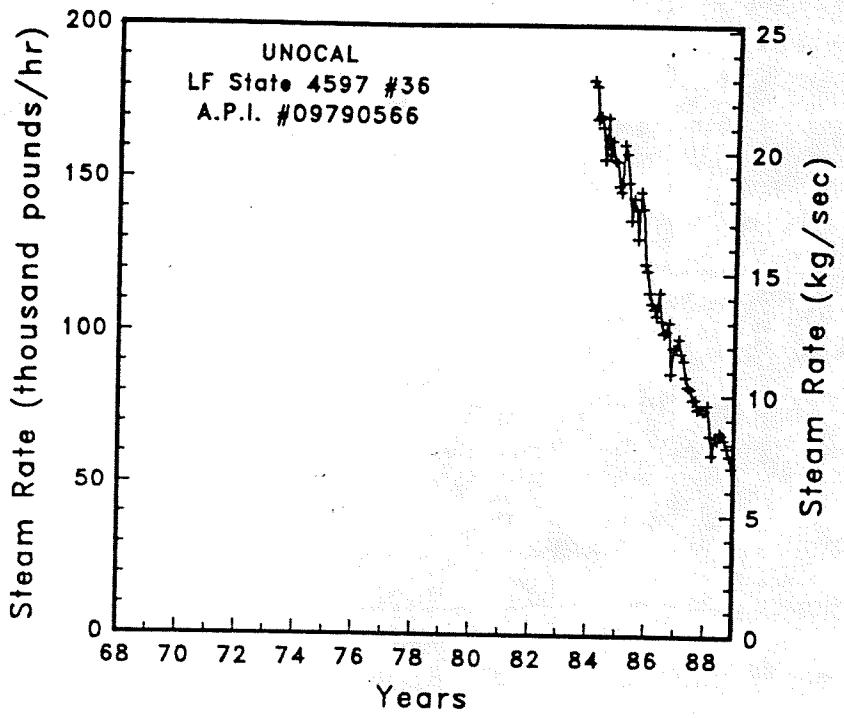

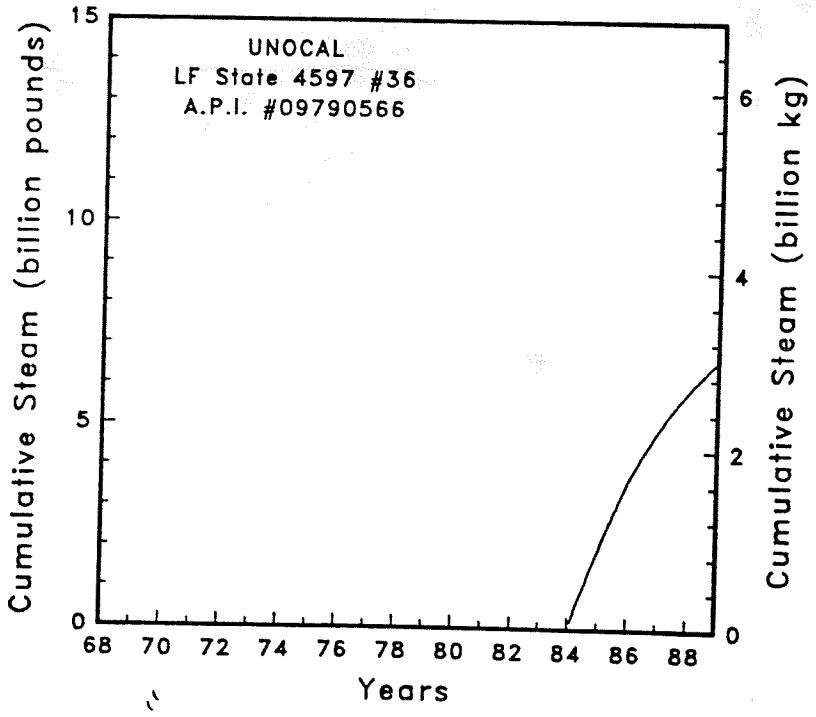

Figure A-143 Steam rate and cumulative mass flow for well LF State 4597 #36

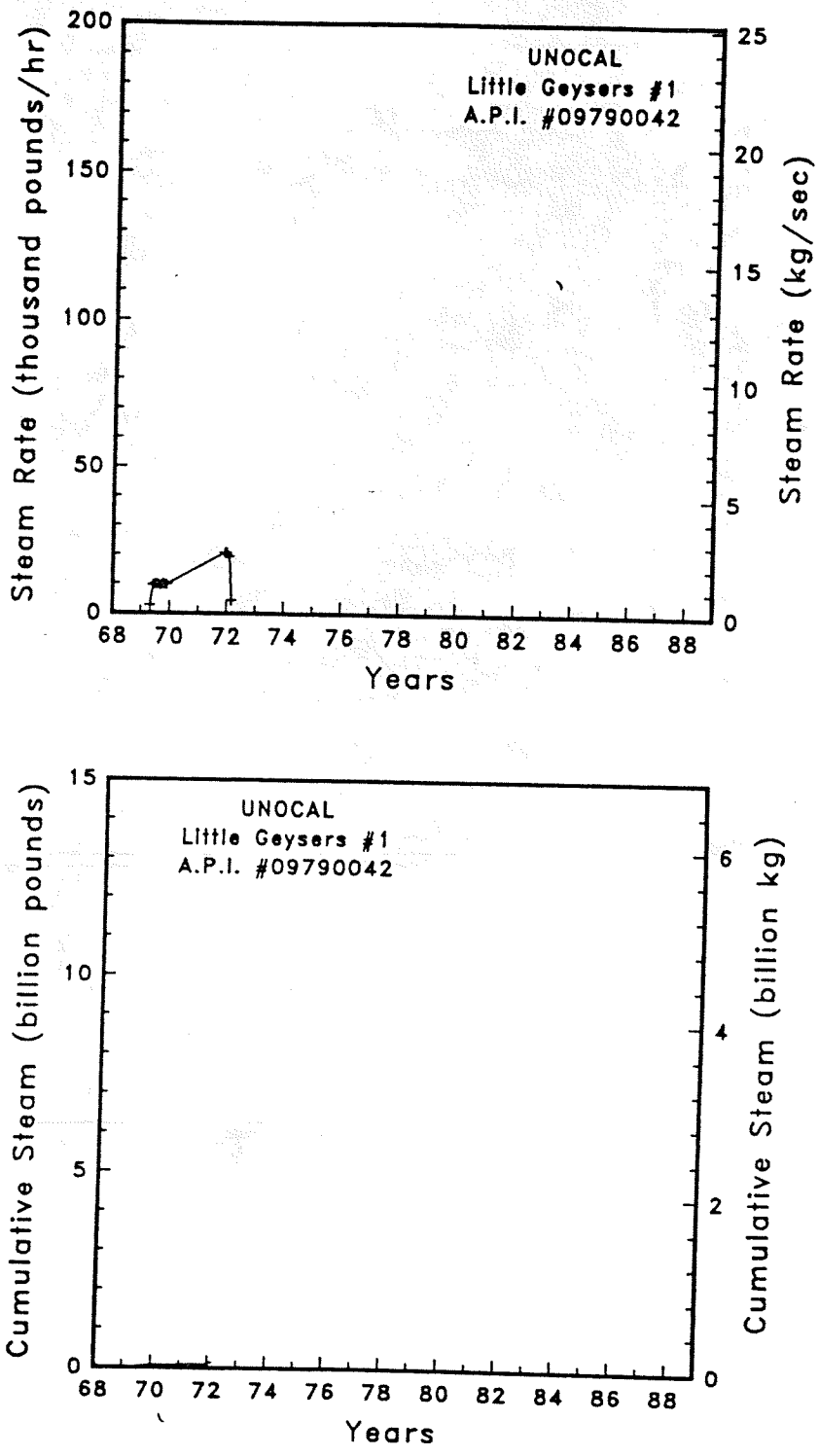

Figure A-144 Steam rate and cumulative mass flow for well Little Geysers #1

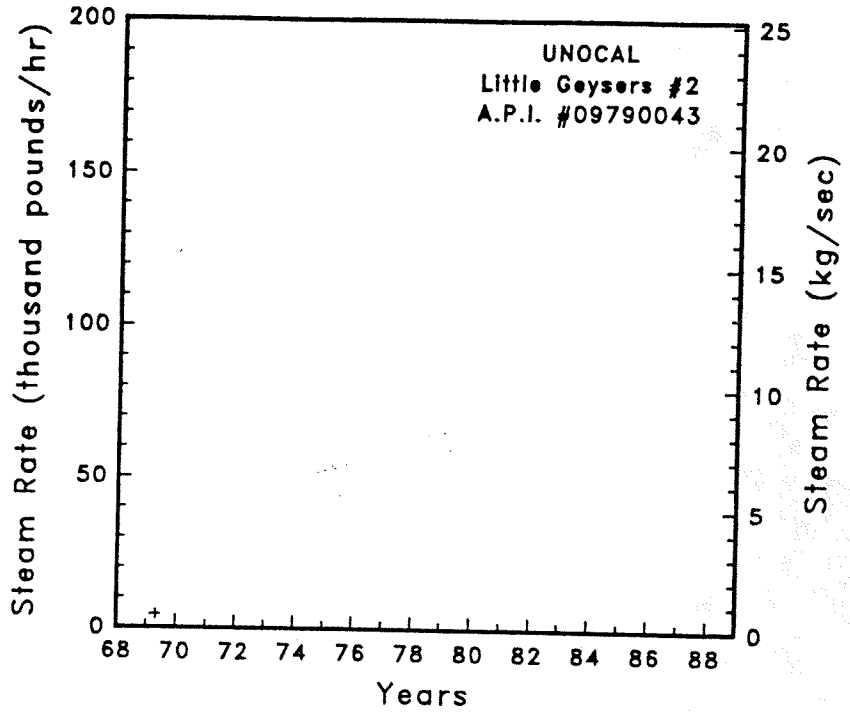

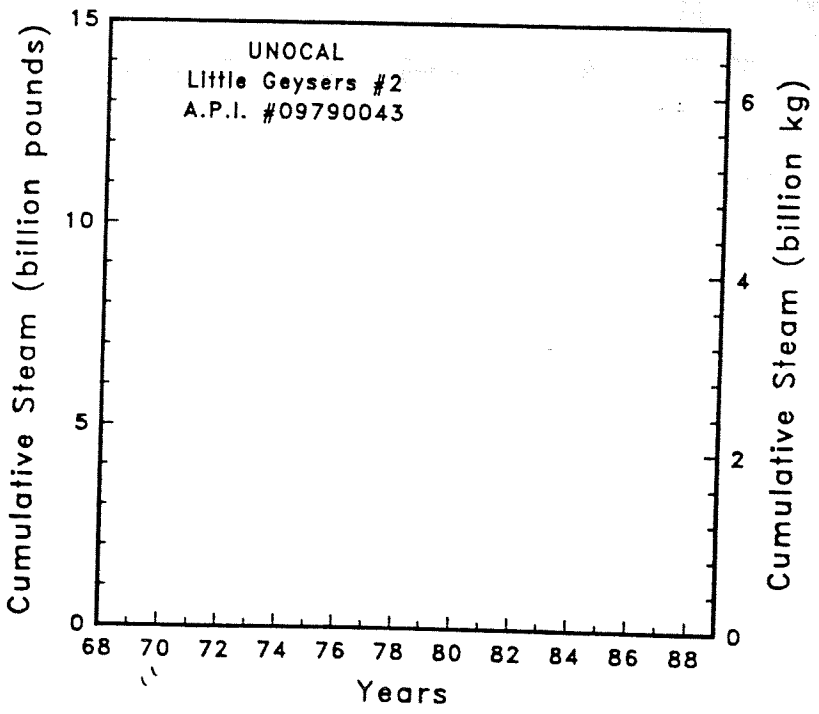

Figure A-145 Steam rate and cumulative mass flow for well Little Geysers #2

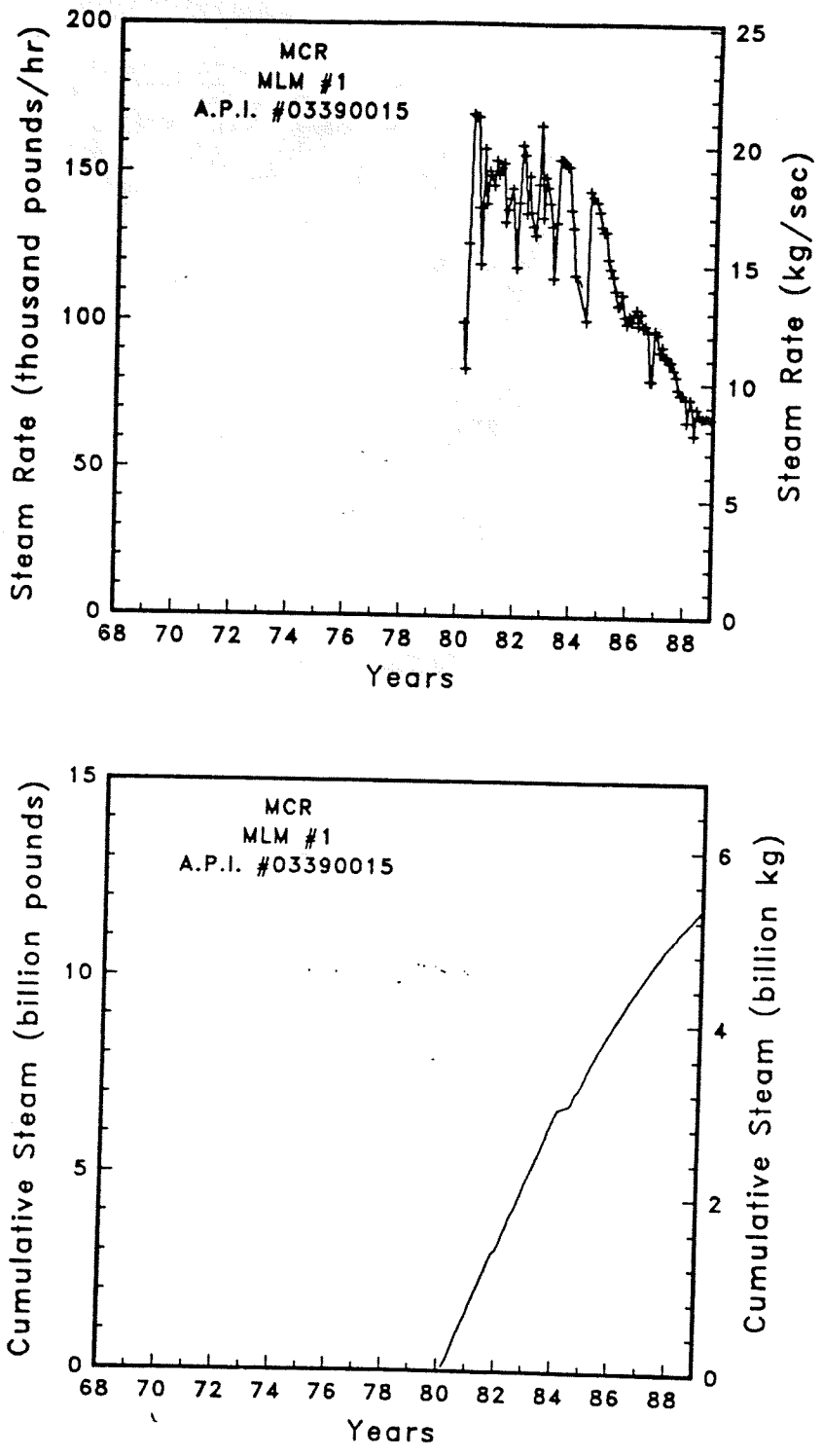

Figure A-146 Steam rate and cumulative mass flow for well MLM #1

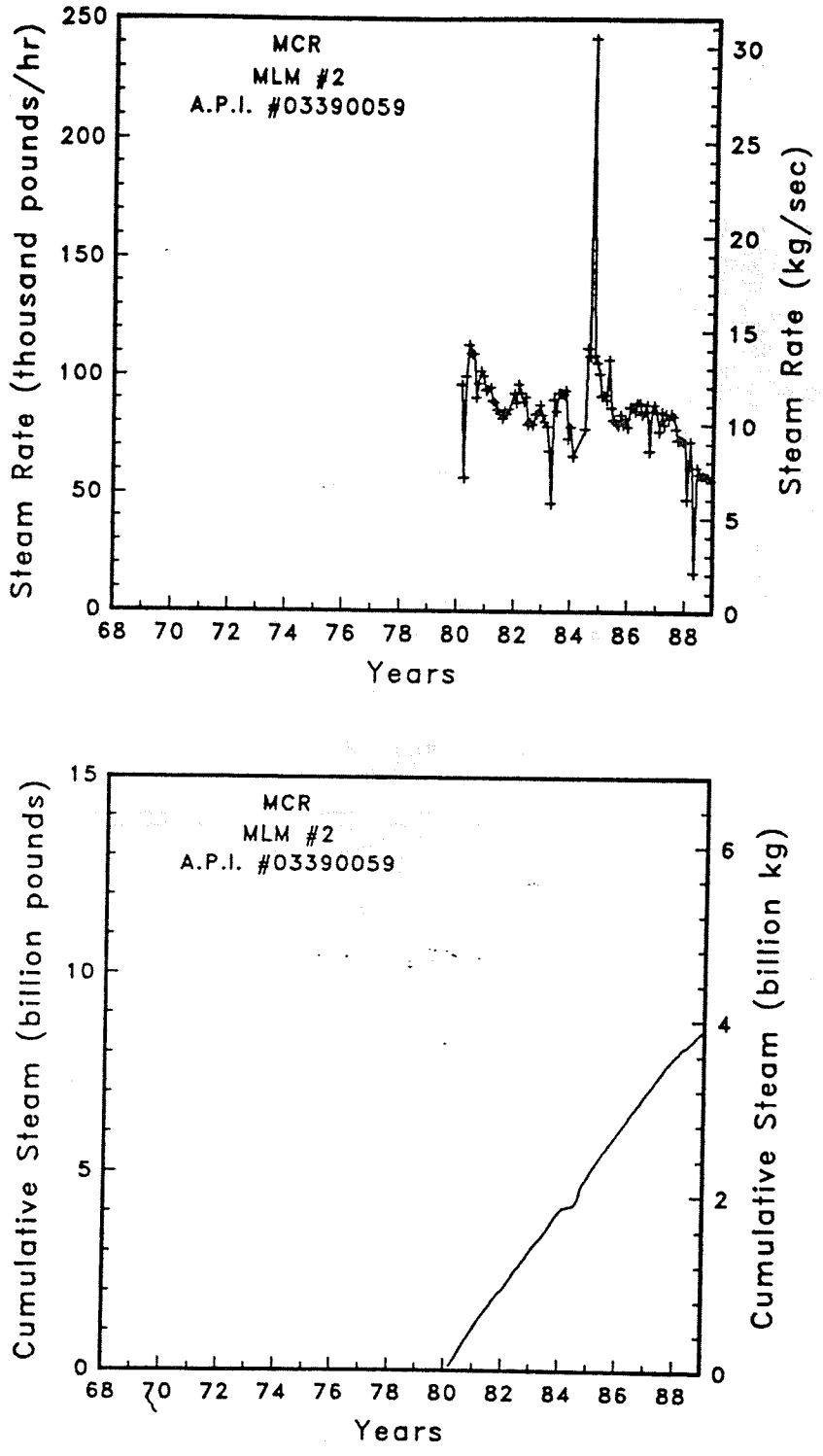

Figure A-147 Steam rate and cumulative mass flow for well MLM #2

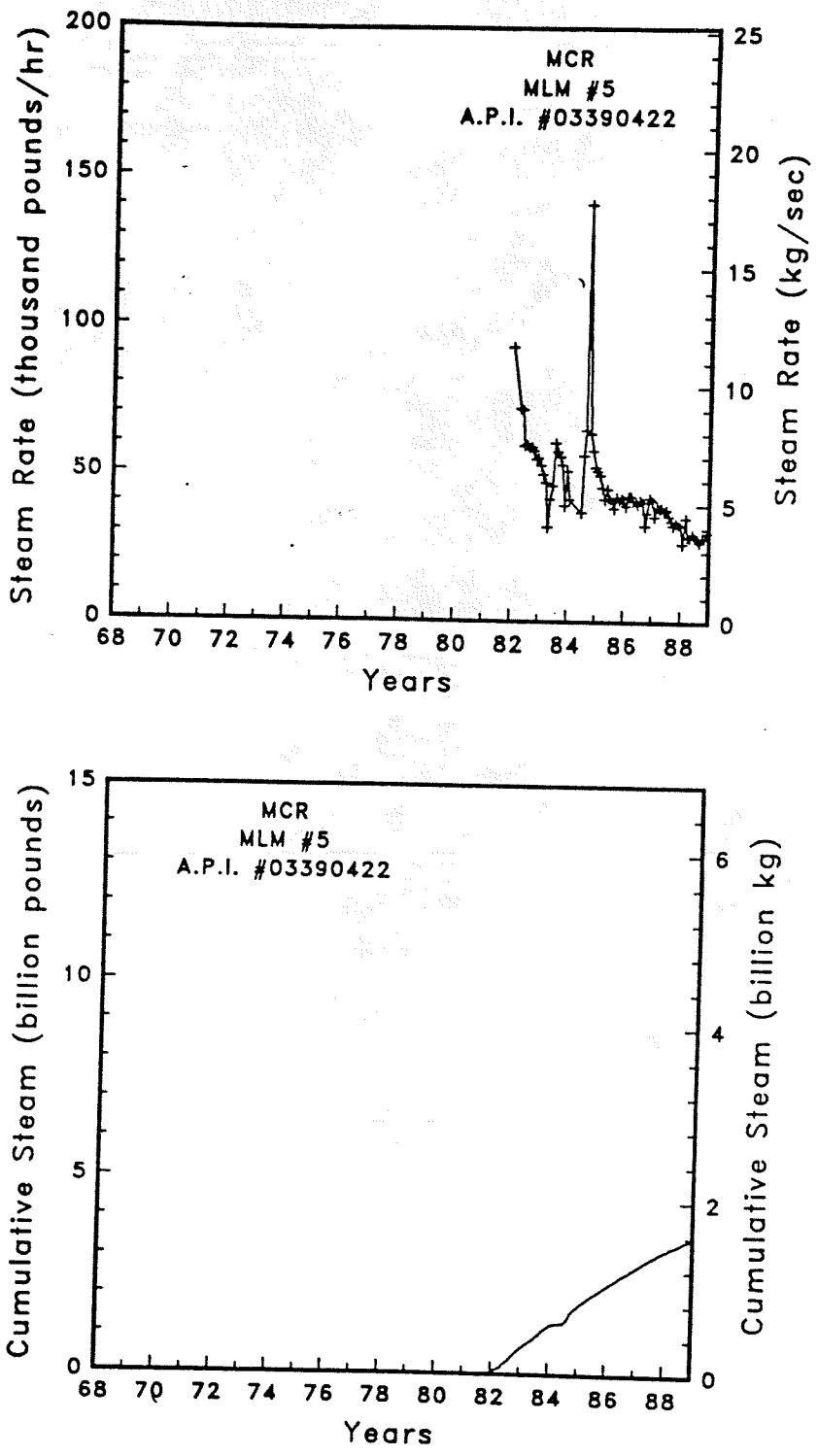

Figure A-148 Steam rate and cumulative mass flow for well MLM #5

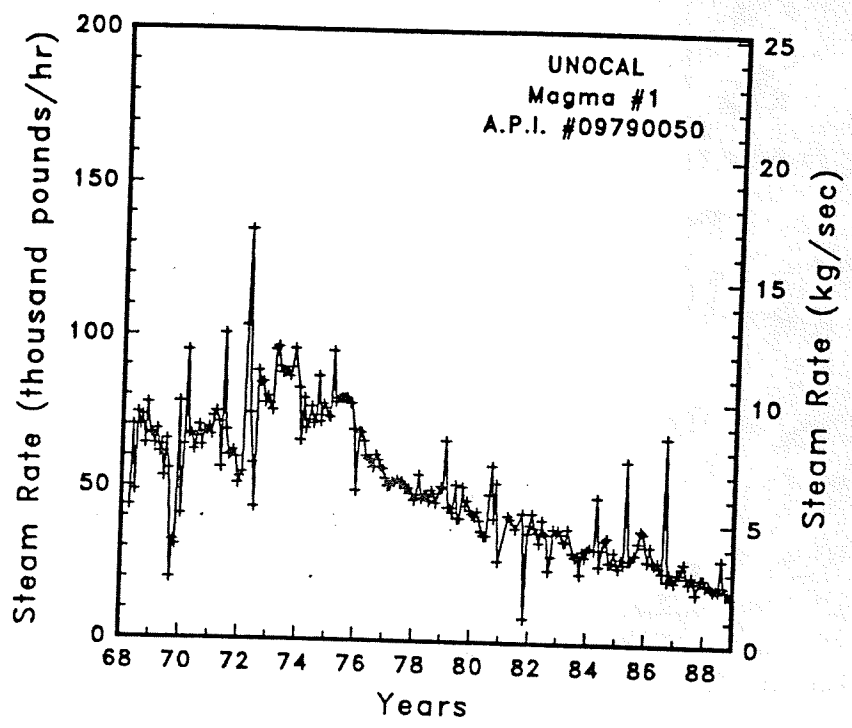

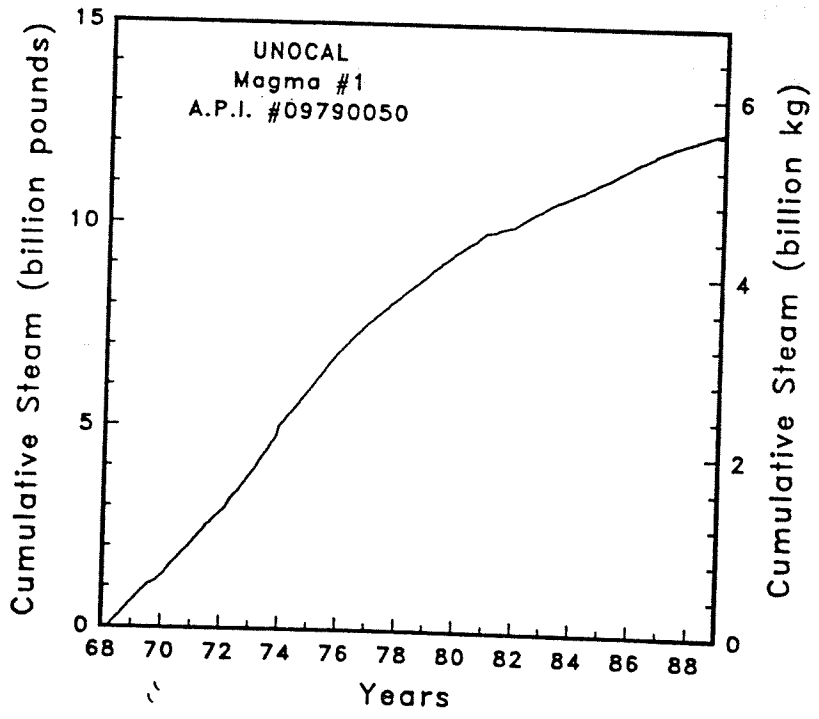

Figure A-149 Steam rate and cumulative mass flow for well Magma #1

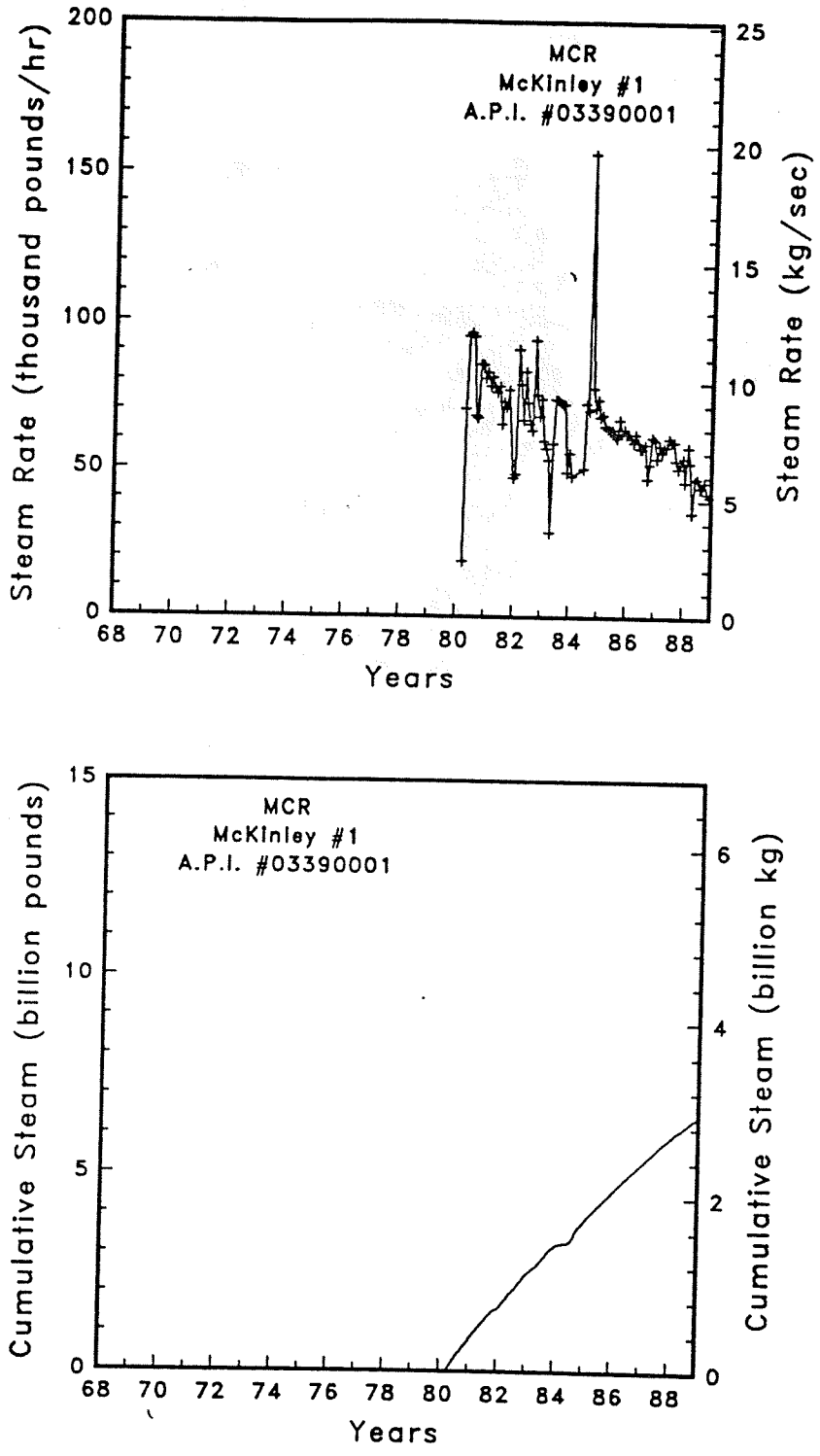

Figure A-150 Steam rate and cumulative mass flow for well McKinley #1

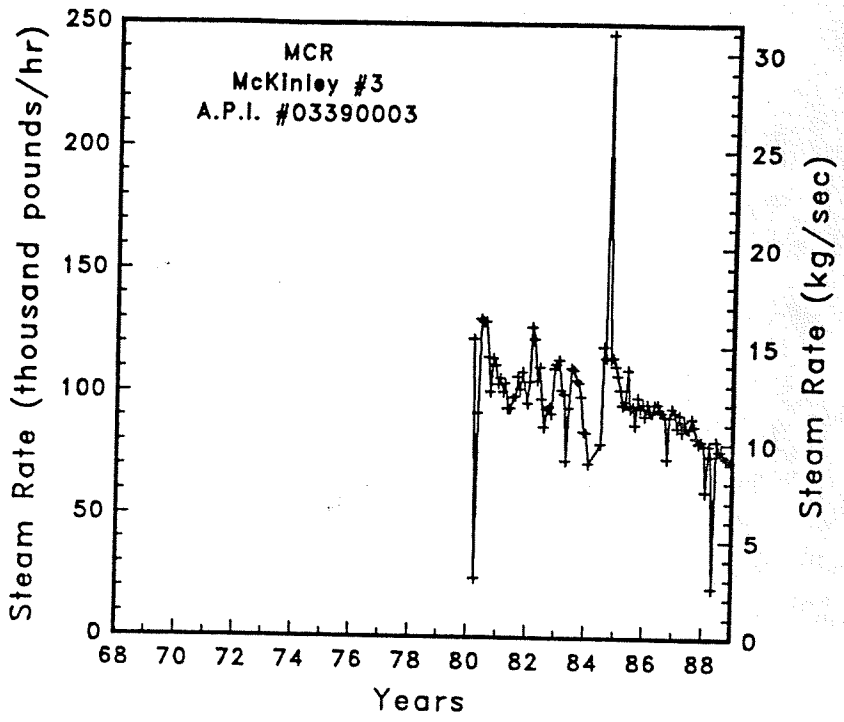

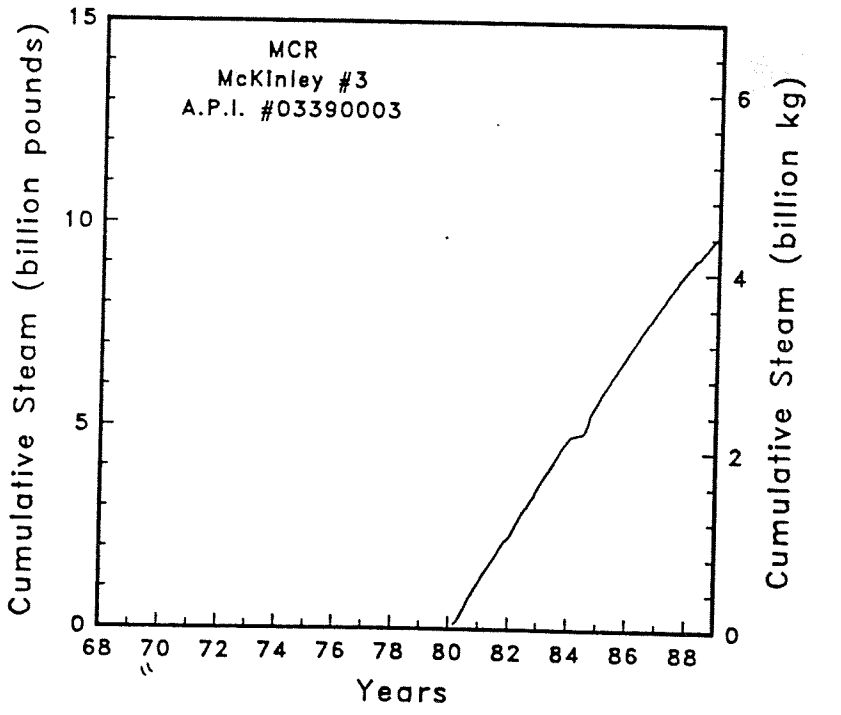

Figure A-151 Steam rate and cumulative mass flow for well McKinley #3

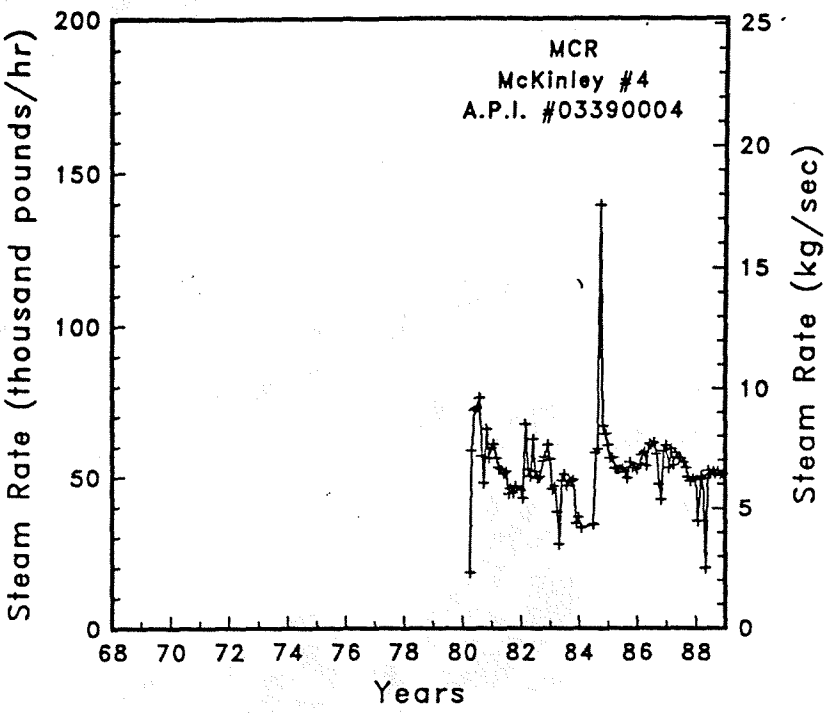

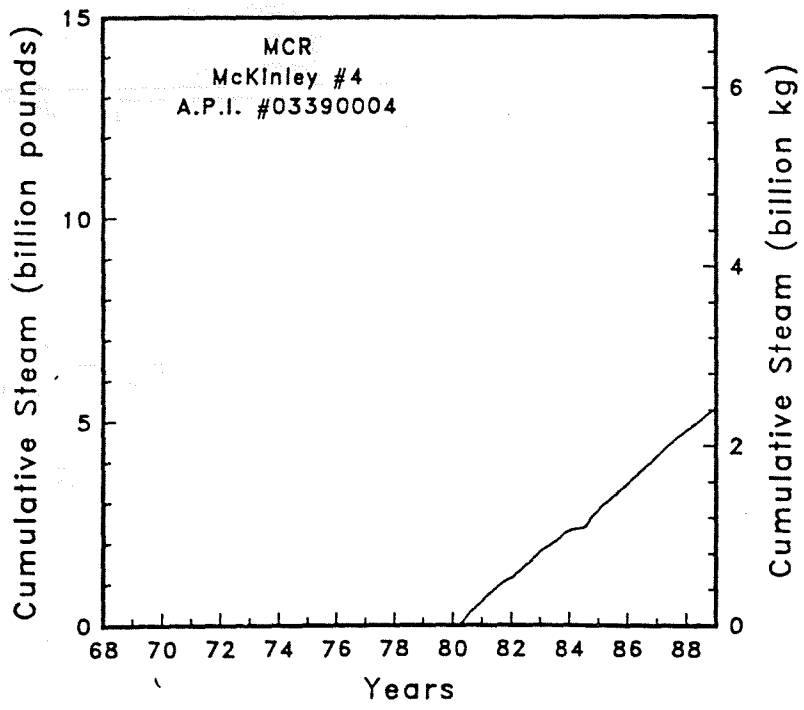

Figure A-152 Steam rate and cumulative mass flow for well McKinley #4

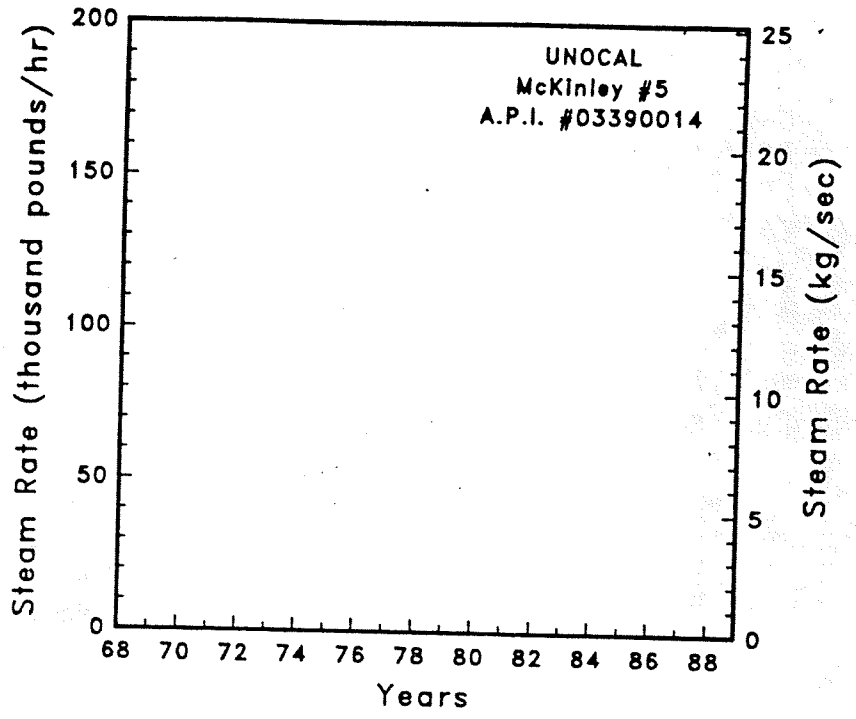

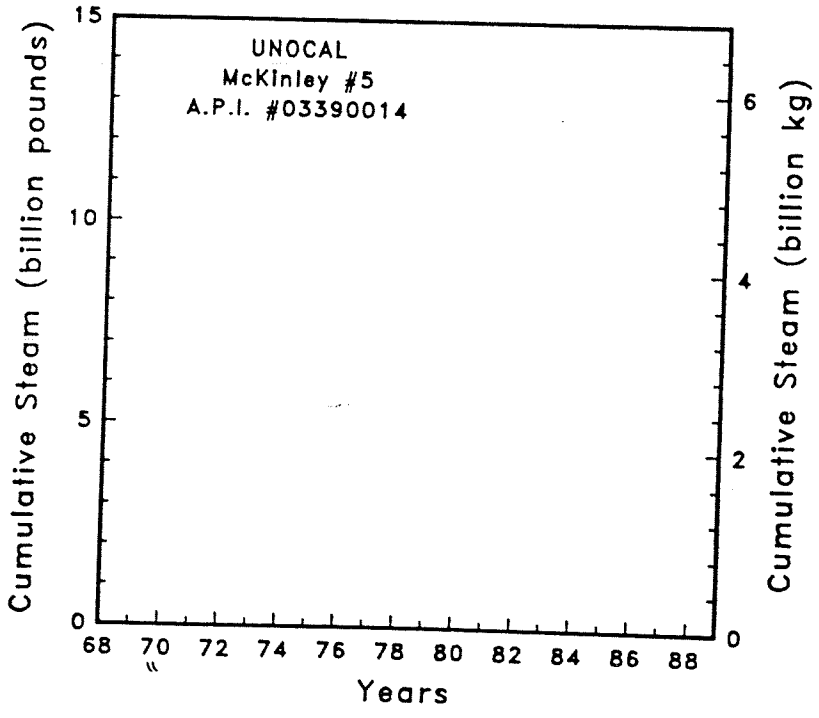

Figure A-153 Steam rate and cumulative mass flow for well McKinley #5

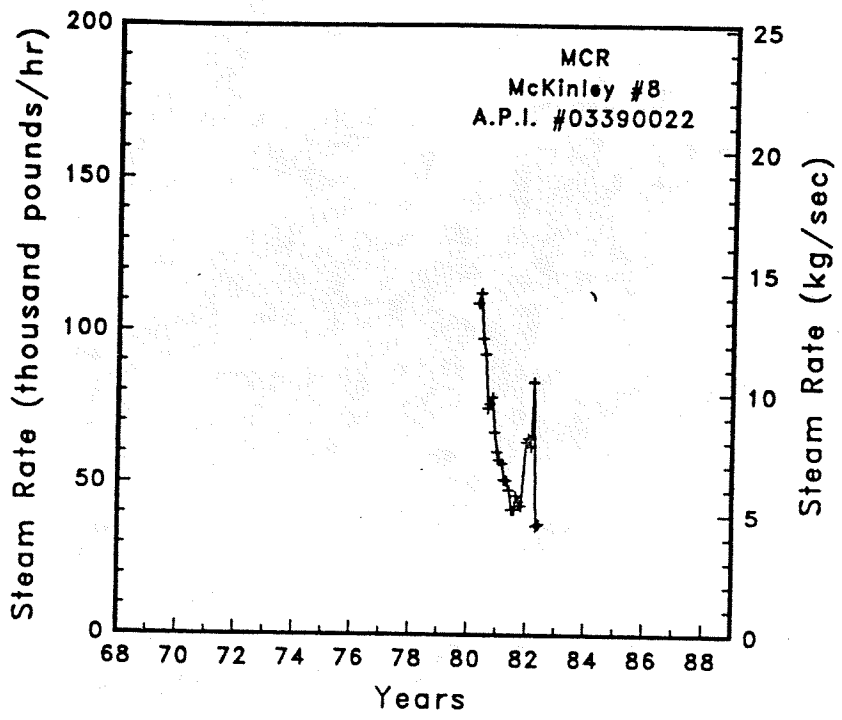

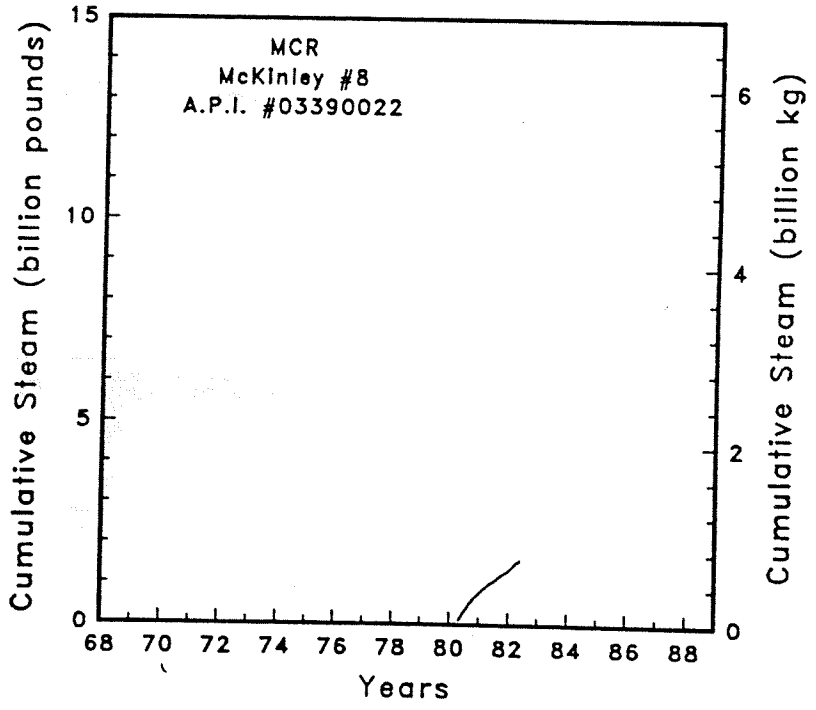

Figure A-154 Steam rate and cumulative mass flow for well McKinley #8

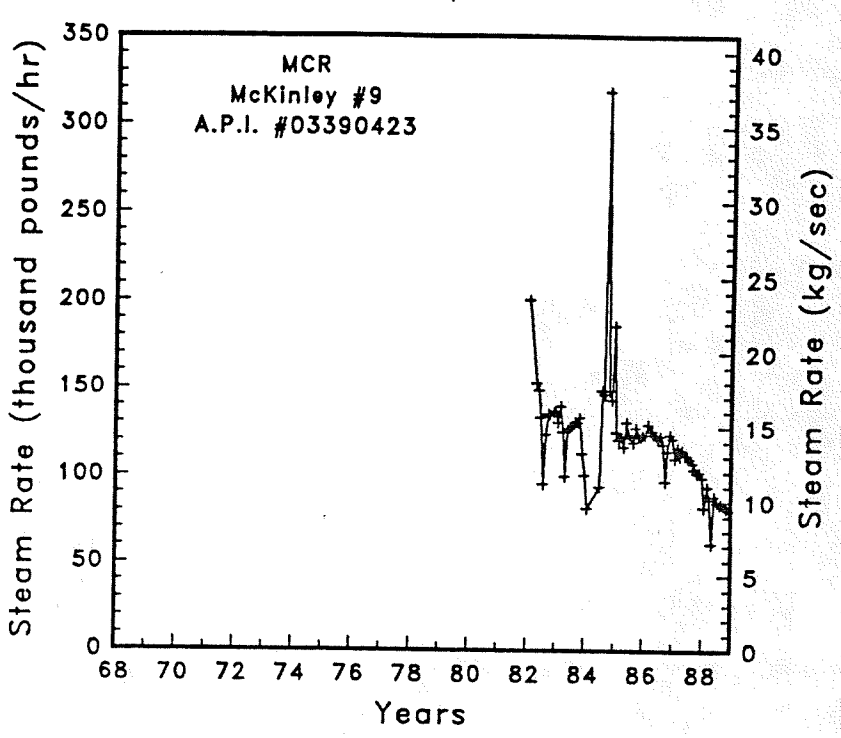

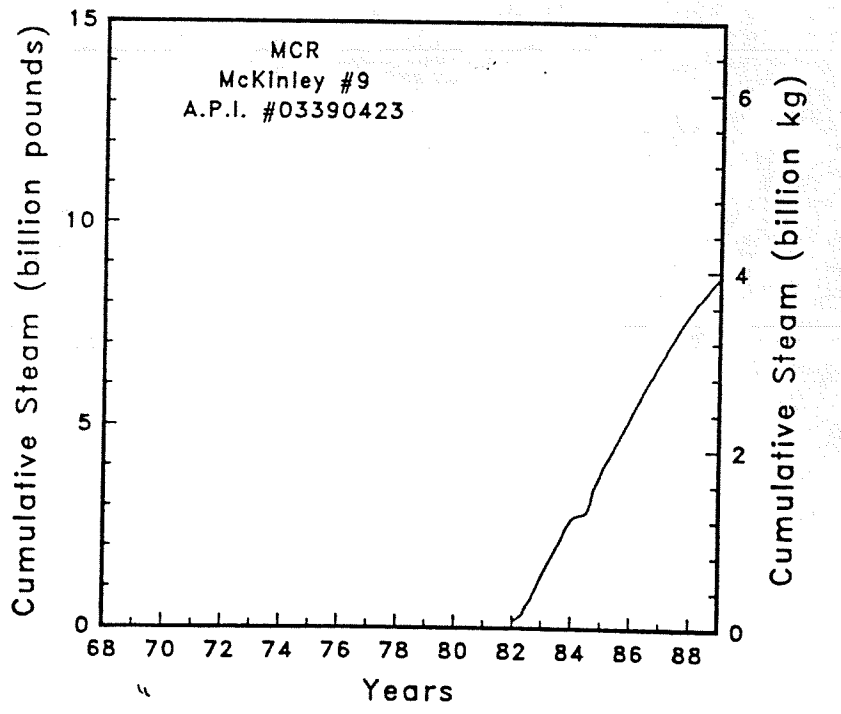

Figure A-155 Steam rate and cumulative mass flow for well McKinley #9

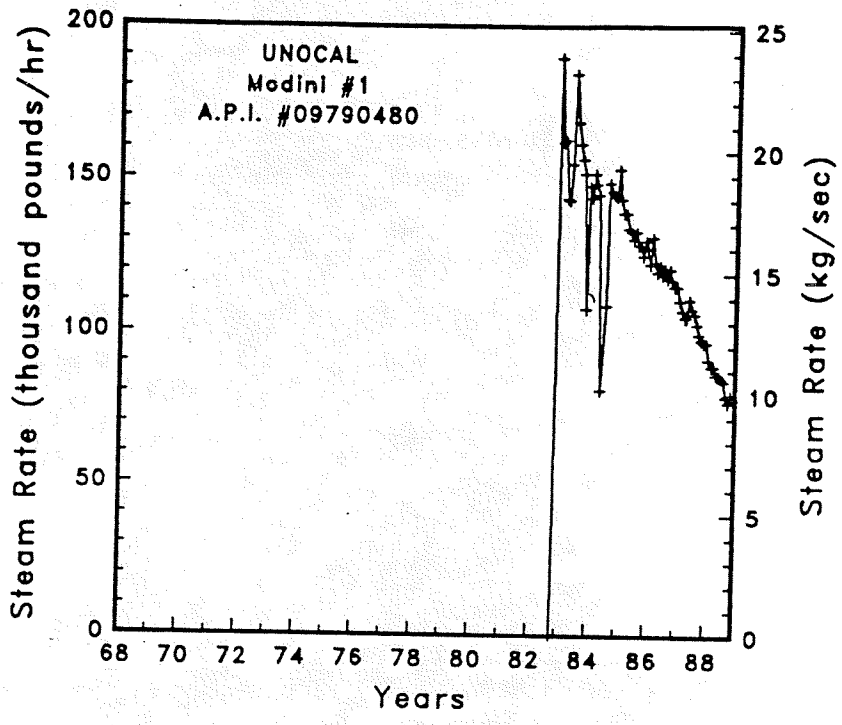

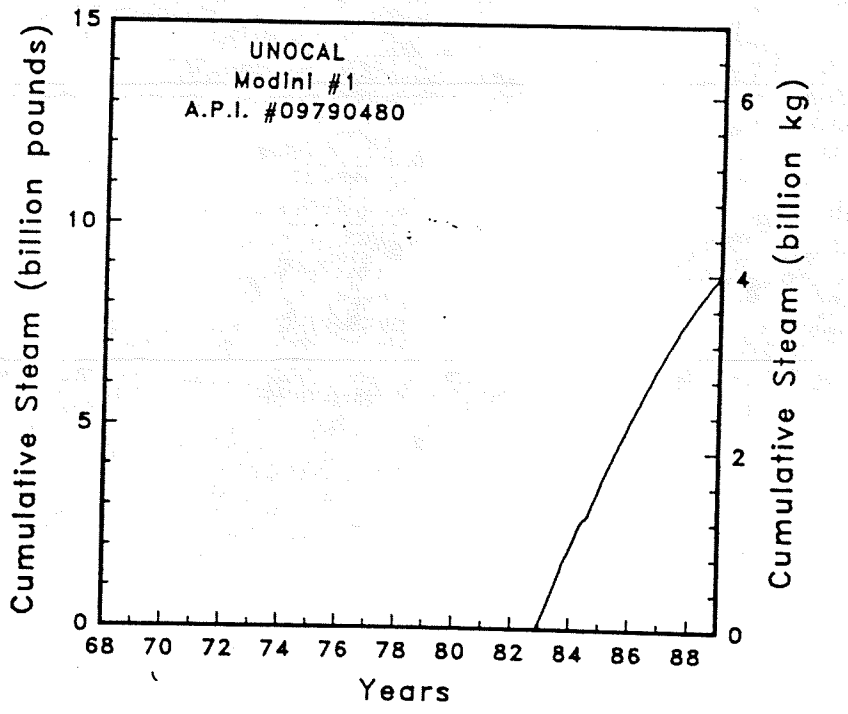

Figure A-156 Steam rate and cumulative mass flow for well Modini #1

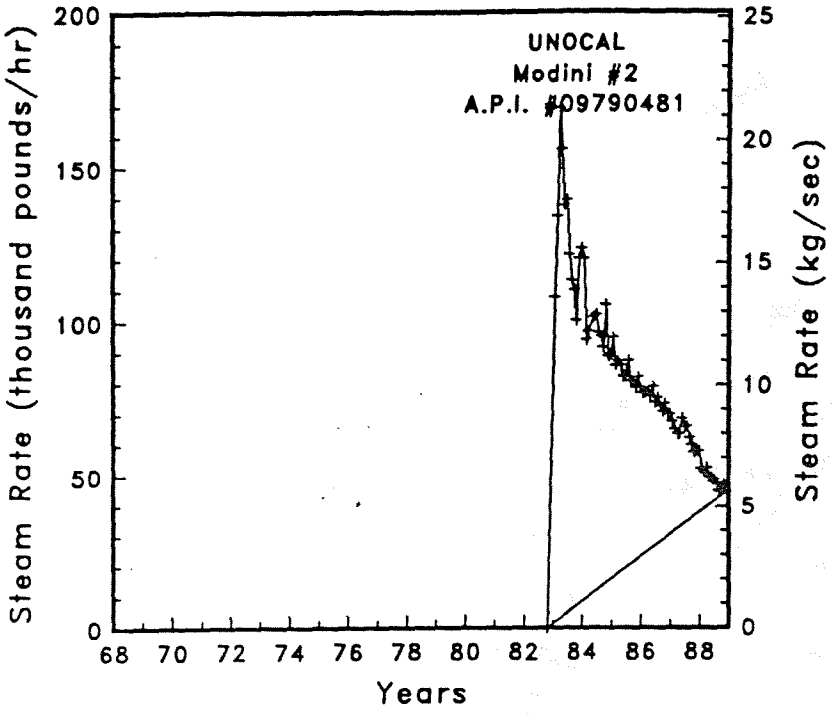

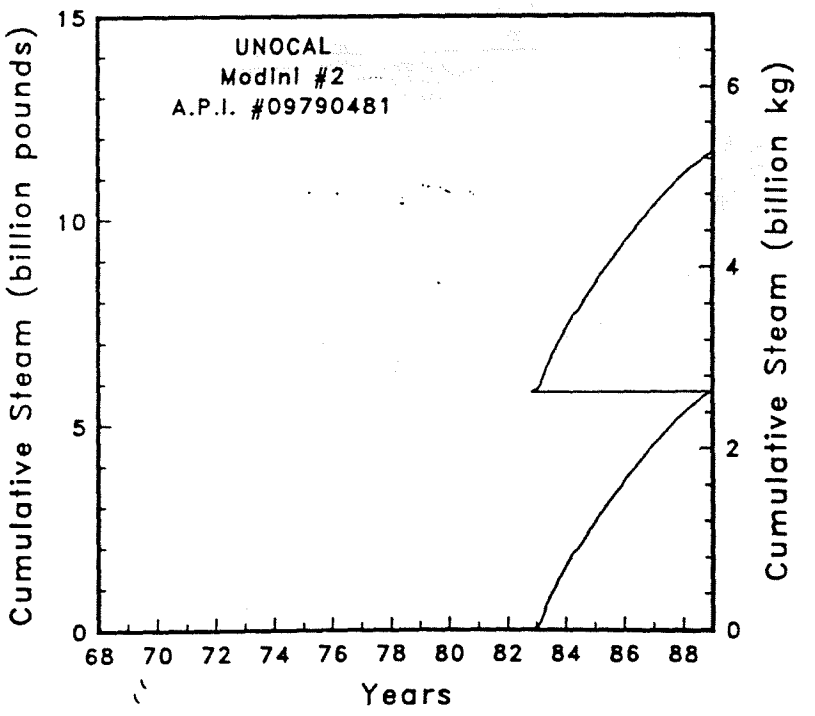

Figure A-157 Steam rate and cumulative mass flow for well Modini #2

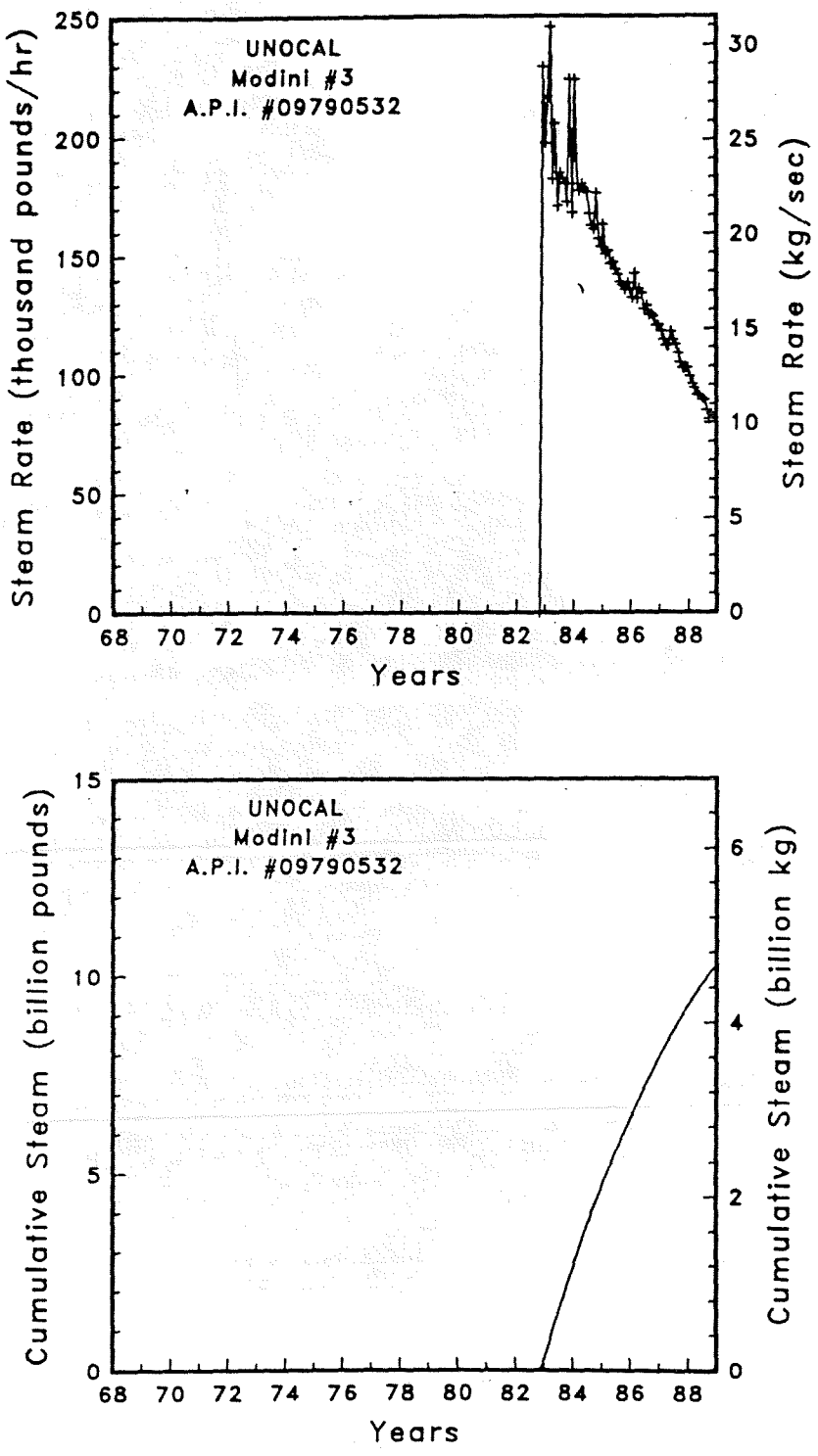

Figure A-158 Steam rate and cumulative mass flow for well Modini #3

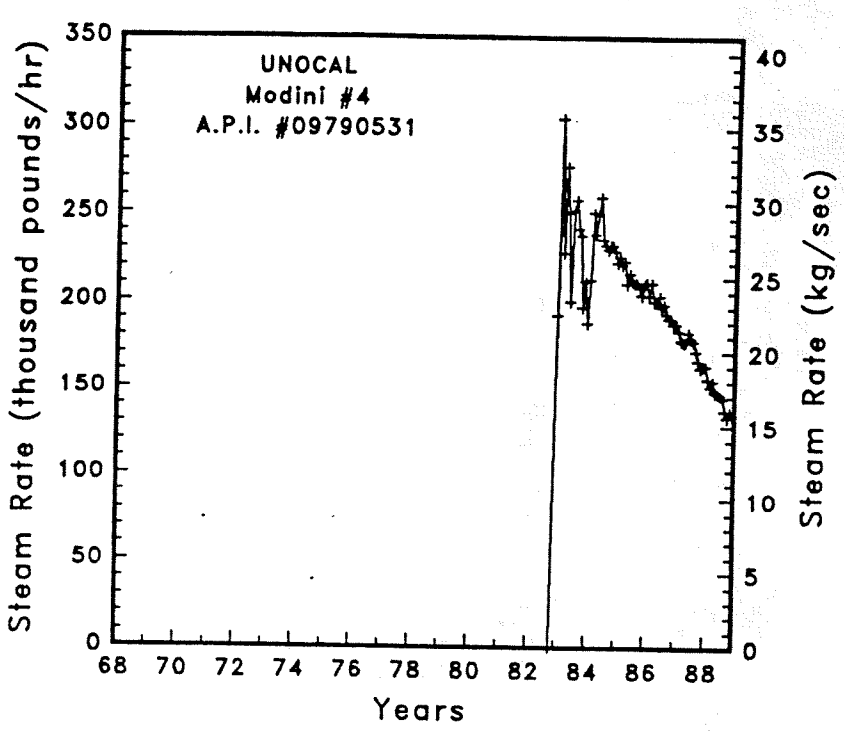

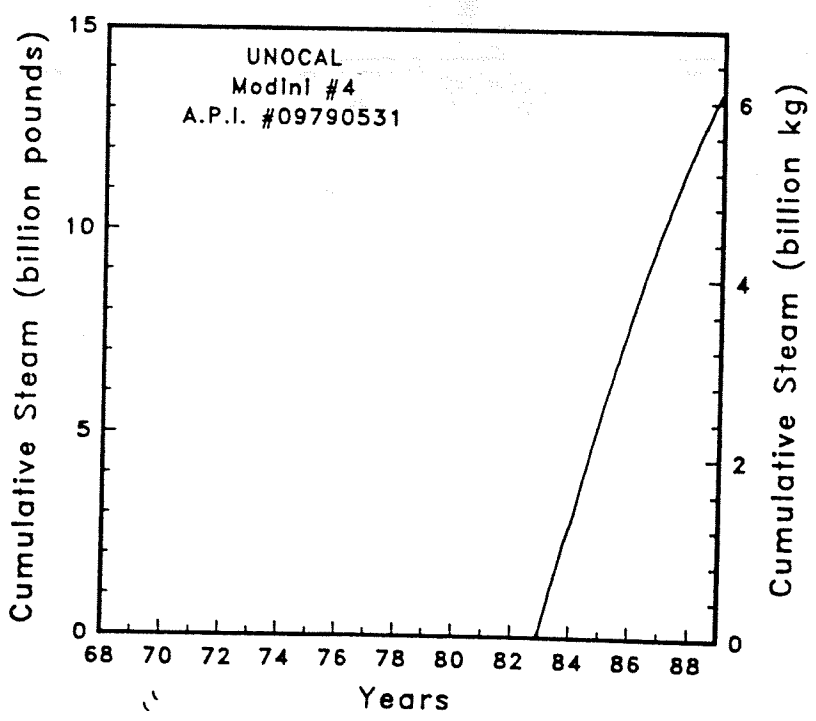

Figure A-159 Steam rate and cumulative mass flow for well Modini #4

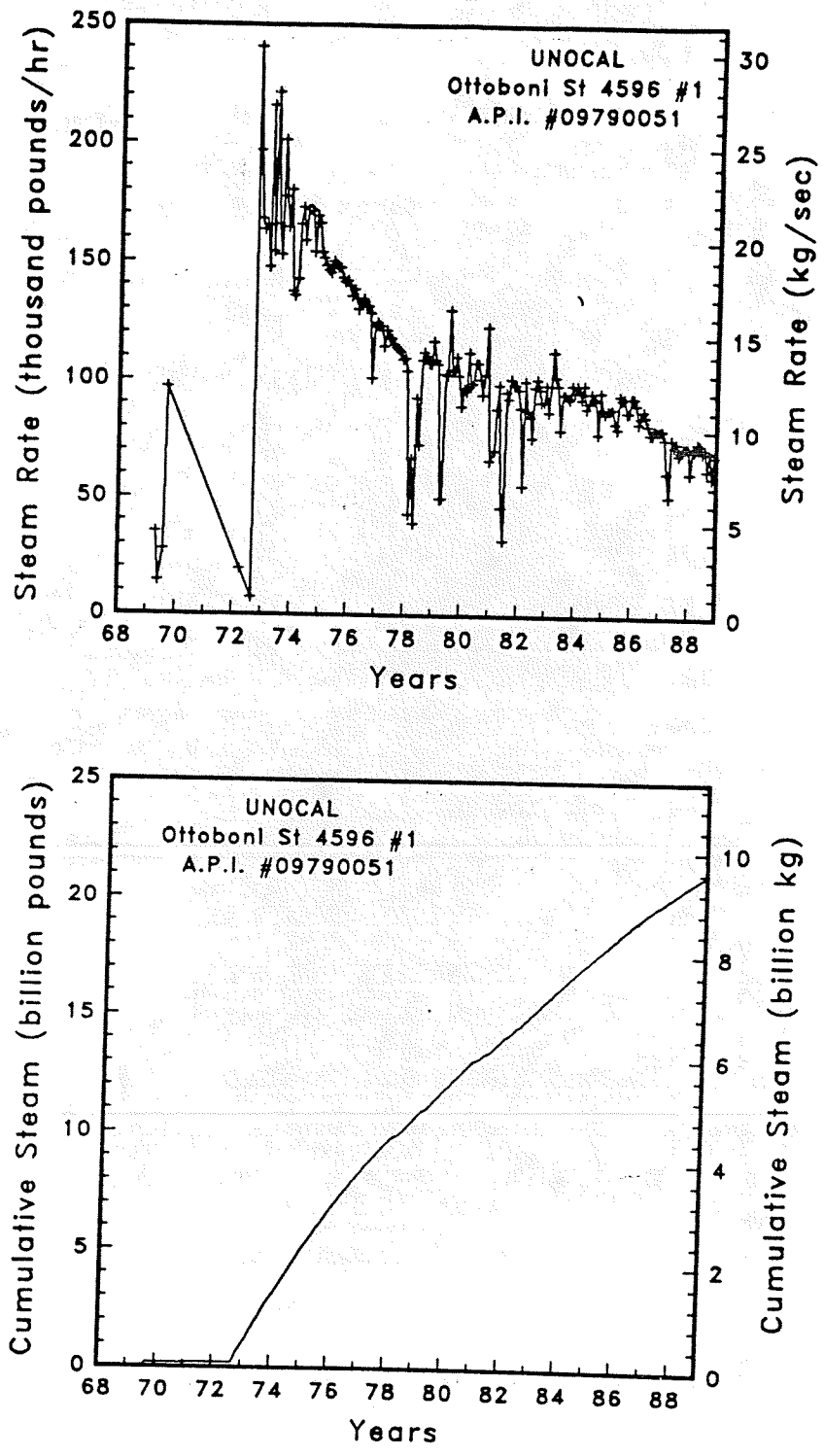

Figure A-160 Steam rate and cumulative mass flow for well Ottoboni St 4596 #1

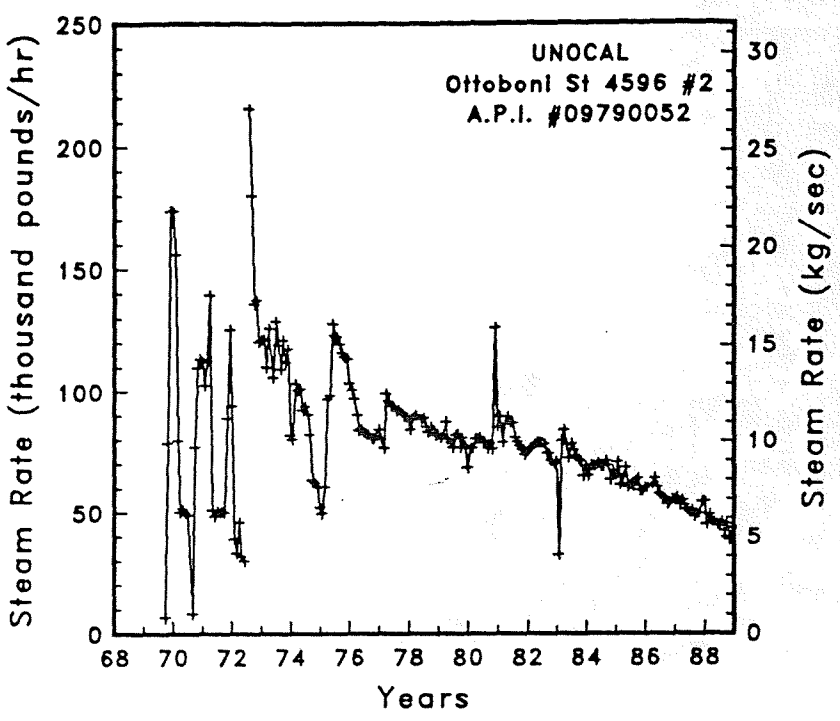

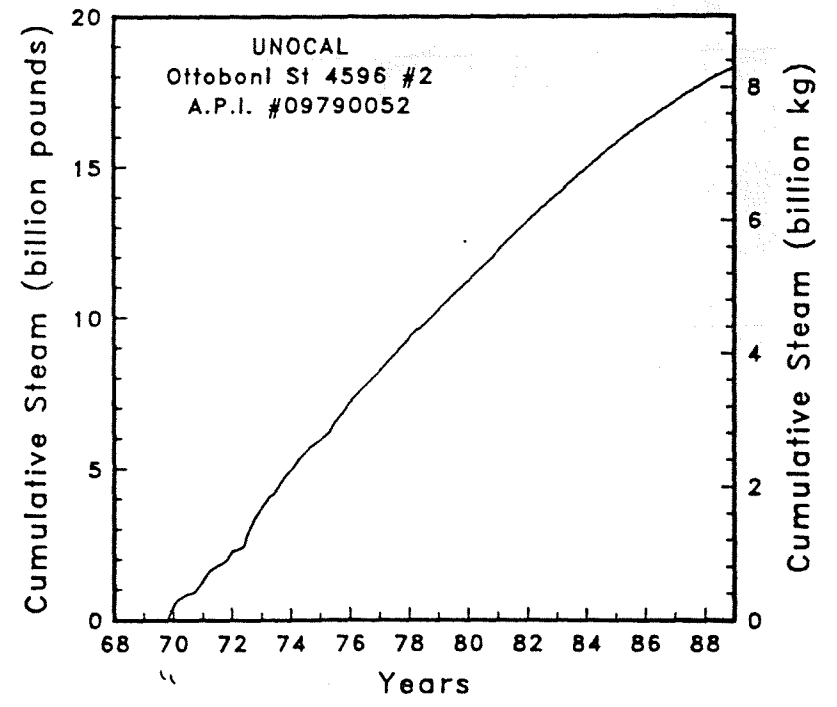

Figure A-161 Steam rate and cumulative mass flow for well Ottoboni St 4596 #2

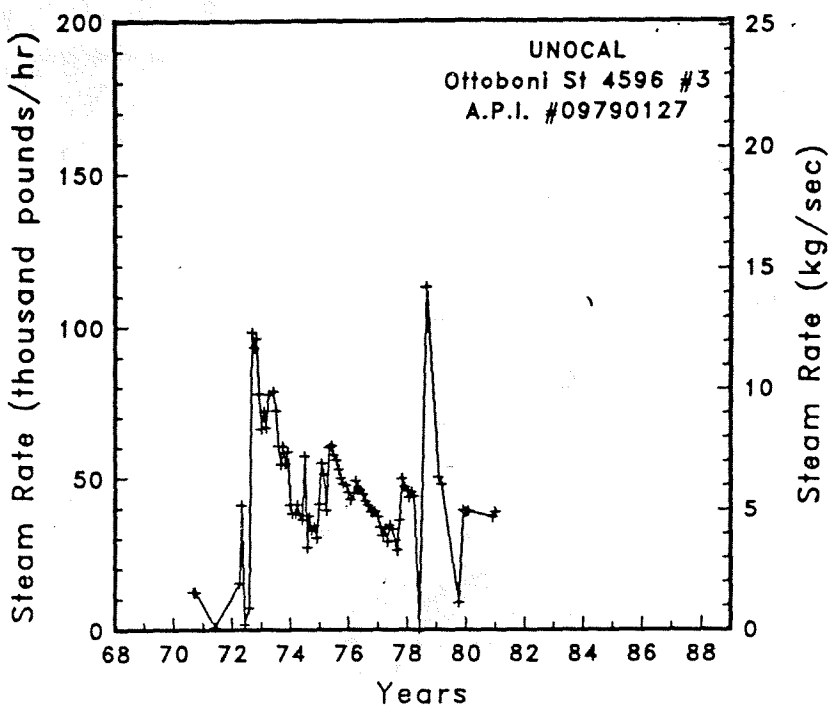

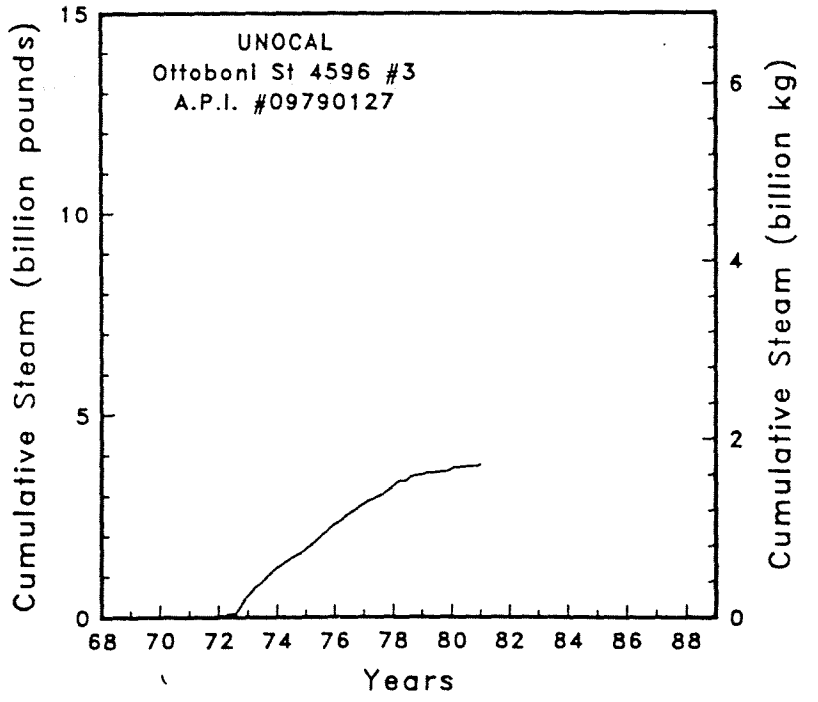

Figure A-162 Steam rate and cumulative mass flow for well Ottoboni St 4596 #3

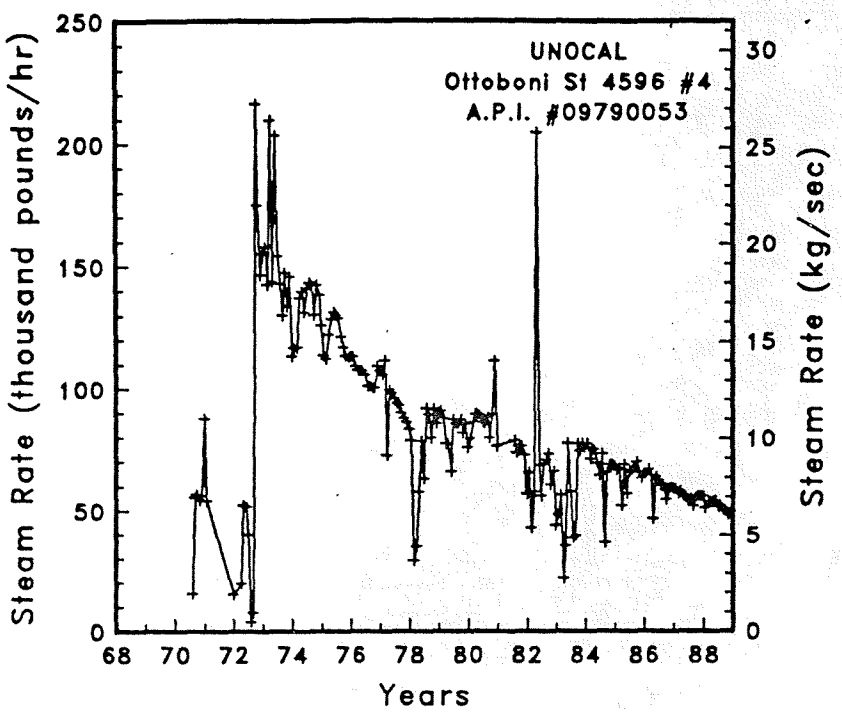

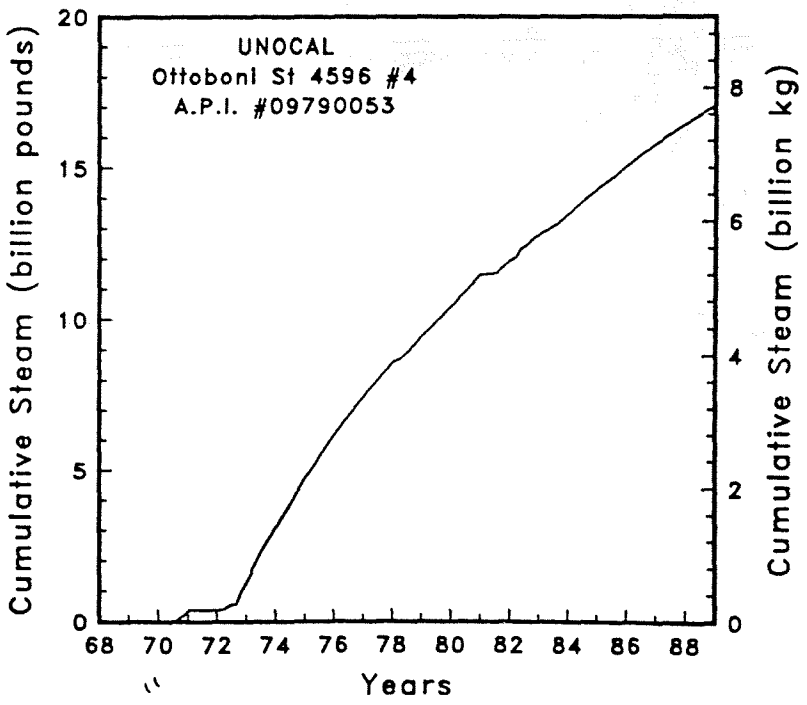

Figure A-163 Steam rate and cumulative mass flow for well Ottoboni St 4596 #4

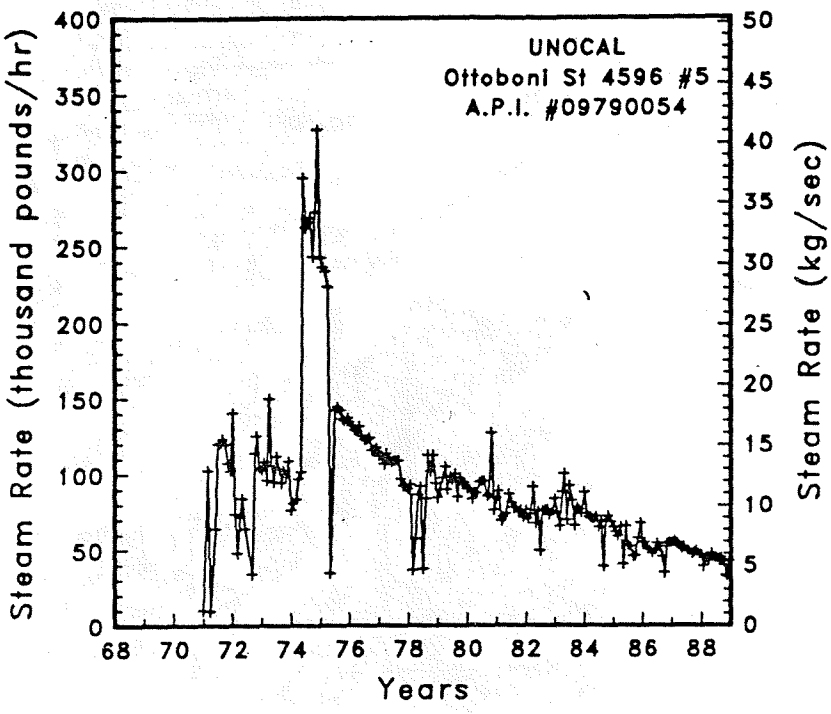

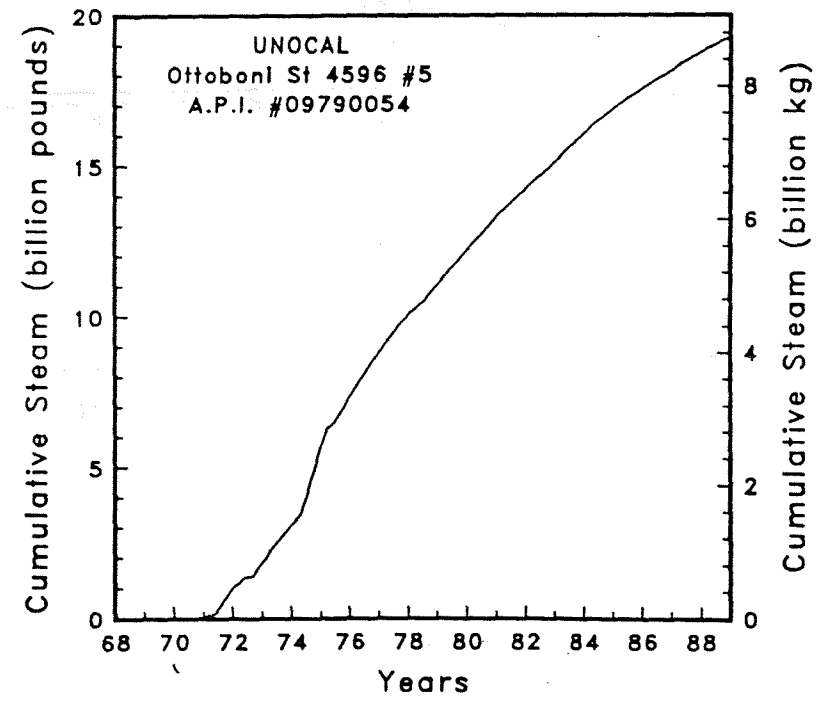

Figure A-164 Steam rate and cumulative mass flow for well Ottoboni St 4596 #5

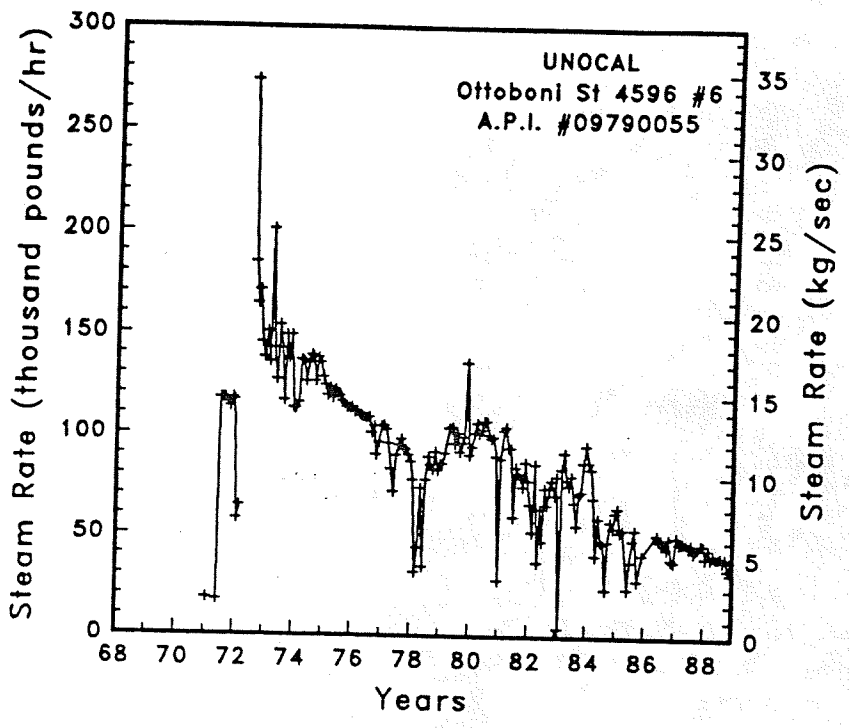

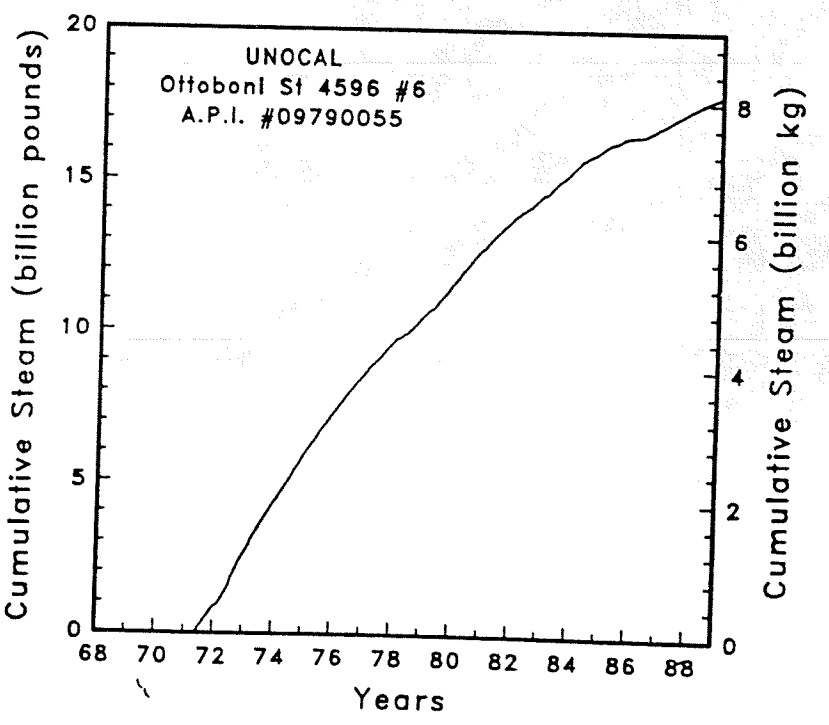

Figure A-165 Steam rate and cumulative mass flow for well Ottoboni St 4596 #6

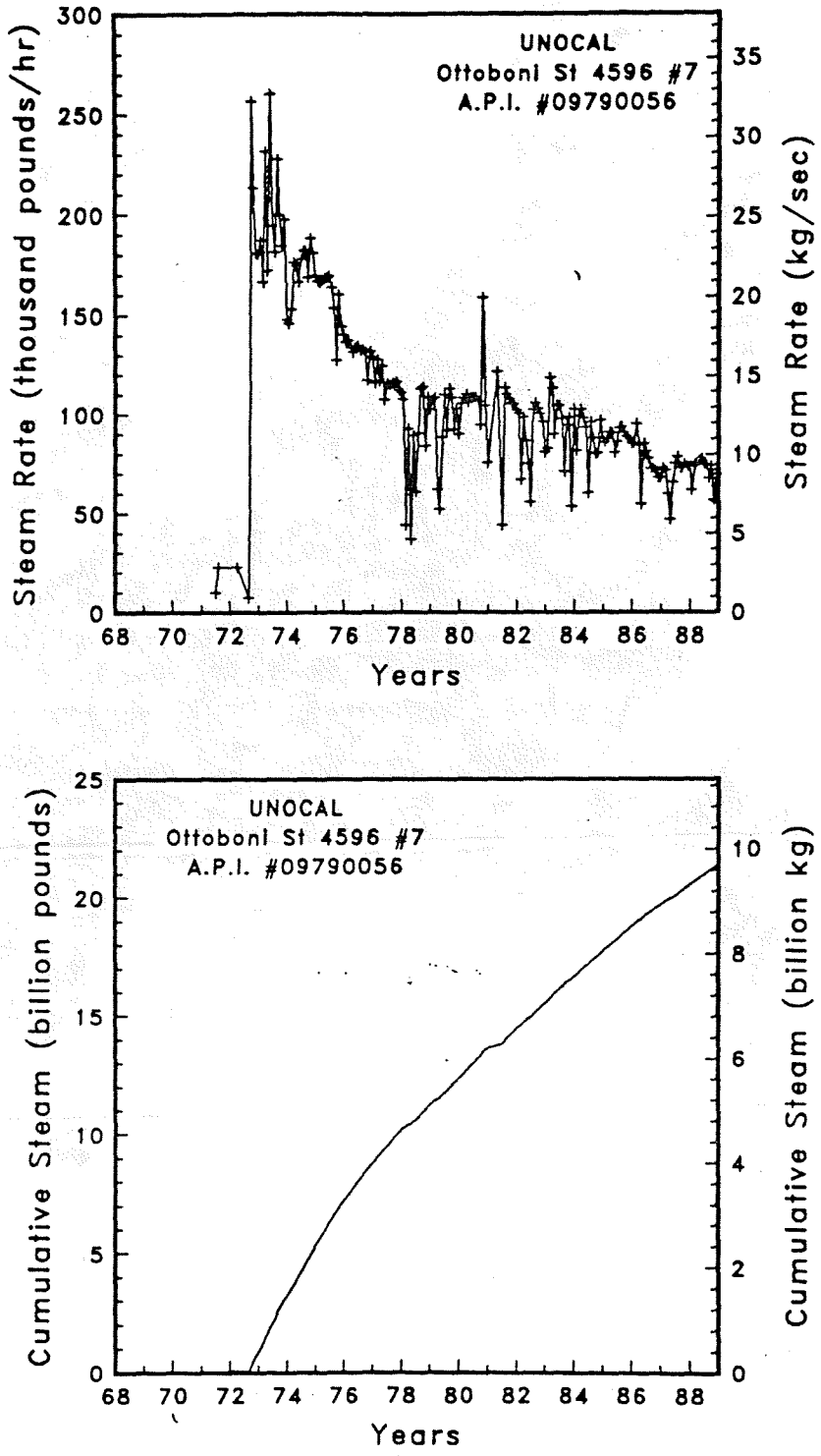

Figure A-166 Steam rate and cumulative mass flow for well Ottoboni St 4596 #7

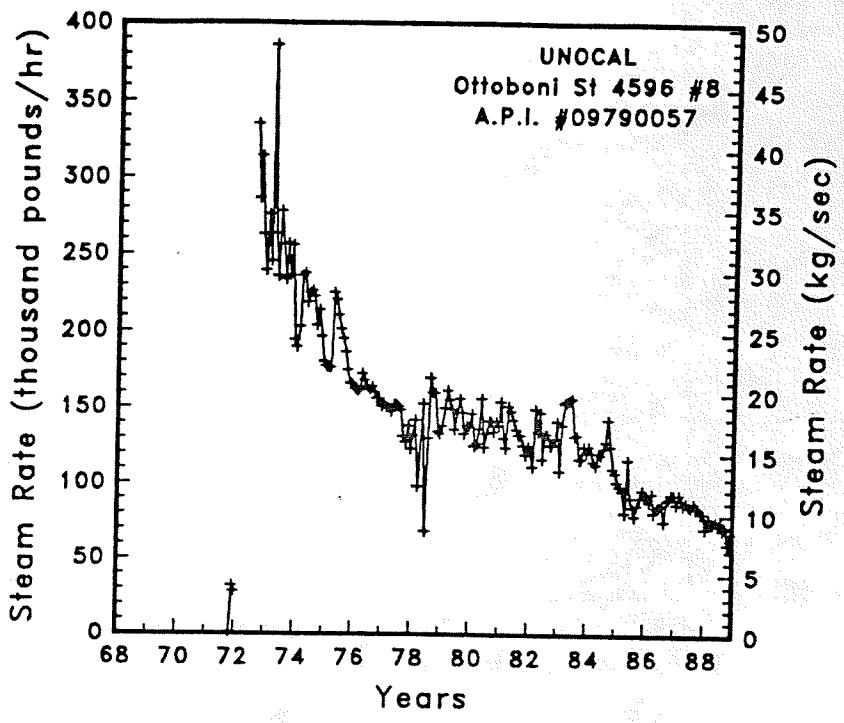

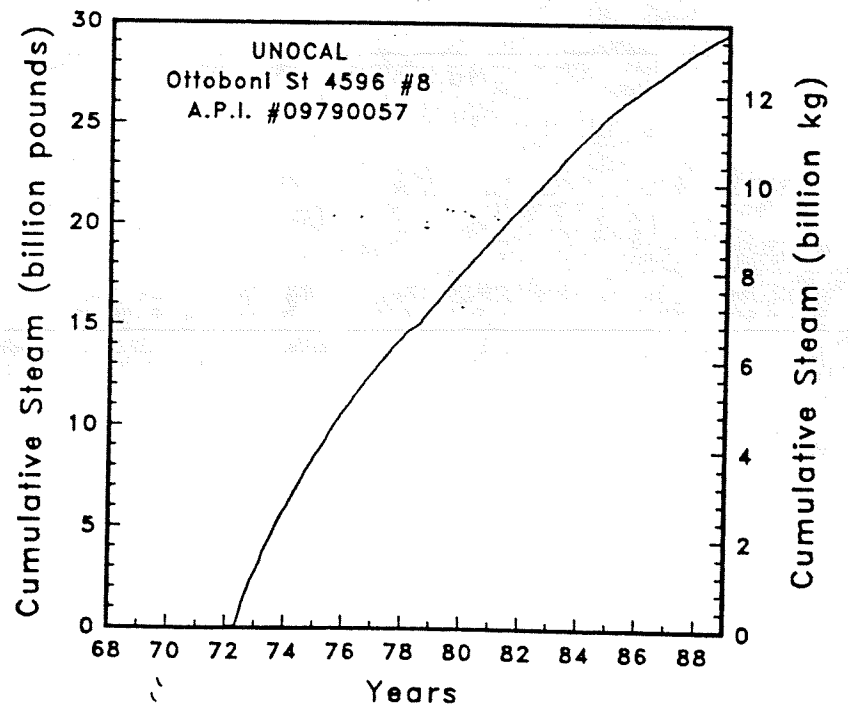

Figure A-167 Steam rate and cumulative mass flow for well Ottoboni St 4596 #8

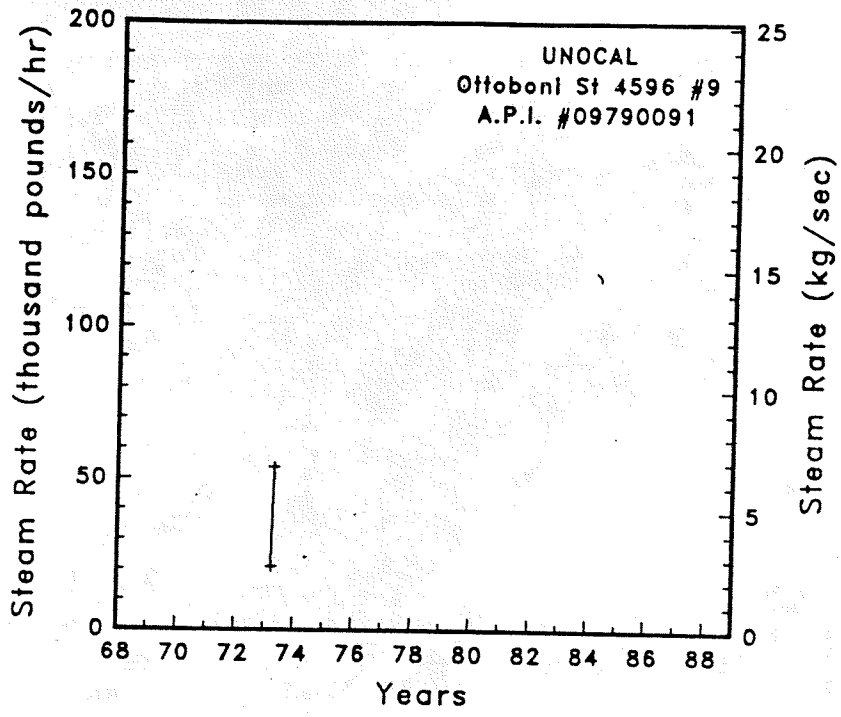

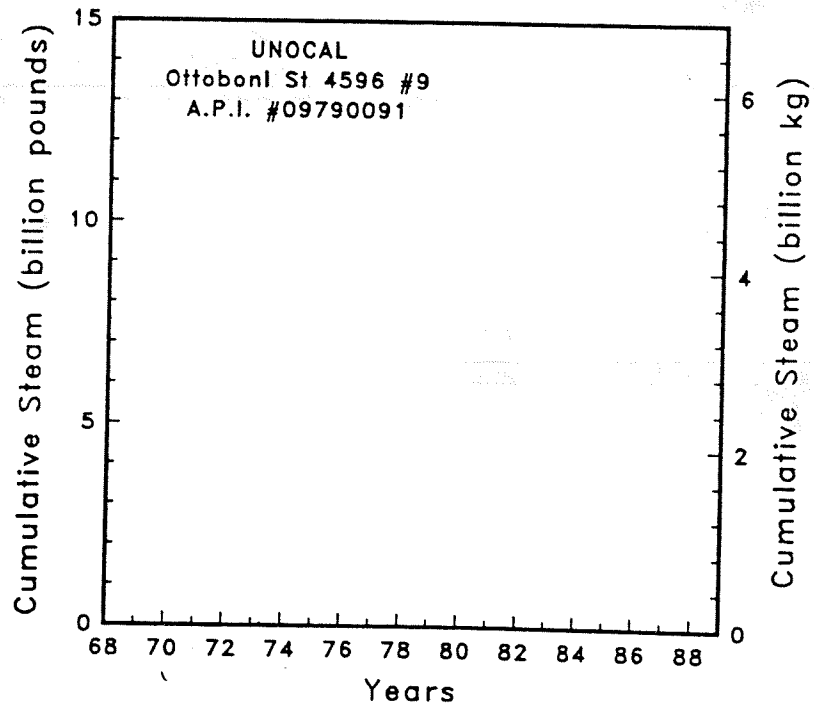

Figure A-168 Steam rate and cumulative mass flow for well Ottoboni St 4596 #9

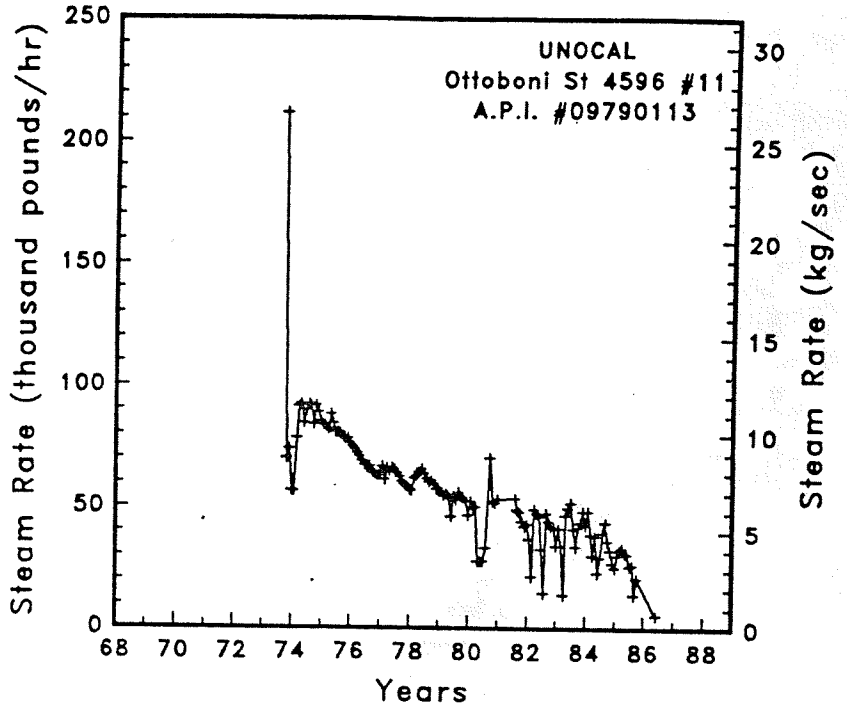

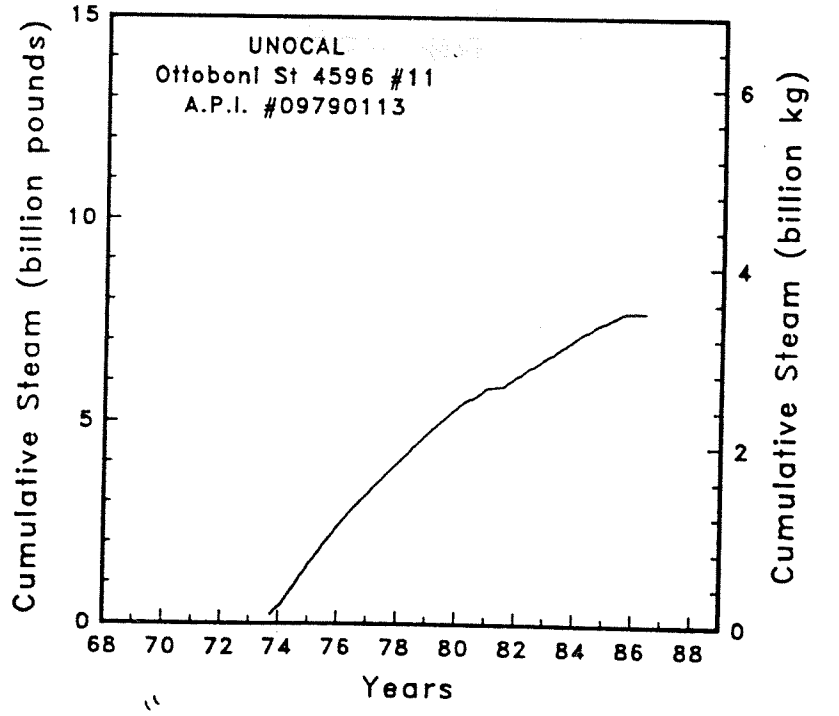

Figure A-169 Steam rate and cumulative mass flow for well Ottoboni St 4596 #11

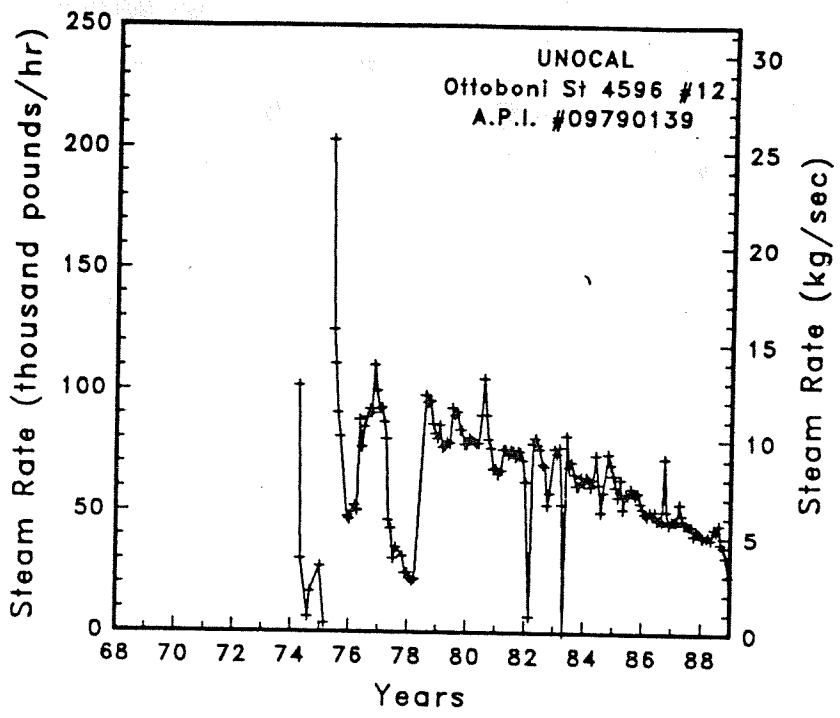

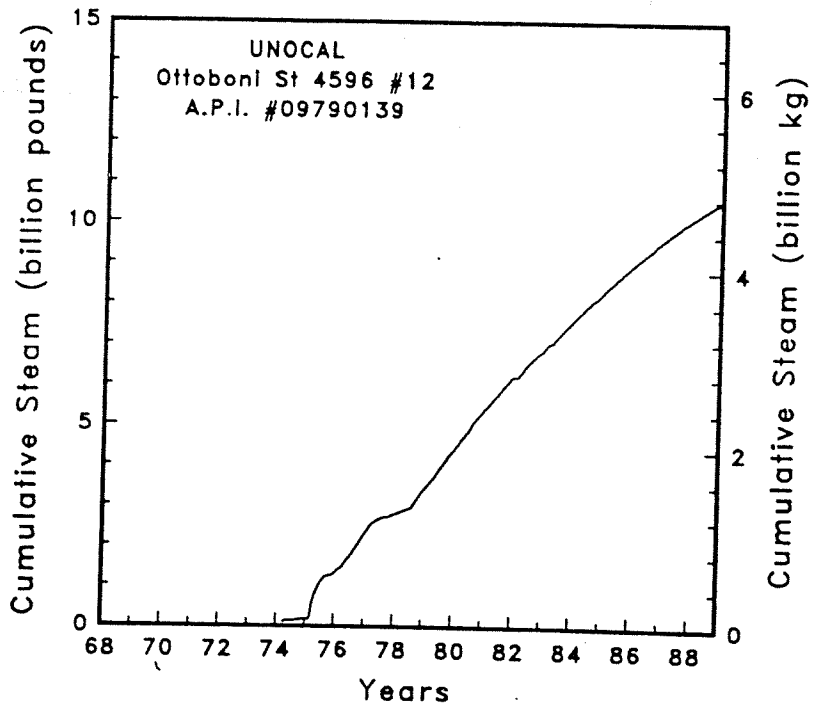

Figure A-170 Steam rate and cumulative mass flow for well Ottoboni St 4596 #12

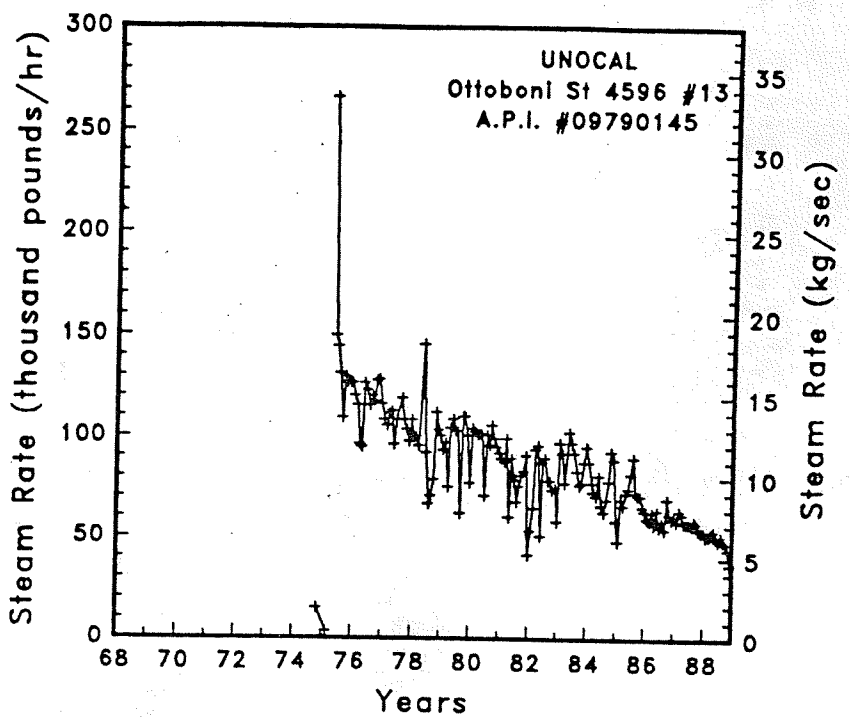

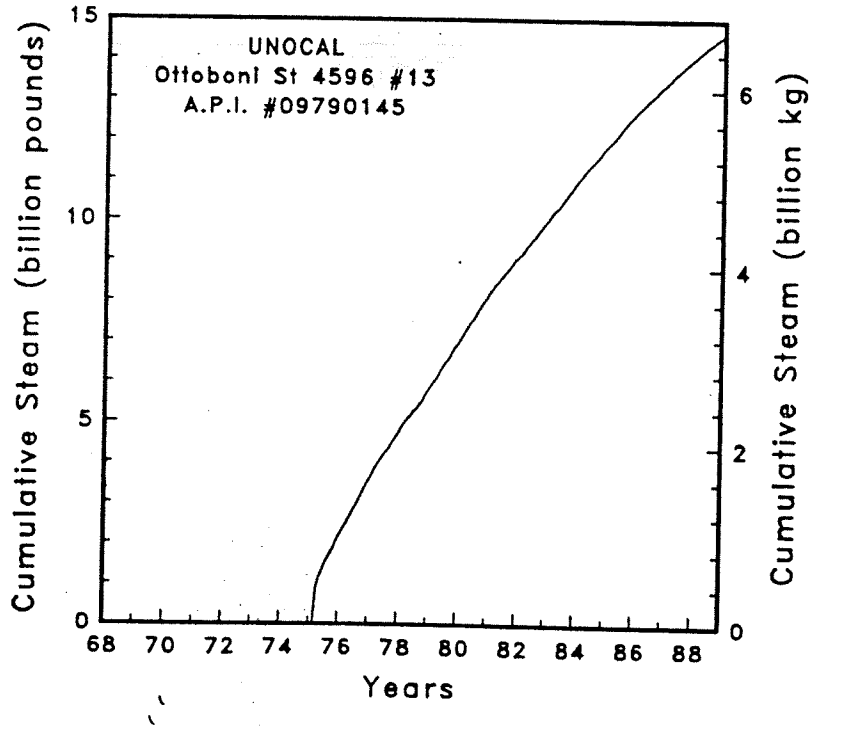

Figure A-171 Steam rate and cumulative mass flow for well Ottoboni St 4596 #13

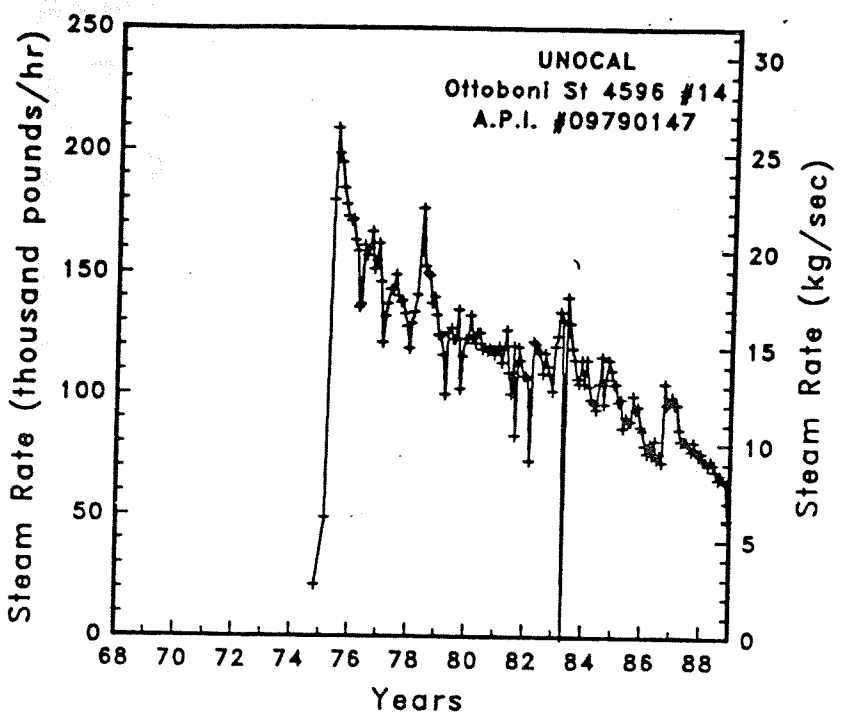

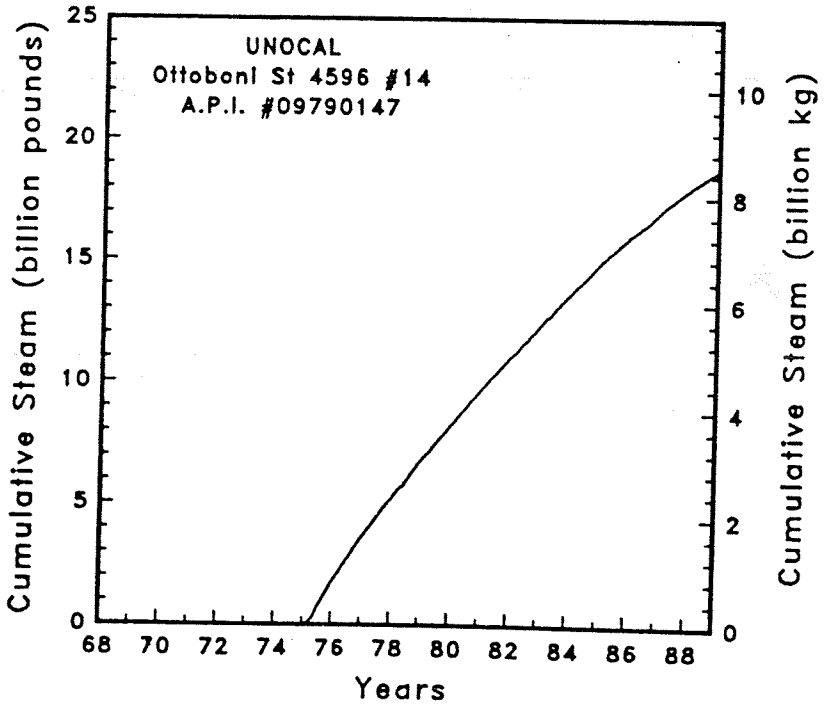

Figure A-172 Steam rate and cumulative mass flow for well Ottoboni St 4596 #14

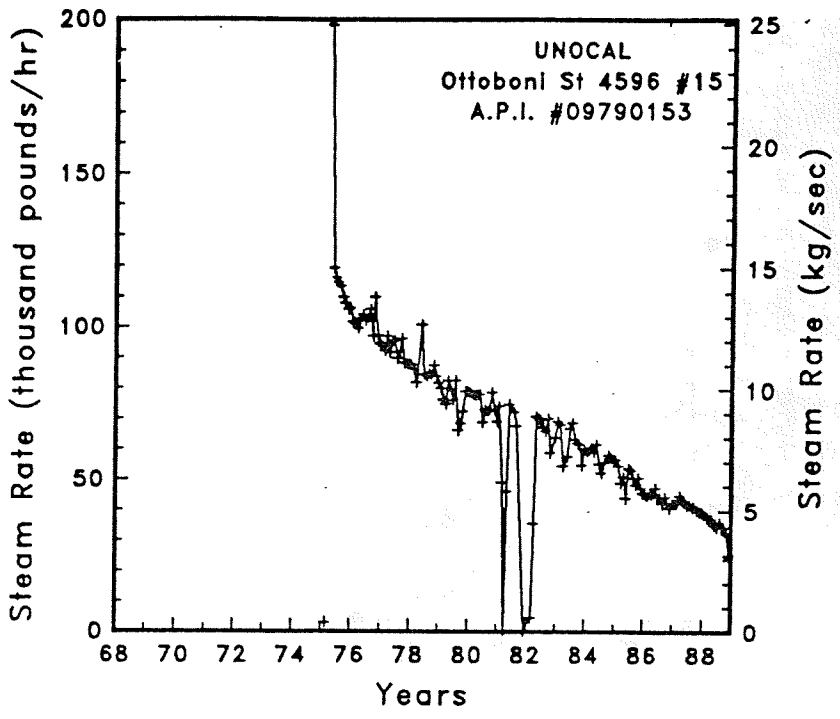

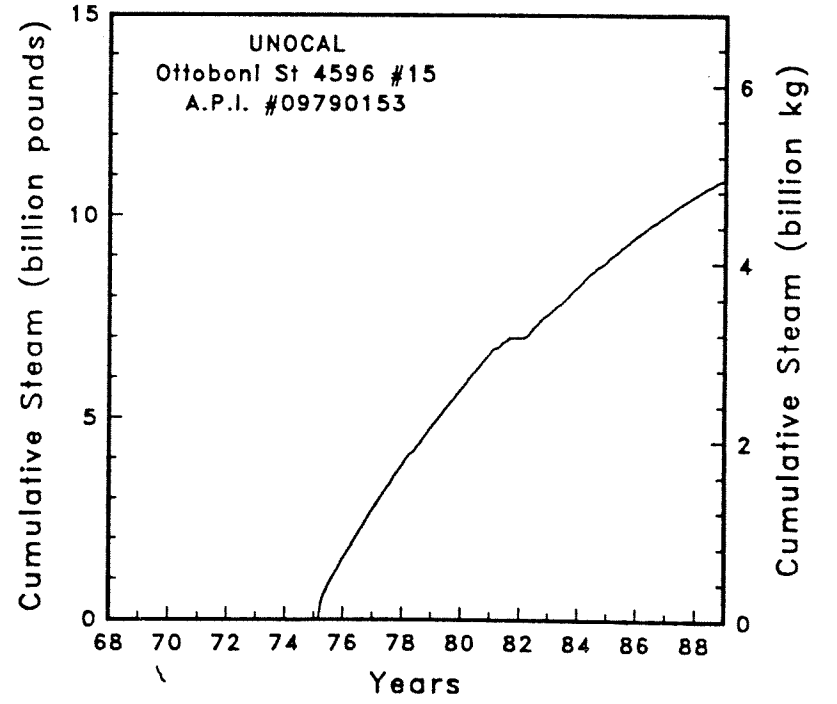

Figure A-173 Steam rate and cumulative mass flow for well Ottoboni St 4596 #15

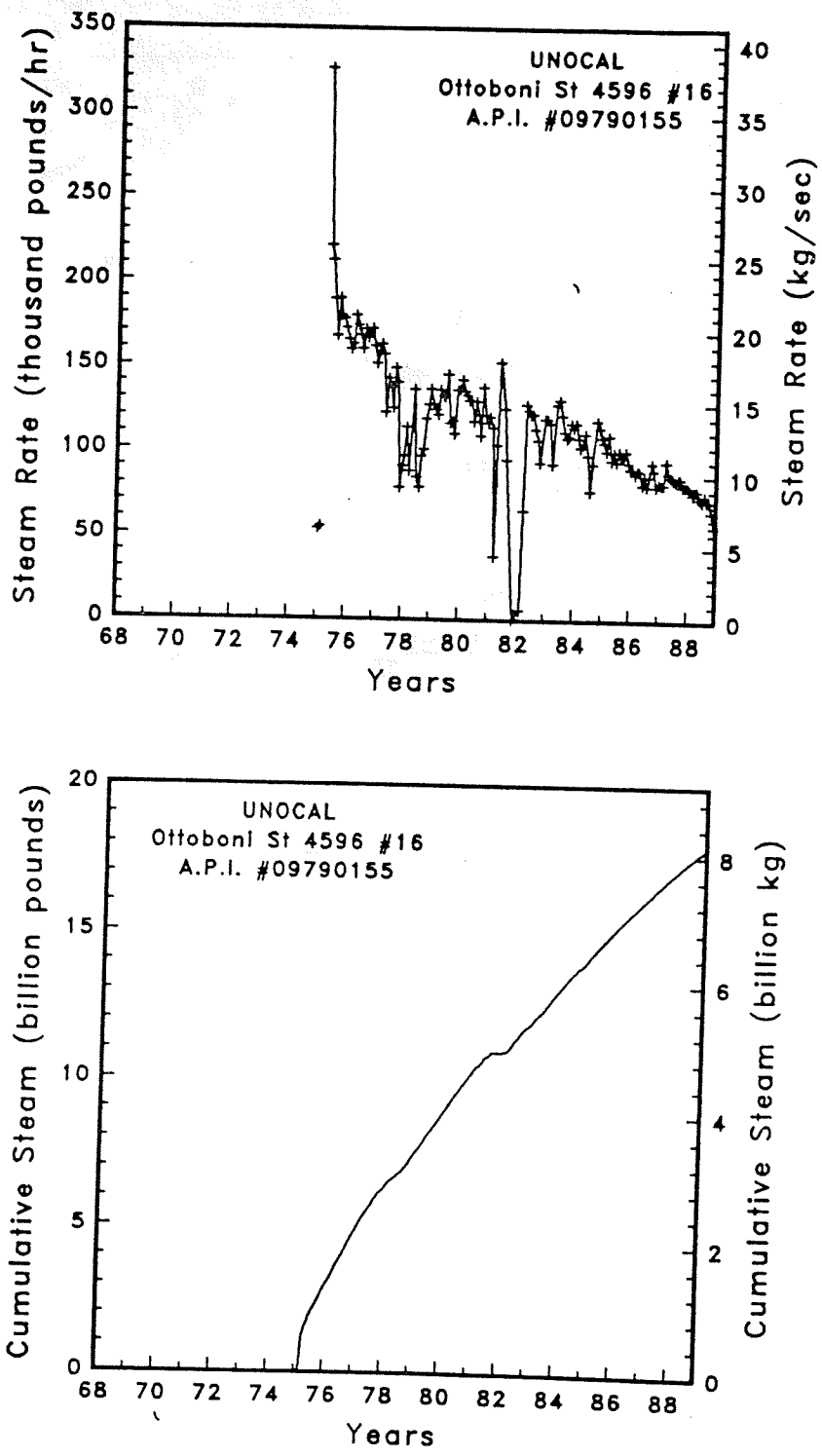

Figure A-174 Steam rate and cumulative mass flow for well Ottoboni St 4596 #16

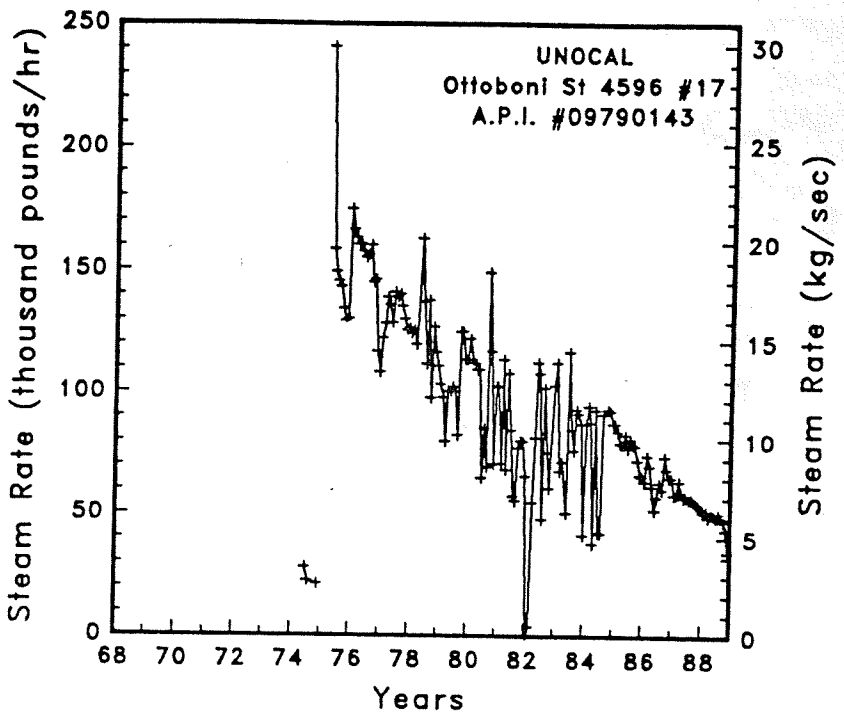

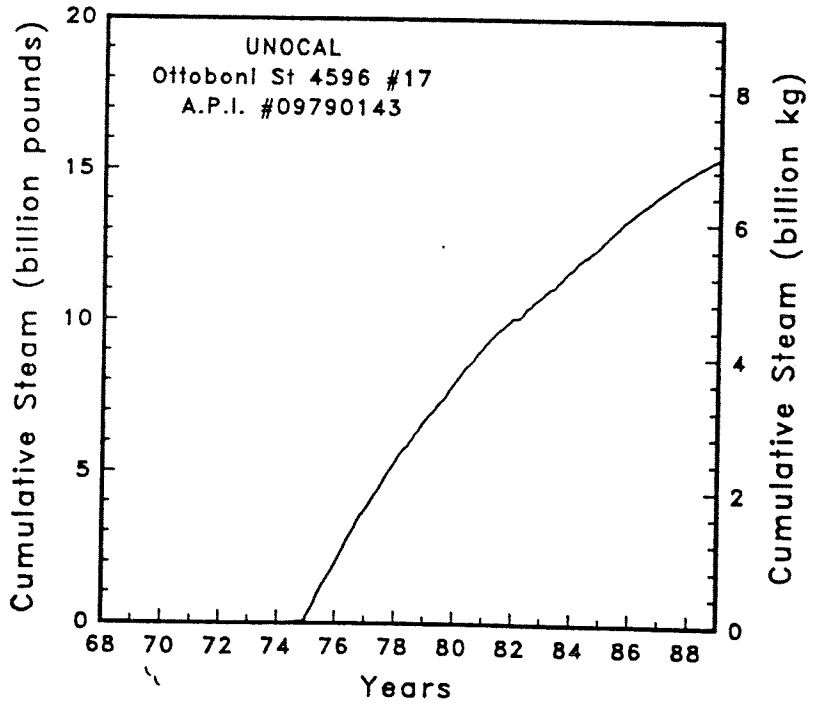

Figure A-175 Steam rate and cumulative mass flow for well Ottoboni St 4596 #17

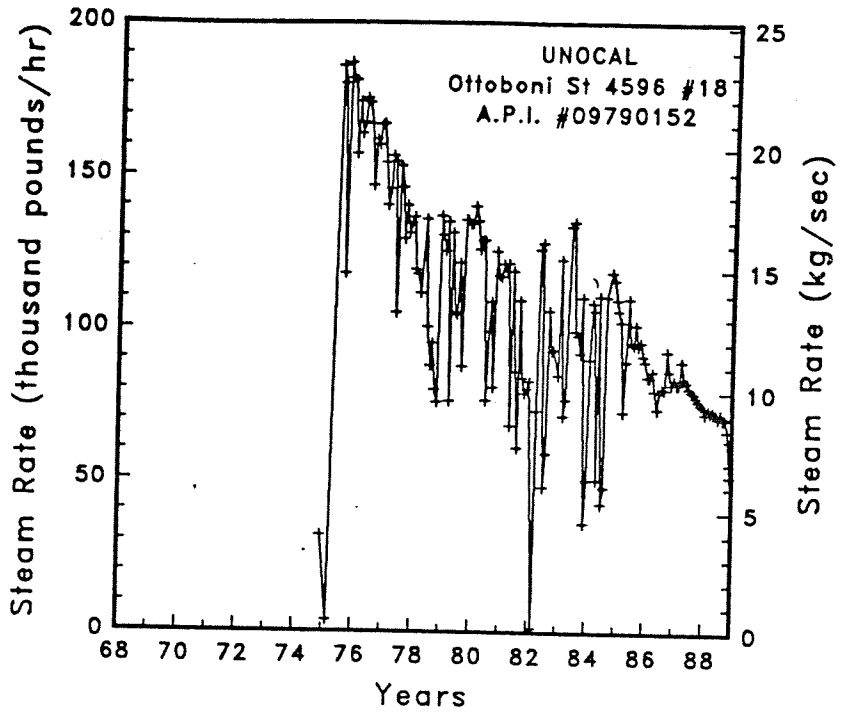

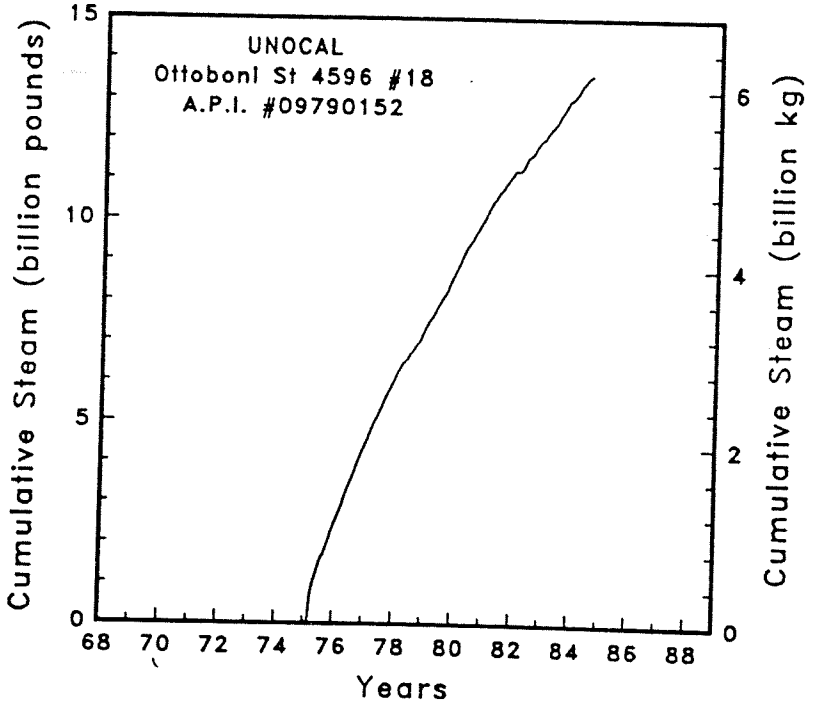

Figure A-176 Steam rate and cumulative mass flow for well Ottoboni St 4596 #18

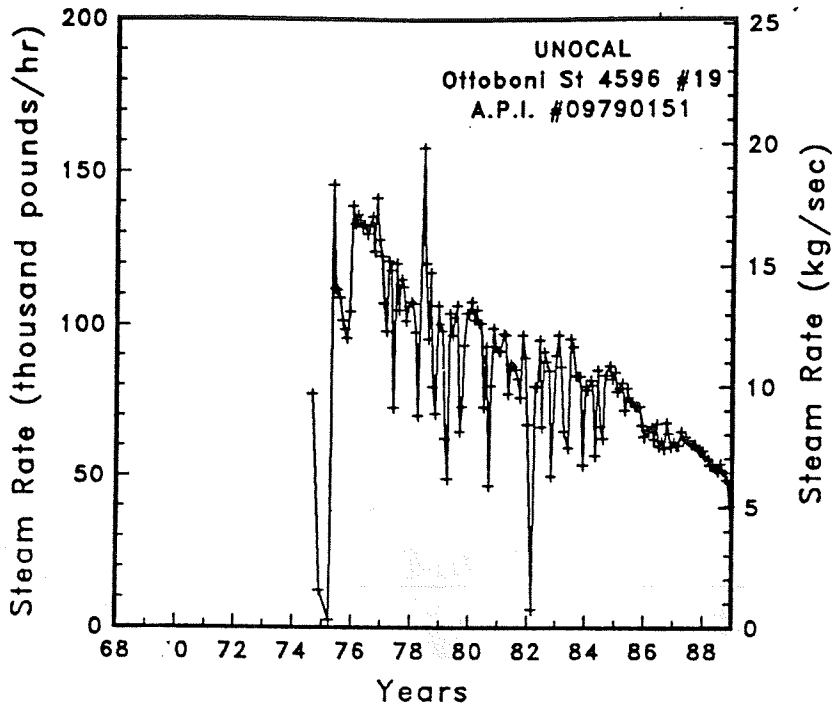

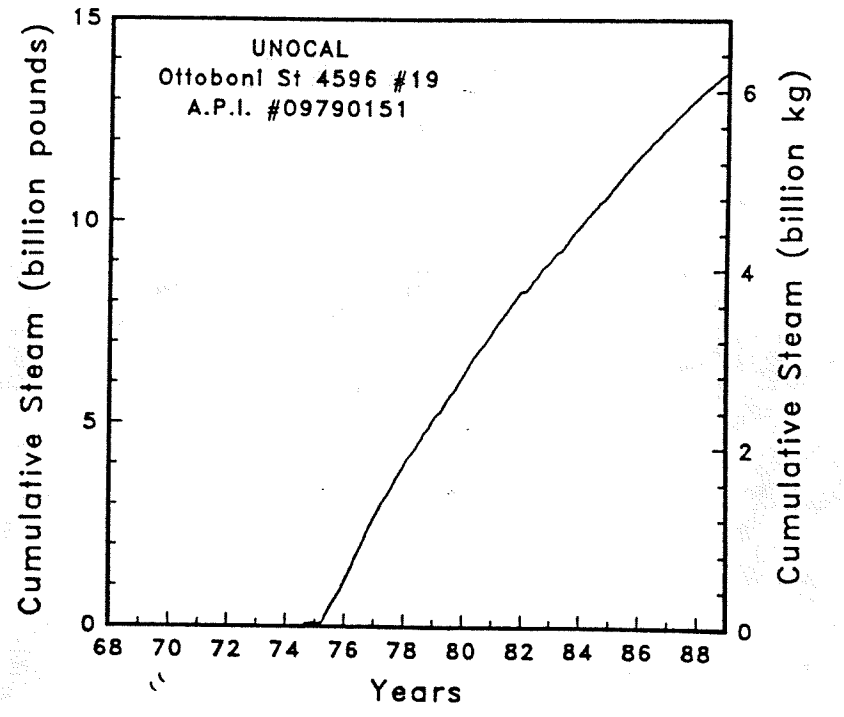

Figure A-177 Steam rate and cumulative mass flow for well Ottoboni St 4596 #19

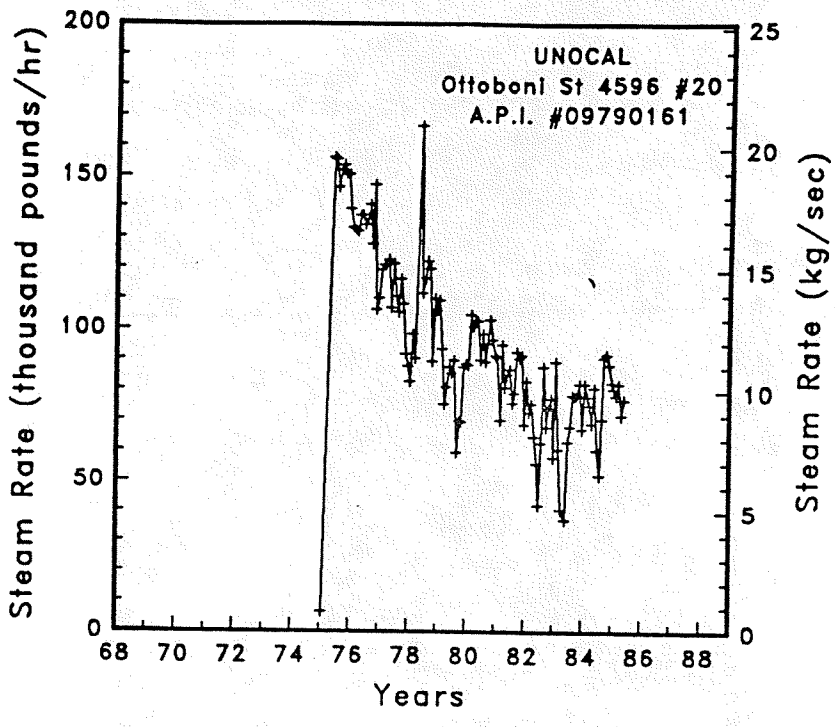

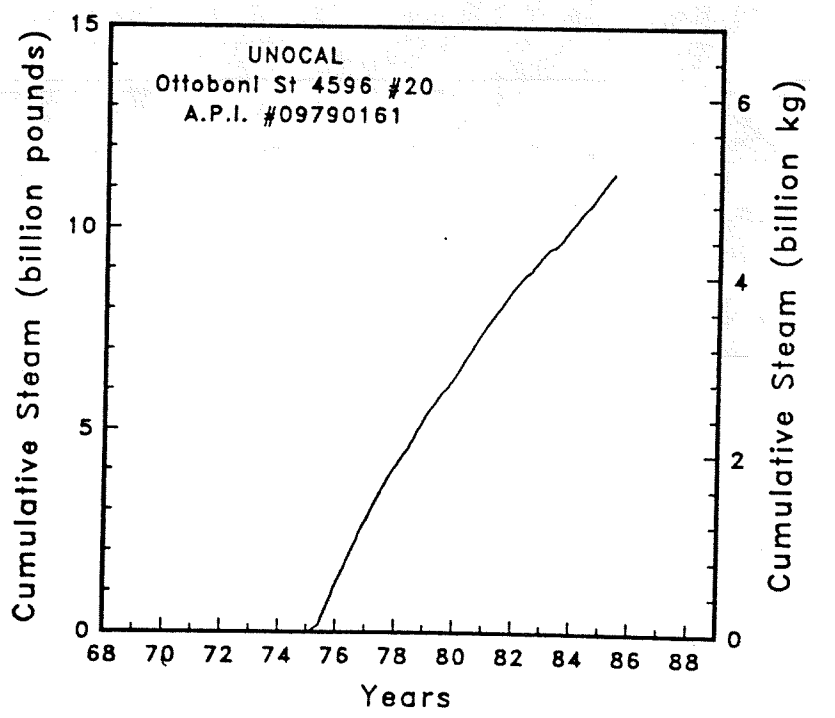

Figure A-178 Steam rate and cumulative mass flow for well Ottoboni St 4596 #20

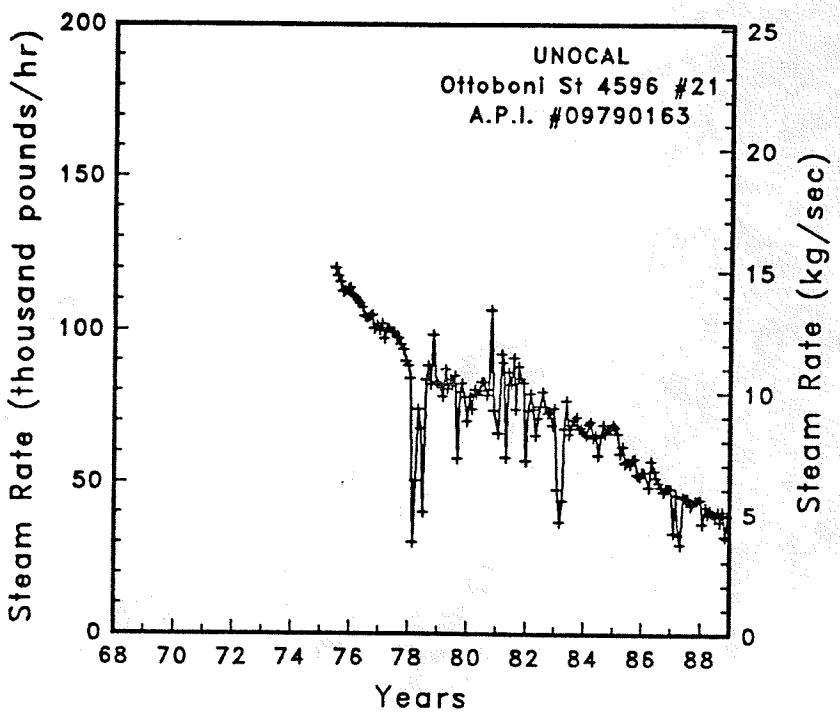

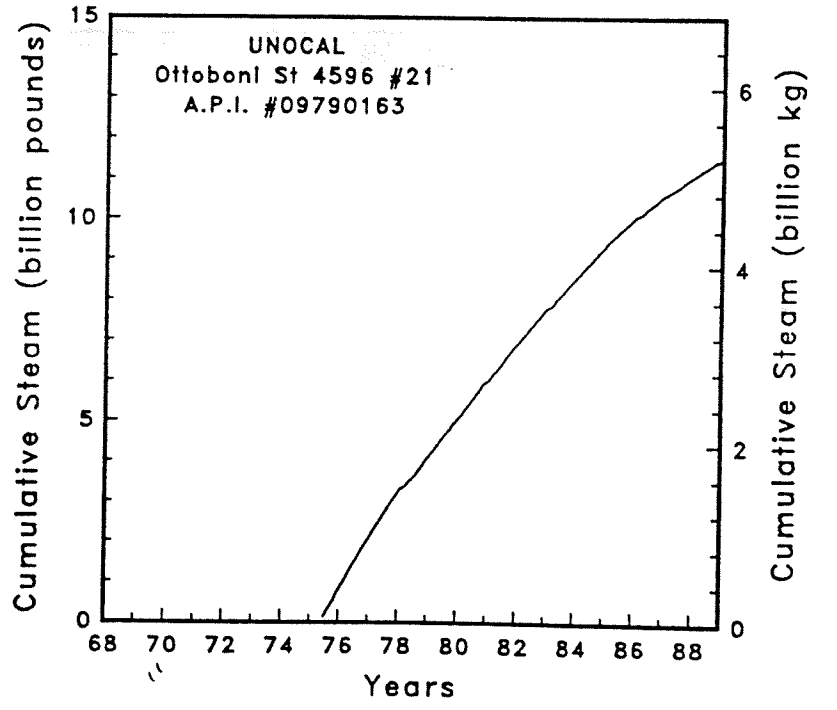

Figure A-179 Steam rate and cumulative mass flow for well Ottoboni St 4596 #21

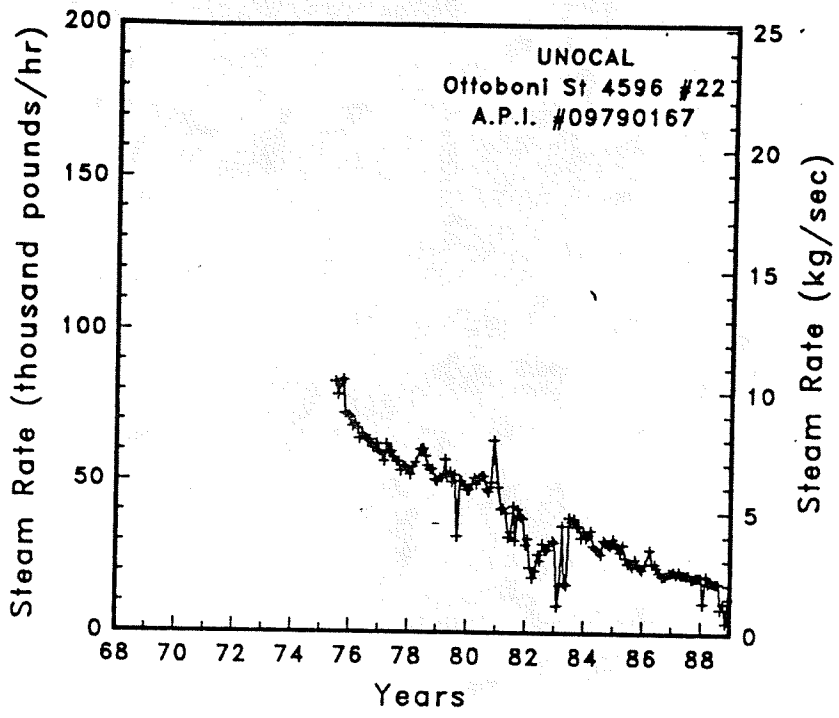

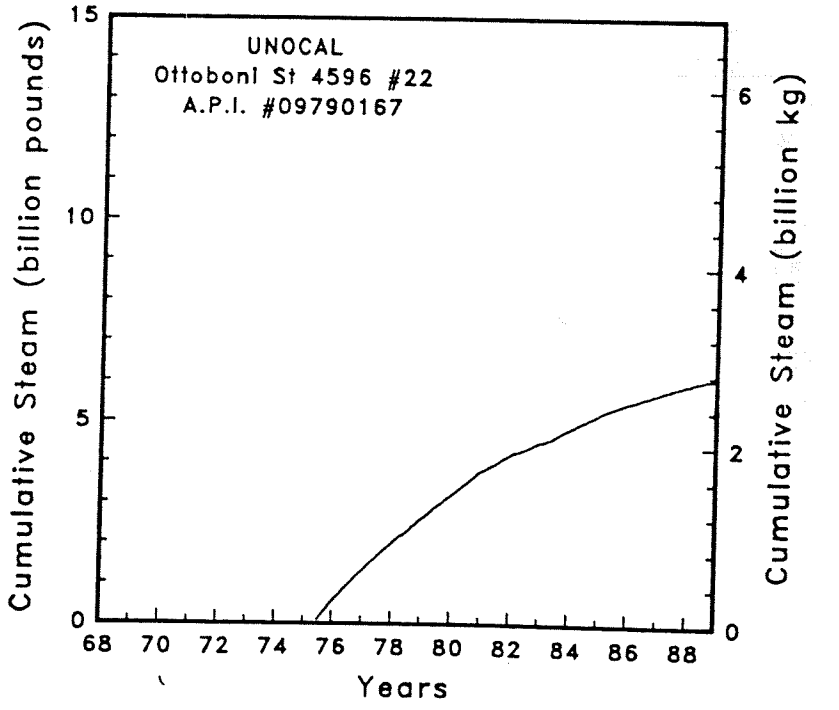

Figure A-180 Steam rate and cumulative mass flow for well Ottoboni St 4596 #22

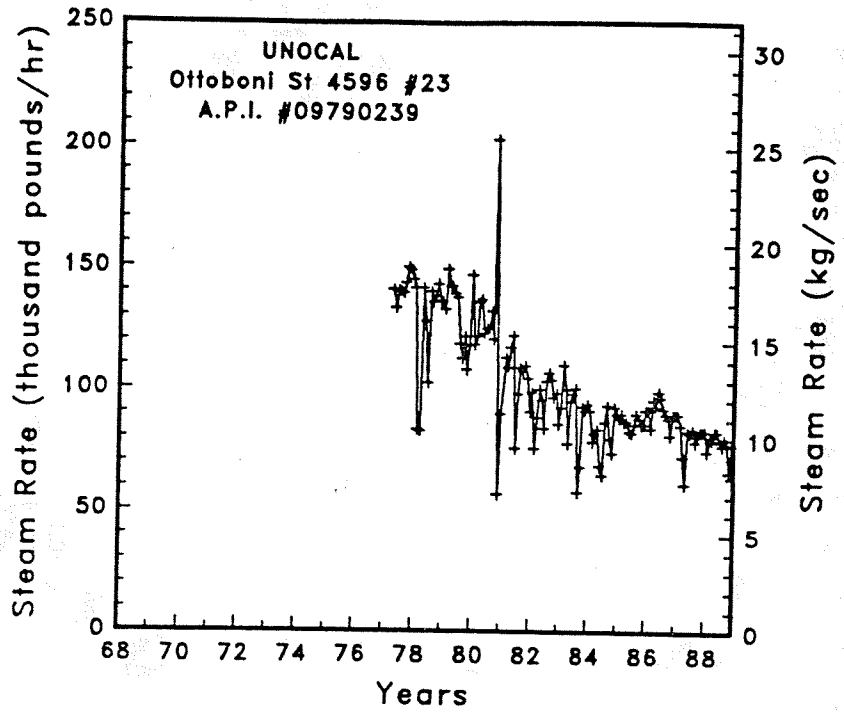

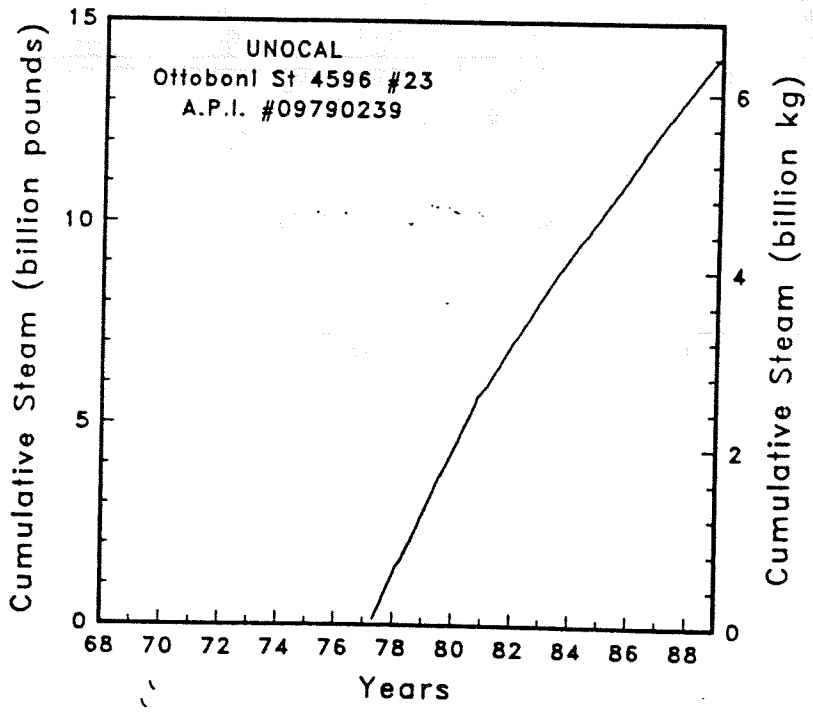

Figure A-181 Steam rate and cumulative mass flow for well Ottoboni St 4596 #23

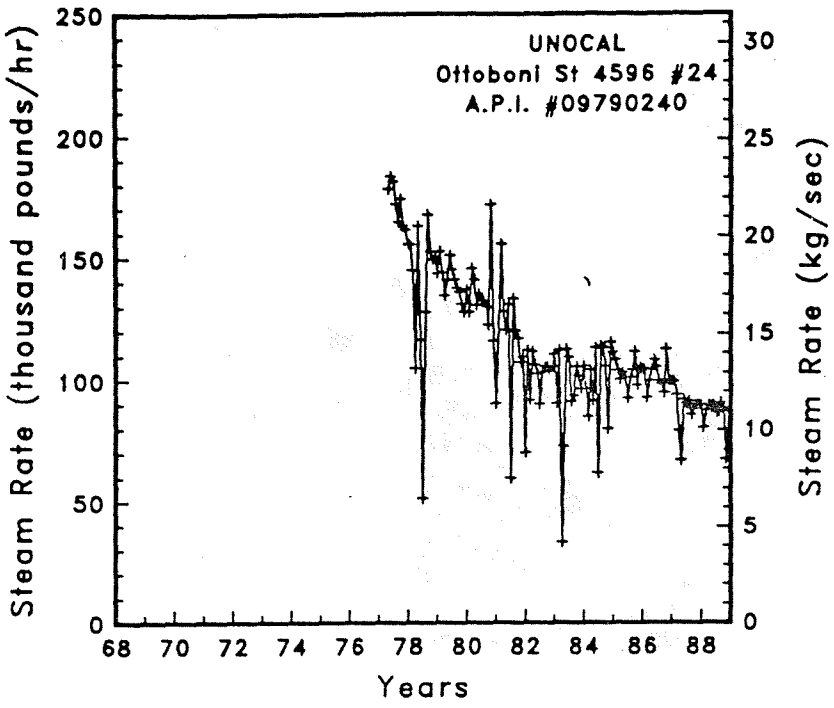

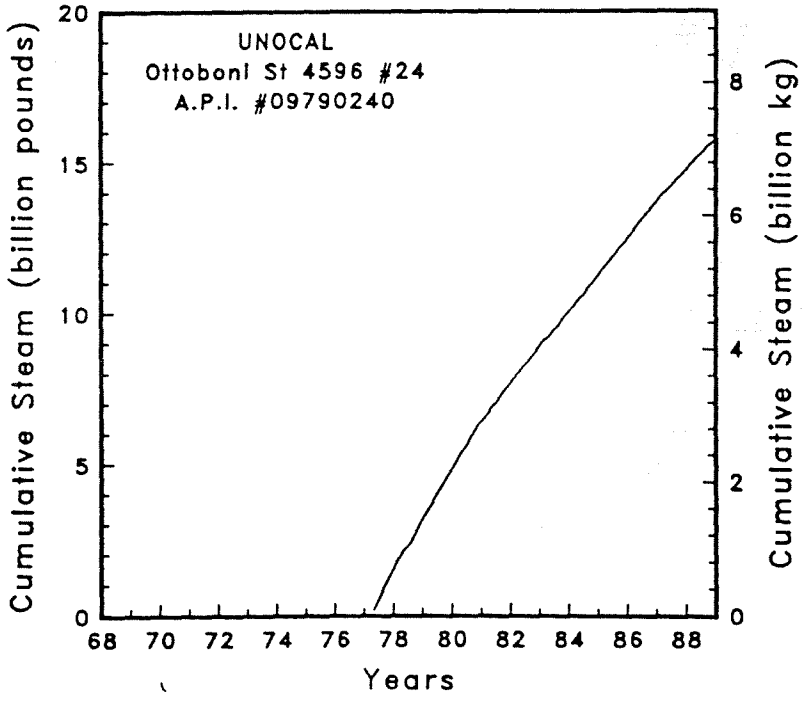

Figure A-182 Steam rate and cumulative mass flow for well Ottoboni St 4596 #24

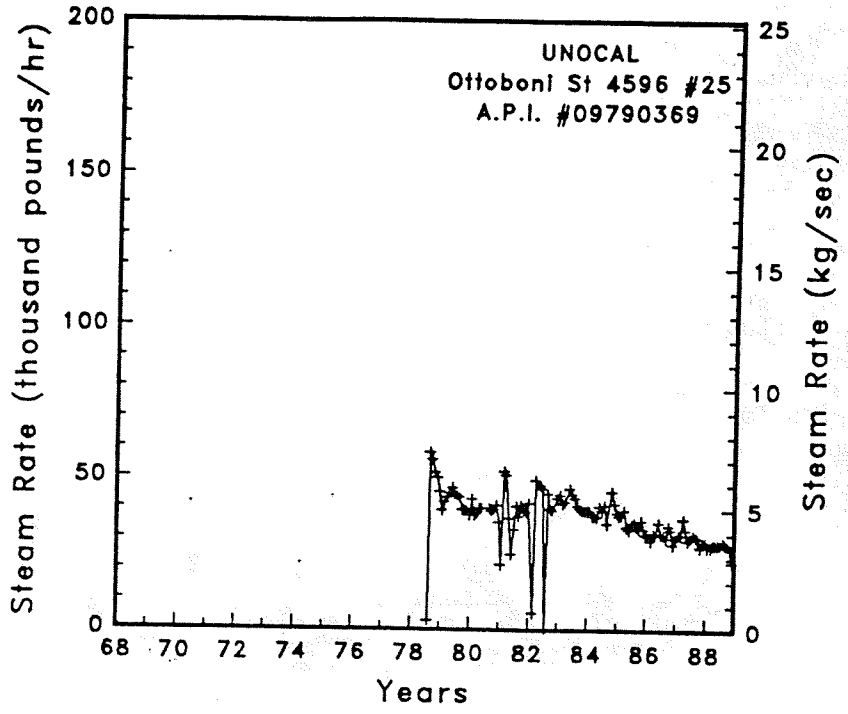

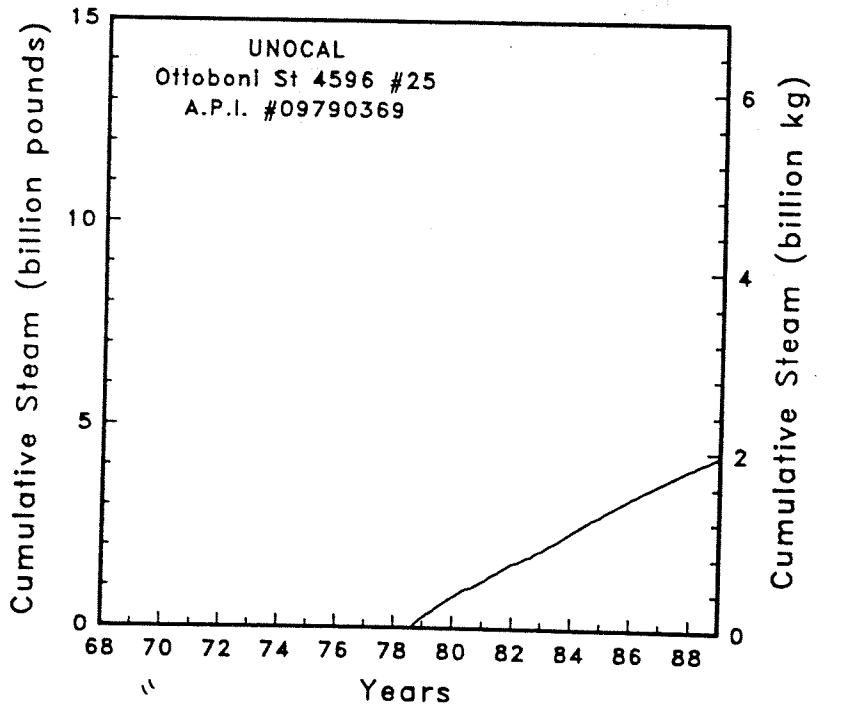

Figure A-183 Steam rate and cumulative mass flow for well Ottoboni St 4596 #25

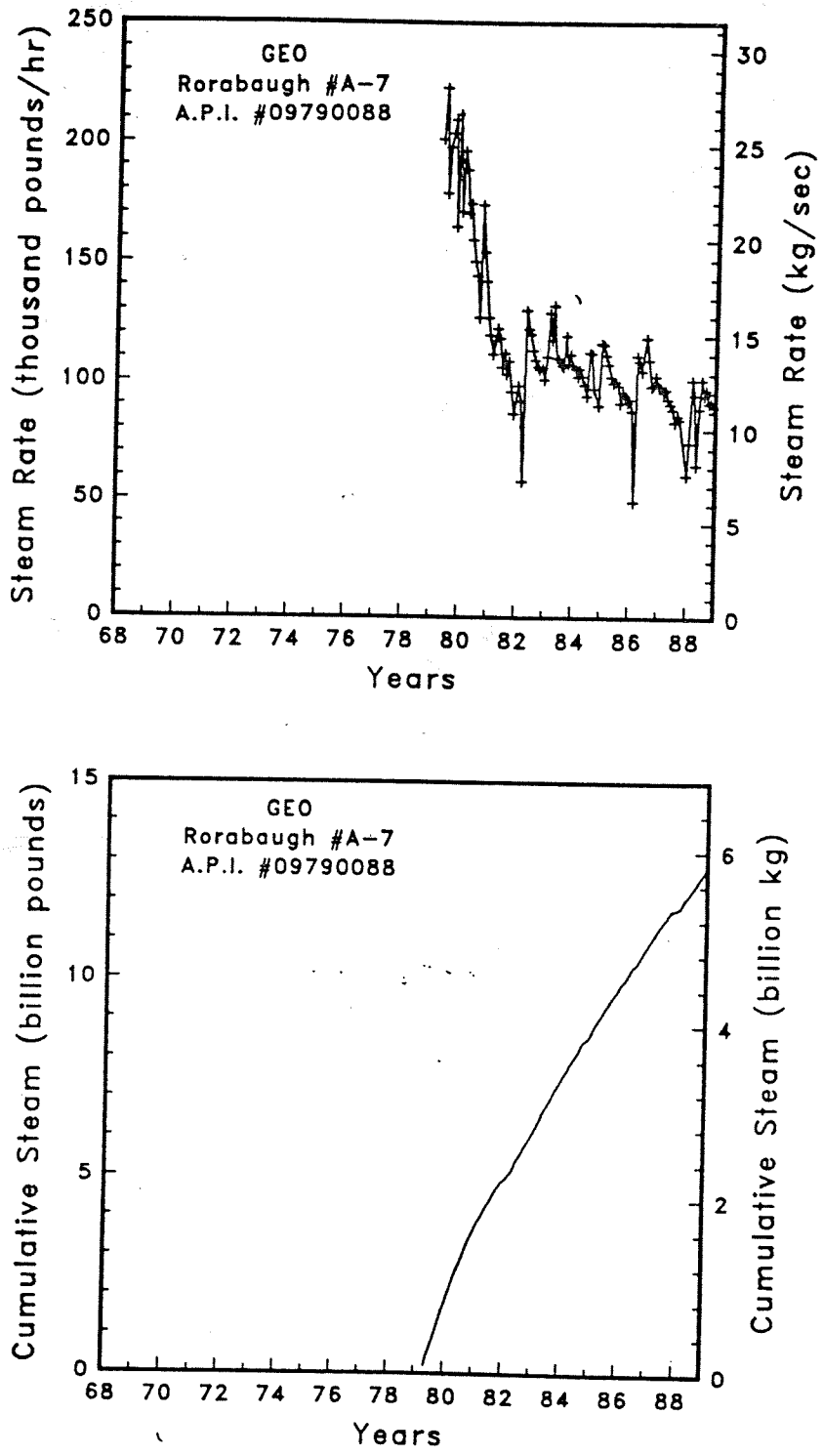

Figure A-184 Steam rate and cumulative mass flow for well Rorabaugh #A-7

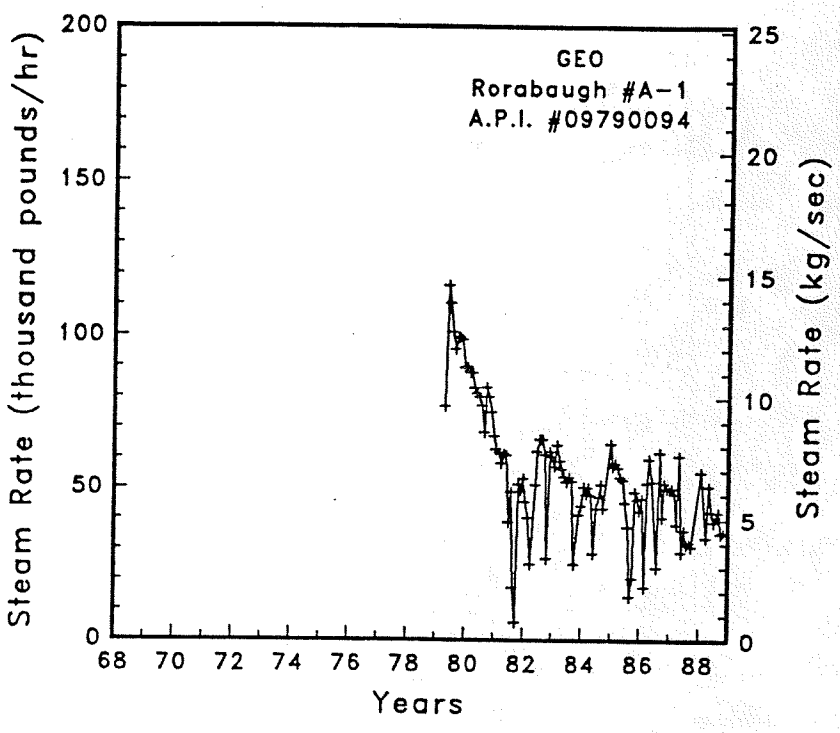

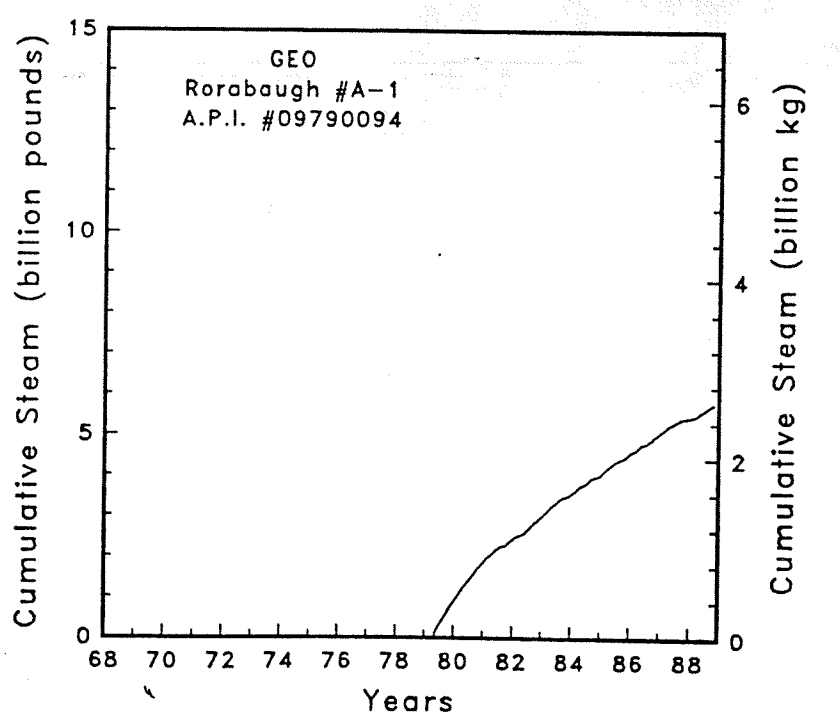

Figure A-185 Steam rate and cumulative mass flow for well Rorabaugh #A-1

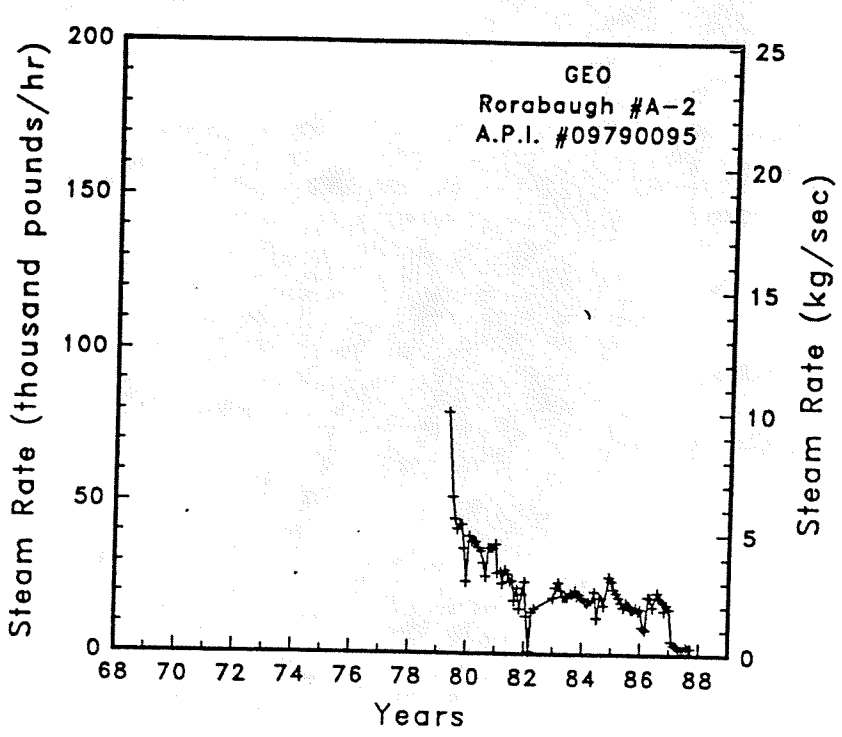

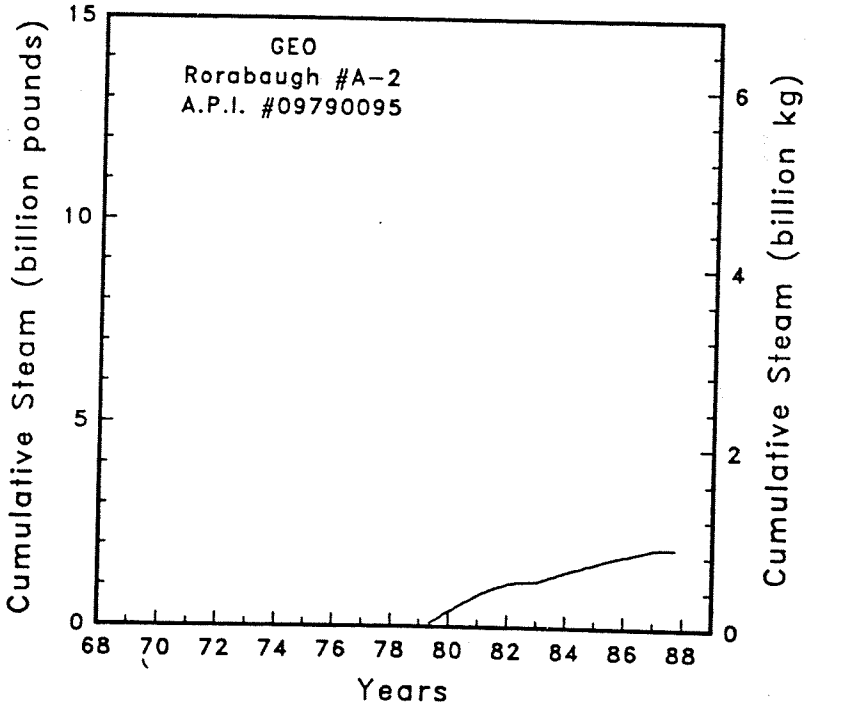

Figure A-186 Steam rate and cumulative mass flow for well Rorabaugh #A-2

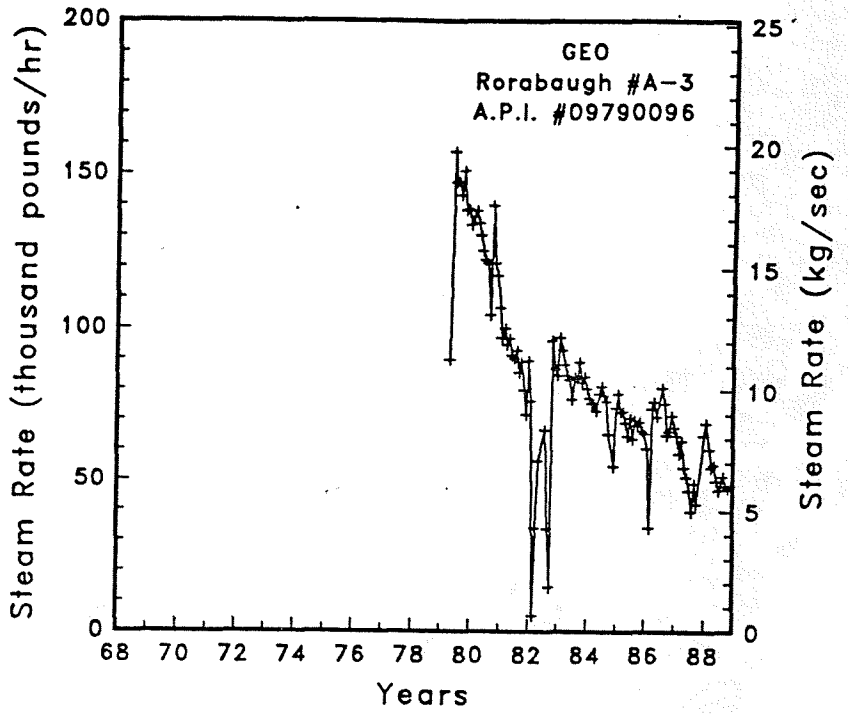

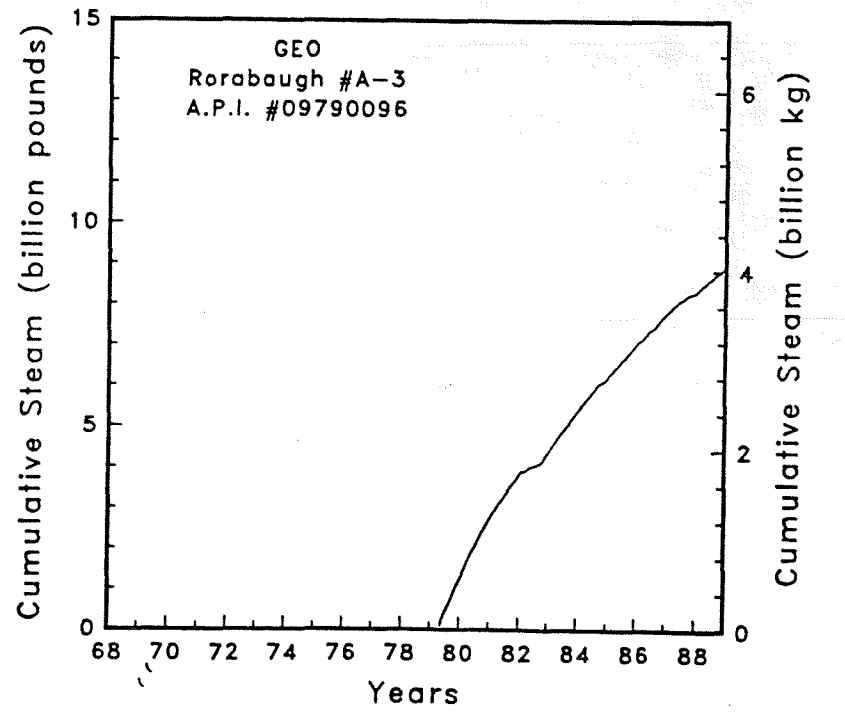

Figure A-187 Steam rate and cumulative mass flow for well Rorabaugh #A-3

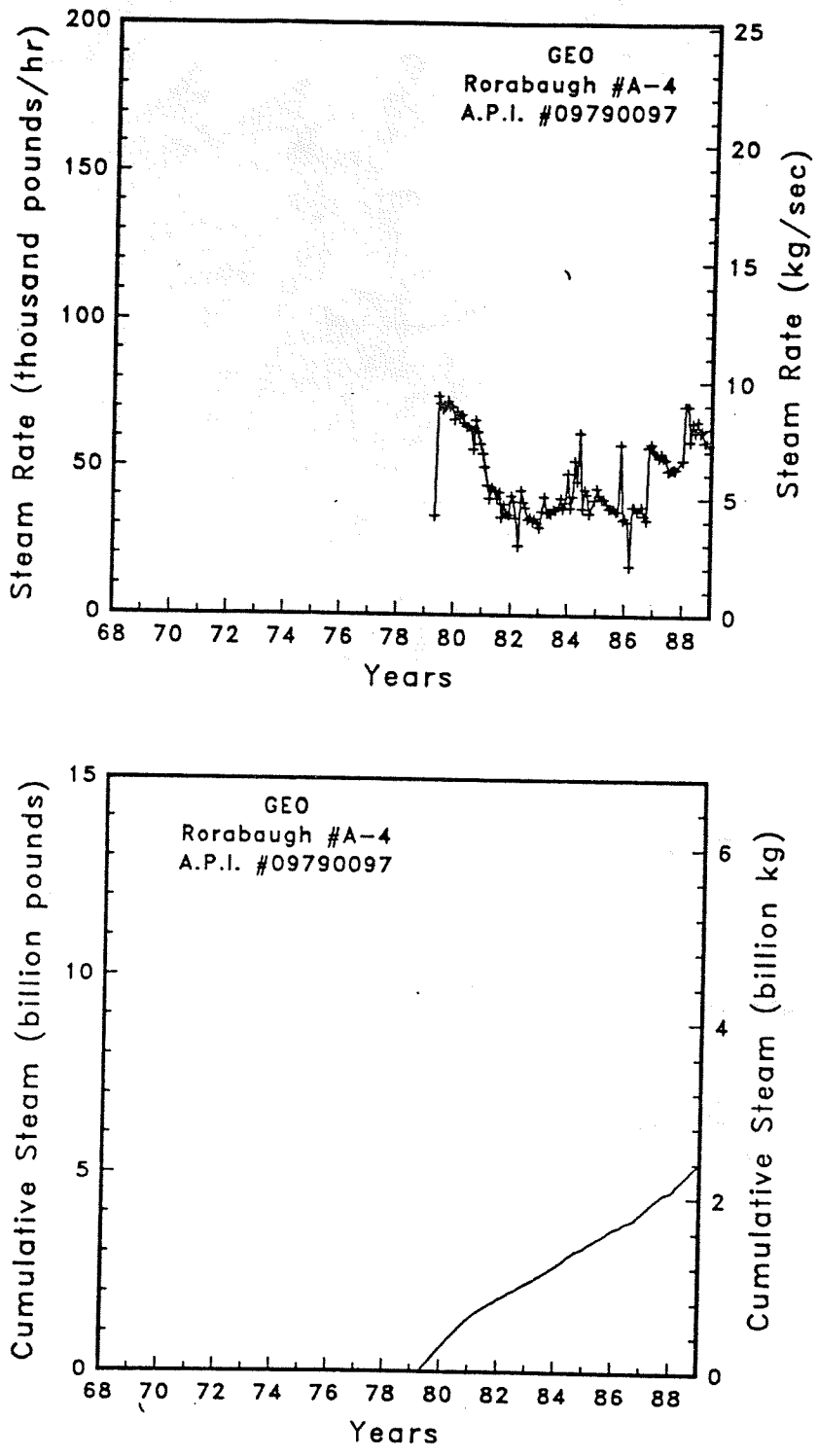

Figure A-188 Steam rate and cumulative mass flow for well Rorabaugh #A-4

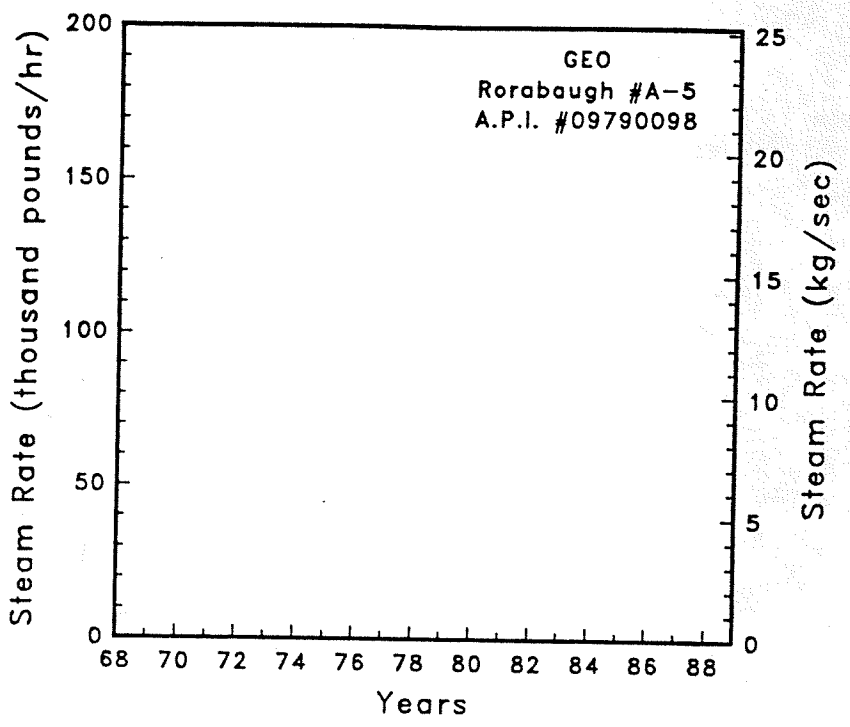

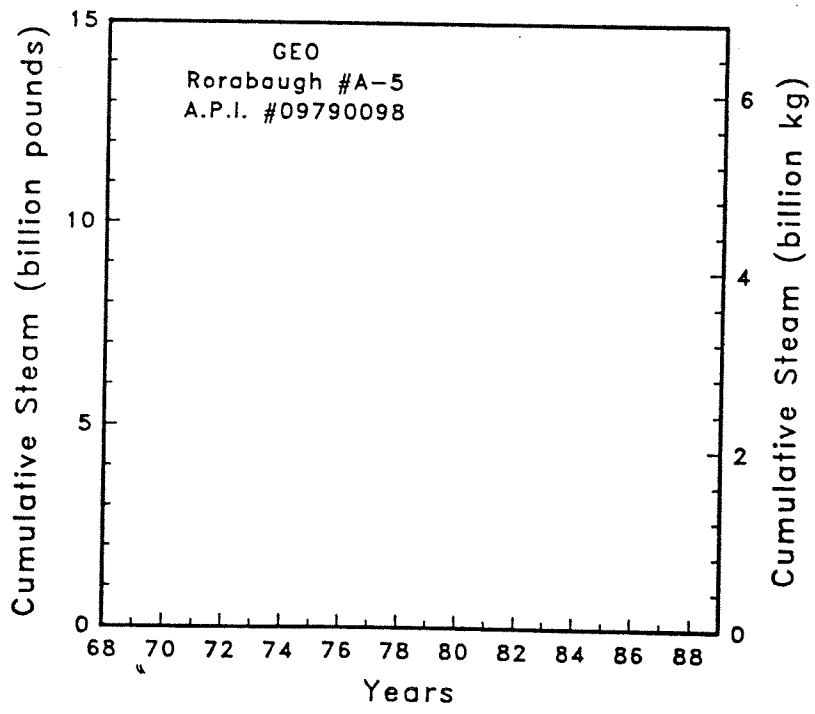

Figure A-189 Steam rate and cumulative mass flow for well Rorabaugh #A-5

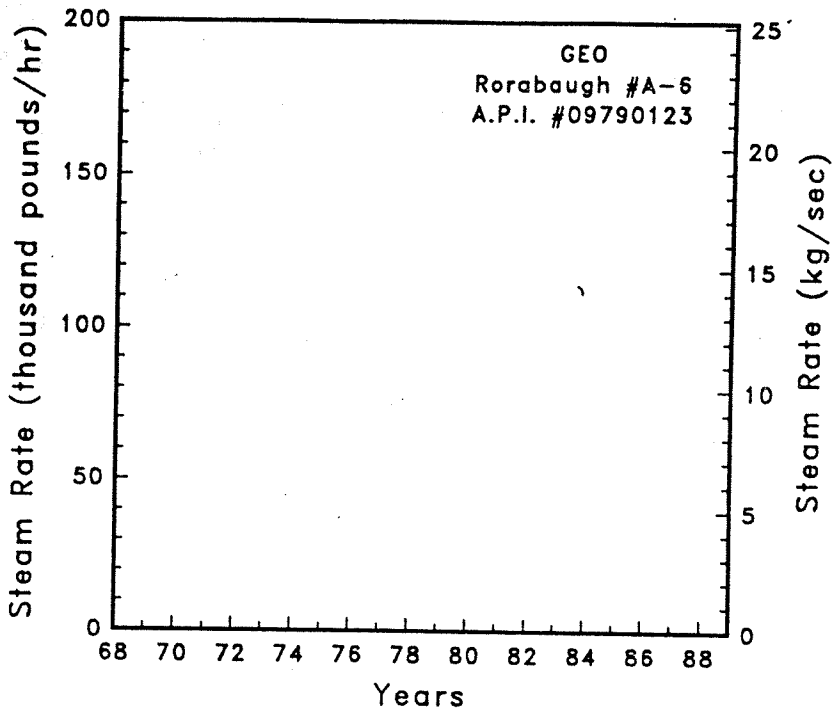

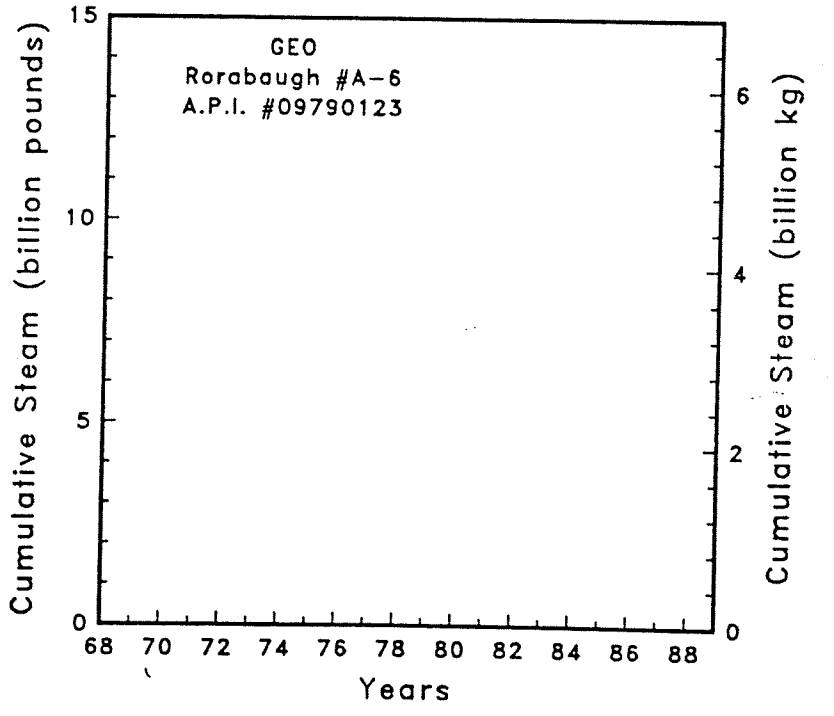

Figure A-190 Steam rate and cumulative mass flow for well Rorabaugh #A-6

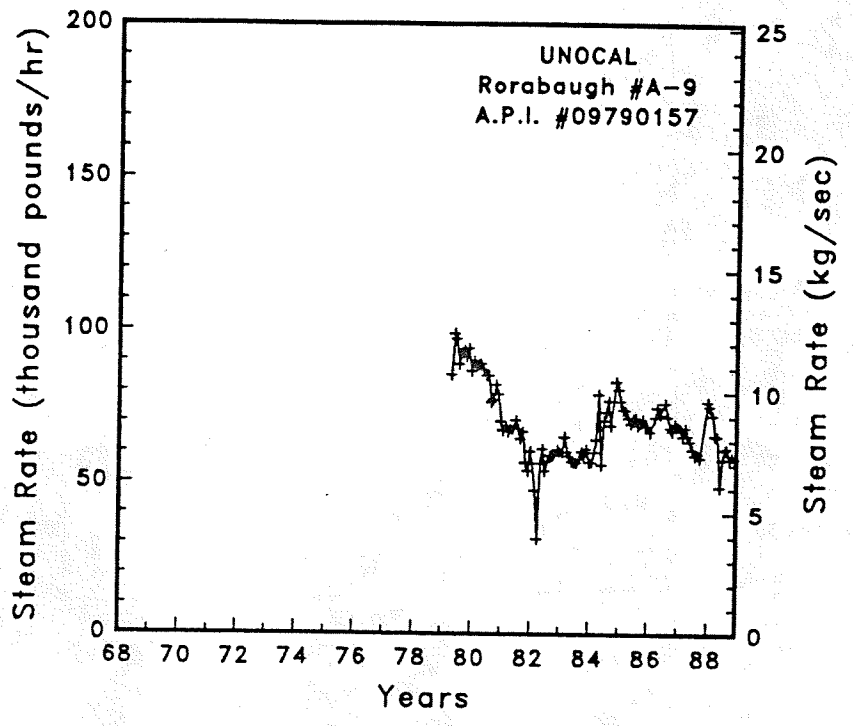

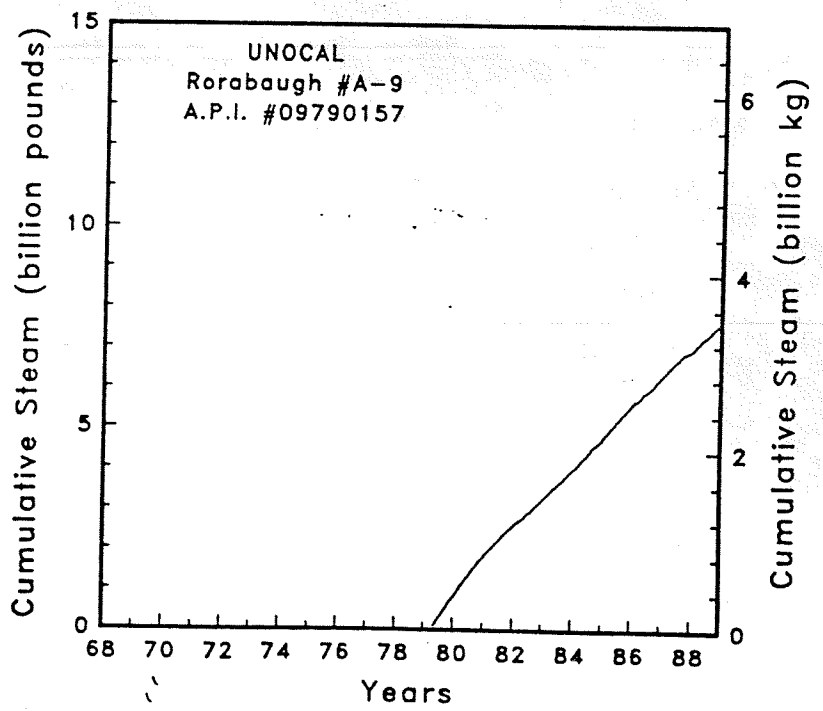

Figure A-191 Steam rate and cumulative mass flow for well Rorabaugh #A-9

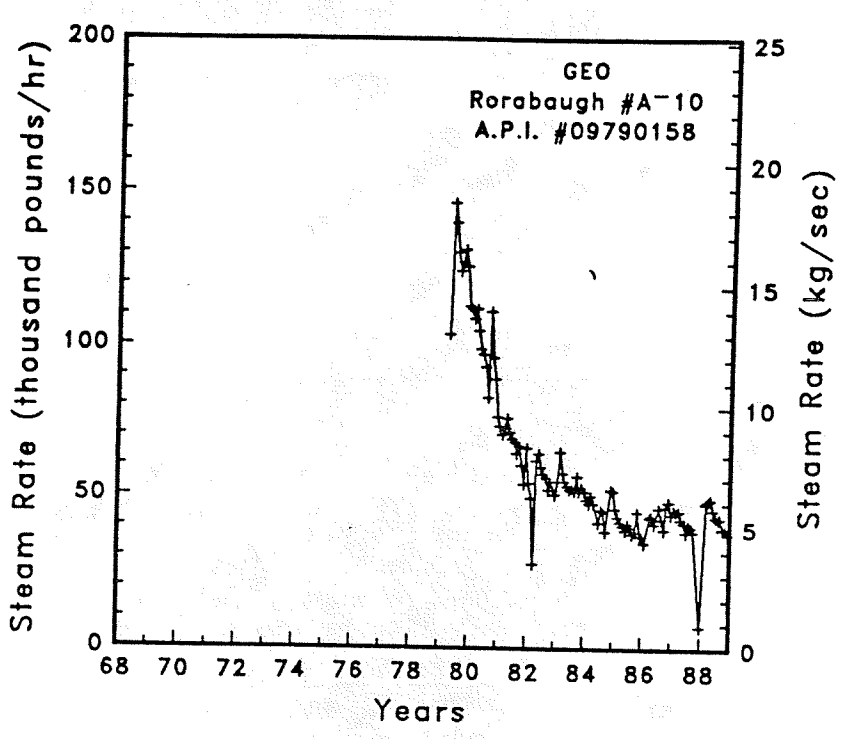

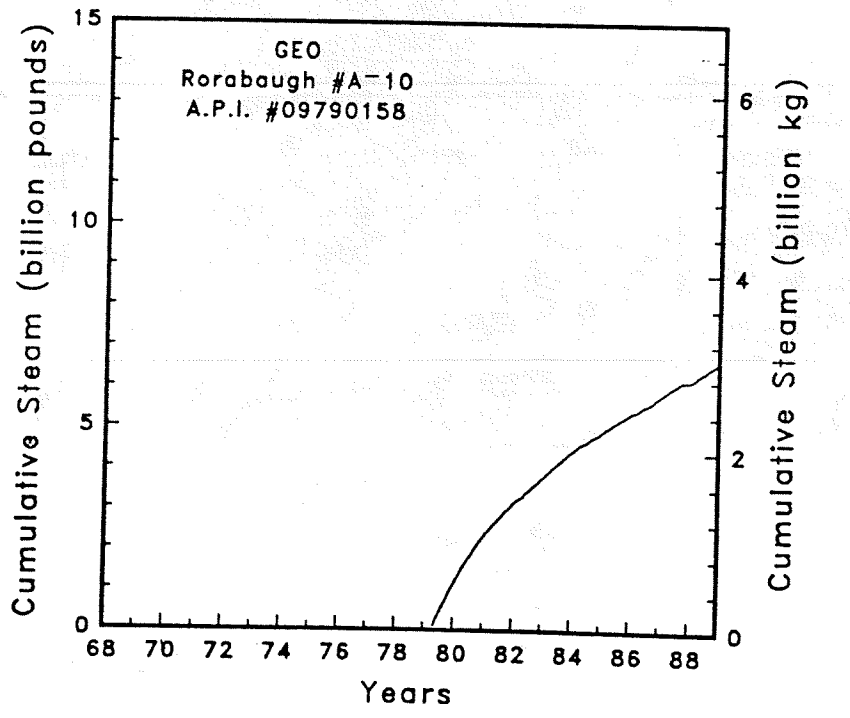

Figure A-192 Steam rate and cumulative mass flow for well Rorabaugh #A-10

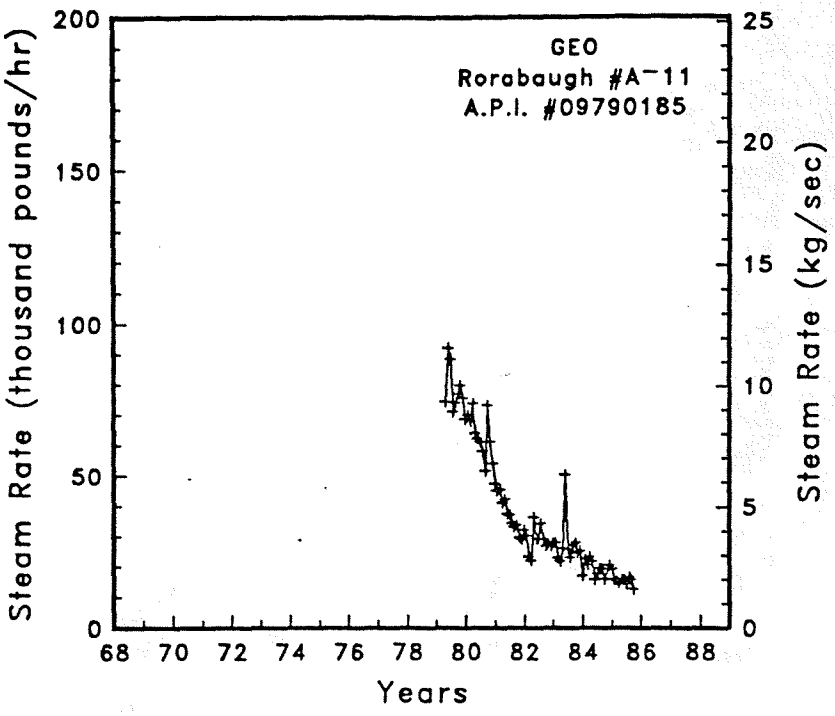

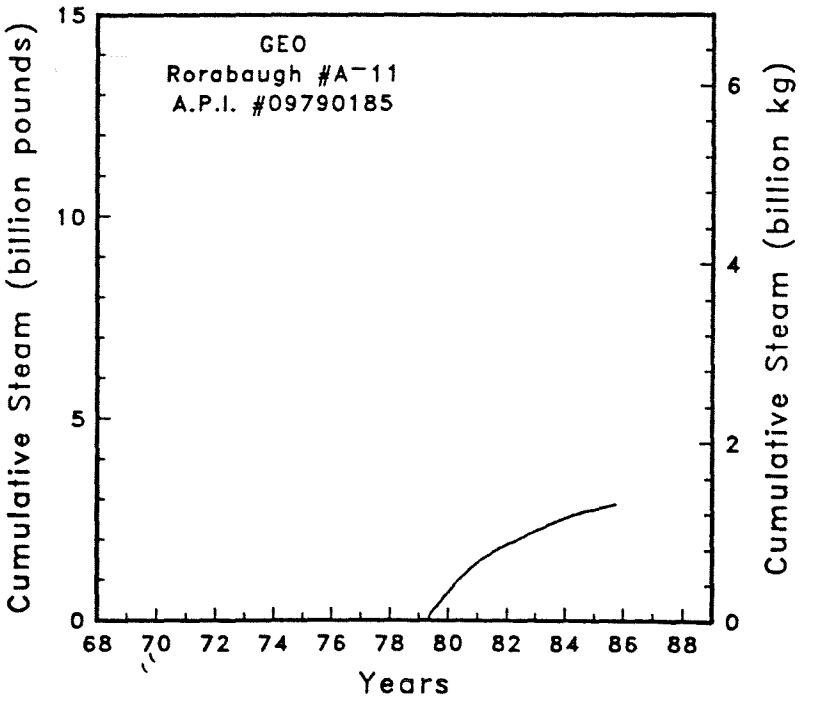

Figure A-193 Steam rate and cumulative mass flow for well Rorabaugh #A-11

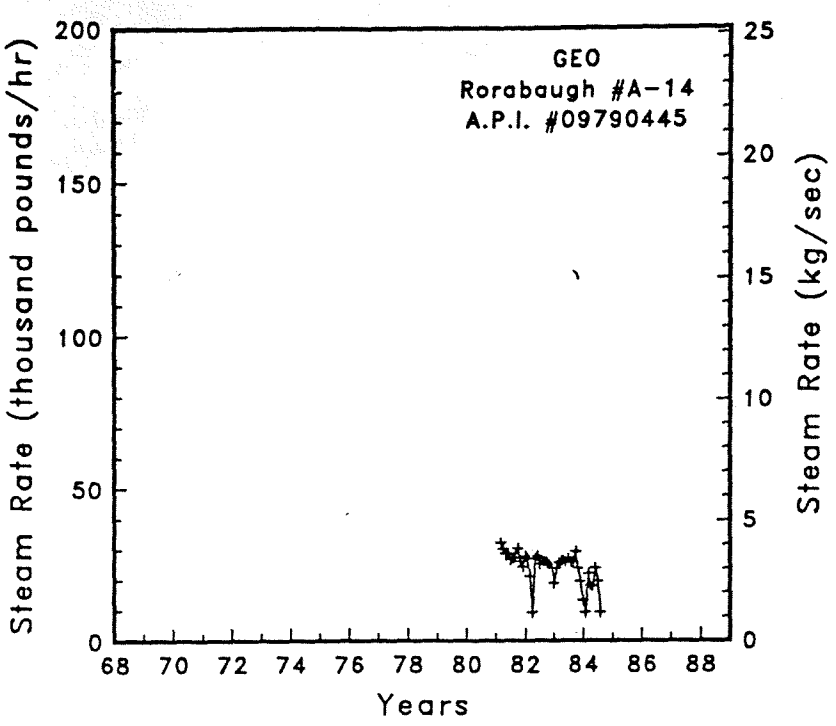

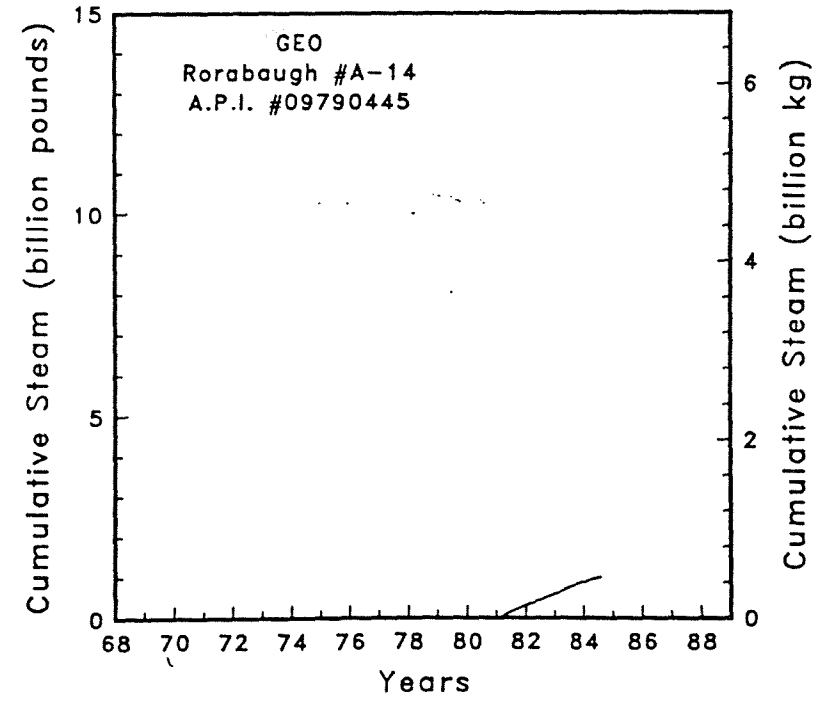

Figure A-194 Steam rate and cumulative mass flow for well Rorabaugh #A-14

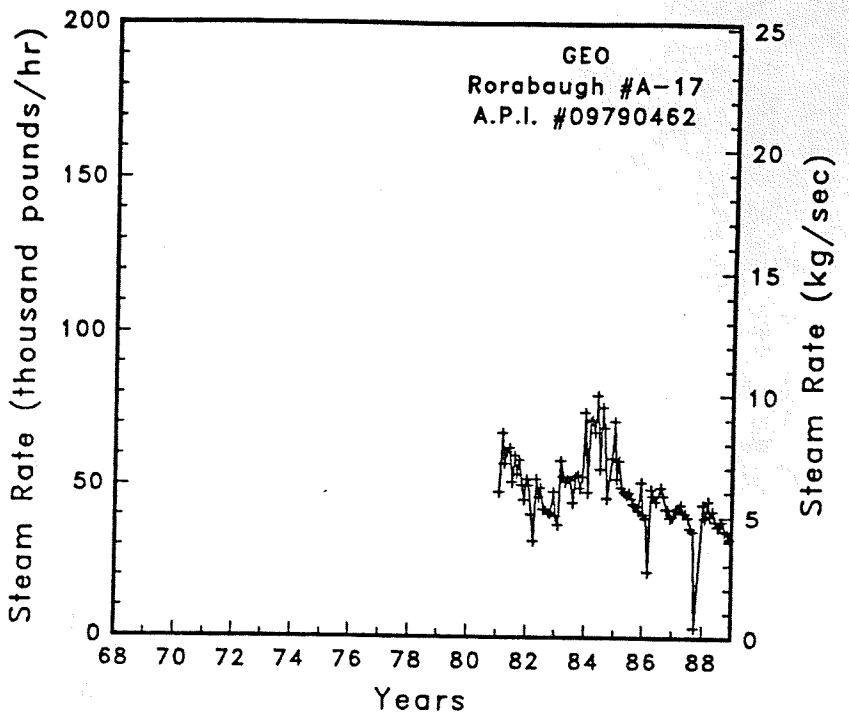

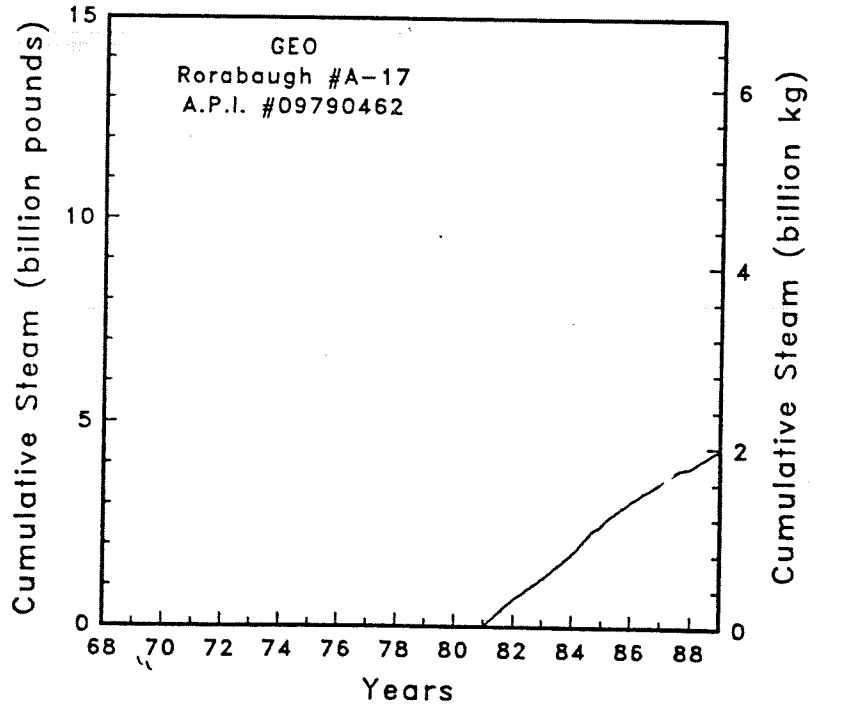

Figure A-195 Steam rate and cumulative mass flow for well Rorabaugh #A-17

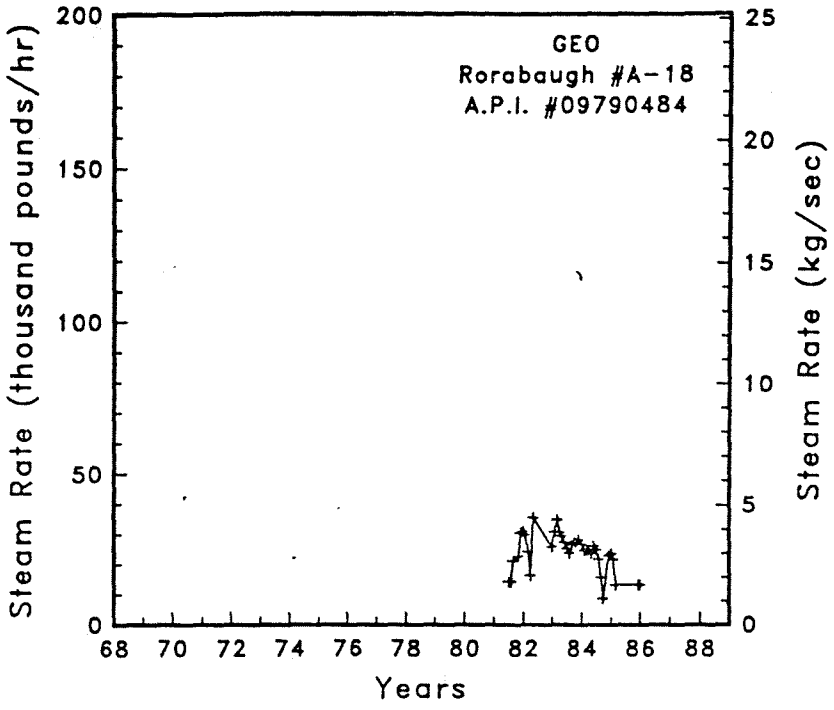

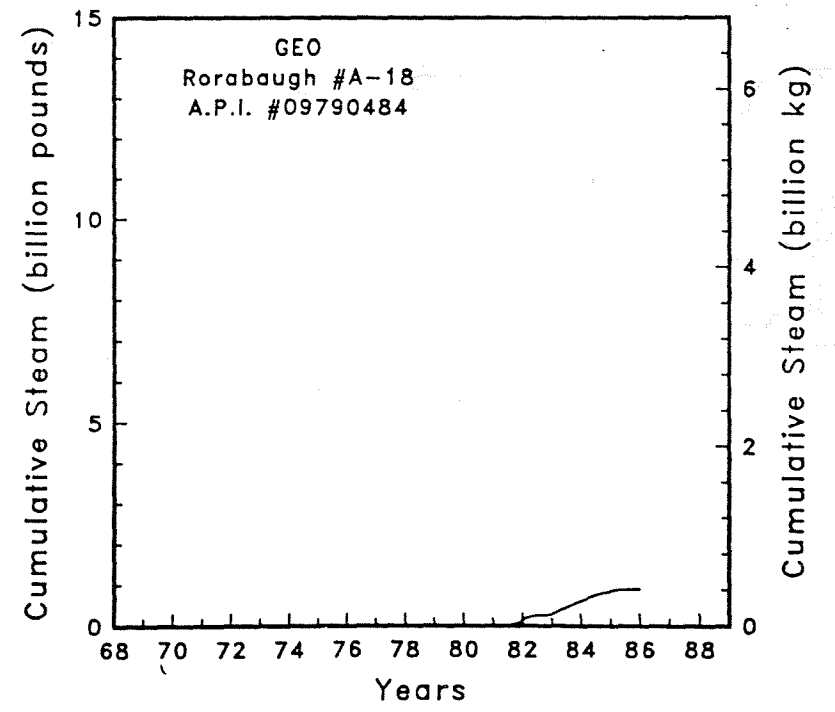

Figure A-196 Steam rate and cumulative mass flow for well Rorabaugh #A-18

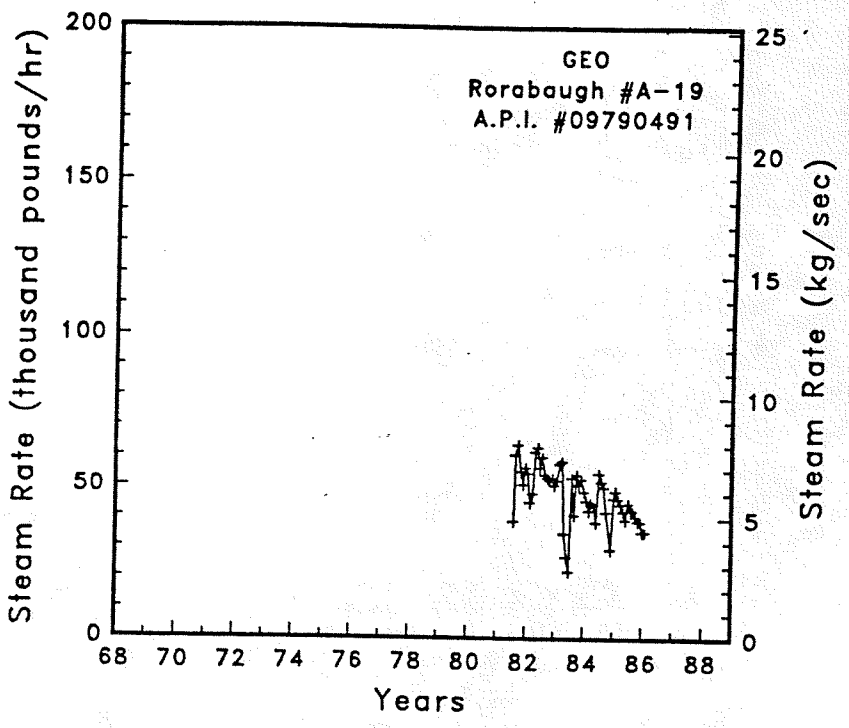

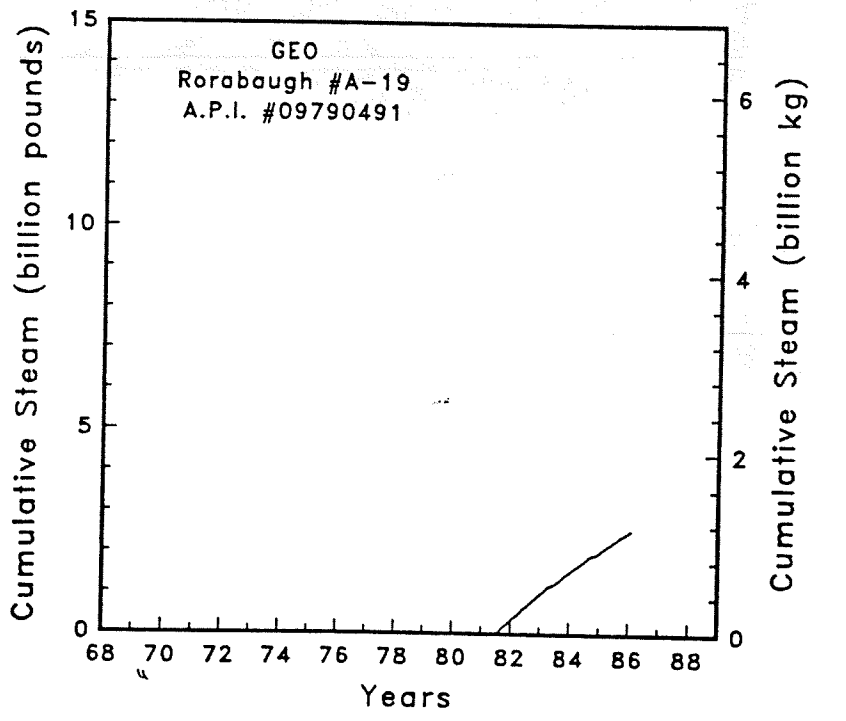

Figure A-197 Steam rate and cumulative mass flow for well Rorabaugh #A-19

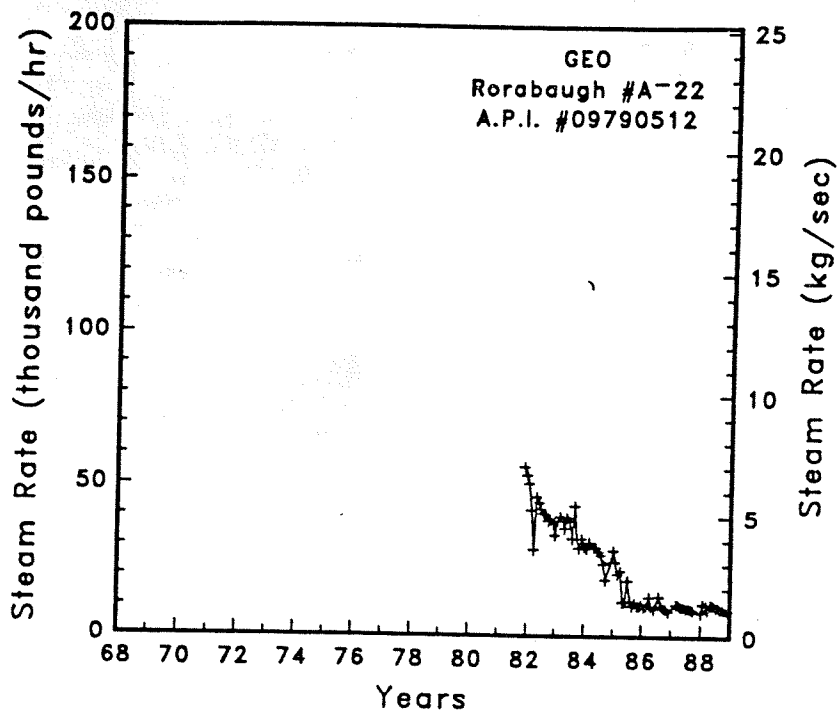

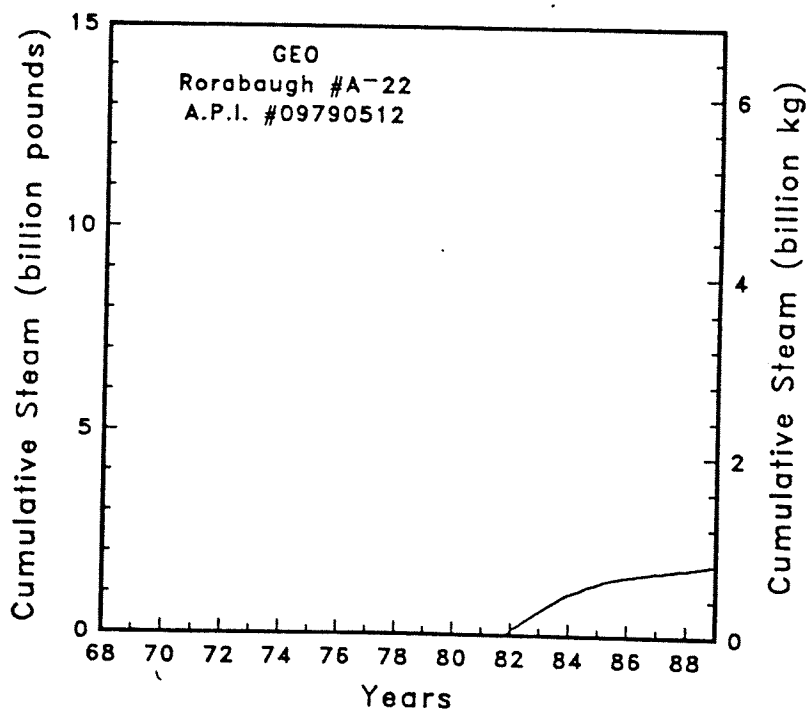

Figure A-198 Steam rate and cumulative mass flow for well Rorabaugh #A-22

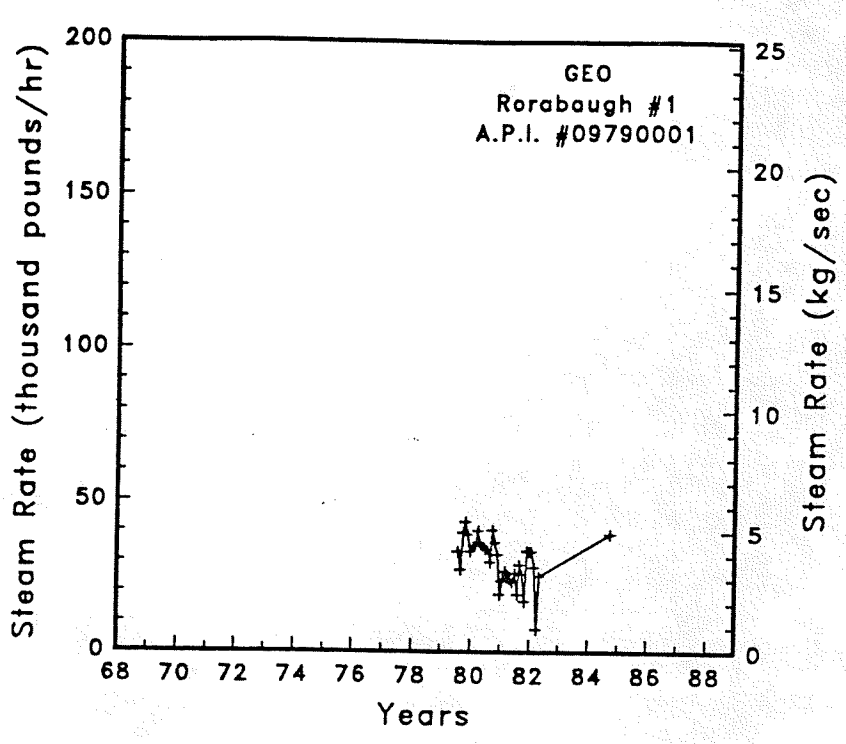

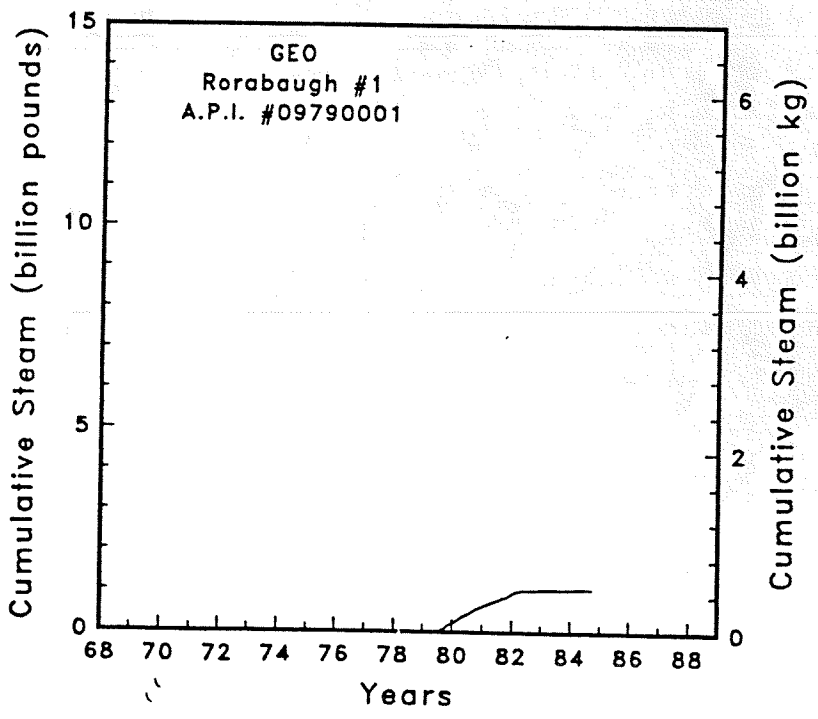

Figure A-199 Steam rate and cumulative mass flow for well Rorabaugh #1

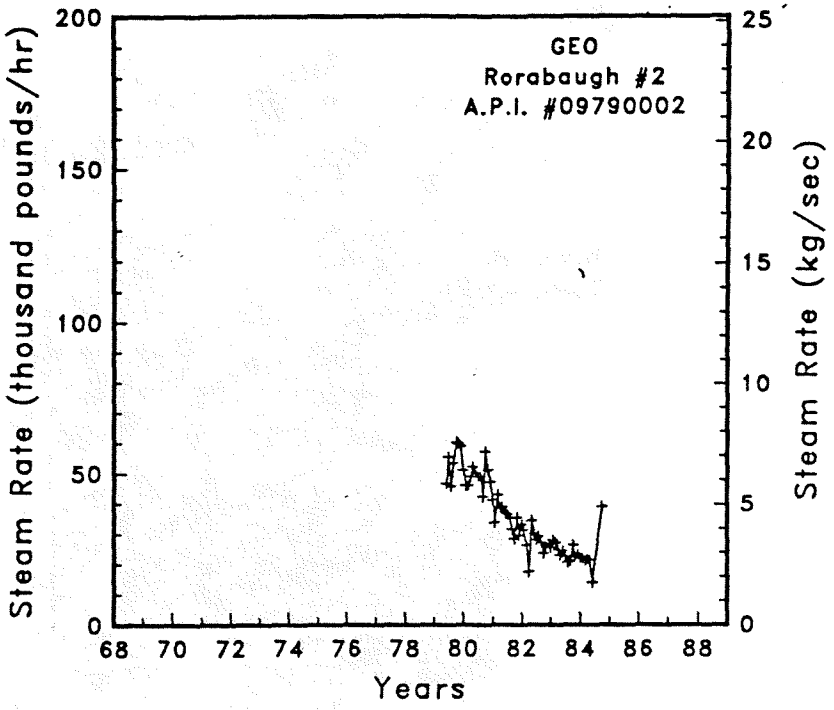

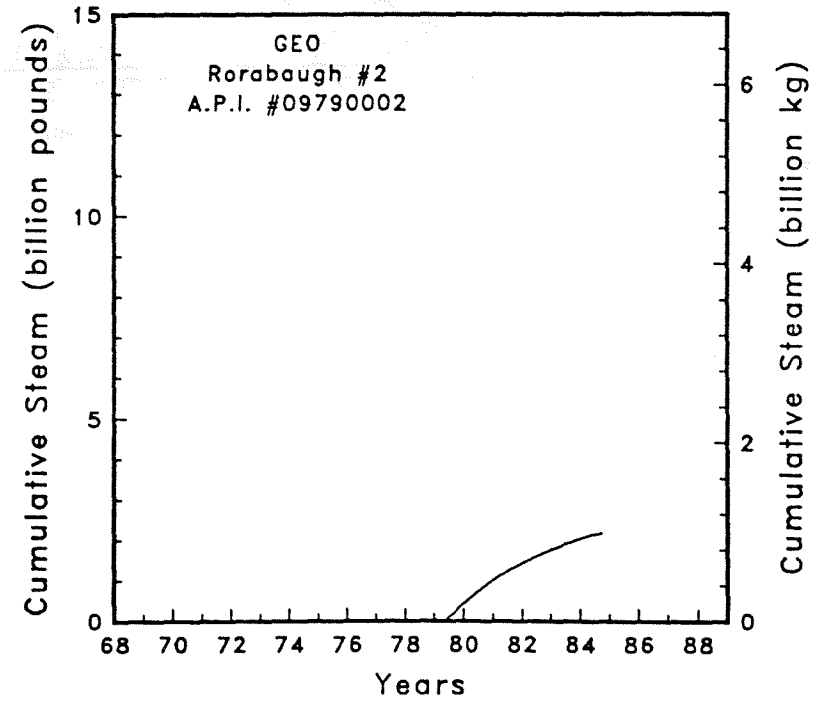

Figure A-200 Steam rate and cumulative mass flow for well Rorabaugh #2

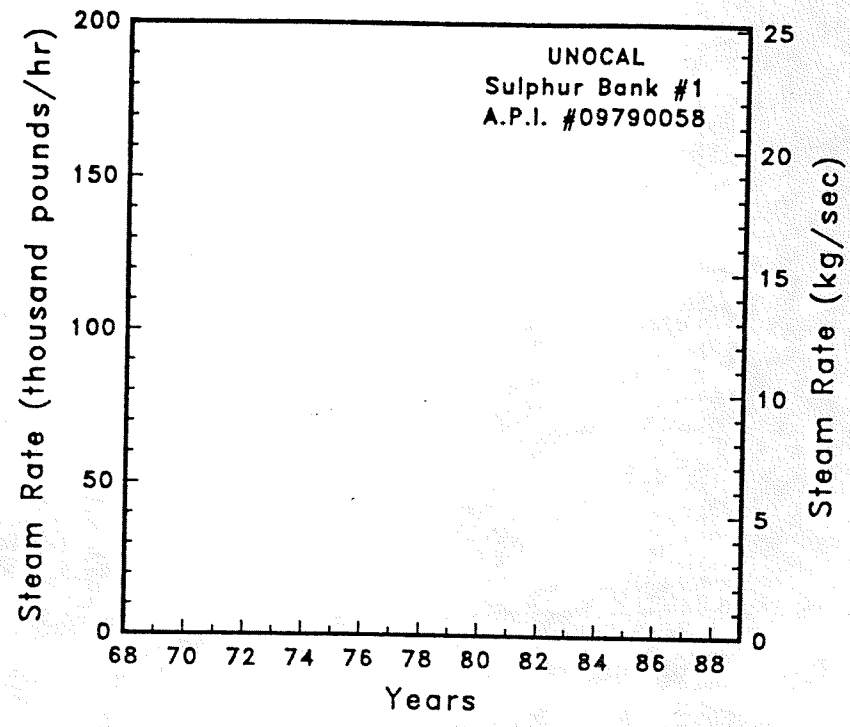

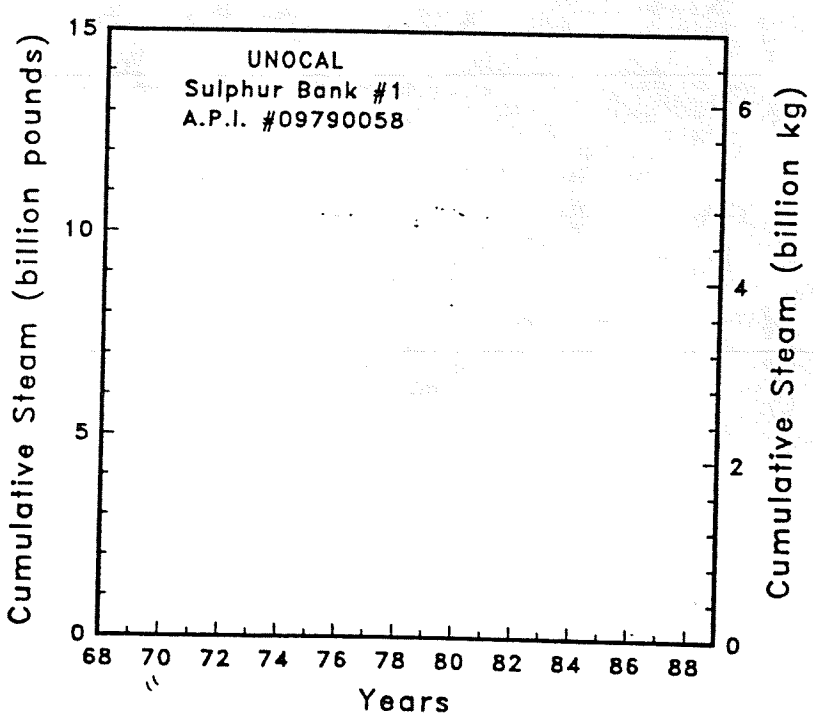

Figure A-201 Steam rate and cumulative mass flow for well Sulphur Bank #1

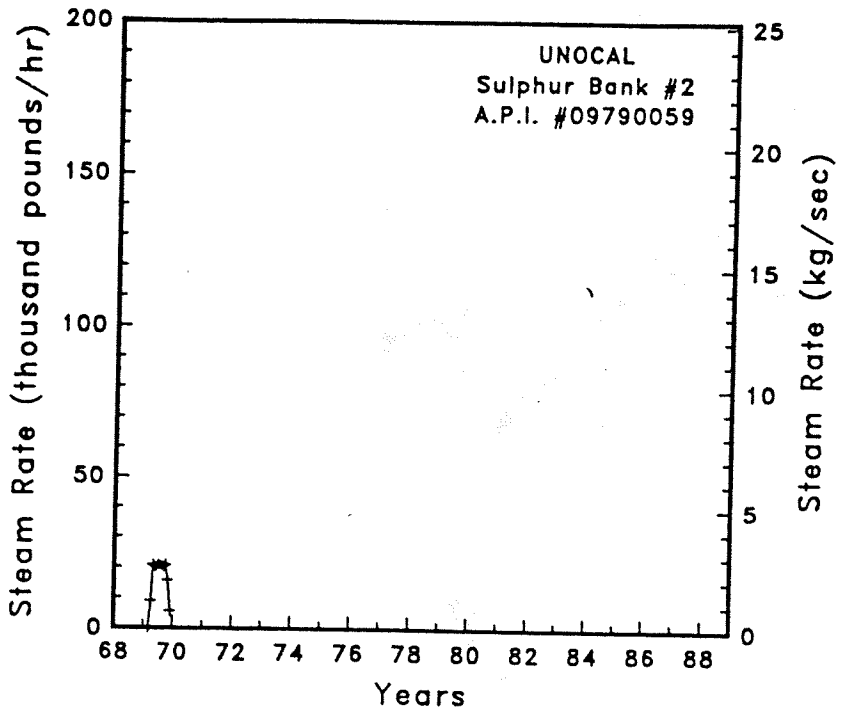

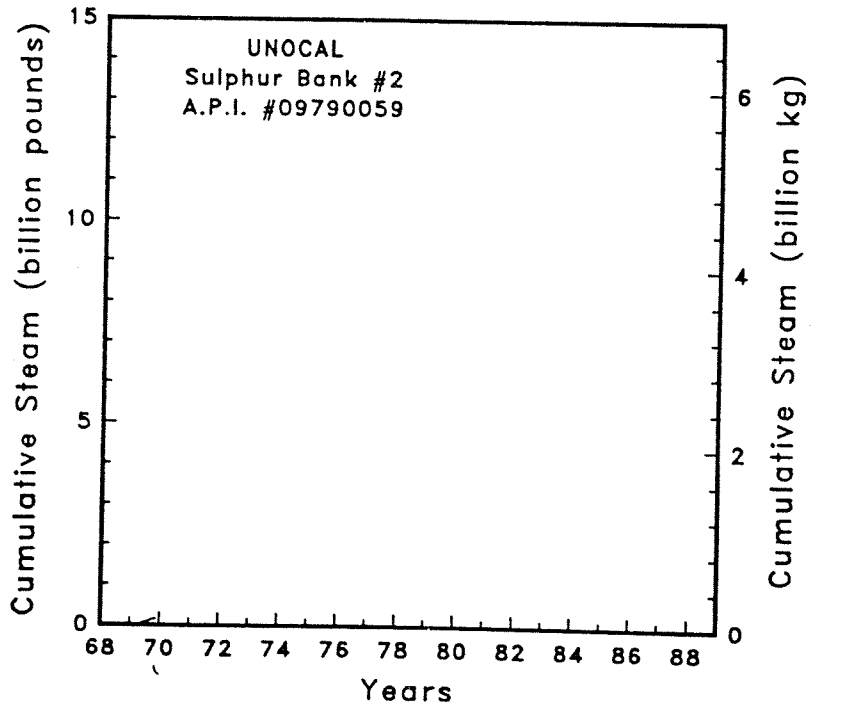

Figure A-202 Steam rate and cumulative mass flow for well Sulphur Bank #2

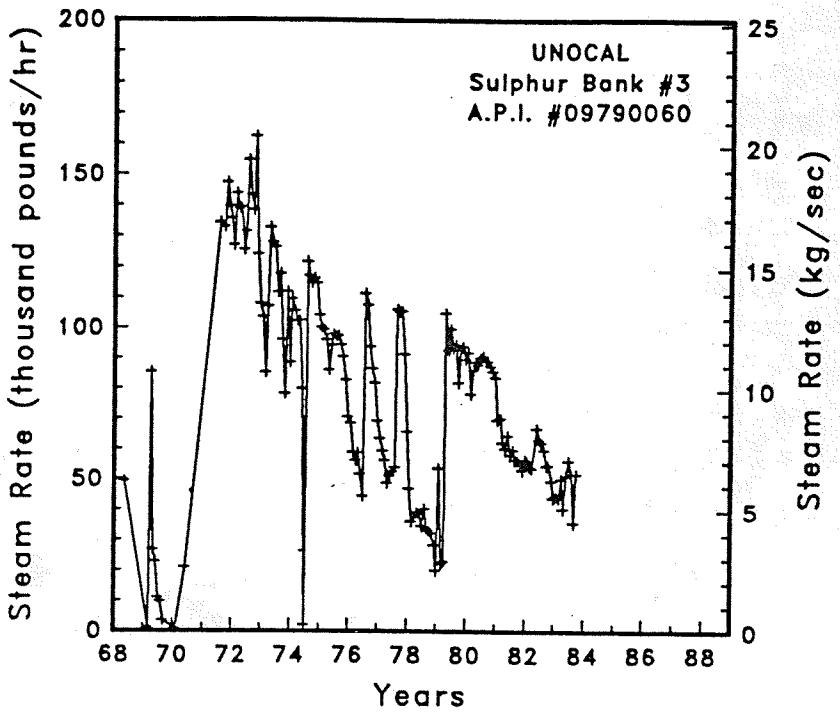

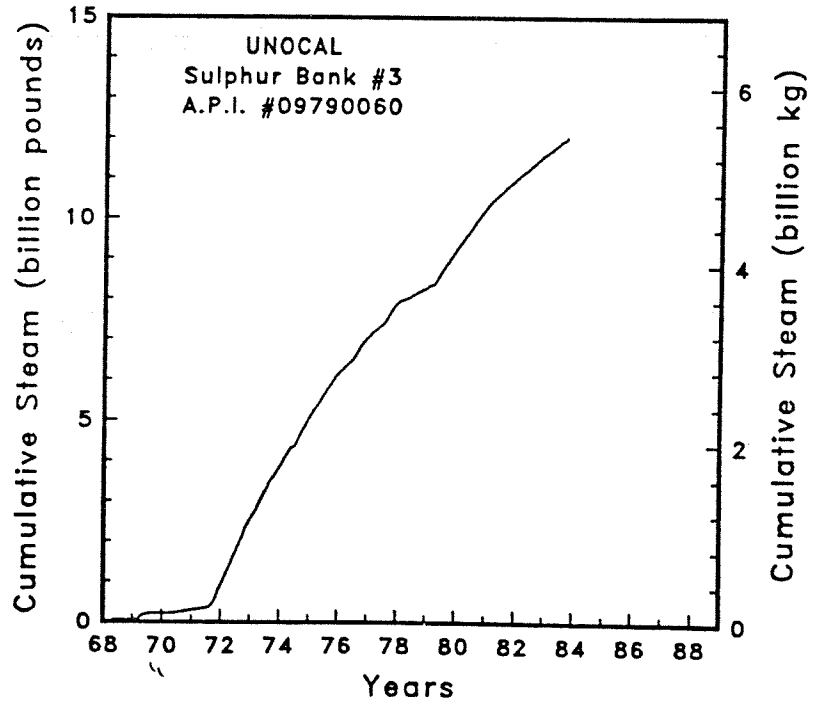

Figure A-203. Steam rate and cumulative mass flow for well Sulphur Bank #3

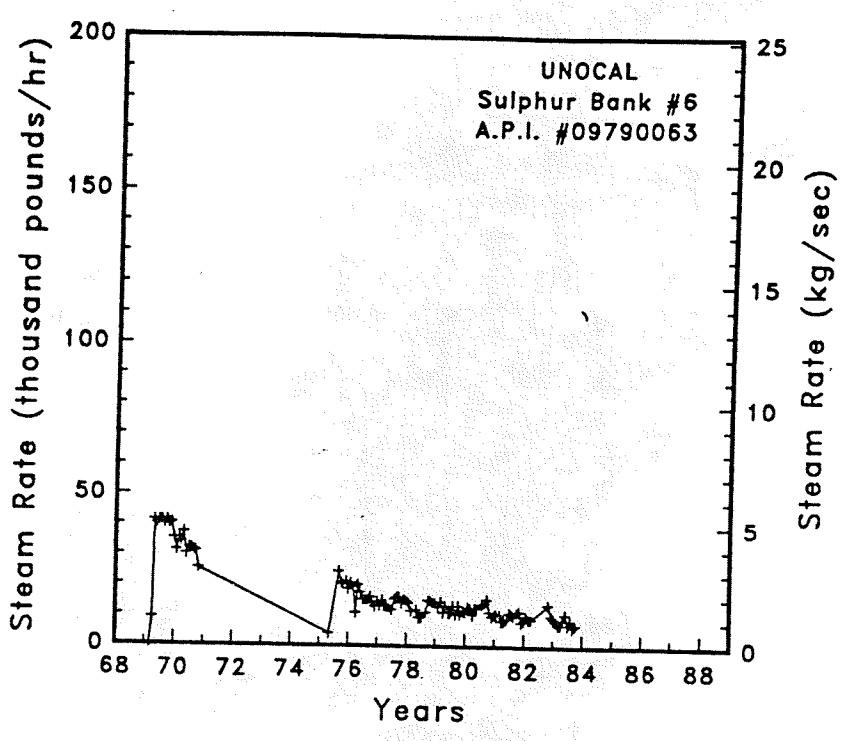

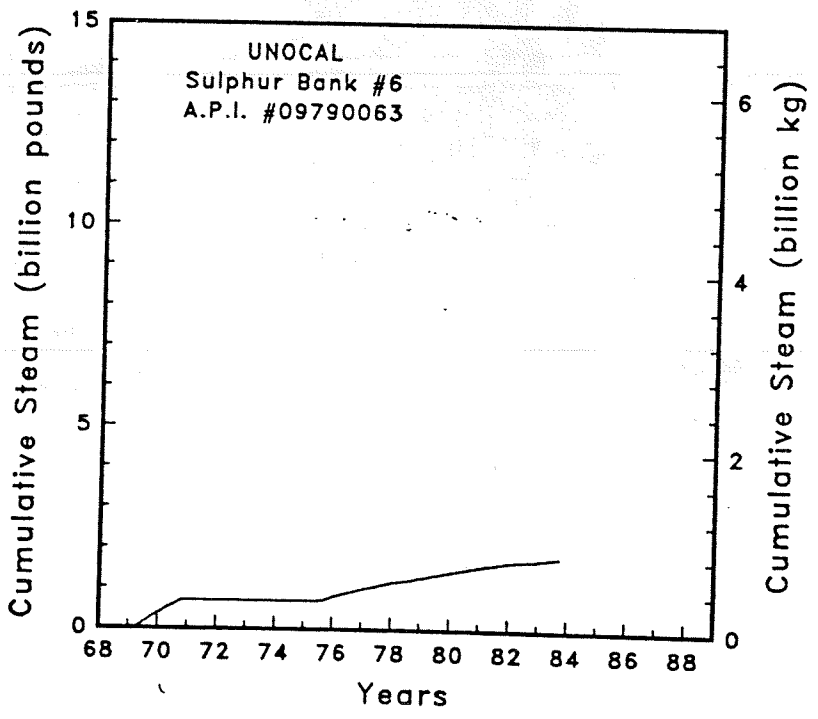

Figure A-204 Steam rate and cumulative mass flow for well Sulphur Bank #6

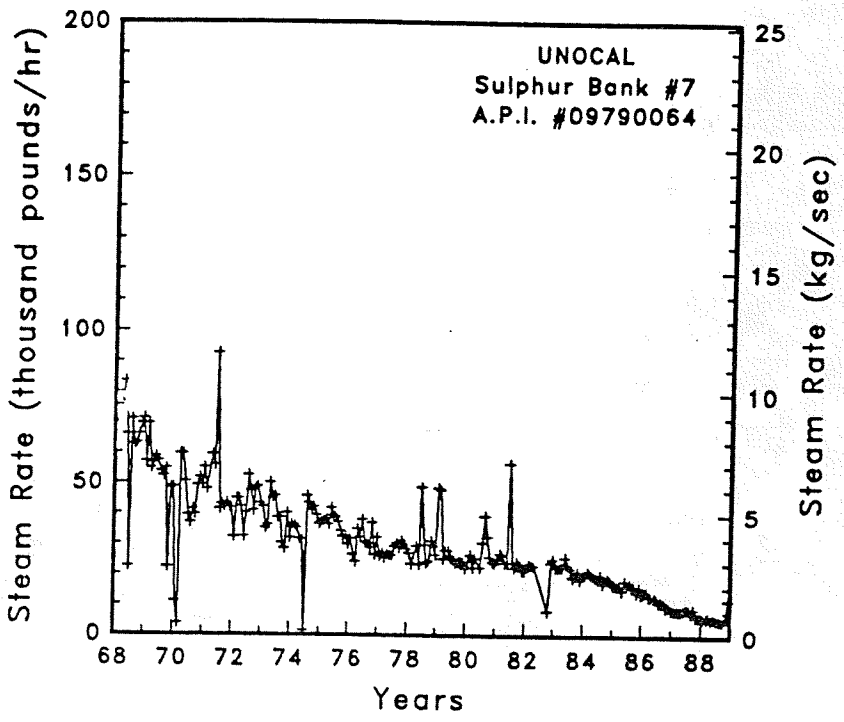

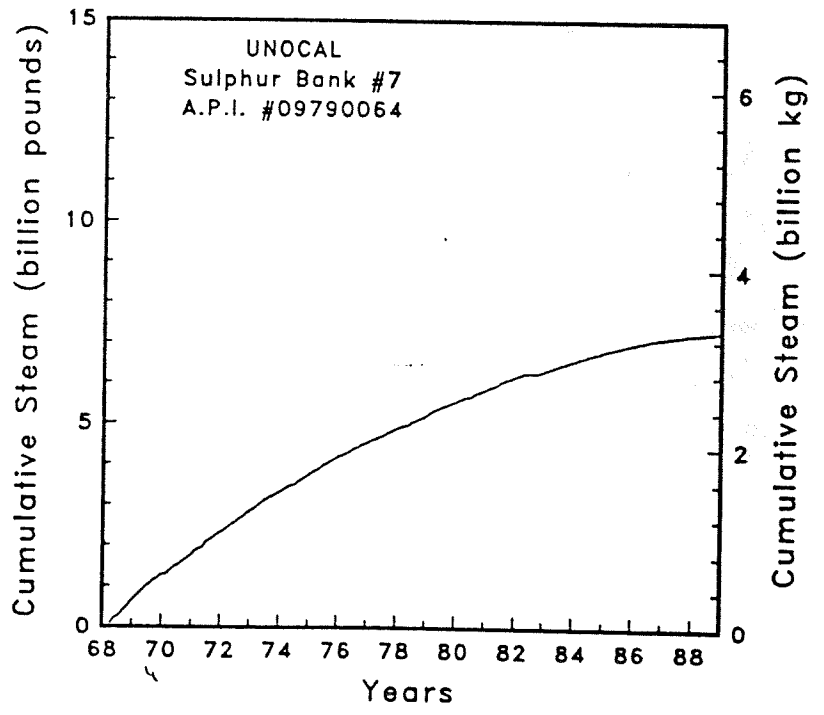

Figure A-205 Steam rate and cumulative mass flow for well Sulphur Bank #7

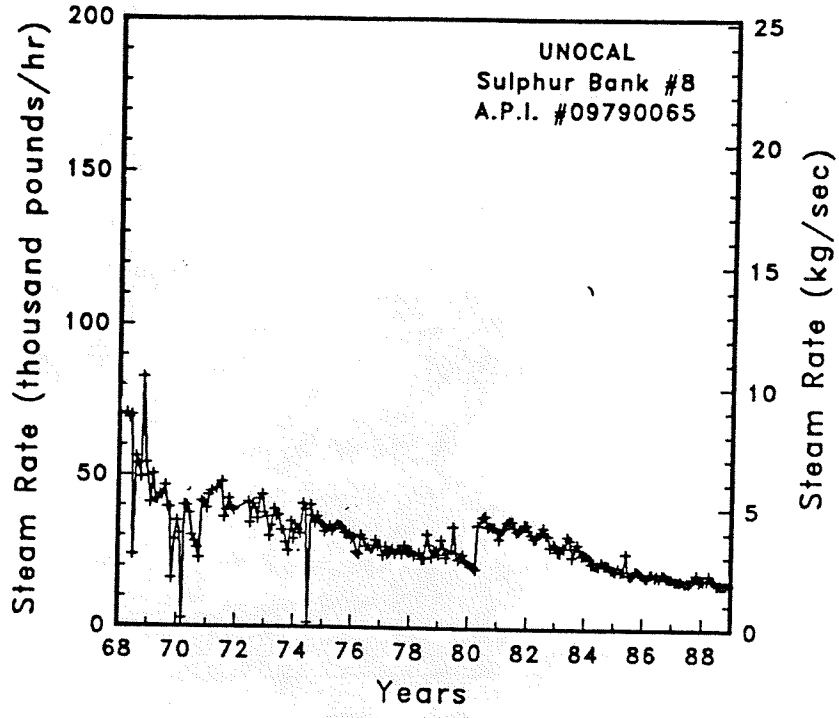

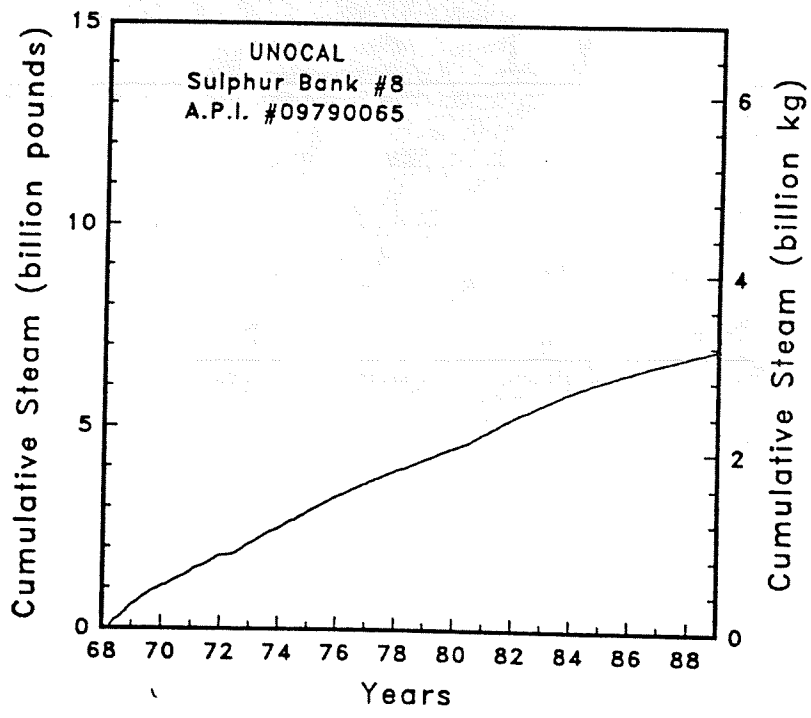

Figure A-206 Steam rate and cumulative mass flow for well Sulphur Bank #8

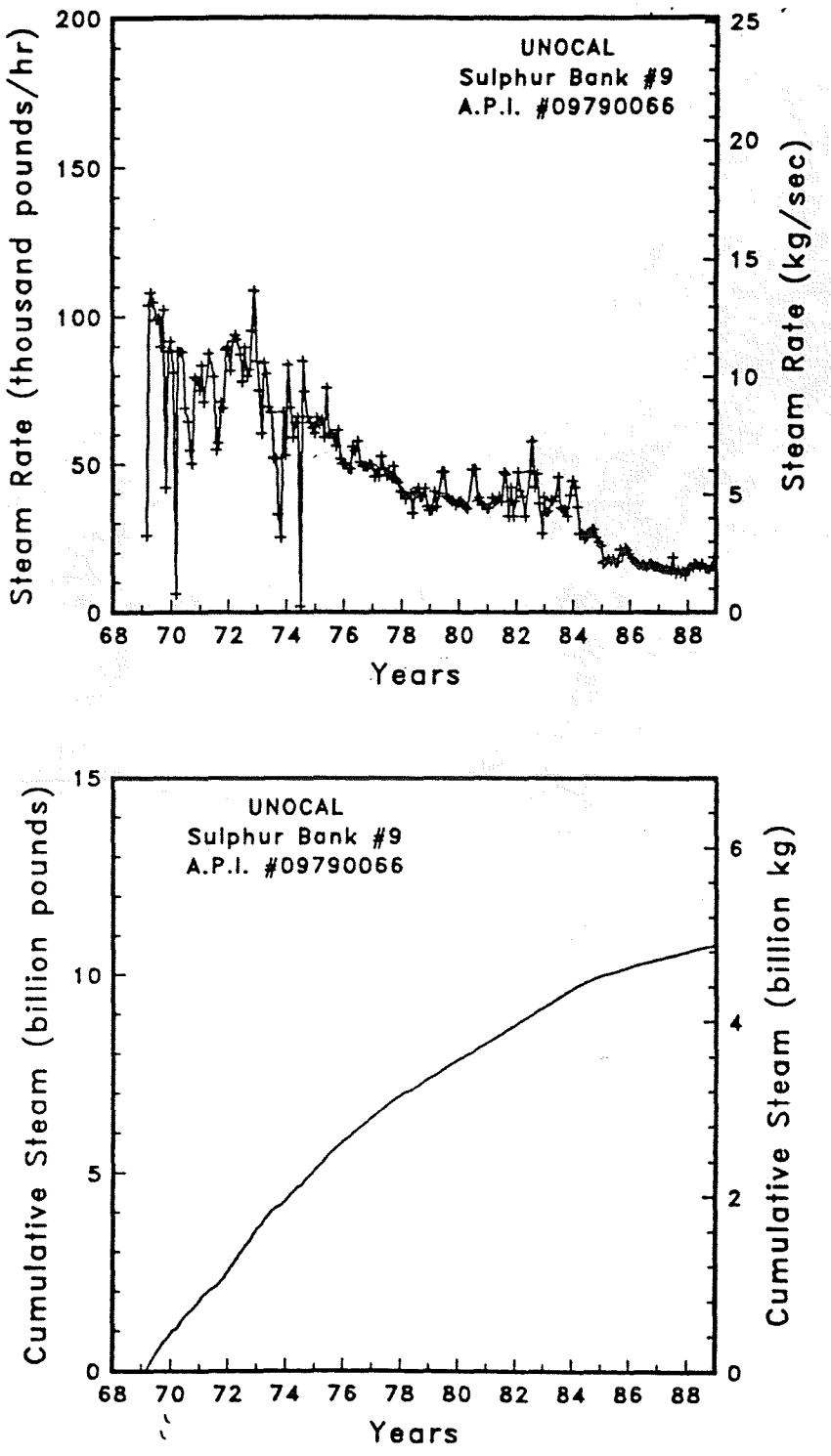

Figure A-207 Steam rate and cumulative mass flow for well Sulphur Bank #9

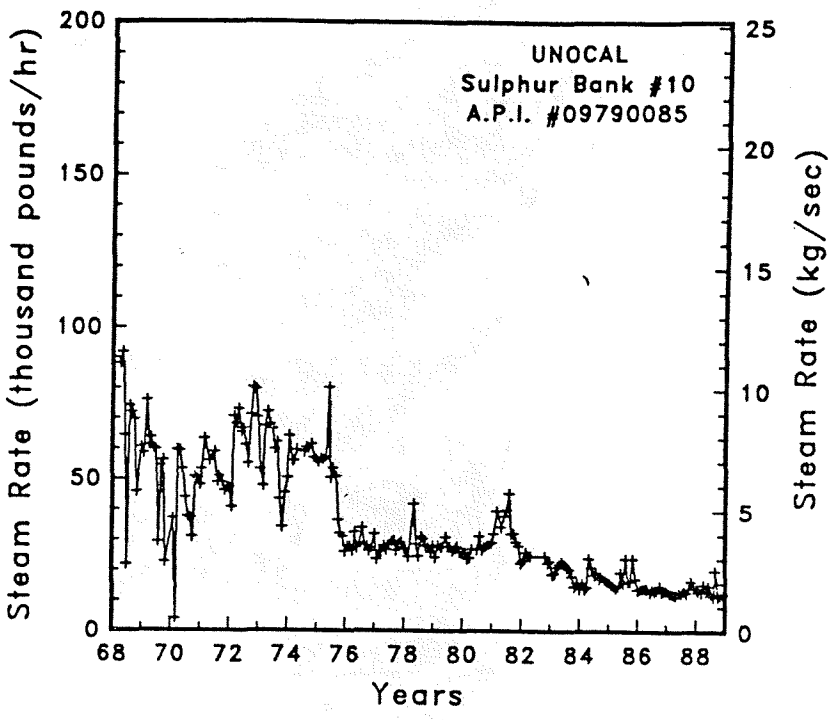

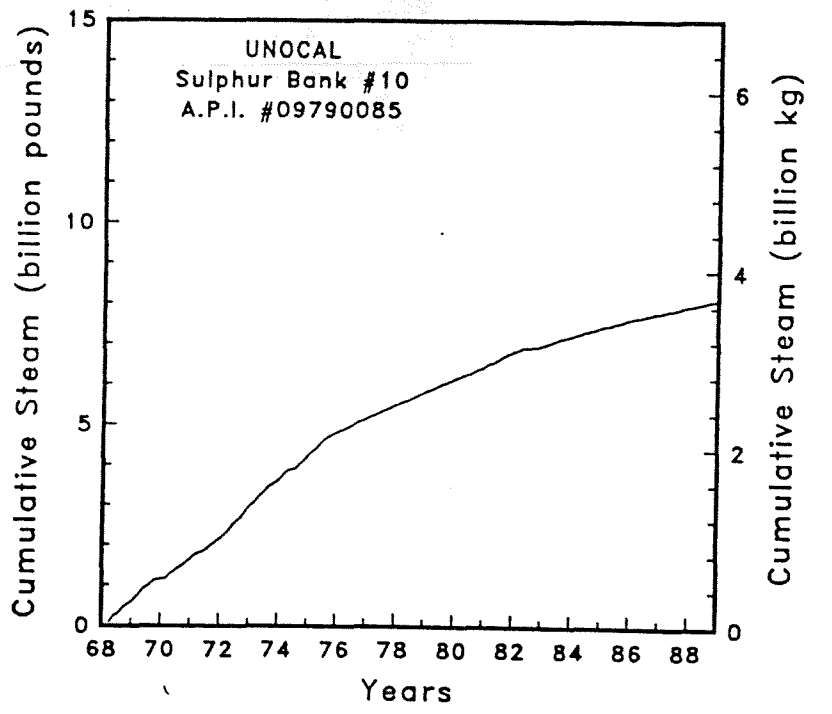

Figure A-208 Steam rate and cumulative mass flow for well Sulphur Bank #10

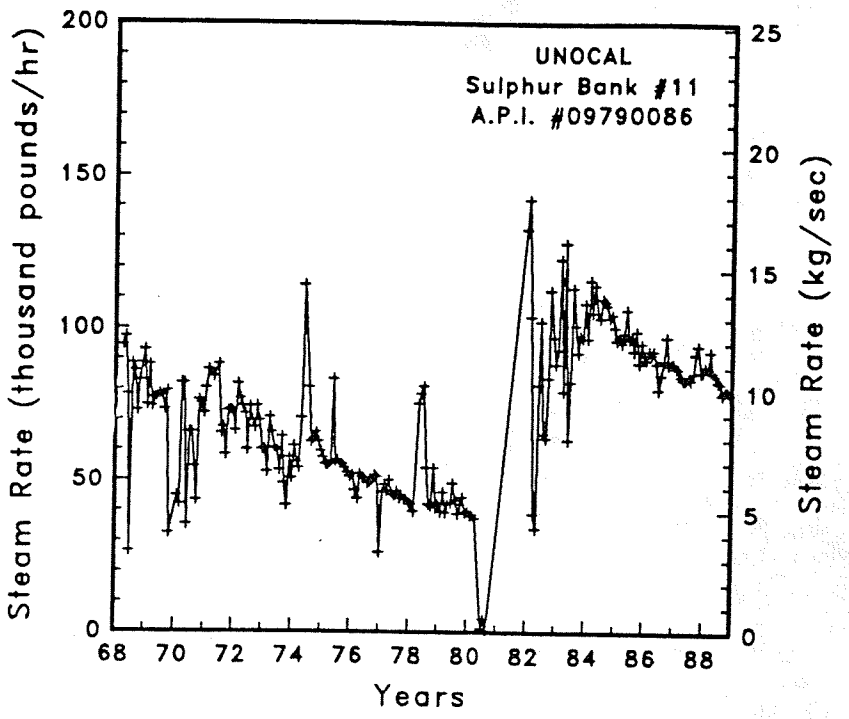

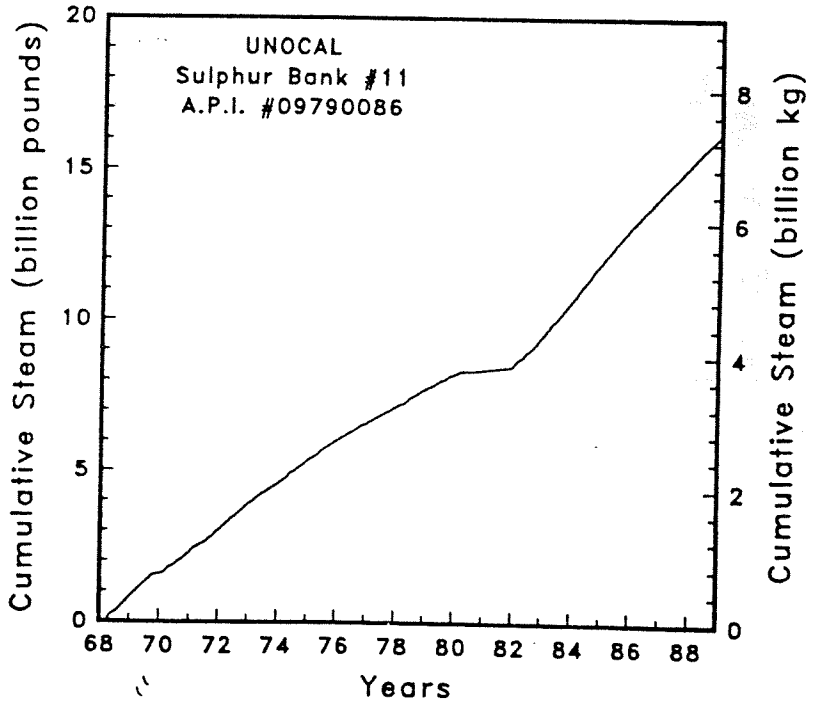

Figure A-209 Steam rate and cumulative mass flow for well Sulphur Bank #11

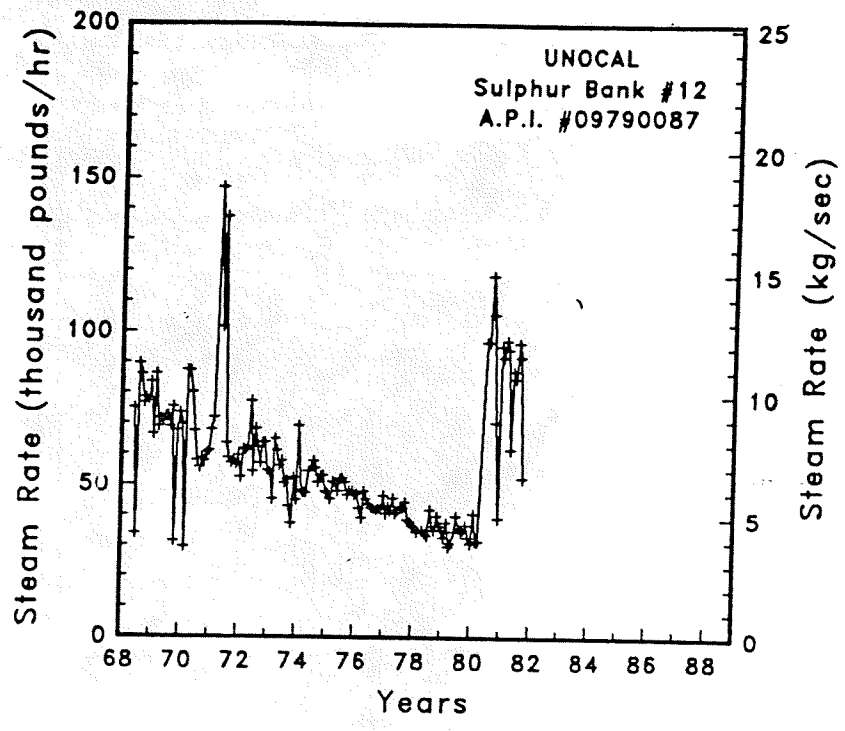

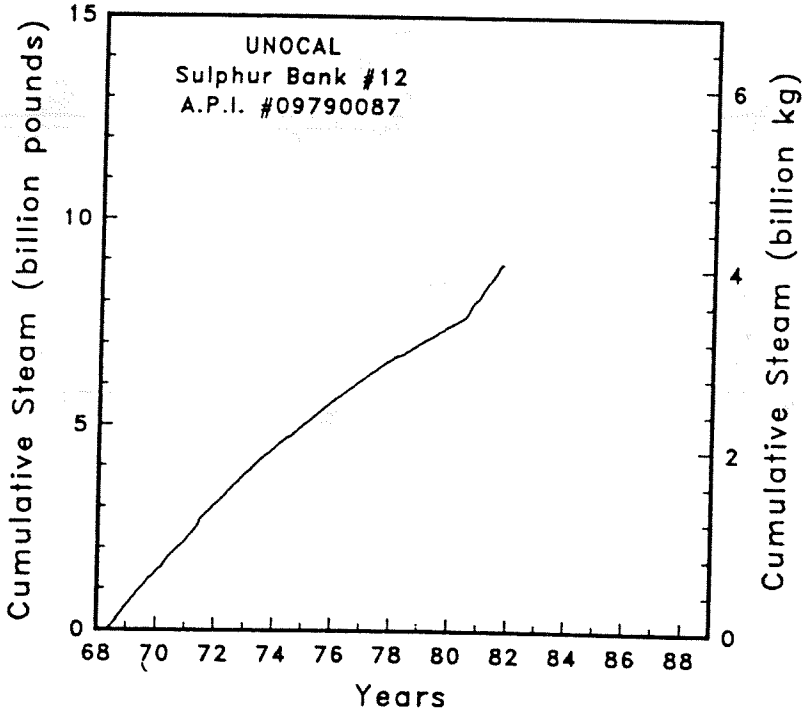

Figure A-210 Steam rate and cumulative mass flow for well Sulphur Bank #12

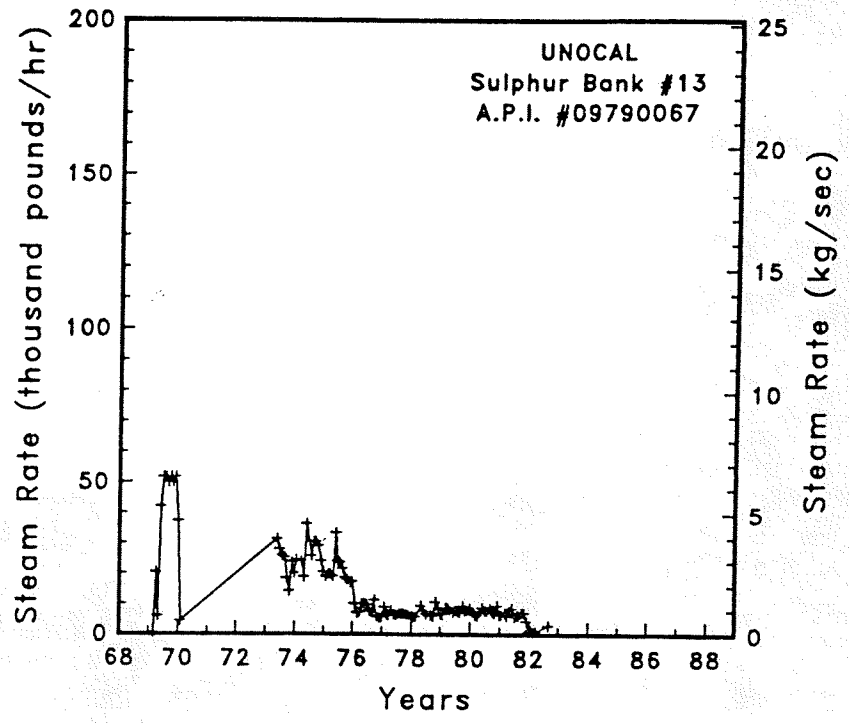

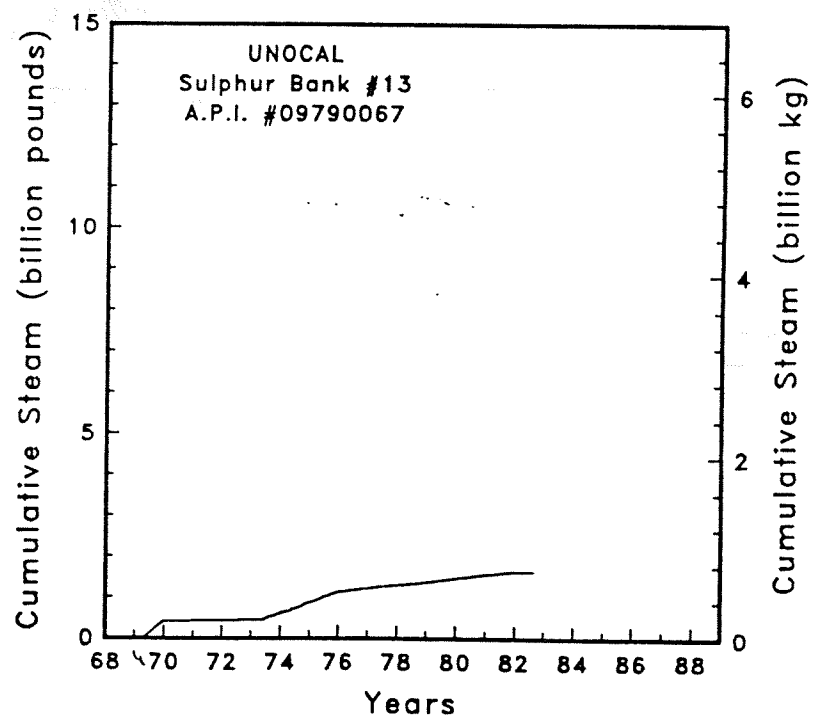

Figure A-211 Steam rate and cumulative mass flow for well Sulphur Bank #13

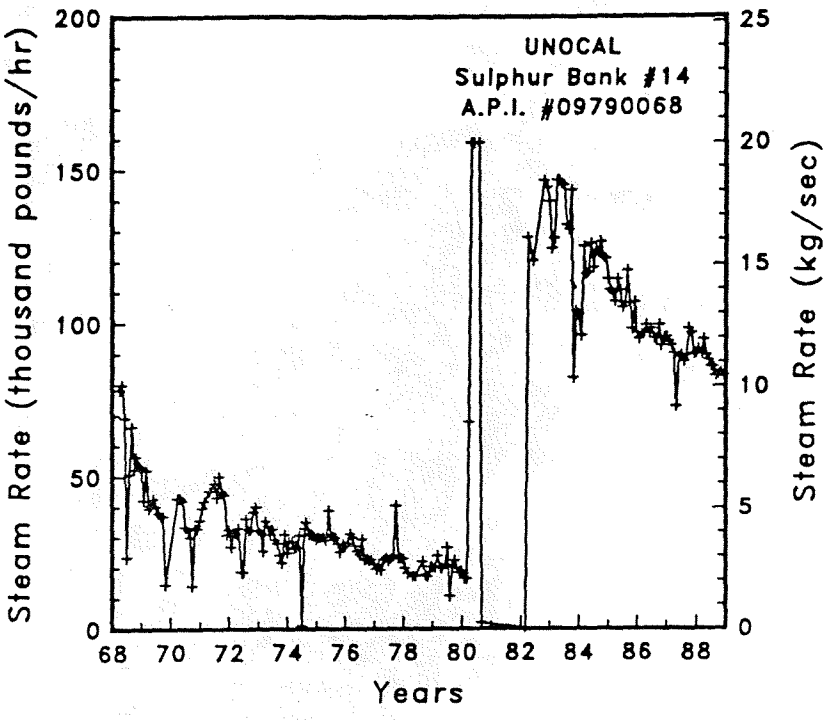

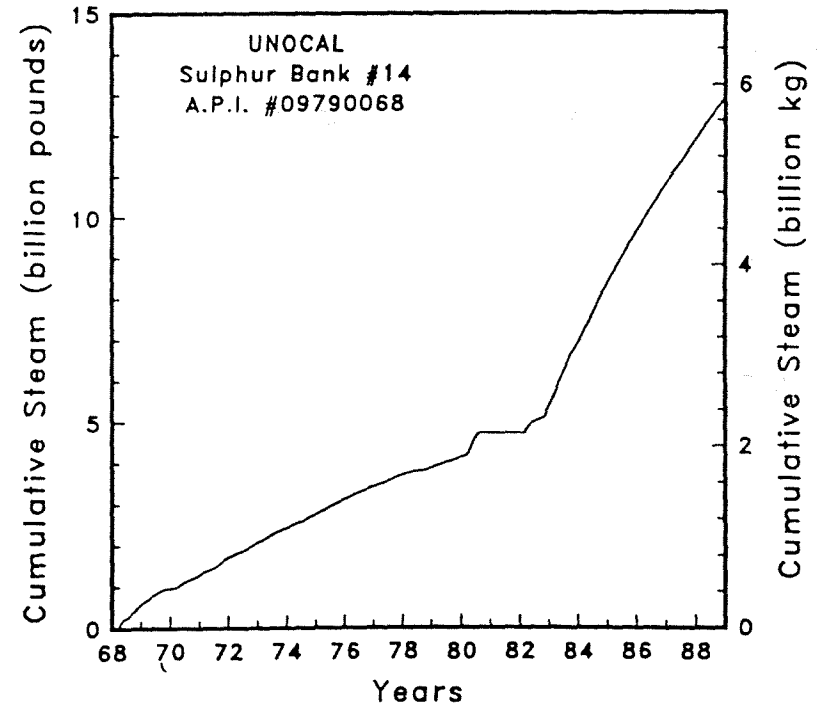

Figure A-212 Steam rate and cumulative mass flow for well Sulphur Bank #14

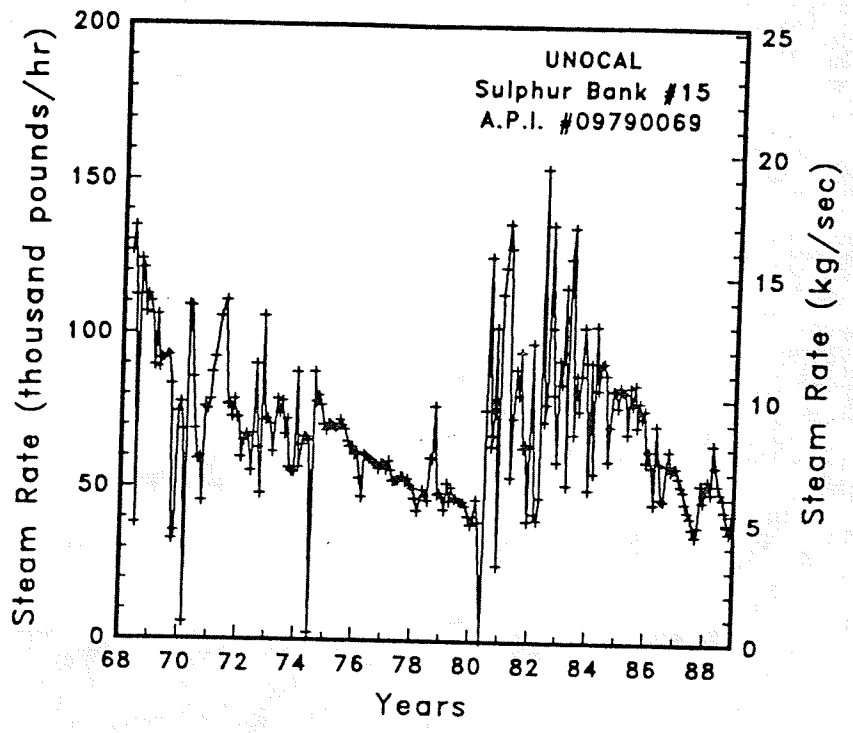

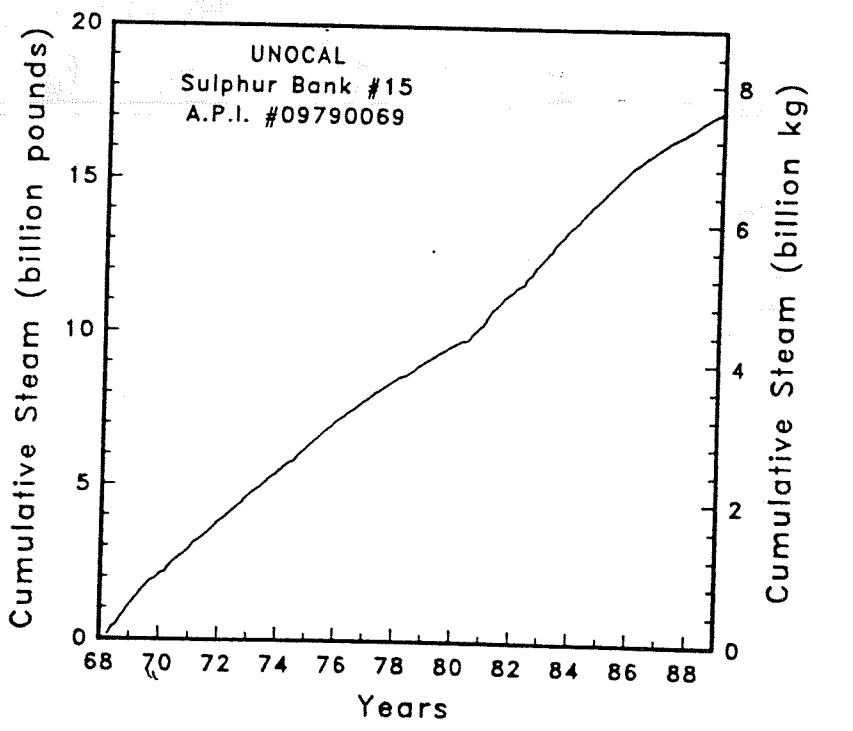

Figure A-213 Steam rate and cumulative mass flow for well Sulphur Bank #15

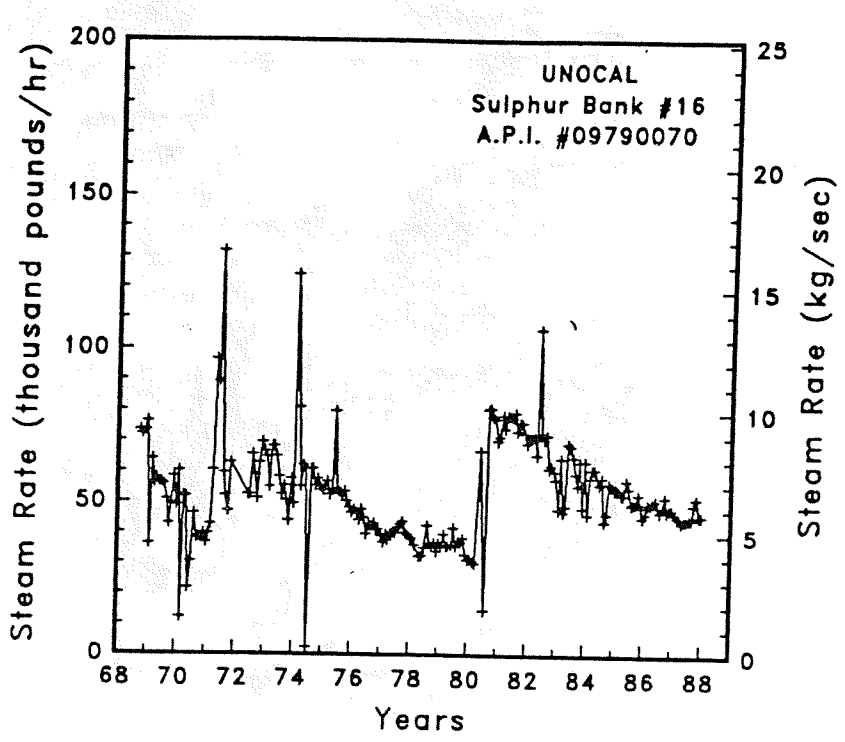

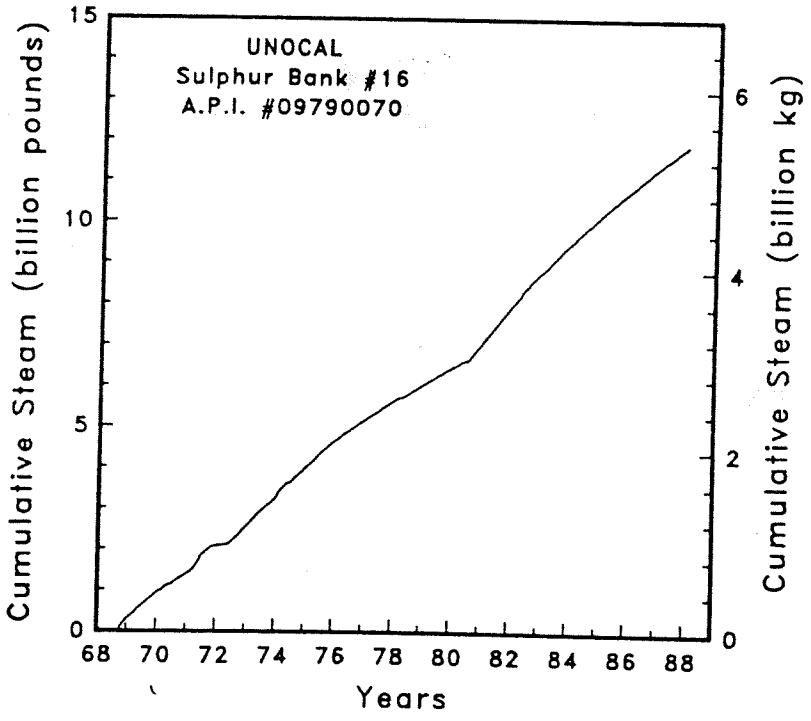

Figure A-214 Steam rate and cumulative mass flow for well Sulphur Bank #16

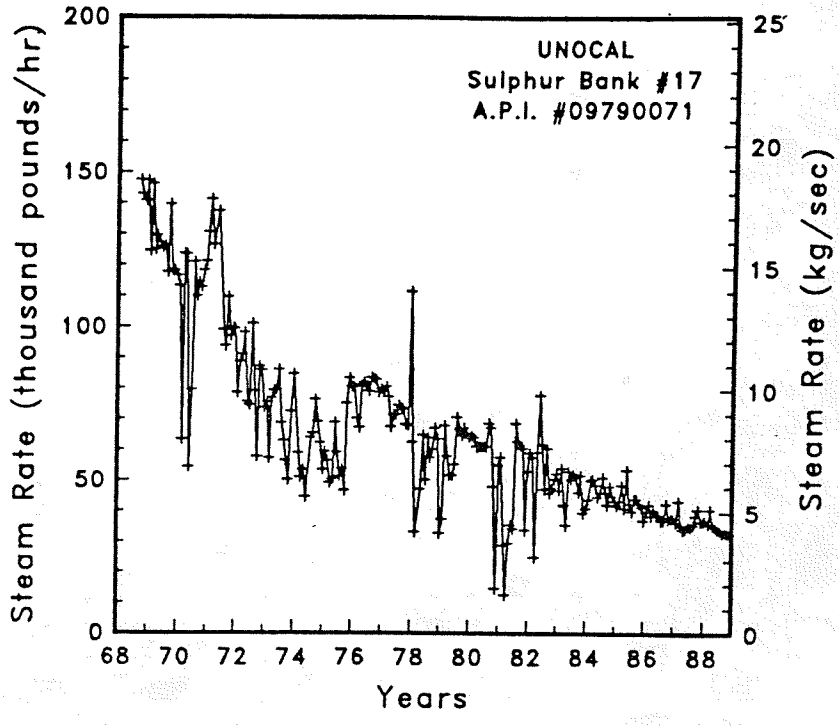

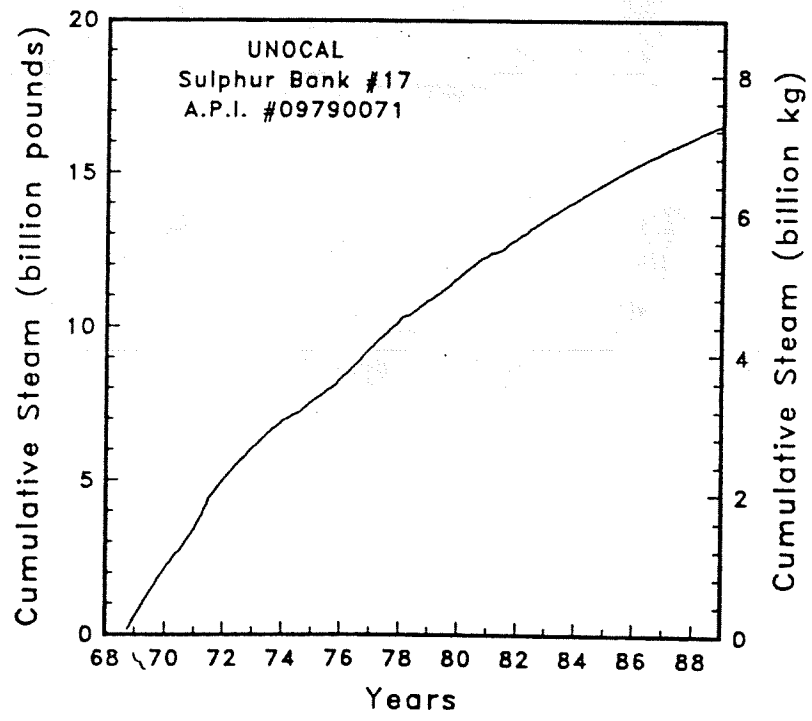

Figure A-215 Steam rate and cumulative mass flow for well Sulphur Bank #17

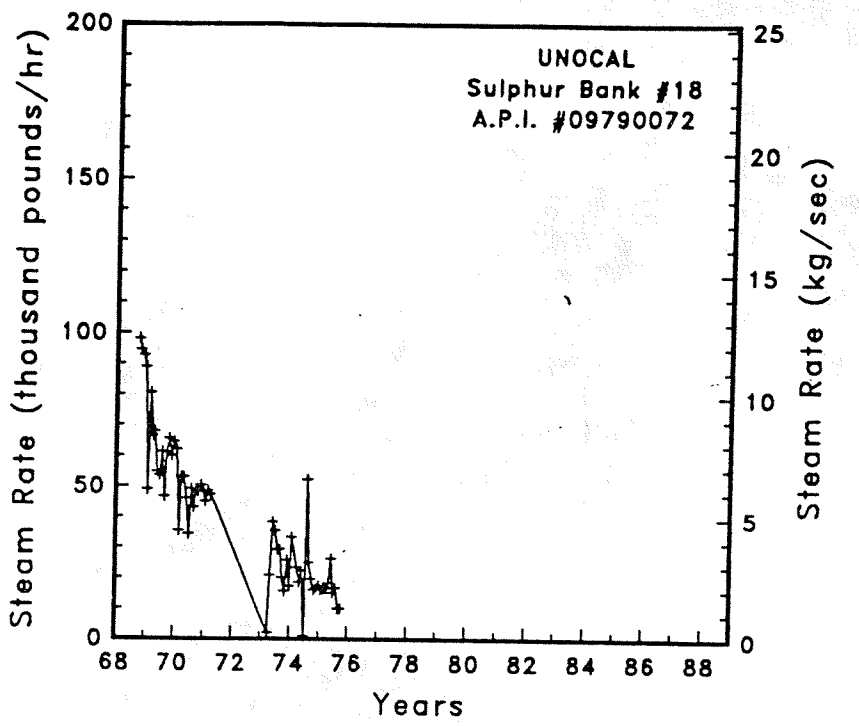

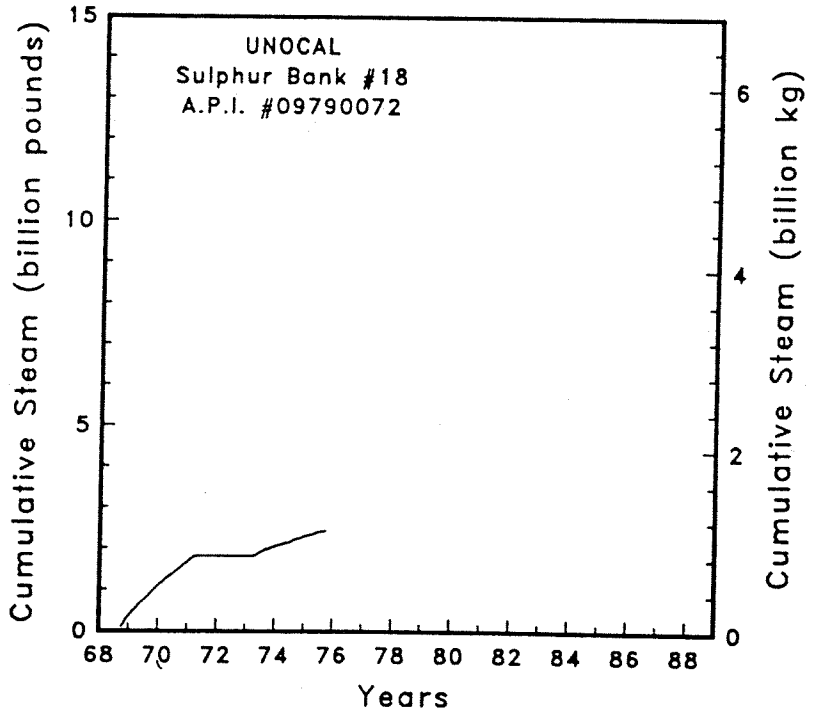

Figure A-216 Steam rate and cumulative mass flow for well Sulphur Bank #18

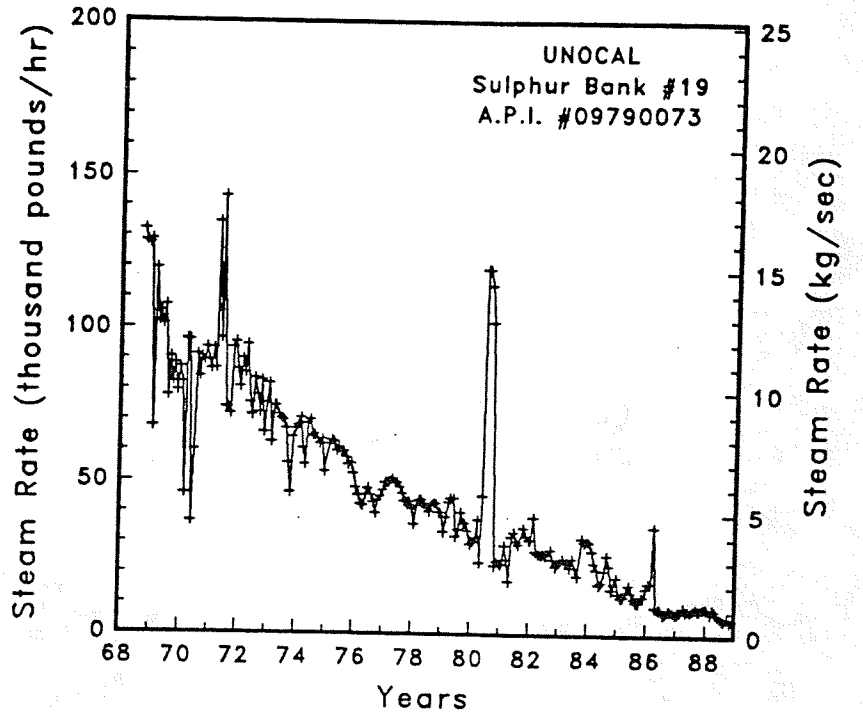

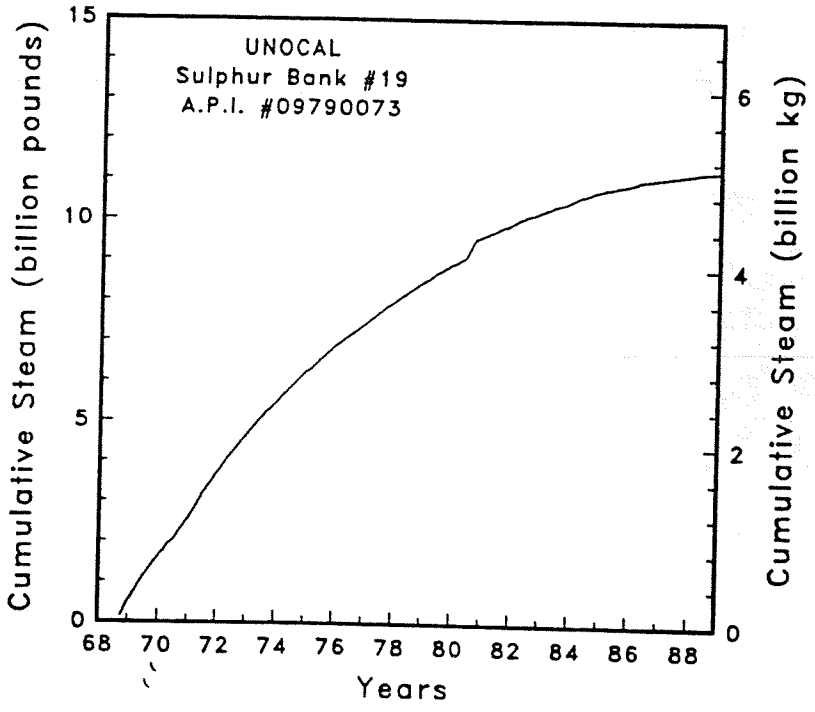

Figure A-217 Steam rate and cumulative mass flow for well Sulphur Bank #19

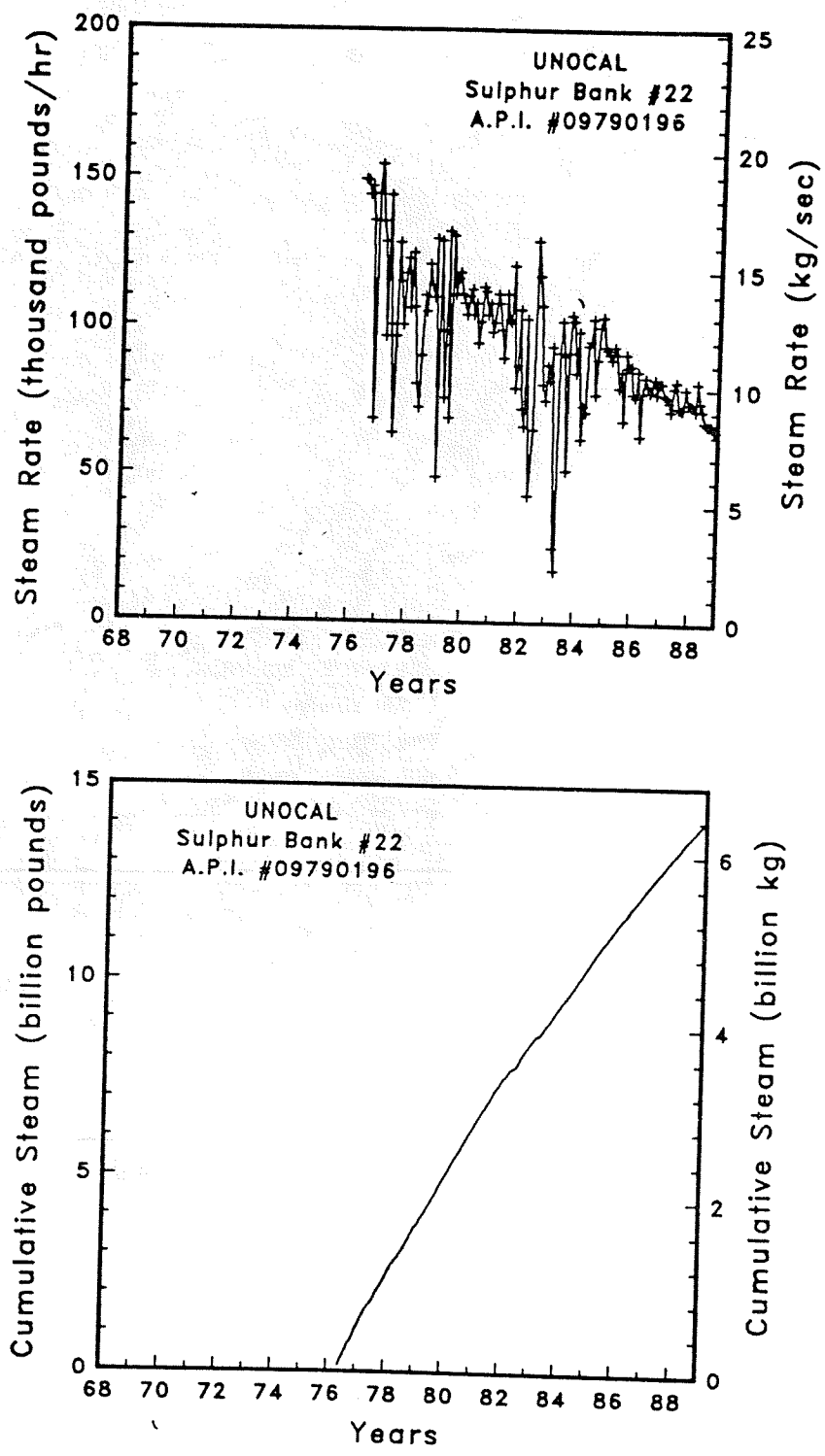

Figure A-220 Steam rate and cumulative mass flow for well Sulphur Bank #22

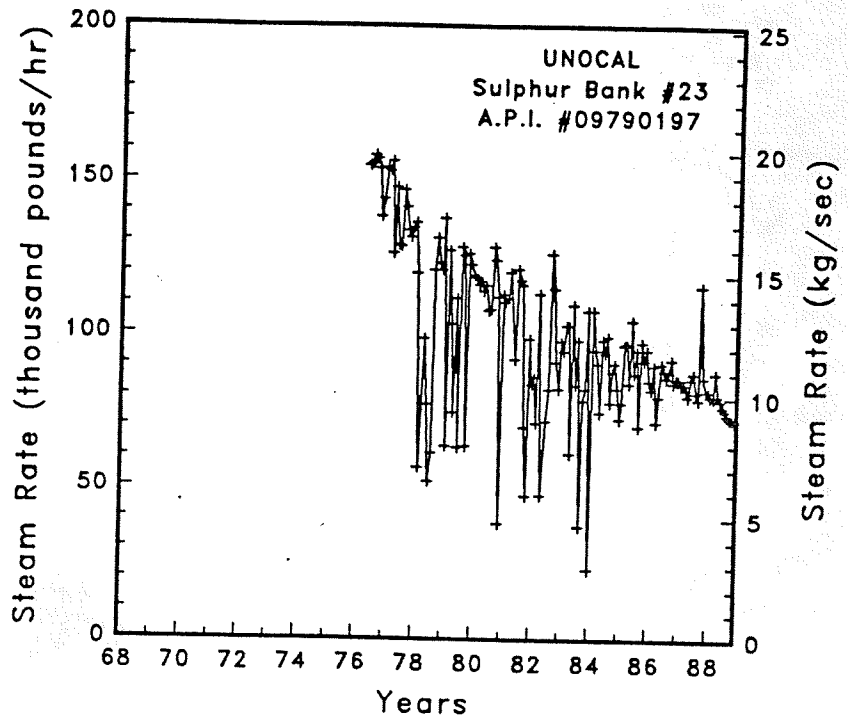

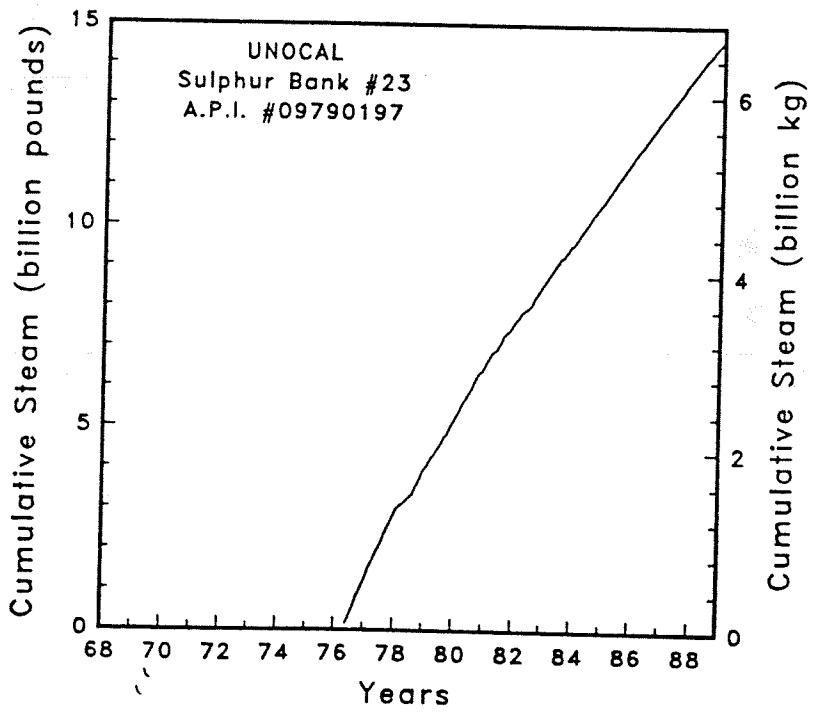

Figure A-221 Steam rate and cumulative mass flow for well Sulphur Bank #23

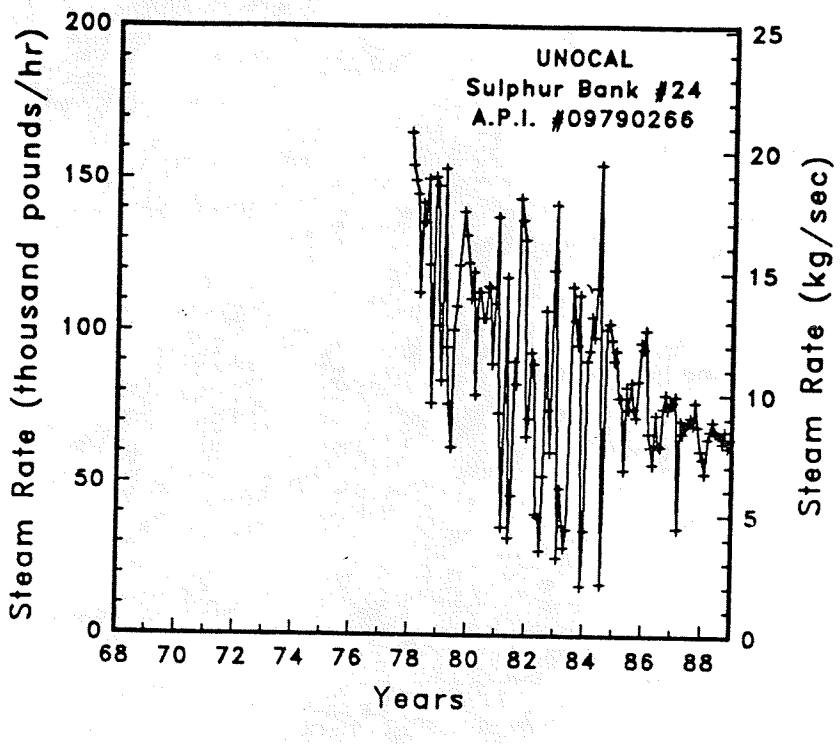

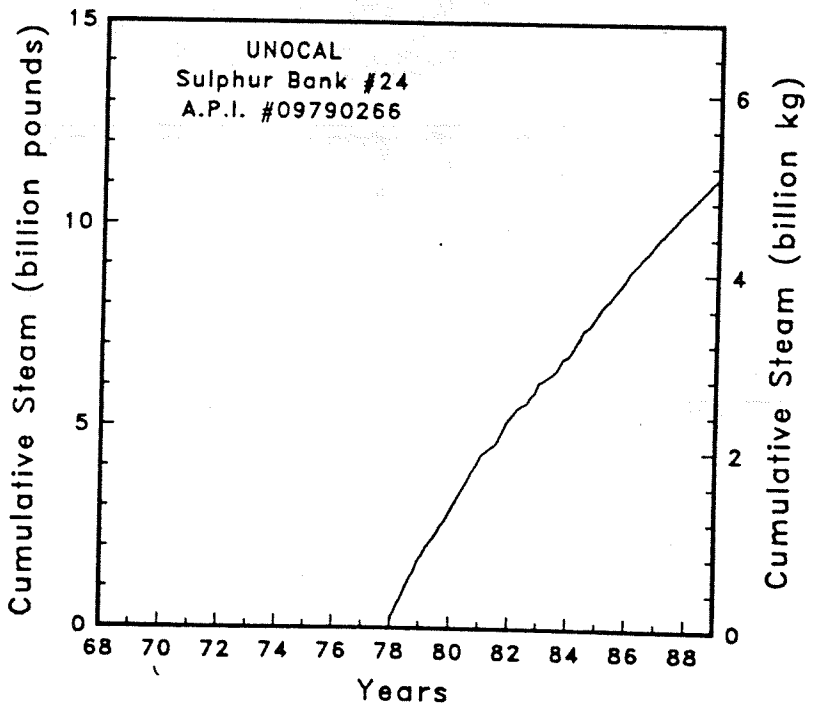

Figure A-222 Steam rate and cumulative mass flow for well Sulphur Bank #24

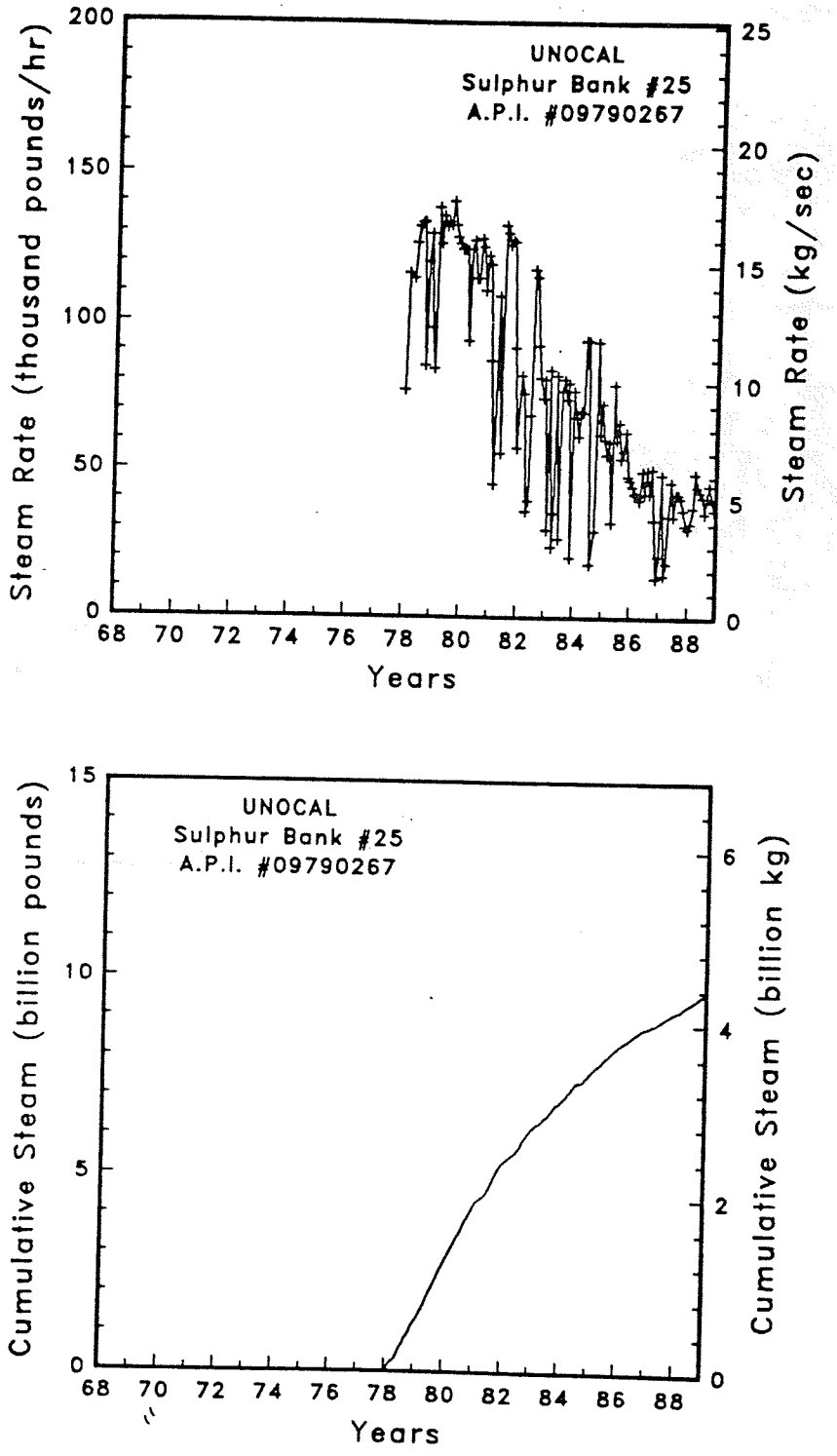

Figure A-223 Steam rate and cumulative mass flow for well Sulphur Bank #25

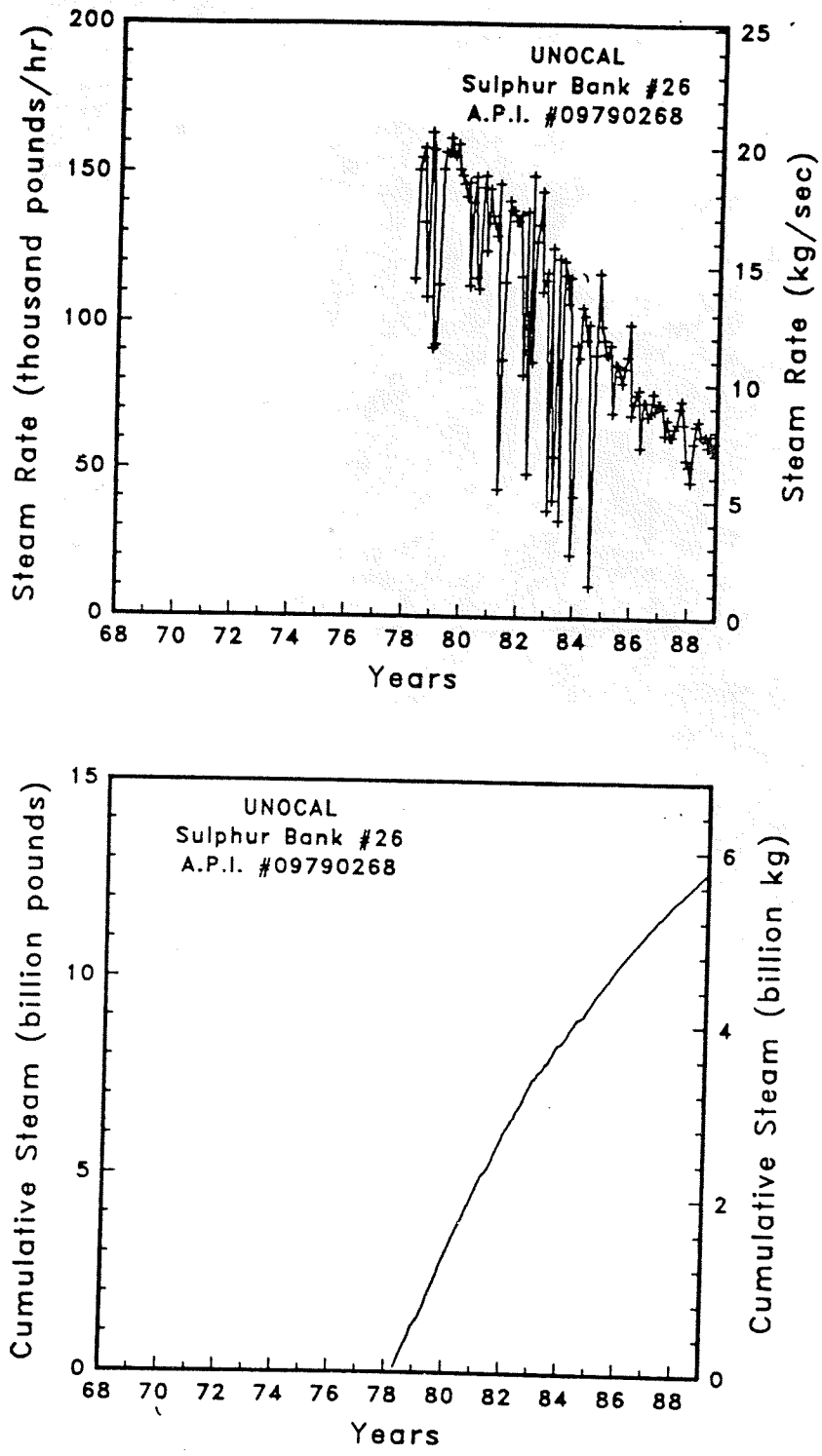

Figure A-224 Steam rate and cumulative mass flow for well Sulphur Bank #26

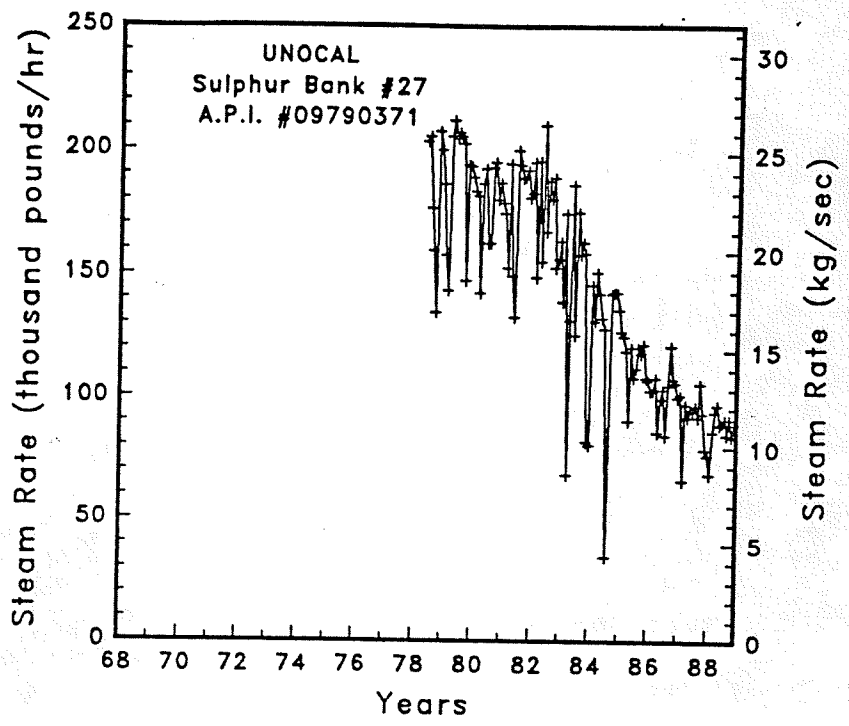

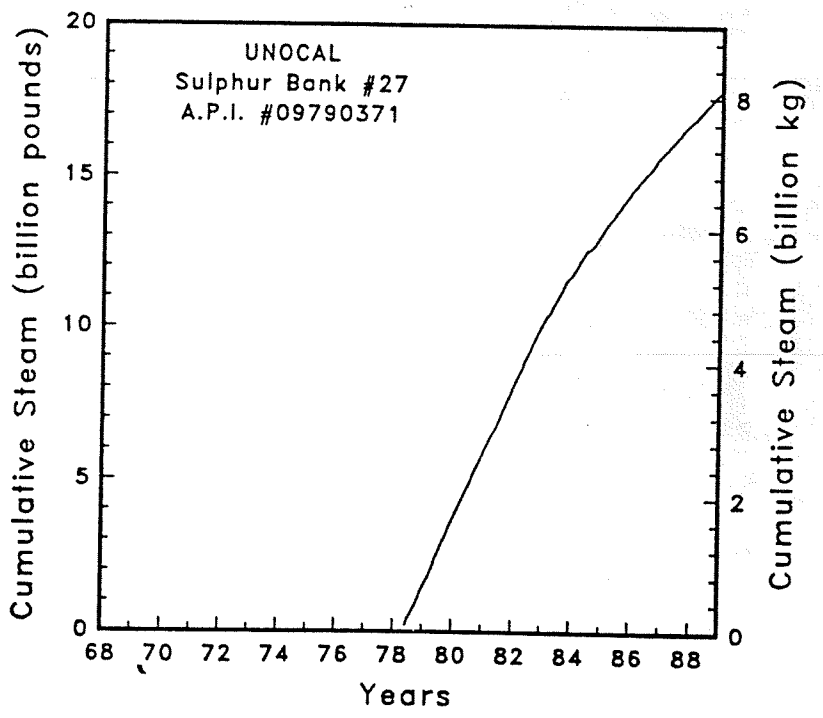

Figure A-225 Steam rate and cumulative mass flow for well Sulphur Bank #27

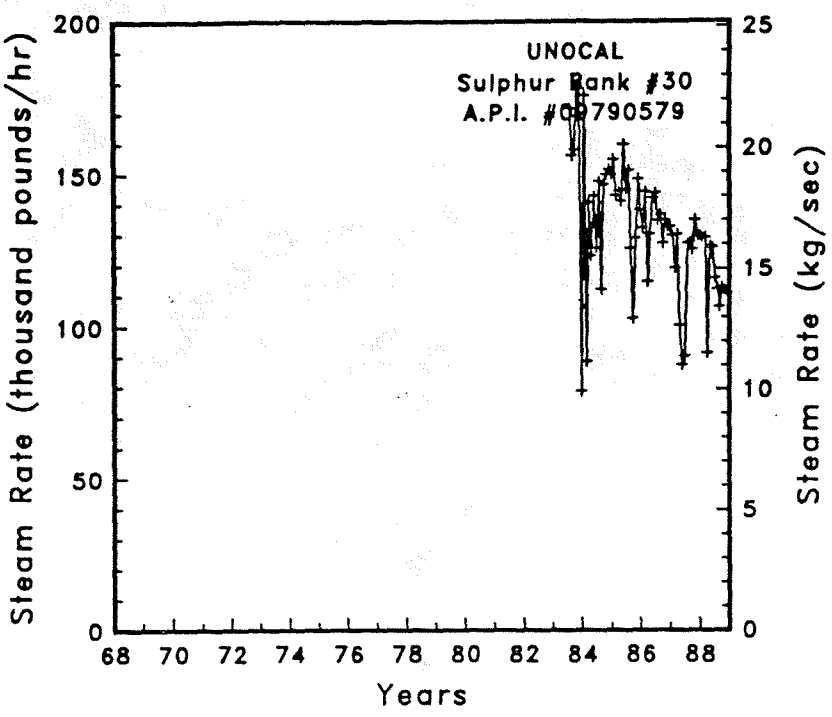

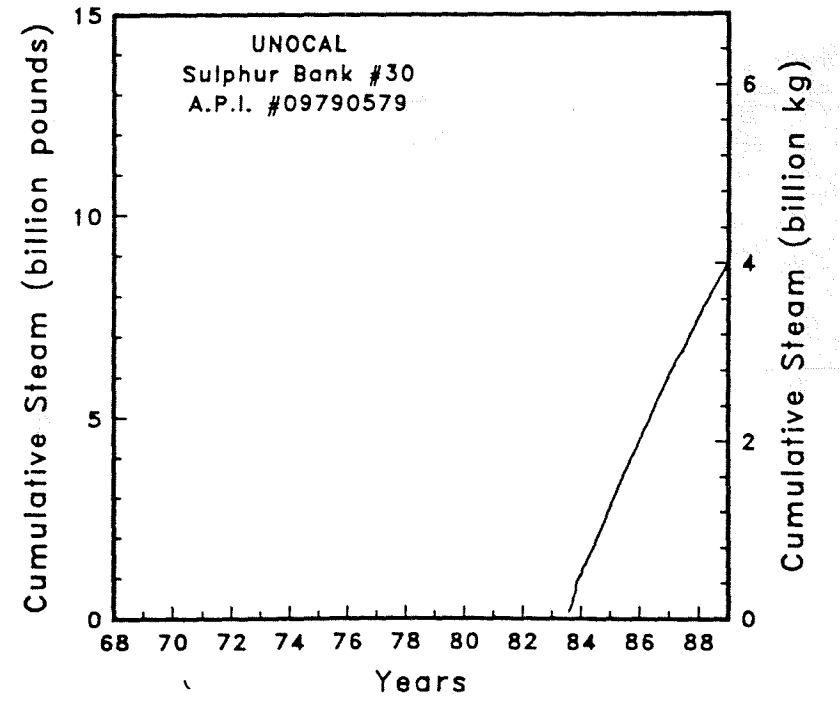

Figure A-226 Steam rate and cumulative mass flow for well Sulphur Bank #30

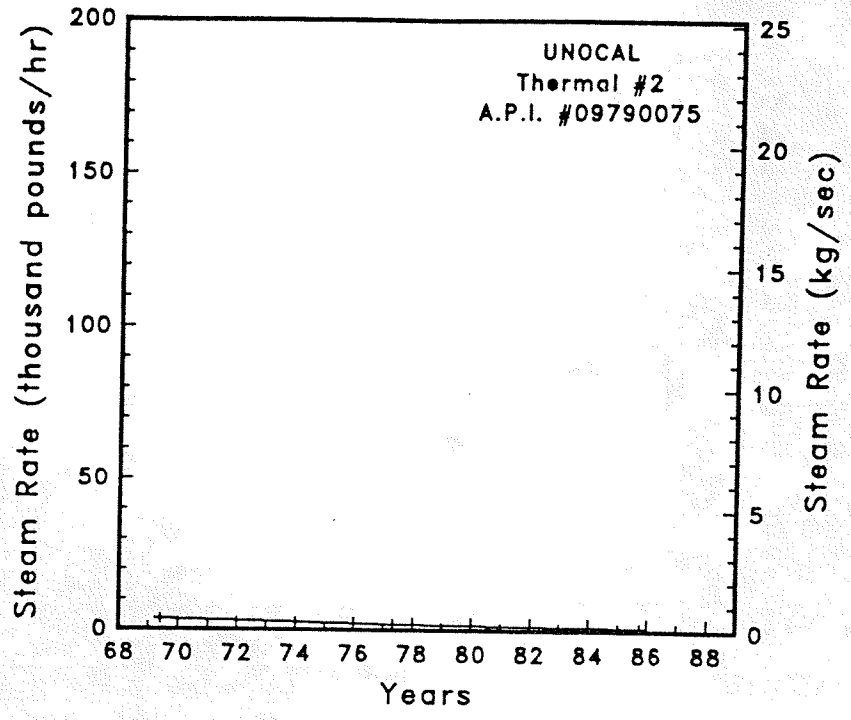

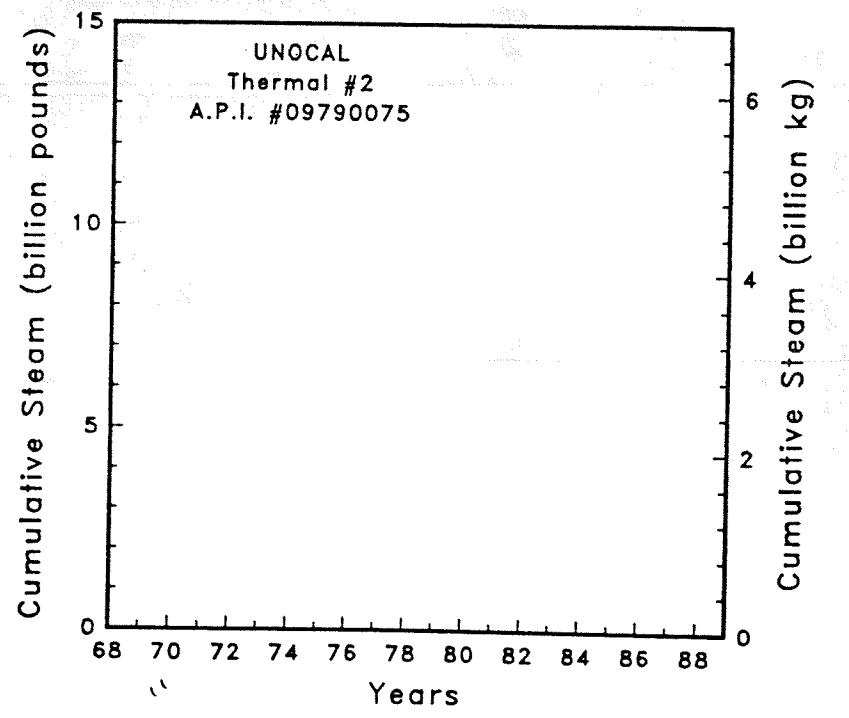

Figure A-227 Steam rate and cumulative mass flow for well Thermal #2

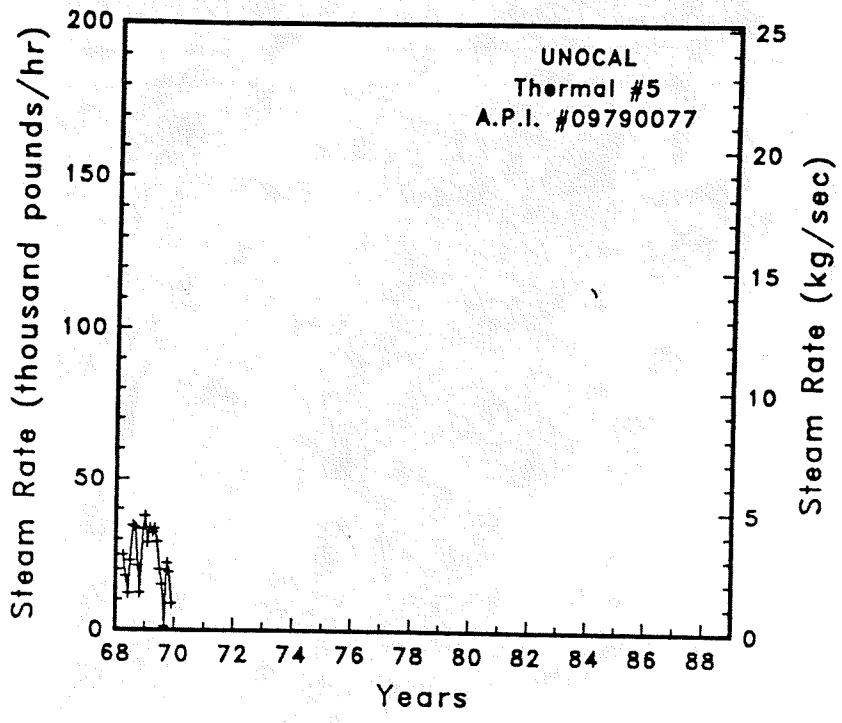

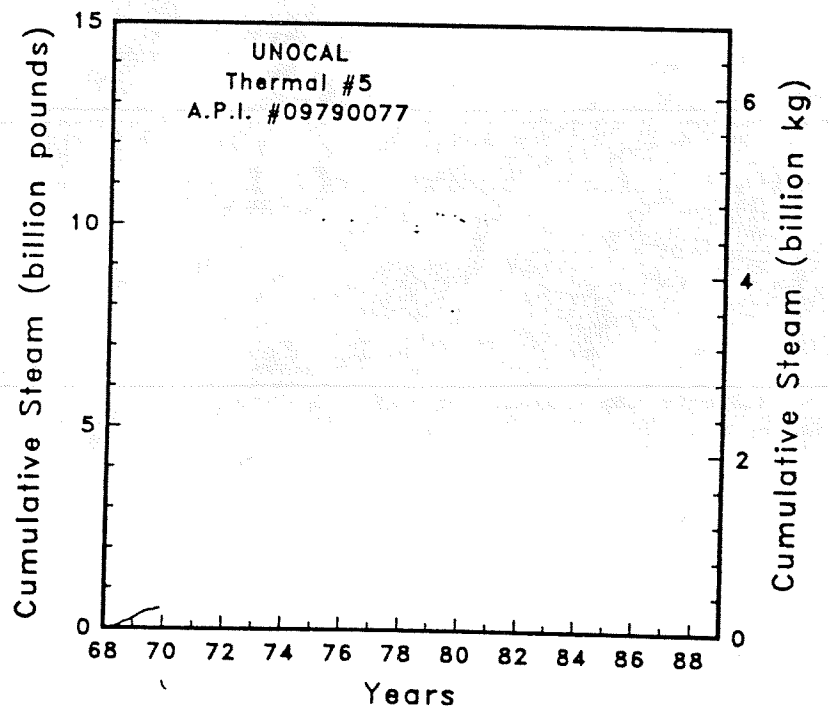

Figure A-228 Steam rate and cumulative mass flow for well Thermal #5

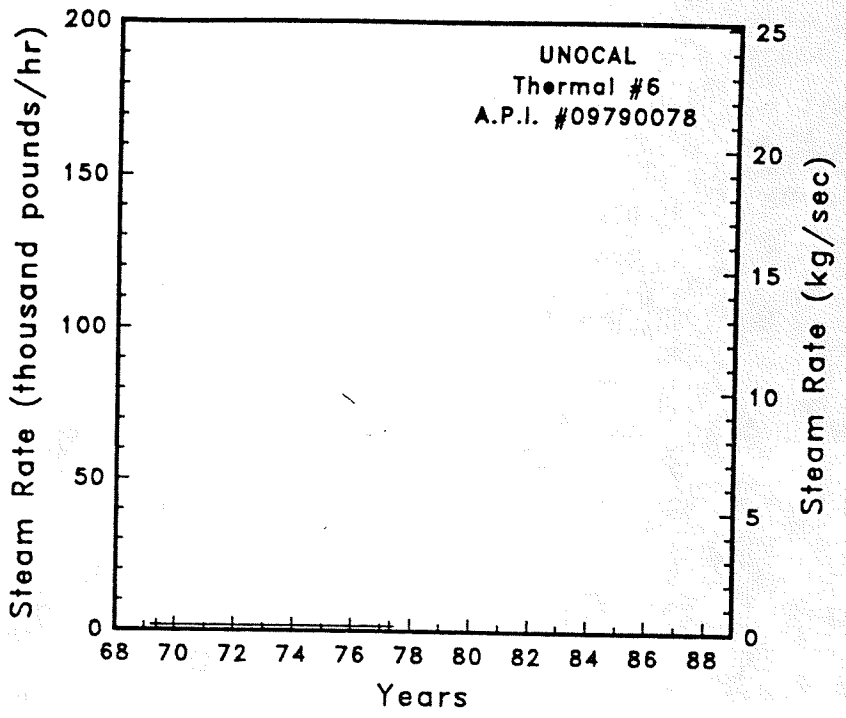

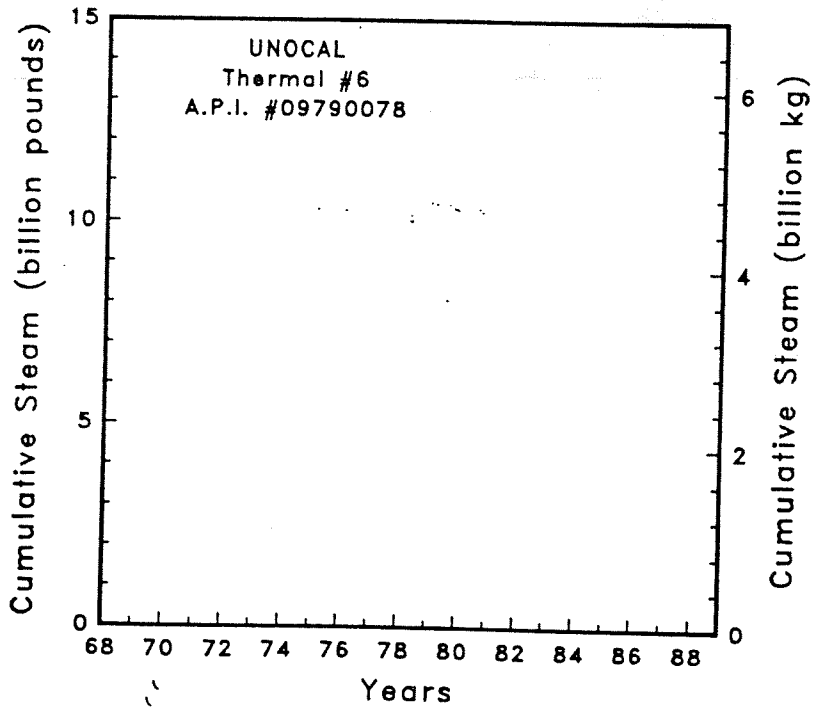

Figure A-229 Steam rate and cumulative mass flow for well Thermal #6

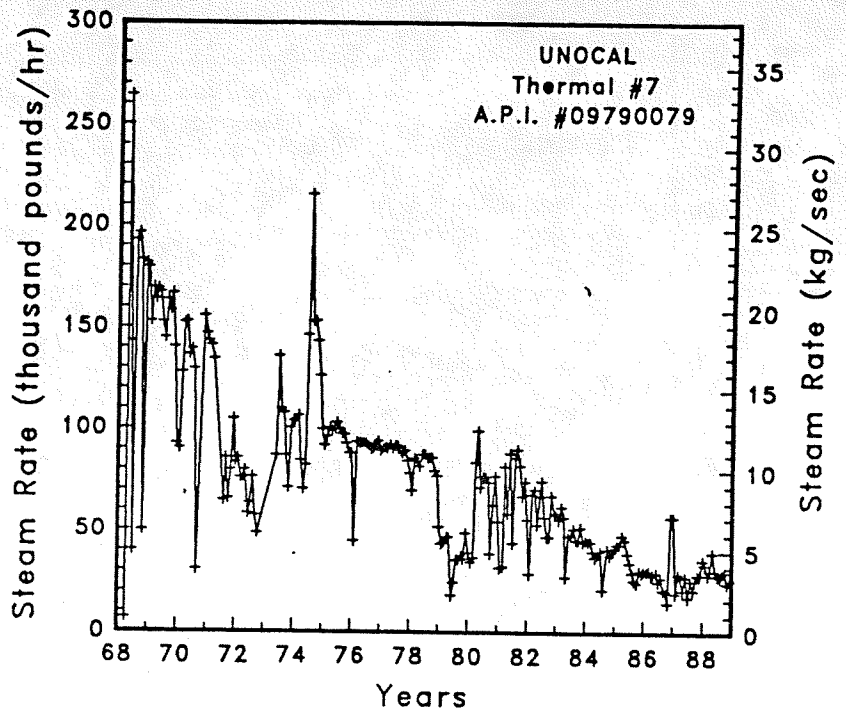

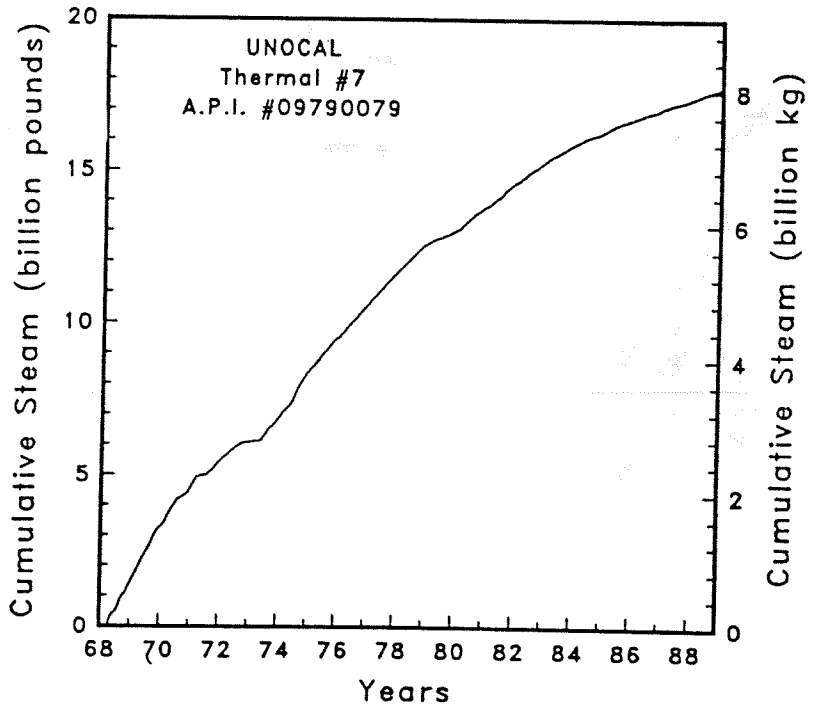

Figure A-230 Steam rate and cumulative mass flow for well Thermal #7

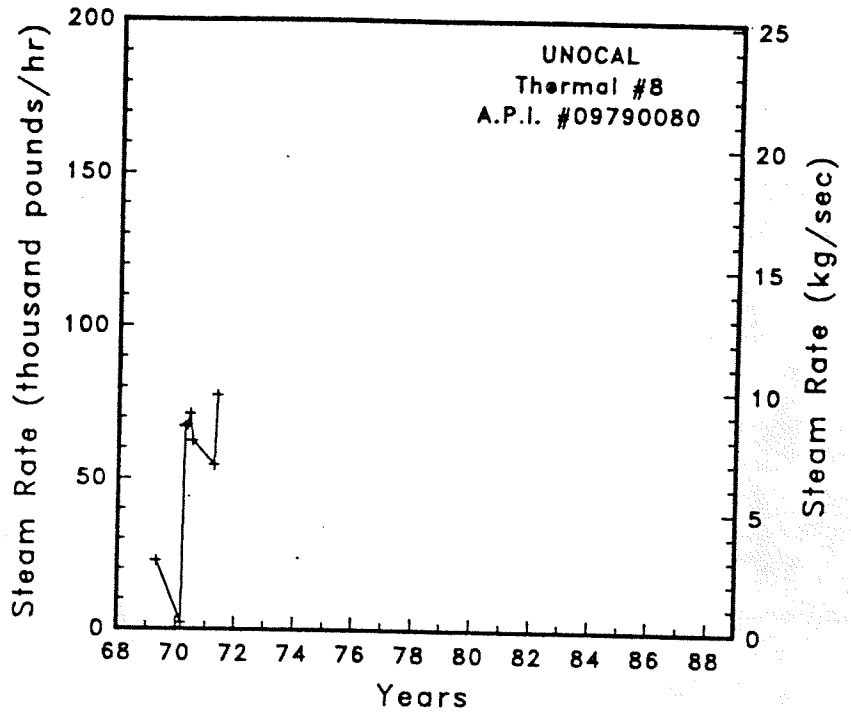

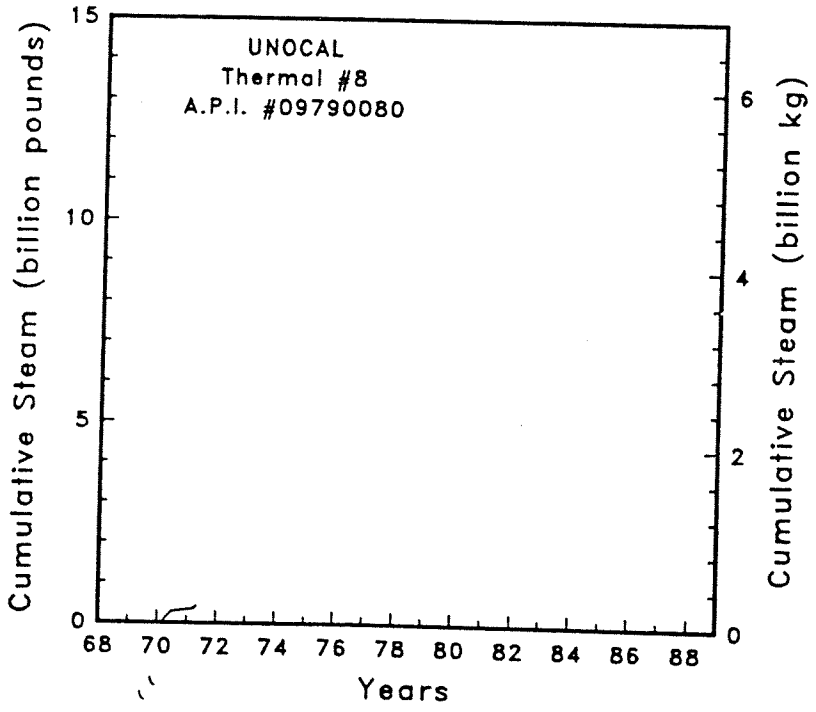

Figure A-231 Steam rate and cumulative mass flow for well Thermal #8

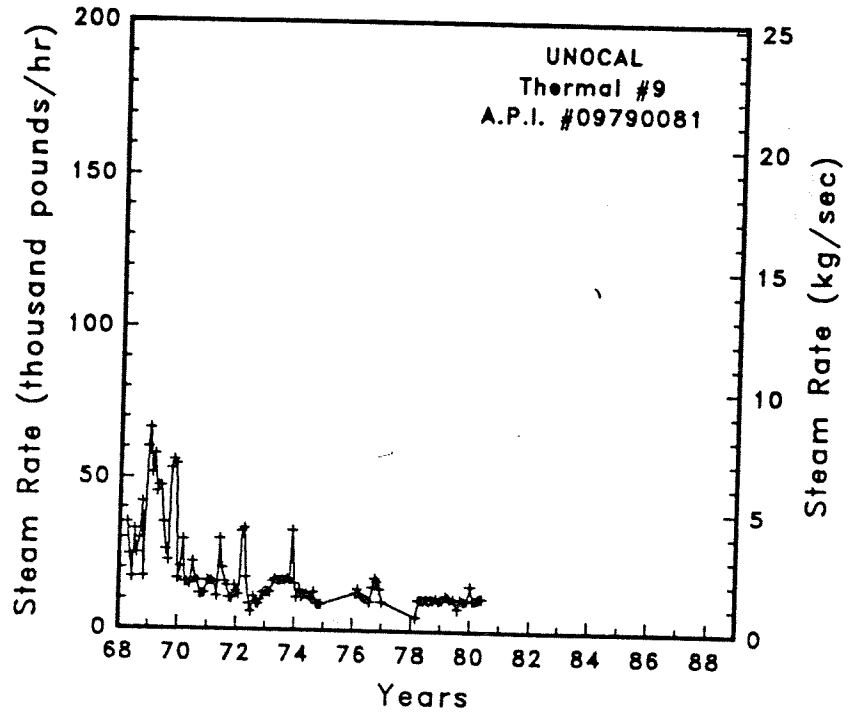

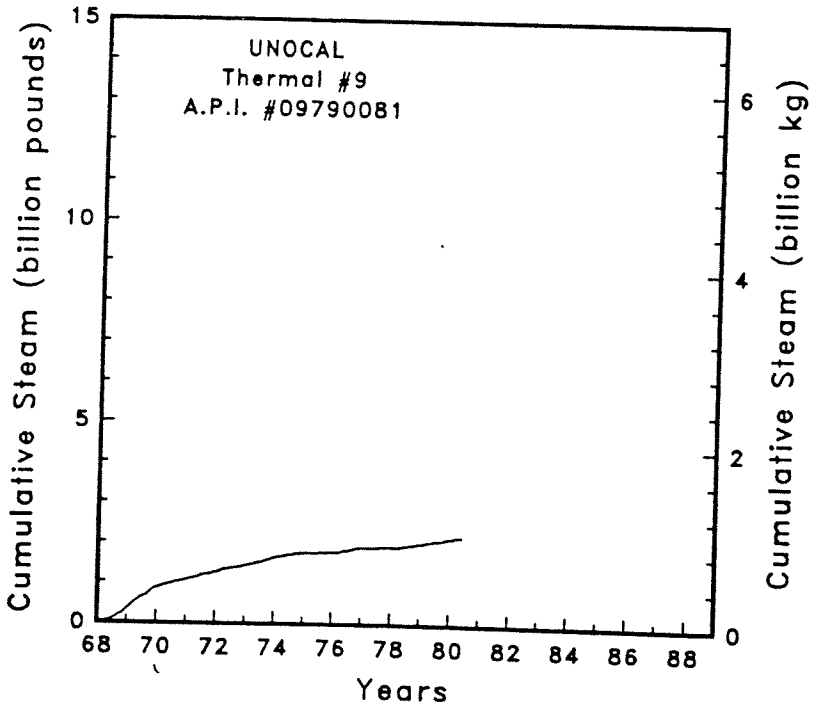

Figure A-232 Steam rate and cumulative mass flow for well Thermal #9

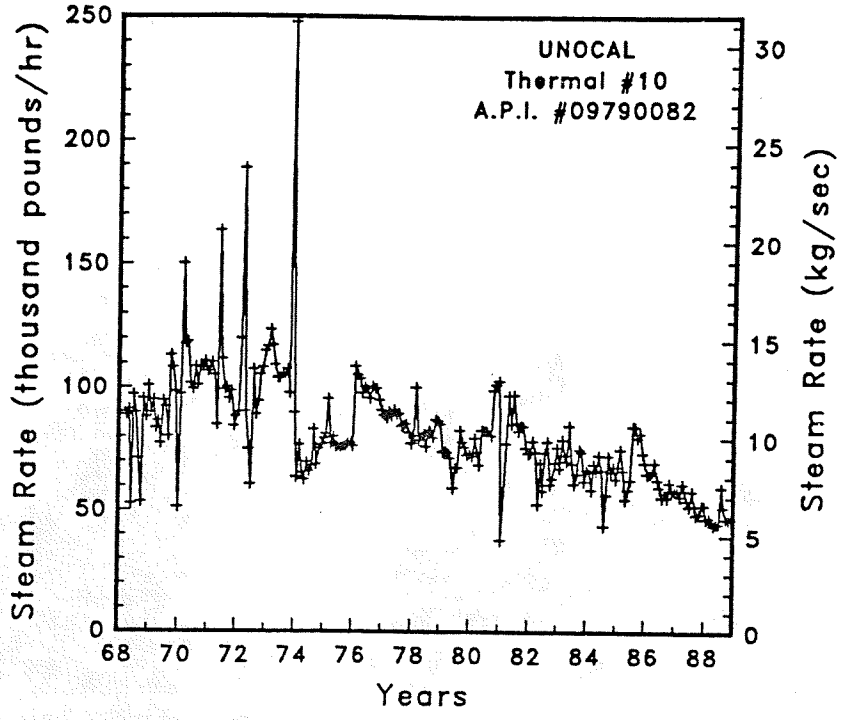

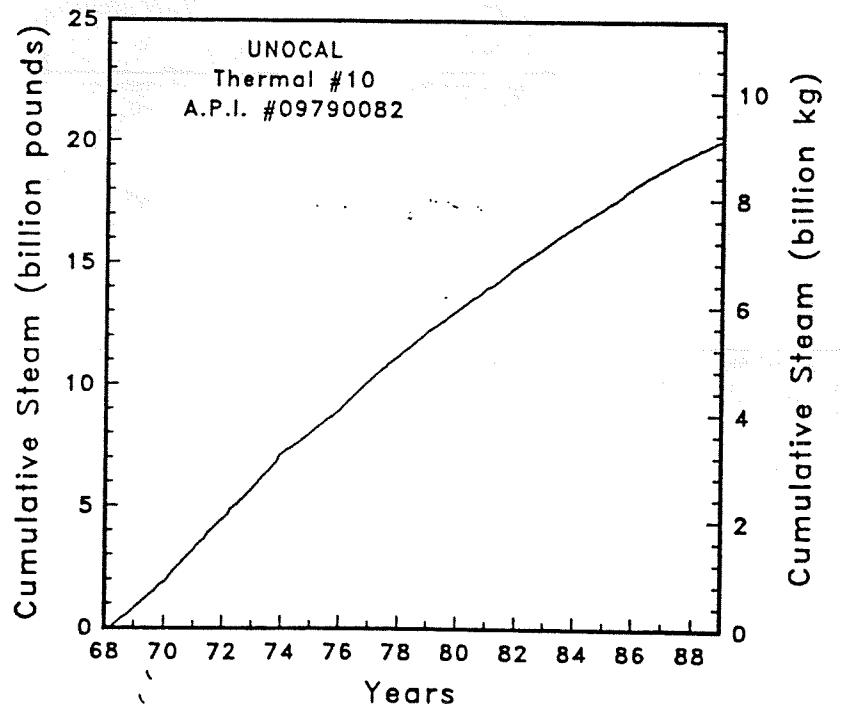

Figure A-233 Steam rate and cumulative mass flow for well Thermal #10

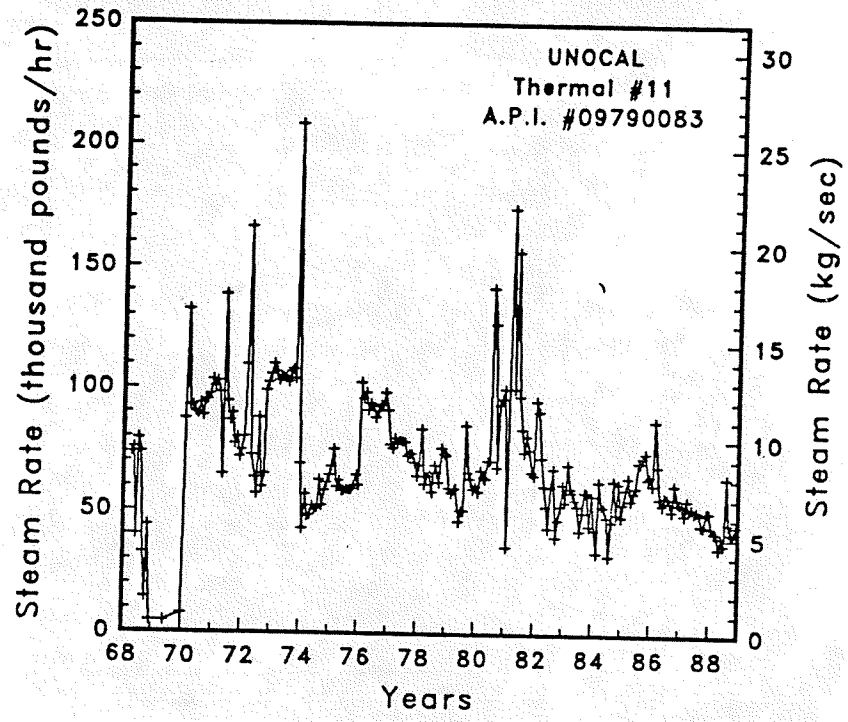

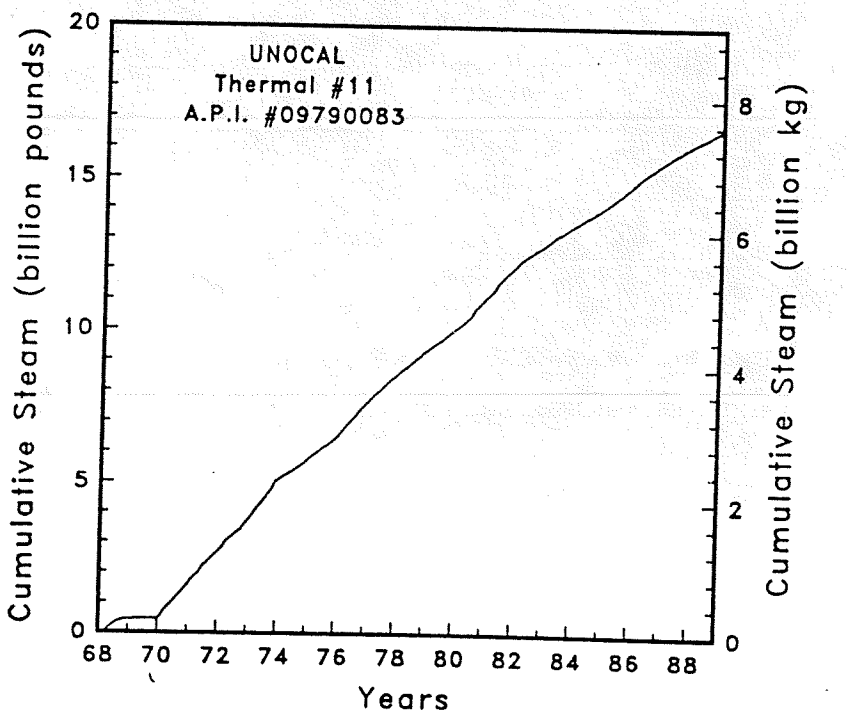

Figure A-234 Steam rate and cumulative mass flow for well Thermal #11

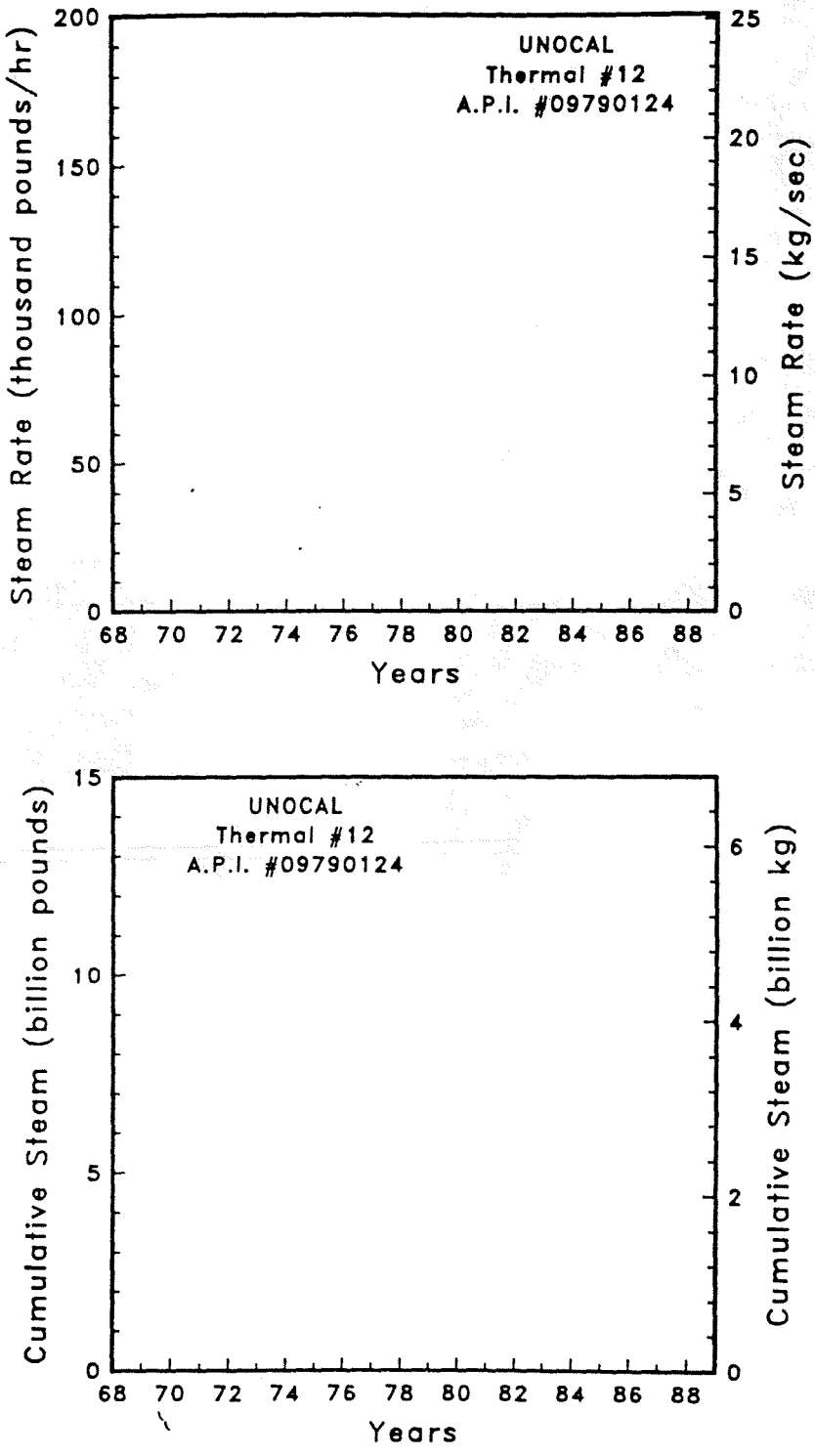

Figure A-235 Steam rate and cumulative mass flow for well Thermal #12

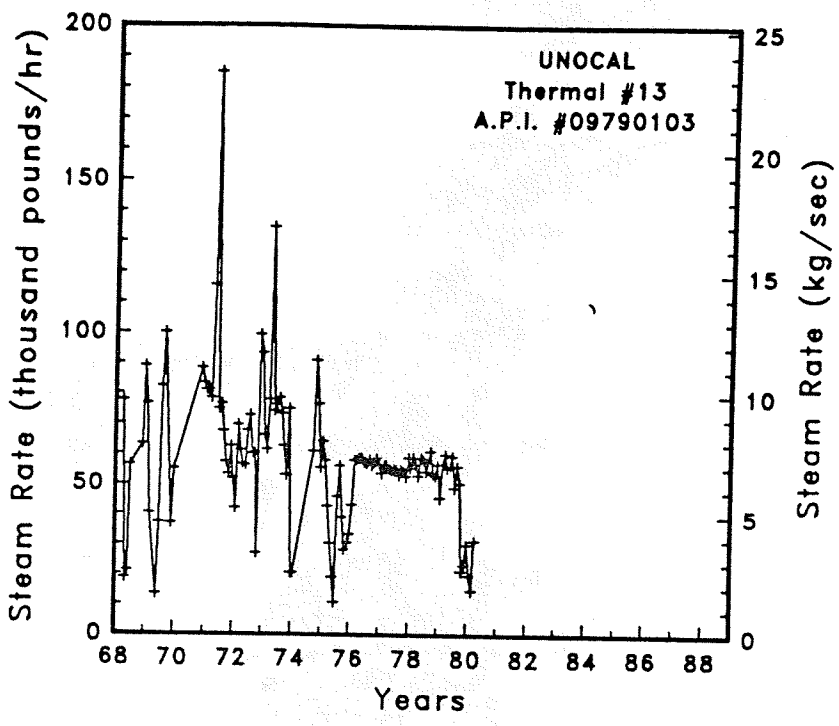

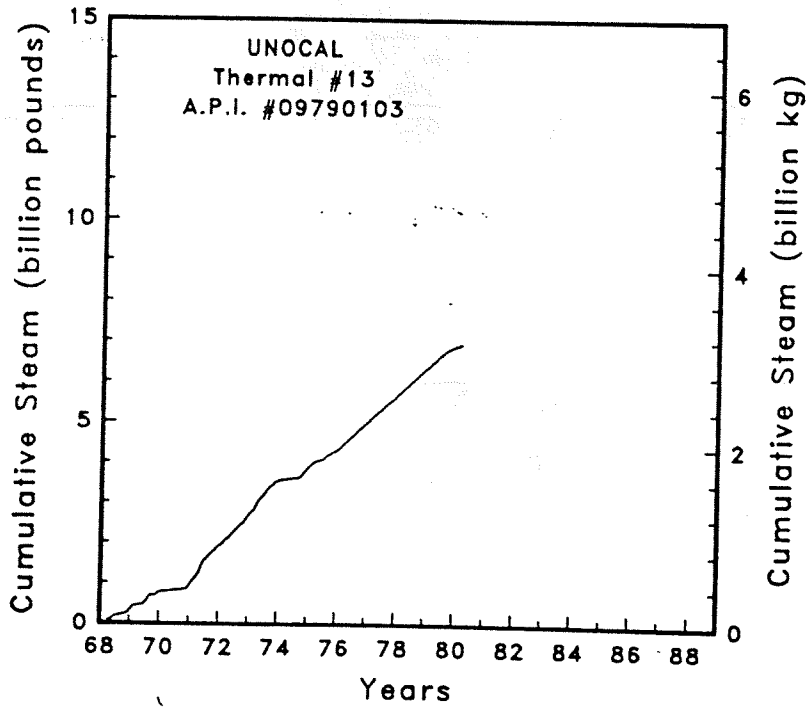

Figure A-236 Steam rate and cumulative mass flow for well Thermal #13

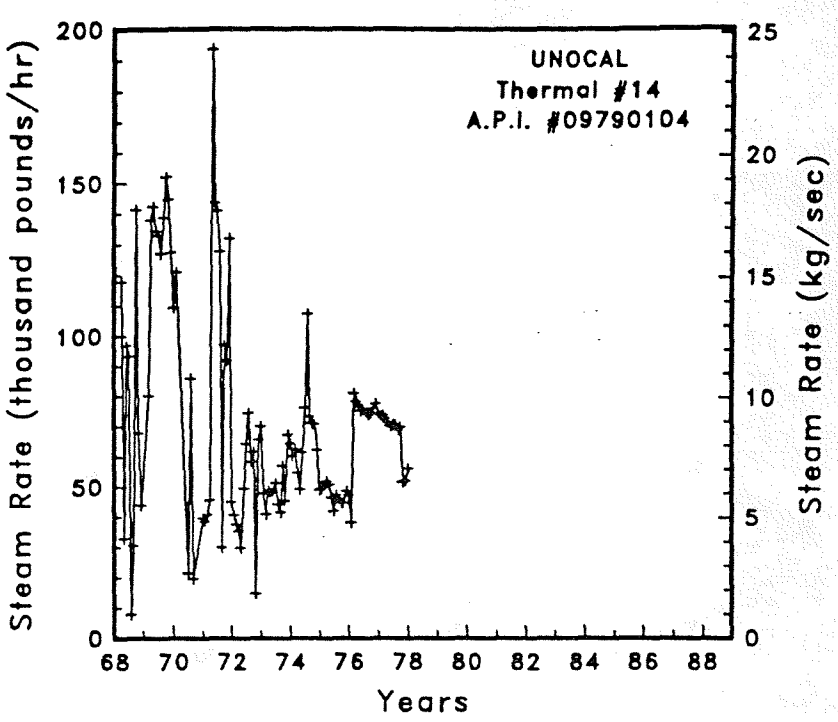

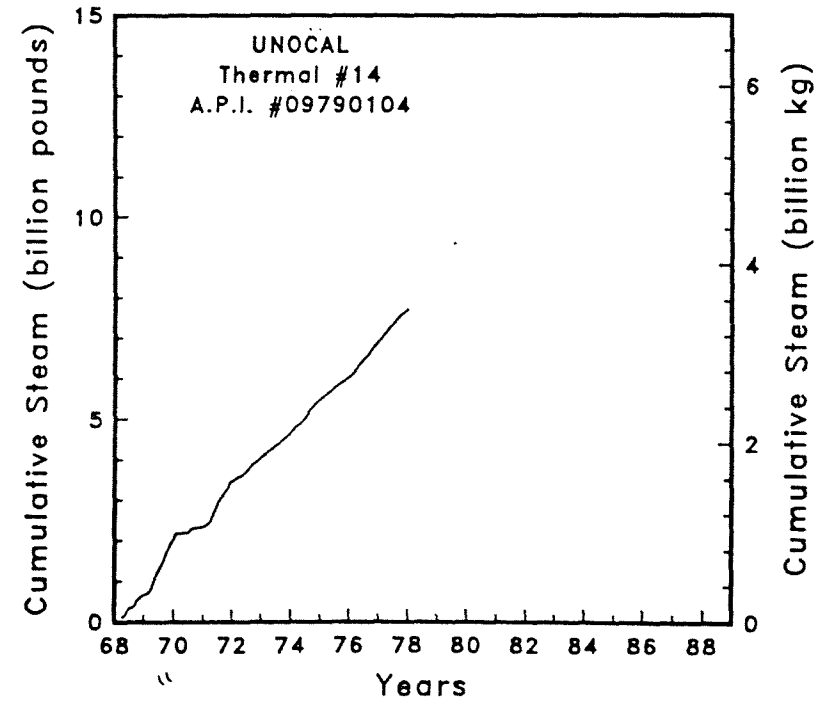

Figure A-237 Steam rate and cumulative mass flow for well Thermal #14

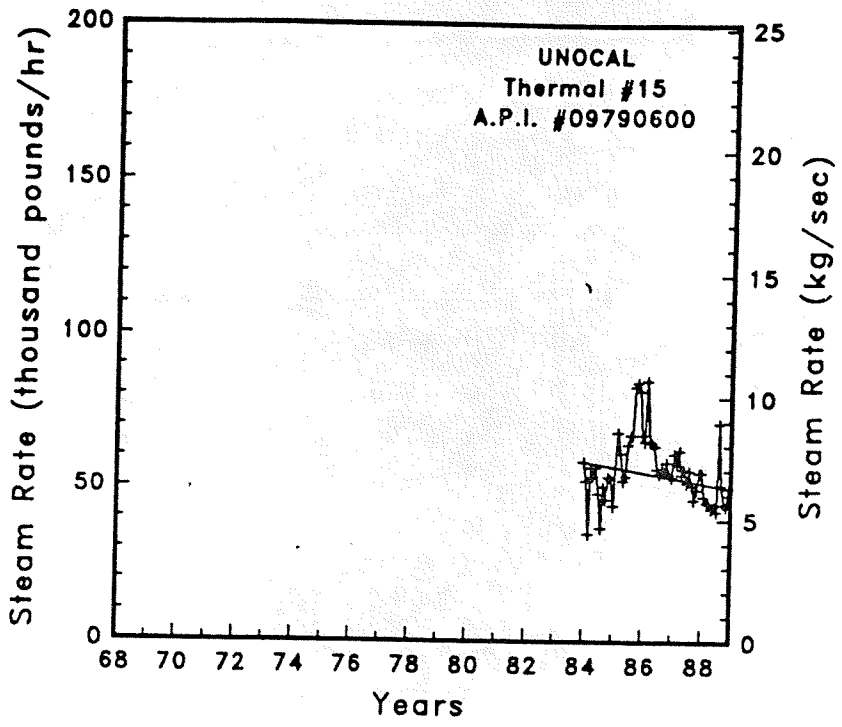

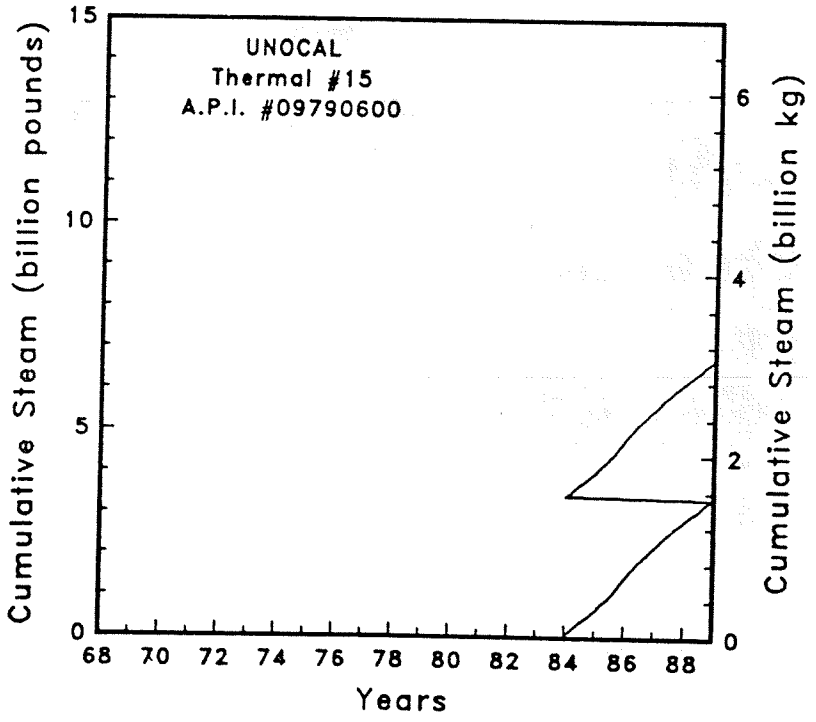

Figure A-238 Steam rate and cumulative mass flow for well Thermal #15

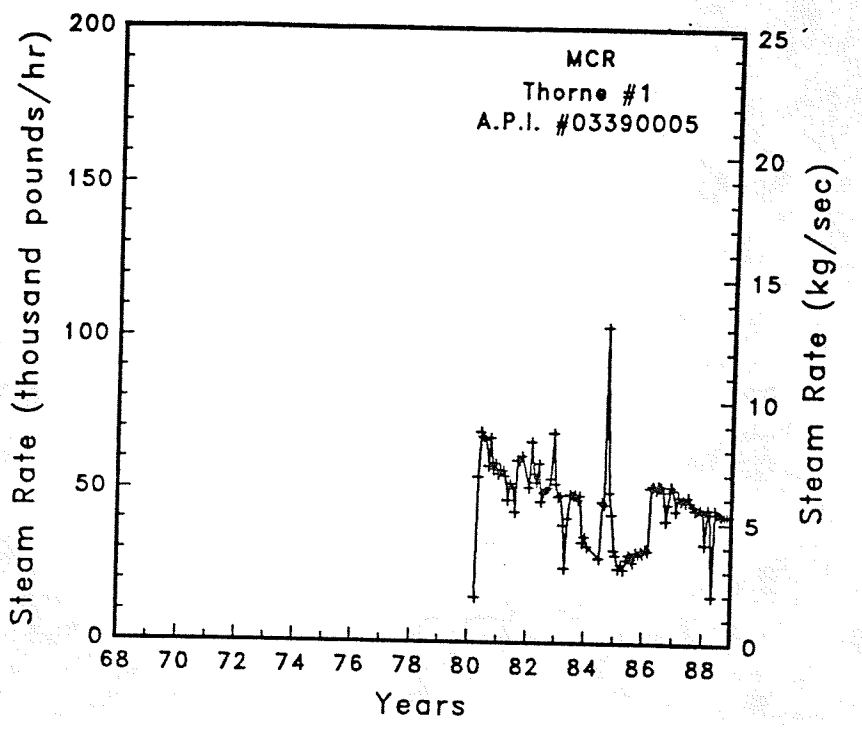

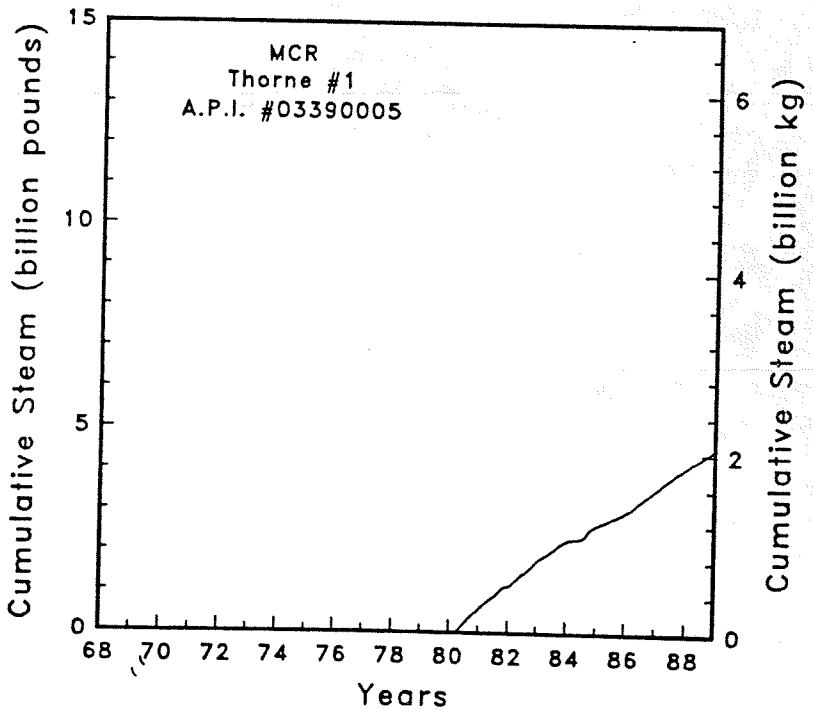

Figure A-239 Steam rate and cumulative mass flow for well Thorne #1

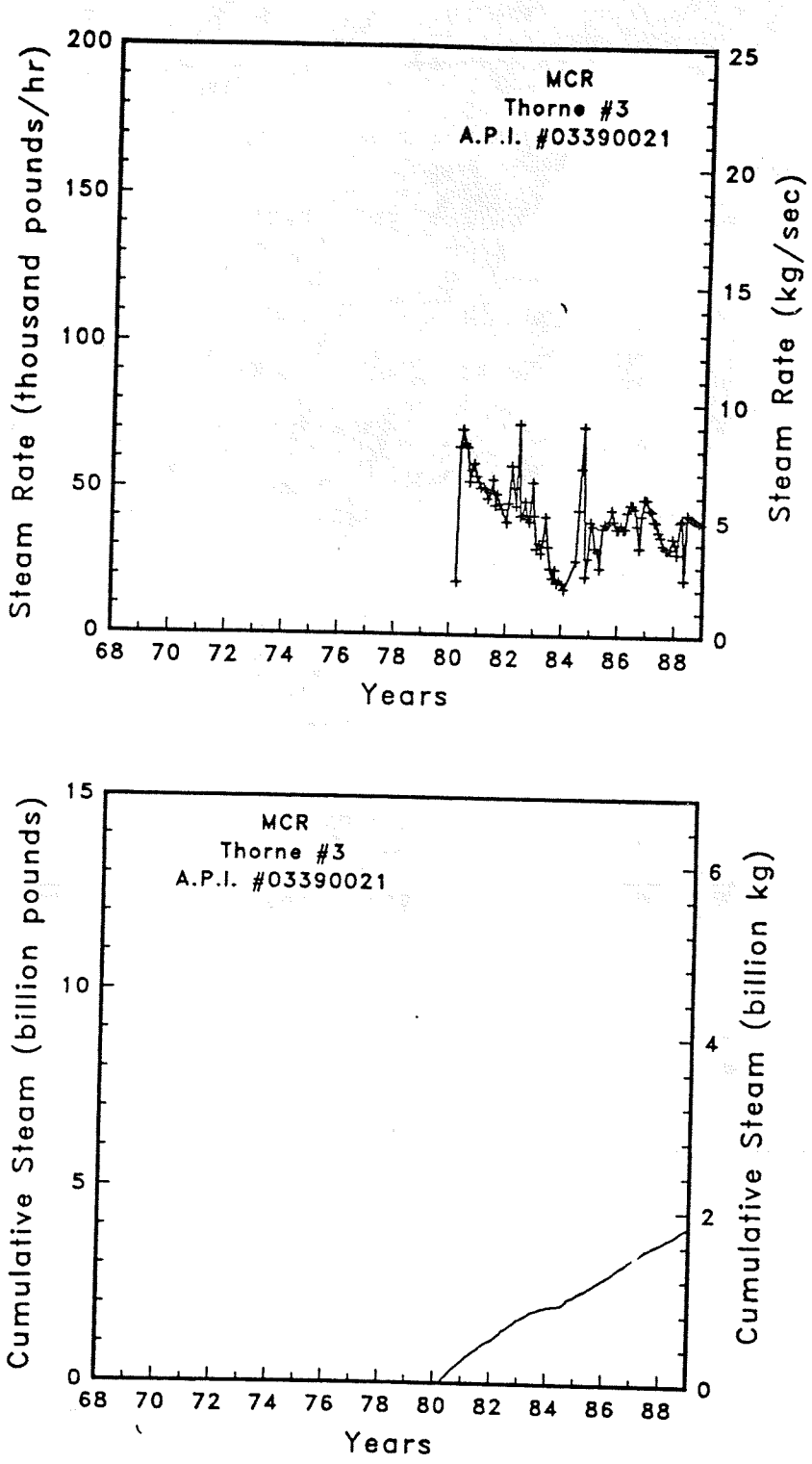

Figure A-240 Steam rate and cumulative mass flow for well Thorne #3

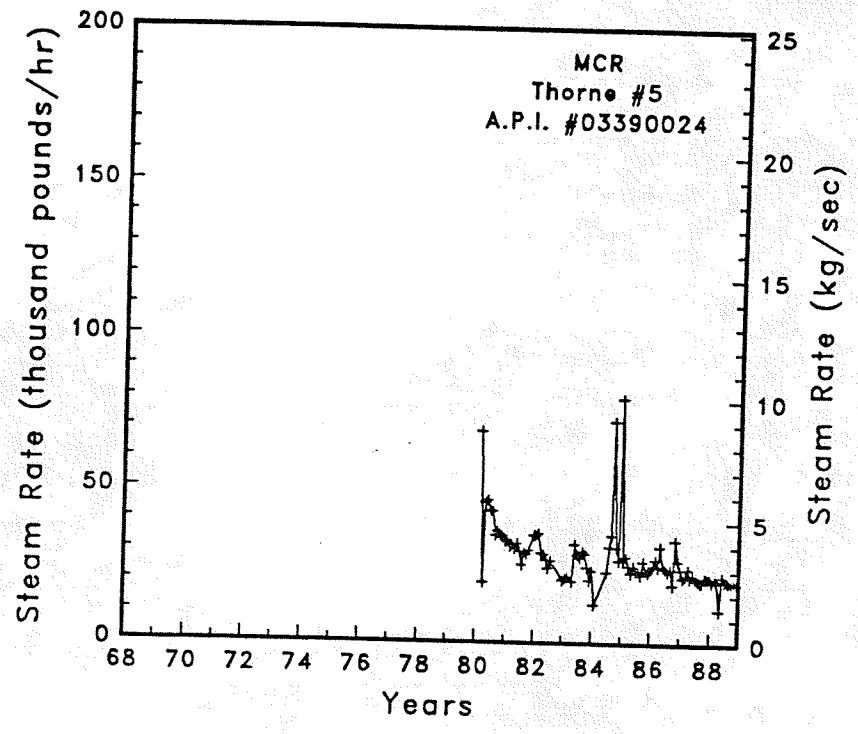

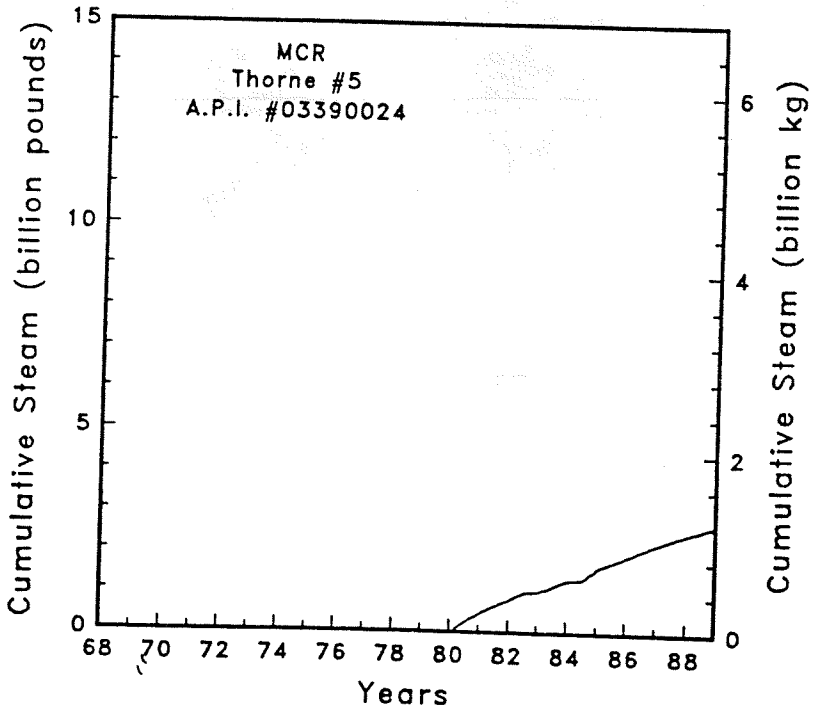

Figure A-241 Steam rate and cumulative mass flow for well Thorne #5